Pecos River-New Mexico Basin Study

Appendices

U.S. Department of the Interior
Bureau of Reclamation
Albuquerque Area Office

New Mexico Office of the State Engineer
Interstate Stream Commission

September 2021

List of Appendices

Figures Appendix	**pdf page 5**
Climate Appendix	**pdf page 85**
Environmental and Recreational Appendix	**pdf page 125**
Extreme Storm Events Appendix	**pdf page 139**
Surface Water Modeling Appendix	**pdf page 149**
Groundwater Modeling Appendix	**pdf page 201**

Pecos River-
New Mexico Basin Study

Figures Appendix

Contents

1. Reservoir Storage 1
2. FSID Entitlement 13
3. FSID Shortages 15
4. CID Allotment 23
5. CID Shortages 35
6. Drying Days at Acme 47
7. Drying at Acme and Artesia Gages...63
8. Potential Settlement Releases...65

1. Reservoir Storage

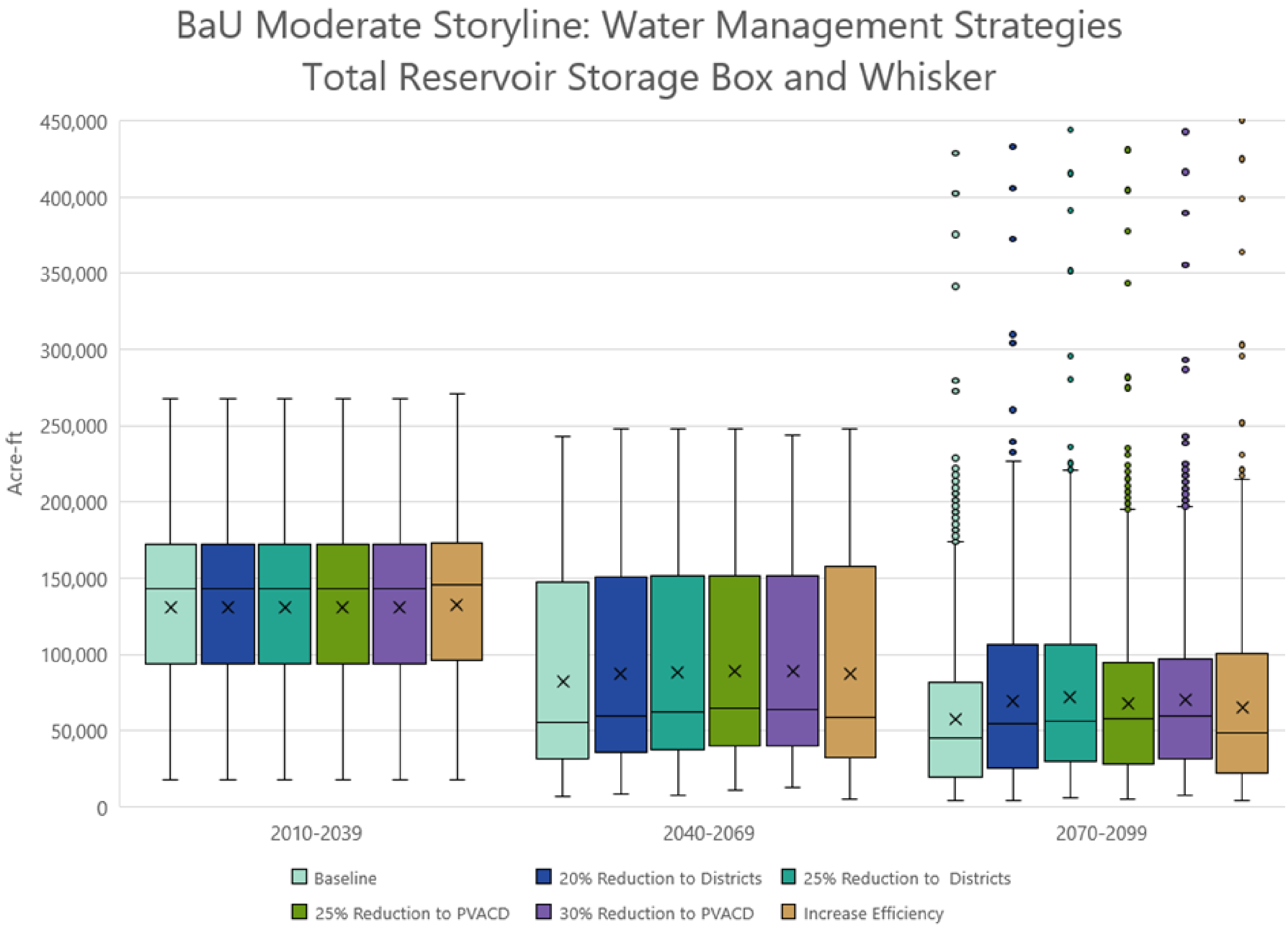

Figure 1. Reservoir Storage: Water Management Strategies in the BaU Moderate Storyline.

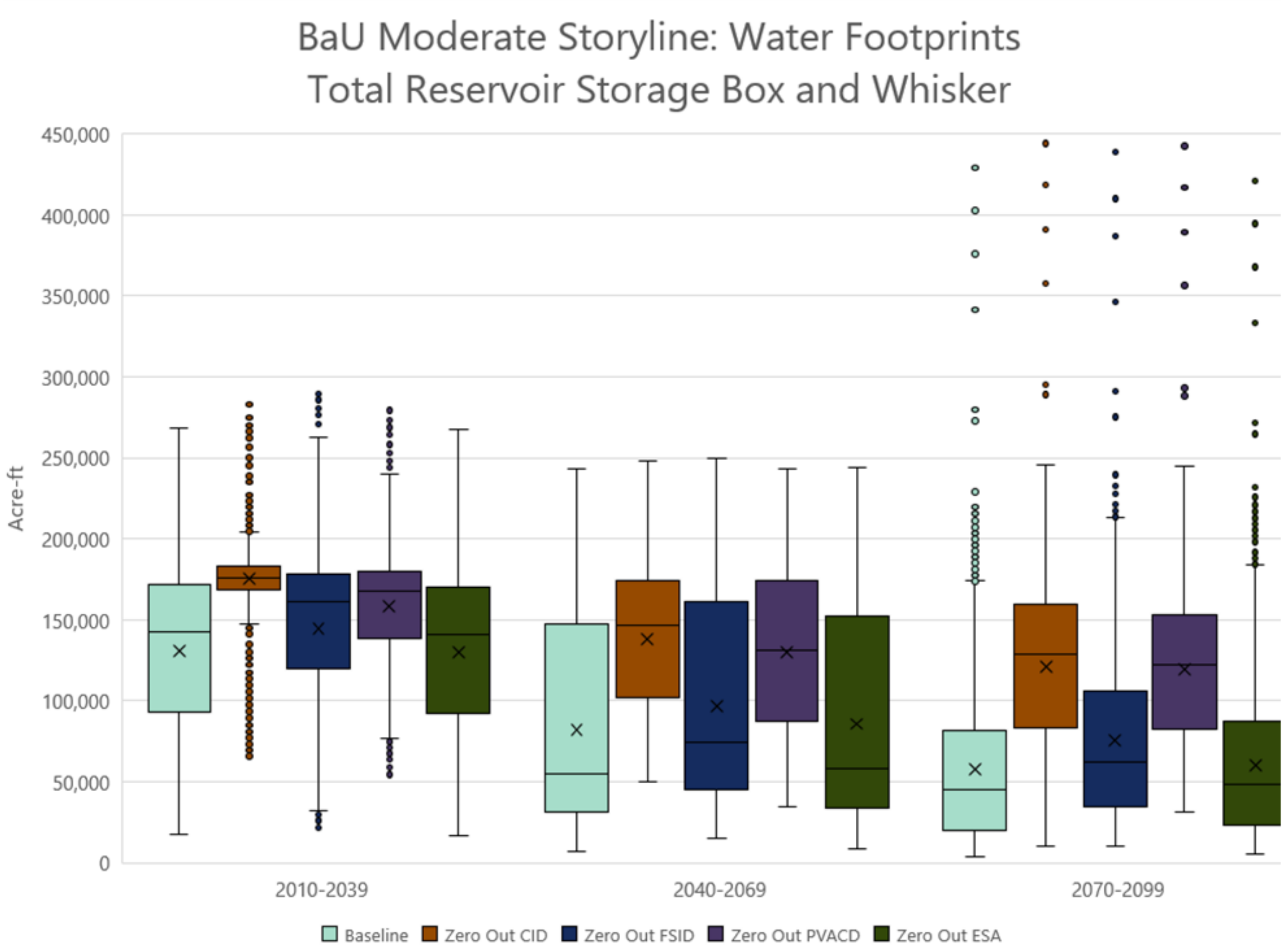

Figure 2. Reservoir Storage: Water Footprints in the BaU Moderate Storyline.

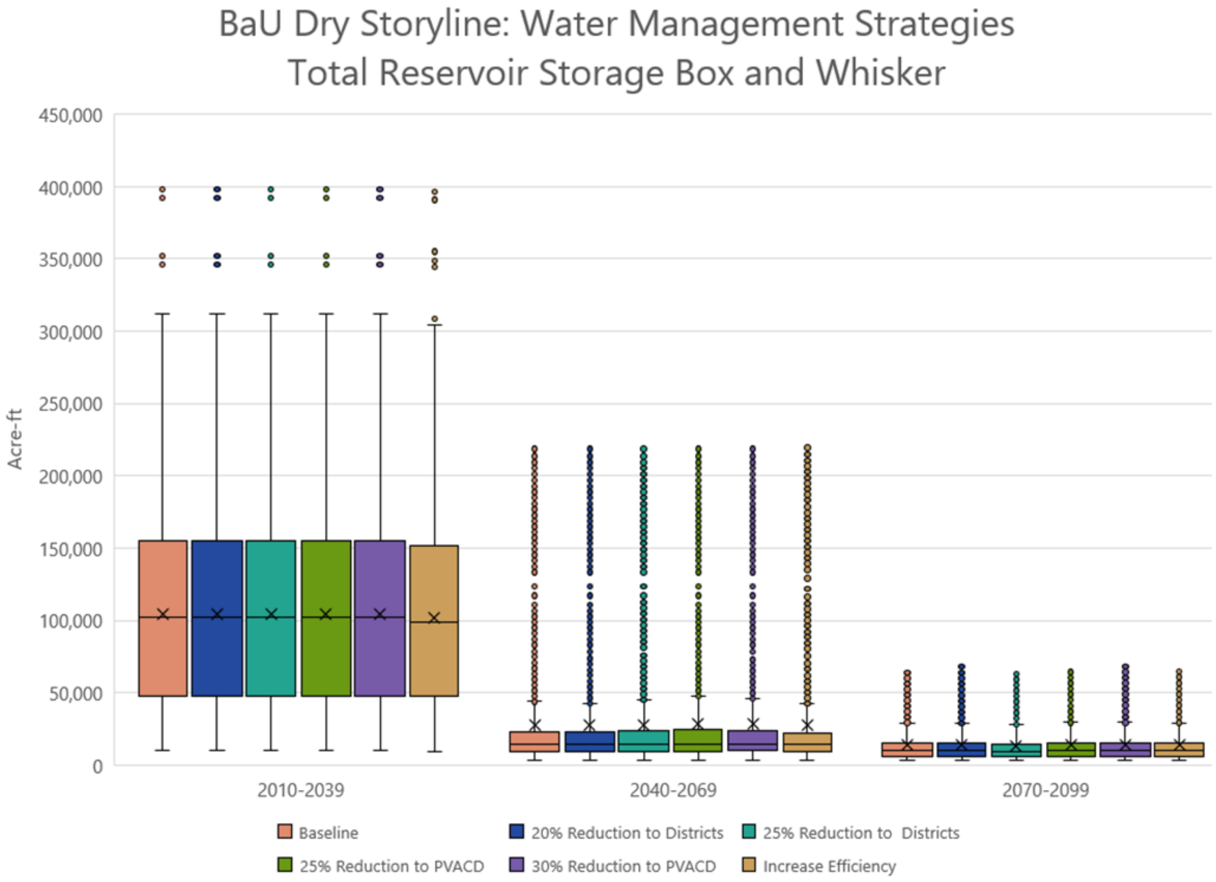

Figure 3. Reservoir Storage: Water Management Strategies in the BaU Dry Storyline.

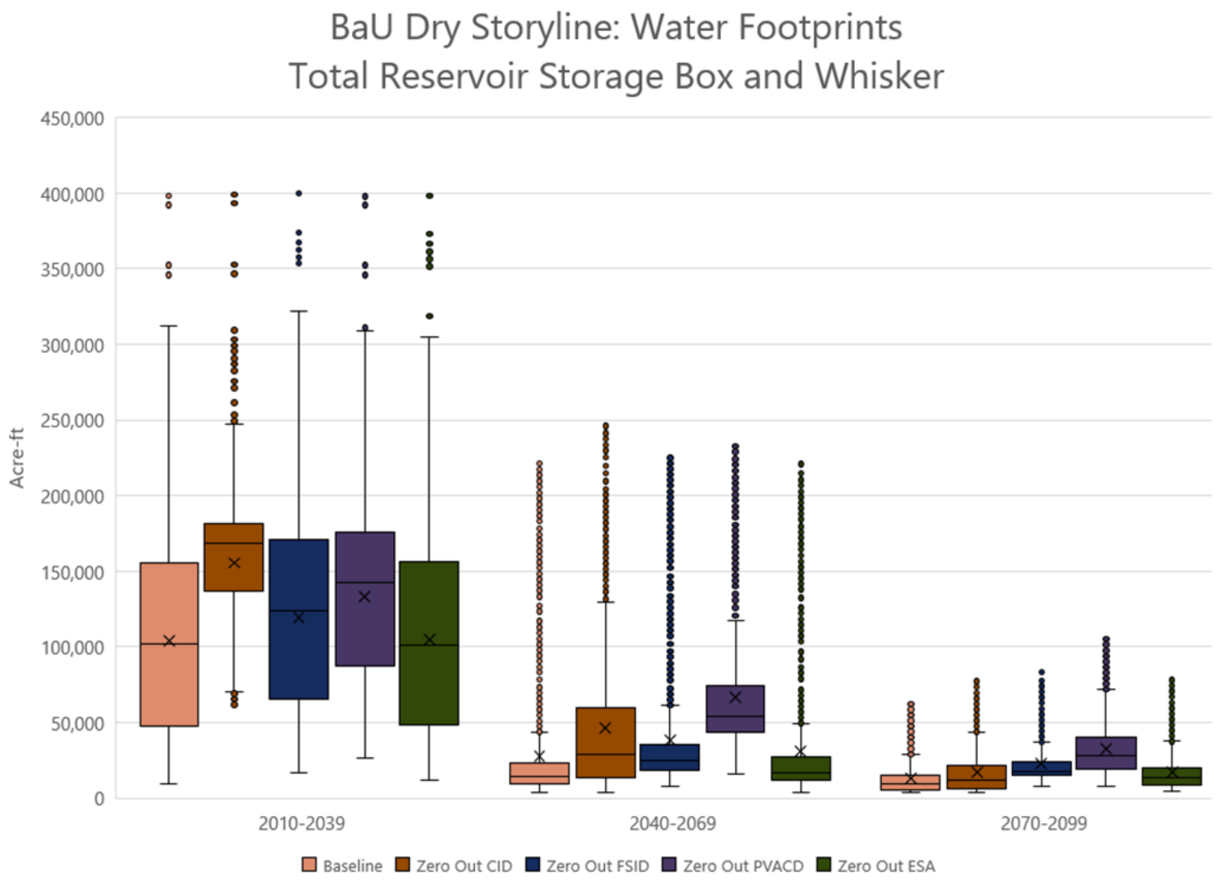

Figure 4. Reservoir Storage: Water Footprints in the BaU Dry Storyline.

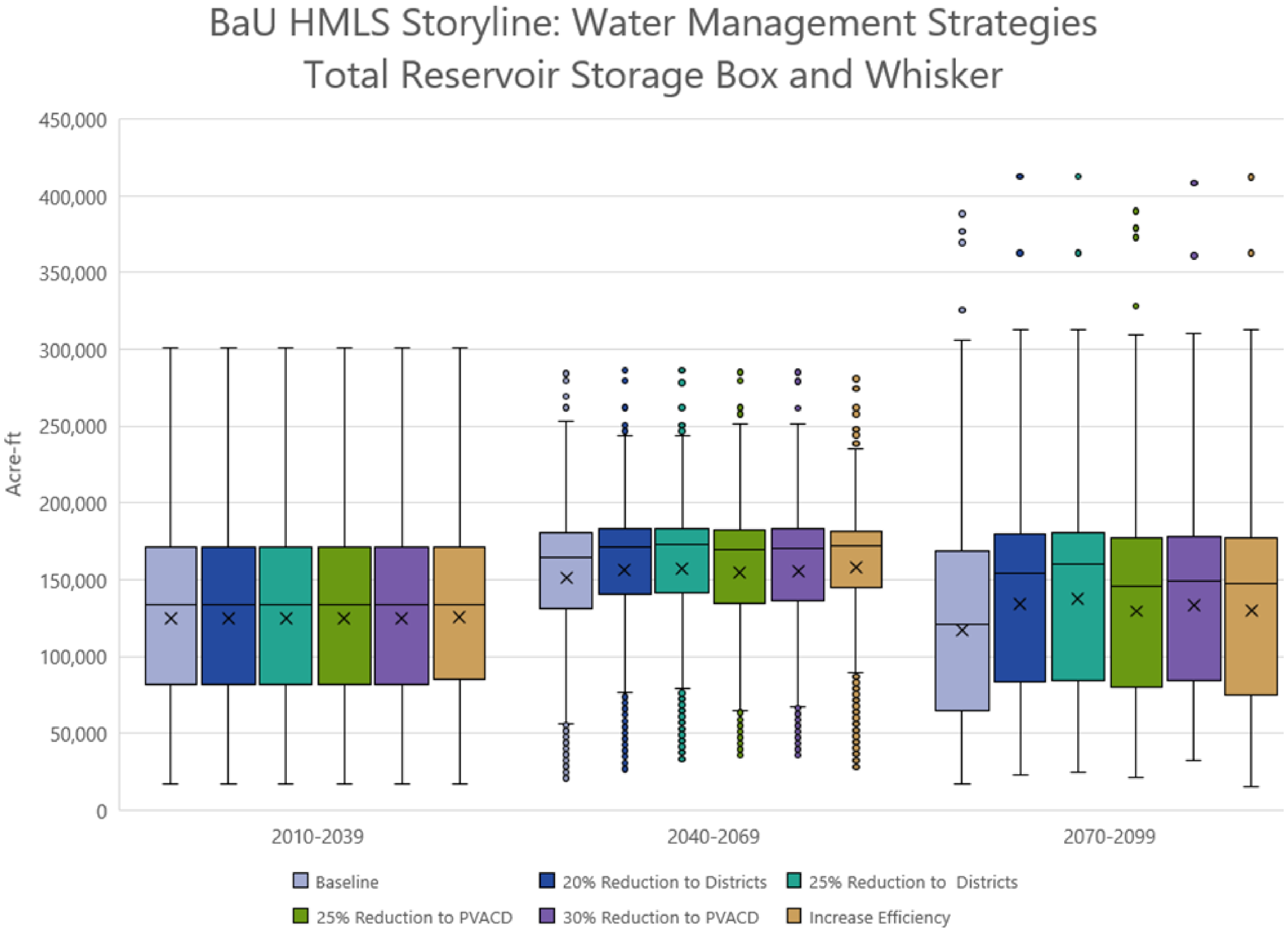

Figure 5. Reservoir Storage: Water Management Strategies in the BaU Dry Storyline.

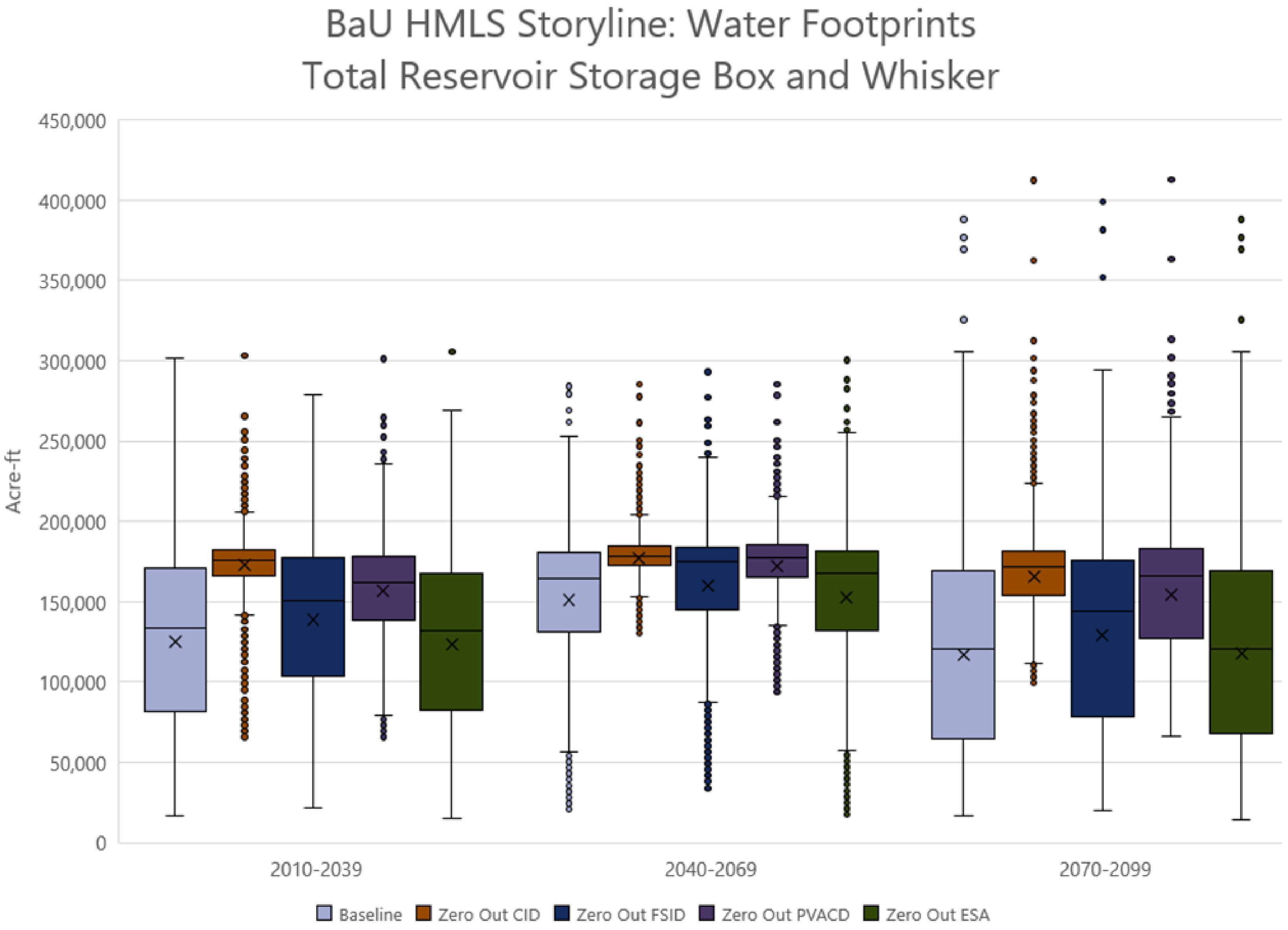

Figure 6. Reservoir Storage: Water Footprints in the BaU HMLS Storyline.

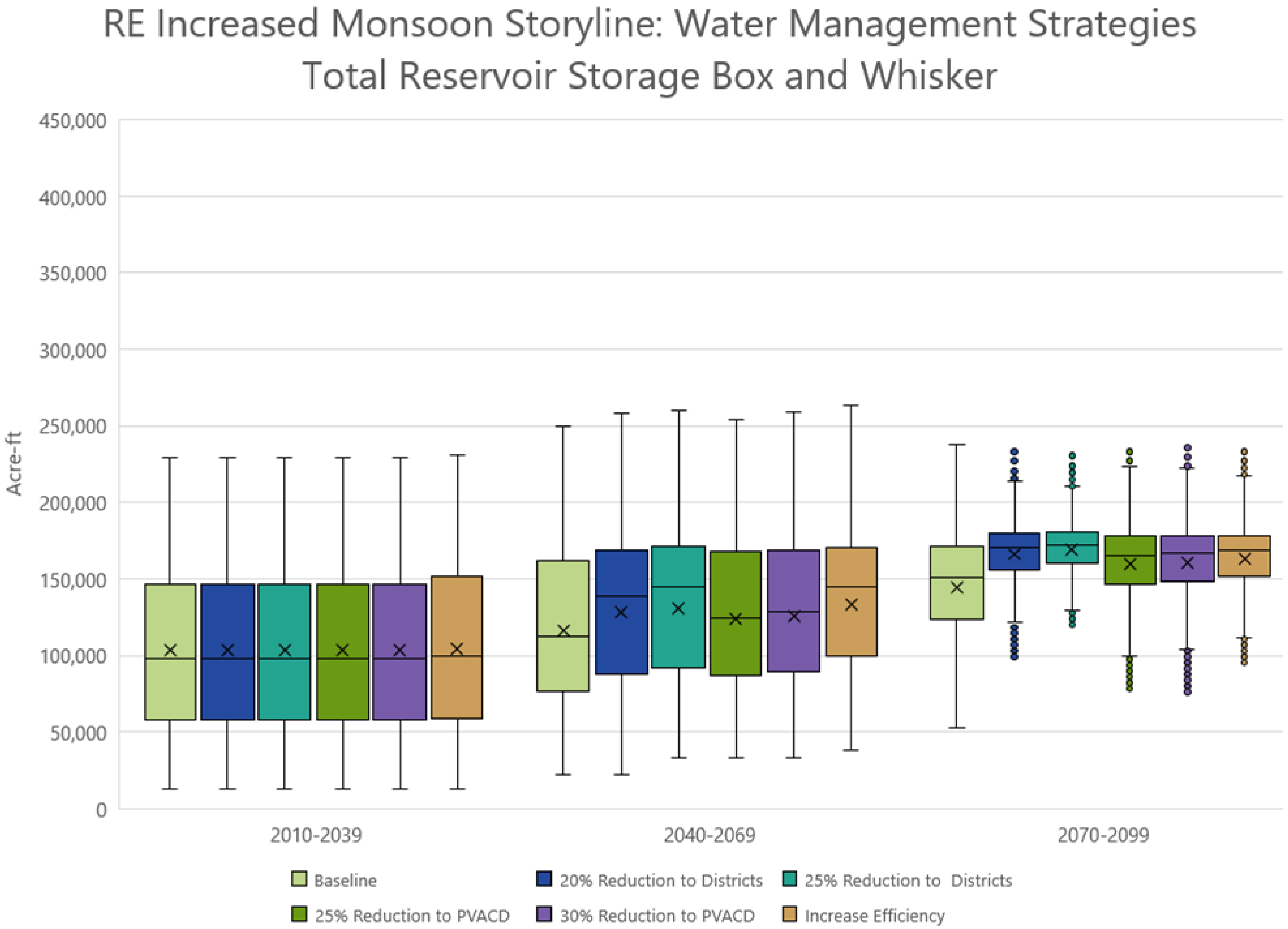

Figure 7. Reservoir Storage: Water Management Strategies in the RE Increased Monsoon Storyline.

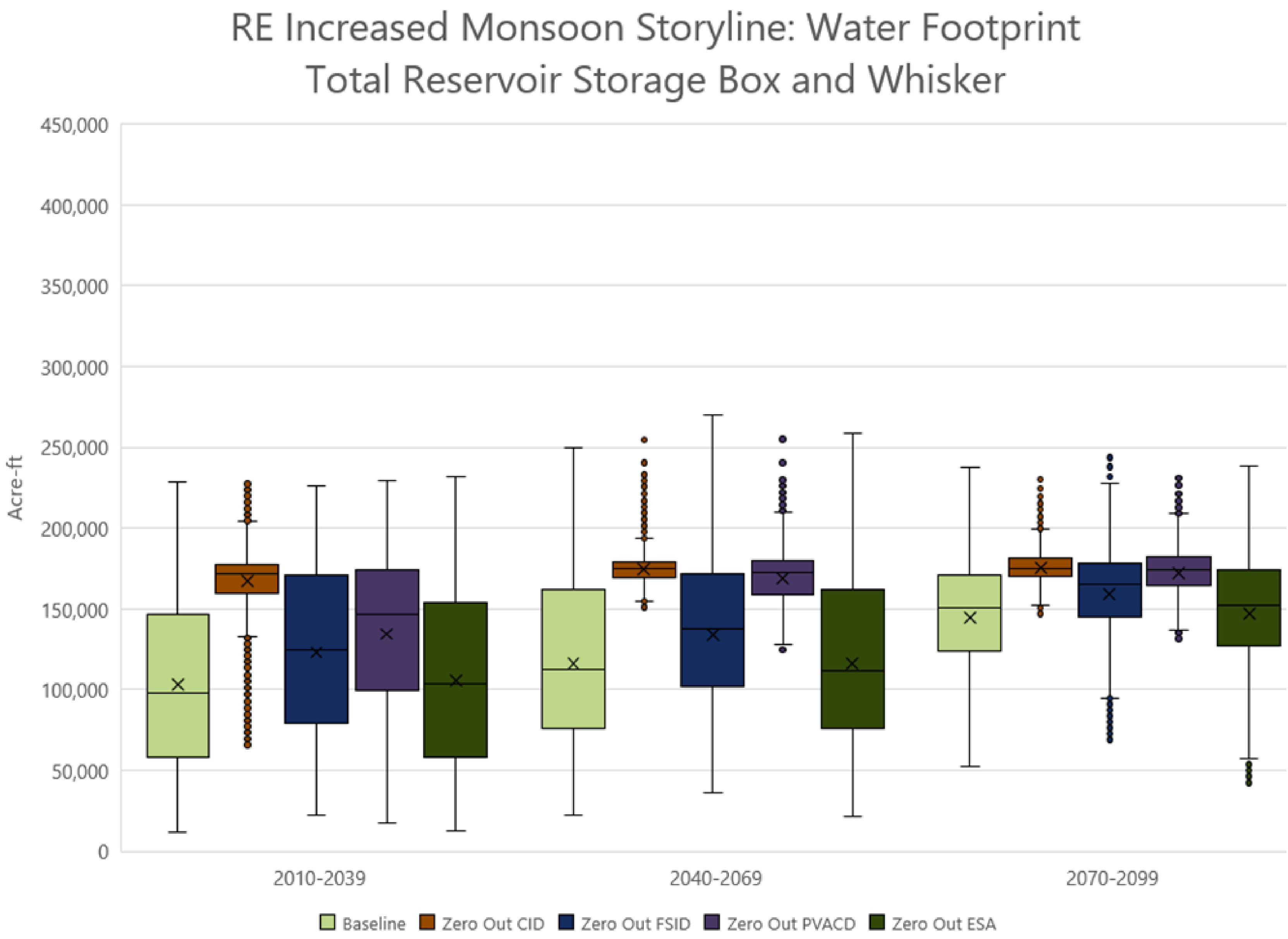

Figure 8. Reservoir Storage: Water Footprints in the RE Increased Monsoon Storyline.

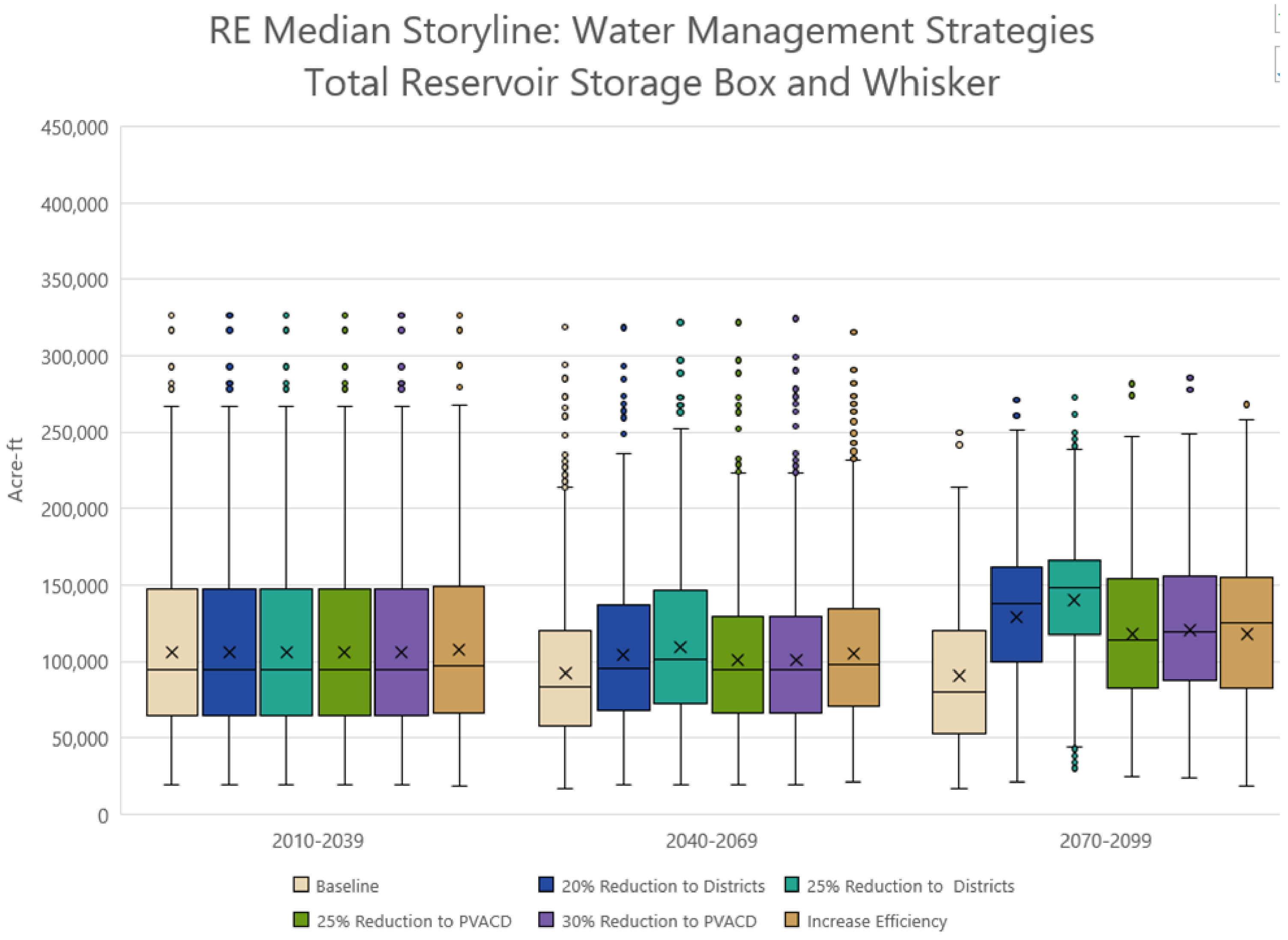

Figure 9. Reservoir Storage: Water Management Strategies in the RE Moderate Storyline.

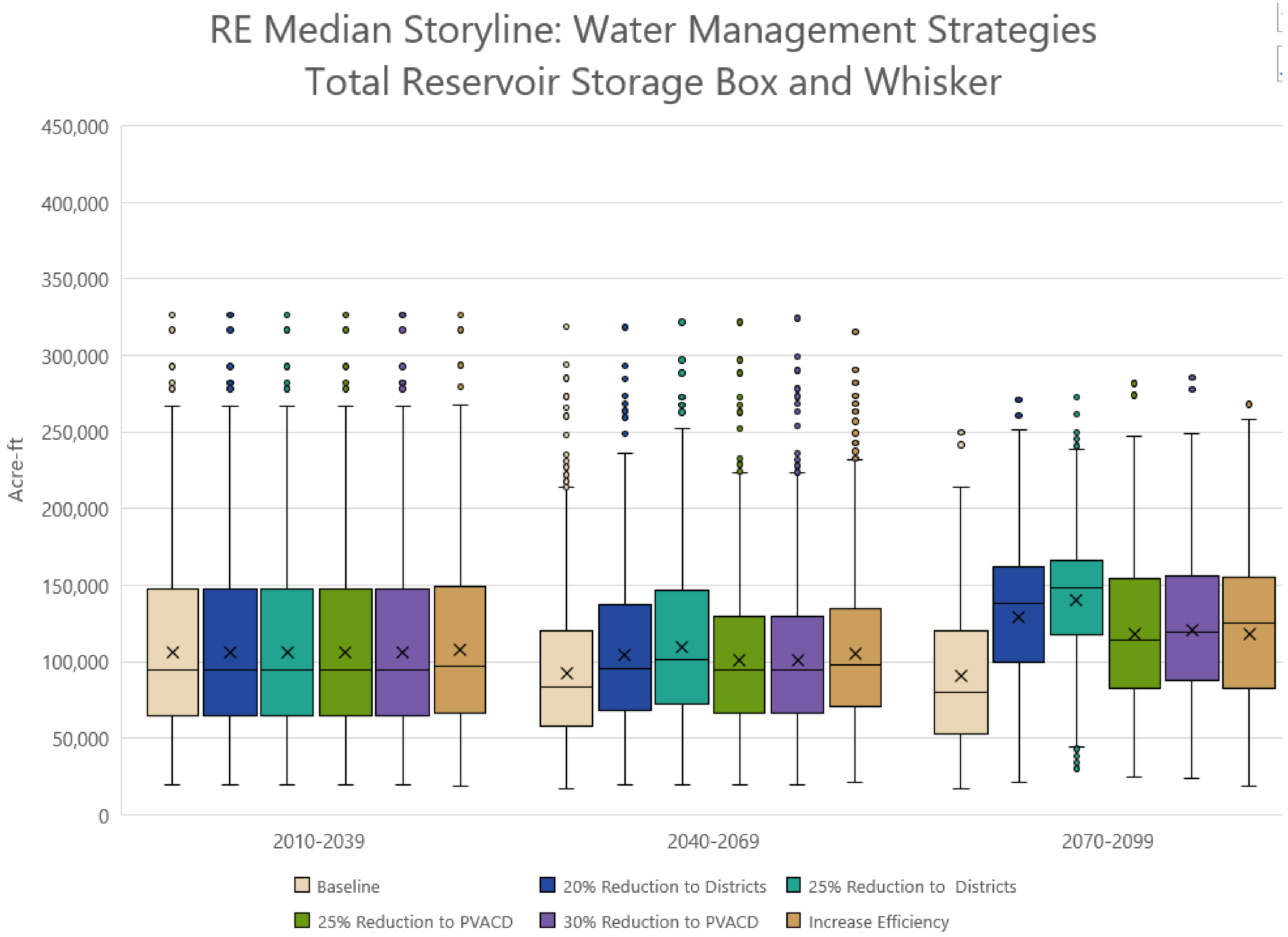

Figure 10. Reservoir Storage: Water Footprints in the RE Median Storyline.

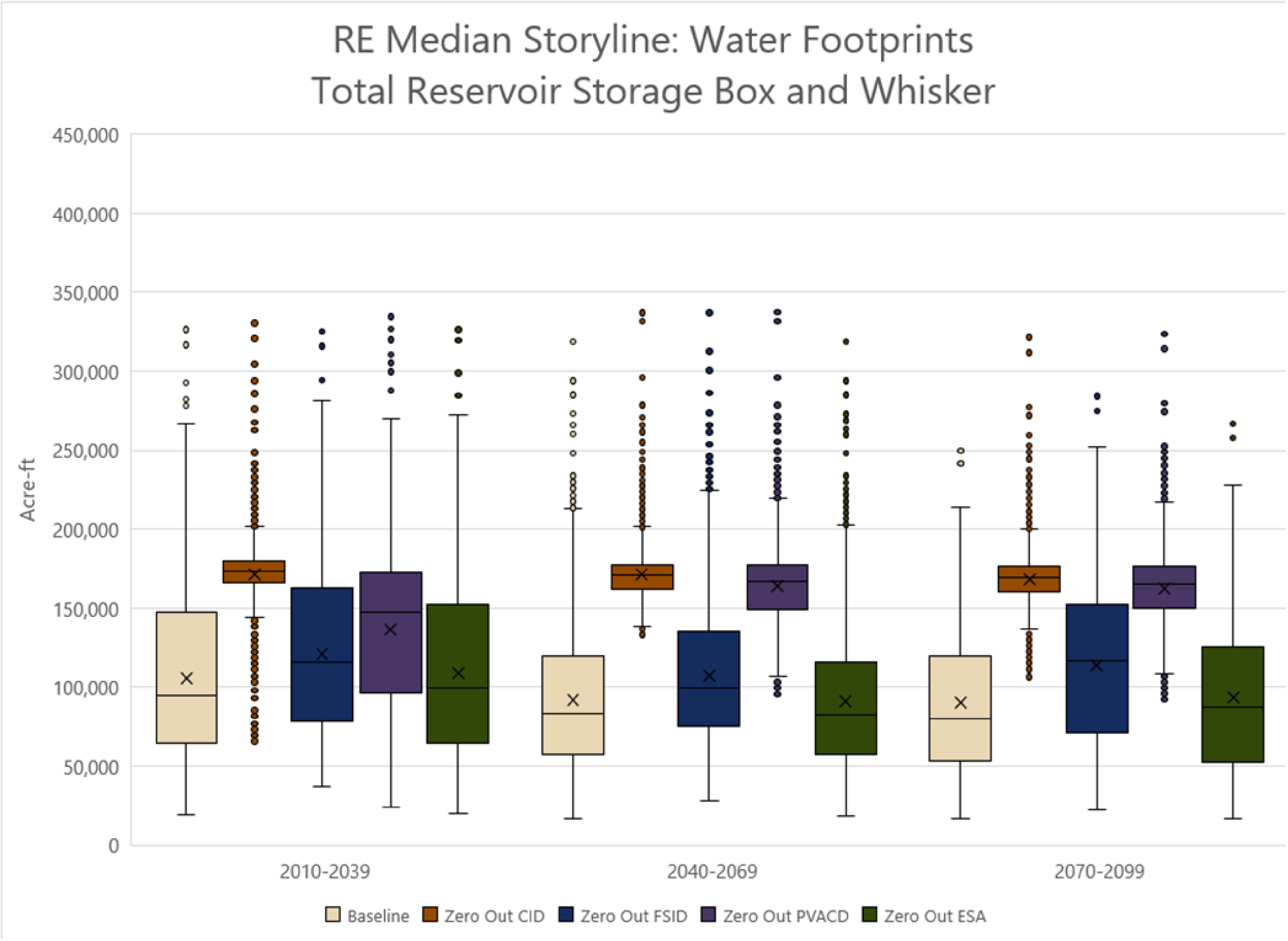

Figure 11. Reservoir Storage: Water Footprints in the RE Median Storyline.

2. FSID Entitlement

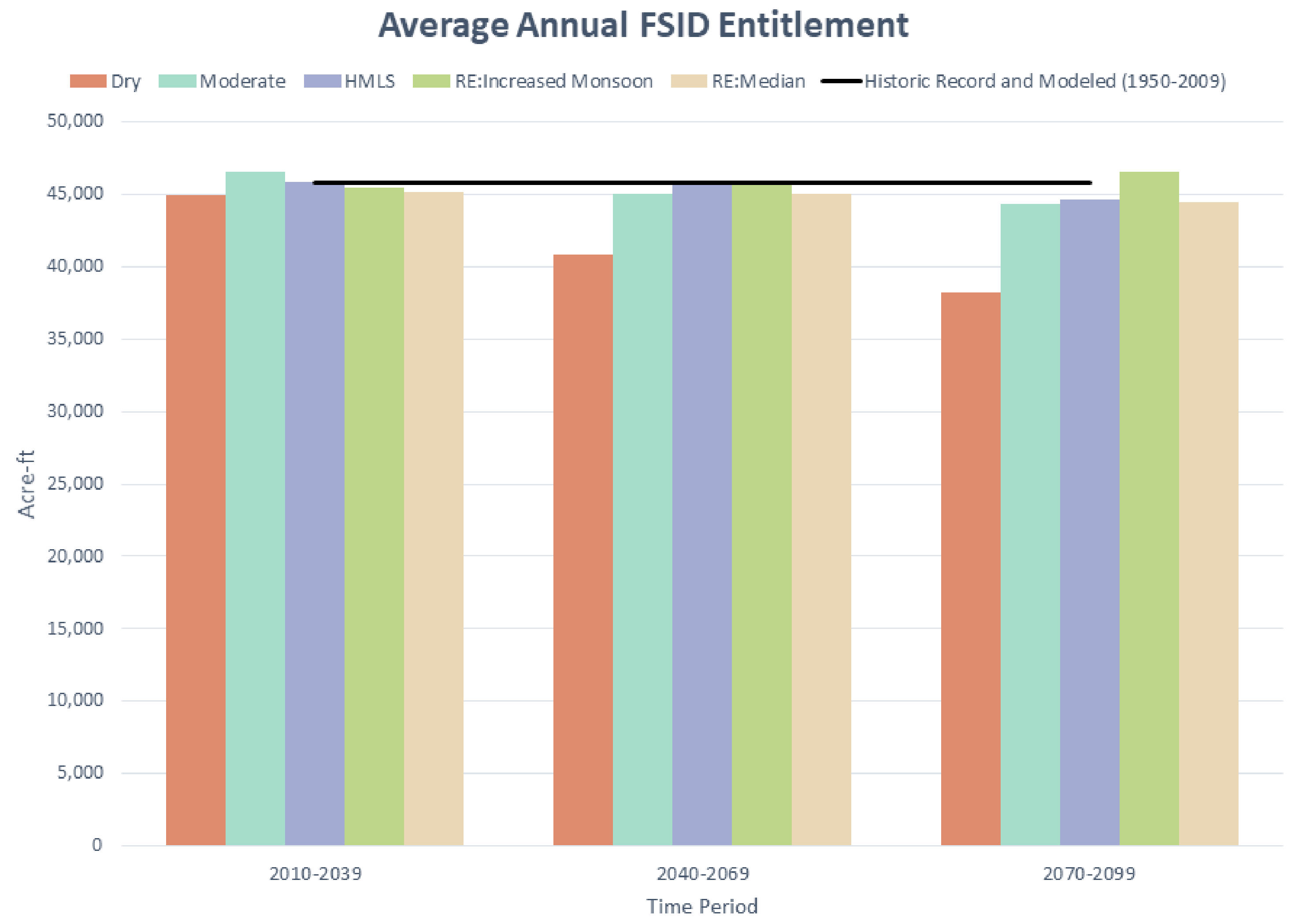

Figure 12. Average Annual FSID Entitlement.

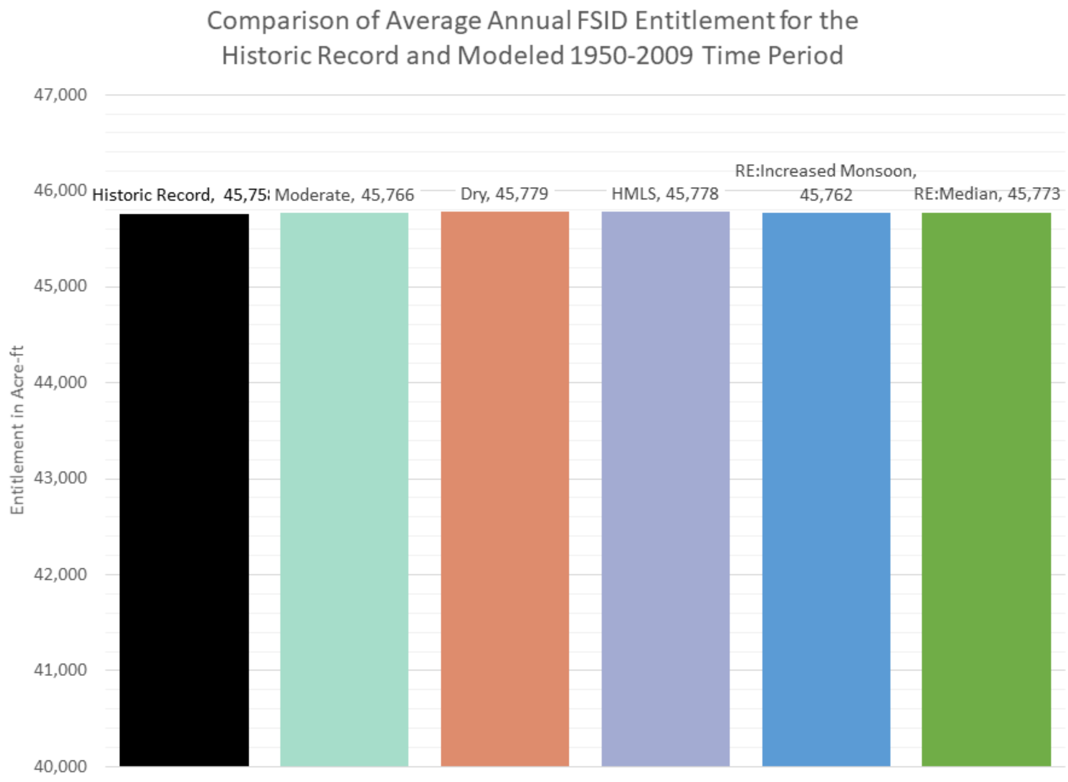

Figure 13. Average Annual FSID Entitlement.

3. FSID Shortages

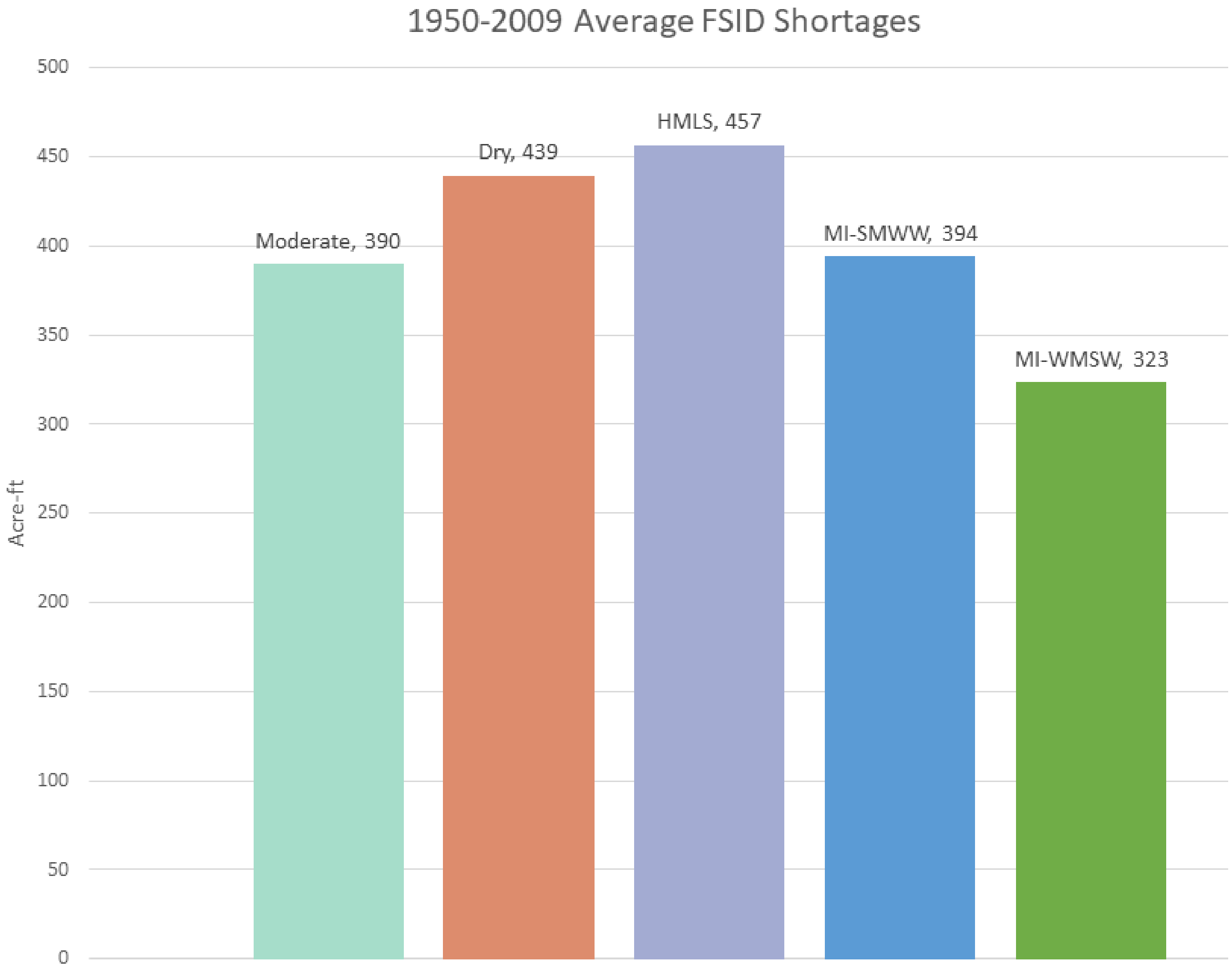

Figure 14. 1950 – 2009 average FSID shortages.

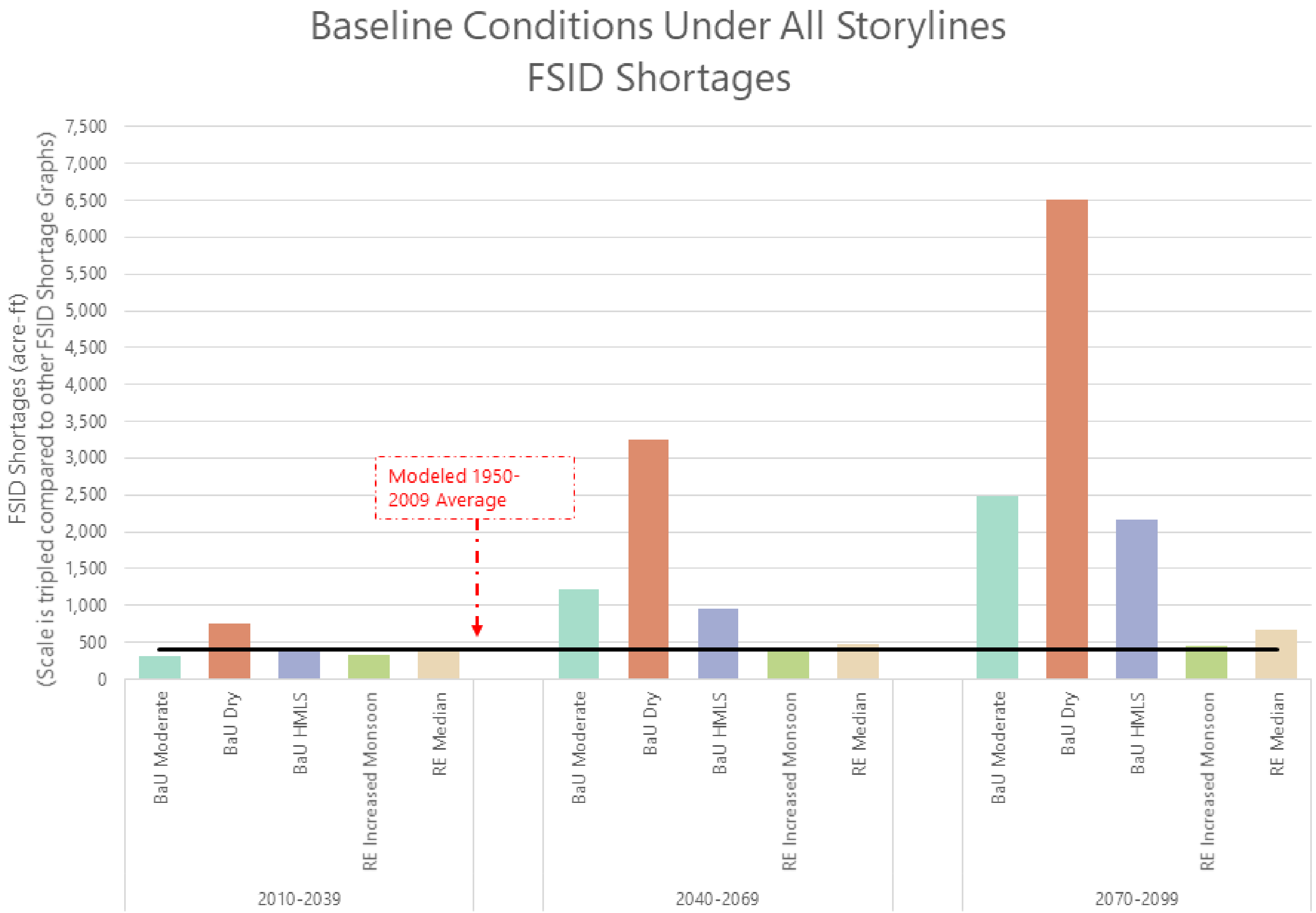

Figure 15. Baseline conditions under all storyline FSID shortages.

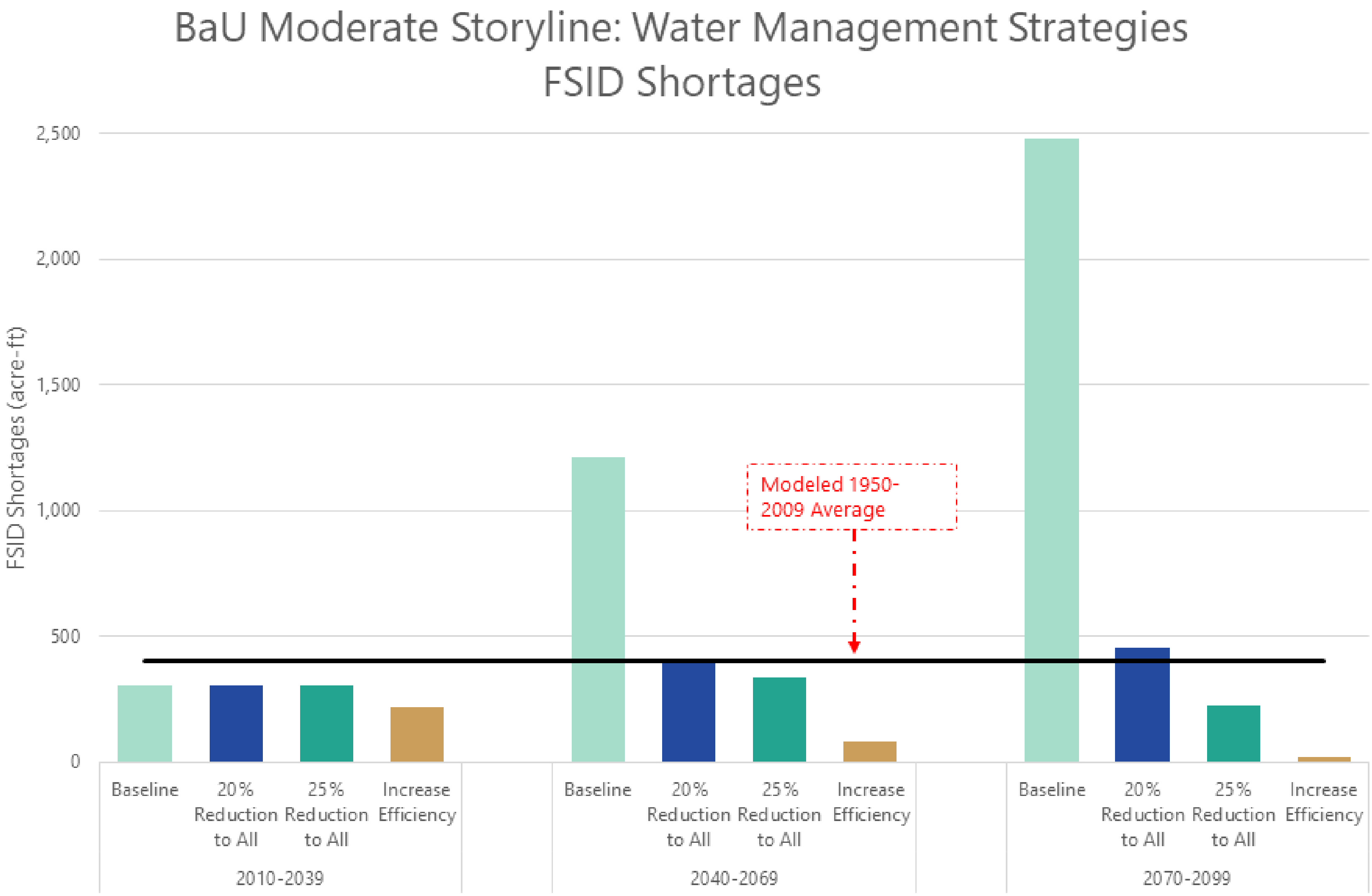

Figure 16. FSID Shortages: Water Management Strategies in the BaU Moderate Storyline.

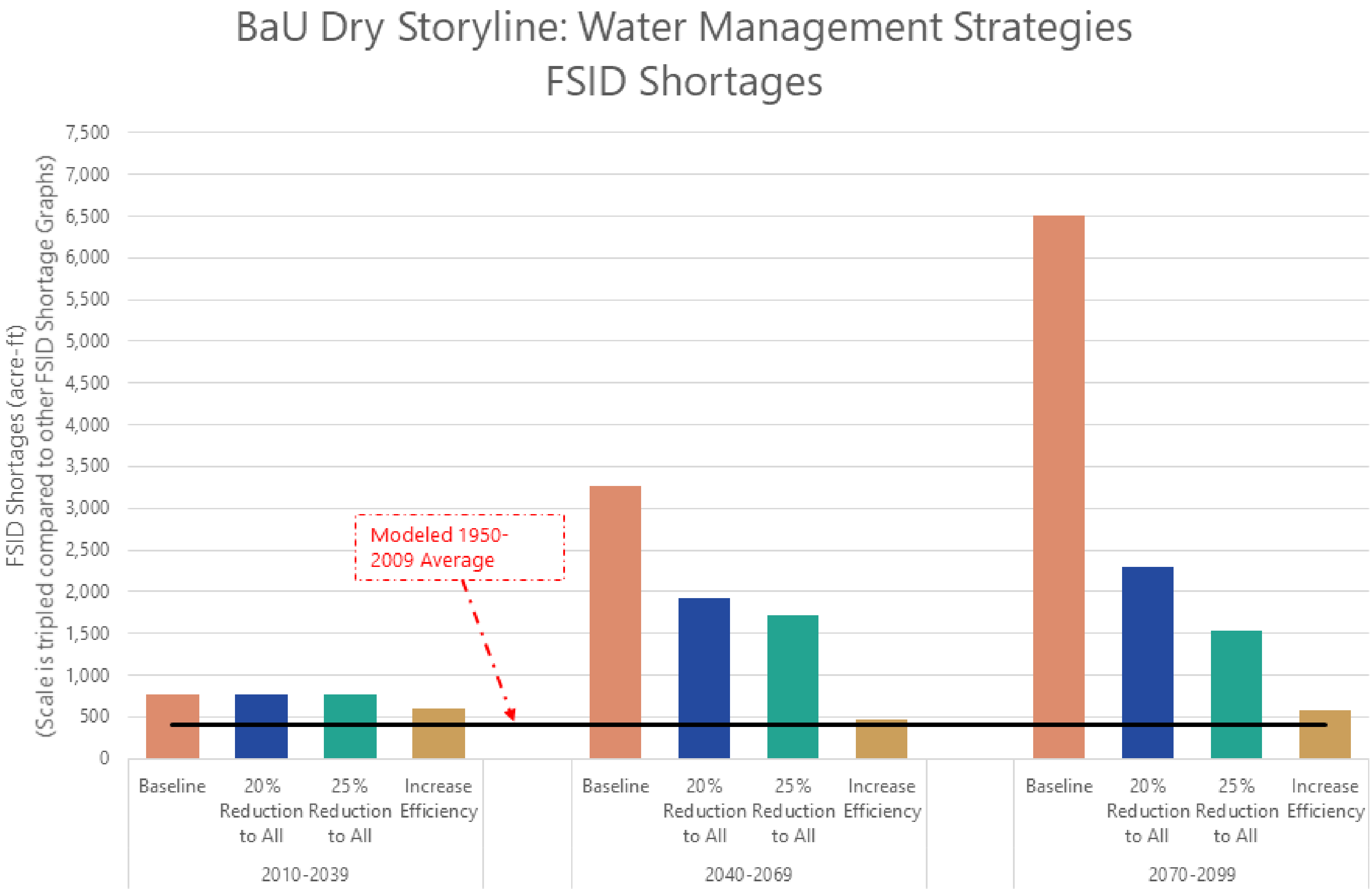

Figure 17. FSID Shortages: Water Management Strategies in the BaU Dry Storyline.

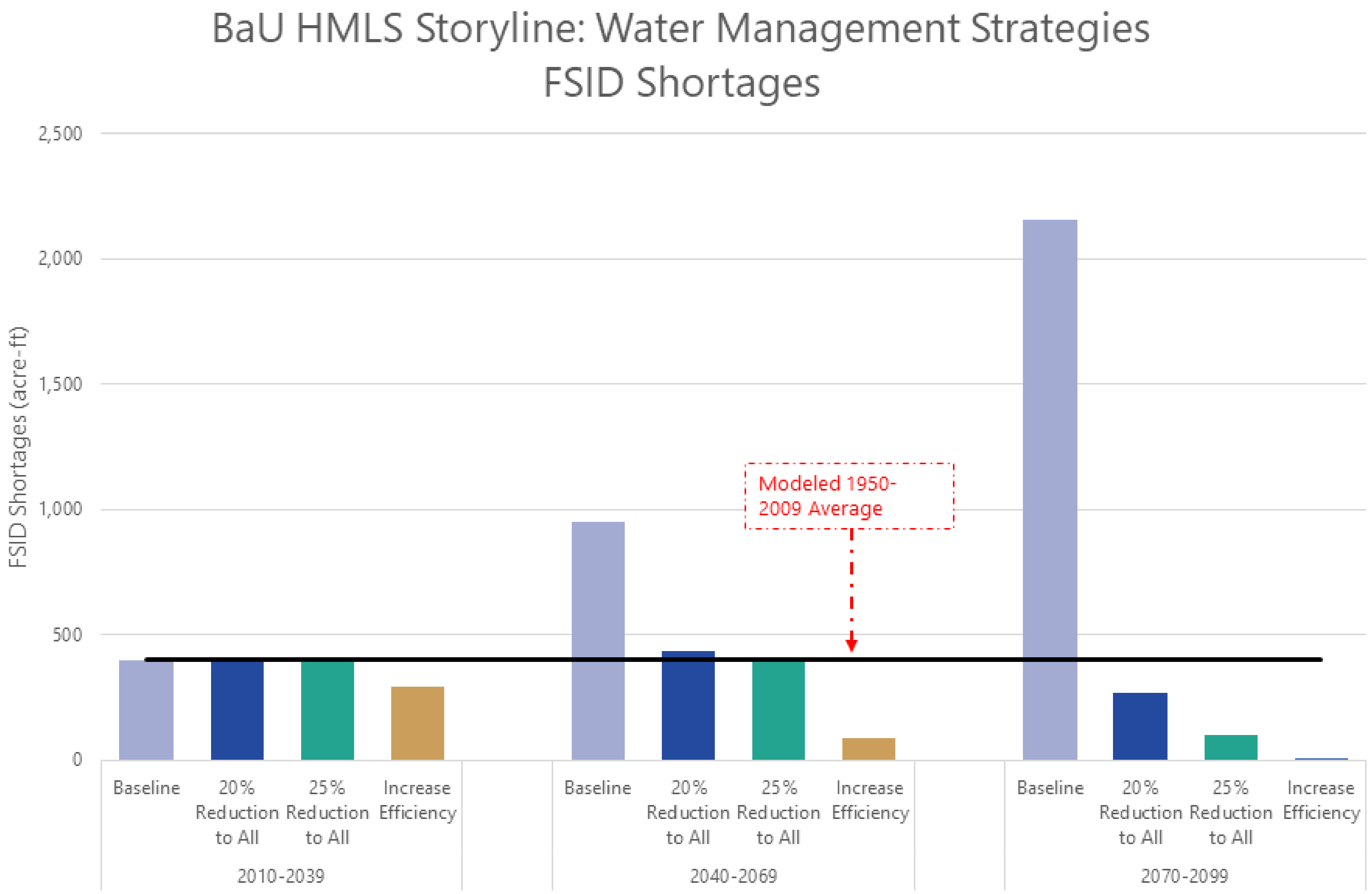

Figure 18. FSID Shortages: Water Management Strategies in the BaU HMLS Storyline.

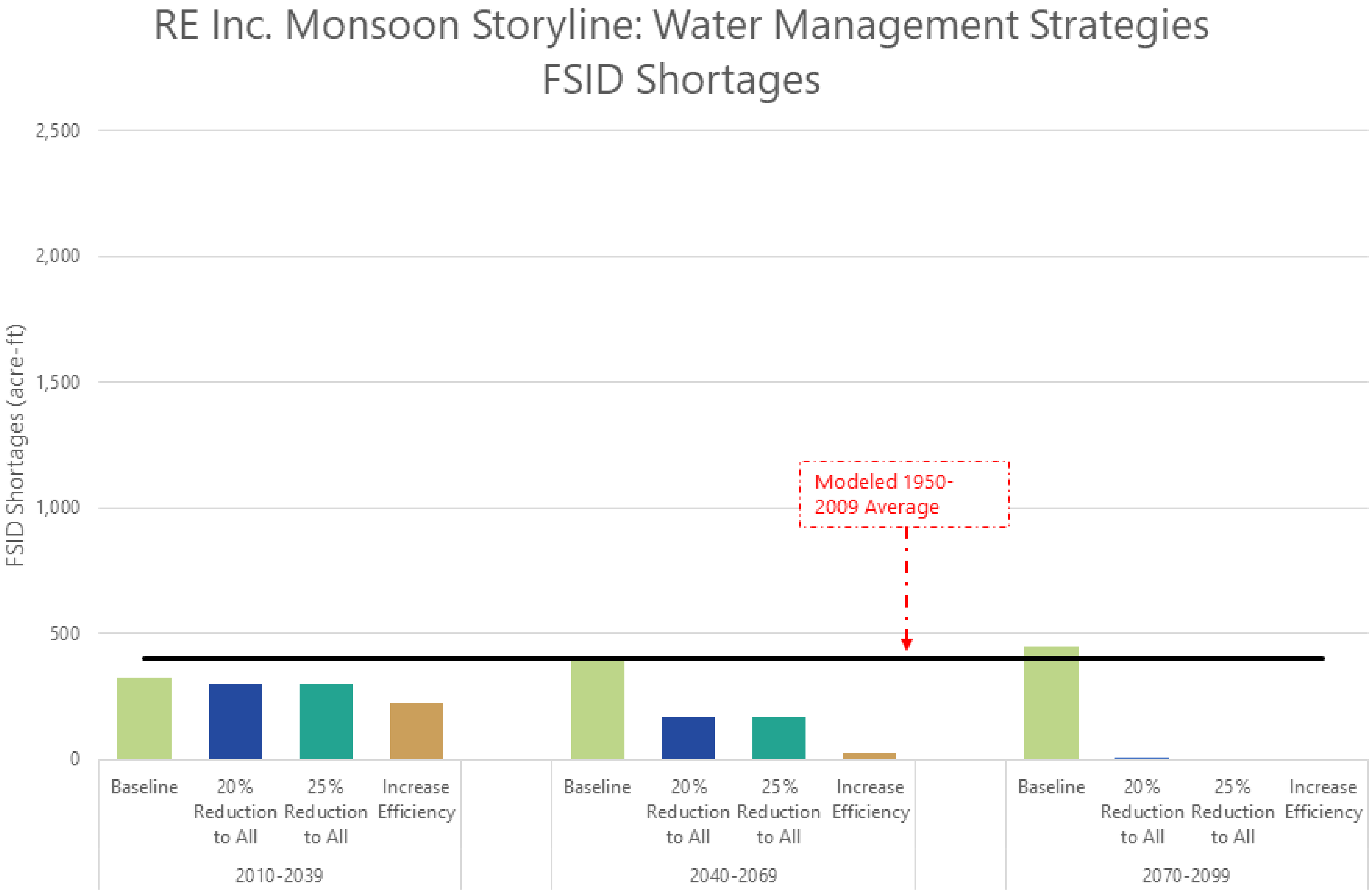

Figure 19. FSID Shortages: Water Management Strategies in the RE Increased Monsoon Storyline.

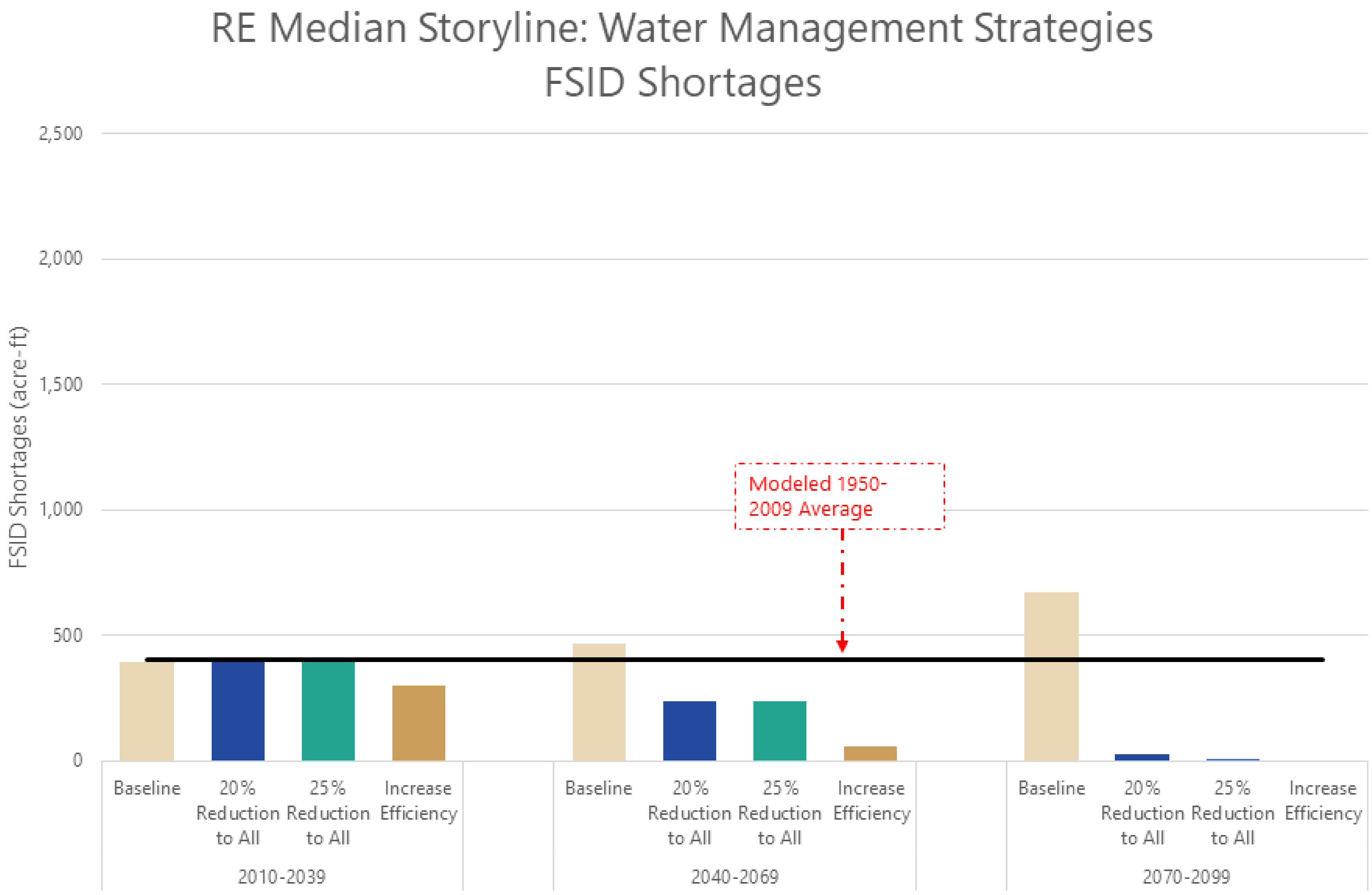

Figure 20. FSID Shortages: Water Management Strategies in the RE Median Storyline.

4. CID Allotment

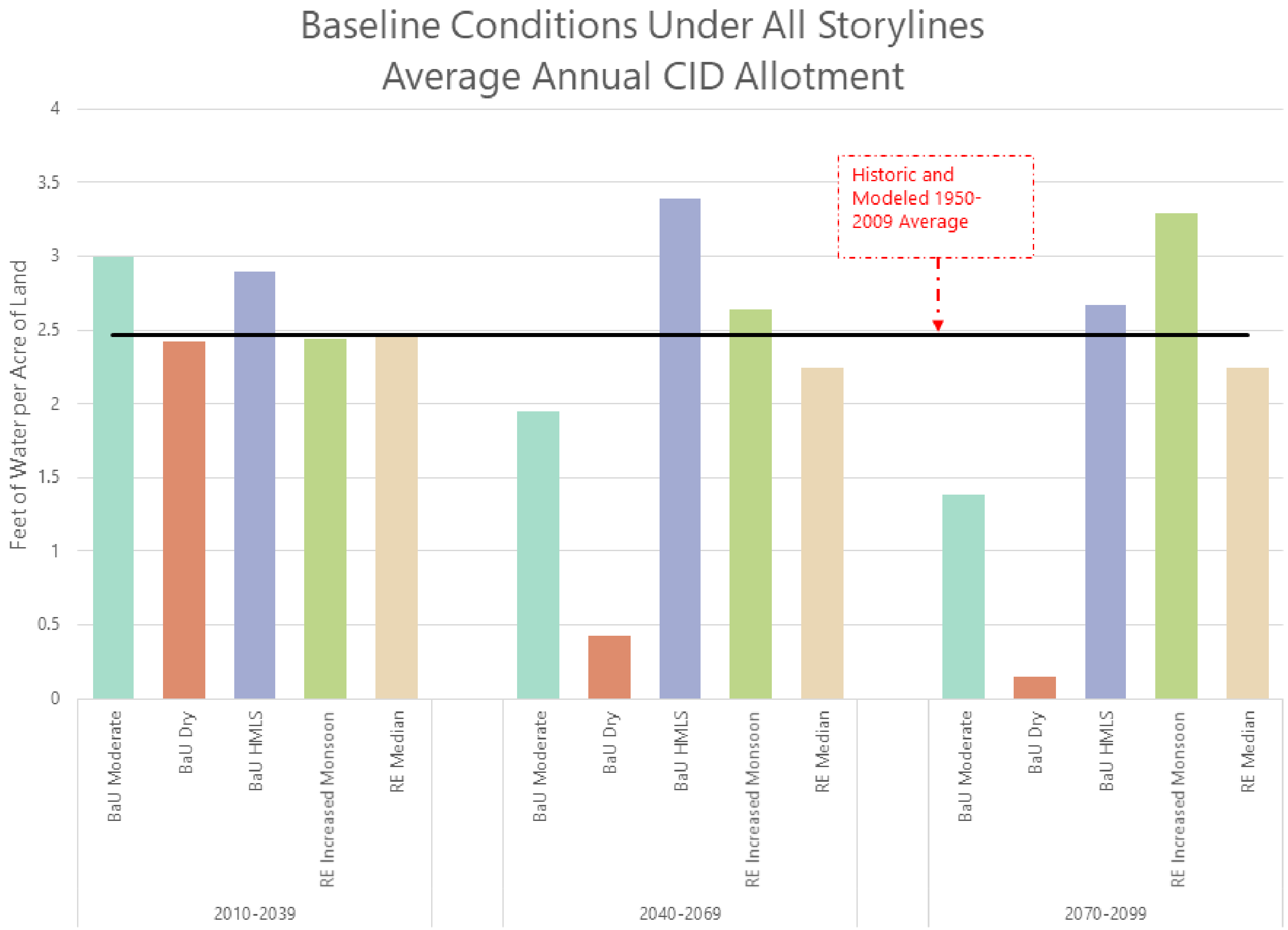

Figure 21. CID Allotment: Baseline conditions under all storylines.

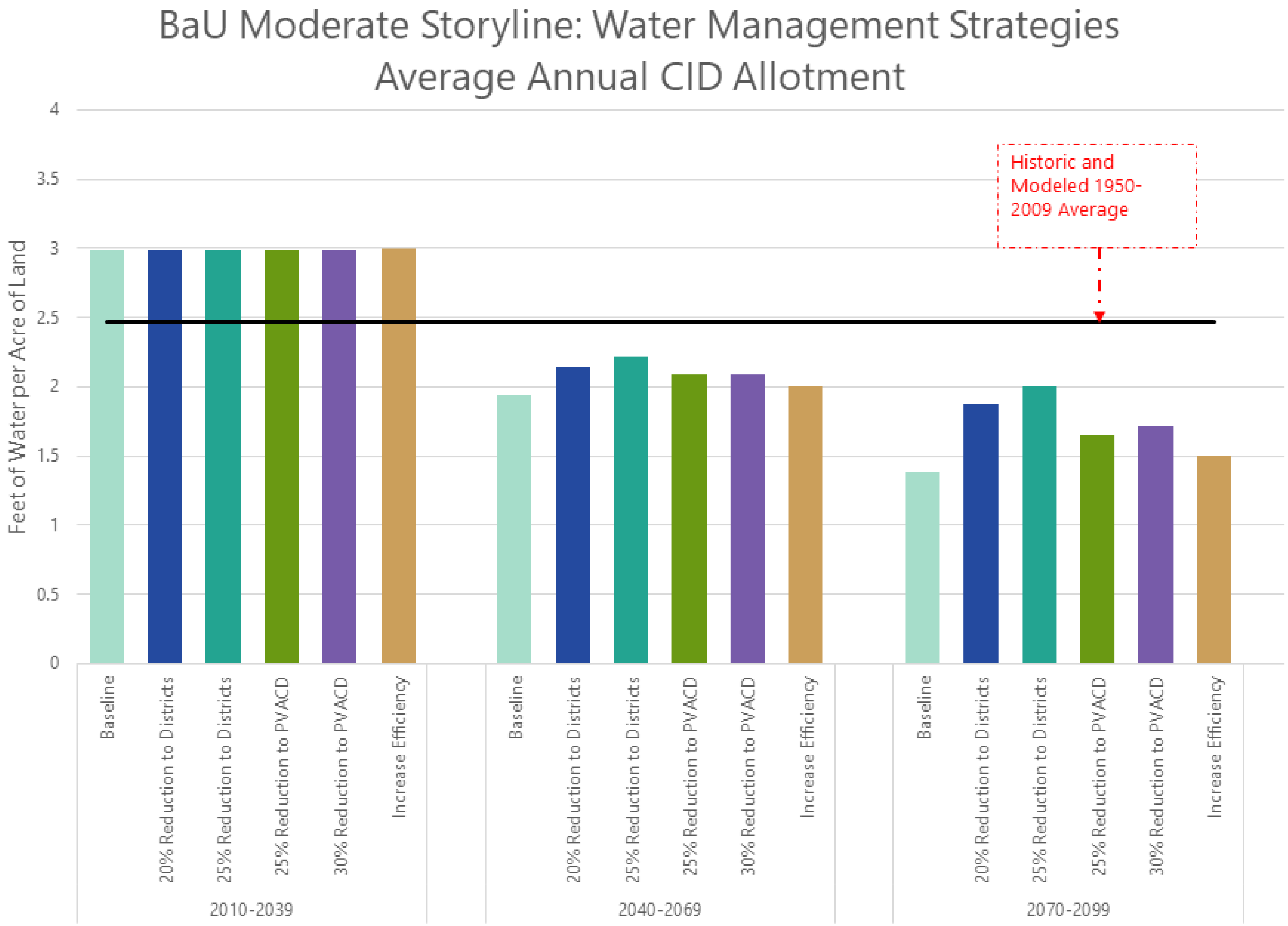

Figure 22. CID Allotment Water Management Strategies in the BaU Moderate Storyline.

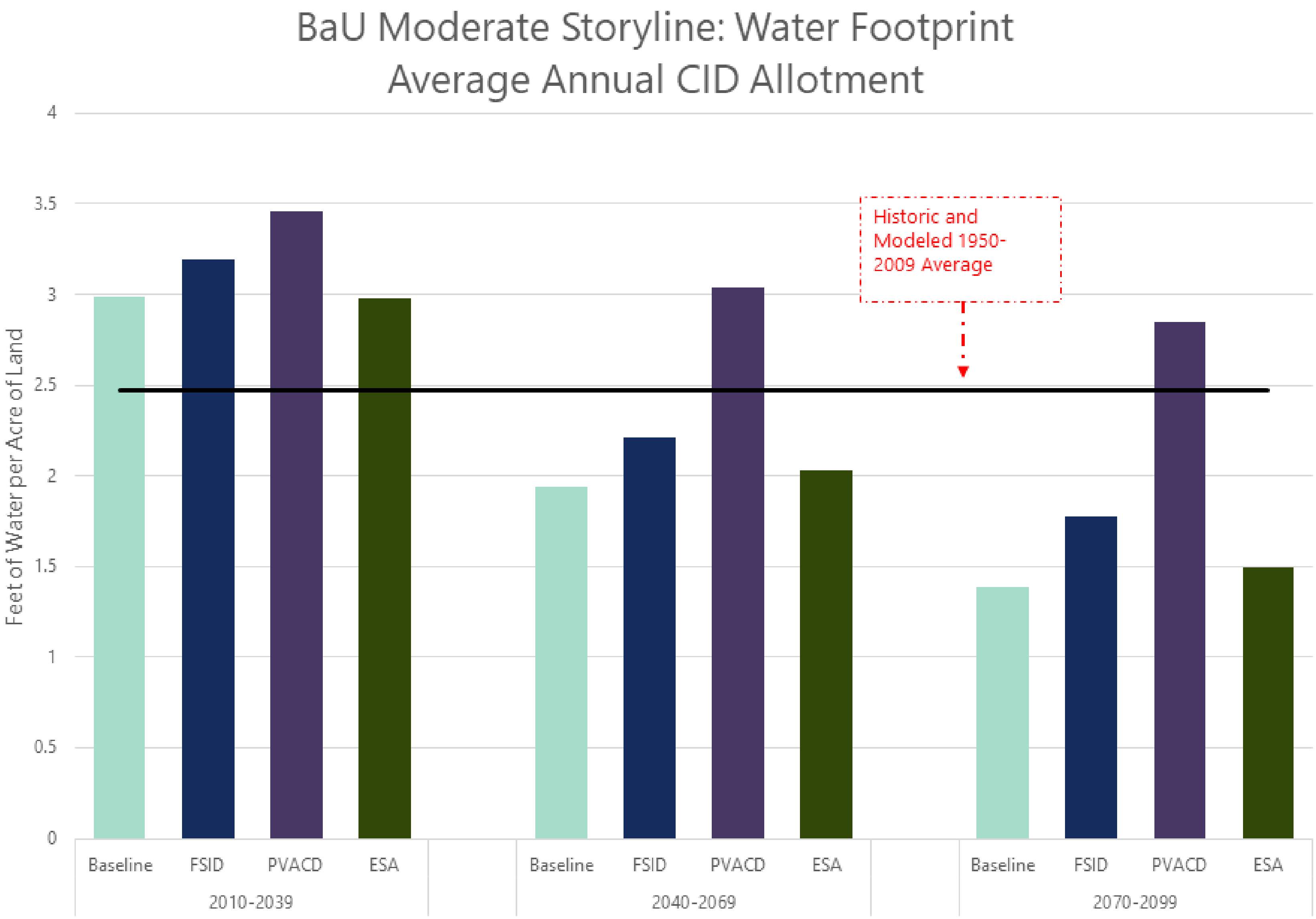

Figure 23. CID Allotment Water Footprint in the BaU Moderate Storyline.

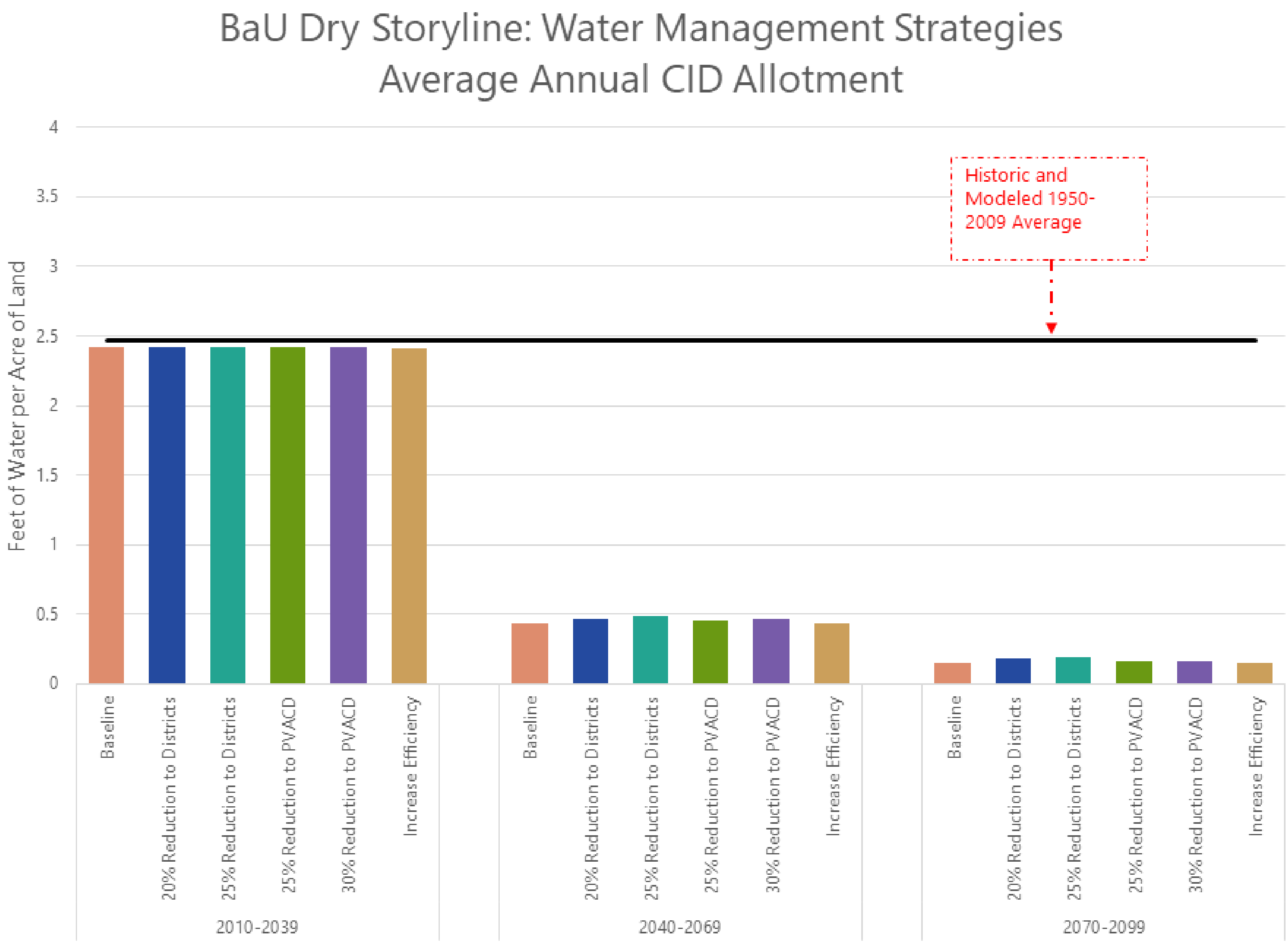

Figure 24. CID Allotment Water Management Strategies in the BaU Dry Storyline.

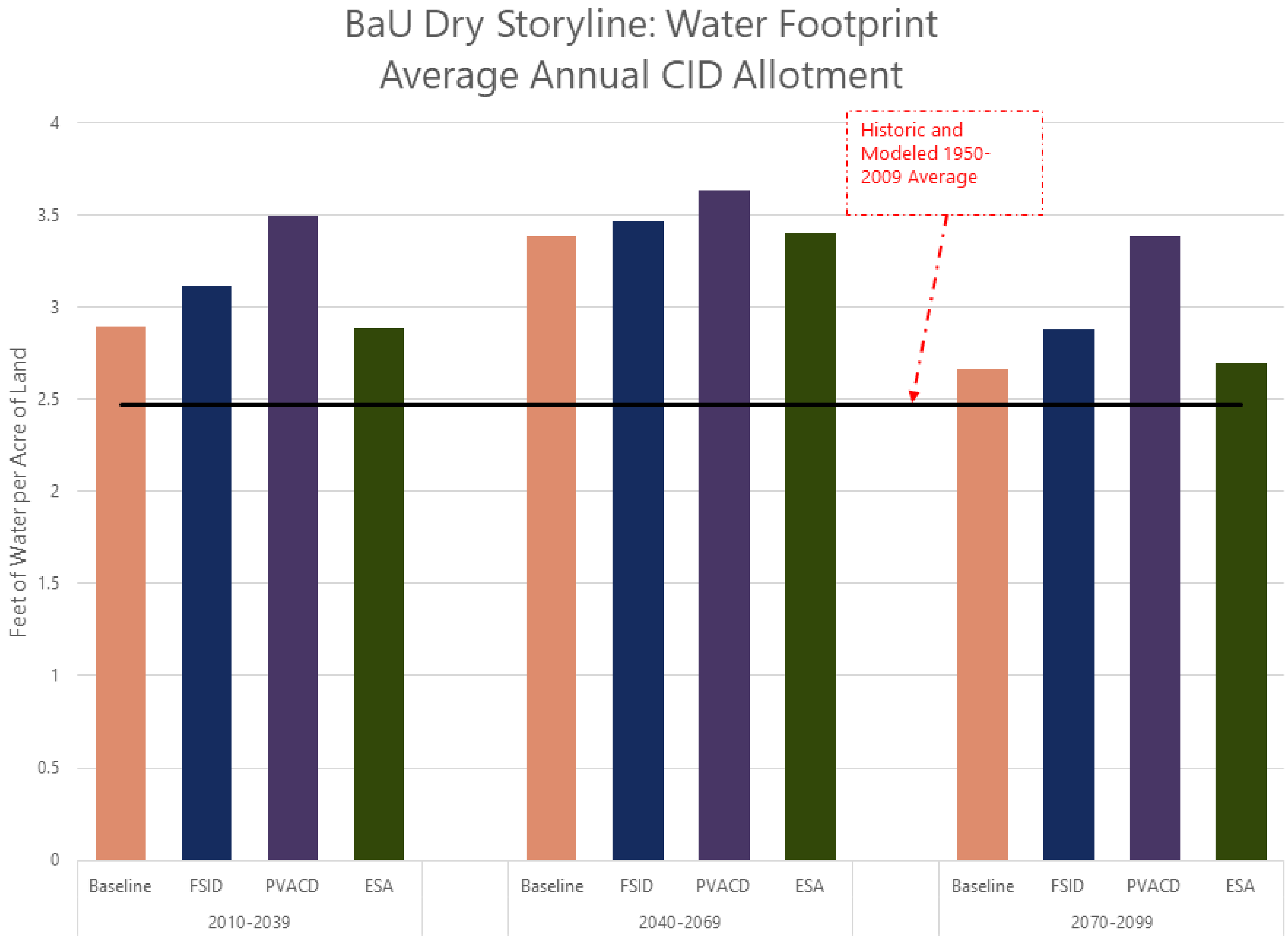

Figure 25. CID Allotment Water Footprint in the BaU Dry Storyline.

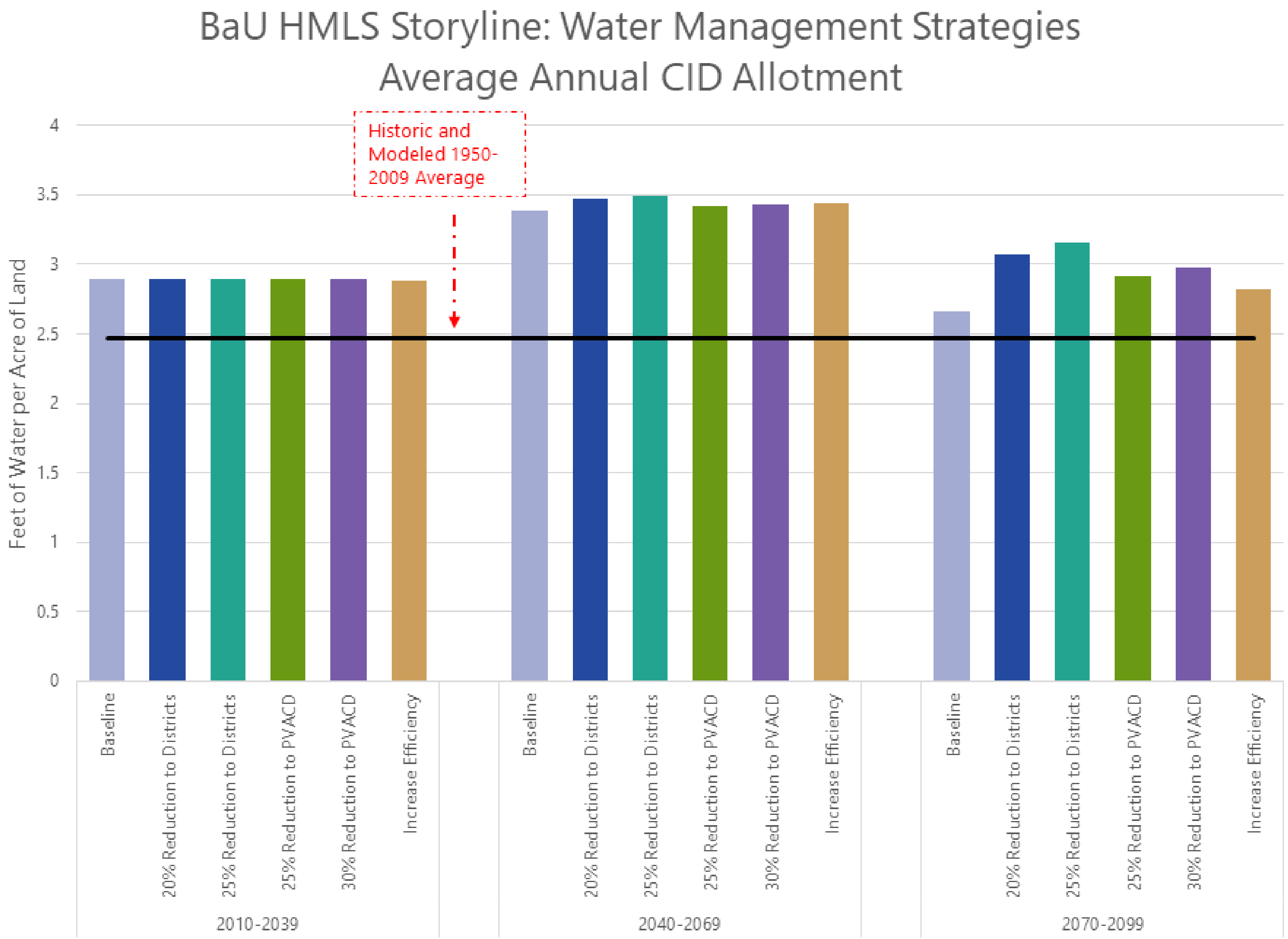

Figure 26. CID Allotment Water Management Strategies in the BaU HMLS Storyline.

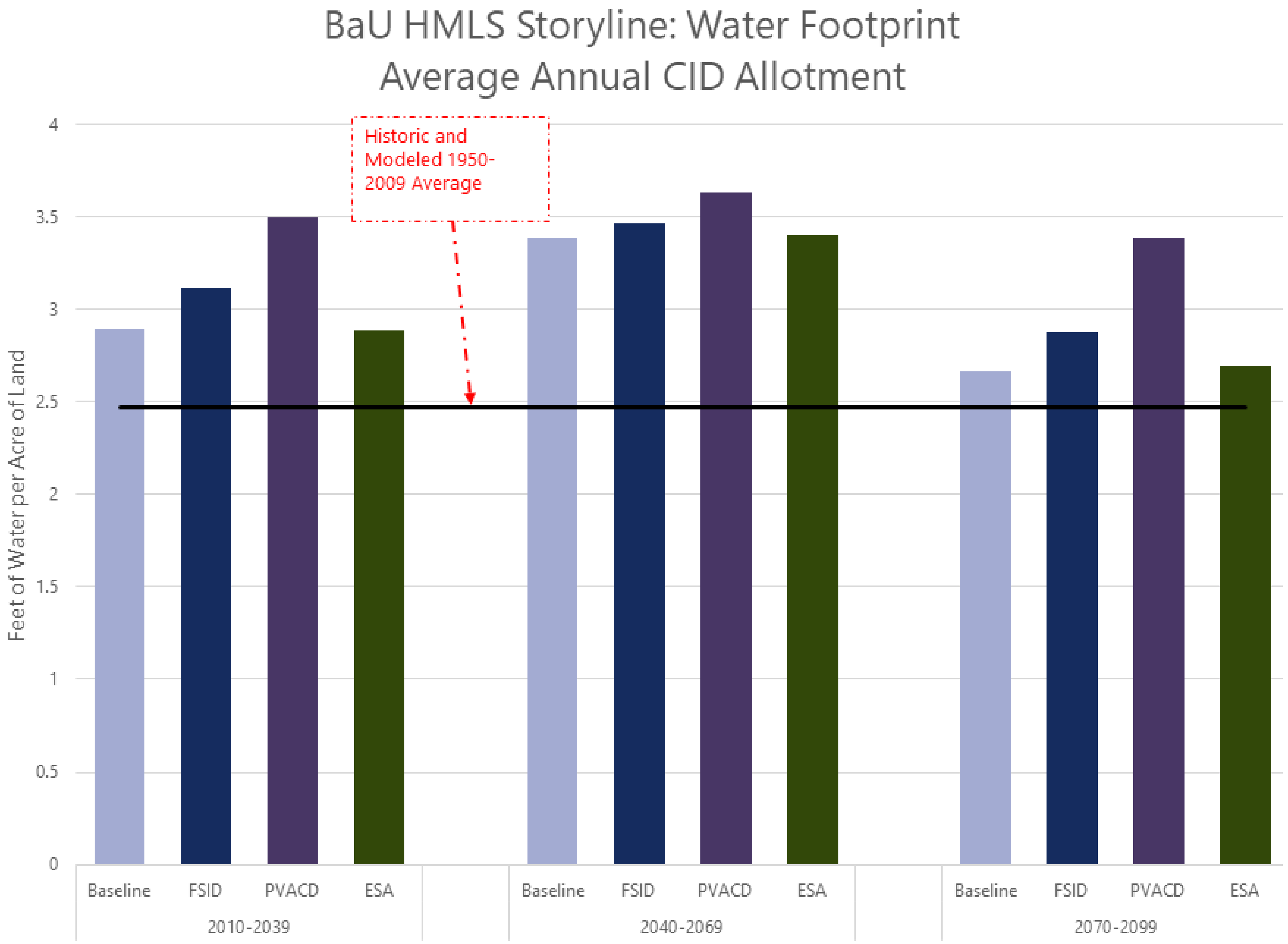

Figure 27. CID Allotment Water Management Strategies in the BaU HMLS Storyline.

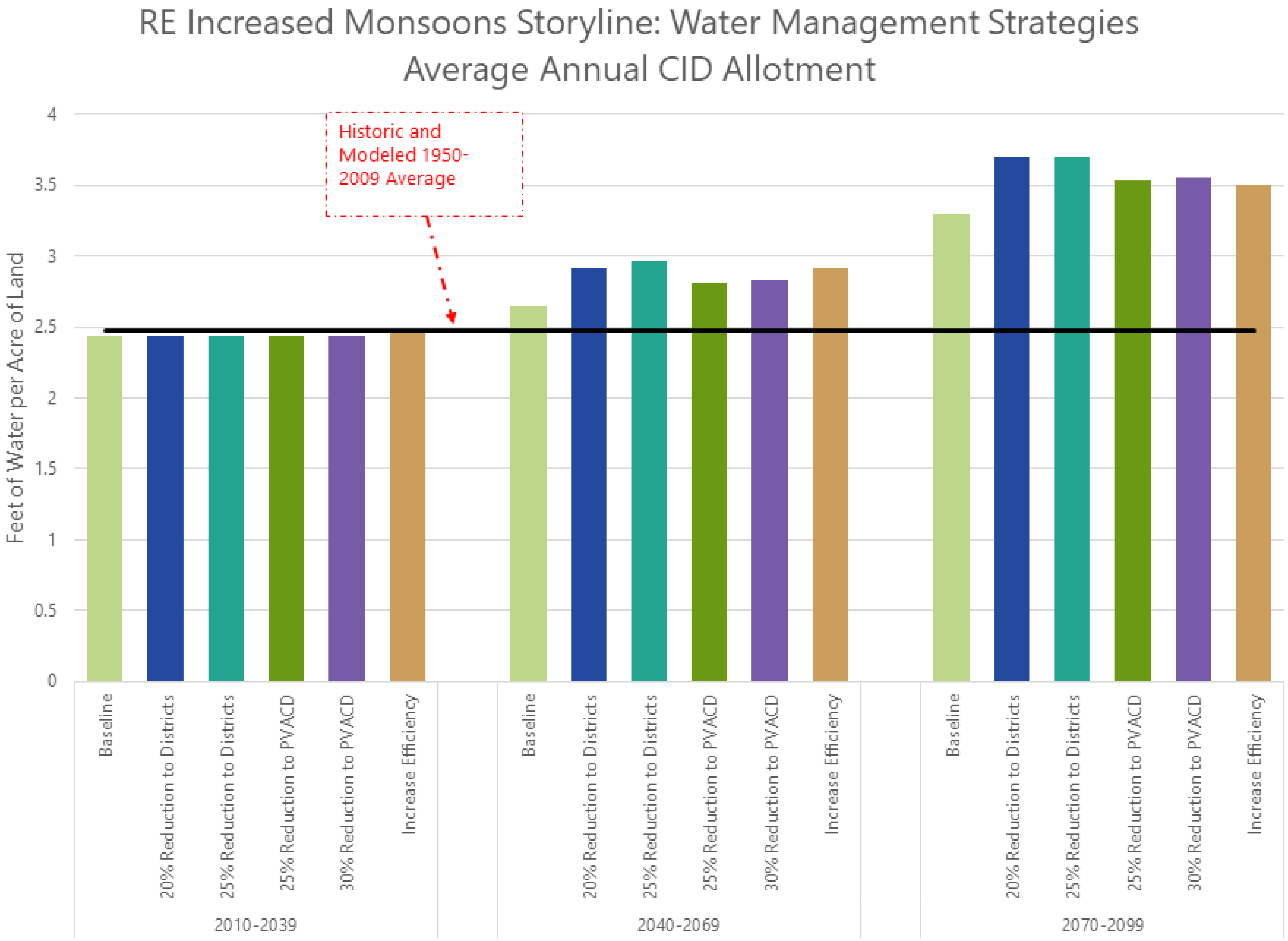

Figure 28. CID Allotment Water Management Strategies in the RE Increased Monsoon Storyline.

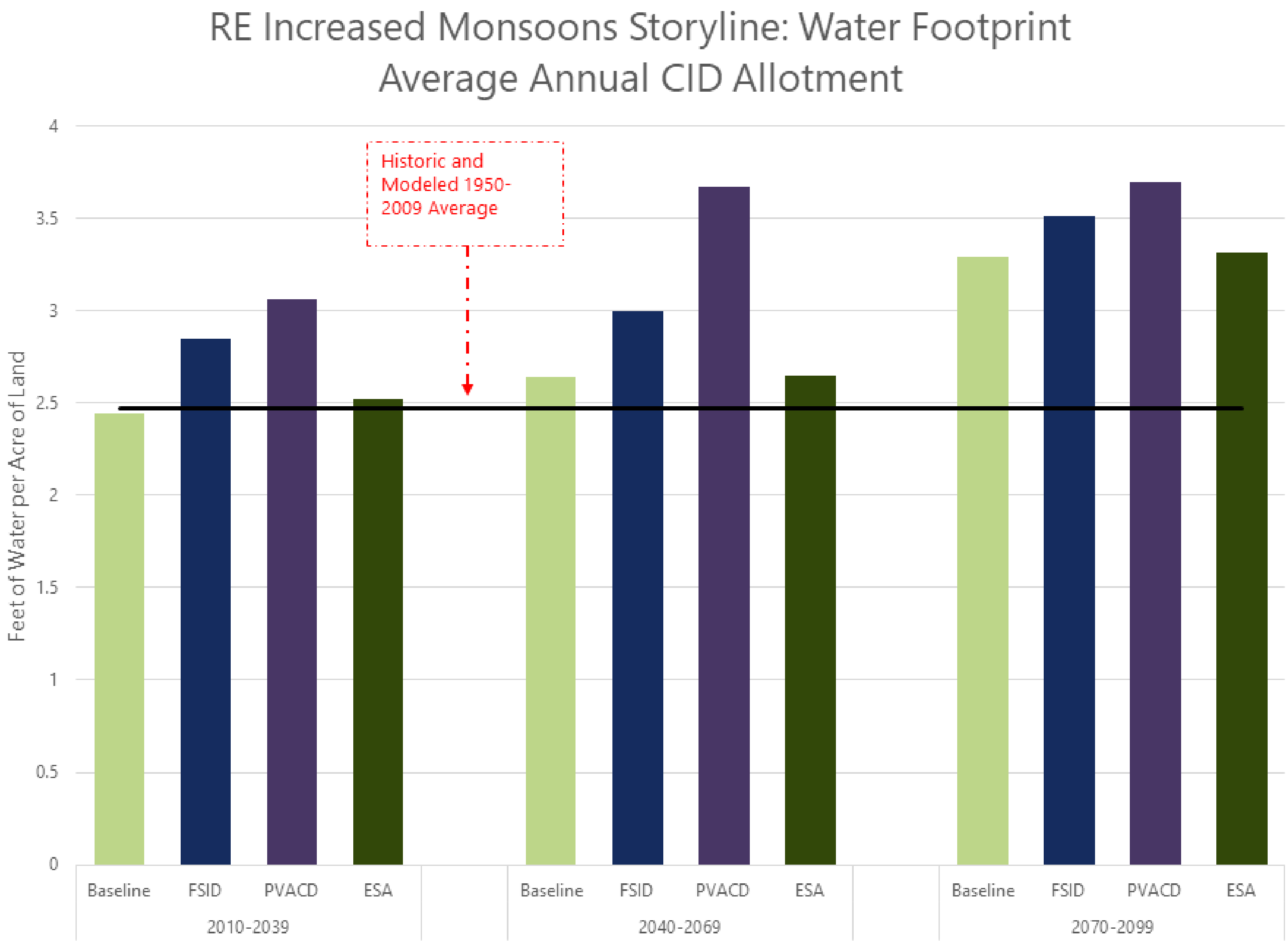

Figure 29. CID Allotment Water Footprint in the BaU Dry Storyline.

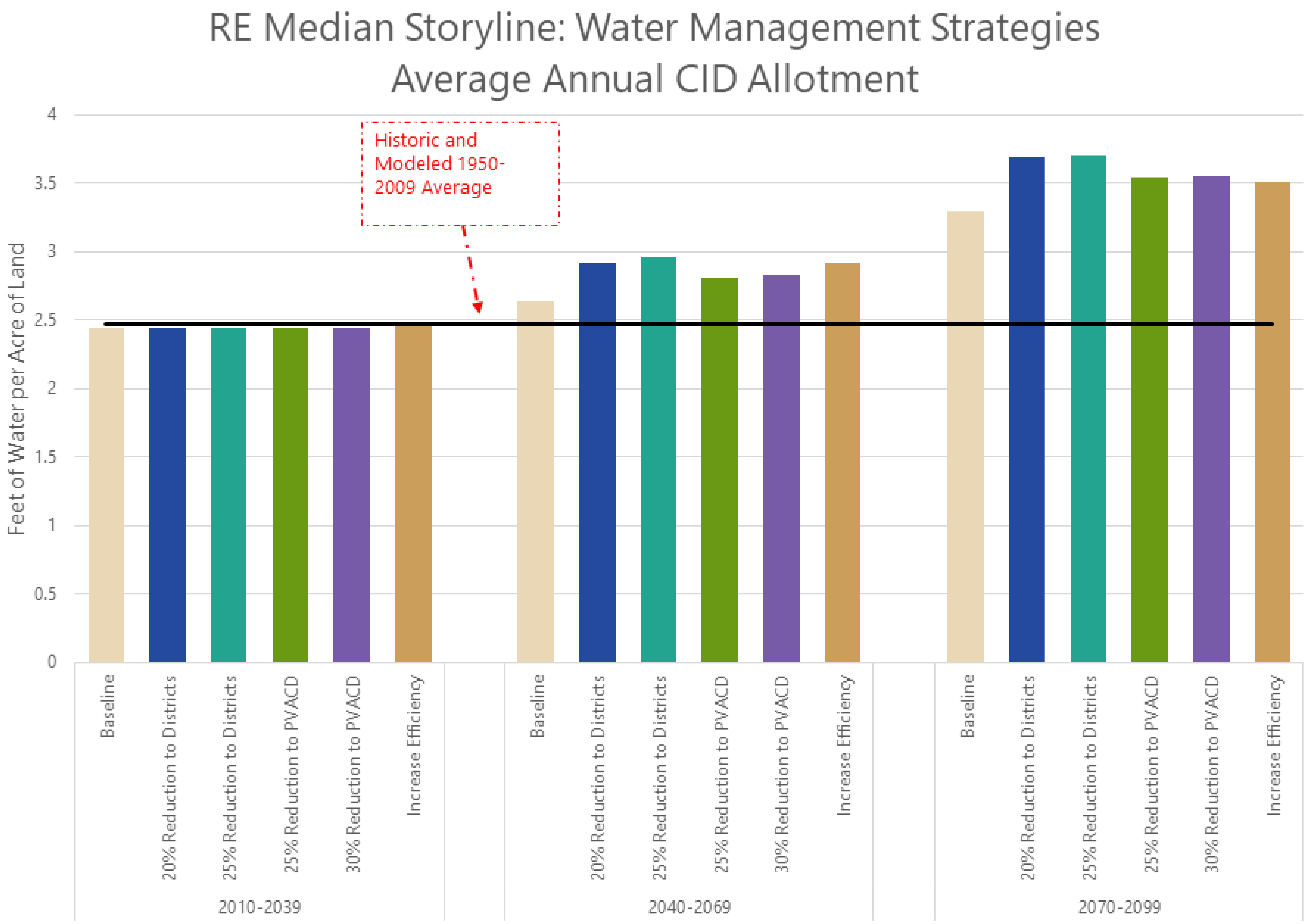

Figure 30. CID Allotment Water Management Strategies in the RE Median Storyline.

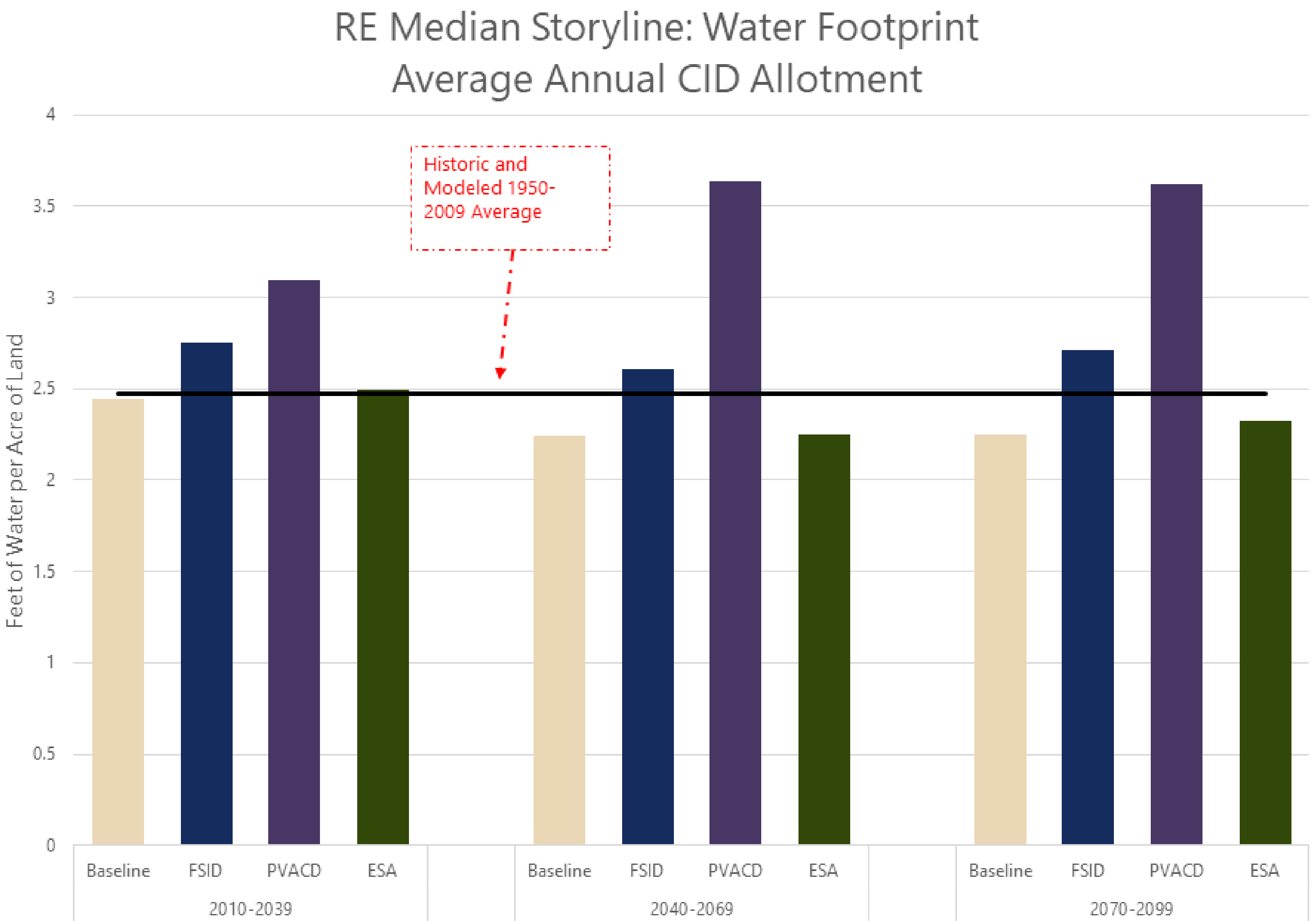

Figure 31. CID Allotment Water Footprint in the RE Median Storyline.

5. CID Shortages

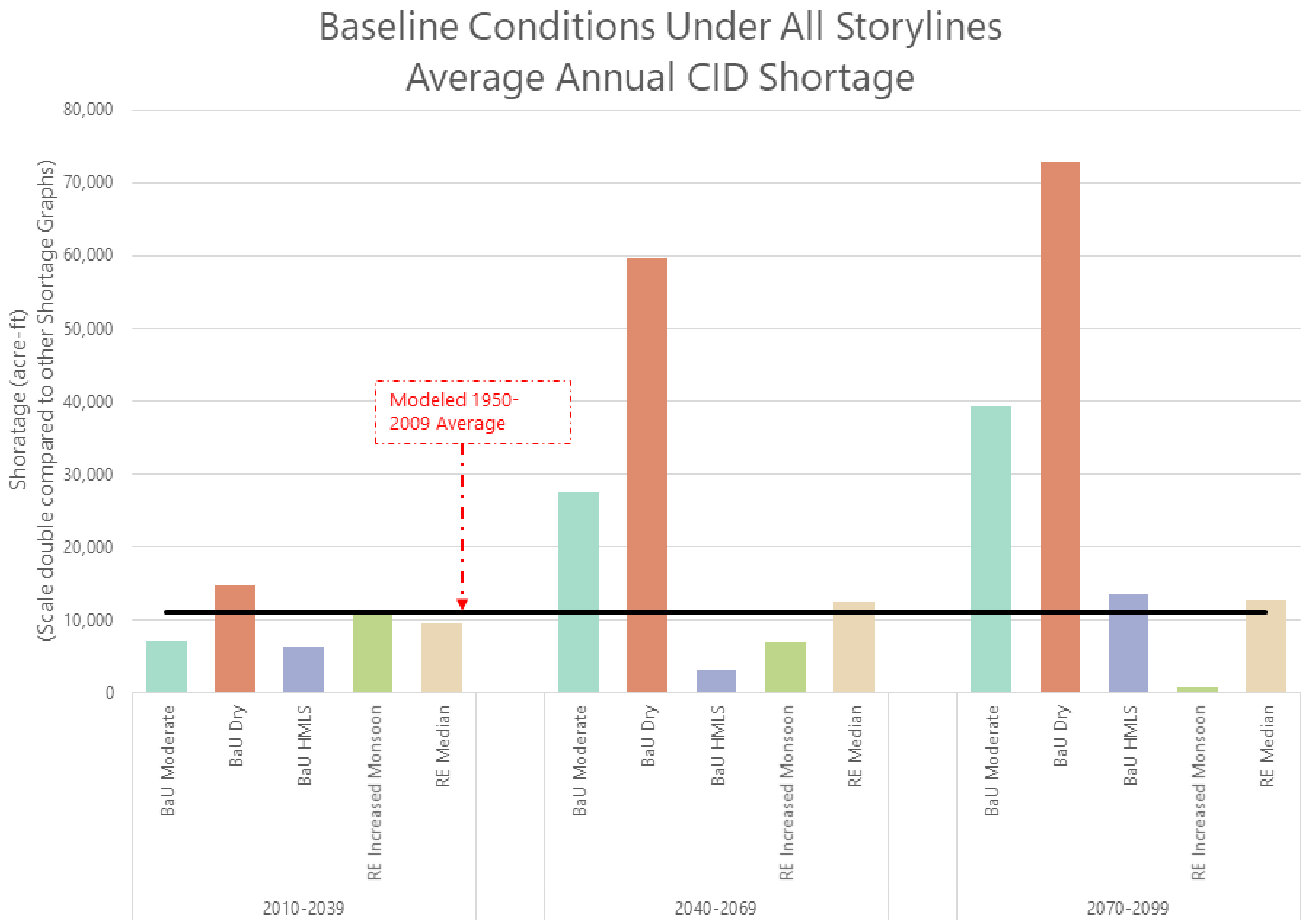

Figure 32. CID Shortages: Baseline condition.

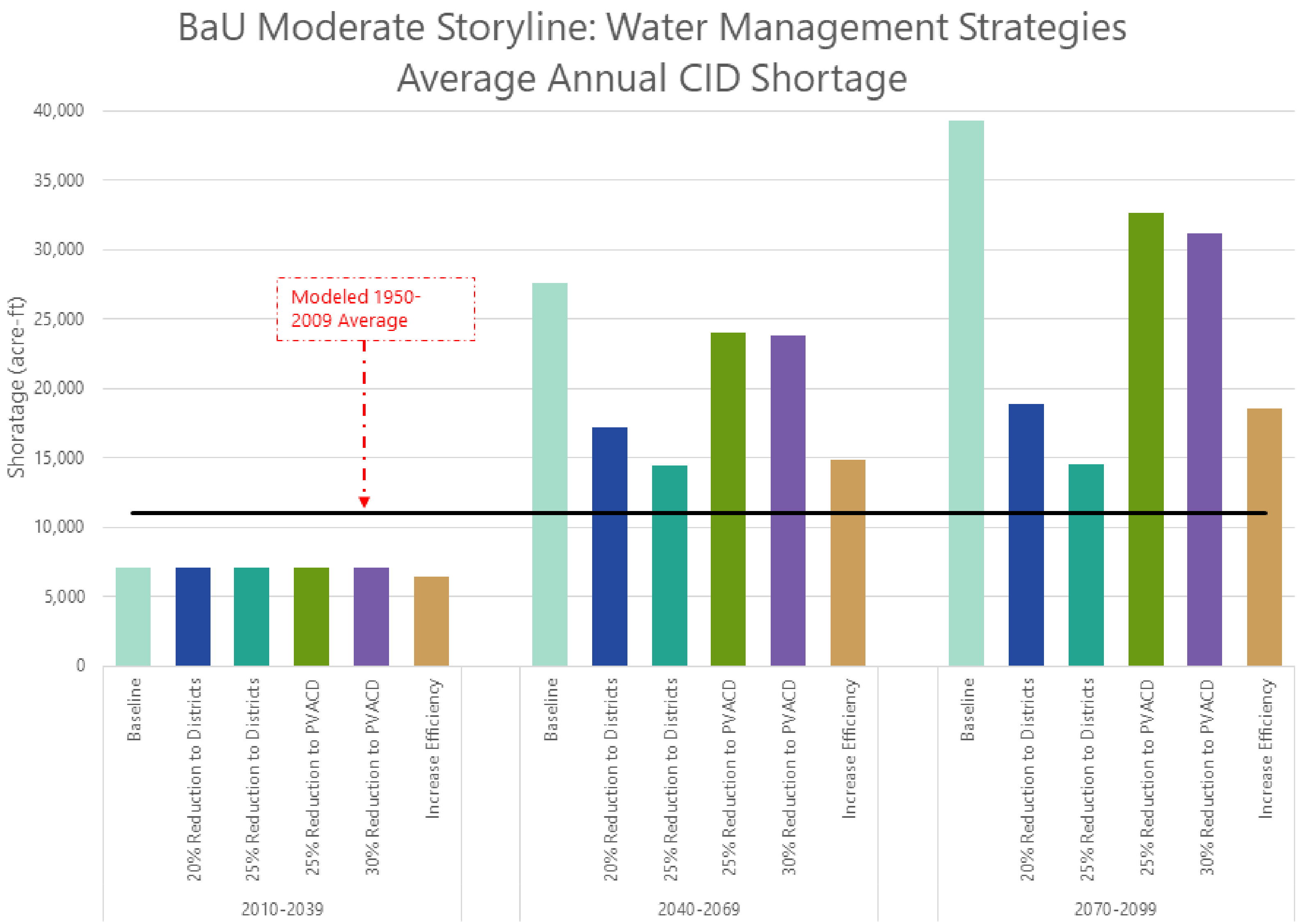

Figure 33. CID Shortages: Water Management Strategies in the BaU Moderate Storyline.

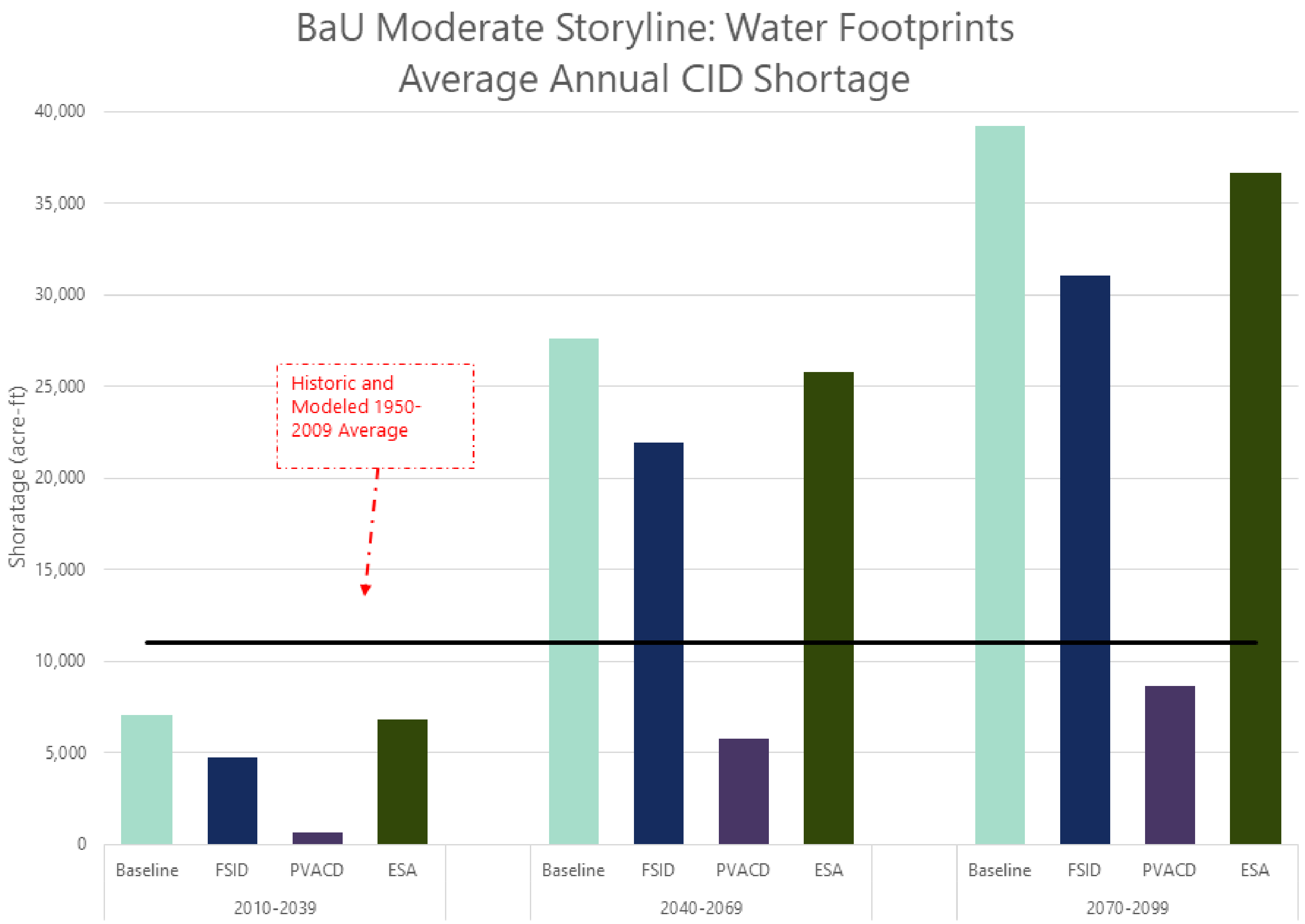

Figure 34. CID Shortages: Water Footprints in the BaU Moderate Storyline.

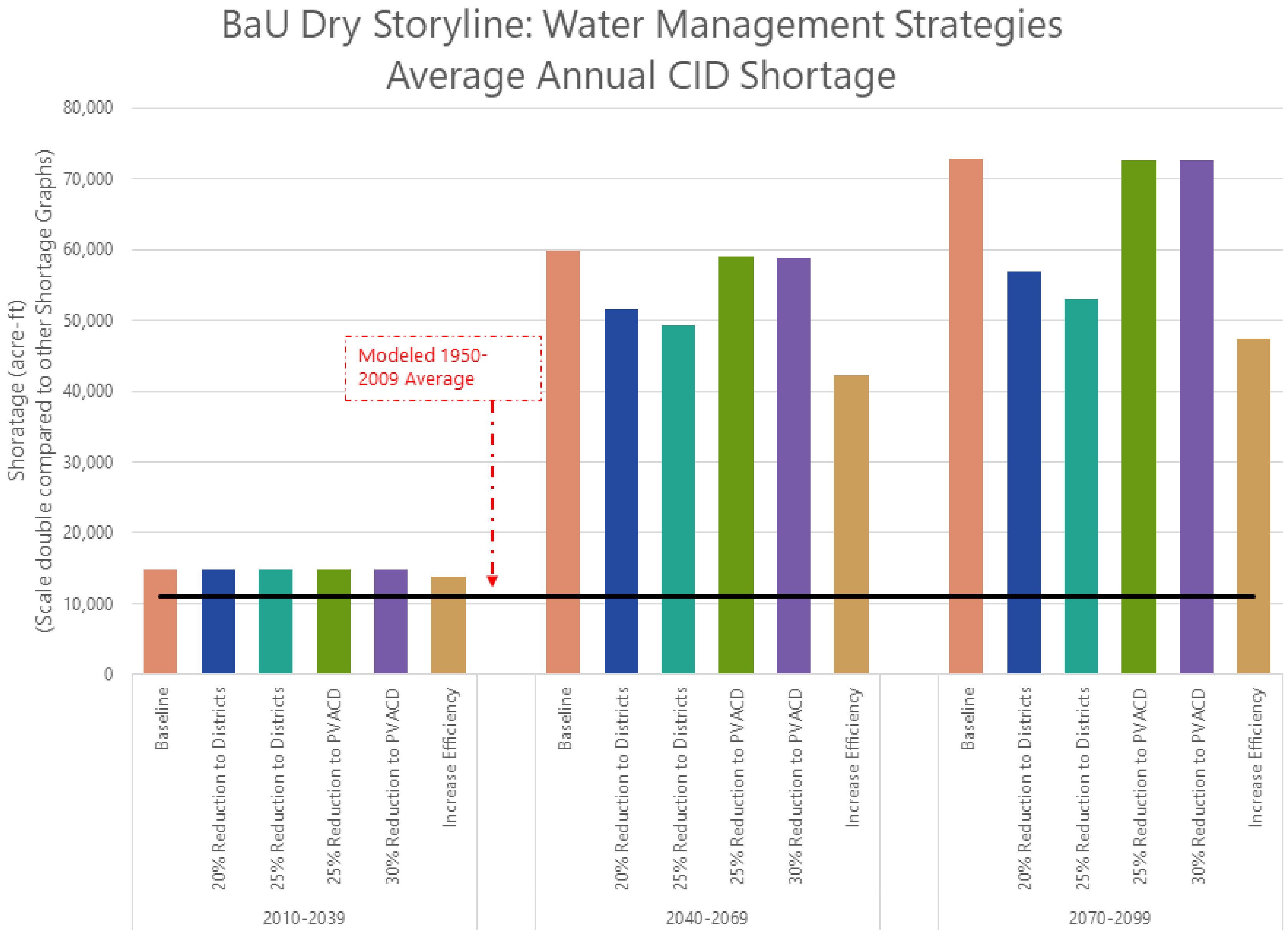

Figure 35. CID Shortages: Water Footprints in the BaU Dry Storyline.

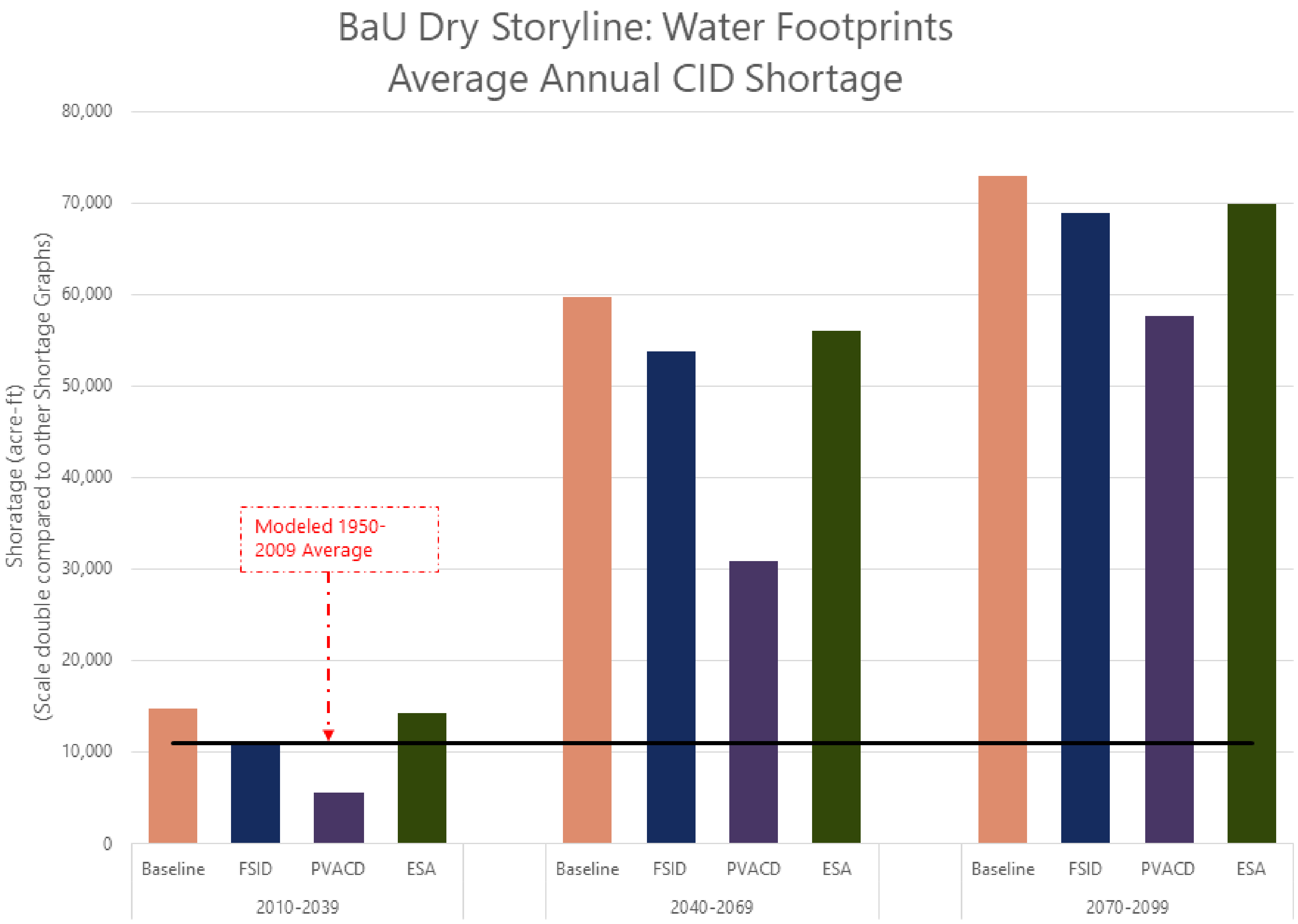

Figure 36. CID Shortages: Water Footprints in the BaU Dry Storyline.

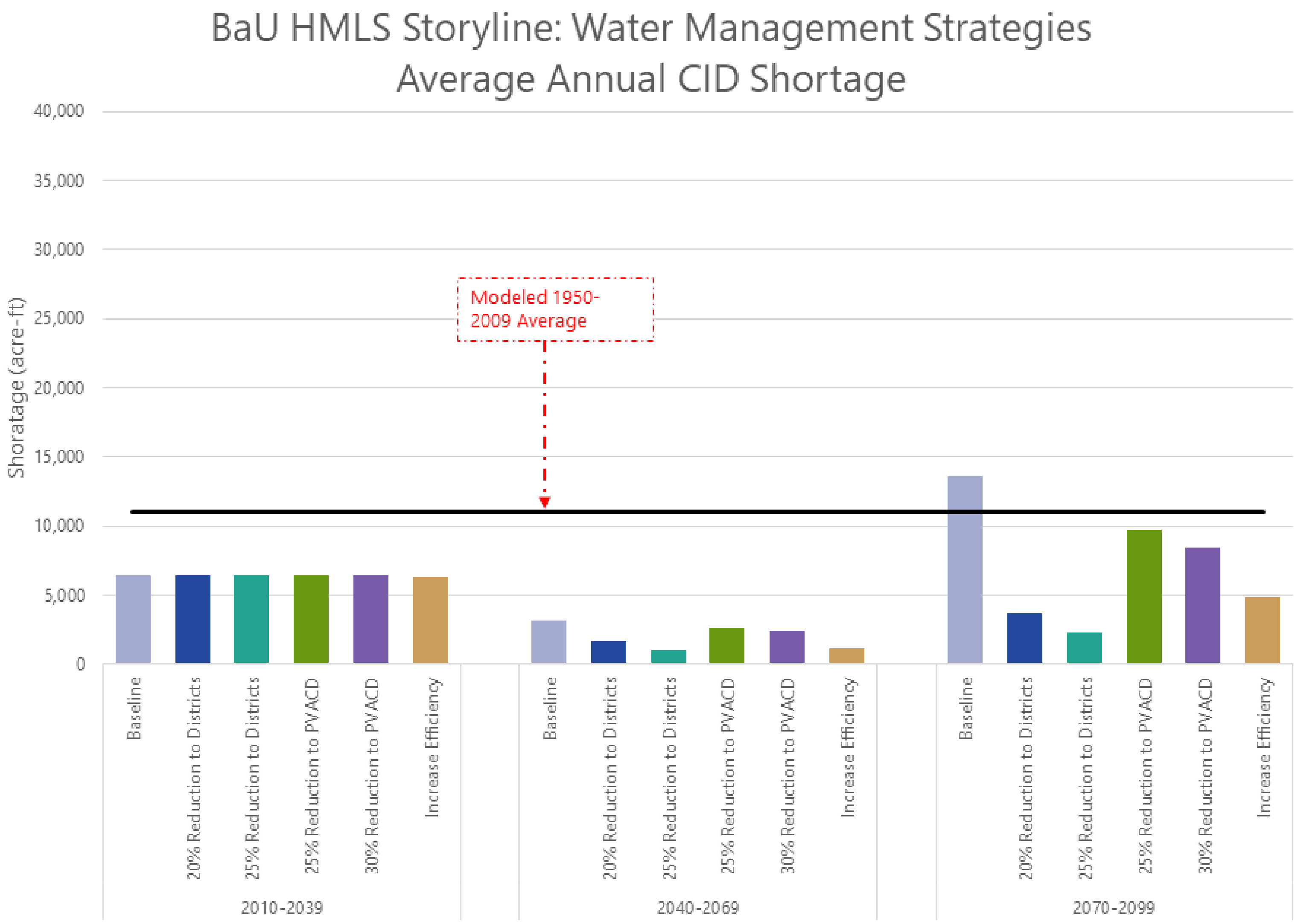

Figure 37. CID Shortages: Water Footprints in the BaU HMLS Storyline.

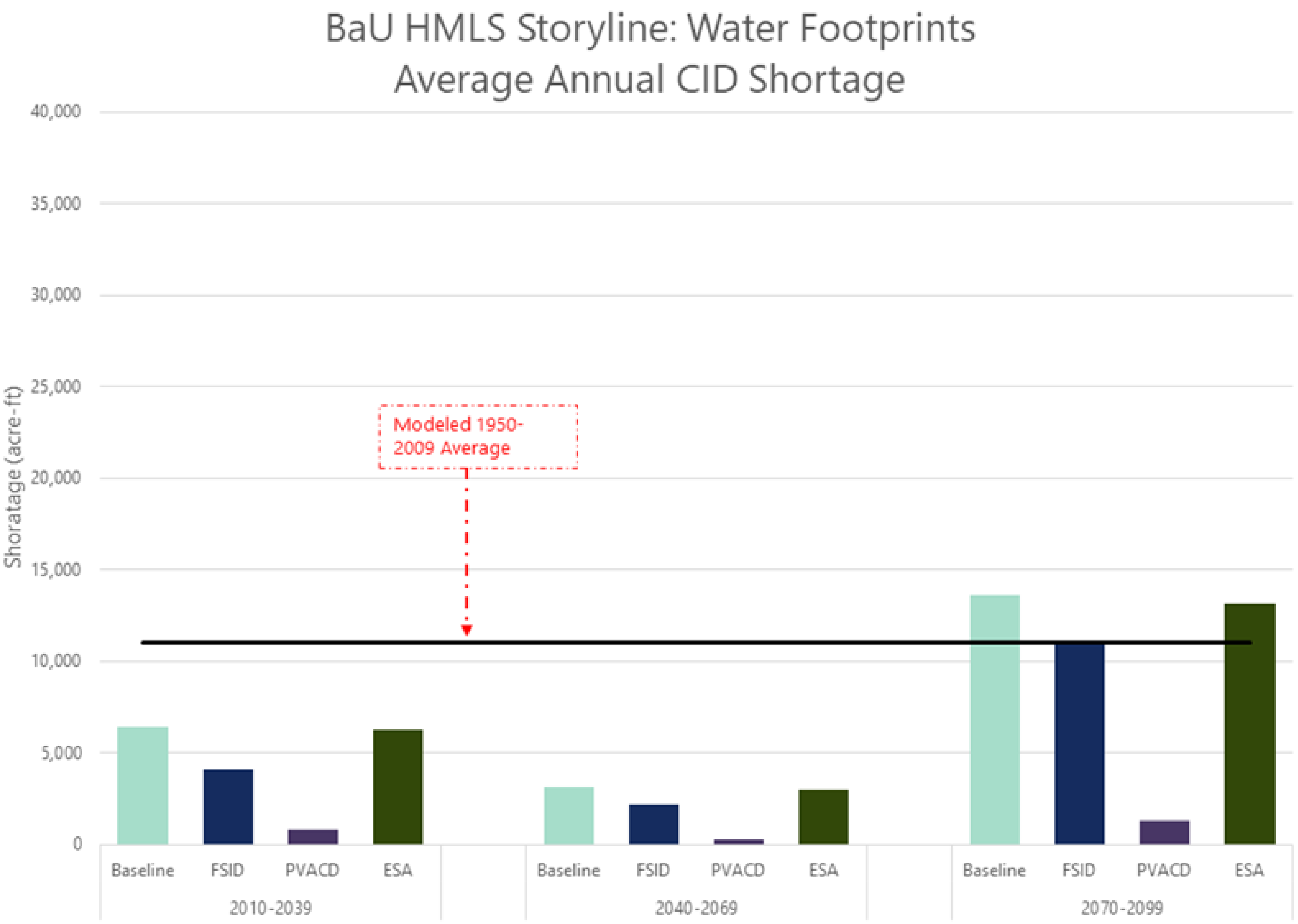

Figure 38. CID Shortages: Water Footprints in the BaU HMLS Storyline.

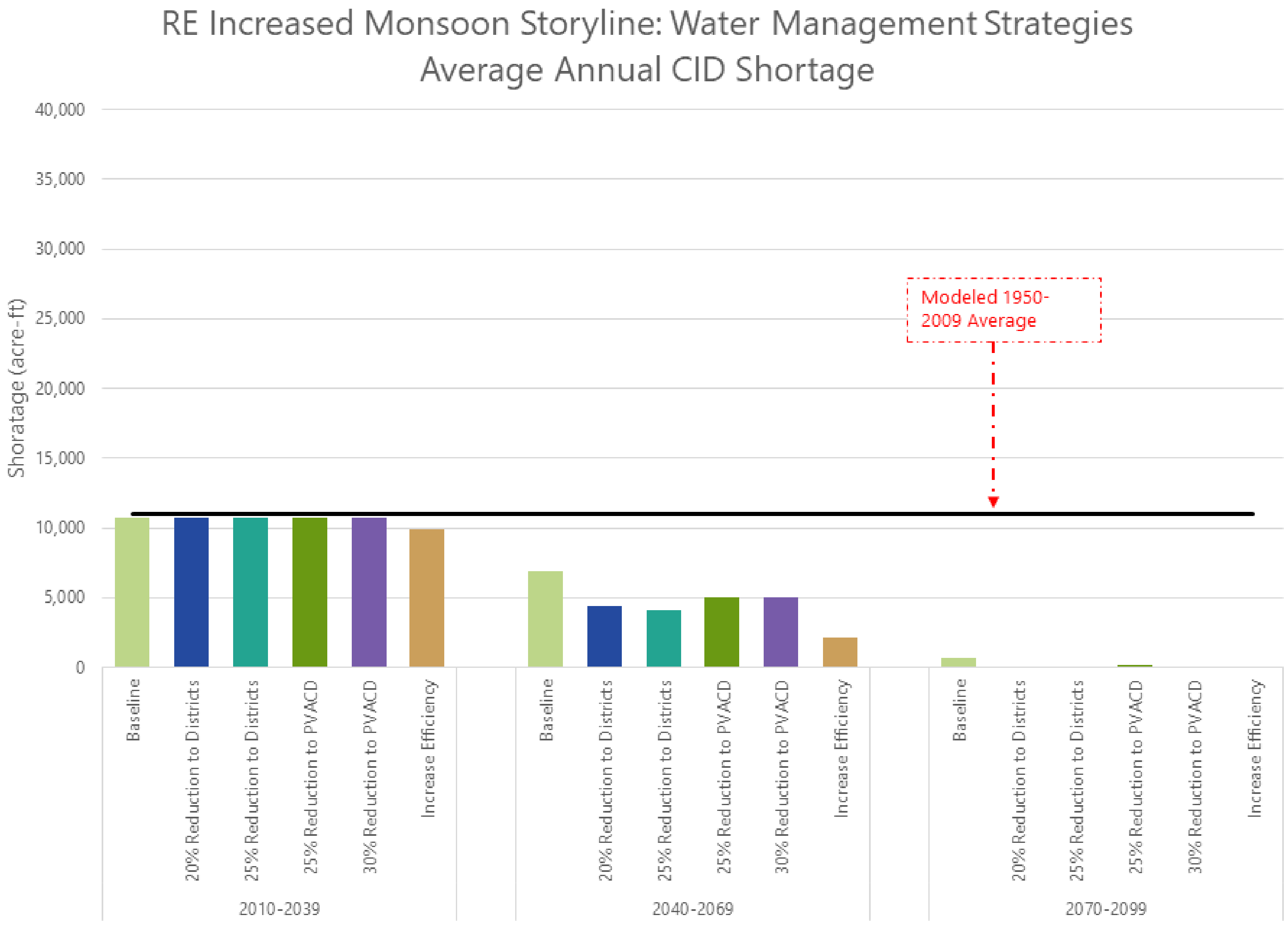

Figure 39. CID Shortages: Water Management Strategies in the RE Increased Monsoon Storyline.

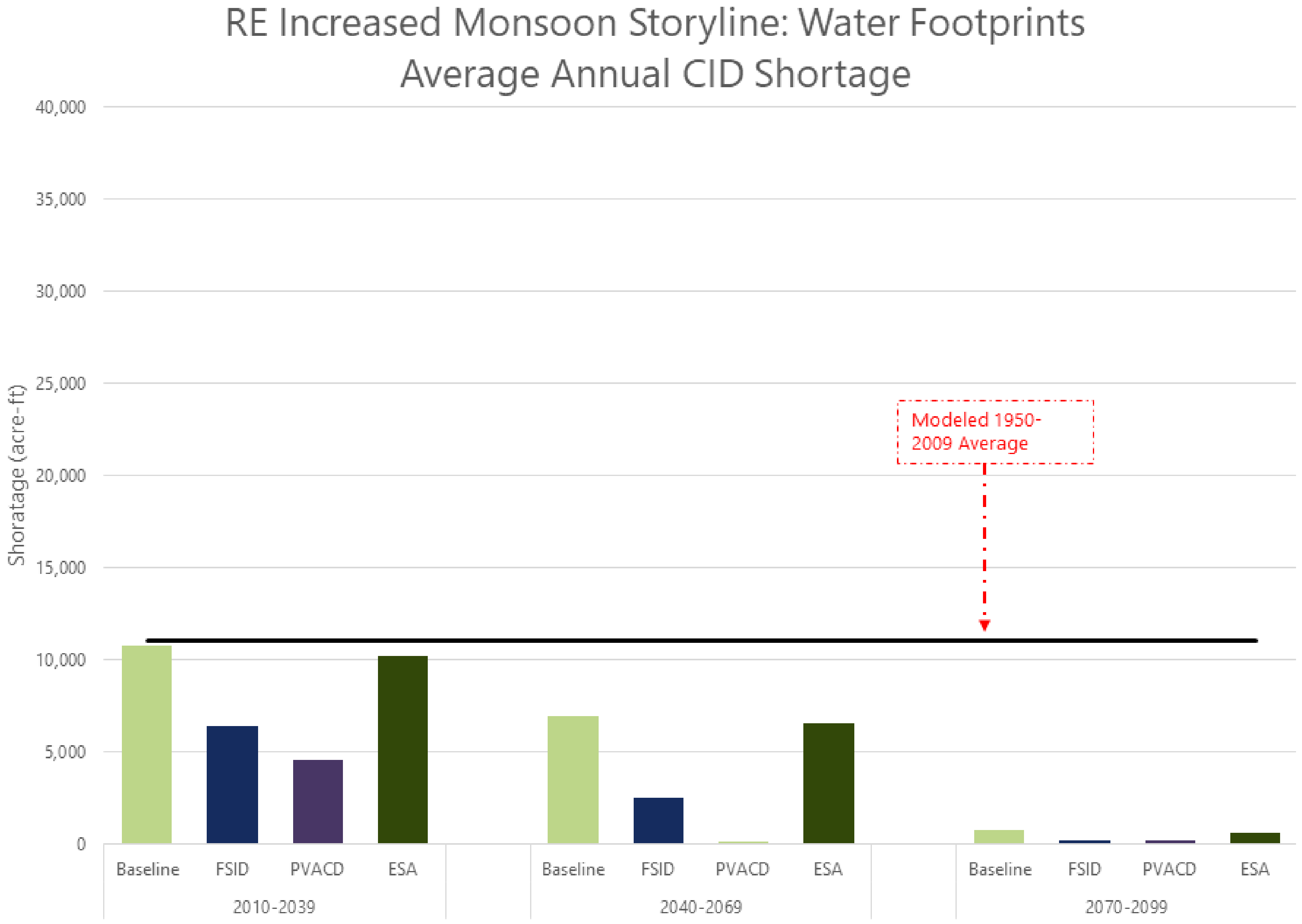

Figure 40. CID Shortages: Water Footprints in the RE Increased Monsoon Storyline.

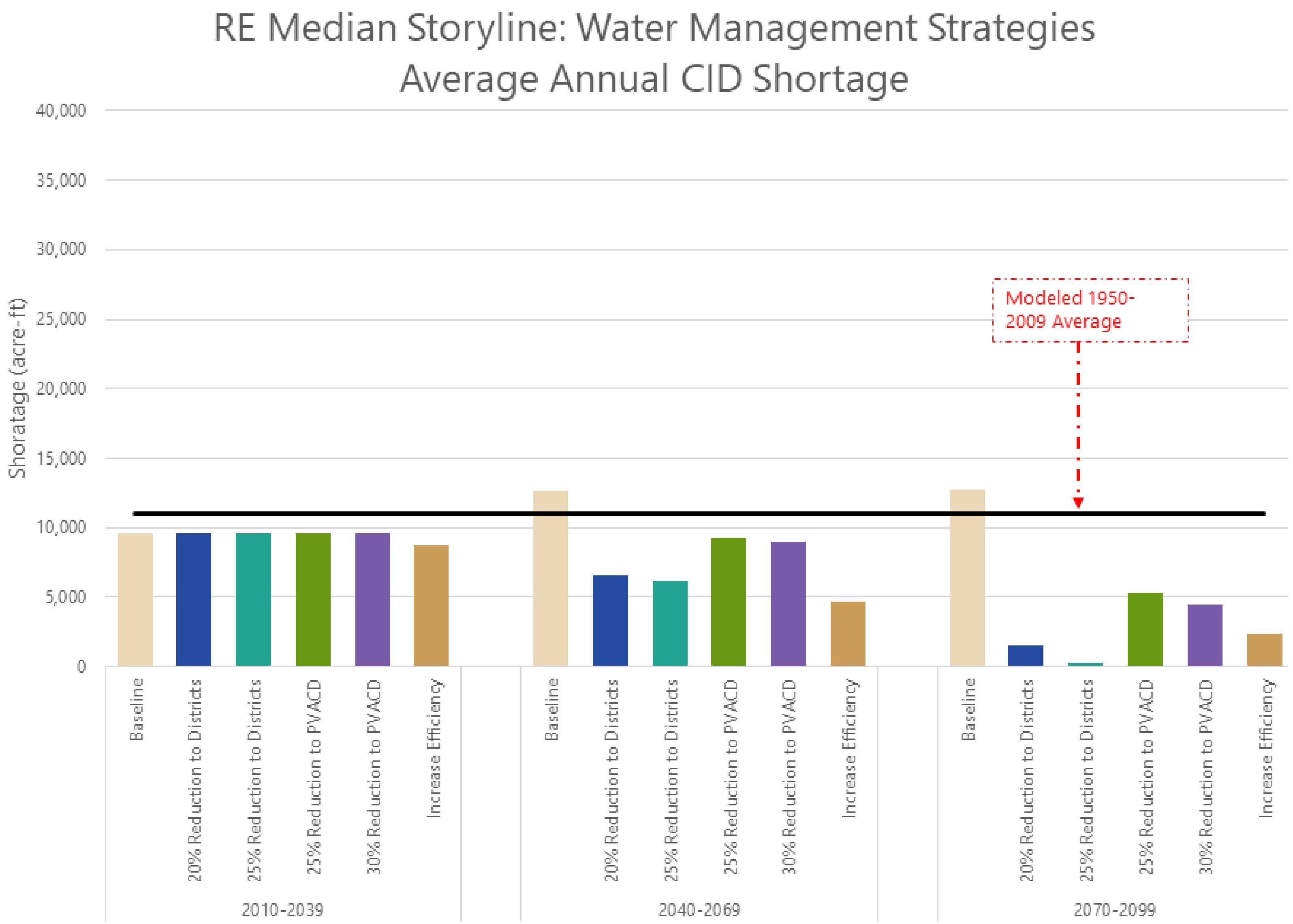

Figure 41. CID Shortages: Water Management Strategies in the RE Median Storyline.

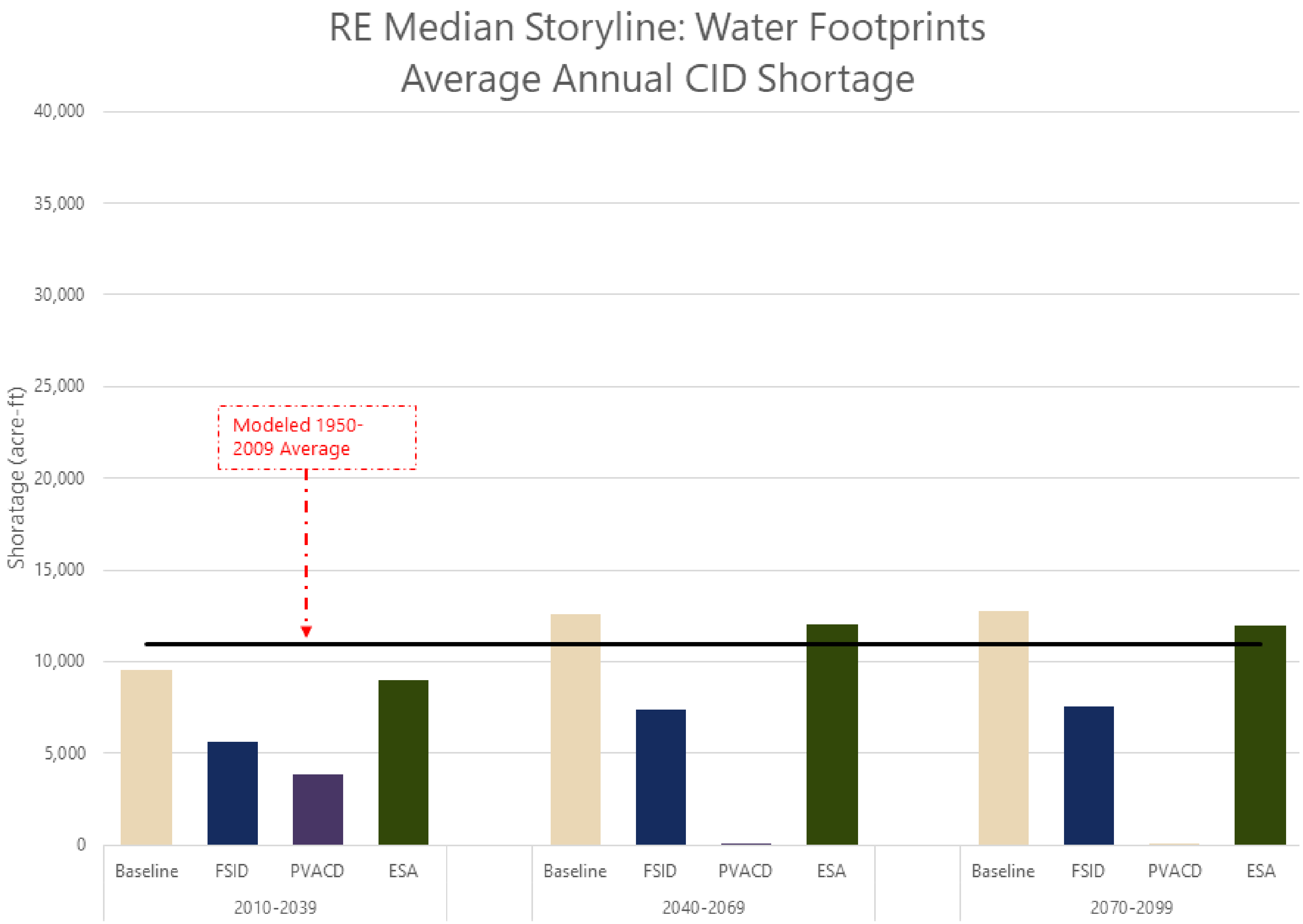

Figure 42. CID Shortages: Water Footprints in the RE Median Storyline

.

6. Drying Days at Acme

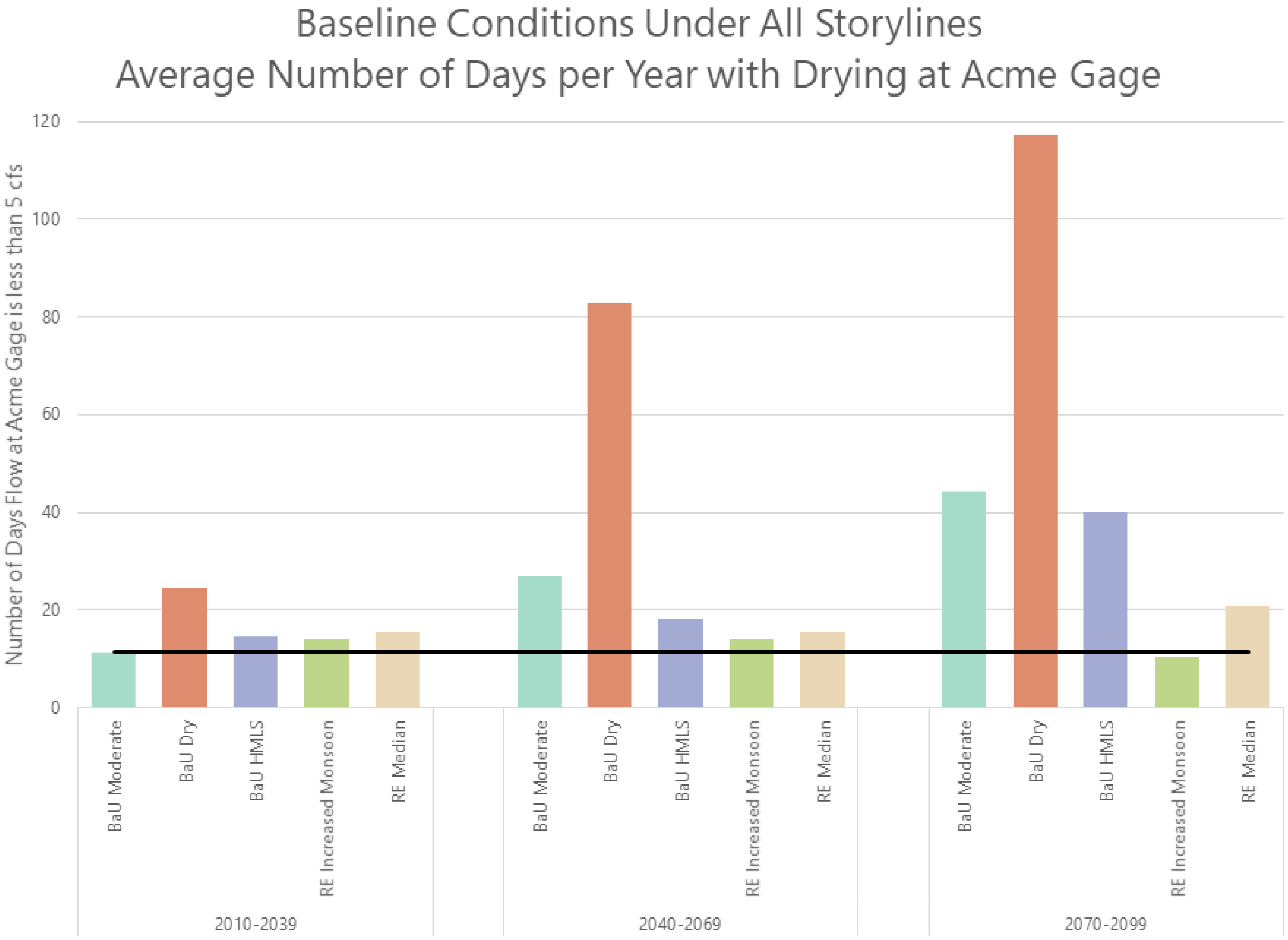

Figure 43. Drying Days at Acme: Baseline condition.

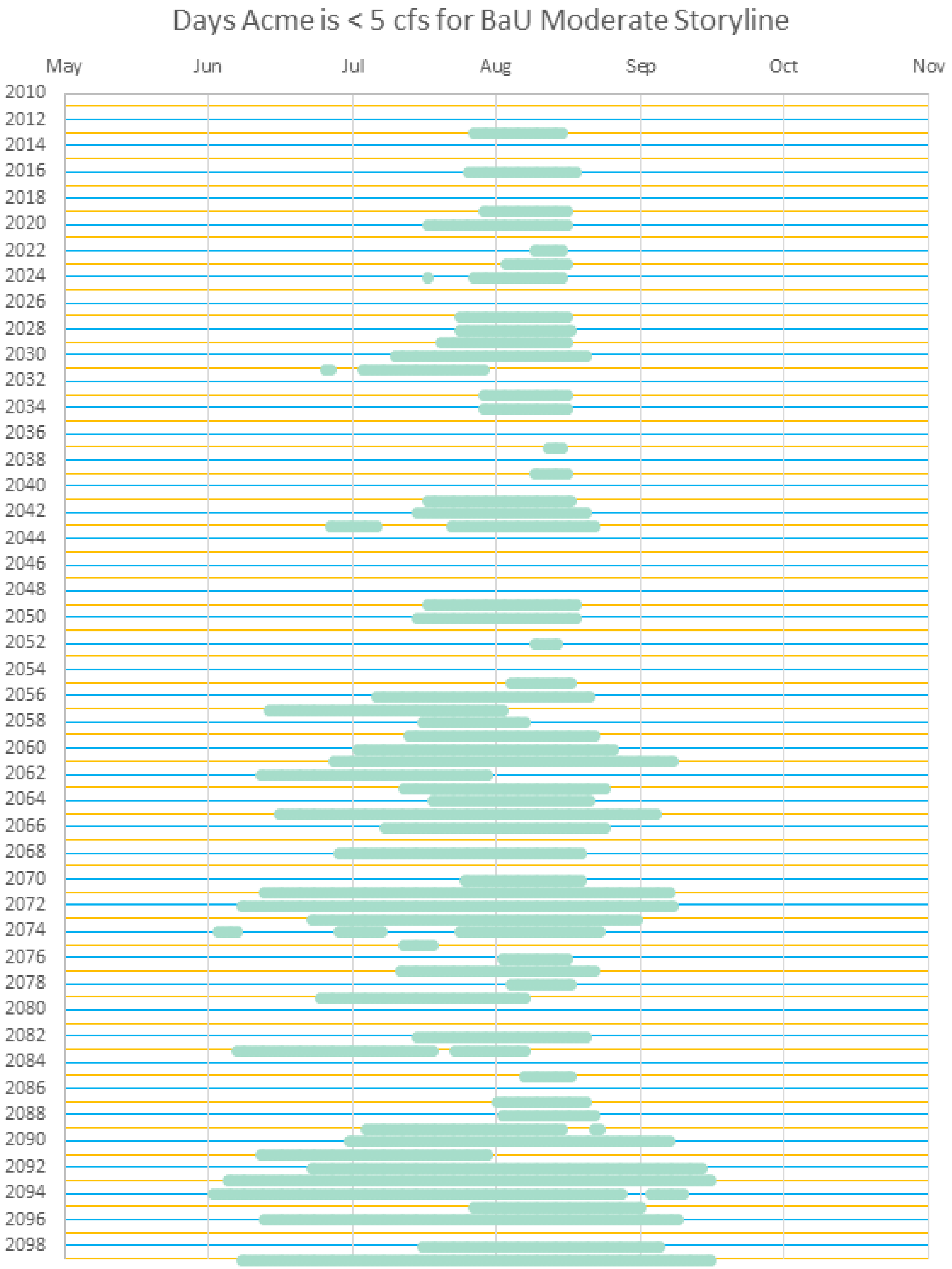

Figure 44. Drying Days: BaU Moderate Storyline baseline.

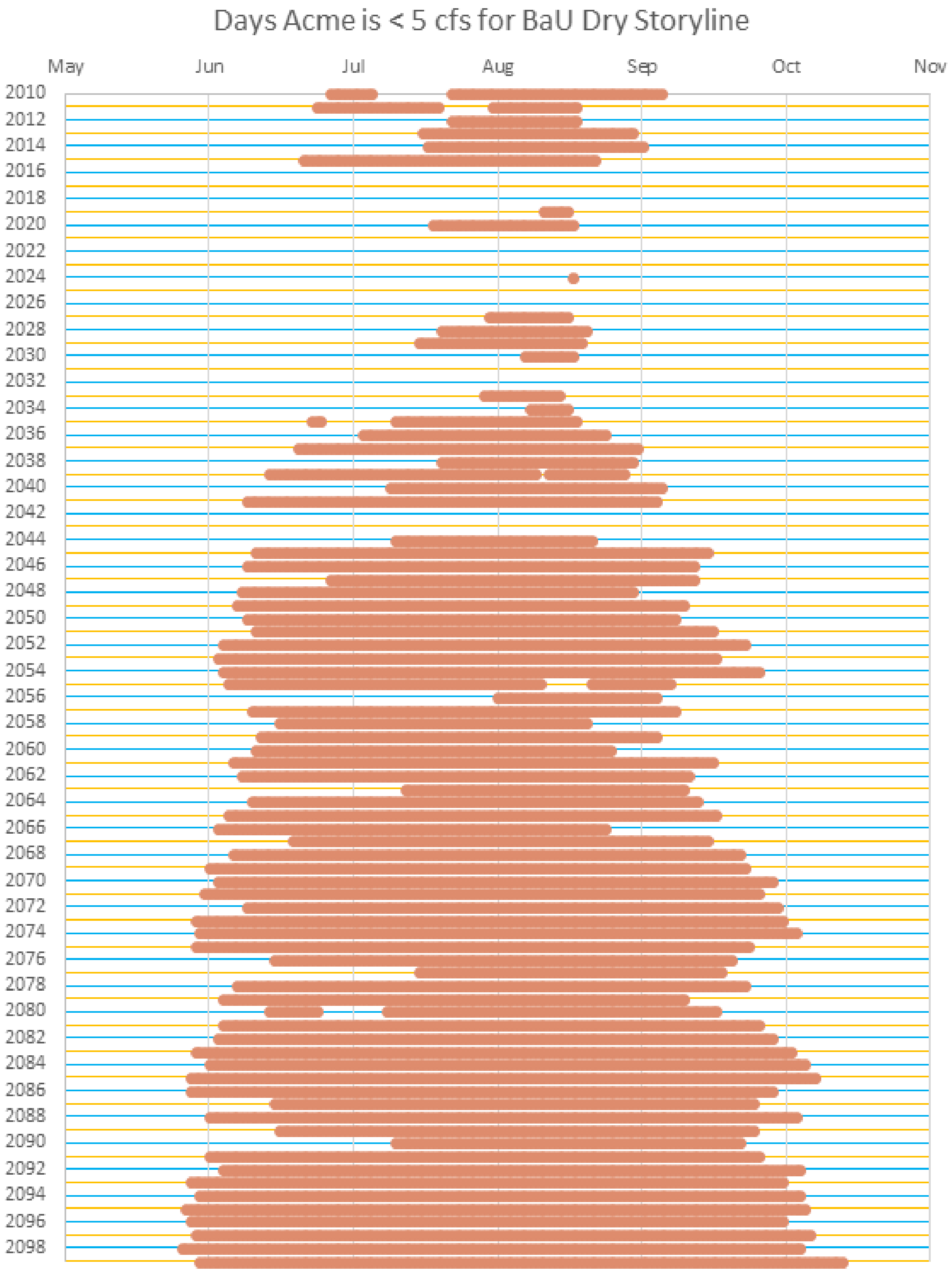

Figure 45. Drying Days: BaU Dry Storyline baseline.

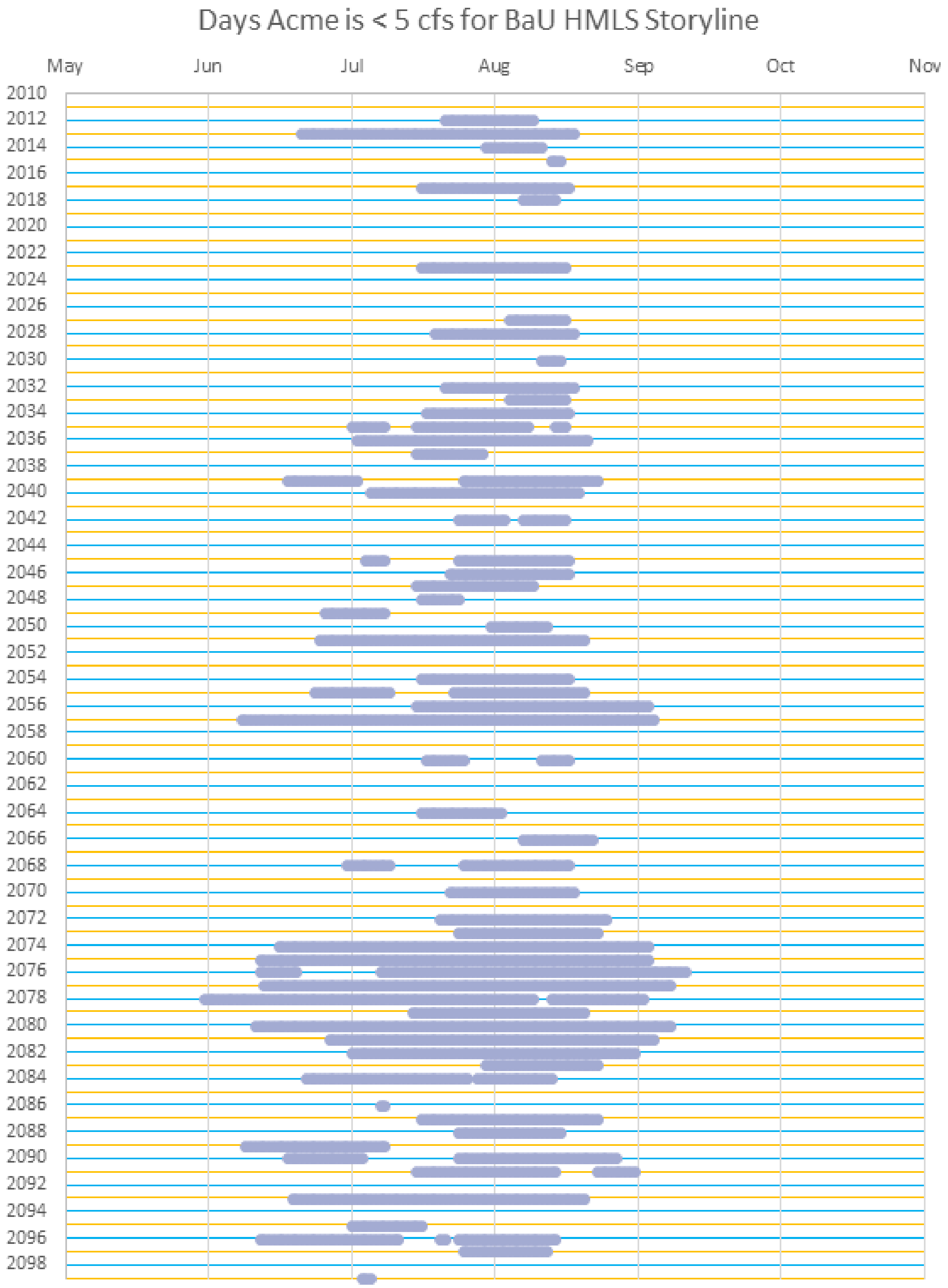

Figure 46. Drying Days: BaU HMLS Storyline baseline.

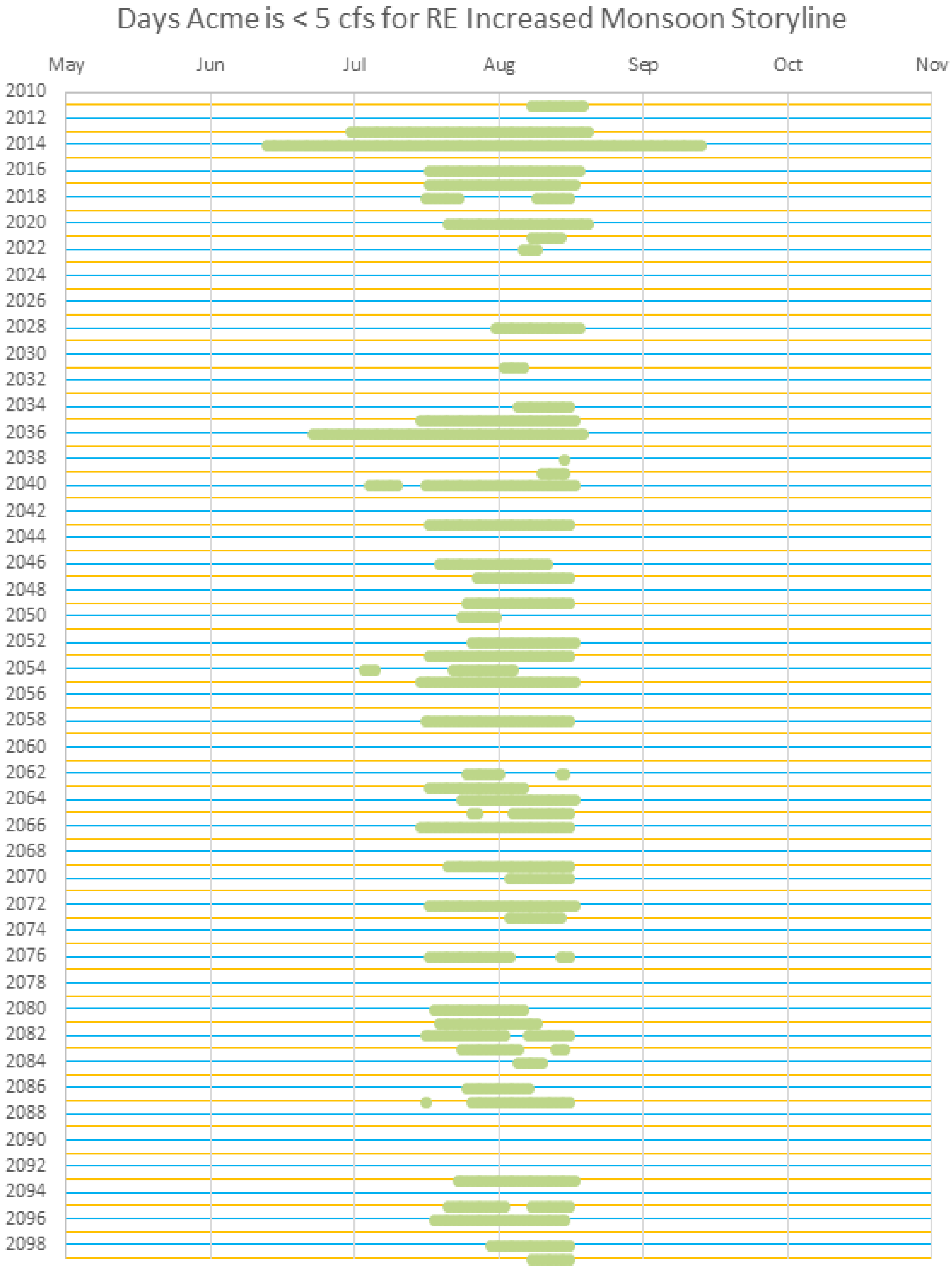

Figure 47. Drying Days: RE Increased Monsoon Storyline baseline.

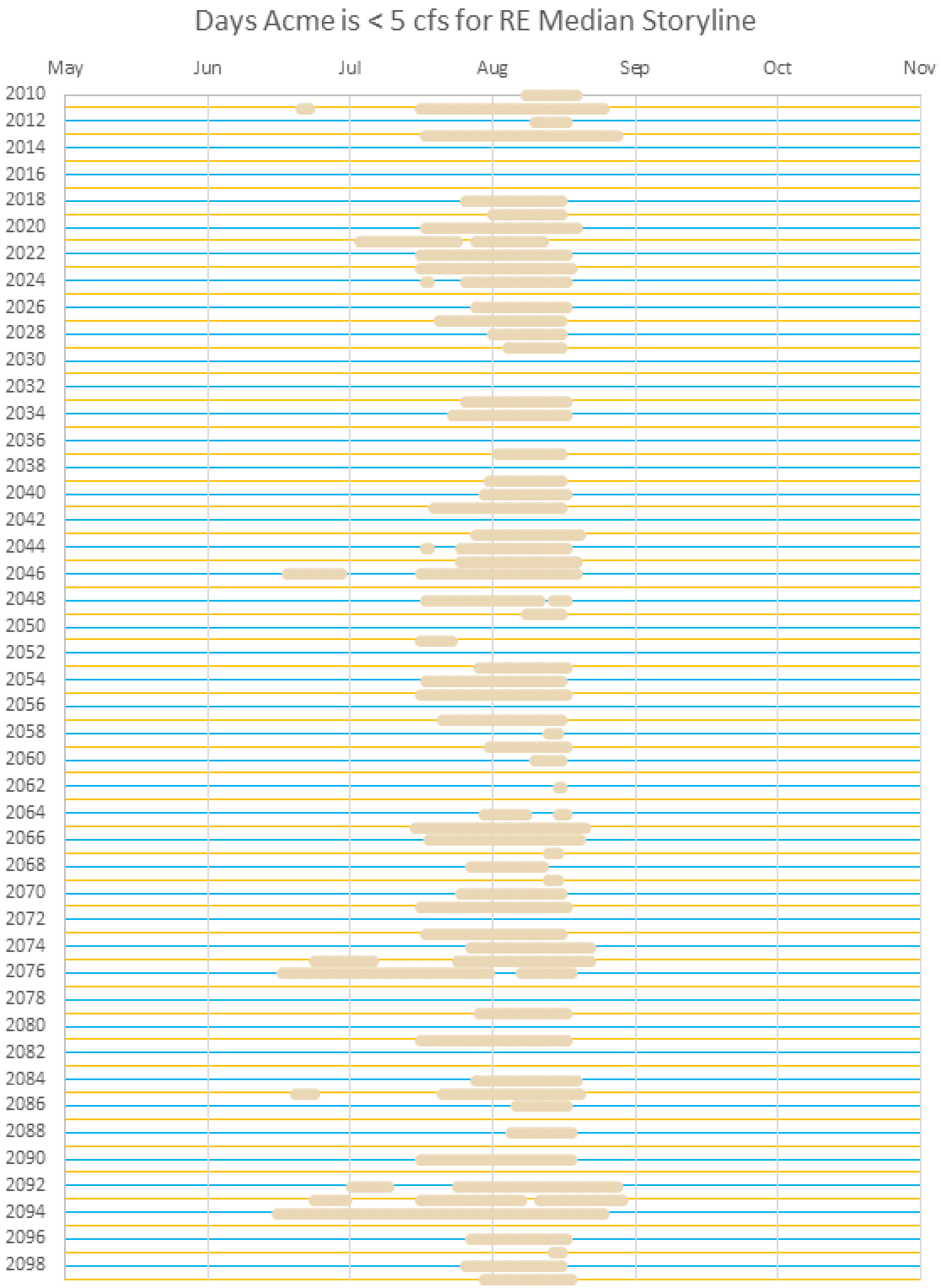

Figure 48. Drying Days: RE Median Storyline baseline.

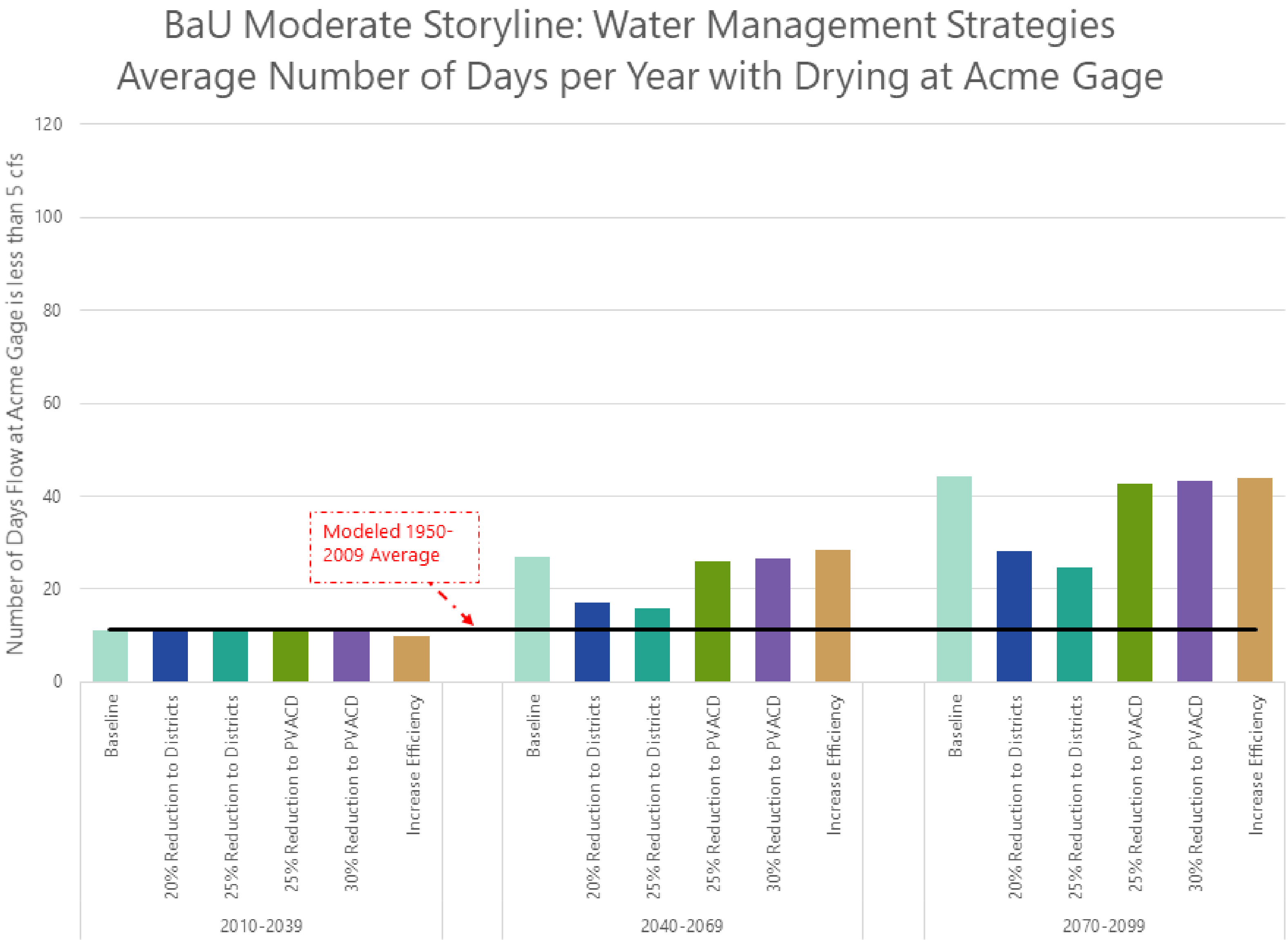

Figure 49. Drying Days: Water Management Strategies in the BaU Moderate Storyline.

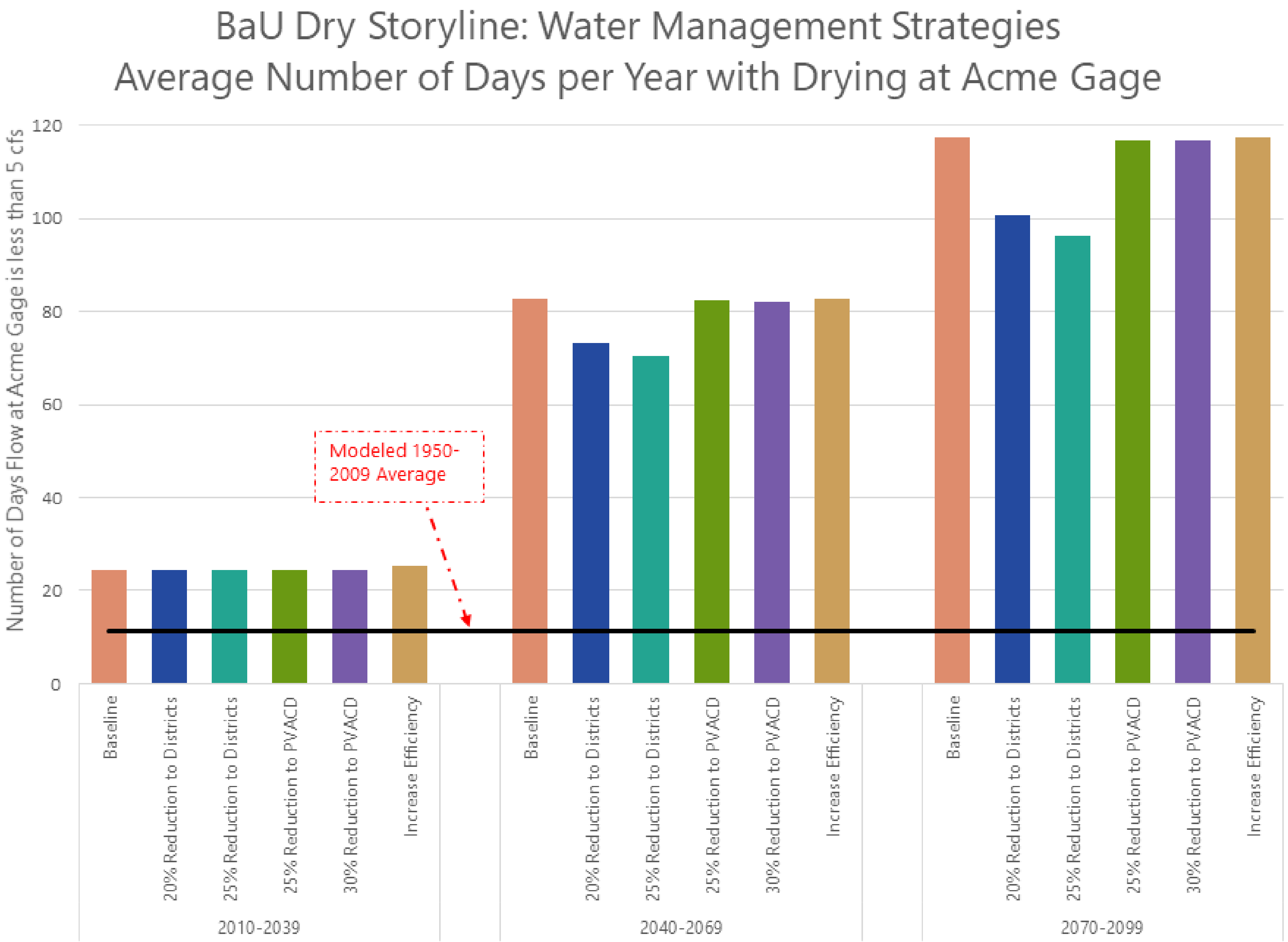

Figure 50. Drying Days: Water Management Strategies in the BaU Dry Storyline.

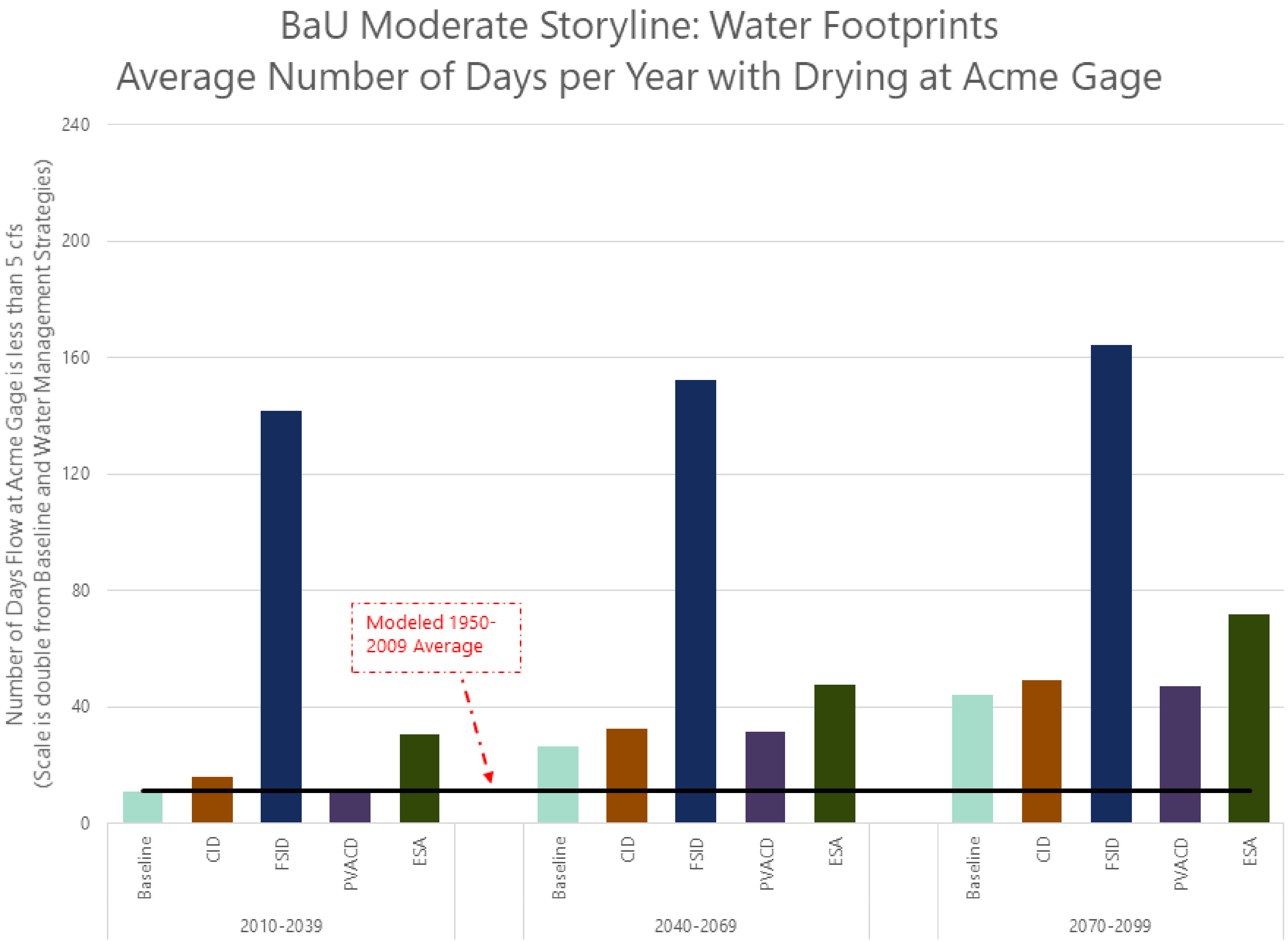

Figure 51. Drying Days: Water Footprints in the BaU Moderate Storyline.

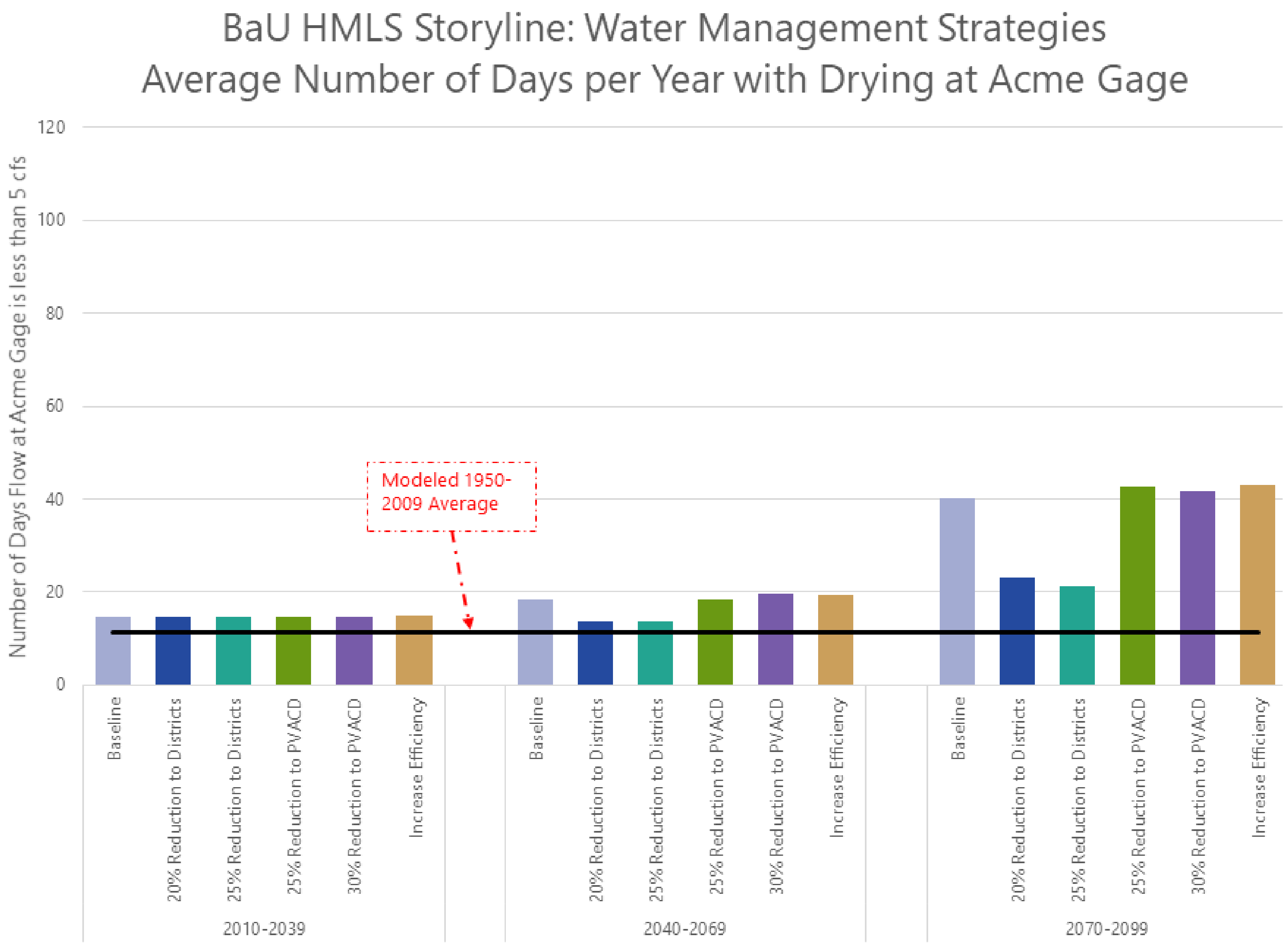

Figure 52. Drying Days: Water Management Strategies in the BaU Dry Storyline.

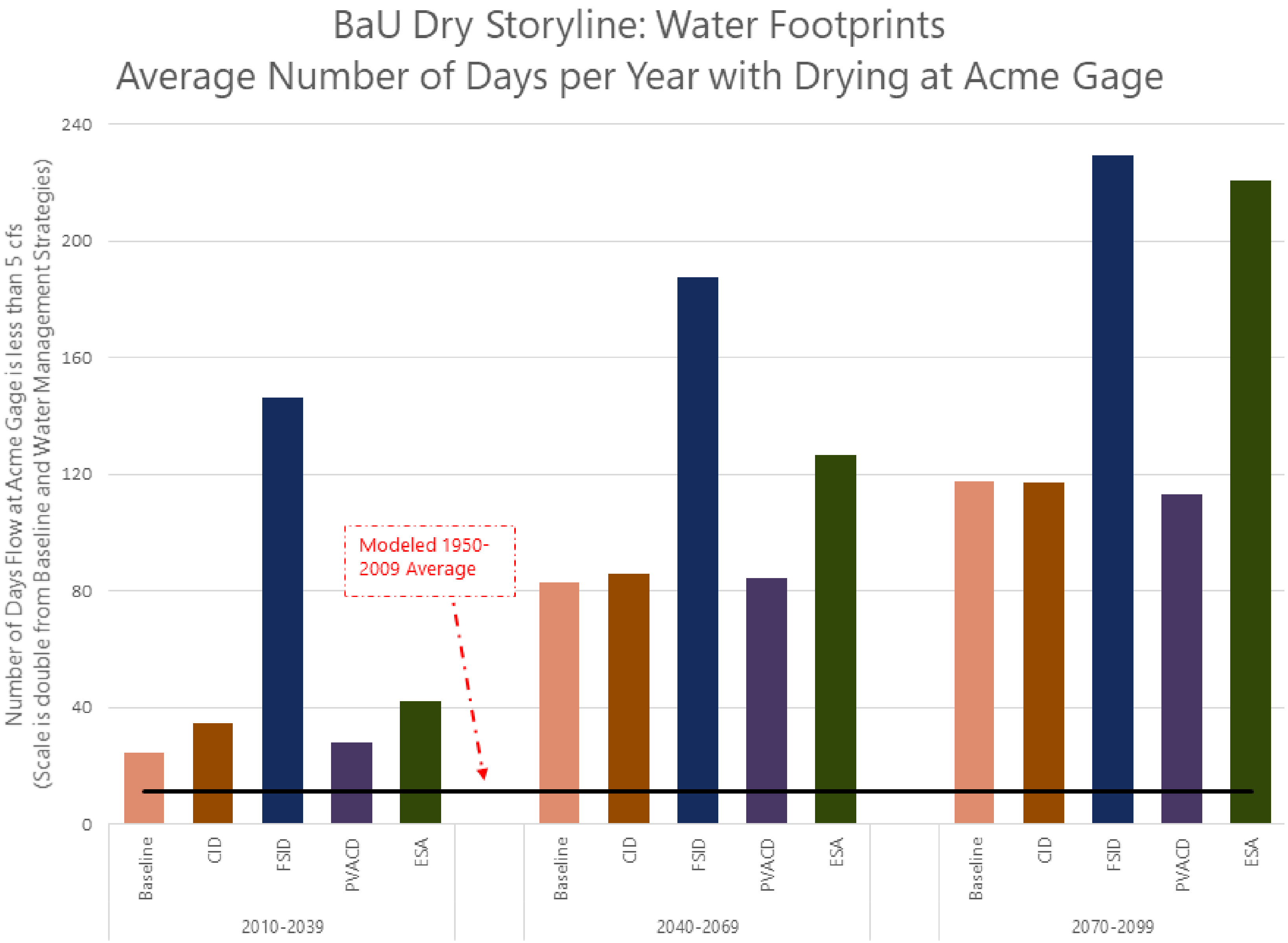

Figure 53. Drying Days: Water Footprint in the BaU Dry Storyline.

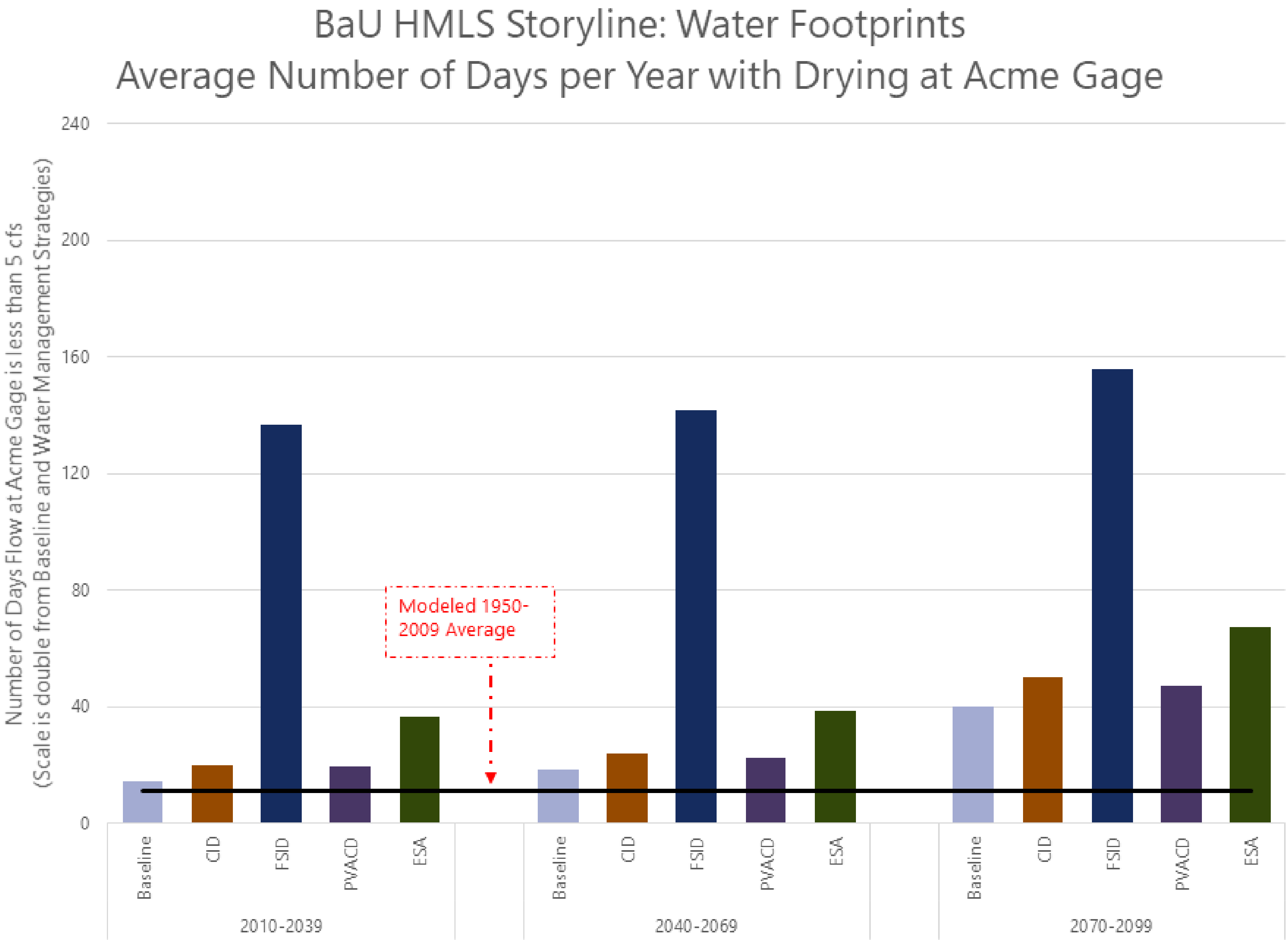

Figure 54. Drying Days: Water Footprint in the BaU Dry Storyline.

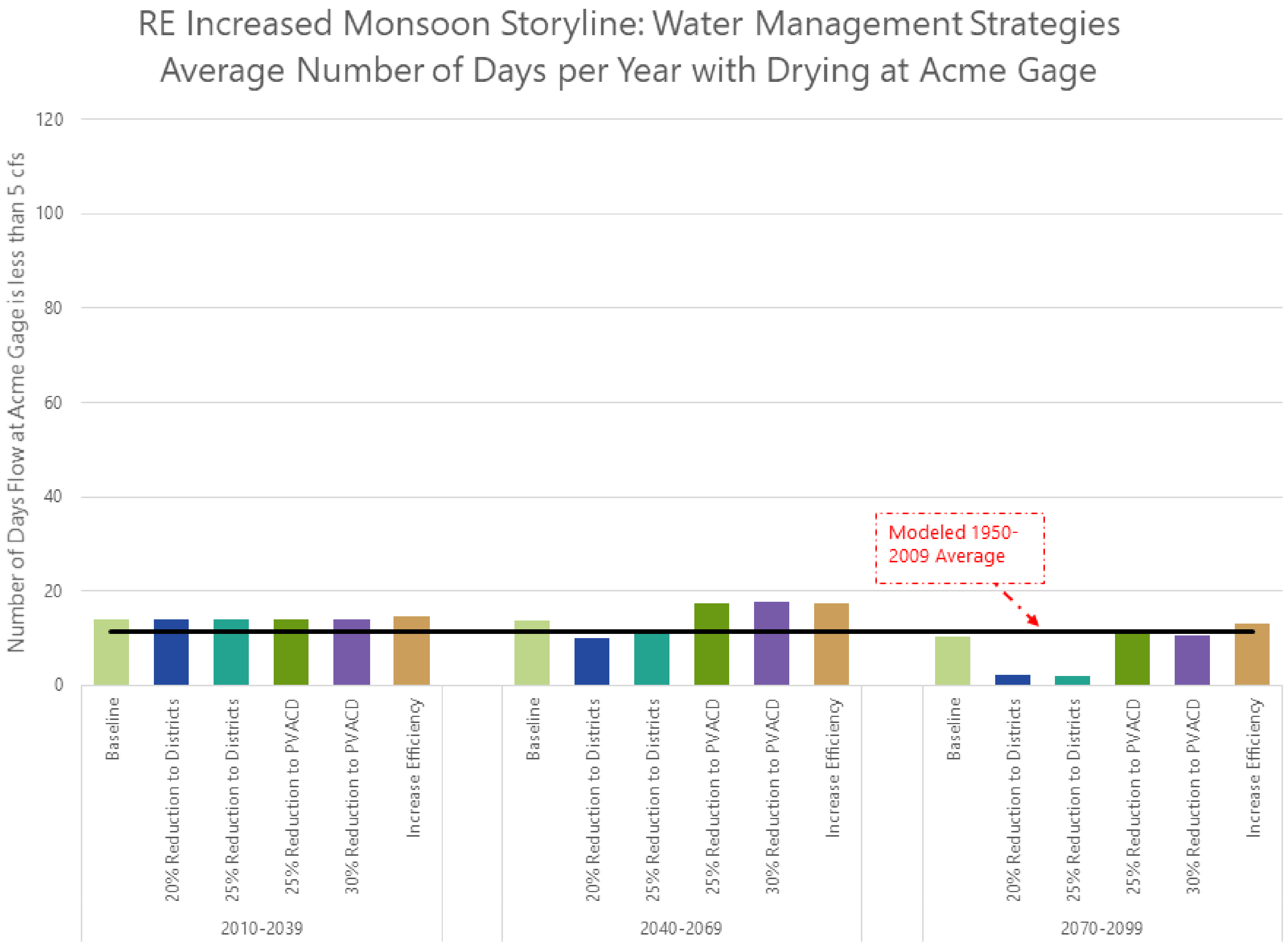

Figure 55. Drying Days: Water Management Strategies in the RE Increased Monsoon Storyline.

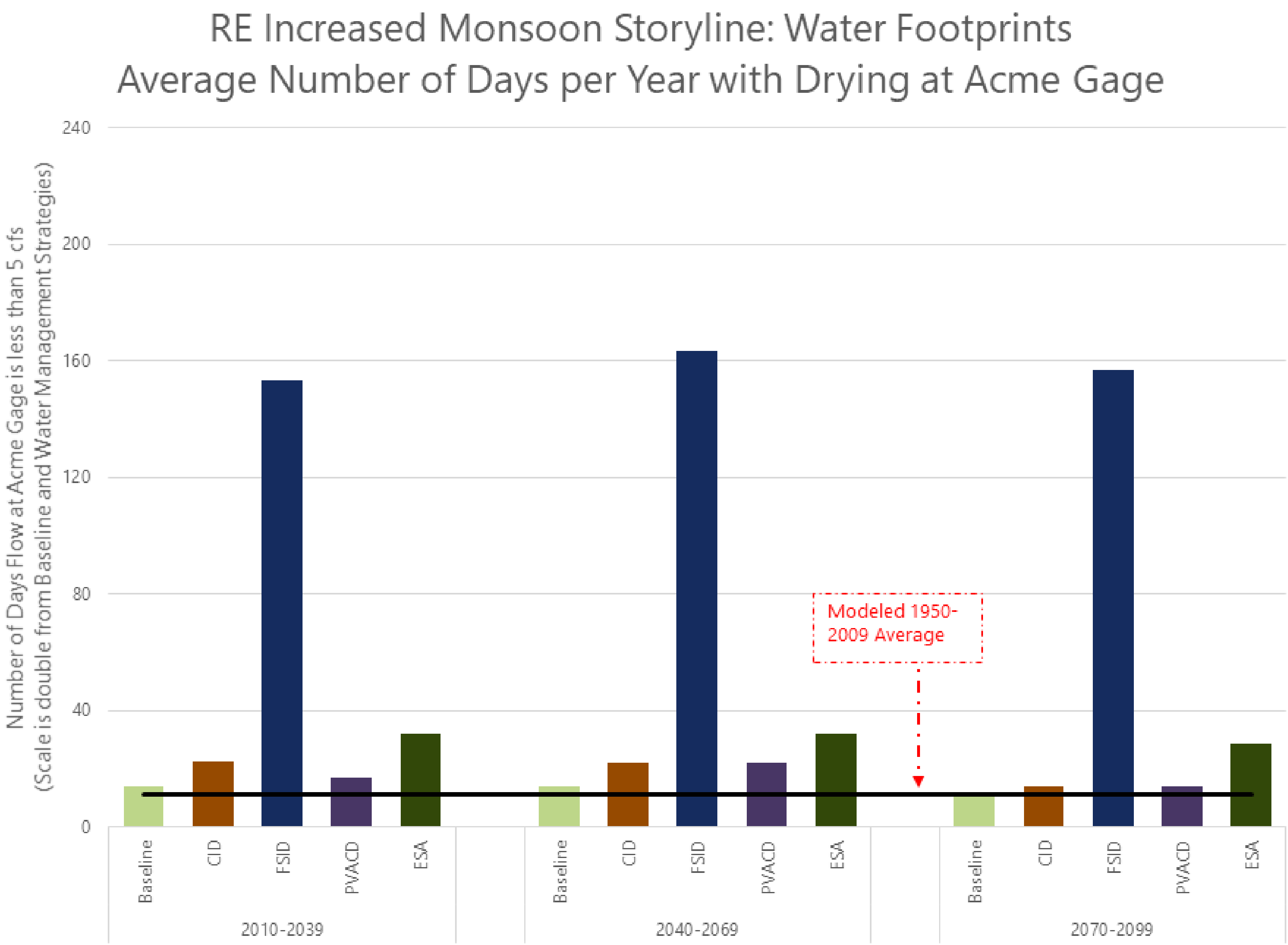

Figure 56. Drying Days: Water Footprint in the RE Increased Monsoon Storyline.

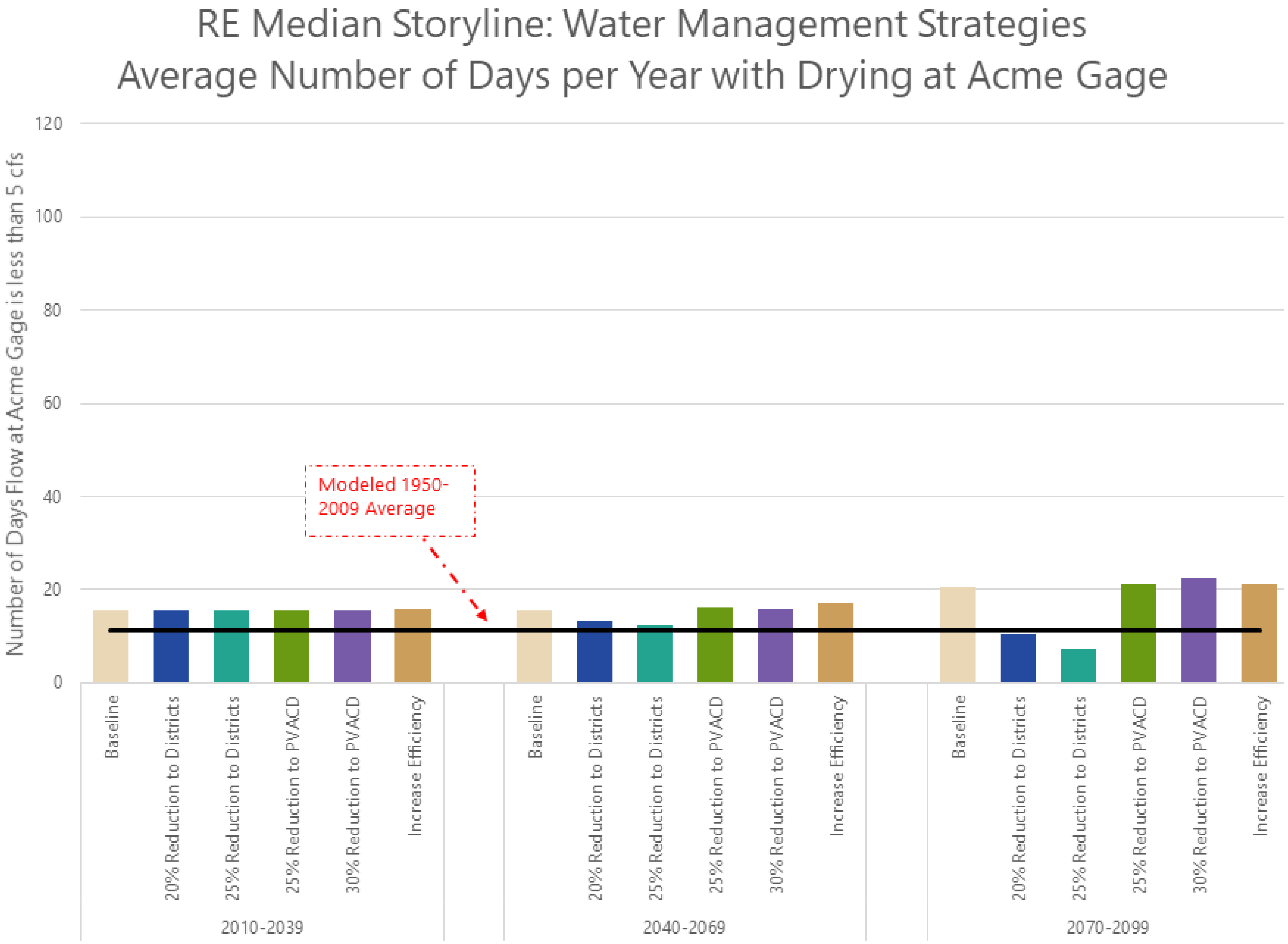

Figure 57. Drying Days: Water Management Strategies in the RE Median Storyline.

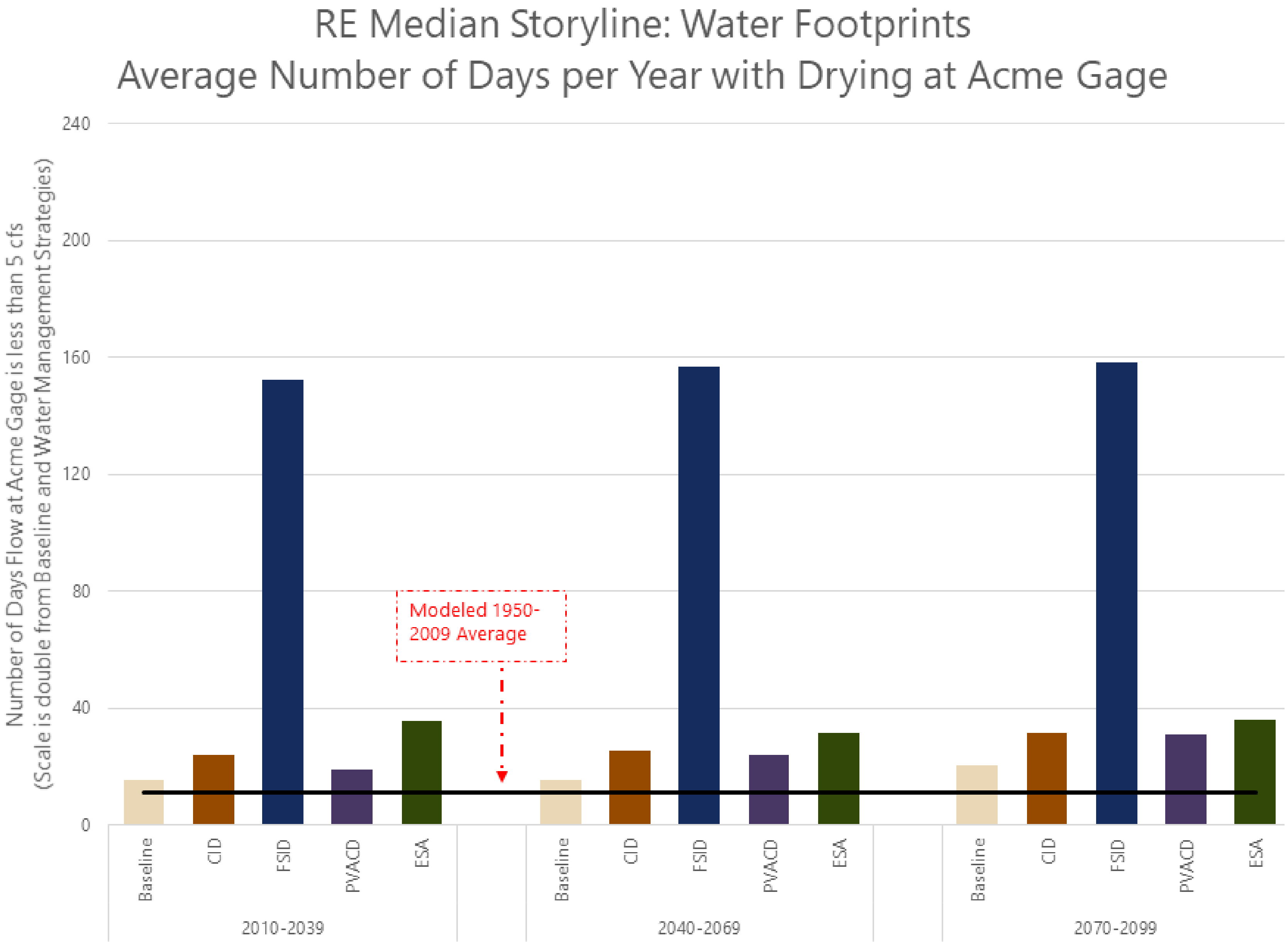

Figure 58. Drying Days: Water Footprint in the RE Median Storyline.

7. Drying at Acme and Artesia Gages

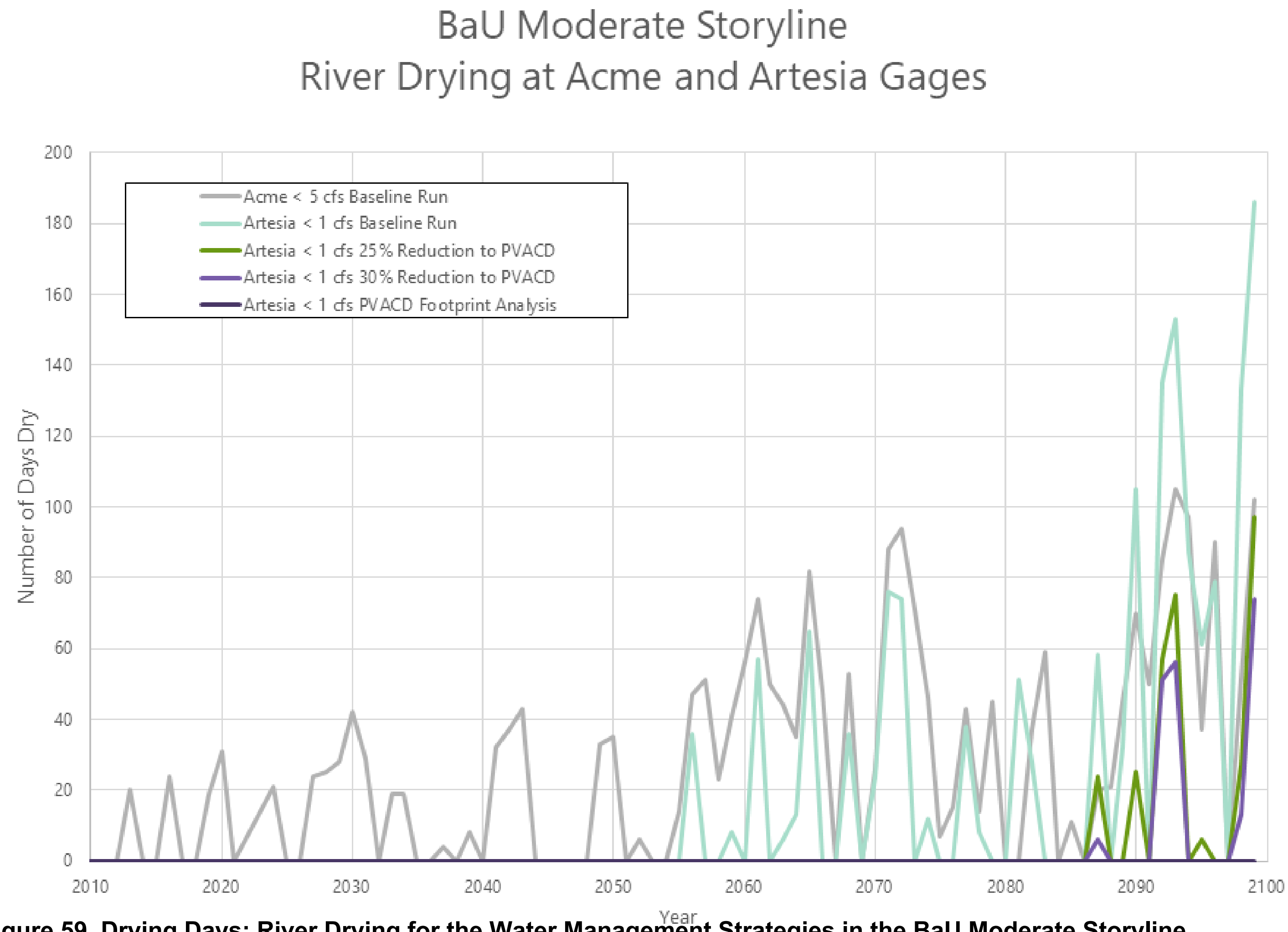

Figure 59. Drying Days: River Drying for the Water Management Strategies in the BaU Moderate Storyline.

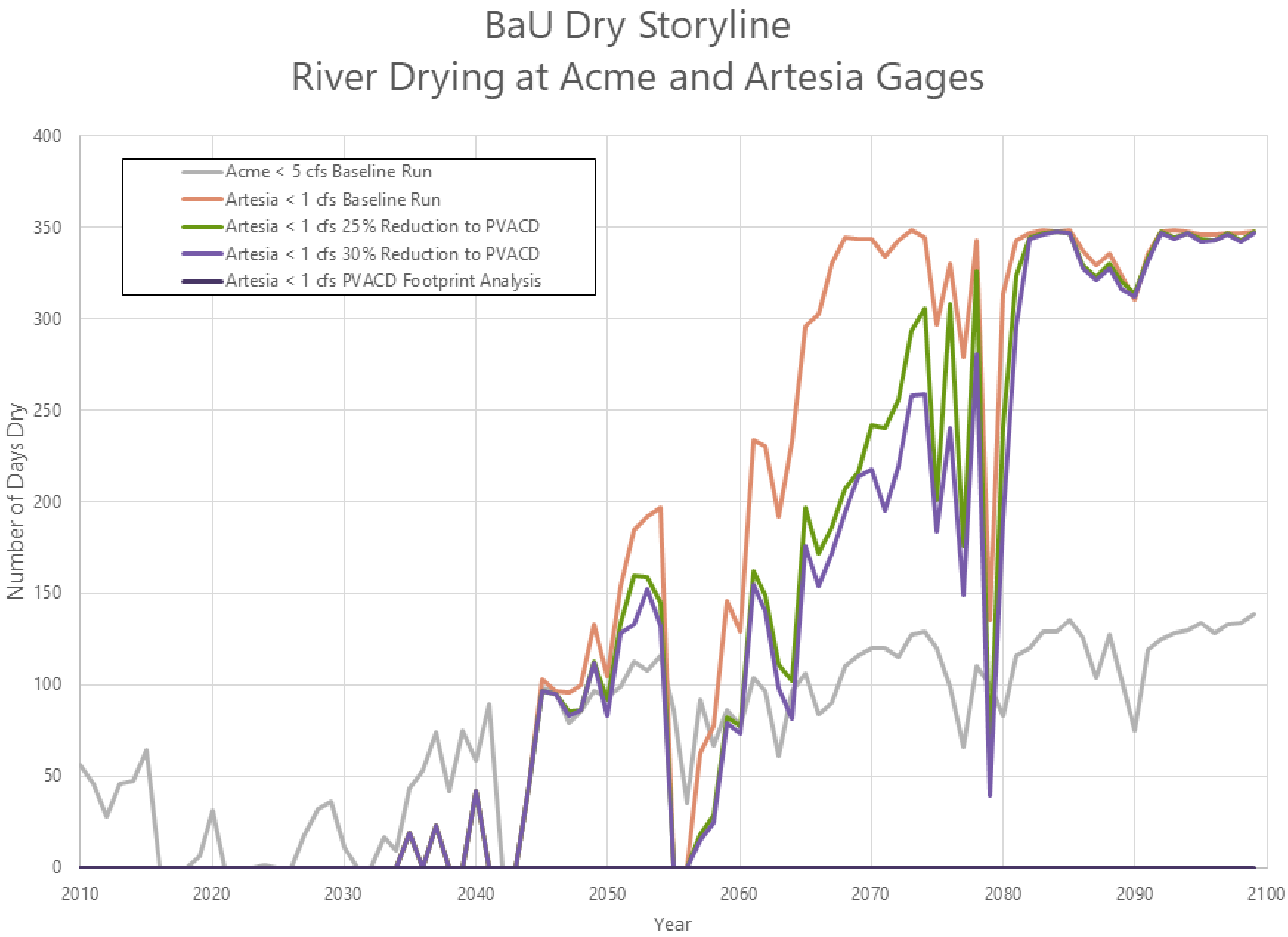

Figure 60. Drying Days: River Drying for the Water Management Strategies in the BaU Dry Storyline.

8. Potential Settlement Releases

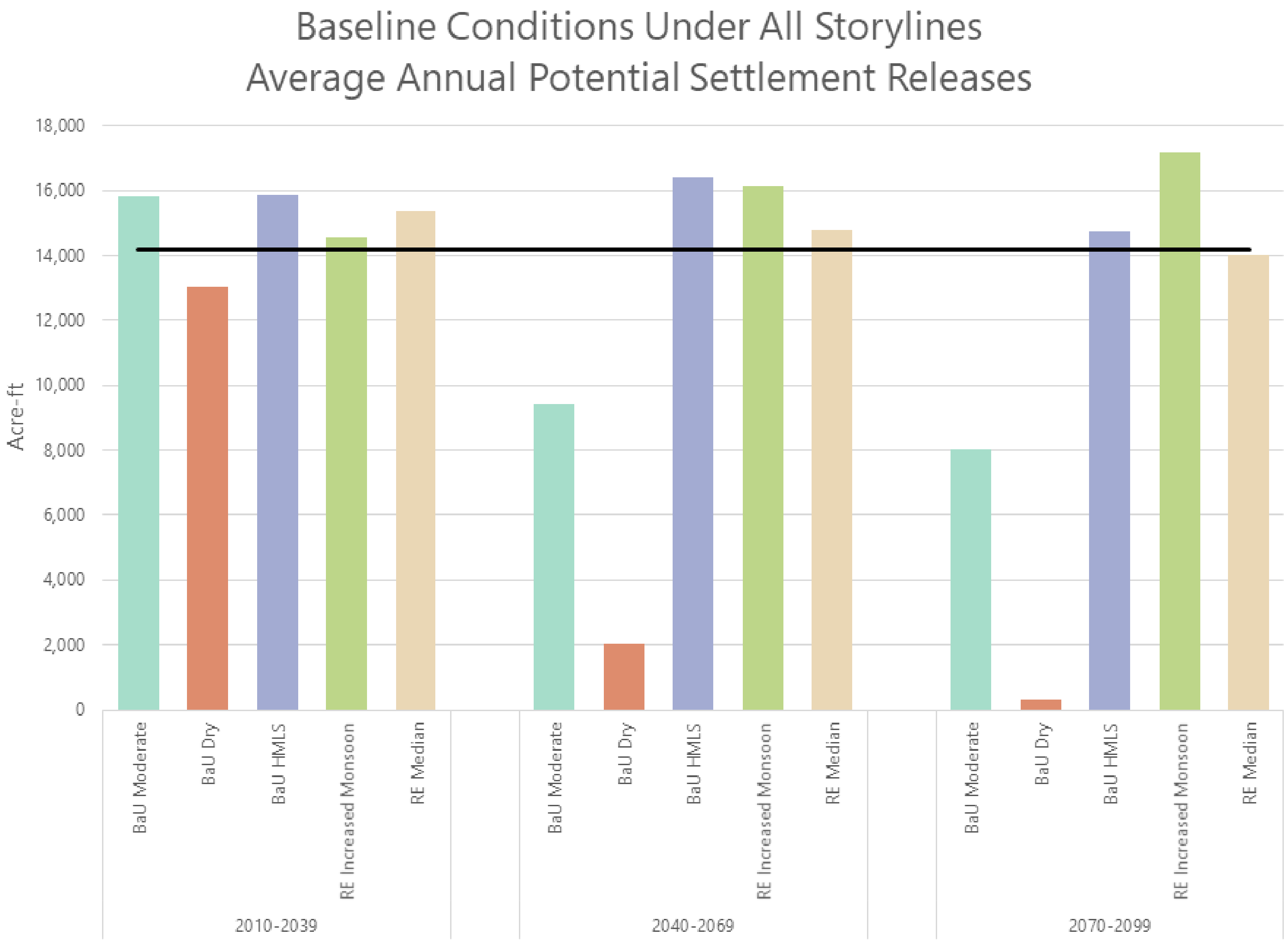

Figure 61. Average annual potential settlement releases: Baseline conditions in all storylines.

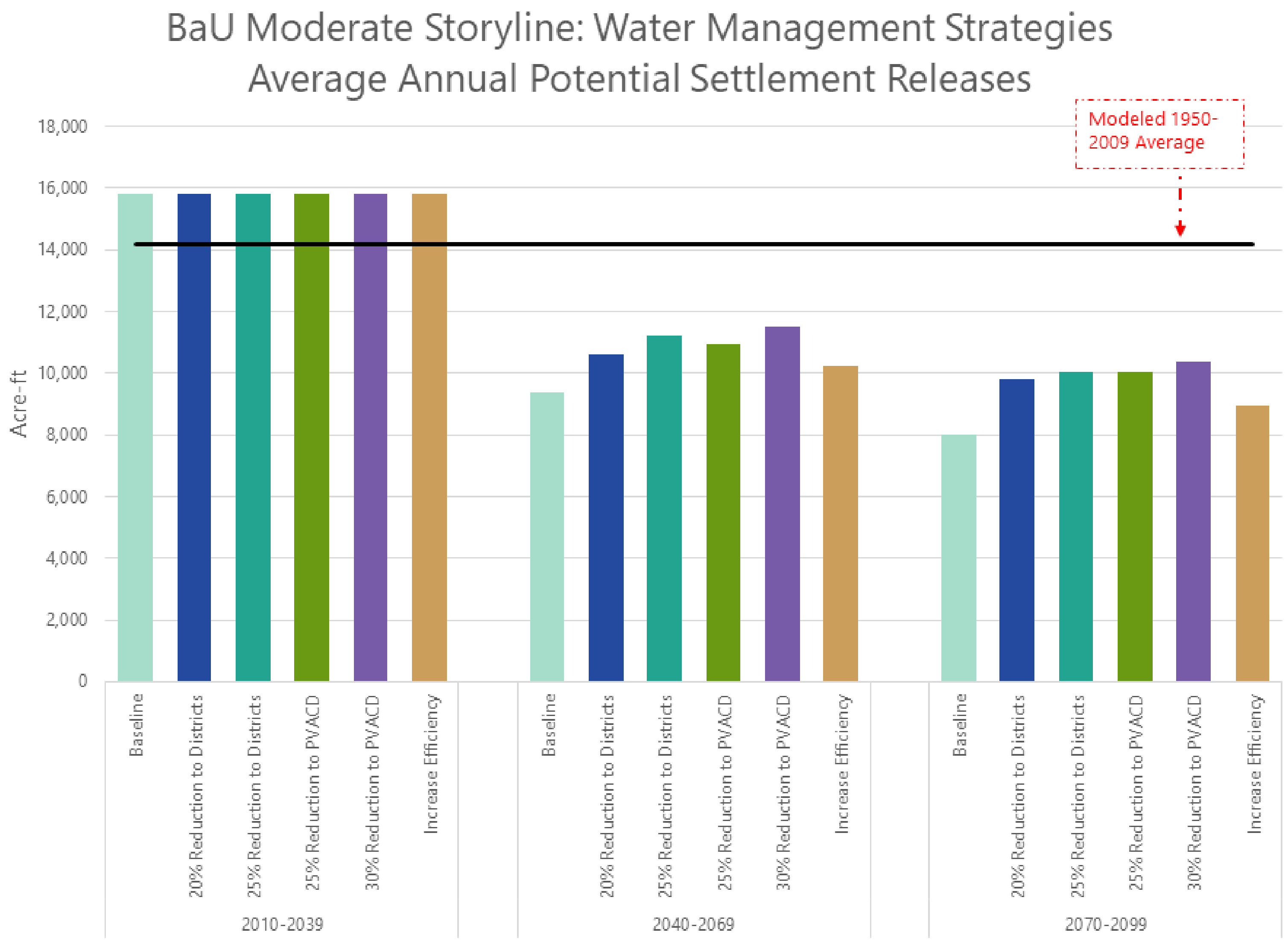

Figure 62. Average annual potential settlement releases: Water Management Strategies in the BaU Moderate Storyline.

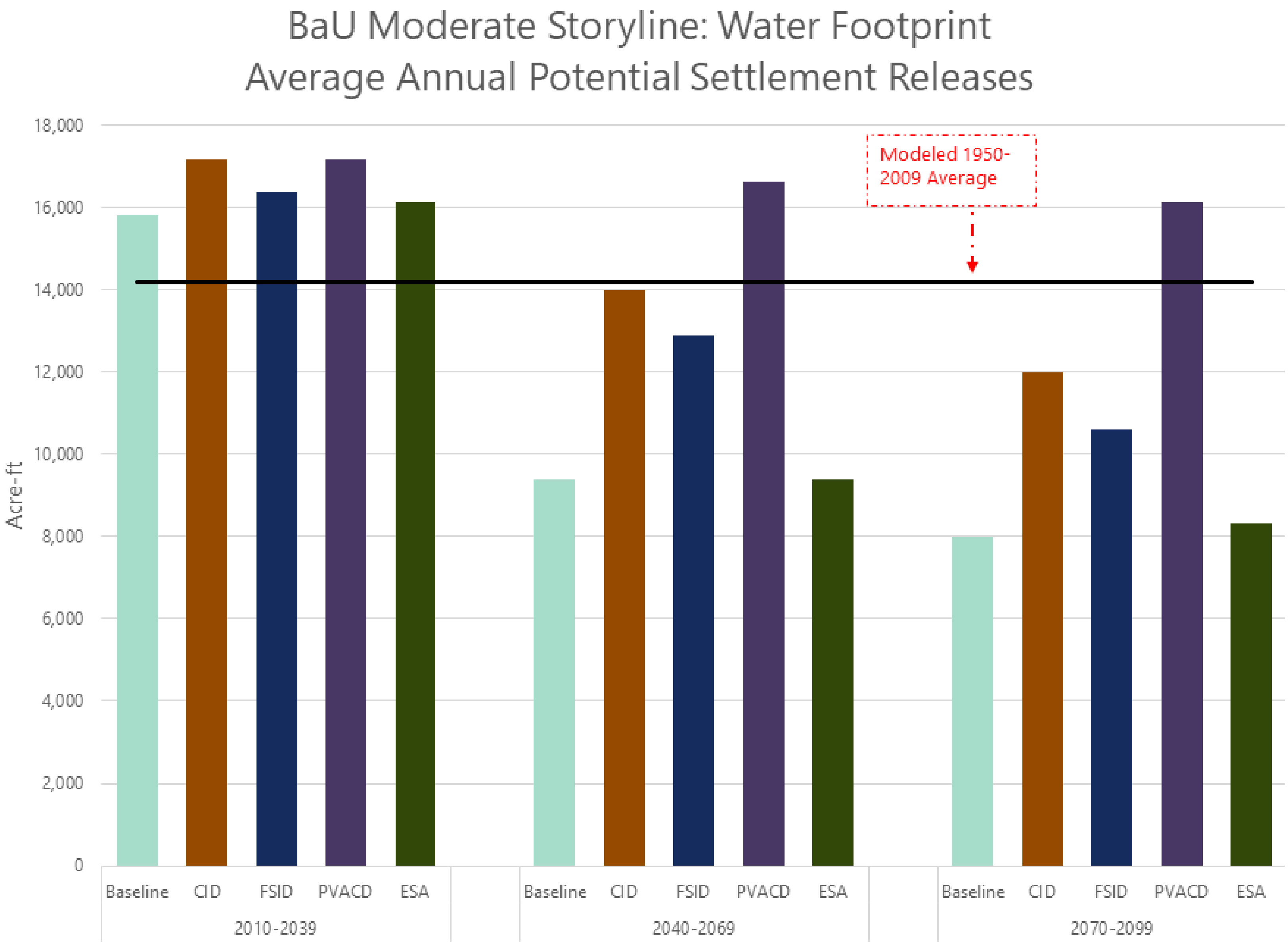

Figure 63. Average annual potential settlement releases: Water Footprint in the BaU Moderate Storyline.

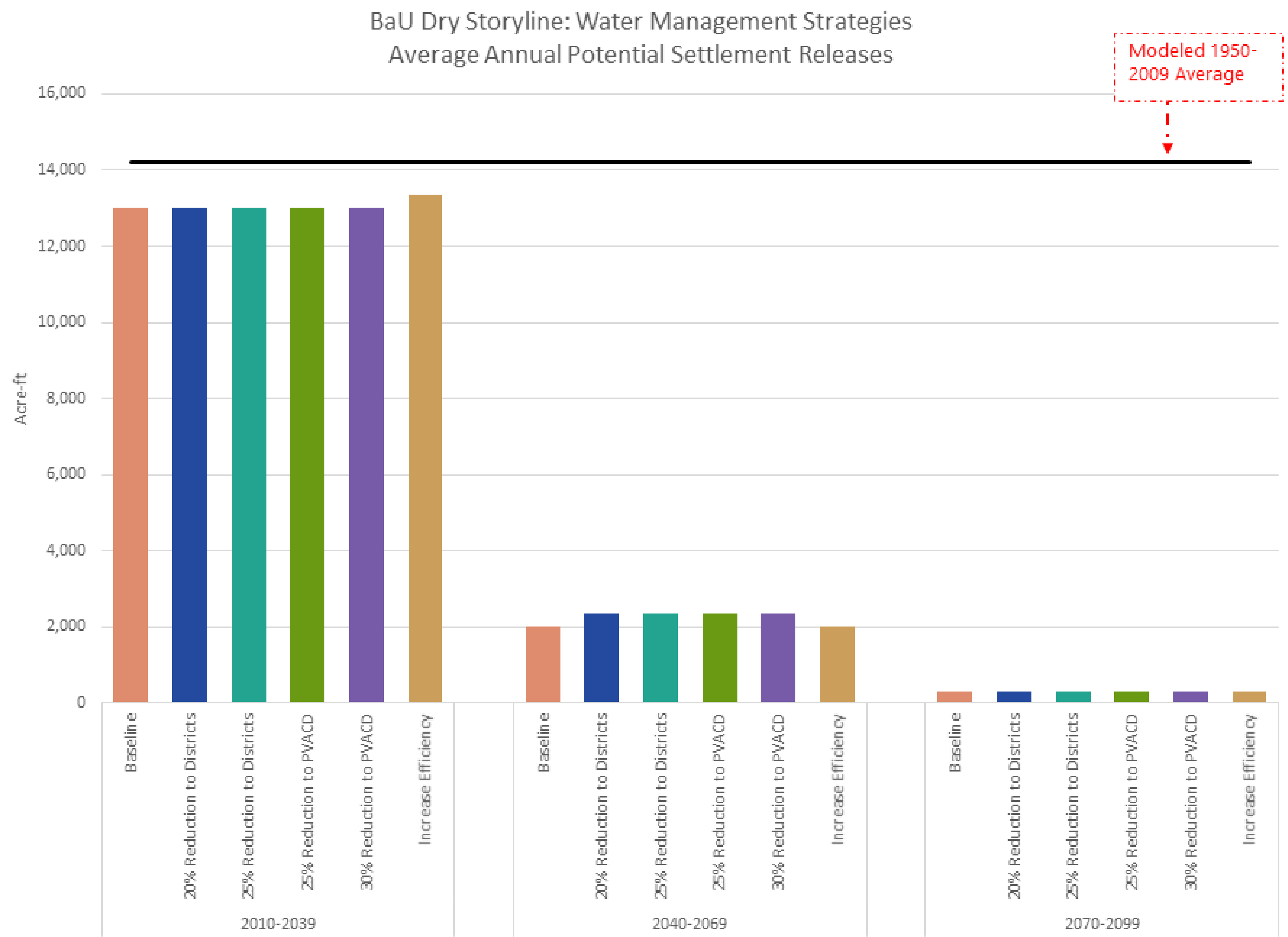

Figure 64. Average annual potential settlement releases: Water Management Strategies in the BaU Dry Storyline.

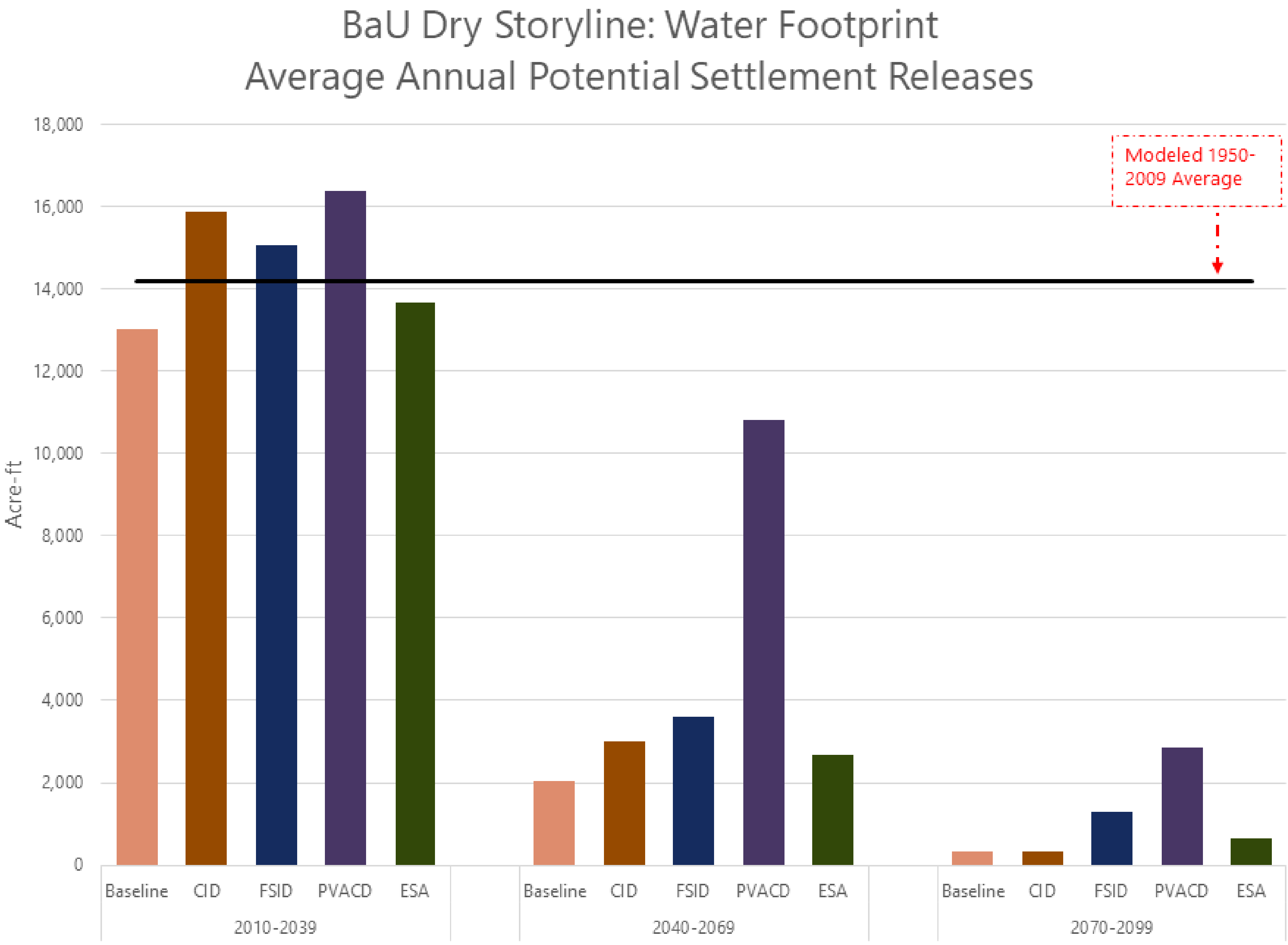

Figure 65. Average annual potential settlement releases: Water Footprints in the BaU Dry Storyline.

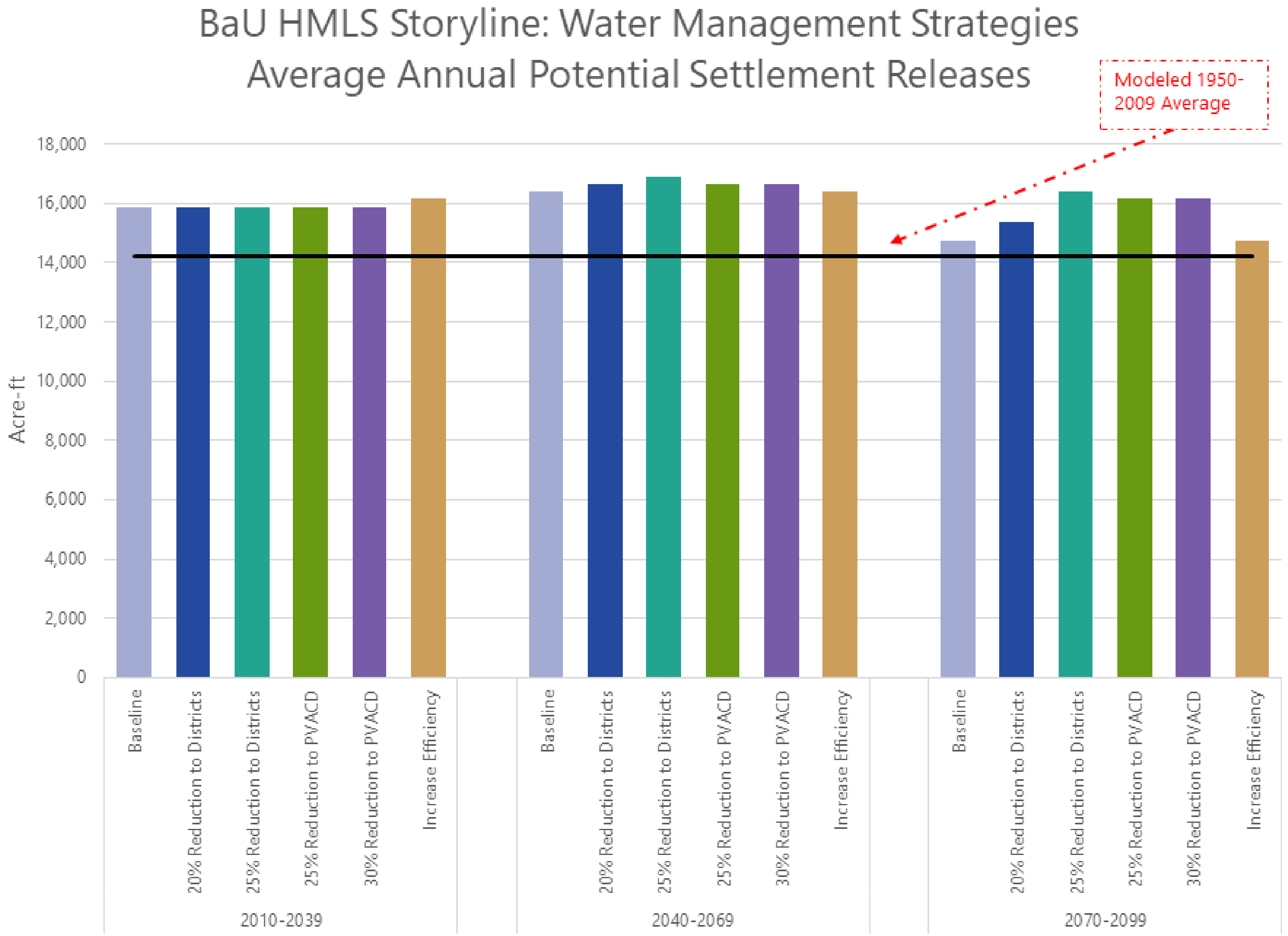

Figure 66. Average annual potential settlement releases: Water Management Strategies in the BaU HMLS Storyline.

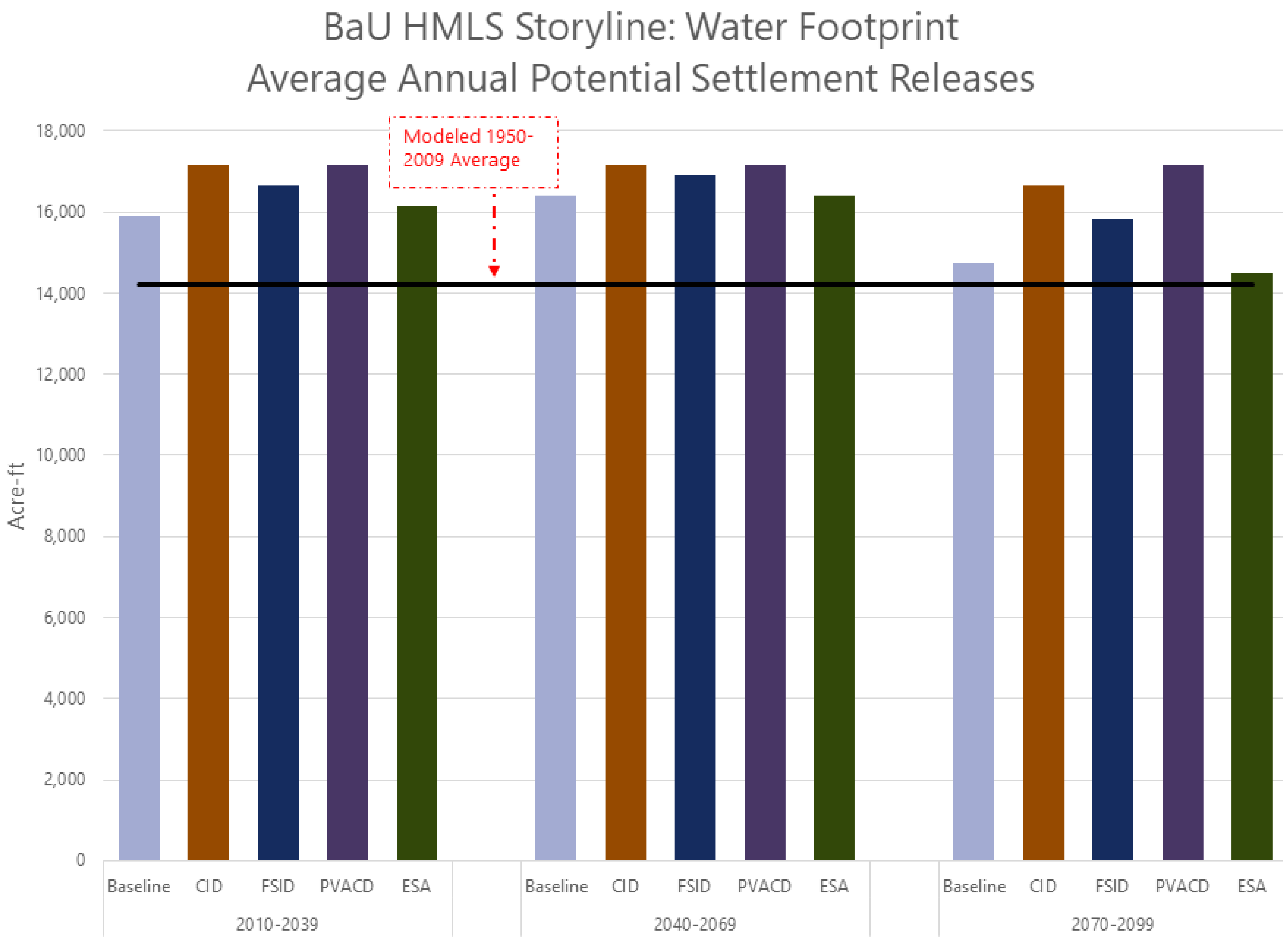

Figure 67. Average annual potential settlement releases: Water Footprint in the BaU HMLS Storyline.

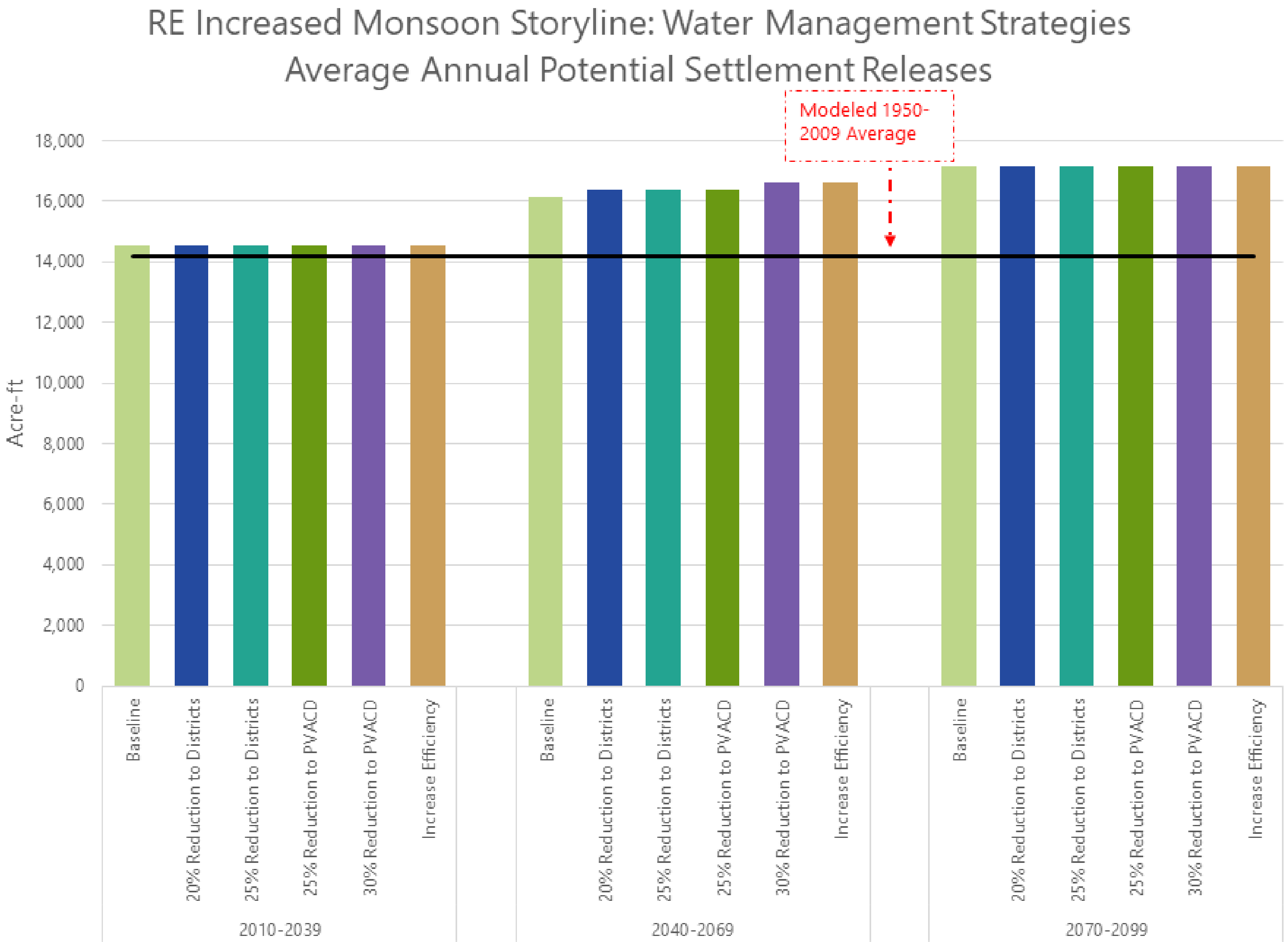

Figure 68. Average annual potential settlement releases: Water Management Strategies in the RE Increased Monsoon Storyline.

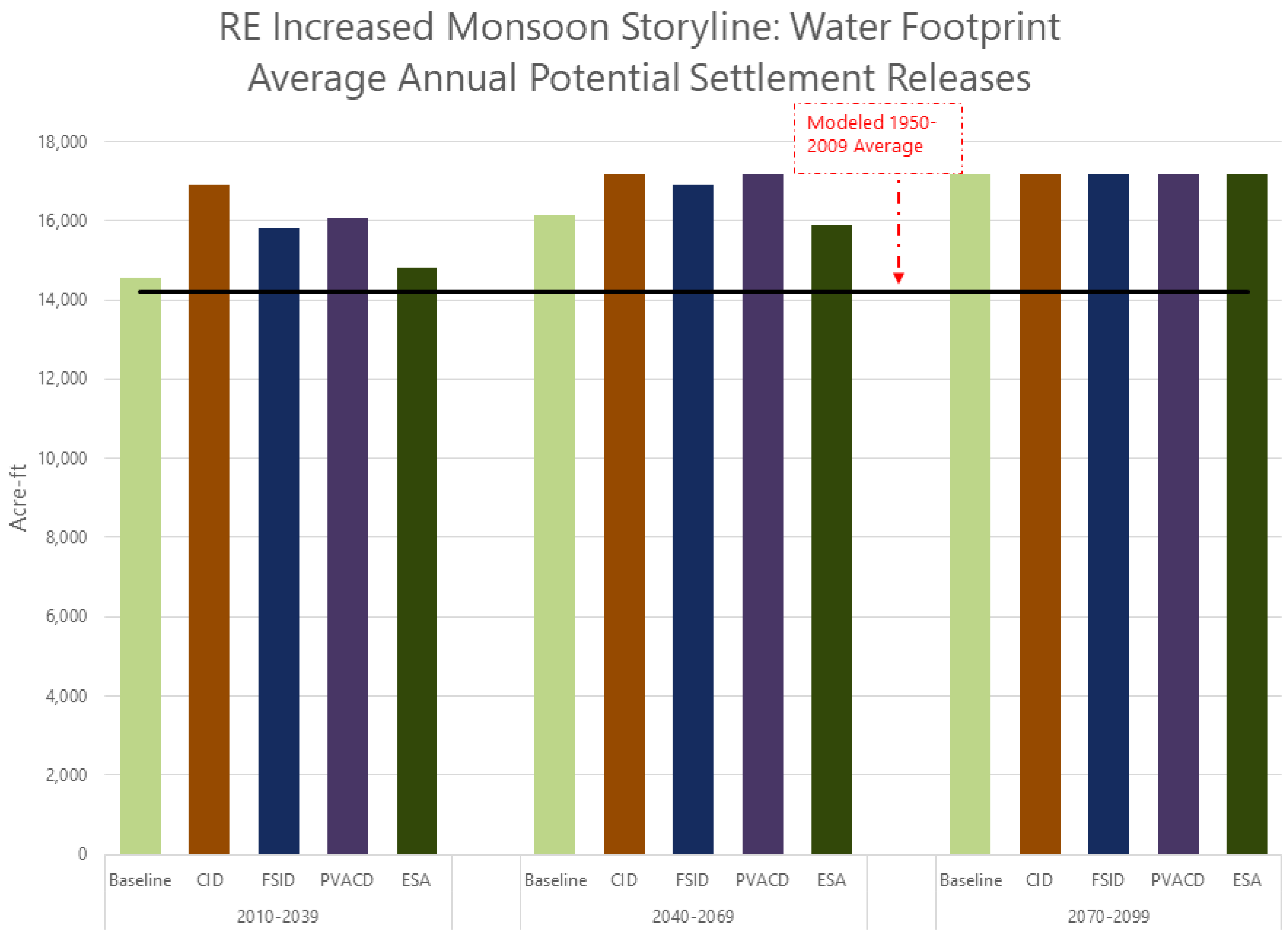

Figure 69. Average annual potential settlement releases: Water Footprint in the RE Increased Monsoon Storyline.

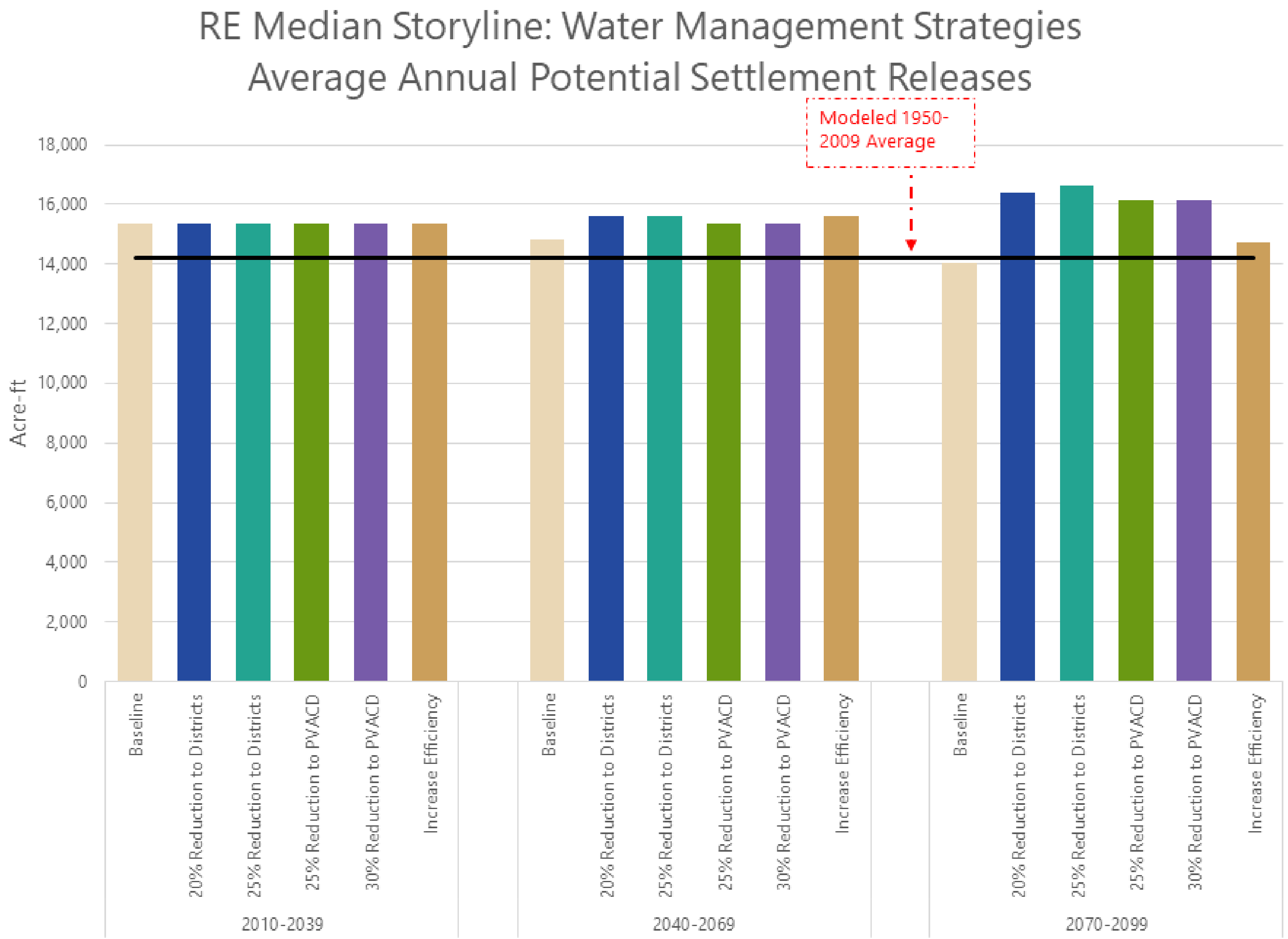

Figure 70. Average annual potential settlement releases: Water Management Strategies in the RE Median Storyline.

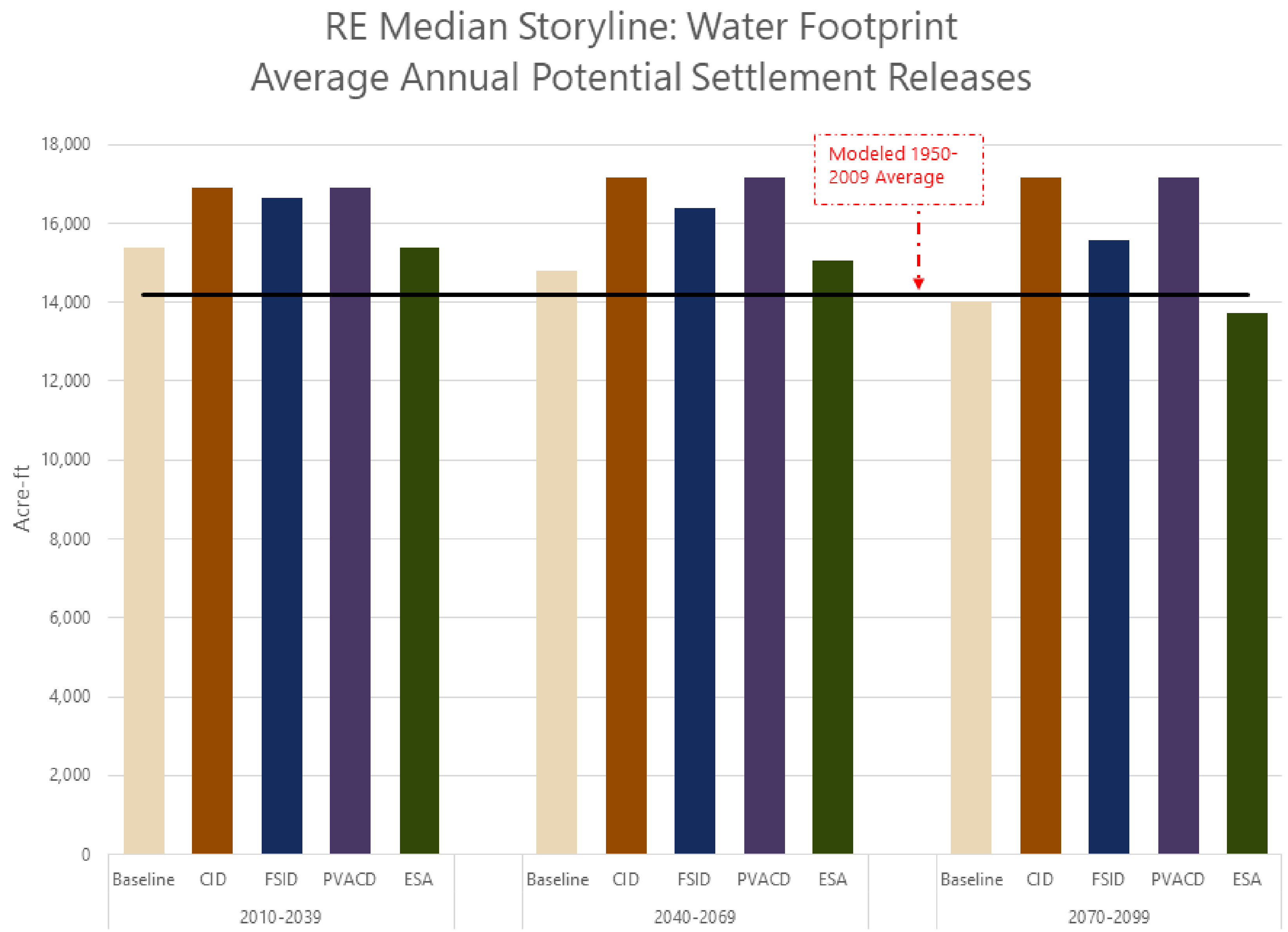

Figure 71. Average annual potential settlement releases: Water Footprint in the RE Median Storyline.

Pecos River-
New Mexico Basin
Study

Climate Appendix

Observed Climate Trends in the Pecos Basin

U.S. Army Corps of Engineers
Albuquerque District

Bureau of Reclamation
Albuquerque Area Office

July 2015

Mission Statements

The U.S. Army Corps of Engineers mission is to deliver vital public and military engineering services; partnering in peace and war to strengthen our Nation's security, energize the economy and reduce risks from disasters.

The U.S. Department of the Interior protects America's natural resources and heritage, honors our cultures and tribal communities, and supplies the energy to power our future.

The mission of the Bureau of Reclamation is to manage, develop, and protect water and related resources in an environmentally and economically sound manner in the interest of the American public.

Photo shows the Giddings Baca diversion dam on Agua Negra Creek, a tributary of the Pecos River, after being damaged by flooding in September 2013.

Acronyms and Abbreviations

cm	centimeter
COOP	Cooperative Observer Network
HCN	Historical Climatology Network 2
km	kilometer
NOAA	National Oceanic and Atmospheric Administration
SNOTEL	SNOwpack TELemetry
Tavg	average annual temperature
Tmax	maximum high temperature
Tmin	minimum temperature
USDA	U.S. Department of Agriculture
USGCRP	U.S. Global Change Research Program

Contents

I. Observed Climate Trends in the Pecos Basin 1
I.A. Pecos Basin Geography 1
I.B. Current Pecos Basin Climate 2
I.B.1. Winter Precipitation Variability... 5

I.B.2. Summer Climate Variability 5

I.B.3. Drought in the Pecos Basin.. 7

II. Data and Methodology 9
III. Observed Trends for the Period 1971 through 2012................................ 13
III.A. Temperature 13
III.B. Precipitation 13
III.C. Literature Review: Observed Southwestern Temperature Change 17
IV. Observed Temperature Trends in Regional Context............................... 21
V. Comparison of Observed Trends with Model Projections......................... 23
VI. Discussion 27
VII. References... 29

I. Observed Climate Trends in the Pecos Basin

Observed climate trends for the Pecos River Basin above Red Bluff Reservoir were analyzed to better understand current rates of climate change in the study area. Topographic diversity is a key factor as this region encompasses the headwaters of the Pecos River in the southern Sangre de Cristo Mountains of New Mexico, with peaks reaching 12,000 feet, gradually sloping to the south to Red Bluff Reservoir in Texas at an elevation of approximately 2,800 feet. Because the Pecos Basin lies east of New Mexico's central mountain chain, moisture from the Gulf of Mexico frequently enhances precipitation in the region.

I.A. Pecos Basin Geography

The Pecos River watershed is located in the states of Texas and New Mexico, in the Rocky Mountains and Great Plains physiographic region. The River has its source in the Sangre de Cristo Mountains in Mora County, New Mexico, and flows in a general southeast direction through eastern New Mexico and western Texas to its confluence with the Rio Grande at Amistad Reservoir The total area of the Pecos River watershed is 44,535 square miles. Of the total, 25,437 square miles constitutes the watershed in New Mexico above Red Bluff Reservoir: 8,160 square miles are considered noncontributing and 17,313 square miles are considered contributing.

The Pecos River Basin above Red Bluff can be divided into two parts at Sumner Dam. From its headwaters near Truchas Peak, the Pecos River flows as a typical mountain stream through narrow valleys and deeply cut gorges. This is characteristic of the main stream from approximately 160 miles from its source to Sumner Lake that comprises the upper basin. It is only in the upper basin that the Pecos River receives a perennial flow derived directly from the snow and precipitation on the mountainous watershed. The major tributaries in this portion of the basin include Cow Creek, Tecolote Creek, Canyon Blanco, the Gallinas River, Pintada Canyon, and Alamogordo Creek. The Pecos River above Sumner Lake is perennial except for short reaches between Anton Chico and Colonias.

Below Sumner Dam, the deep gorges, narrow valleys and canyon sections give way to wider valleys between low hills, and these in turn open out into broad expanses of gently rolling plains that extend southward for 130, the latter half in the gently undulating plain that constitutes the lowland portion of the Roswell artesian basin. Below the Roswell basin, narrow canyon stretches alternate with open basins (e.g., the Carlsbad basin) until Red Bluff Reservoir is reached. The major tributaries below Sumner Dam, upstream of Red Bluff Reservoir, are Salt Creek, Rio Hondo, Rio Felix, Rio Penasco, Dark Canyon, and Delaware River. The Rio Hondo is the largest tributary in this reach. Numerous tributaries, normally dry, contribute flow to the Pecos River between Roswell and Red Bluff Reservoir. The most notable is Dark Canyon near Carlsbad, New Mexico.

I.B. Current Pecos Basin Climate

The Pecos Basin has a semi-arid climate characterized by relatively dry winters and relatively wet summers. The climate is cooler and wetter at the higher elevation headwaters area, as exemplified by the Pecos Ranger Station and Las Vegas NWS Cooperative Observer (COOP) station records (Tables I-1 and I-2), becoming warmer and drier at lower elevation, downstream locations (Santa Rosa and Carlsbad COOP sites). The overall arid climate typically produces large diurnal temperature differences.

The Pecos Basin lies south of the usual winter westerly storm tracks across the western U.S., and passage of these systems is typically marked by high wind and cloudy skies, but little to no precipitation in the valleys (although precipitation over higher terrain occurs more frequently). Storms of exceptionally large size, or ones that may follow a more southerly track, are responsible for the majority of winter precipitation in the region. This precipitation typically falls as steady rain or snow at lower elevations and snow at higher elevations. In the Pecos Basin, very little snow falls outside the high terrain in the headwaters and in the mountains near Capitan, Ruidoso and Cloudcroft, west of Artesia, NM.

Because the Pecos Basin lies east of the central mountain chains, the interaction between cold, dry spring air masses to the north and warm, humid air masses originating over the Gulf of Mexico can produce relatively more spring rain than is typical in other portions of New Mexico. These convective storms are associated with large frontal systems, and may include storms with heavy rain, damaging hail, and tornados.

As temperatures warm into the summer, greater heating draws in more moisture from the Gulf of Mexico, fueling strong convective storms independent of the passage of fronts. During the July-September monsoon season, regional temperatures and precipitation peak, with more northern reaches of the basin receiving as much as 8 inches of precipitation during this three month period on average. Interannual precipitation variability is typical, ranging in some years from virtually no monsoon precipitation to years in which precipitation may be significantly above average. As with winter precipitation, summer precipitation is greatest in the higher elevation, upstream areas and is typically lower in the lower elevation, downstream reaches.

Table I-1 Temperature Data, Average Monthly Maximum and Minimum, and Annual Mean Temperature (°F)

Month	**Pecos Ranger Station, NM (6,900 ft)**		**Las Vegas, NM (6,877 ft)**		**Santa Rosa, NM (4,600 ft)**		**Carlsbad, NM (3120 ft)**	
	Ave. Max.	**Ave. Min.**	**Ave. Max.**	**Ave. Min.**	**Ave. Max.**	**Ave. Min.**	**Ave. Max.**	**Ave. Min.**
January	47.2	14.9	48.1	16.3	53.3	24.8	58.6	27.9
February	49.9	19.1	50.4	19.9	58.1	27.5	64.1	31.9
March	54.9	23.2	55.5	24.9	64.6	32.6	70.8	37.7
April	63.5	30	63.3	32.2	73.4	40.5	79.9	46.5
May	73.2	38.1	71.2	40.6	81.5	49.3	87.6	55.5
June	82.7	47.1	81.5	48.9	90.3	58	95.1	63.8
July	85.2	52.6	84.1	53.5	91.9	62.7	95.8	67.1
August	82	51.3	82.3	52.1	89.9	61.2	94.4	66
September	77	44.2	76.5	45.6	84.3	53.9	88.2	59.3
October	67.3	33.6	68.1	35.1	74.8	42.6	79.2	48
November	55	23	56.8	23.4	62.4	31.9	67	35.5
December	48.7	16.4	50.4	18.3	54.3	25.8	59.2	28.8
Annual Mean	65.6	32.8	65.7	34.2	73.2	42.6	78.3	47.3
Record	1916 – 2006		1914 – 1983		1914 – 2005		1914-2006	
Data was obtained from the Western Regional Climate Center (http://www.wrcc.dri.edu/summary/climsmnm.html)								

Table I-2 Precipitation Data, Total Monthly and Annual Mean, Average Maximum and Average Minimum (inches)

Month	Pecos Ranger Station, NM (6,900 ft)			Las Vegas, NM (6,877 ft)			Santa Rosa, NM (4,600 ft)			Carlsbad, NM (3120 ft)		
	Monthly Averages			Monthly Averages			Monthly Averages			Monthly Averages		
	Max	Min	Mean	Max	Min	Mean	Max	Min	Mean	Max	Min	Mean
January	3.58	0.0	0.74	3.24	0.0	0.52	2.67	0.0	0.40	2.31	0	0.41
February	2.13	0.0	0.66	2.83	0.0	0.47	2.59	0.0	0.44	2.26	0	0.44
March	3.31	0.0	0.88	4.07	0.0	0.80	3.75	0.0	0.66	4.39	0	0.46
April	4.23	0.0	0.83	3.62	0.0	0.88	4.20	0.0	0.83	5.04	0	0.64
May	4.55	0.0	1.07	5.38	0.0	1.79	7.25	0.0	1.58	12.28	0	1.3
June	4.09	0.57	1.26	6.73	0.06	1.68	5.51	0.0	1.61	6.24	0	1.39
July	5.96	1.19	2.88	7.66	0.21	3.01	5.35	0.0	2.35	7.48	0	1.61
August	7.06	0.0	3.38	11.60	0.21	3.06	8.64	0.0	2.64	7.7	0.01	1.81
September	5.03	0.0	1.73	8.03	0.0	2.08	6.74	0.0	1.66	12.27	0	2.15
October	5.29	0.0	1.18	4.57	0.0	1.12	5.68	0.0	1.28	6.13	0	1.4
November	3.75	0.0	0.75	4.55	0.0	0.62	3.80	0.0	0.53	4.58	0	0.56
December	1.94	0.0	0.68	2.13	0.0	0.51	4.13	0.0	0.60	3.79	0	0.5
Annual Mean	25.34	9.82	16.5	32.29	6.29	16.53	34.97	6.63	14.57	33.94	2.95	12.59
Record	1916 – 2006			1914 – 1983			1914 – 2005			1914-2006		
Data was obtained from the Western Regional Climate Center (http://www.wrcc.dri.edu/summary/climsmnm.html)												

Although uncommon, tropical cyclone remnants may enter the Pecos Basin as decaying storms, or moisture from storms decaying elsewhere in the eastern Pacific or Gulf of Mexico can be drawn into the region. When this moisture is entrained in monsoonal flows, or encounters a front passing through the region, significant rain and flooding may occur.

I.B.1. Winter Precipitation Variability

Winter precipitation varies from year to year, depending primarily on the Pacific Ocean sea surface temperature. Areas of the ocean with warm sea surface temperatures add a great deal of heat (energy) and moisture to overlying air masses, creating larger storms with greater precipitation potential. Areas with cool sea surface temperatures fail to heat the air much and produce small, weak storms with low or no precipitation potential. Ocean temperatures in areas that matter for Southwestern climate—eastern Pacific, Gulf of Mexico—vary in temperature from year to year, with direct consequences for climate in the Upper Rio Grande.

The most important source of variation is the El Niño-Southern Oscillation (ENSO) cycle, characterized by the shift in warm surface waters between the eastern and western Pacific, and an associated shift in atmospheric pressure. During El Niño years, eastern Pacific sea surface temperatures warm significantly and allow the overlying air mass to warm and hold more moisture. In addition, the winter westerly flow shifts southward, with storms that follow this more southerly tracking bringing precipitation to the Southwest. Storms following this more southerly track can tap into the unusually warm, moist air masses over the eastern Pacific, resulting in greater winter precipitation across the Southwest. During La Niña years, lower-than-average sea surface temperatures in the eastern Pacific act to reduce regional moisture supplies, and the storm track is shifted away from the Southwest, resulting in drier-than-average winter conditions across the Southwest. Although ENSO primarily affects winter precipitation, in some El Niño years precipitation in other seasons is also enhanced.

The frequency of El Niño and La Niña events may have increased since the 1970s. Before 1970, El Niño and La Niña events occurred in roughly equal frequencies, and were separated by several normal (ENSO-neutral) years. Since the late 1970s, the frequency of El Niño and La Niña events has increased, El Niño events have outnumbered La Niña events by 2:1, the number of "normal" years separating the two have decreased, and El Niño events have increased in strength. The reasons for these changes are poorly understood. They may relate to other large-scale climate phenomena, including long-cycle changes in sea surface temperatures in the north Pacific which operate on multi-decadal (50 to 80 year) cycles, and which can serve to amplify or dampen the different phases of the ENSO cycle. Since the 1970s, Central Pacific El Niño events have become more common, in which the warm pool occurs in the central rather than eastern Pacific. During Central Pacific El Niño events, precipitation in the U.S. is reduced relative to Eastern Pacific El Niño events, leading to winter precipitation in the Upper Rio Grande that is at or only slightly above normal (Jin-Yi and Yuhao 2013).

Since 1990, five of the last seven El Niño events have been Central Pacific El Niño events.

The strength of El Niño and La Niña are also affected by the interplay of long- and short-term climate cycles. Long-term wet and dry cycles in the Southwest are controlled primarily by Pacific sea surface temperatures (SST), particularly the multi-decadal Pacific Decadal Oscillation (PDO), and Atlantic sea surface temperatures via the Atlantic Multidecadal Oscillation (AMO). The phase of the PDO in particular acts to amplify and dampen portions of the ENSO cycle. The negative (cool) phase of the PDO enhances La Niña effects and dampens the increase in precipitation during El Niño events, while the reverse is true under during positive PDO cycles. Historically, the driest periods in the Southwest were associated with cool Pacific sea surface temperatures (negative PDO) and warm Atlantic sea surface temperatures (positive AMO) (McCabe et al. 2004).

I.B.2. Summer Climate Variability

The North American Monsoon is driven by daytime heating of the land surface that, in turn, warms the lower atmosphere leading to atmospheric convection. The rising air cools and, if moisture is present, can lead to precipitation. The monsoon is initiated in mid-summer when surface heating is strong enough over a large enough area to draw in moisture from the Gulf of Mexico and, secondarily, the eastern Pacific/ Gulf of California. The monsoon onset is time-transgressive, beginning mid-June in areas in the southern part of the Southwest, and in mid-July in areas in the north.

Monsoon strength increases with elevation, in direct proportion to the amount of increase in daytime air mass rise. All things being equal, higher elevation areas will receive greater, and more consistent, monsoonal precipitation, with many high mountain areas experiencing daily downpours. Lower elevation areas will tend to see less midday precipitation but more evening precipitation, and there will be greater day-to-day and place-to-place variation in precipitation.

The strength of the monsoon varies greatly from year to year for reasons that are not well understood. The strength of the monsoon appears to depend on 1) how hot the Southwest gets (how much heat is available to drive air convection); 2) how warm the sea surface temperatures are the eastern Pacific and Gulf of Mexico, which serve as the principal sources for moist air and therefore determine the amount of moisture in air masses being pulled into the Southwest ; and, 3) how active the cyclone/hurricane season is in the eastern Pacific and Gulf of Mexico, which can push tremendous amounts of moisture into the Southwest during the late summer and early fall. Monsoon strength is also affected by sea surface temperatures at the hemispheric scale that govern large-scale movements of air masses at different latitudes.

NAM is associated with a subtropical ridge that shifts poleward during the summer months over the northwestern Mexican plateau and southwestern United States. ENSO conditions influence the strength and path of the subtropical ridge: under El Niño (La Niña) conditions, a weaker (stronger) southward (northward) displacement of this ridge occurs (Castro et al. 2001). A strong relationship also exists between ENSO and the frequency of Atlantic hurricanes, with El Niño (La Niña) correlated with a decrease (increase) in activity (Pielke and Landsea 1999).

Monsoon precipitation is typically intense but localized, and rarely has a uniform effect across a large drainage basin area, such as the Pecos Basin. However, precipitation can be more widespread if the monsoon is able to tap moisture from a tropical cyclone in the moisture source regions.

I.B.3. Drought in the Pecos Basin

Drought is a regular occurrence in the Pecos Basin. In the period 1895-2012, there were five major droughts (South Central Climate Science Center 2013; South Central Climate Science Center. 2013. Drought History for the Southeastern Plains of New Mexico). Although the region was in drought during the Dust Bowl years, the 1930s drought was most severe and intense in Oklahoma and eastern Colorado. T Peak dryness occurred from 1950 through 1956 when average annual precipitation remained below the long term average (Swetnam and Betancourt 1998, Sheppard et al. 2002, Gutzler 2003).

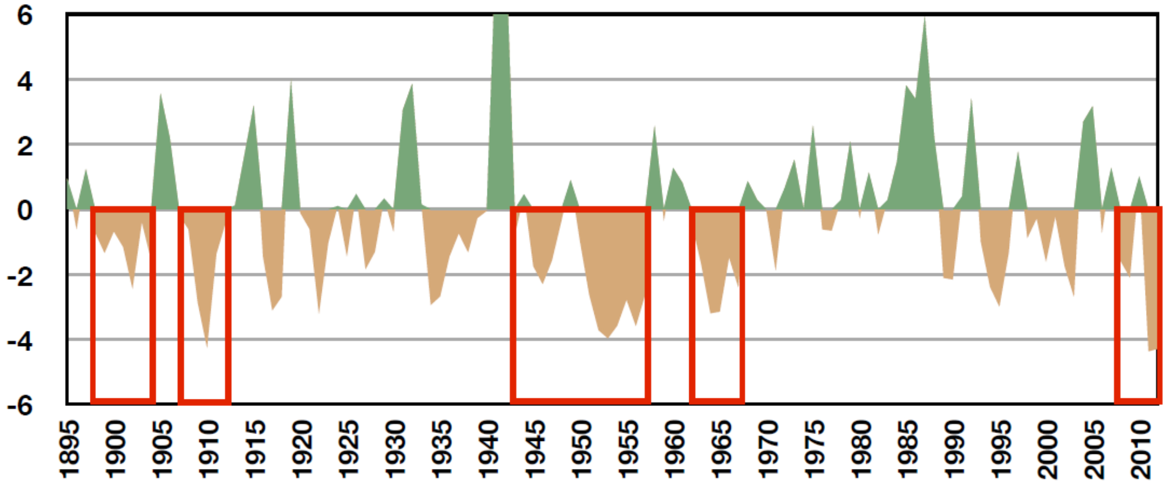

Figure 1 Palmer Drought Severity Index for the Southeastern Plains of New Mexico from 1895 to 2012 (South Central Climate Science Center 2013)

II. Data and Methodology

Twenty two (22) NOAA National Weather Service Cooperative Observer Network (COOP) sites provided the bulk of the data from lower elevation settings. COOP sites are located to collect agriculturally-relevant climate data. Data are collected on a voluntary basis. COOP data at most sites contain recording gaps, notably during World War I, the Great Depression, and World War II. Consequently, although data exist prior to 1950, it is mainly discontinuous. The data collected since 1950 are more complete, and therefore the year 1950 is taken as the earliest reliable date for most COOP site data in the study area. Monthly average values for temperature and precipitation were obtained from the National Climate Data Center (NOAA National Climate Data Center 2013). The period of record for COOP sites in this study is January 1971 through December 2012.

Mountain climates are complex and vary over short distances due to aspect and relief, which influence temperature and precipitation via cold air drainage, down and up-canyon winds, variation in the duration of direct vs. indirect insolation, vegetation cover, duration of snow cover, and other factors (Beniston 2006, Barry 2008). Changes at individual stations may differ from regional climate trends (Pepin et al. 2005) in ways that are strongly influenced by landscape position, topography and elevation (Lundquist and Cayan 2007). Valley floors may lag behind regional warming trends, particularly in winter months, due to the increasing frequency and severity of temperature inversions under more stable, anticyclonic conditions (Daly et al. 2010), which are anticipated to become more common in the southwestern United States (Seth et al. 2011).

Because of these complexities, additional data processing was not undertaken: some locations in each data set exhibited trends counter to the remainder of the sites, and these data may reflect real—but local—climate differences. They may also reflect changes to station equipment, setup and location, and National Climate Data Center data are corrected for many of these factors.

Because the distribution of monthly means is skewed, trends are assessed nonparametrically using the Regional Kendall Test (Helsel and Frans 2006). For this analysis, the Regional Kendall Test yields the annual trend (Thiel-Sen’s slope) and statistical significance of the trend by physiographic unit. All analyses are conducted using the RKT package in R (an open-source statistical software) (Marchetto 2012). Statistical significance was evaluated at the 0.1 (90% confidence) level. Annual trends are computed as the median of the monthly trends.

Table II-1 COOP Sites Used in this Study (keyed to Figure I-X)

No.	Station	Station Name	Elev. (m)	Latitude	Longitude	Use*
1	USC00290600	ARTESIA 6 S NM US	1026	32.7547	-104.384	TP
2	USC00290992	BITTER LAKES WL REF NM US	1117	33.4594	-104.404	TP
3	USC00291440	CAPITAN NM US	1975	33.5311	-105.595	P
4	USW00093033	CARLSBAD CAVERN CITY AIRPORT NM US	985	32.3375	-104.263	TP
5	USC00291480	CARLSBAD CAVERNS NM US	1352	32.1783	-104.443	TP
6	USC00291469	CARLSBAD NM US	951	32.3478	-104.223	TP
7	USC00291918	CLINES CORNERS 7 SE NM US	2110	34.9319	-105.587	P
8	USC00292510	DILIA NM US	1570	35.1841	-105.057	TP
9	USC00292865	ELK NM US	1809	32.916	-105.338	TP
10	USC00293296	FORT SUMNER 5 S NM US	1234	34.3942	-104.25	P
11	USC00293294	FORT SUMNER NM US	1227	34.4667	-104.232	TP
12	USC00293586	GLORIETA NM US	2292	35.5816	-105.773	P
13	USC00294112	HOPE NM US	1247	32.8111	-104.734	P
14	USC00294175	HOUSE NM US	1471	34.6344	-103.89	P
15	USW00023054	LAS VEGAS MUNICIPAL AIRPORT NM US	2095	35.6542	-105.142	TP
16	USC00296676	PECOS NATIONAL MONUMENT NM US	2096	35.5488	-105.689	TP
17	USC00296804	PICACHO NM US	1521	33.3503	-105.14	TP
18	USW00023009	ROSWELL INDUSTRIAL AIR PARK NM US	1112	33.3075	-104.508	TP
19	USC00297649	RUIDOSO NM US	2112	33.3589	-105.665	TP
20	USC00298107	SANTA ROSA NM US	1405	34.9358	-104.681	TP
21	USC00298596	SUMNER LAKE NM US	1313	34.6033	-104.381	TP
22	USC00299851	YESO 2 S NM US	1478	34.4031	-104.613	P

**TP = Station temperature and precipitation data were both used in this study; P=Only station precipitation data was used in this study (typically because temperature data was not available).*

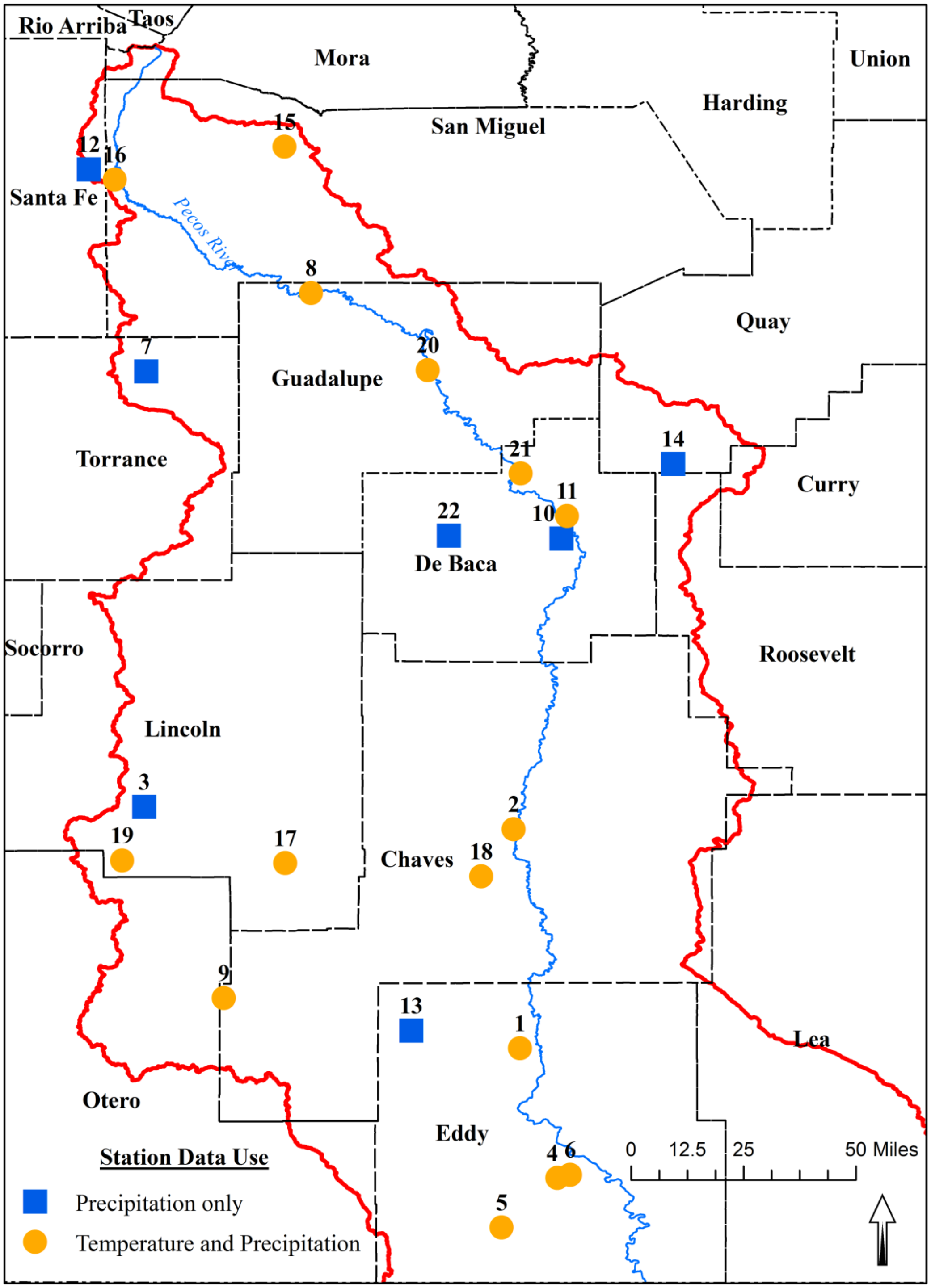

Figure 2.—Map Showing Sites Used in this Study (Site Numbers Keyed to Table II-1).

III. Observed Trends for the Period 1971 through 2012

Despite the noise in the data introduced by measurement changes, errors, instrumentation, changes in station microclimate due to movement and wildfire, and other problems, a coherent regional picture of temperature and precipitation emerges when the data are aggregated for the Pecos Basin above Red Bluff Reservoir.

III.A. Temperature

Over the period 1971-2013, temperatures have risen significantly[1] in the Pecos Basin in all months except December (Table III-1). The rate of increase has been greatest in January and in late spring and summer. Mean monthly maximum (daytime) temperatures are rising at approximately double the rate of mean monthly minimum (nighttime) temperatures. In June, July and August, there has been a significant increase in the hottest days (with temperatures in excess of 90°F). Extreme temperatures also exhibit a significant increasing trend in most months.

Over the course of the year, average temperatures are increasing at an average rate of 0.57°F/decade, mean monthly minimum temperatures are increasing at a rate of 0.42°F/decade, and mean monthly maximum temperatures are rising at a rate of 0.72°F/decade.

III.B. Precipitation

Precipitation exhibited a small but statistically-significant downward trend in 8 of 12 months, and a comparably small increasing trend in March and December. The largest decreasing trends are in August (-0.263 in/decade) and September (-0.165 in/decade), and coincide with significant decreasing trends in the days with trace precipitation (days with >0.1 inch of precipitation), but not in the number of days with >0.5 in precipitation). There is no detectable change in the frequency of large precipitation events (days with precipitation >0.5 or 1.0 in).

---

[1] Tables III-1 and III-2 denote statistically significant changes. Statistical significance takes into account the magnitude of the change and the amount of normal variation in that month. If there’s typically a wide range of temperatures in a month, then a large change may not be identified as “significant,” whereas the same-size change might be statistically significant in a month where the range of variation is small.

Table III-1.—Trend in Average Monthly Temperature (Tavg) in °F/Decade for 1971 Through 2012*

Variable	Jan	Feb	Mar	Apr	May	Jun	Jul	Aug	Sept	Oct	Nov	Dec
Mean monthly minimum temperature (1 F units)	0.5760	0.3600	0.3600	0.4966	0.5539	0.6858	0.4500	0.6750	0.3913	0.1636	0.2160	0.1125
Mean monthly maximum temperature (1 F units)	1.1129	0.3001	0.8307	0.8249	0.9000	0.9529	0.3406	0.9360	0.9486	0.5539	0.9529	0.0000
Mean monthly temperature (1 F units)	0.9000	0.3600	0.6260	0.5999	0.7715	0.8307	0.3913	0.8181	0.6428	0.3001	0.5625	0.0643
Cooling degree days (1 F units)	0.0000	0.0000	0.0000	0.0000	6.8000	17.0527	11.3999	19.2119	4.6364	0.0000	0.0000	0.0000
Heating degree days (1 F units)	-30.0001	-11.1600	-20.7391	-13.8946	-5.5125	0.0000	0.0000	0.0000	-7.2000	-7.6000	-17.8490	-3.9089
Days minimum temperature <00.0F	0.0000	0.0000	0.0000	0.0000	0.0000	0.0000	0.0000	0.0000	0.0000	0.0000	0.0000	0.0000
Days minimum temperature < 32.0F	0.0000	0.0000	0.0000	0.0000	0.0000	0.0000	0.0000	0.0000	0.0000	0.0000	-0.2860	0.0000
Days maximum temperature >90.0F	0.0000	0.0000	0.0000	0.0000	0.0000	0.9520	0.3120	0.7690	0.0000	0.0000	0.0000	0.0000
Days maximum temperature >32.0F	0.0000	0.0000	0.0000	0.0000	0.0000	0.0000	0.0000	0.0000	0.0000	0.0000	0.0000	0.0000
Extreme maximum temperature (1 F units)	0.3334	0.0000	1.2857	0.5323	1.2375	0.6352	0.0000	0.6352	0.4738	0.5143	0.7474	0.0000
Extreme minimum temperature (1 F units)	2.1600	1.2375	0.0000	0.7072	0.5294	0.9000	0.5400	0.5625	0.5625	0.0000	0.0000	0.0000

**Warm tones indicate statistically-significant positive trends; grey tones indicate statistically-significant negative trends.*

Table III-2.—Trend in Precipitation (Inches/Year) by Region for 1971 Through 2012

Variable	Jan	Feb	Mar	Apr	May	Jun	Jul	Aug	Sept	Oct	Nov	Dec
Precipitation (in)	-0.041	-0.017	0.021	-0.033	-0.128	-0.056	-0.017	-0.263	-0.165	-0.028	-0.079	0.021
Total snow fall (in)	0.000	0.000	0.000	0.000	0.000	0.000	0.000	0.000	0.000	0.000	0.000	0.000
Extreme maximum daily precipitation (in)	-0.027	-0.010	0.009	-0.018	-0.062	-0.024	0.005	-0.065	-0.033	-0.013	-0.046	0.012
Maximum snow depth (in)	0.000	0.000	0.000	0.000	0.000	0.000	0.000	0.000	0.000	0.000	0.000	0.000
Number of days with >1.0 in precipitation	0.000	0.000	0.000	0.000	0.000	0.000	0.000	0.000	0.000	0.000	0.000	0.000
Number of days with >0.5 in precipitation	0.000	0.000	0.000	0.000	0.000	0.000	0.000	0.000	0.000	0.000	0.000	0.000
Number of days with >0.1 in precipitation	0.000	0.000	0.000	0.000	0.000	0.000	0.000	-0.476	-0.323	0.000	0.000	0.000

**Tan tones indicate statistically-significant positive trends; blue tones indicate statistically-significant negative trends.*

Table III-3 Upper Rio Grande Impact Study Observed Temperature Trends

Region	Jan	Feb	Mar	Apr	May	Jun	Jul	Aug	Sep	Oct	Nov	Dec	Annual °F/decade
All Mountain Sites	***1.350***	***0.000***	***0.900***	***0.648***	***0.792***	***0.702***	***0.666***	***0.594***	***0.666***	***0.360***	***1.386***	***0.540***	***0.666***
All Valley Sites	***0.900***	***0.216***	***0.540***	***0.648***	***0.900***	***0.594***	***0.558***	***0.702***	***0.576***	***0.252***	***0.594***	***0.000***	***0.594***
Region (All Sites)	***1.044***	***0.126***	***0.648***	***0.648***	***0.900***	***0.612***	***0.594***	***0.666***	***0.594***	***0.270***	***0.774***	***0.198***	***0.630***

III.C. Literature Review: Observed Southwestern Temperature Change

Recent overviews of climate change in the Southwestern United States (SWUS) have been provided in (Garfin et al. 2013), U.S. Global Change Research Program (USGCRP) (2013), and NOAA (2013). Important syntheses of climate change impacts to New Mexico and Colorado include New Mexico Office of the State Engineer (2006) and Ray et al. (2008). There are no Pecos Basin-specific syntheses currently available. Temperature changes are assumed to be broadly similar between the Pecos Basin above Red Bluff Reservoir and the Rio Grande from the Colorado border to Elephant Butte Dam, given the similarity in latitudinal extent and elevation between the two adjacent streams.

III.C.1.1 Global, National and Western U.S. Temperature Trends

Globally, 2014 was the warmest year on record, with global temperatures averaging 1.4°F (0.8°C) warmer than 1880 (NASA 2015).

Temperatures in the Western U.S. have shown a relatively steady rise beginning in the early 20th Century. The rise stalled during the middle part of the century during the post-war economic boom as increasing atmospheric pollution reduced the amount of sunlight entering the lower atmosphere, and then continued to rise following implementation of laws regulating environmental and atmospheric pollution. The consensus view is that recent increases in temperature in the Western U.S. exceed observations in the historic record beginning in the late 19th Century (USGCRP 2009). In the mountainous West, average annual temperatures for 2001-2009 were 1.4°F (0.8°C) higher relative to the average for 1895-2000 (MacDonald 2010). Temperature increases were greater in areas to the south and at lower elevation.

Particularly notable are increases in winter (January, February, March, or JFM) temperatures throughout the mountainous West. The observational record of 1950-1999 shows an increase in maximum average JFM temperatures of 2.8°F (1.53°C) and an increase in minimum average JFM temperatures of 3°F (1.72°C) (Bonfils et al. 2008). Rising winter temperatures have contributed to a contraction of 8 days in the number of days below freezing, and a corresponding lengthening of the frost-free period. Detection and attribution modeling studies indicate that these patterns cannot be replicated in models of natural climate forcing (models that exclude human greenhouse gas emissions but include the effects of ENSO, Pacific Decadal Oscillation, solar variation and changes in volcanic aerosol concentrations), but are robustly replicated in models that also include human greenhouse gas emissions (Bonfils et al. 2008).

III.C.1.2 Southwestern U.S. and Upper Rio Grande Temperature Trends

In the Southwestern U.S. as a whole, encompassing New Mexico, Colorado, Arizona, Utah, Nevada, and California, the decade 2001-2010 was the warmest of all decades from

1901-2010, with temperatures increasing approximately 1.6°F±0.5°F (0.9°C±0.3°C) over the period 1901-2010 (Hoerling et al. 2013). Rising temperatures increased the frequency of heat waves, reduced the frequency of cold waves, and contributed to the expansion of the growing season by 17 days (7%) during 2001-2010 compared to the average season length for the 20th Century. The period since 1950 in the Southwest has been warmer than any comparable period in at least 600 years, according to paleoclimate records (Hoerling et al. 2013).

At the regional level, several recent studies have examined trends in temperature. Tebaldi et al. (2012) use low elevation National Weather Service Cooperative Observer Program (COOP) station data and corrected climate data from the NOAA Historical Climatology Network (HCN) to estimate that average annual temperatures in New Mexico rose at an average rate of 0.219°F (0.10°C) per decade from 1912 to 2011 but at the faster rate of 0.678°F (0.34°C) per decade since 1970. The same pattern of faster recent warming was also observed in annual average daytime maximum high temperature (Tmax) and annual average nighttime minimum temperature (Tmin).

In the Upper Rio Grande Basin, a comparison of average monthly temperatures over the 1995-2004 period with average monthly temperatures for the period 1961-2000 showed increases of 3-4°F (1.5-2.5°C) in winter, with increases in the April through November period less than approximately 2.0°F (1.1°C) in all months but May (Saunders and Maxwell 2005). The increase in average annual temperatures between 2001 and 2009 was 1.5 to 2 standard deviations above the 20th Century average in the Rio Grande valley in New Mexico (see Figure 1, MacDonald 2010).

Rates of warming in high elevation areas may be considerably greater than the regional average. In a recent analysis of National Weather Service and SNOTEL site data in the San Juan Mountains, Rangwala and Miller (2010) detect a rate of warming of 1.8°F (1°C) per decade from 1990 to 2005. Elevation plays an important role in determining the season of greatest warming in the mountains. Lower elevation sites experienced greatest warming during the winter months, warming in winter at an average rate of 2.7°F (1.5°C) per decade. Higher elevation sites experienced their greatest warming during the summer months, with temperatures increasing at a rate of 2.7°F (1.5°C) per decade during this season. The differences in the season of greatest warming are due to the cooling effects on air temperatures of snow on the ground. Increases in winter minimum temperatures increased faster than winter maximum temperatures at lower elevations, while summer maximum temperatures rose faster than summer minimum temperatures at higher elevations.

A temperature trend analysis comparable to this study was conducted as part of the Upper Rio Grande Impact Assessment (U.S. Bureau of Reclamation (Reclamation) 2013). This study employed a mix of data from COOP and National Resources Conservation Service SNOTEL (snow telemetry) sites. The sites were analyzed for the region as a whole, and differences between mountain and valley sites discussed. For the entire Upper Rio Grande study area, temperatures increased substantially over the four decade period 1971 through 2012. Average annual temperatures increased at a rate of 0.63°F (0.35°C) per decade, with a faster increase in nighttime minimum temperature (Tmin) of 0.67°F (0.37°C) per decade offset by a slower increase in daytime high temperature (Tmax) of 0.45°F (0.25°C) per decade. Precipitation was unchanged at the regional scale. Temperature changes were significant in most months for the region as a whole.

Mountain and valley regions analyzed for the Upper Rio Grande Impact Assessment (U.S. Bureau of Reclamation (Reclamation) 2013) responded differently to warming. Mountain average annual temperatures increased at a rate of 0.67°F (0.37°C) per decade over the period 1971 through 2012. This change was driven by increases in nighttime minimum temperatures (Tmin) of 1.21°F (0.67°C) per decade that were significant in every month but February. Daytime high temperatures (Tmax) rose at the slow rate of 0.25°F (0.14°C) decade, and this trend was not significant in most areas. By contrast, valley Tavg temperatures increased at a rate of 0.39°F (0.33°C) per decade over the period 1971 through 2012, driven by both increases in Tmax (0.61°F [0.34°C] per decade) and Tmin (0.50°F [0.28°C] per decade). At valley sites, increases in May through September temperatures were statistically significant, increasing at a rate of 0.54 to 0.90°F (0.3 to 0.5°C) per decade in these months.

III.C.1.3 Pecos Basin Studies

Only one study has addressed recent trends in Pecos Basin temperature and precipitation incidental to studies of changing regional hydrology. Hall et al. (2006) investigated changes in temperature, precipitation and streamflow in the Rio Grande and Pecos River Basins for the period 1960-2000 using temperature records from 35 COOP stations, precipitation records from 63 COOP stations, and hydrometric records from 15 Hydro-Climatic Data Network stations. Trends were determined using Mann-Kendall tests, and clustered using the pattern of significance of the monthly trends. The stations in this study demonstrate strong, coherent warming in winter (JFM) but significant divergence in the rest of the year, with some sites showing strong warming, others cooling. There was no spatial coherence between the two groups of sites within the Pecos Basin or regionally. One group of 4 Pecos Basin sites showed strong, significant warming for April through September, and less warming, a less consensus on warming, for October-December. The other group of three sites showed cooler temps for April-July with less model consensus, little change in July-August, and a strong negative trend for fall (OND). Specific trend values were not specified.

IV. Observed Temperature Trends in Regional Context

Temperature rises observed in this study are comparable to those observed in the regional studies discussed above (Table IV-1), particularly the 0.68°F/decade observed by Tebaldi et al. (2012) for New Mexico as a whole over the 41 year period 1970-2011.

Table IV-1 Regional temperature increases in the historic record

Area	Comparison	Temperature Change	Source
Western U.S.	2001-2009 vs. 1895-2000	Average annual temperature: 1.4°F	MacDonald 2010
Western U.S.	1950-1999	JFM temperature increase of 2.8-3.0°F	Bonfils et al. 2008
Southwest U.S.	2001-2010 vs. 1901-2010	Average annual temperature: 1.6°F±0.5°F	Hoerling et al. 2013
New Mexico	1912-2011 1970-2011	0.22°F / decade 0.68°F / decade	Tebaldi et al. 2012
Upper Rio Grande Basin	1971-2012	Average annual temperature: 0.63°F / decade	Reclamation et al. 2013
Upper Rio Grande Basin	1995-2004 vs. 1961-2000	3-4°F Winter 2.0°F April-November	Saunders and Maxwell 2005

The rate of observed warming is similar in magnitude between the Pecos Basin and the Upper Rio Grande Basin, with similar patterns of rise and fall among the months. In both basins, December has warmed relatively little, and the change is not statistically-significant. The slowest rates of mean monthly temperature increases in the Pecos Basin occur in February and October, a pattern also seen the Upper Rio Grande where temperature trends in these two months are both small and not statistically-significant.

V. Comparison of Observed Trends with Model Projections

Comparison of observed trends with model projections provides a means of assessing the significance of current rates of change, should they continue, with respect to responses of the natural environment. Observed trends in annual average temperature are compared to trends projected by models for areas encompassing the Upper Rio Grande (Table IV-1) in New Mexico, as there are no comparable studies for the Pecos Basin. The table homogenizes information on observed and modeled projected changes, either by estimating a rate of change (°F/decade) based on period-change projects, or using a projected trend to estimate a period change from the year 2000. Comparisons are meant to be illustrative rather than definitive.

The rates of future change in stream flow and vegetation models depend on the rates of change in the climate model(s) driving them. In other words, projections of vegetation and stream flow change for particular decades make critical assumptions about the rate of future change in temperature and precipitation. In short, vegetation and streamflow display a given sensitivity[2] to a given amount of temperature and precipitation change—changing faster if under faster climate change and slower under slower rates of climate change. Thus, it is important to understand how fast climate is actually changing relative to climate model projections to better understand the likely rates of resulting environmental change.

If temperatures in the Pecos Basin continue to rise at current rates, average warming for the period 2010 through 2039 would be 1.40°F; net warming by 2050 would approach 2.85°F. Observed rates of change in the Pecos Basin, if multiplied out, are at the low end of model estimates for the period 2020-2039 for a net average warming of 1.68°F compared to a range of future

---

[2] The amount of response to a stimulus of a given magnitude – in this case, a 1°C temperature change is anticipated in a particular model to result in so much change in evaporation, soil moisture, plant growth, etc.

Table V-1.—Observed Rates of Change and Net Warming vs. Model Projections in °F (converted from original units, reatlive to the year 2000)

Area	Source	Tavg Change (°F/decade)	Tavg Change 2010-2039 (°F)	Tavg Change 2020-2039 (°F)	Tavg Change 2041-2070 (°F)	Tavg Change 2050 (°F)	Notes
Model Projections (SRES scenario)							
Rio Grande Basin (A1B)	Hurd and Coonrod (2007)	--	--	4.23	--	--	Dry model, baseline 1971-2000
Rio Grande Basin (A1B)	Hurd and Coonrod (2007)	--	--	2.29	--	--	Medium model, baseline 1971-2000
Rio Grande Basin (A1B)	Hurd and Coonrod (2007)	--	--	4.16	--	--	Wet model, baseline 1971-2000
New Mexico (A1B)	Gutzler et al. (2006)	0.54	1.35	1.62	2.97	--	At least 3°C by 2100 ≈0.30C/decade
Observed Trends							
New Mexico and Colorado	Tebaldi et al. (2012)	0.22	0.52	0.63	1.21	1.08	Average of rates for NM and CO HCN sites, 1912-2011.
New Mexico and Colorado	Tebaldi et al. (2012)	0.56	1.37	1.64	3.10	2.79	Average of rates for NM and CO HCN sites, 1970-2011.
San Juan Mountains	Rangwala and Miller 2010	0.81	1.98	2.40	4.50	4.05	Average of rates for NWS sites, 1976-2005.
Upper Rio Grande	Reclamation et al. 2013	0.63	1.55	1.85	3.50	3.15	Across all HCN, COOP and SNOTEL sites, 1971-2012.
Pecos Basin*	This study	0.57	1.40	1.68	3.16	2.85	This study

**Average temperatures are increasing at an average rate of 0.57°F/decade, mean monthly minimum temperatures are increasing at a rate of 0.42°F/decade, and mean monthly maximum temperatures are rising at a rate of 0.72°F/decade.*

The observed regional trend is in line with the most recent North American Regional Climate Change Assessment Program model projections used in the 2013 National Climate Assessment (U.S. Global Change Research Program [USGCRP] 2013). These models project that the Upper Rio Grande area will warm by 4.1 to 4.9°C (7.5 to 8.5°F) by 2070 through 2099 under the A2 (high emissions) scenario and by 2.5 to 3.1°C (4.5 to 5.5°F) by 2070 through 2099 under the B1 (low emissions) scenario.

VI. Discussion

The observed trends in temperature indicate warming is occurring at the middle end of model projections. However, whether the true average regional rate of change is 0.35°C (0.63°F)/decade, or higher as some models project, warming of 1 to 2.5°C (1.8 to 4.5°F) by 2040 is likely to exert profound changes on every part of the landscape and is likely to cause significant changes to the availability and quality of surface and ground water in the region. Warming in early spring and late fall contributes to an expansion of the growing season and, therefore, greater transpiration demand and more demand for soil moisture. Declines in soil moisture are likely to contribute to altered fire regimes and changes in vegetation communities, changes that are likely to alter existing rainfall-runoff relationships. Concomitant changes to flood frequency curves and other relationships are likely, with increases in both the frequency of low flow and highest flow years. The current rate of warming exceeds the rate of warming at the end of the last Ice Age (15,000 years ago), and, as during that time, the changes are widely expected to contribute to both species and habitat loss on both global and local scales.

Although mitigation measures may yet reduce net warming by 2100, significant reductions in anticipated warming by 2030 or 2040 are much less likely as much of the warming that will occur in this time frame will be due to greenhouse gases already in the atmosphere. Thus, adaptation will likely be necessary to address climate changes in a region that is likely to be 1 to 2.5°C (1.8 to 4.5°F) warmer by 2040.

VII. References

Barry, R. G. 2008. Mountain Weather and Climate. Cambridge University Press, Cambridge, United Kingdom.

Beniston, M. 2006. Mountain weather and climate: a general overview and a focus on climatic change in the Alps. Hydrobiologia **562**:3-16.

Bonfils, C., B. D. Santer, D. W. Pierce, H. G. Hidalgo, G. Bala, T. Das, T. P. Barnett, D. R. Cayan, C. Doutriaux, A. W. Wood, A. Mirin, and T. Nozawa. 2008. Detection and attribution of temperature changes in the mountainous western United States. Journal of Climate **21**:6404-6424.

Castro, C. L., T. B. McKee, and R. A. Pielke. 2001. The Relationship of the North American Monsoon to Tropical and North Pacific Sea Surface Temperatures as Revealed by Observational Analyses. Journal of Climate **14**:4449-4473.

Daly, C., D. R. Conklin, and M. H. Unsworth. 2010. Local atmospheric decoupling in complex topography alters climate change impacts. International Journal of Climatology **30**:1857-1864.

Garfin, G., A. Jardine, R. Merideth, M. Black, and S. LeRoy, editors. 2013. Assessment of Climate Change in the Southwest United States: A Report Prepared for the National Climate Assessment. A report by the Southwest Climate Alliance. Island Press, Washington, D.C.

Gutzler, D. S. 2003. Drought in New Mexico: history, causes and future prospects. Pages 101-105 *in* P. S. Johnson, L. A. Land, L. G. Price, and F. Titus, editors. Water Resources of the Lower Pecos Region, New Mexico—Science, Policy, and a Look to the Future Decision-Makers Field Guide New Mexico Bureau of Geology and Mineral Resources, Socorro, New Mexico.

Hall, A. W., P. H. Whitfield, and A. J. Cannon. 2006. Recent Variations in Temperature, Precipitation, and Streamflow in the Rio Grande and Pecos River Basins of New Mexico and Colorado. Reviews in Fisheries Science **14**:51-78.

Helsel, D. R., and L. M. Frans. 2006. The regional Kendall test for trend. Environmental Science and Technology **40**:4066-4073.

Hoerling, M. P., M. D. Dettinger, K. Wolter, J. Lukas, J. Eischeid, R. Nemani, B. Liebmann, and K. E. Kunkel. 2013. Present weather and climate: evolving conditions. Pages 74-100 *in* G. Garfin, A. Jardine, R. Merideth, M. Black, and S. LeRoy, editors. Assessment of Climate Change in the Southwest United States: A Report Prepared for the National Climate Assessment. NCA Regional Input Reports. Island Press, A report by the Southwest Climate Alliance. Washington, D.C.

Jin-Yi, Y., and Z. Yuhao. 2013. The enhanced drying effect of Central-Pacific El Niño on US winter. Environmental Research Letters **8**:014019.

Lundquist, J. D., and D. R. Cayan. 2007. Surface temperature patterns in complex terrain: Daily variations and long-term change in the central Sierra Nevada, California. J. Geophys. Res. **112**:D11124.

MacDonald, G. M. 2010. Water, climate change, and sustainability in the southwest. Proceedings of the National Academy of Sciences of the United States of America **107**:21256-21262.

Marchetto, A. 2012. Package 'rkt': Mann-Kendall test, seasonal and regional Kendall tests. R-project. Online at http://cran.r-project.org/web/packages/rkt/index.html, Accessed March 11, 2013.

McCabe, G. J., M. A. Palecki, and J. L. Betancourt. 2004. Pacific and Atlantic Ocean influence on multidecadal drought frequency in the United States. Proceedings of the National Academy of Sciences of the United States of America **101**:4136-4141.

NASA. 2015. NASA, NOAA find 2014 warmest year in modern record. Press Release 15-010 (16 January 2015).

New Mexico Office of the State Engineer, editor. 2006. The impact of climate change on New Mexico's water supply and ability to manage water resources. New Mexico Office of the State Engineer/Interstate Stream Commission, Santa Fe., New Mexico.

NOAA. 2013. Regional climate trends and scenarios for the U.S. National Climate Assessment: Part 5. Climate of the Southwest U.S., U.S. Department of Commerce, National Oceanic and Atmospheric Administration, Washington, D.C.

NOAA National Climate Data Center. 2013. Climate Data Online. Online at http://www.ncdc.noaa.gov/cdo-web/search;jsessionid=B1442CA4064331E19DB7BF2A05517AC5.lwf1, Accessed April 1 and 2, 2013.

Pepin, N. C., M. Losleben, M. Hartman, and K. Chowanski. 2005. A comparison of SNOTEL and GHCN/CRU surface temperatures with free-air temperatures at high elevations in the western United States: data compatibility and trends. Journal of Climate **18**:1967-1985.

Pielke, R. A., and C. N. Landsea. 1999. La Niña, El Niño and Atlantic Hurricane Damages in the United States. Bulletin of the American Meteorological Society **80**:2027-2033.

Rangwala, I., and J. R. Miller. 2010. Twentieth century temperature trends in Colorado's San Juan Mountains. Arctic Antarctic and Alpine Research **42**:89-97.

Ray, A. J., J. J. Barsugli, K. B. Averyt, K. Wolter, M. Moerling, N. Doesken, B. Udall, and R. S. Webb. 2008. Climate change in Colorado: a synthesis to support water resources management and adaptation. A report for the Colorado Water Conservation Board, Boulder, Colorado.

Saunders, S., and M. Maxwell. 2005. Less snow, less water: climate disruption in the West. Rocky Mountain Climate Organization (RMCO), Louisville, CO.

Seth, A., S. A. Rauscher, M. Rojas, A. Giannini, and S. J. Camargo. 2011. Enhanced spring convective barrier for monsoons in a warmer world? Climatic Change **104**:403-414.

Sheppard, P. R., A. C. Comrie, G. D. Packin, K. Angersbach, and M. K. Hughes. 2002. The climate of the US Southwest. Climate Research **21**:219-238.

Swetnam, T. W., and J. L. Betancourt. 1998. Mesoscale disturbance and ecological response to decadal climatic variability in the American Southwest. Journal of Climate **11**:3128-3147.

Tebaldi, C., D. Adams-Smith, and N. Heller. 2012. The Heat is On: U.S. Temperature Trends. Page 17. Climate Central, Palo Alto, California.

U.S. Bureau of Reclamation (Reclamation), U.S. Army Corps of Engineers (USACE) and Sandia National Laboratories (Sandia),. 2013. West-Wide Climate Risk Assessment: Upper Rio Grande Impact Assessment. U.S. Bureau of Reclamation, Upper Colorado Region, Albuquerque Area Office (December 2013), Albuquerque, NM.

U.S. Global Change Research Program (USGCRP). 2013. Draft Third National Climate Assessment Report.

Pecos River-
New Mexico Basin Study

Environmental and Recreational Appendix

Acronyms

ACEC	Areas of Environmental Concern
BLM	Bureau of Land Management
BLNWR	Bitter Lake National Wildlife Refuge
IUCN	International Union for Conservation of Nature
NMDGF	New Mexico Department of Game and Fish
OHV	off-highway vehicle
RNA	Research Natural Area
USFS	U.S. Forest Service
USFWS	U.S. Fish and Wildlife Service
WSA	Wilderness Study Areas

Contents

1.Listed Species **1**
1.1. Birds 1
1.1.1.Interior Least Tern *1*
1.1.2.Southwestern Willow Flycatcher. *1*
1.2. Reptiles 1
1.2.1.Western River Cooter *1*
1.3. Fish 5
1.3.1.Gray Redhorse *2*
1.3.2.Pecos Gambusia *2*
1.3.3.Pecos Bluntnose Shiner *2*
1.3.4.Pecos Pupfish *2*
1.3.5.Greenthroat Darter *2*
1.3.6.Bigscale Logperch *3*
1.4. Crustaceans 3
1.4.1.Noel's Amphipod *3*
1.5. Mollusks 3
1.5.1.Texas Hornshell *3*
1.5.2.Koster's Springsnail *4*
1.5.3.Roswell Springsnail *4*
1.5.4.Pecos Assiminea *4*
1.5.5.Pecos Springsnail *4*
2.Environmentally Protected Areas **5**
2.1. Wildernesses and Wilderness Study Areas 5
2.2. Other Protected Areas 6
3.Recreation **7**
4.References 9

1. Listed Species

1.1. Birds

1.1.1. Interior Least Tern

Least terns are the smallest members of the subfamily Sterninae and family Laridae of the order Charadriiformes. The least tern is recognized as a distinct species of tern, and the interior least tern as a subspecies, based on studies of vocalizations and behavior, but genetic analysis has not validated the subspecies. Interior least tern were first reported from the Rio Grande drainage (including the Pecos River) in 1949, occupying salt flats on Bitter Lake National Wildlife Refuge (BLNWR), adjacent to the Pecos. From 1987 through 2006 numbers of Interior least terns on BLNWR increased, then stabilized to around 5 nests per year through 2016. In the Rio Grande basin, interior least terns are known to nest only on reservoirs, and there are no data to demonstrate historical occupation of natural riverine habitat. It is possible that the Rio Grande is outside of the historical range of the species, and that reservoir construction provided an opportunity for range expansion into the basin. Interior least terns generally nest on the ground, in open areas, and near appropriate feeding habitat. Vegetation-free sand or gravel islands are preferred for nesting, although, sand banks, point bars, and beaches may also be used.

Flooding was historically, and remains, a primary cause of interior least tern nest failure in both unregulated and regulated river channels (U.S. Fish and Wildlife Service [USFWS] 2017 [2016 BO]).

1.1.2.Southwestern Willow Flycatcher

The southwestern willow flycatcher *(Empidonax traillii extimus*), a willow flycatcher subspecies, is a small insectivorous migrant bird of the tyrant flycatcher family. The USFWS listed the southwestern willow flycatcher as endangered in 1995; the New Mexico Department of Game and Fish (NMDGF) listed the flycatcher as threatened in 1988 and reclassified it as endangered in 1996. The bird breeds primarily in New Mexico, Arizona, and southern California, including small populations in the Pecos River Basin. It nests in riparian areas with dense vegetation. The flycatcher has been threatened by diverting and pumping water—altering, fragmenting, and destroying its habitat; grazing livestock, which inhibits vegetation growth; and efforts to remove non-native vegetation, particularly tamarisk. (NMDGF 2016, p. 37).

1.2. Reptiles

1.2.1. Western River Cooter

The western river cooter (*Pseudemys gorzugi*) is a large primarily herbivorous turtle. The turtle's range is limited to isolated areas in New Mexico, Texas, and northern Mexico. In New Mexico it is confined to the Pecos River below Brantley Dam, the Black River, the Delaware River, and Rocky Arroyo. The turtle is threatened by habitat loss and degradation, recreational hunters who use it for target practice and fishermen who use it for bait, wildfires, and pollution runoff from oil and gas wells.

1.3. Fish

Drought in 2012 dried the Pecos River and eliminated permanent water, from about 0.5 kilometers (0.3 miles) of upper critical habitat.

1.3.1. Gray Redhorse

The gray redhorse (*Moxostoma congestum*) is a freshwater sucker of the family catostomidae. It is a host to the larval stage of the Texas hornshell (discussed below). The NMDGF listed the gray redhorse as threatened in 1976 and reclassified as endangered in 2008. The range of this fish is limited to streams in New Mexico, Texas, and Mexico. In New Mexico, it inhabits the lower Rio Grande, the Pecos River below Roswell, and the Black River. It is threatened by habitat fragmentation due to dams, modification of stream flow patterns, and outbreaks of golden algae which has drastically diminished its population in the Pecos River. (NMDGF 2016, pp. 101-102).

1.3.2. Pecos Gambusia

The Pecos gambusia (*Gambusia nobilis*) is a small, about 2 inch (5 cm) long, omnivorous freshwater fish of the Poeciliidae family. The USFWS listed the Pecos gambusia as endangered in 1970, and the NMDGF did so in 1975. The fish is endemic to springs in the Pecos River Basin in southeast New Mexico and Texas. Primary threats to the gambusia are depletion of groundwater, habitat modification by livestock grazing, and predation by non-native species. (NMDGF 2016, pp. 102-103).

1.3.3. Pecos Bluntnose Shiner

The Pecos bluntnose shiner (*Notropis simus pecosensis*) is a small freshwater minnow of the family cyprinidae. The USFWS listed the Pecos bluntnose shiner as threatened in 1987. The NMDGF listed the shiner as threatened in 1986 and as endangered in 2006. USFWS adopted a recovery plan for the shiner in 1992. The shiner formerly inhabited the Pecos River from near the city of Santa Rosa downstream to near the city of Carlsbad. Currently its range has decreased from near the town of Fort Sumner to the Brantley Reservoir. Major threats to the shiner are block releases from reservoirs during summer spawning season, which carries eggs and larvae into unsuitable habitat, reduced river flow at other times, habitat degradation and fragmentation, and pollution from agricultural runoff. (NMDGF 2016, pp. 104-106).

1.3.4. Pecos Pupfish

The Pecos pupfish (*Cyprinodon pecosensis*) is a small, about 2-inch (5 cm) long omnivorous freshwater fish of the Cyprinodontidae family. NMDGF listed the pupfish in 1988. It ranges on the Pecos River and its floodplain from Bitter Lake National Wildlife Refuge to the Texas state line, although it is now confined to lakes in the Pecos River Basin. The primary threat to the pupfish is displacement by the non-native sheephead minnow. Golden algae blooms are also a threat. (NMDGF 2016, pp. 109-111).

1.3.5. Greenthroat Darter

The greenthroat darter (*Etheostoma lepidum*) is a small, about 1 to 1.5-inch (3 centimeters) long omnivorous fish in the perch family. The NMDGF listed the greenthroat darter as threatened in 1975. The darter lives in the lower Pecos River watershed, as well as in a disjointed habitat on the Edwards Plateau in south-central Texas. In New Mexico. It is now primarily confined to portions of the BLNWR and two springs on the Black River: Blue Spring and Rattlesnake Spring. Pumping groundwater and diverting spring surface flow are the primary threats to the darter (NMDGF 2016, p. 113).

1.3.6. Bigscale Logperch

The bigscale logperch (*Percina macrolepida*) is a 3 to 4-inch (8-10 cm) darter, also in the perch family. The NMDGF listed the bigscale logperch as threatened in 1975. The habitat for the logperch includes coastal streams in Texas, the Red River in Texas and Oklahoma, and the Pecos River. In New Mexico its range is now limited to the Pecos River between the cities of Santa Rosa and Fort Sumner, the Pecos River near the city of Carlsbad, and the Black River. The fish prefer fast-flowing, non-turbulent moderately deep water with a large cobble substrate. Major threats to the logperch are reduced river flow, diversions, which reduce flow velocity, and degradation of water quality (NMDGF 2016, pp. 113-114).

1.4. Crustaceans

1.4.1. Noel’s Amphipod

Noel’s amphipod (*Gammarus desperatus*) is a medium-sized detritivorous – meaning it feeds on decaying plant and animal matter – amphipod, a shrimp-like crustacean. NMDGF listed Noel’s amphipod, which was identified as a separate species only in 1979 (Cole 1981) and reclassified it as endangered in 1990. The USFWS listed the amphipod as endangered in 2006. Its habitat is limited to the BLNWR and adjacent private land and, historically, to two springs near the city of Roswell, although it was extirpated from the two springs by 1988.Threats to the *desperatus* amphipod – a name that suggested its precarious situation even at the time of its discovery – are mostly from groundwater pumping and surface water diversions, which have altered its habitat, as well as from pollution and wildfires. (NMDGF 2016, pp. 115-116).

1.5. Mollusks

1.5.1. Texas Hornshell

The Texas hornshell (*Popenaias popeii*) is a freshwater mussel. The NMDGF listed the Texas hornshell as endangered in 1983, and as endangered in 2018 (USFWS 2016). The Texas hornshell was once prevalent on the Pecos River from North Spring River near the city of Roswell to the confluence of the Pecos River and the Rio Grande, on the Black River and Delaware River, and on the Rio Grande from its confluence with the Pecos River to the Gulf of Mexico, and in several Texas and Mexican tributaries to the Rio Grande (USFWS 2017). It is now confined to isolated locations on the Black River in New Mexico, the Rio Grande downstream of Big Bend National Park in Texas, the Devil’s River, a Texas tributary to the Rio Grande, and a stretch of the Rio Grande near the city of Laredo, Texas (USFWS 2016).

Hornshells habituate seams of fine sediment in crevices, undercut riverbanks, travertine shelves, and large boulders in riverine ecosystems with flowing water (USFS 2016). Hornshells also require the presence of river fish, as hornshell larvae, or glochidia, attach to fish as parasites (USFS, 2016). Threats to the hornshell include excessive sedimentation, caused by reduced river flows; impairment of water quality due to agricultural and urban runoff, and pollution from oil and gas operations and associated vehicular traffic; reduction in flowing water, due to diversions and management of dams; and barriers to the movement of fish that serve as hosts to the hornshell glochidia (USFWS, 2016 and NMDGF 2016).

1.5.2. Koster's Springsnail

Koster’s springsnail (*Juturnia kosteri*) is a miniature snail about the size of a pencil eraser, which feeds on algae, bacteria, and decaying organic matter. The NMDGF listed Koster's springsnail (*Juturnia kosteri*) as threatened in 1983 and reclassified it as endangered in 2000; the USFWS listed the snail as endangered in 2005. The snail is endemic to the Pecos River Basin, with habitat in and around BLNWR. The primary threat to the snail and its habitat is pumping groundwater for irrigation, municipal water supplies, and oil and gas operations (NMDGF, 2016, pp. 124-125).

1.5.3. Roswell Springsnail

The Roswell springsnail (*Pyrgulopsis roswellensis*) is another miniature snail. The NMDGF listed the Roswell springsnail as endangered in 1983, and the USFWS did so in 2005. This snail is also endemic to the Pecos River Basin, with its current habitat in the Bitter Lake National Wildlife Refuge, and a spring, North Spring, near the city of Roswell. Again, pumping of groundwater for irrigation, municipal water supplies, and oil and gas operations is the primary threat to this snail. (NMDGF, 2016, pp. 131-132).

1.5.4. Pecos Assiminea

The Pecos assiminae (*Assiminea pecos*) is an amphibious snail. The NMDGF listed the Pecos assiminea as endangered in 1983, and the USFWS listed the snail as endangered in 2005. The snail’s habitat is localized along the Pecos River and in sporadic locations in Texas and Mexico. Its habitat in New Mexico is limited to the Bitter Lake National Wildlife Refuge and North Spring near the city of Roswell. As with the other endangered New Mexico snails, the primary threat to its survival is groundwater pumping for irrigation, municipal water supplies, and oil and gas operations (NMDGF, 2016, pp. 134-136).

1.5.5. Pecos Springsnail

The Pecos springsnail (*Pyrgulopsis pecosensis*) is another small snail. The NMDGF listed the Pecos springsnail as threatened in 1983. The snail is endemic to two perennial tributaries to the Black River, Blue Spring and Castle Spring. Again, groundwater withdrawal for irrigation and oil and gas operations presents the primary risk to this snail (NMDGF, 2016, pp. 144-146).

2. Environmentally Protected Areas

2.1. Wildernesses and Wilderness Study Areas

The Pecos Basin contains five units of the U.S. Wilderness Preservation System. Wilderness areas permit only non-mechanized recreation and are generally managed for both ecological and recreational functions.

The Pecos Wilderness protects nearly 100,000 acres of the headwaters of the Pecos River in the southern Sangre de Cristo Mountains. The wilderness preserves ecosystems of ponderosa pine forest, subalpine spruce-fir forests, and alpine tundra. The high peaks of the wilderness remain snowbound until late spring or early summer, and the wilderness and surrounding mountains provide snowmelt runoff that is critical to the water supply of downstream communities. The wilderness also supports diverse wildlife, including one of America's healthiest herds of Rocky Mountain Bighorn Sheep (U.S. Forest Service [USFS] 2019).

The 35,000-acre Capitan Mountains Wilderness, part of Lincoln National Forest, encompasses most of the small Capitan Range, west of Roswell. The wilderness preserves pinyon-juniper, ponderosa, and subalpine spruce-fir forests on the slopes of the range. The wilderness is famous for being the location where Smokey Bear, the mascot for the US Forest Service, was rescued from a devastating fire.

The nearby White Mountain Wilderness, also in Lincoln National Forest, encompasses the northern portion of the Sierra Blanca Range and features terrain and vegetation similar to that in the Capitan Mountains Wilderness. Roughly 18,000 acres protect the headwaters of the Rio Bonito. Snowmelt and rainfall in the wilderness and surrounding forest of the Sierra Blancas and the neighboring Sacramento Range provides a steady source of water for the Roswell Artesian Basin.

The Salt Creek Wilderness protects 9,600 acres of riparian wetlands, native grassland and shrubland, as well as several large sinkholes. The wilderness is part of the nearly 27,000 acre BLNWR, whose extensive wetlands provides winter habitat for migratory waterfowl. The refuge provides habitat for many threatened and endangered species, including the least shrew, Noel's amphipod, least tern, Pecos sunflower, and Roswell spring snail (USFWS 2018)

Carlsbad Caverns National Park protects the numerous caves of the northeastern Guadalupe Mountains, include the centerpiece Carlsbad Caverns and the pristine Lechuguilla Cave. The Carlsbad Caverns Wilderness makes up about 70% of the roughly 47,000 acre park.

Wilderness Study Areas (WSA) are areas that have been identified by federal agencies as candidates for wilderness designation but have not yet been designated by congress. WSAs are generally managed similarly to wildernesses, despite the lack of formal designation. There are four wilderness study areas in the Pecos Basin. The 360-acre Mathers WSA, one of the smallest WSAs nationwide, is managed by the Bureau of Land Management (BLM) for the protection of the lesser prairie chicken. Three other WSAs, Mudgetts (BLM), Lonesome Ridge (BLM), and Guadalupe Escarpment (WSA), collectively protect about 27,500 acres of the Guadalupe Mountains, connecting the existing Carlsbad Caverns Wilderness to the Guadalupe Mountains Wilderness across the Texas border.

2.2. Other Protected Areas

One of the most highly protected area in the basin is the 600-acre Mesita de los Ladrones Research Natural Area (RNA) in the Santa Fe National Forest near the small community of Tecolotito. Research Natural Areas represent relatively pristine examples of native ecosystems and are used for scientific and educational purposes. They are similar to wildernesses, but recreational use is generally discouraged, and managing agencies generally do not construct trails or other amenities within them. The Mesita de los Ladrones RNA serves as an excellent example of a relatively undisturbed juniper savannah, a rarity in New Mexico, as this type of ecosystem has generally been historically grazed.

Pecos National Historical Park mainly exists to protect the historic Pecos Pueblo and nearby Glorieta Battlefield, its 6,700 acres protect pinyon-juniper forest and savannah, as well as 3 miles of the Pecos River.

Las Vegas National Wildlife Refuge protects almost 8,700 acres of wetlands and prairies southeast of the town of Las Vegas, serving as a major refuge for migratory waterfowl.

The first 20.5 miles of the Pecos River, from its source to the townsite of Terrero, is designated as a The Pecos Wild and Scenic River. Wild and Scenic River designations protect rivers from shoreline development and ensure they remain undammed.

Four small parcels of NMDGF land in the near the easternmost edge of the basin protect mixed-grass prairie and shinnery oak scrubland used as habitat by the lesser prairie chicken. This land makes up about 2,600 acres of the almost 22,000-acre NMDGF Prairie Chicken Wildlife Areas, most of which are located further east.

The William S. Huey Wildlife Area is also managed by the NMDGF and protects about 3,000 acres of riparian wetlands and floodplain along the Pecos River near the town of Artesia

The roughly 25,000-acre Fort Stanton – Snowy River Cave Natural Conservation Area, managed by BLM, protects Ft. Stanton Cave, the second longest cave in New Mexico, as well as the historic Ft. Stanton. Ft. Stanton Cave features the Snowy River formation, a 11-mile long streambed of brilliant white calcite that is the nation’s longest cave formation.

BLM designates certain lands as Areas of Environmental Concern (ACEC). Management of these lands involves restrictions on use that may vary widely depending on specific qualities of the land and the resource being protected. Not all ACECs are included in the International Union for Conservation of Nature IUCN database, but within the Pecos six ACECs are listed: Dark Canyon ACEC, Pecos River Canyons Complex ACEC, Blue Springs ACEC, Mescalero Sands ACEC (which has a separate Grazing Exclusion Area ACEC within it), and Lonesome Ridge ACEC.

3. Recreation

In the uppermost part of the basin, the Santa Fe National Forest encompasses over 400,000 acres of the headwaters of the Pecos River and the Gallinas River. At the northernmost point of the basin roughly 100,000 acres of the vast Pecos Wilderness lie within the basin. The wilderness features hundreds of miles of hiking trails and dozens of mountain lakes and streams and is popular with hikers, backpackers, horseback riders, and cross-country skiers, due to its proximity to Santa Fe and Albuquerque. Outside of the wilderness, the Santa Fe National Forest features several campgrounds and additional hiking trails, as well as opportunities for mountain biking and off-highway vehicle (OHV) use. The Pecos National Historical Park, which preserves a historic mission and pueblo near the town of Pecos, and the 21-mile long Pecos Wild and Scenic River, are also in this area.

Further downstream, the Pecos River passes through Villanueva State Park, which offers hiking, camping, horseback riding, and a launching point for canoeing/kayaking on the river. Within the watershed of the Gallinas River, the main tributary of the Pecos above Santa Rosa Reservoir, boating and camping occur at Storrie Lake State Park near Las Vegas. The Las Vegas National Wildlife Refuge preserves rare high plains wetlands. The McAllister Lake Wildlife Area is surrounded by the refuge, and provides opportunities for hiking, birding, and hunting, and fishing.

Downstream of the mountains, the Pecos River flows through Santa Rosa Reservoir and Sumner Reservoir, which are the primary recreational sites along this stretch of the river. Santa Rosa Lake State Park and Sumner Lake State Park both offer camping, boating, and fishing on their respective reservoirs, as well as short hiking trails. In the town of Santa Rosa, a series of perennial, spring-fed lakes support swimming and fishing, and in the case of the famous Blue Hole, high-altitude scuba diving. Just south of the town of Fort Sumner, the Fort Sumner State Monument and Bosque Redondo Memorial preserves the history of the Navajo internment at Fort Sumner in the 1860s.

Near Roswell, the Bitter Lake National Wildlife Refuge features wildlife viewing and hunting, as well as hiking and horseback riding in the Salt Creek Wilderness, which lies within the refuge. Further downstream, the Pecos River passes near Bottomless Lakes State Park, where another series of spring-fed lakes support swimming, diving, and fishing. Several BLM Recreation Areas in the region provide opportunities for OHV use.

North of Carlsbad, Brantley Lake State Park offers fishing, boating, and camping, and the smaller Avalon Reservoir offers boating and fishing. Near Carlsbad, the Living Desert Zoo and Gardens State Park has no connection to the river. Several city parks in Carlsbad, as well as the Carlsbad Riverwalk, flank the small Lake Carlsbad, which is popular for swimming, fishing, and boating.

South of Carlsbad, the major recreational attraction is Carlsbad Caverns National Park. While the park is not directly connected to the river, it does contain a picnic area and historic site at Rattlesnake Springs, near the headwaters of the Black River. The nearby BLM Black River Recreation Area provides fishing and a short trail. The Carlsbad Caverns Wilderness and adjacent areas of the Guadalupe Mountains also provide hiking and camping opportunities. Other attractions in this area include Sitting Bull Falls Recreation Area, a popular day use swimming and hiking area within Lincoln National Forest, and two other BLM Recreation Areas: the La Cueva Non-

Motorized Trail System along Dark Canyon Draw just outside of Carlsbad, and the Pecos River Corridor Recreation Area near the state line.

In addition to the recreational activities along and near the main river corridor, there are ample recreational activities in the Sacramento Mountains, whose streams supply the Rio Hondo, the Rio Peñasco, and the Roswell Artesian Basin. Most of the Sacramento Range, along with the neighboring Capitan and Guadalupe Ranges, is contained within Lincoln National Forest, which features extensive options for hiking, camping, and fishing. The Capitan Mountains Wilderness spans most of the smaller Capitan Range and lies within the forest. The White Mountain Wilderness also lies within the forest and encompasses the headwaters of the Rio Bonito. Fort Stanton State Monument and Lincoln State Historic Site preserve historic Fort Stanton and the town of Lincoln, both located along the banks of the Rio Bonito. Fort Stanton is surrounded by the 25,000-acre Fort Stanton-Snowy River Cave National Conservation Area, a BLM recreation area featuring hunting opportunities and a 70-plus mile trail system. The Sacramento Mountains also contain the resort town of Ruidoso and ski areas at Ski Apache and Cloudcroft. North of the Sacramento Mountains, a tiny portion of Cibola National Forest near Gallinas Peak lies in the basin and contains a few campgrounds.

Apart from these primary recreation areas, vast amounts of BLM land are available for hunting and fishing. Much of the Pecos River can be canoed or kayaked at certain times of year, though some areas are exceedingly remote and fence crossings can be potential hazards.

4. References

Cole, G.A., 1981. *Gammarus desperatus*, a new species from New Mexico (*Crustacea: Amphipoda*). Hydrobiologia, January 1981 76: 27–32.

New Mexico Department of Game and Fish (NMDGF), 2016. Threatened and Endangered Species of New Mexico, 2016 Biennial Review.

U.S. Fish and Wildlife Service (USFWS), 2016. Proposed Rule: Endangered and Threatened Wildlife and Plants; Endangered Species Status for Texas Hornshell, 51 Fed. Reg. 52,796 (Aug. 10, 2016).

USFWS, 2017 (2016 BO). Final Biological Opinion for the Carlsbad Project Water Operations and Water. Supply Conservation, 2016-2026. Consultation Number 02ENNM00-2016-F-0506. Field Supervisor, Fish and Wildlife Service, New Mexico Ecological Services Field Office (NMESFO), Albuquerque, New Mexico December 5, 2017.

USFWS, 2018. Bitter Lake National Wildlife Refuge, New Mexico. https://www.fws.gov/refuge/Bitter_Lake/map.html.

U.S. Forest Service (USFS), 2019. Pecos Wilderness. https://www.fs.usda.gov/detail/santafe/specialplaces/?cid=fsbdev7_021062. Accessed 9/28/2019.

Pecos River-
New Mexico Basin
Study

Extreme Storm
Events Appendix

Recent Trends in Warm Season Extreme Precipitation for the Pecos River Basin

Prepared by:

Maryam Pournasiri Poshtiri,
National Center for Atmospheric Research (NCAR),
Boulder, CO, pournasiri.m@gmail.com

Erin Towler,
National Center for Atmospheric Research (NCAR),
Boulder, CO,
towler@ucar.edu

Andreas F Prein,
National Center for Atmospheric Research (NCAR),
Boulder, CO,
prein@ucar.edu

Dagmar Llewellyn,
Bureau of Reclamation,
Albuquerque, NM,
dllewellyn@usbr.gov

Acknowledgements

This work was supported by the Bureau of Reclamation Science and Technology award No. 1782: “Detecting, Interpreting, and Modeling Hydrologic Extremes to Support Flexible Water Management and Planning.”

NCAR is sponsored by the National Science Foundation

1. Introduction

Although winter snowpack is the dominant water source for many river basins in the Western states, it has been suggested that potential increases in warm season precipitation, including heavy precipitation, could provide a more substantial contribution to water supply as temperatures increase and snowpack decreases. In a previous study, Pournasiri et al. (2018 WSC) examine recent trends in warm season precipitation characteristics within the state of New Mexico and southern Colorado. The study documented some increasing precipitation trends, which were mainly concentrated in the southeastern parts of New Mexico that include the Pecos basin. In this Appendix, we repeat these analyses, but only focus on this southeastern part of New Mexico. Specifically, we quantify precipitation trends, looking at the upper quantiles and extremes.

1.1. Data and Methods

The data and methods are adapted from Pournasiri et al. (2018): This study focuses on the area surrounding the Pecos basin in the state of New Mexico (Longitude: 105.75 to 103.5 W & Latitude: 32 to 36 N, and see Figure 2 at the end of this section). Daily precipitation data from PRISM Gridded Climate Data Group (prism.oregonstate.edu) is used, which can be downloaded from http://www.prism.oregonstate.edu/documents/PRISM_downloads_FTP.pdf. The 4 km daily precipitation data is processed by averaging 10 x 10 grid cells. We examine data from 1981-2017, with a focus on June through October, i.e., the warm season.

For precipitation, magnitude and frequency characteristics are both examined. For magnitude, five precipitation magnitude indicators are examined for the upper (higher value) quantiles: q50, q75, q90, q95, and q99 (i.e., the 50th percentile to the 99th percentile), as well as the average (avg) and maximum (max) values. For each magnitude indicator, a time series of the daily value for each year's warm season (or individual month) is constructed for each grid cell. For frequency, five thresholds of the upper quantiles (i.e., q50, q75, q90, q95, and q99) are considered, which are calculated over the entire precipitation record for the warm season (or individual month) in each grid cell. As such, the frequency indicators are defined as the time series of the number of days above each of the thresholds in each grid cell.

To see if there is a monotonic temporal trend in the magnitude, the nonparametric Mann-Kendall test is used (Kendall, 1975, Mann, 1945). This is undertaken for the magnitudes for each precipitation indicator at each grid cell. To see if there is any trend in the frequency of days above the threshold, Poisson regression is used, since the response variables are discrete (e.g., Dobson & Barnett, 2008, Fox, 2015). For both, trends with p-values <0.05 are considered statistically significant.

2. Results and Discussions

2.1. Trend Results

Trend results for the precipitation indicators from June through October, and each individual month, are presented in Table 1. The table summarizes the percentage of grid cells where the precipitation trends are statistically significant (p-values <0.05). For June-October, there is not a consistent trend. For example, positive trends dominate for q50, q75, and q99 for magnitude and q50 and q99 for frequency; but negative trends dominate for q75, q90, and q95 for frequency. Indicators in June and August (except for q50 indicators) mainly show drying trends, though many of the percentages are not that high. July shows increasing trends, especially for the q50 indicators (80% and 90% for magnitude and frequency indicators, respectively).

An important point is that many grid cells have a q50 of zero (i.e., more than half the days don’t receive any precipitation), so for this, the trend increase indicates an increase in the non-zero precipitation days. For July, we also see that positive (wetter) trends dominate all of the July frequency indicators. Most of September and October indicators don’t have many cells with significant trends (many indicators detect trends at less than 5% of the grid cells), with a notable exception: in September, the q99 frequency indicator shows an increasing trend at 31% of the grid cells. However, it is important to note that the majority of locations in the study area did not show any significant trends. Further, this study focuses on trends in the recent period (1981-2017), but Pournasiri Poshtiri & Pal (2016) have shown that trends are dependent on time period analyzed.

2.2. Comparing the Trend in Magnitude and Frequency Characteristics

Figure 1A-C compares the percent of grid cells with statistically significant negative trends between the magnitude and frequency quantile indicators. In June-October (Figure 1A), June (Figure 1B), and August (Figure 1C), we see that across quantiles, there is a higher percentage of grid cells with negative trends in frequency than in magnitude (i.e., the red bars are higher than the orange bars). This suggests that the trend is more detectable in the frequency of extreme precipitation rather than the magnitude, similar to results from Mallakpour & Villarini (2017).

We do see some positive trends for June-October, July, and September (Table 1), so Figure 1D-F compares the percent of grid cells with statistically significant positive trends for these three periods. In July, we see the dominant positive trend across all indicators (Figure 1E) and dominant positive trend for q50, q95, and q99 in September (Figure 1F). This shows how in recent years, the sign of the precipitation trend is sensitive to the season or month examined. In the next section, we explore the spatial patterns of the precipitation trends during June-October, July, and September.

Table 1. Percentage of grid cells with a statistically significant trend (p-values <0.05) for each precipitation indicator.
+Sig indicates a statistically significant increasing (wetter) trend, and -Sig indicates a statistically significant decreasing (drying) trend. Bold values indicate where the percentage of grid cells is greater than 5% and is also higher than that of the opposite sign.

Characteristic	Indicator	June-October		June		July		August		September		October	
		+Sig	-Sig	+Sig	-Sig	+Sig	-Sig	+Sig	-Sig	+Sig	-Sig	+Sig	-Sig
Magnitude	avg	2.86	0	0	**5.7**	**13**	0	0	**10**	0	0	0	0
	q50	**23**	0	2.9	0	**80**	0	**10**	8.6	**8.6**	0	0	0
	q75	**7.0**	1.4	0	1.4	**26**	0	0	**10**	0	0	0	0
	q90	0	0	0	2.9	**8.7**	0	0	**20**	0	1.43	0	0
	q95	1.4	1.4	0	**8.6**	**11.4**	0	0	**19**	0	0	0	0
	q99	**5.7**	1.4	0	**8.6**	4.3	0	1.4	**13**	1.4	0	0	0
	max	2.9	1.4	0	**8.6**	2.9	1.4	2.9	**11**	2.9	0	0	0
Frequency	q50	**51**	2.9	**12.9**	0	**90**	0	**17**	10	**8.6**	0	**7.1**	2.9
	q75	8.6	**11.4**	1.4	**10**	**56**	0	0	**11**	0	0	2.9	1.4
	q90	2.9	**23**	0	**22.9**	**30**	0	0	**26**	0	0	0	1.4
	q95	1.4	**11**	0	**30**	**30**	0	1.4	**19**	4.3	0	0	0
	q99	**10**	7.1	0	**12.9**	**21**	0	0	**7.0**	**31**	0	0	4.3

2.3. Examining the Spatial Trend Patterns

In this section, we illustrate the spatial patterns in the magnitude and frequency of the indicators for June-October (Figure 2), July (Figure 3), and September (Figure 4) within the study region. These figures show that the spatial pattern of both increasing and decreasing trends vary across the different quantiles and seasons/months. Over the warm season (Figure 2), the study area shows a mixed bag of increasing and decreasing trends. In July, q50 (Figure 3A) shows positive trends over much of the domain. As we move from lower quantiles (i.e., q50, Figure 3A) to higher quantiles (i.e., q99, Figure 3E), the spatial coverage decreases, but we only see positive trends. In Figure 4, only the positive trends in September for q99 (Figure 4E) are notable.

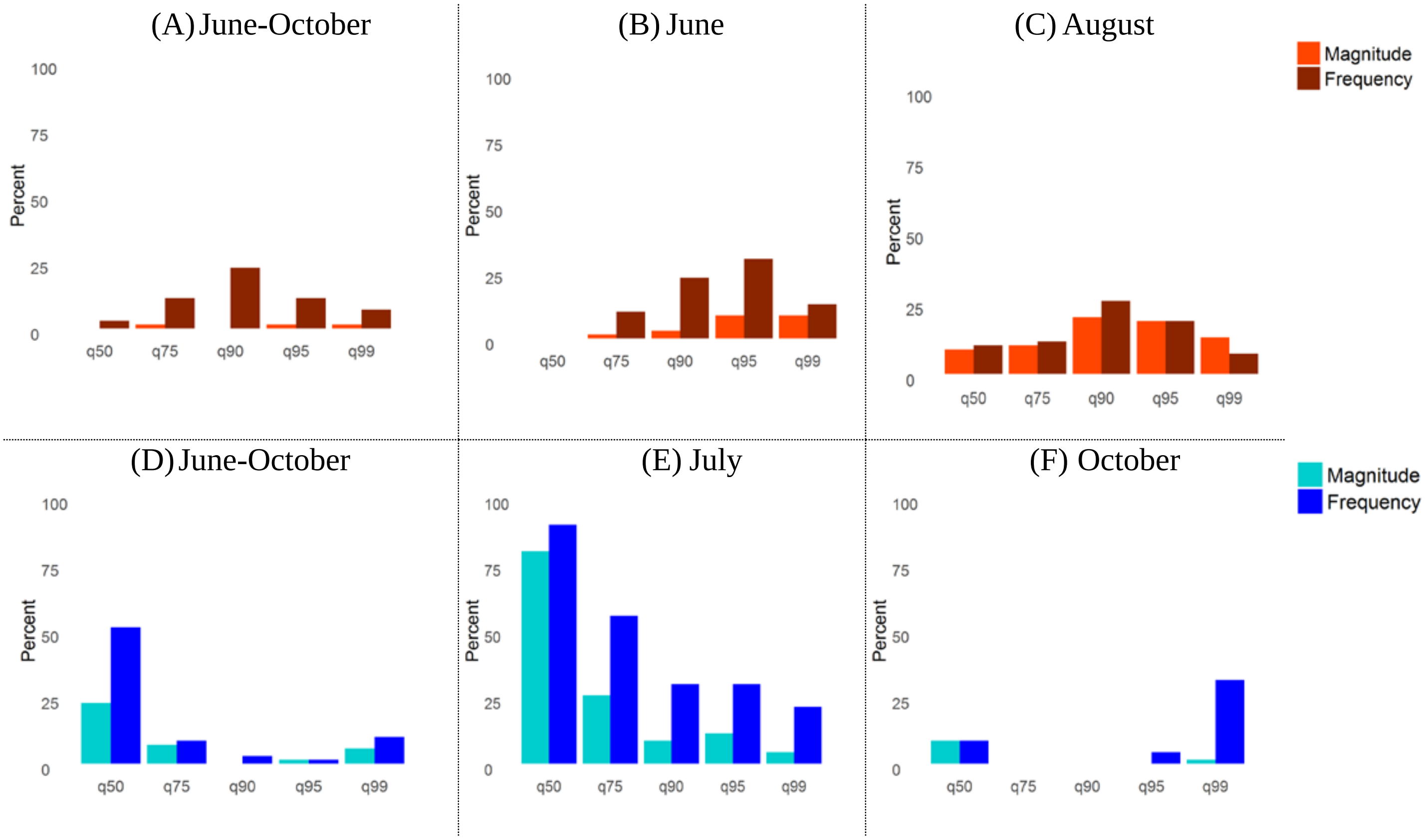

Figure 1. Percent of grid boxes with statistically significant trends (p-values <0.05, Table 1) for different quantiles of the magnitude and frequency precipitation indicators. Panels (A) to (C) show the dominant negative significant trend (drying tendency: red colors) and Panels (D) to (F) show the dominant positive significant trend (wetting tendency: blue colors).

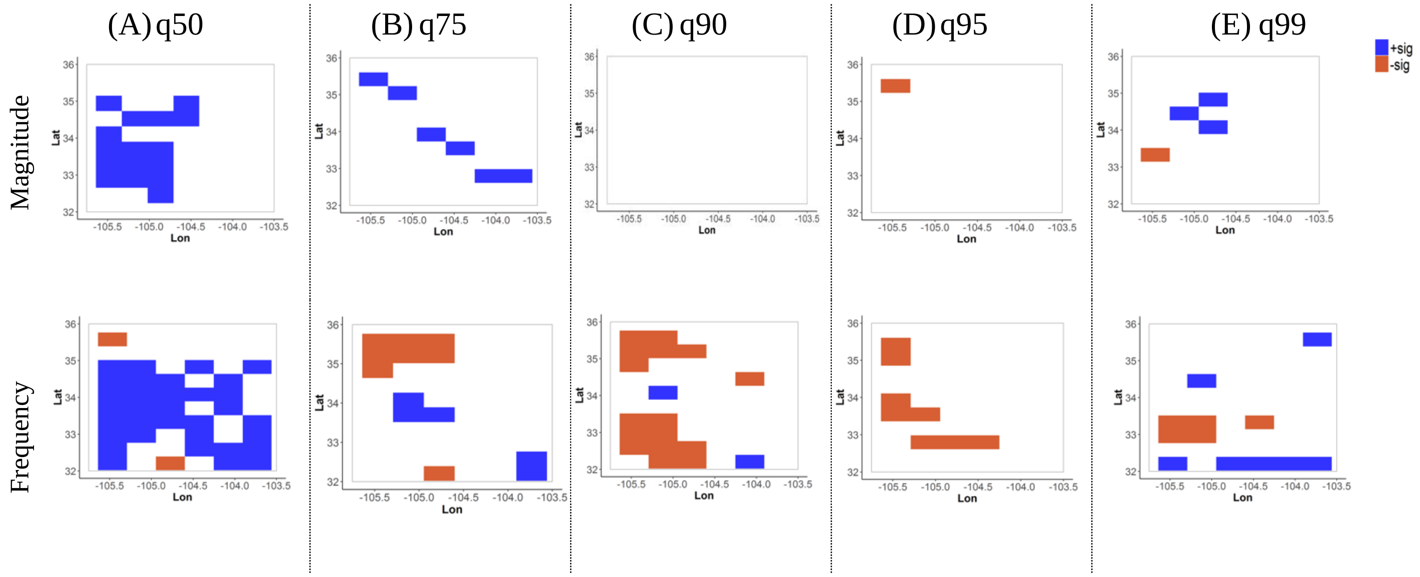

Figure 2. Spatial trend pattern in magnitude (top row) and frequency (bottom row) precipitation indicators for the warm season (June – October). The blue (red) areas indicate the location of the stations with increasing (decreasing) trends (p-values <0.05).

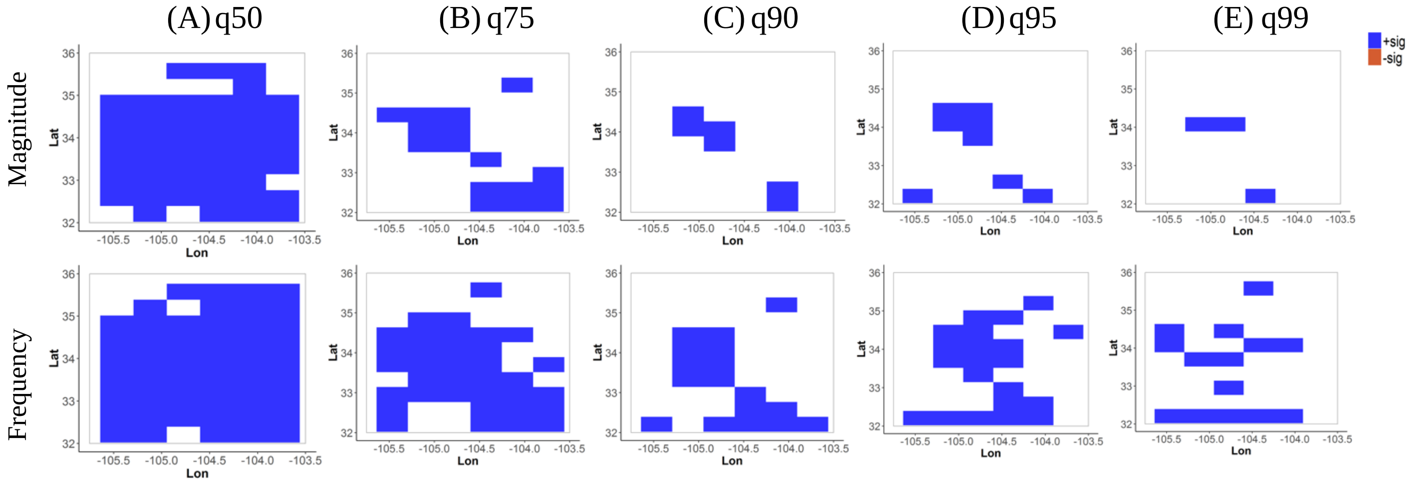

Figure 3. Spatial trend pattern in magnitude (top row) and frequency (bottom row) precipitation indicators for July. The blue (red) areas indicate the location of the stations with increasing (decreasing) trends (p-values <0.05).

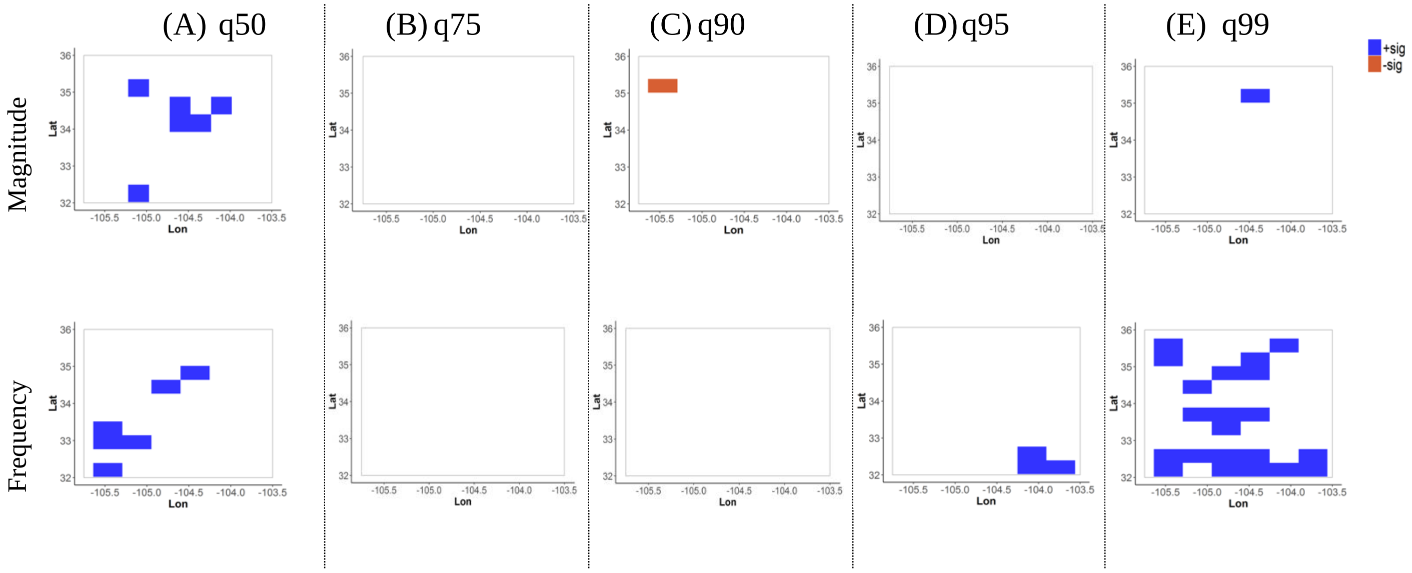

Figure 4. Spatial trend pattern in magnitude (top row) and frequency (bottom row) precipitation indicators for September. The blue (red) areas indicate the location of the stations with increasing (decreasing) trends (p-values <0.05).

3. Conclusion

In this study, we explore the trends in precipitation magnitude and frequency characteristics within an area of New Mexico containing the Pecos basin. We examine both magnitude and frequency characteristics for the warm season (June - October) and individual months therein, with a focus on the upper quantiles and extremes. The purpose of this is to determine how changing precipitation could potentially help mitigate decreases in water supply due to increasing temperatures and decreasing snowpack. For the period analyzed (1981-2017), we found that the dominant sign of the precipitation trend depends on the season/month examined, although the majority of the locations did not show any significant trend:

- The warm season (June - October) shows a mix of positive and negative trends; negative trends dominate June and August, and positive trends dominate July and for some September indicators. The increasing trends across many of the July indicators in the Pecos Basin show the most potential for water supply.

- The frequency of days above q99 for September also showed increasing trends, but this very heavy precipitation could be difficult to capture.

However, across most characteristics examined, we find that significant trends are more detectable in the frequency indicators than the magnitude. For times and locations showing increasing trends, this suggests that water managers looking to exploit changes in precipitation might not need to plan for larger events, but rather more frequent events.

Finally, we note that trend analysis provides important insight for water managers, especially in terms of where to focus further analysis. To this point, it is also critical to understand the drivers of the trends. In future work, the authors plan to investigate some of the factors that may be contributing to these trends, such as large-scale climate phenomena (e.g., the El Nino Southern Oscillation) or changes in the frequency of weather conditions (e.g., Prein *et al.*, 2016).

4. References

Dobson, A.J. and A. Barnett. (2008) An introduction to generalized linear models.

Fox, J. (2015) Applied regression analysis and generalized linear models.

Kendall, M.G. (1975) Rank Correlation Methods; Charles Griffin: London, 1975.

Mallakpour, I. and G.Villarini. (2017) Analysis of changes in the magnitude, frequency, and seasonality of heavy precipitation over the contiguous USA. Theor. Appl. Climatol. **130**(1–2), 345–363.

Mann, H.B. (1945) Non-Parametric Tests against Trend. Econmetrica, 13, 245-259.

Pournasiri Poshtiri, M. and I.Pal. (2016) Patterns of hydrological drought indicators in major US River basins. Clim. Change **134**(4), 549–563. https://doi.org/10.1007/s10584-015-1542-8

Pournasiri Poshtiri, M., E. Towler, D. Llewellyn, and A.F. Prein. (2018) Extremes of opportunity: Examining recent trends in warm season extreme precipitation for New Mexio River Basins, Proceedings from the 86th Western Snow Conference, Albuquerque, NM, in press.

Prein, A.F., G.J. Holland, R.M. Rasmussen, M.P. Clark, and M.R. Tye. (2016) Running dry: The US Southwest's drift into a drier climate state. Geophys. Res. Lett. **43**(3), 1272–1279.

Pecos River-
New Mexico Basin Study

Surface Water Modeling Appendix

Acronyms and Abbreviations

HDB	Hydrologic Data Base
HMLS	BaU High Monsoon/Low Snowpack
NMISC	New Mexico Interstate Stream Commission
Reclamation	Bureau of Reclamation
QUANT	Quantile Mapping,
PET	potential evapotranspiration
PRMS	Precipitation Runoff Modeling System,
PROM	Pecos River Operations Model
PVACD	Pecos Valley Artesian Conservancy District
VIC	Variable Infiltration Capacity,
RAB	Roswell Artesian Basin
RCP	Representative Concentration Pathways
RE	Reduced Emissions
USACE	U.S. Army Corps of Engineers

Contents

1. Global Climate Model (GCM) Selection Process 1
1.1. Methodology Background 1
Transient Projections and Period-Change Projections 1
Storyline Approach 2
1.2. Range Selection 2
Storyline Selection 2
Temperature 6
Precipitation 7
2. Unregulated Inflows to the Pecos River Operations Model 13
3. PROM Set-up for the Baseline Runs for Each Storyline for the Pecos River Basin Study 15
3.1. Inputs 15
Global Climate Model Input Flows 15
Precipitation 15
Evapotranspiration 19
Gains and Losses from Acme to Brantley 25
Local Inflows and Additional Bias Correction 26
3.2. Surface Water Irrigation Districts Implementation 32
Fort Sumner Irrigation District 32
Carlsbad Irrigation District 33
3.3. Settlement Implementation 34
3.4. Drought and Drying Analysis 34
Drying at Acme 34
FSID Bypass Flows 35
3.5. CMIP Acknowledgements and Permissions 36
Acknowledgements 36
Modeling Groups and Their Terms of Use 36
4. PROM Set-up for Strategy Runs of the Pecos River Basin Study 39
4.1. Strategies and Water Footprints Overview 39
4.2. Reducing Irrigation Water Consumption within Each Irrigation District 39
4.3. Increased Irrigation Efficiency Strategy 41
4.4. Water Footprint Analyses 43
PVACD 43
FSID 43
CID 43
ESA Operations 43
5. References 45

1. Global Climate Model (GCM) Selection Process

This appendix describes the methodology and approach used to select the Global Climate Model (GCM) projections used in the Pecos River Basin Study in New Mexico. This approach for evaluating and modeling potential responses to future water supply and demand challenges results in a range of potential futures (termed “storylines”). This method avoids describing the likelihood of potential future changes, and therefore avoids the need to characterize uncertainty associated with water supply and demand projections.

1.1. Methodology Background

Since the passage of the SECURE Water Act in 2009, the Bureau of Reclamation (Reclamation) has been developing state-of-the art methodologies for characterizing future climate and hydrology within the river basins of the Western United States that are served by Reclamation water projects. These methodologies have been developed by Reclamation’s West Wide Climate Risk Assessment Team and applied in Reclamation’s Basin Studies, which are partnerships with local water-management entities to characterize potential future water supply and demand and develop and model adaptations to the projected system changes. Under the Basin Study Program, Reclamation has developed methodologies for ensembling forecasts of future water supply and demand based on large suites (compiled by the World Climate Research Programme’s Coupled Model Intercomparison Project [CMIP]) for GCM simulations, which have been bias-corrected and downscaled, and then run through hydrologic models in an attempt to capture the range of likely future water supply conditions. These ensembling methods are meant to help comprehend the results of the many GCM runs, and the range of variability of these results.

1.1.1. Transient Projections and Period-Change Projections

So far, these Basin Studies have primarily relied on two ensembling approaches: transient projections and period-change projections. Transient projections are traces of the changes in climatic or hydrologic parameters over time (usually over the course of the 21st century). Transient projections are ensembled through the generation of statistics describing the full suite of these traces that are generated from a suite of GCMs. Period-change projections are projections of the likely range of climate and hydrology parameters at a specific future year. To develop ensemble period-change projections, Reclamation has clustered the hydrologic projections by the degree of change in temperature and precipitation, by the specified year, and then analyzed groups of projections according to their location in the precipitation-temperature space: central tendency, hot and wet, hot and dry, warm and wet, and warm and dry. Monthly change factors are applied to historic records for each of these groups, generating 5 sets of statistics characterizing the range of variability in the projections for the selected future year.

Both of these methods attempt to capture the degree of hydrologic change that could be expected in the future, both in terms of means and extremes, as well as the degree of uncertainty in the projection of future conditions, based on the range of variability within the ensembles. However, these projection sets come with considerable uncertainty, especially for precipitation. This uncertainty can complicate planning of adaptation measures by water managers and stakeholders.

1.1.2. Storyline Approach

In the Pecos River Basin in New Mexico, the small portion of the basin's water supply that comes from snowpack, as well as the dominance of groundwater in the water supply, have made the Pecos Basin poorly suited for Reclamation's developed methodologies. Therefore, an alternative approach was developed using individual projections that tell particular stories about the way that the basin may develop. This approach has the added benefit that it avoids describing the likelihood of potential future changes, and therefore avoids the need to characterize uncertainty associated with water supply and demand projections. It also allowed Reclamation, its study partner, and basin stakeholders to play a game of "what if", which allowed consideration of different ways that the basin might change in the future. For example, we could contrast a future in which snowpack declines, but summer monsoonal precipitation increases with a future in which precipitation declines in both seasons, and another in which the seasonal distribution of precipitation doesn't change significantly. This provided a tool for visioning of different potential futures, which helped with developing adaptation strategies, and also highlighted the adaptation strategies that are common between the different potential futures. See Section 4.3. *Storyline Projections* in the main report.

1.2. Range Selection

1.2.1. Storyline Selection

Modelling 930 traces (93 GCMs, 2 hydrologic models, and 4 bias-correction techniques plus raw output) takes high-end computing power and a large amount of time and effort for computation and analysis. Therefore, the storyline approach selected a few statistically reasonable traces to describe varying futures for the basin rather than attempting to create a deterministic forecast that shows an envelope of many different traces. This approach narrowed down the immense number of possible traces to analyze for the Pecos River Basin Study. The multistep process of narrowing down those 930 traces to a manageable number of storylines is shown in Figure 1 shows the modeled GCMs provide data that characterize future evapotranspiration, temperature, and precipitation in the basin.

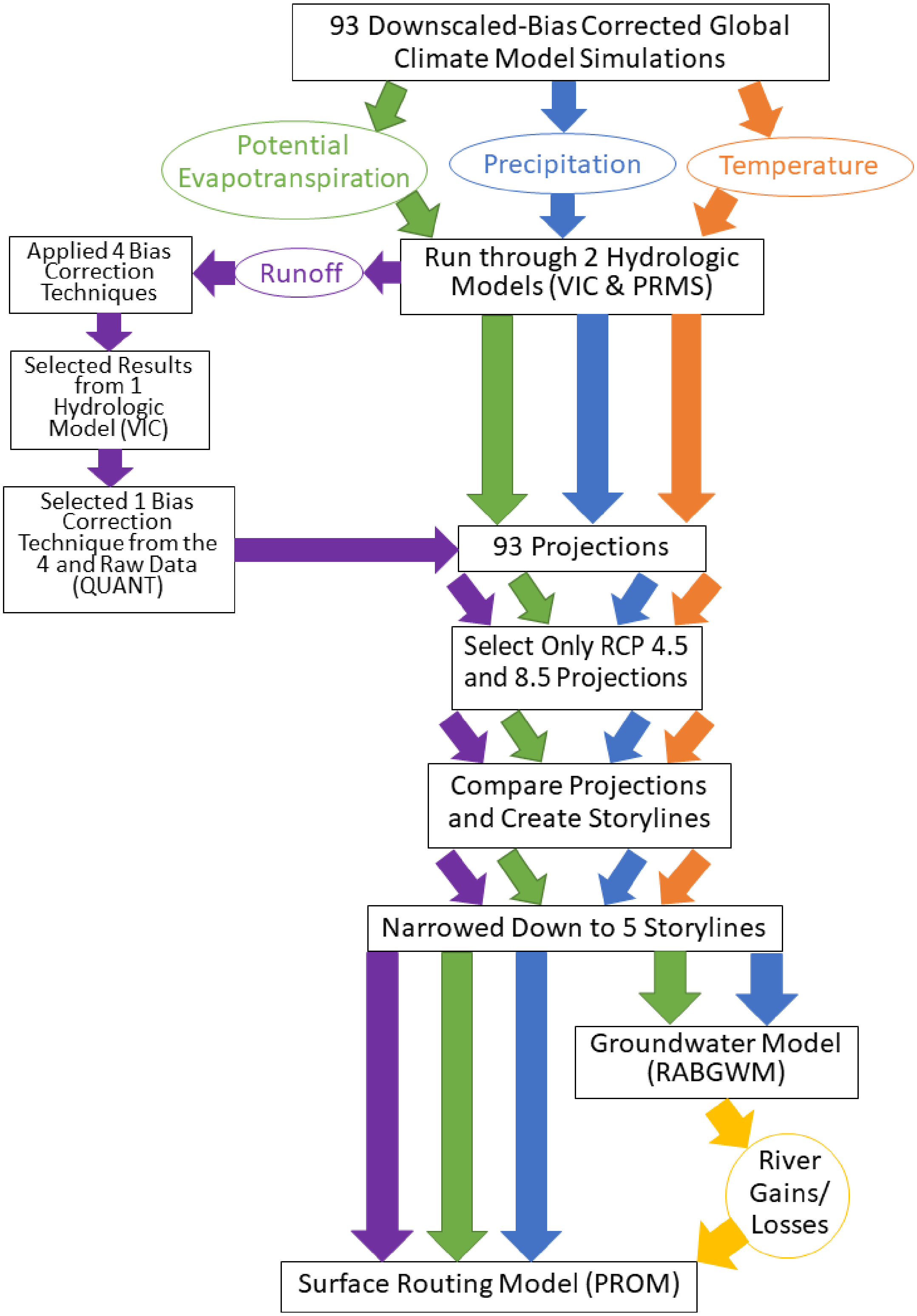

Figure 1. Simplified diagram depicting the steps that were taken to narrow the 930 traces to five storylines. (VIC = Variable Infiltration Capacity, PRMS = Precipitation Runoff Modeling System, QUANT = Quantile Mapping, RAB = Roswell Artesian Basin, and PROM = Pecos River Operations Model).

The process of developing the storylines for the Pecos River Basin in New Mexico began with the evaluation of 93 sets of climatic and hydrologic projections developed from the CMIP5 suite of GCM simulations (https://esgf-node.llnl.gov/projects/cmip5/). The projections provided on this website have been bias corrected for climate parameters and spatially downscaled to 1/8th degree of latitude/longitude (through the statistical Bias Correction and Spatial Downscaling process (BCSD) (Wood et al. 2004), and processed through two hydrologic modeling codes (the Variable Infiltration Capacity (VIC) modeling code (Liang et al. 1994), and the US Geological Survey's Precipitation Runoff Modeling System (PRMS) (Leavesley et al. 1983).

The resulting hydrologic projections were then routed by the U.S. Army Corps of Engineers (USACE) using a hydrologic routing tool known as mizuRoute (Mizukami et. al 2016) to provide projections of streamflow at specific gage locations within the basin. This process provided a more complete projection set for the projections processed through the VIC model code (i.e. it provided hydrologic projections for each of the headwater locations in the operations model for the Pecos Basin in New Mexico), and for that reason, only projections processed through the VIC model code were carried forward in this study. USACE also performed bias correction on the routed streamflows using four bias correction techniques, and allowed us access to an in-house tool that compared the robustness of the routed streamflows using each technique for hindcast streamflows. Projections processed using the Quant (Quantile Mapping) streamflow bias correction technique were deemed the most robust and were carried forward in this study.

These processes provided 93 climate and hydrology projection traces for the 21st century. The number of projections under consideration in this study was then reduced by selecting only the projections based on the greenhouse-gas emissions scenarios referred to as Representative Concentration Pathways (RCP) 8.5 and 4.5. RCP 8.5 represents a "business as usual" future. In contrast, RCP 4.5 shows what would happen if our global society begins to strongly reduce greenhouse gas emissions. More conservative greenhouse-gas emissions groupings, including RCP 2.6, are broadly outside the projected range of future conditions considered by major climate assessments, including those produced by the Intergovernmental Panel on Climate Change (Sun et al., 2015). Further, the Fourth National Climate Assessment (U.S. Global Change Research Program 2018) which was underway at the time of this study, considers CMIP5 4.5 and CMIP5 8.5 projections only. This process narrowed the number of hydrologic projections under consideration to 58 (28 RCP 8.5 projections, and 30 RCP 4.5 projections).

A detailed comparative analysis was then performed on the remaining projection traces in order to characterize the story that each tells about the projected future climate and hydrology in the basin. The overarching goal was to select storylines that were not only plausible representations of our future, but also that were distinct from each other, so that a wide range of plausible futures can be modeled within a small select group.

We characterized and compared snowmelt runoff and timing, monsoon intensity, seasonal and spatial runoff and precipitation patterns, temperatures, evapotranspiration rates, and total streamflow in the mainstem and key tributaries. Reclamation and the New

Mexico Interstate Stream Commission (NMISC) then evaluated these projections and selected five storylines to be carried forward in the study:

- **Business as Usual (BaU) Moderate:** a Moderate Storyline that showed a mild amount of drying across the entire basin and was close to the median of all the RCP 8.5s that were analyzed.
- **BaU Dry:** a Dry Storyline that showed extreme drying and increased temperatures across the basin.
- **BaU High Monsoon/Low Snowpack (HMLS):** a storyline that show an increase to the monsoon intensity great enough to make up for the decrease in snowpack.
- **Reduced Emissions (RE) Increased Monsoon:** a storyline that is around the average and median of the 4.5 projections and shows minor increases in monsoon activity and temperature.
- **RE Median:** a storyline that is close to the median of the 4.5 projections and shows minor decrease in precipitation and temperature over time.

Table 1 shows the overall storyline trends for temperature, precipitation, and runoff.

Table 1. Storyline Trends from 2010 to 2099

Storyline	Temperature (°F)		Precipitation (inches [in])		Runoff (acre-feet [af])	
	Per Year Trend	Change from 2010 to 2099	Per Year Trend	Change from 2010 to 2099	Per Year Trend	Change from 2010 to 2099
Business as Usual (RCP 8.5)						
BaU Moderate	0.098	8.82 °F	-0.040	-3.6 in	-673	-60,570 af
BaU Dry	0.148	13.32 °F	-0.093	-8.37 in	-1557	-140,130 af
BaU HMLS	0.137	12.33 °F	0.022	1.98 in	903	81,270 af
Reduced Emissions (RCP 4.5)						
RE Increased Monsoon	0.045	4.05 °F	0.035	3.15 in	403	36,270 af
RE Median	0.028	2.52 °F	-0.007	-0.63 in	-289	-26,010 af

1.2.2. Temperature

Figure 2 shows the range of average temperatures for what is defined in the study as the Pecos River Basin in New Mexico. In this figure, there is a clear branching of the RCP 4.5 and 8.5 GCMs and also an overlapping portion of the two. The BaU Dry and BaU HMLS storylines are in the upper range of temperatures where only RCP 8.5 GCMs are at by the end of the century. The BaU Moderate and RE Increased Monsoon storylines are near the center of the entire range of possible temperatures at the end of the century, where both RCP 4.5 and 8.5 GCMs overlap. The RE Median is at the lower end of the potential temperature increases at the end of the century.

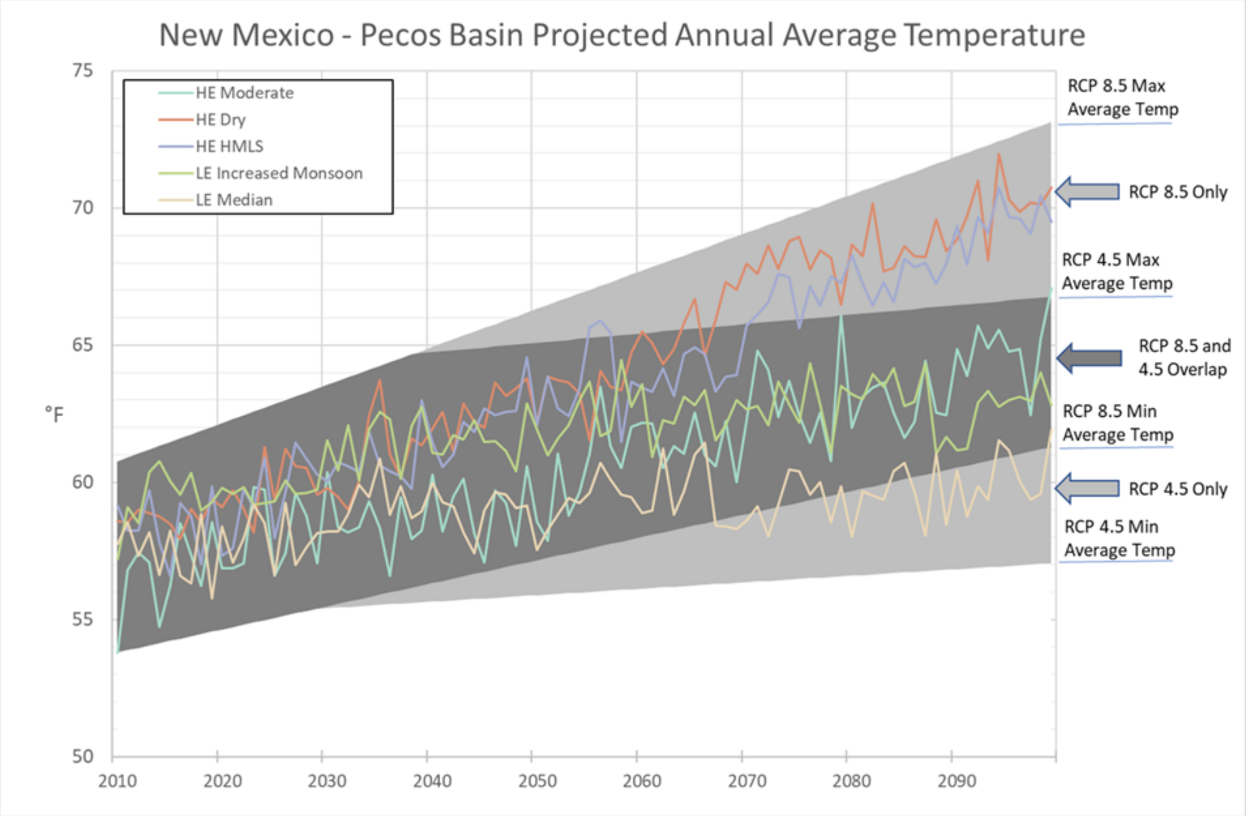

Figure 2. Trends for average temperatures in the Upper Pecos Basin compared with the range for RCP 8.5 and RCP 4.5.

Figure 3 shows a more in-depth look at the temperature trends of all the GCMs annually and seasonally and how the 5 selected storylines compare. Annually, the 5 selected storylines show a similar pattern to Figure 2, with the BaU Dry and BaU HMLS storylines at or near, respectively, the top of the range of potential average temperature increases, the BaU Moderate and RE Increased Monsoon storylines closer to the middle of the range and the RE Median Storyline toward the bottom of the range. This pattern stays almost the same across all seasons. The BaU Dry has the highest trending average temperature across all seasons except for spring, where the BaU HMLS is the highest. The BaU HMLS is always in the top 25% of average temperature increases across all seasons. The BaU Moderate is generally in the 50-25%, with the RE Increased monsoon generally in the 75-50% range of temperature increases throughout all the seasons. The RE Median is always on the lowest 25% range of temperature increases.

When looking at the entire range of GCMs, summer and fall show the greatest average increases in temperatures, but also the largest range. In contrast, winter has the lowest average increase in temperatures, but has the smallest range. These seasonal patterns hold true even when separating them by RCPs. Even when separating them by RCPs, the BaU HMLS and BaU Dry storylines are still in the uppermost 25% of the GCMs in terms of increasing temperatures, while the BaU Moderate is around or slightly below the median of the RCP 8.5 GCMs temperature trends. Analyzing only the RCP 4.5 GCMs, the RE Increased Monsoon is near or slightly above the median temperature trends, while the RE Median is more on the lower end of increasing temperatures.

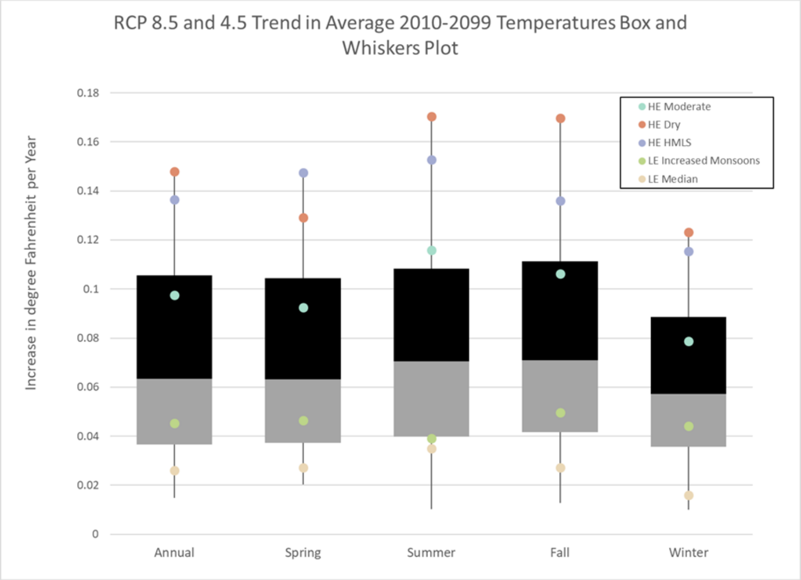

Figure 3. Seasonal breakdown of per-year trends in temperature for RCP 8.5 and 4.5 CMIP5 GCMs.

1.2.3. Precipitation

Changes in precipitation are associated with more future uncertainty than changes in temperature. Figure 4 is a box and whisker plot showing future projections of annual and seasonal precipitation. As is the case with temperature changes, the five selected storylines encompass a broad range of future precipitation changes from across the entire spectrum of RCP 4.5 and RCP 8.5 GCMs. The BaU HMLS and RE Increased Monsoon storylines show an increase in annual rainfall, while the other three storylines show a decrease—and the BaU Dry Storyline has the largest decrease in annual precipitation of all the RCP 4.5 and 8.5 GCMs. The RE: Increased Monsoon Storyline is the only storyline with increases of precipitation in the spring and has the largest increase in precipitation during the summer of the storylines. The BaU HMLS Storyline has slight decreases in precipitation in the spring and winter, slight increases in precipitation in the summer, and the largest increase In Fall precipitation of any. The RE Median Storyline shows a slight decrease in precipitation overall and is the only storyline featuring increasing winter precipitation. The BaU Moderate Storyline shows overall decreases in the lowest 25% of the GCMs, while the BaU Dry Storyline shows the most dramatic decrease in precipitation in the summer and fall, which results in the largest decrease in annual precipitation.

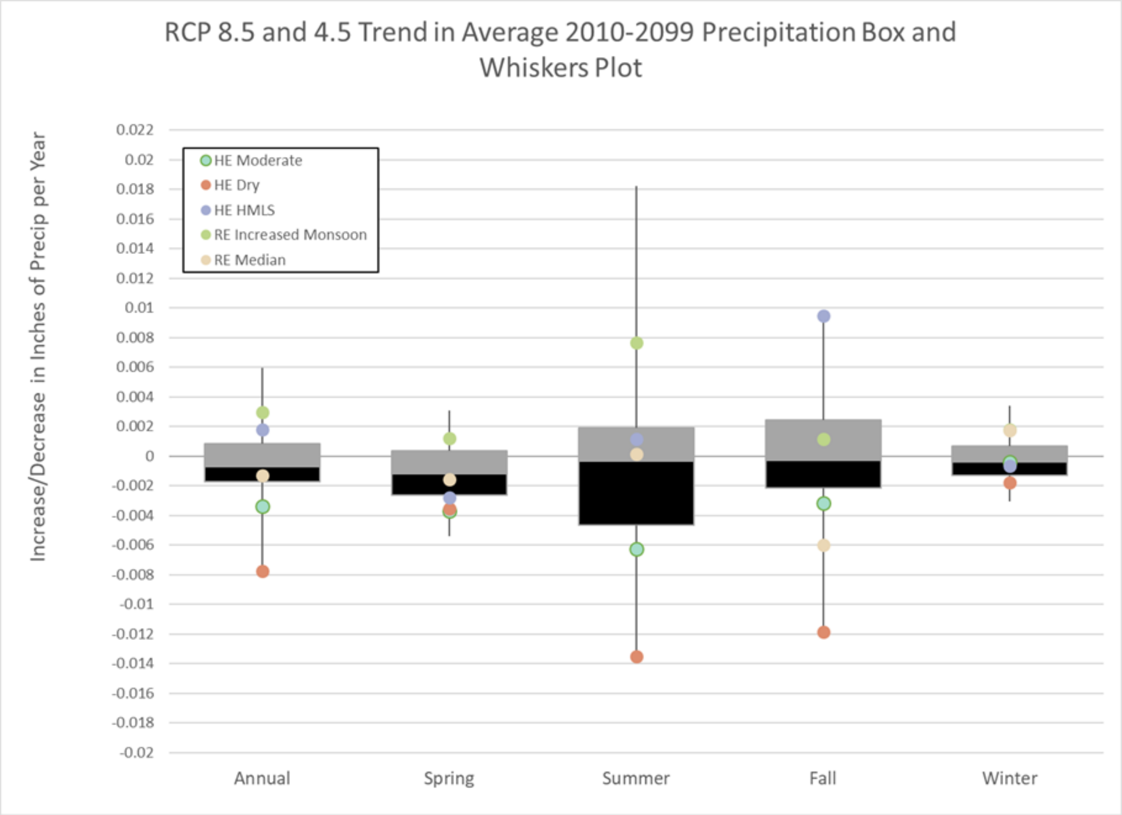

Figure 4. Seasonal breakdown of per-year trends in precipitation for RCP 8.5 and 4.5 CMIP5 GCMs.

The storyline selection process attempted to choose storylines that would appropriately represent the range of potential future outcomes predicted by the GCMs. Figure 5 shows that, with respect to temperature and precipitation, the storylines are distinct and wide ranging. The BaU Dry Storyline is somewhat of an outlier due to its significant decrease in precipitation, serving as an effective “worst-case scenario” storyline, while the other four storylines reflect the range of possible temperatures and precipitation projected by the RCP 4.5 and 8.5 GCMs.

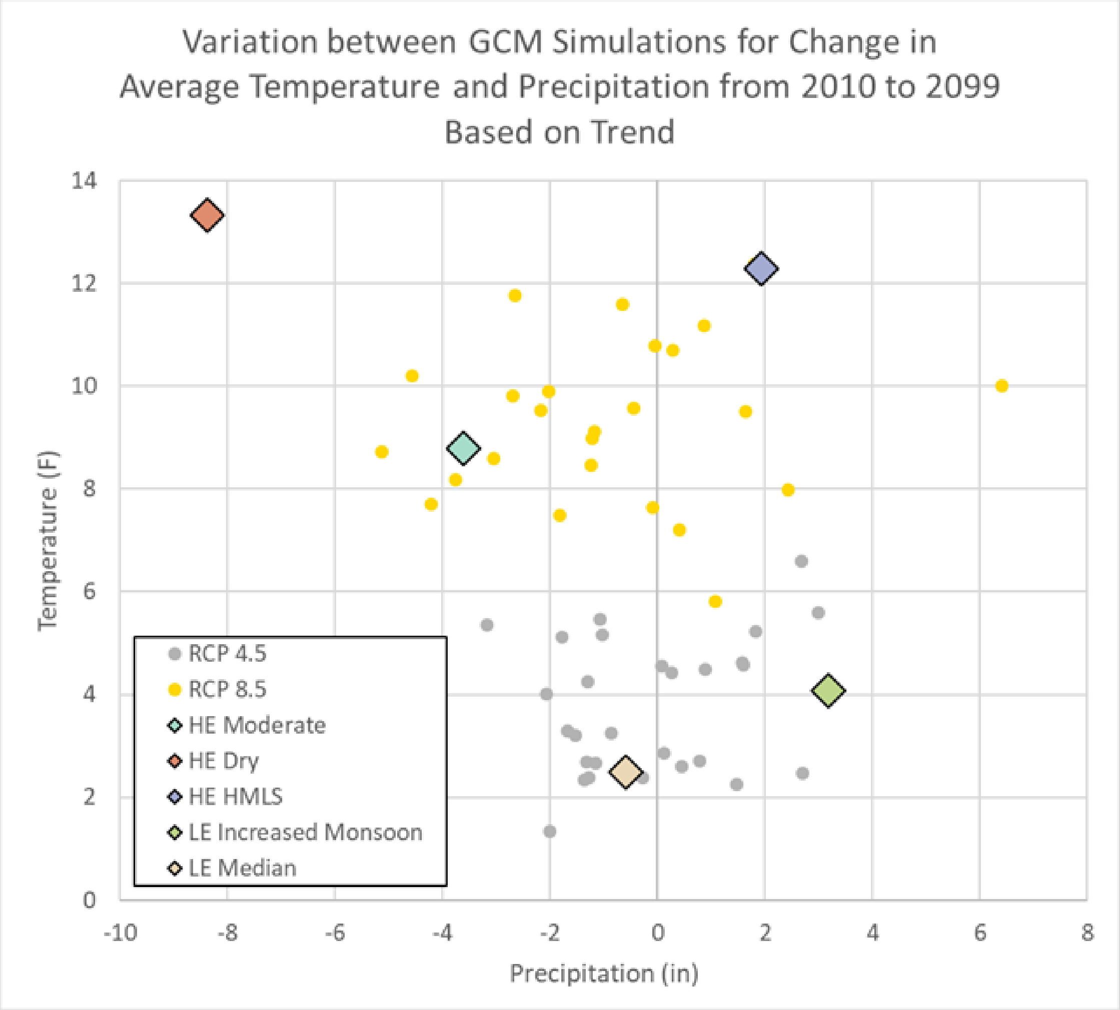

Figure 5. Per-year trends for average temperatures and precipitation in the Upper Pecos Basin in New Mexico.

Comparing precipitation and runoff at gaged locations (Figure 6) again shows a representative spread of storylines within the selected GCMs. Although the BaU Dry Storyline is an outlier in terms of precipitation, Figure 7shows that the BaU Dry Storyline is still in line with other GCMs for runoff at gaged locations. There are several possible explanations for this, but likely the result of either the bias-correction techniques in the modeling process, or an artifact of spatial and temporal variations in overall precipitation and runoff in the basin. Still, even though the BaU Dry Storyline is not an outlier with respect to runoff, it still has the second largest decrease in runoff volume of all RCP 4.5 and 8.5 GCMs. Similarly, even though the RE Increased Monsoon Storyline projects a higher increase in annual precipitation than the BaU HMLS Storyline, the BaU HMLS projects higher runoff. The RE Median Storyline is close to the median projected runoff, while the BaU Moderate storyline is slightly lower than median projected runoff. Figure 8 shows increases/decreases in temperature, precipitation, and runoff from 2010 to 2099 for each of the 5 selected GCMs.

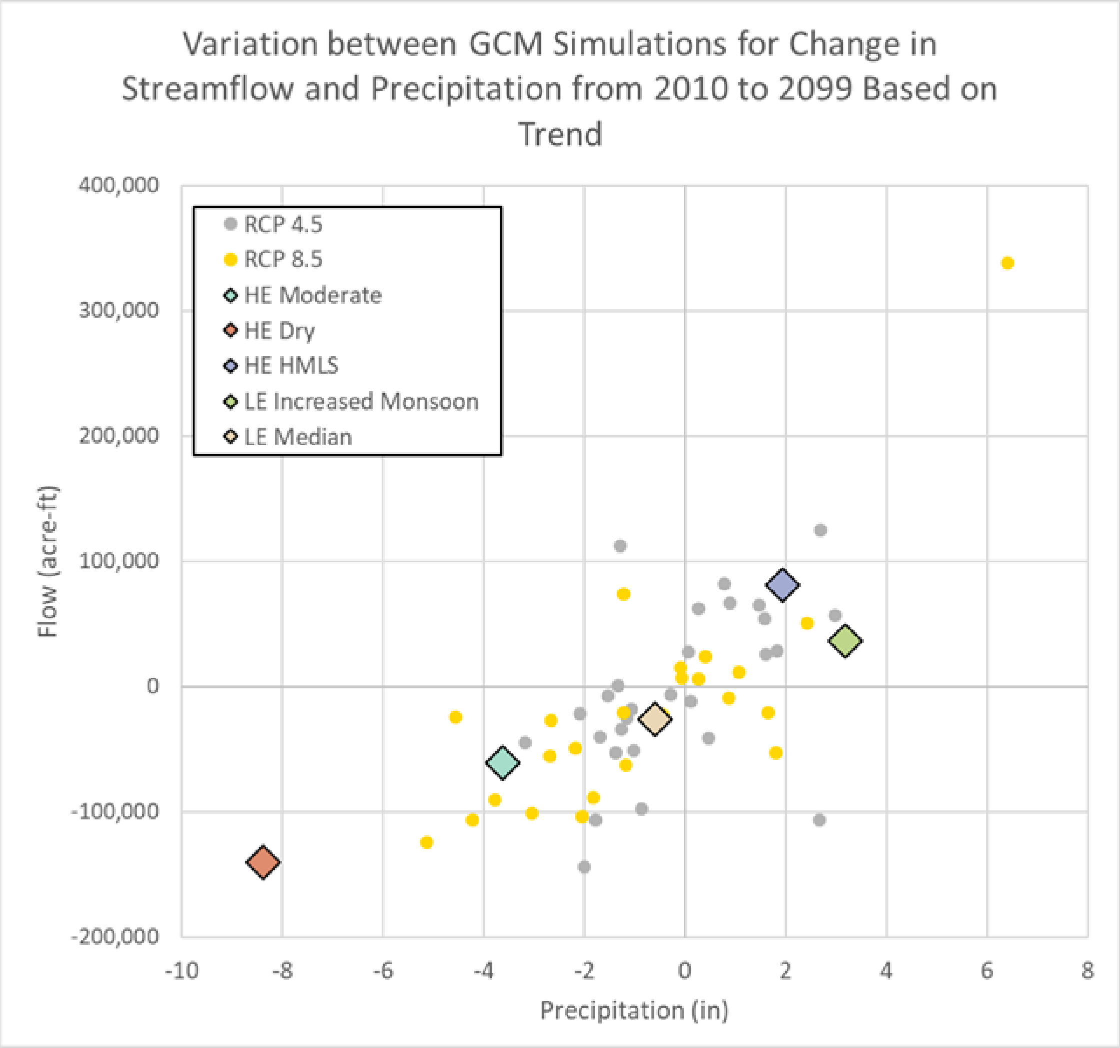

Figure 6. Total change in precipitation and gaged flows. Gaged flows include the Above Santa Rosa Gage and 8 tributary gages from Sumner Reservoir to Red Bluff. Results show comparison between storylines used in this Basin Study and the remaining RCP 4.5 and RCP 8.5 simulations in the CMIP5 archive.

Flows at Pecos gages were further broken into spring runoff and monsoon season flows (Figure 7). Again, analyzing the trends, each storyline appears very distinctive. The BaU HMLS Storyline has the lowest spring runoff of all the GCM projections, followed by the BaU Dry Storyline, with a decreasing annual trend in spring runoff above 500 acre feet per year in both cases (a total decrease of over 45,000 acre-feet/year by 2099). For both winter precipitation and spring runoff, the RE Median storyline is the only storyline that experiences an increasing annual trend—almost 200 acre feet/year in spring runoff, (a total increase of about 18,000 acre feet/year by 2099). This increase in spring runoff indicates that the increase in precipitation during the winter is likely falling mostly as additional snow, an unsurprising outcome given the RE Median Storyline’s relatively low increases in temperature compared to other RCP 4.5 and 8.5 GCMs.

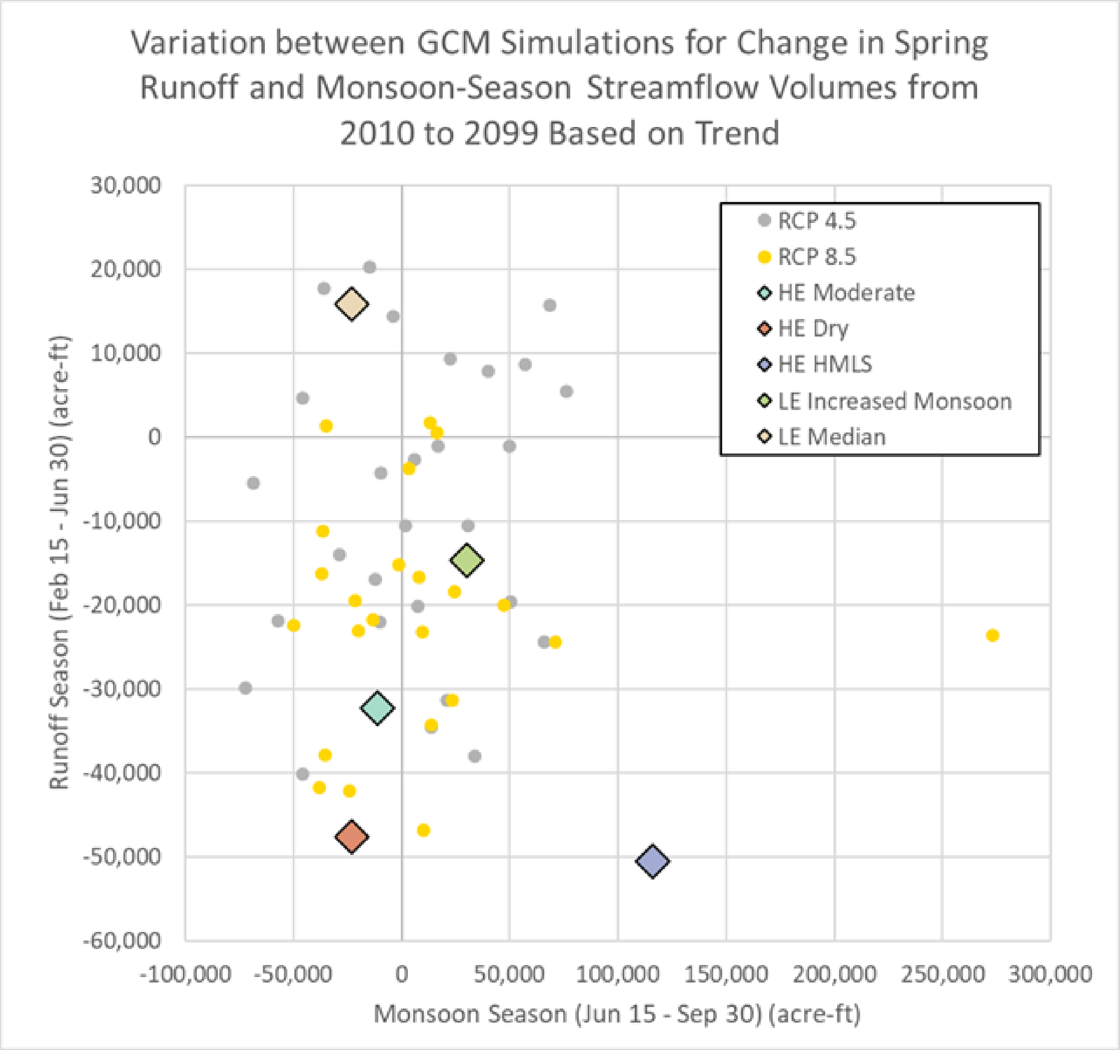

Figure 7. Total change in modeled annual spring runoff compared to monsoon flows from 2010-2099 in the Pecos River Basin in New Mexico. The spring runoff was based on the Above Santa Rosa Gage, and the monsoon flows were based on 6 main monsoon-driven tributaries between Sumner Reservoir and Avalon Reservoir. Results show comparison between storylines used in this Basin Study and the remaining RCP 4.5 and RCP 8.5 simulations in the CMIP5 archive.

The BaU HMLS and RE Increased Monsoon Storylines both show increases to flow during the monsoon season. The BaU HMLS Storyline has the second largest increasing trend in monsoon flows of all the GCMs, about 1,300 acre feet/year (a total increase of approximately 120,000 acre-feet/year by 2099), while in the RE Increased Monsoon Storyline flows trend upwards by about 300 acre feet per year (a total increase of approximately 27,000 acre feet/year by 2099). The BaU Dry Storyline has the biggest projected decrease in monsoon flows of the 5 storylines, with a decreasing trend of about 250 acre feet per year (a total decrease of over 22,000 acre-feet per year by 2099), but several other RCP 4.5 and 8.5 GCMs project even greater reductions in monsoon flows.

Lastly, runoff was analyzed with respect to intensity of extreme storms (>99th percentile) and days of significant flows (Figure 8). With respect to these parameters, the selected storylines are slightly less reflective of the range of GCM projections than in the case of temperature, precipitation, and overall runoff. The BaU Moderate, BaU Dry, and RE Median Storylines all project decreases in the number of days with gaged monsoon storm flows over 1,000 acre feet. These three storylines also show similar decreases, of between 10-50 acre feet per year, in the intensity of the 99th percentile of storm flows. In contrast, the BaU HMLS Storyline projects a significant increase in the intensity of the 99th percentile of storm, and the RE Increased Monsoon Storyline projects a significant increase in the number of days of monsoon storm flows above 1,000 acre feet. See Section 4.3.5. *Frequency and Intensity of Extreme Events* in the main report for further comparisons for extreme storms.

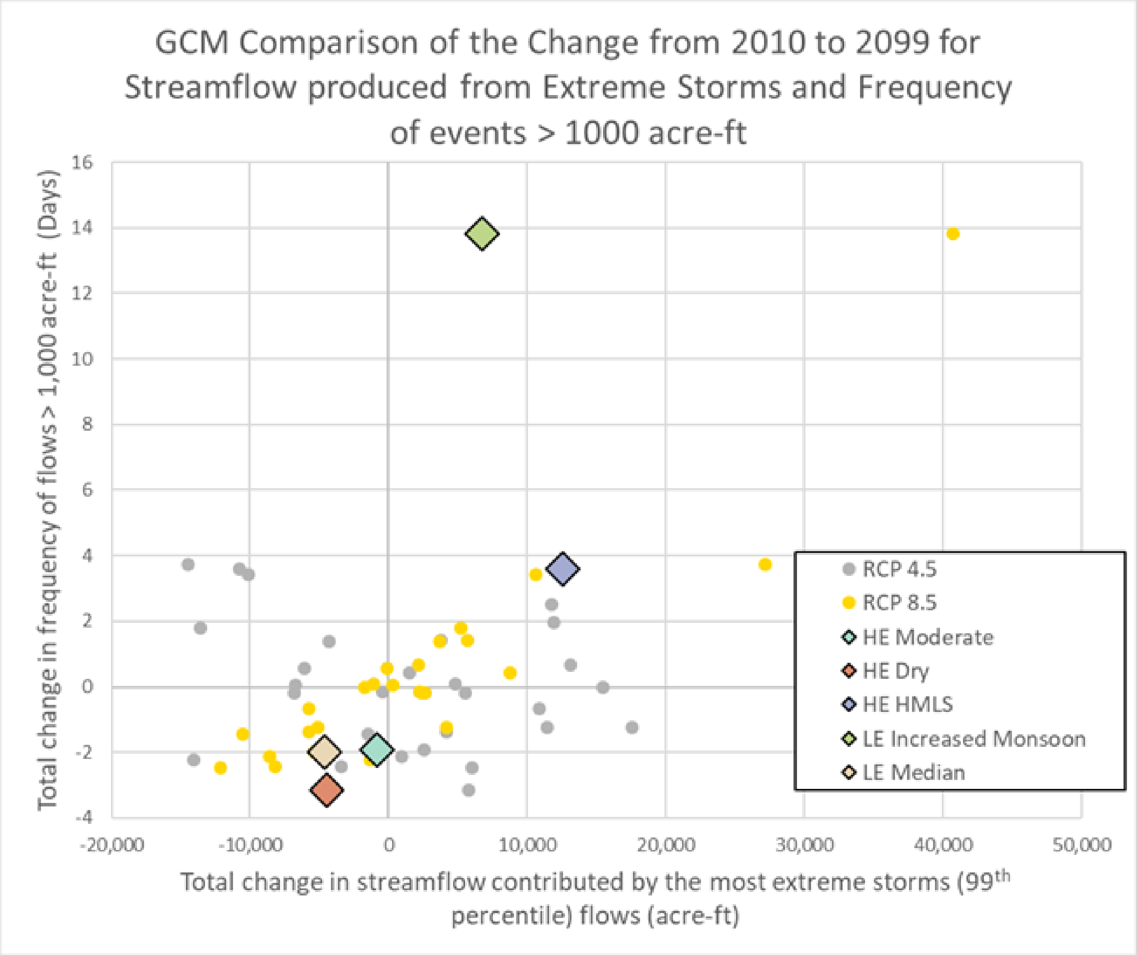

Figure 8. Total change in streamflow (acre-feet) contributed by the most extreme storms (99th percentile) from 2010 to 2099 compared to the frequency of flows greater than 1,000 acre-feet per day. Results show comparison between storylines used in this Basin Study and the remaining RCP 4.5 and RCP 8.5 simulations in the CMIP5 archive.

2. Unregulated Inflows to the Pecos River Operations Model

Routing points for which USACE provided values for headwater flows into PROM for the Pecos Basin Study (Table 2). These were the main points used for selecting the GCM projections that became the storylines. The PROM model does go beyond Avalon and supports those gages. USACE data for these points were entered into the model but had no overall impact on any of the results upstream.

Table 2. Routing Points for Headwater Flows into PROM

Name (USGS)	**Basin Area (mi^2)**	**Routing Point on Pecos River**		**USGS Gage URL**	**HUC 8 or 10 Name (Approximate)**
		Latitude (NAD 83)	Longitude (NAD 83)		
Pecos River Above Santa Rosa	2,340	35°03'34"	104°45'40"	http://waterdata.usgs.gov/nm/nwis/inventory/?site_no=08382650&agency_cd=USGS	Pecos Headwaters (H8-13060001)
Rio Hondo Near Roswell	2,900	33°24'32"	104°28'18"	http://waterdata.usgs.gov/nm/nwis/inventory/?site_no=08393610&agency_cd=USGS	Rio Hondo (H8-13060008)
Rio Felix at Old Hwy Brd Nr Hagerman	932	33°07'30"	104°20'40"	http://waterdata.usgs.gov/nm/nwis/inventory/?site_no=08394500&agency_cd=USGS	Rio Felix (H8-13060009)
Rio Peñasco at Dayton	1,060	32°44'36"	104°24'51"	http://waterdata.usgs.gov/nm/nwis/inventory/?site_no=08398500&agency_cd=USGS	Rio Penasco (H8-13060010)
Fourmile Draw Nr Lakewood	265	32°40'22"	104°22'08"	http://waterdata.usgs.gov/nm/nwis/inventory/?site_no=08400000&agency_cd=USGS	Fourmile Draw (H10-1306001104)
South Seven Rivers	220	32°35'19"	104°25'17"	http://waterdata.usgs.gov/nm/nwis/inventory/?site_no=08401200&agency_cd=USGS	South Seven Rivers (H10-1306001105)
Rocky Arroyo	285	32°30'22"	104°22'30"	http://waterdata.usgs.gov/nm/nwis/inventory/?site_no=08401900&agency_cd=USGS	Rocky Arroyo (H10-1306001107)
Dark Canyon	451	32°24'12"	104°13'46"	http://waterdata.usgs.gov/nm/nwis/inventory/?site_no=08405150&agency_cd=USGS	Dark Canyon (H10-1306001109)
Black River	350	32°14'27"	104°03'53"	http://waterdata.usgs.gov/nm/nwis/inventory/?site_no=08406000&agency_cd=USGS	Black River (H10-1306001111)

3. PROM Set-up for the Baseline Runs for Each Storyline for the Pecos River Basin Study

This appendix details specific analyses made with the overall RiverWare®, Pecos River Operations Model (PROM) for the Pecos River Basin Study in New Mexico. For additional information about PROM, see Reclamation 2020.

3.1. Inputs

3.1.1. Global Climate Model Input Flows

As discussed in Section 1. *Global Climate Selection Process* in this appendix, five traces from the VIC runoff model runs of the RCPs 8.5 and 4.5 GCMs were downscaled using the QUANT bias correcting technique were chosen to provide daily series flow data between 1950-2099 to eight tributary gages to the Pecos and one gage along the main stem of the Pecos above Santa Rosa (shown in Section 2. *Unregulated Inflows to the Pecos River Operations Model*). PROM has objects below Avalon Dam for the Dark Canyon and Black River tributaries, but anything that is currently simulated in the model below Avalon Dam will not have any impact on the above Avalon Dam portion of the model. This means that although data was added for these two locations into the model, that data did not affect anything above Avalon Dam, including any Settlement calculations.

To provide a consistent basis for comparison, the baseline runs assumed that operations in 2017 were continual throughout the entire modeled period—both past and future. Thus, the historical portion of the model runs were not altered to reflect actual historic operations or structures (e.g., Santa Rosa Reservoir is in the model from the start of the runs in 1950, even though it did not begin storing water until 1979). The model was run at a daily timestep for all model runs.

3.1.2. Precipitation

Precipitation in RiverWare is only simulated over reservoirs. Precipitation for each GCM was downloaded from "Downscaled CMIP3 and CMIP5 Climate and Hydrology Projections" archive at http://gdo-dcp.ucllnl.org/downscaled_cmip_projections/ (Reclamation 2014). From this site BCSD CMIP5 hydrologic projections for monthly precipitation over the locations in the Santa Rosa (Figure 9), Sumner (Figure 10), and Brantley and Avalon Reservoirs' areas (Figure 11) were downloaded.

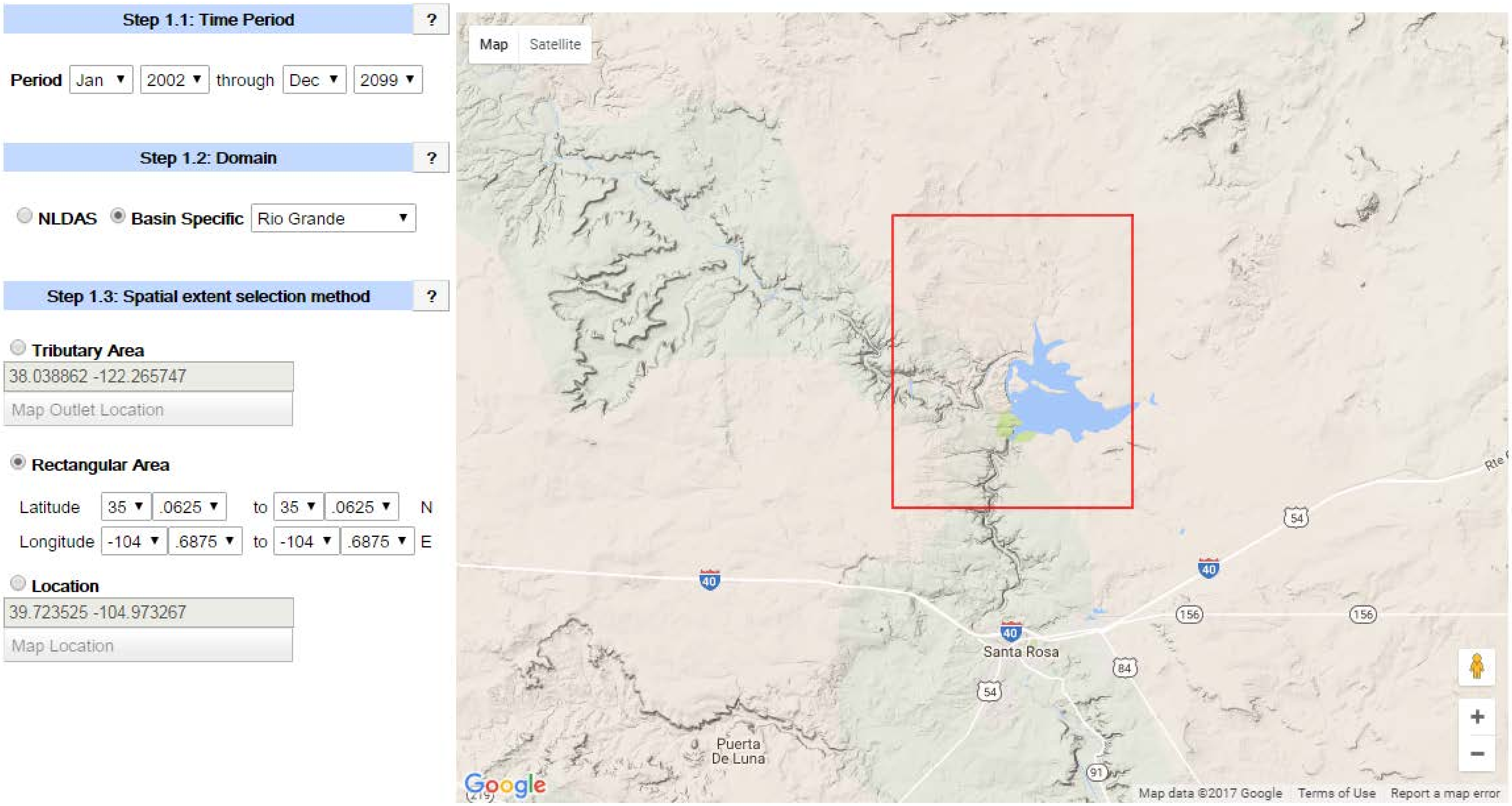

Step 1.1: Time Period ?

Period Jan ▾ 2002 ▾ through Dec ▾ 2099 ▾

Step 1.2: Domain ?

○ NLDAS ● Basin Specific Rio Grande ▾

Step 1.3: Spatial extent selection method ?

○ Tributary Area

38.038862 -122.265747

Map Outlet Location

● Rectangular Area

Latitude 35 ▾ .0625 ▾ to 35 ▾ .0625 ▾ N

Longitude -104 ▾ .6875 ▾ to -104 ▾ .6875 ▾ E

○ Location

39.723525 -104.973267

Map Location

Figure 9. Screenshot depicting the Santa Rosa grid boundary used when downloading precipitation and open water and tall reference potential evapotranspiration data (Reclamation 2014).

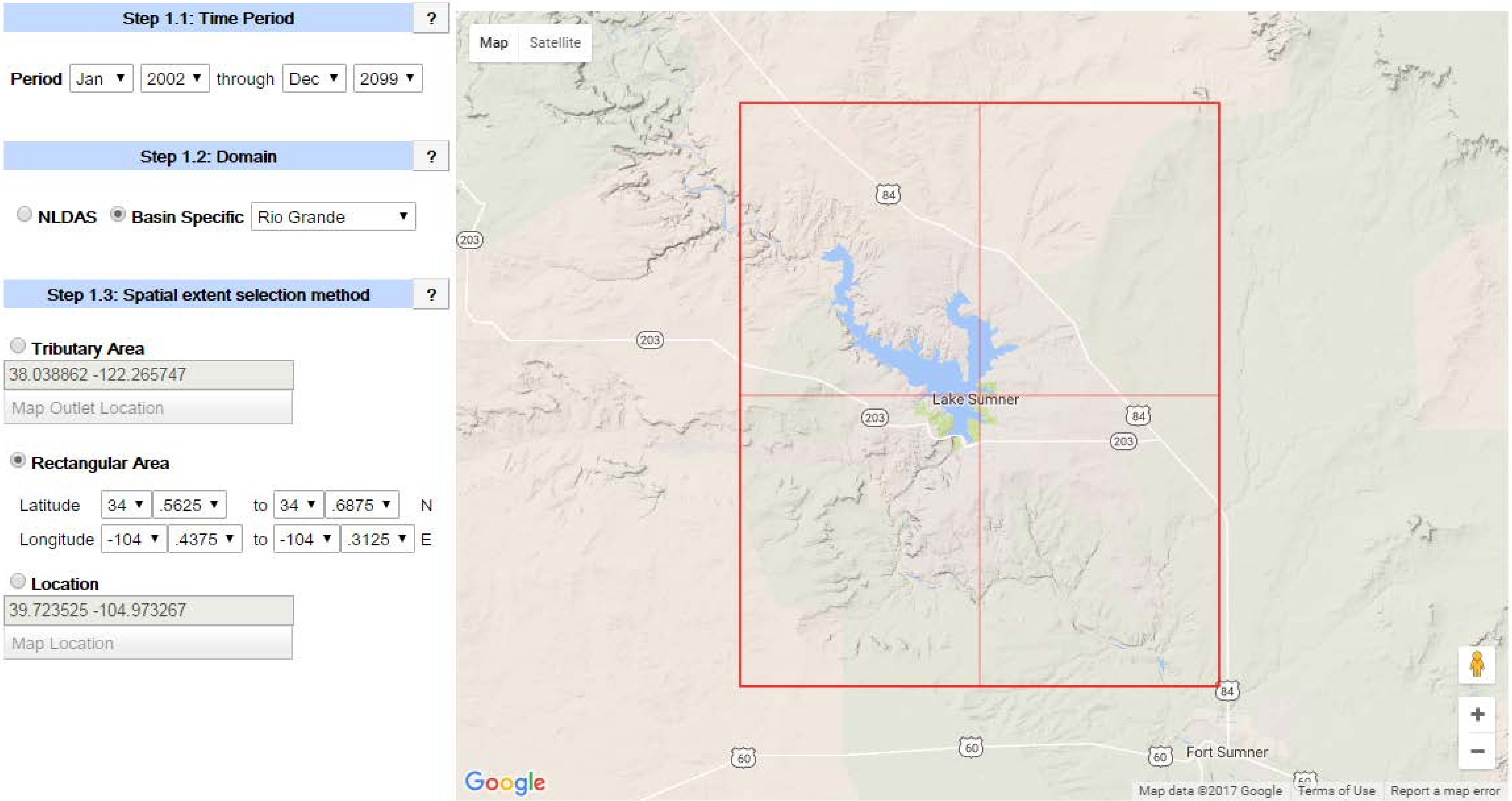

Step 1.1: Time Period ?

Period Jan ▼ 2002 ▼ through Dec ▼ 2099 ▼

Step 1.2: Domain ?

○ NLDAS ● Basin Specific Rio Grande ▼

Step 1.3: Spatial extent selection method ?

○ Tributary Area

38.038862 -122.265747

Map Outlet Location

● Rectangular Area

Latitude 34 ▼ .5625 ▼ to 34 ▼ .6875 ▼ N

Longitude -104 ▼ .4375 ▼ to -104 ▼ .3125 ▼ E

○ Location

39.723525 -104.973267

Map Location

Figure 10. Screenshot depicting the Sumner grid boundary used when downloading precipitation and open water and tall reference potential evapotranspiration data (Reclamation 2014).

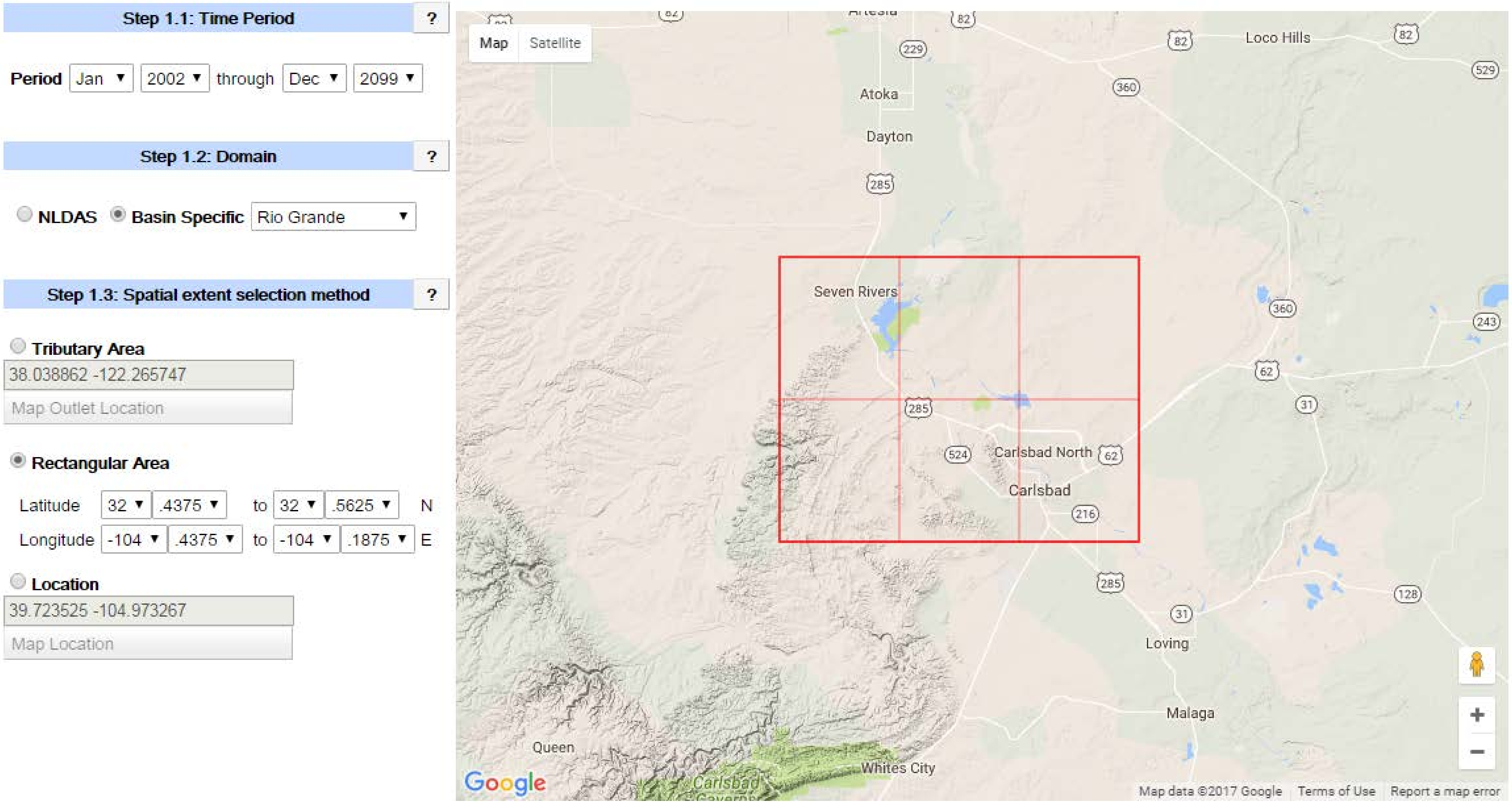

Step 1.1: Time Period ?

Period Jan ▾ 2002 ▾ through Dec ▾ 2099 ▾

Step 1.2: Domain ?

○ **NLDAS** ● **Basin Specific** Rio Grande ▾

Step 1.3: Spatial extent selection method ?

○ **Tributary Area**
38.038862 -122.265747
Map Outlet Location

● **Rectangular Area**

Latitude 32 ▾ .4375 ▾ to 32 ▾ .5625 ▾ N
Longitude -104 ▾ .4375 ▾ to -104 ▾ .1875 ▾ E

○ **Location**
39.723525 -104.973267
Map Location

Figure 11. Screenshot depicting the Brantley and Avalon grid boundary used when downloading precipitation and open water and tall reference potential evapotranspiration (PET) (Reclamation 2014).

To transform the modeled monthly precipitation into daily precipitation for PROM, the nearest tributary flows for each reservoir were used to dictate on which days the precipitation will fall over the reservoir. For the two northern reservoirs (Santa Rosa and Sumner) the two northernmost tributary flows in the modeling area with available gages were used (Rio Hondo and Rio Felix). The flow data from VIC of these two tributaries were first summed together for each GCM. Using the summed flows, precipitation was disaggregated so that the monthly rainfall fell proportionally on the days that the Rio Hondo and Rio Felix had flows. If neither the Rio Hondo nor Rio Felix flowed in a given month, the precipitation was disaggregated evenly throughout all the days of the month. Precipitation at Brantley and Avalon was modeled using the same process, with flows in Rocky Arroyo taking the place of flows in Rio Hondo and Rio Felix.

3.1.3. Evapotranspiration

Evapotranspiration values are required in multiple objects throughout the model. To calculate these values for PROM, GCM data for monthly tall reference and open water potential evapotranspiration (PET) for the five GCMs over the 2010-2099 time period were downloaded from the same sites and projections as precipitation. From the downloaded data, a linear annual trend was developed for the open water potential evapotranspiration at Santa Rosa, along with a tall reference and open water potential evapotranspiration at Sumner and Brantley. To create the trend, the following process was completed for each GCM.

The five downloaded potential evapotranspiration datasets were annually summed and their slope and y-intercept calculated. The slope and y-intercept were used to calculate the percent difference between the beginning and ending years (i.e., 2010 and 2099) and then divided by the total number of years to get the average percent difference per year. This percent difference was then applied to synthetic data to create linear trends.

Evapotranspiration analysis was based on seven different annual synthetic datasets for evapotranspiration. Five of these datasets were already incorporated in the PROM, and the other two obtained from USACE, with some data sets being used for multiple objects in the model.

The dataset used for evapotranspiration from both the Fort Sumner Irrigation District (FSID) and the Carlsbad Irrigation District (CID) was altered as discussed in the next section, for CID, resulting in eight different annual synthetic datasets. Two datasets, Sumner pan evaporation and Brantley/Avalon pan evaporation, were replaced with the USACE's monthly estimates for pan evaporation, as these estimates were much closer when compared to averaged historical data within Reclamation's Hydrologic Data Base (HDB) than what was already in the model.

Santa Rosa pan evaporation used the average monthly values that are within PROM. The datasets within PROM were used during planning runs if no other data is inputted for the pertinent evapotranspiration slot. The annual synthetic datasets are used and repeated in the PROM runs for the 1950-2010 period. For the 2011-2099 period, a linear trend was extracted from one of the five downloaded potential evapotranspiration datasets and applied to one of the eight PROM synthetic datasets for each GCM based on location and potential evapotranspiration type, resulting in eight synthetic evapotranspiration datasets for each individual GCM. The percent differences are applied to the synthetic data using the following equation to create a trend:

$$\boldsymbol{Y_i^j = Y_{2010}^j + (Y_{2010}^j * \beta * (i - 2010))}$$

Where $\boldsymbol{Y_i^j}$ is the new rate for year, and $\boldsymbol{i}$ is the year and $\boldsymbol{j}$ the day of the year; $\boldsymbol{i}$ ranges from 2011-2099 and $\boldsymbol{j}$ ranges from 1-365. For years with a leap day, the leap day (February 29th) is set to equal the value of the previous day (February 28th). $\boldsymbol{Y_{2010}^j}$ is the rate for day j during the year 2010 and $\boldsymbol{\beta}$ is the associated calculated percent increase between any two years for the GCM open water and the tall reference potential evapotranspiration trendline.

Table 3 shows the breakdown on the synthetic evapotranspiration datasets with their associated appendix, model objects, and trends that are applied to them. Figure 12 and Figure 13 show evaporation rates.

Table 3. Synthetic Evapotranspiration Rates

Synthetic Evaporation Data ($\boldsymbol{Y_{2010}^j}$)	Appendix Figure	Associated Model Objects	GCM Calculated Trend Applied ($\boldsymbol{\beta}$)
Santa Rosa Pan Evaporation	Figure 4	• Santa Rosa	Santa Rosa Open Water Trend
USACE's Sumner Pan Evaporation	Figure 4	• Sumner	Sumner Open Water Trend
USACE's Brantley and Avalon Pan Evaporation	Figure 4	• Brantley • Avalon	Brantley/Avalon Open Water
FSID Evapotranspiration	Figure 5	• UpperFSID • LowerFSID	Sumner Tall Reference Trend
CID Evapotranspiration	Figure 5	• CIDDiversion	Brantley/Avalon Tall Reference Trend
Sumner Groundwater Evapotranspiration	Figure 5	• Eastside 1 • Eastside 3 • Eastside 4 • Sumner to FSID • FSID to Sand Gates • Sand Gates to Main Drain • Main Drain to Taiban	Sumner Tall Reference Trend
Sumner Groundwater Pan Evaporation	Figure 5	• Sumner to FSID • FSID to Sand Gates • Sand Gates to Main Drain • Main Drain to Taiban	Sumner Tall Reference Trend
Sumner to Taiban Pan Evaporation	Figure 5	• SumnerToTaiban LossSumnerToFSID • SumnerToTaiban LossFSIDToSandGates • SumnerToTaiban LossSandGatesToMainDrain • SumnerToTaiban LossMainDrainToTaiban	Sumner Tall Reference Trend

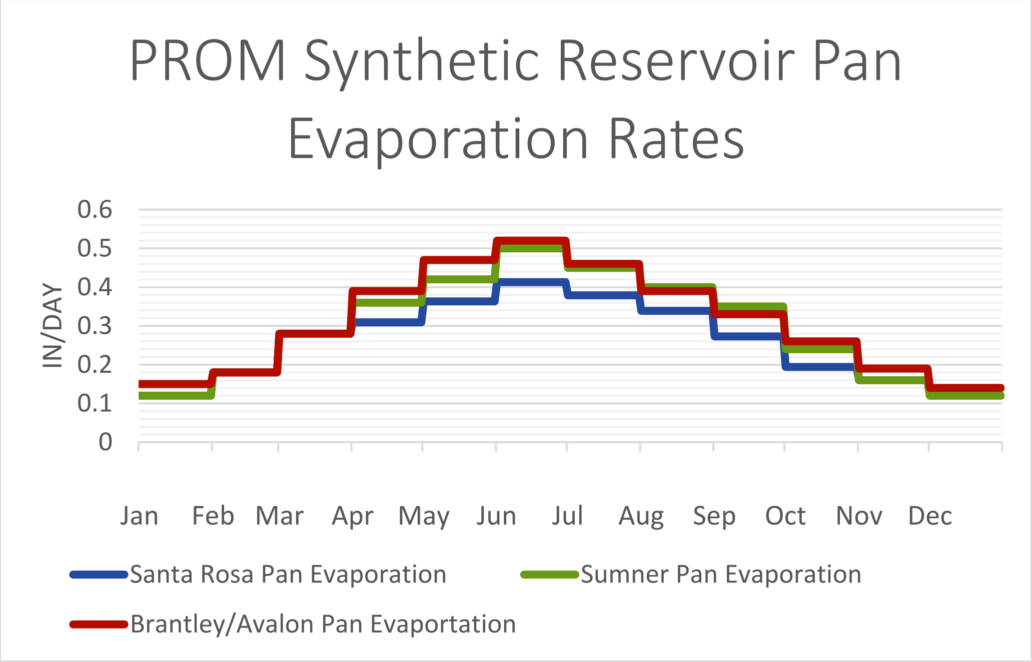

Figure 12. Synthetic data used for the four reservoirs' pan evaporation.

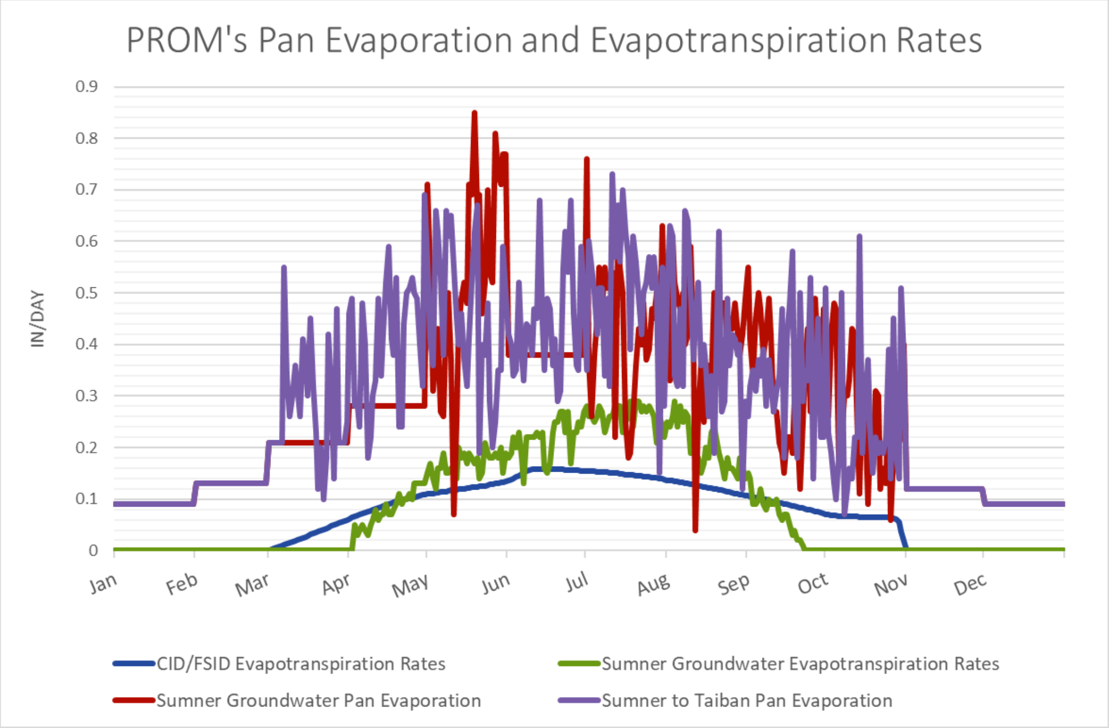

Figure 13. PROM's synthetic data for evapotranspiration and non-reservoir pan evaporation rates.

3.1.3.1. CID Evapotranspiration Data

As an example of the projected evapotranspiration, Figure 14 depicts the end result of projecting CID evapotranspiration into the future, which is then inputted into the RiverWare model. Future changes in irrigation demand for FSID and CID are dependent on changes in evapotranspiration. With increasing evapotranspiration in every storyline, and all else being equal, demand for crop irrigation will increase as a function of increased evapotranspiration. The model runs demonstrate that principle with the following equation used to calculate “requested depletion”:

$$\boldsymbol{Depletion = Irrigated\ Area * Evapotranspiration\ Rate * (1 + Incidental\ Loss\ Rate)}$$

(CADSWES, 2017)

Where ***Incidental Loss Rate*** (conveyance loss from the point of diversion) is a constant. ***Depletion*** in the model is a rough calculation of the needed water to fully irrigate a specified area. ***Depletion*** is then divided by an efficiency factor to get the total amount of water needed to be diverted on any day, known as “requested diversion” in the model. Figure 15 depicts 2010-2099 CID baseline demand (or “requested diversion”) for the five selected storylines.

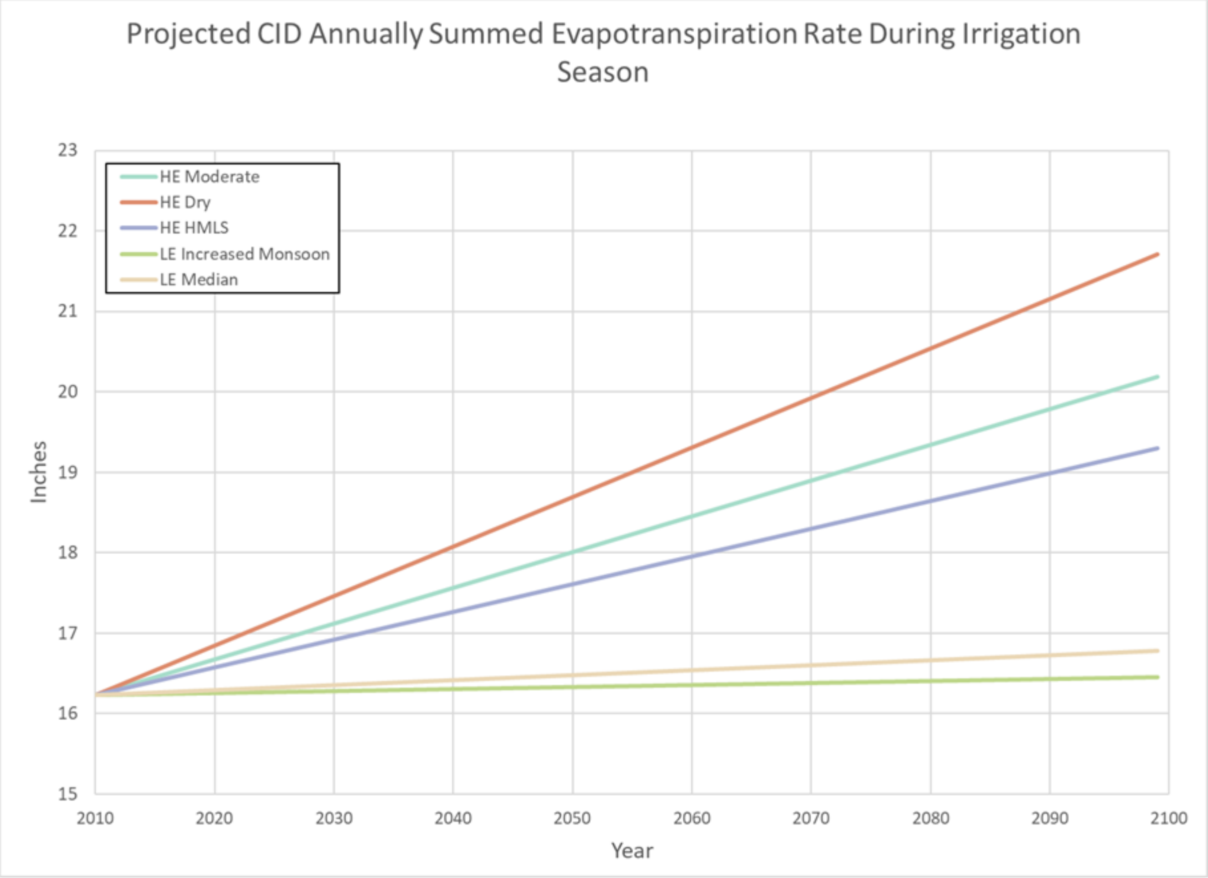

Figure 14. Calculated projected synthetic CID evapotranspiration rates used in the CID diversion object within PROM for the five storylines.

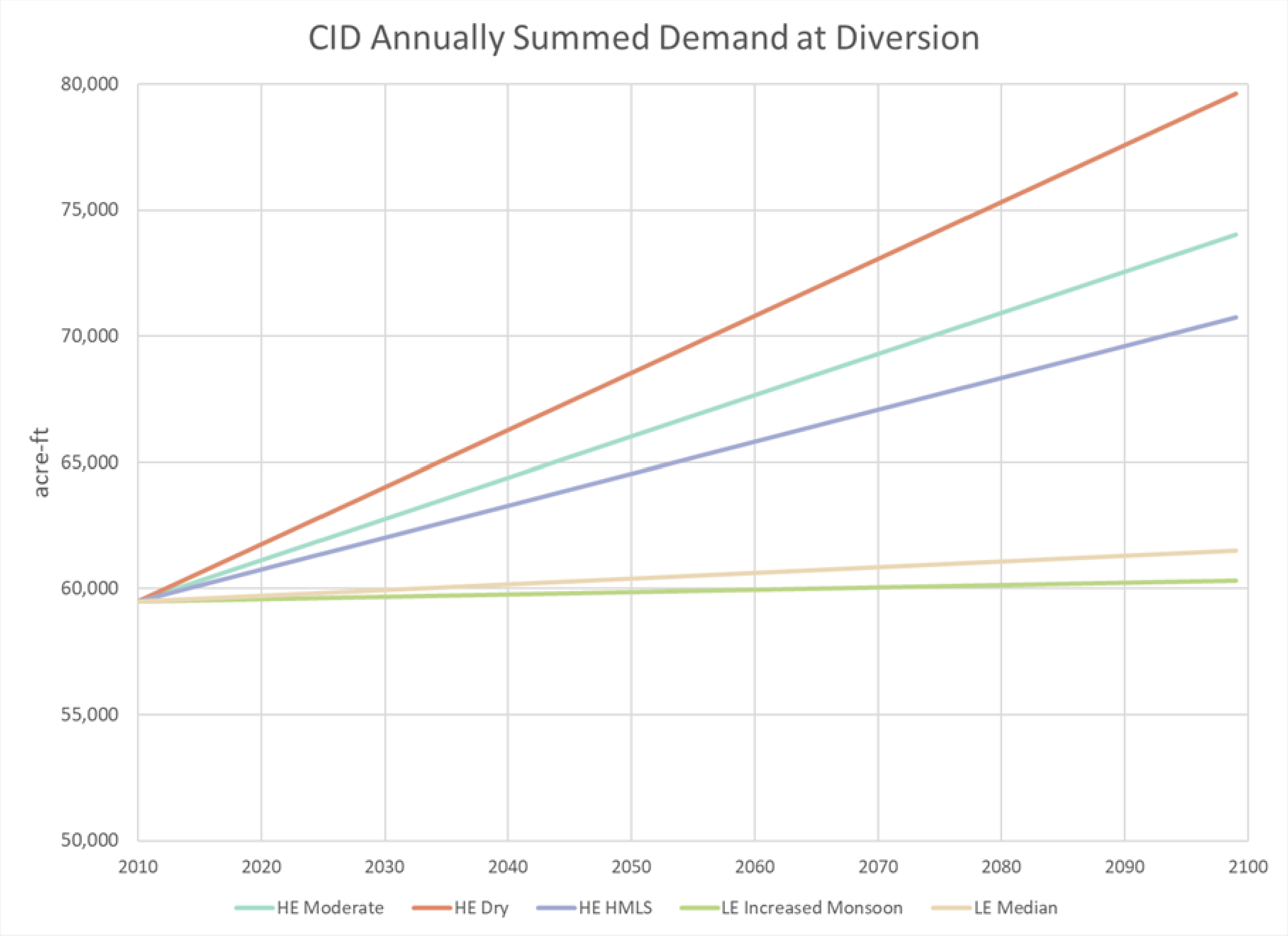

Figure 15. PROM calculated CID demand (requested diversion) for the five storylines.

3.1.3.2. CID Synthetic Evapotranspiration Data

Preliminary runs showed that the synthetic data that was already in PROM produced unrealistically high crop demands, and in turn, unrealistically high shortages. Therefore, CID synthetic evapotranspiration data described in the previous section was altered before going through the process described in Section 3.1.3.1. Using PROM's original synthetic year, it took approximately the maximum CID allotment to have enough water to irrigate ~20,000 acres for the full year. To remedy this issue, a graph was created that showed historic CID diversions and corresponding CID allotments.

When analyzing the years post-2003 Settlement, there seemed to be a slowdown in how much water is taken once CID reaches an allotment of 3 feet-per-acre, which is equivalent to about 60,000 acre-feet passing through CID Main Canal for a given year. Based on that, 60,000 acre-feet passing through CID Main Canal was used as the assumed point at which CID will have a full irrigation season and not have any shortages during an average year. This volume is a broad assumption, as many factors play a role in how much water is needed to fully irrigate a certain amount of crops, but should give a more realistic approximation when analyzing CID shortages. Using how the model calculated depletion, see the equation in section above, and the PROM's CID synthetic evapotranspiration data, a factor was applied to the synthetic evapotranspiration data so that the total amount of diversion requested for an entire year is equal to 30,000 cfs. The final calculated multiplication factor applied to PROM's synthetic CID evapotranspiration data was 0.65 to achieve the 30,000 cfs per year (Figure 16).

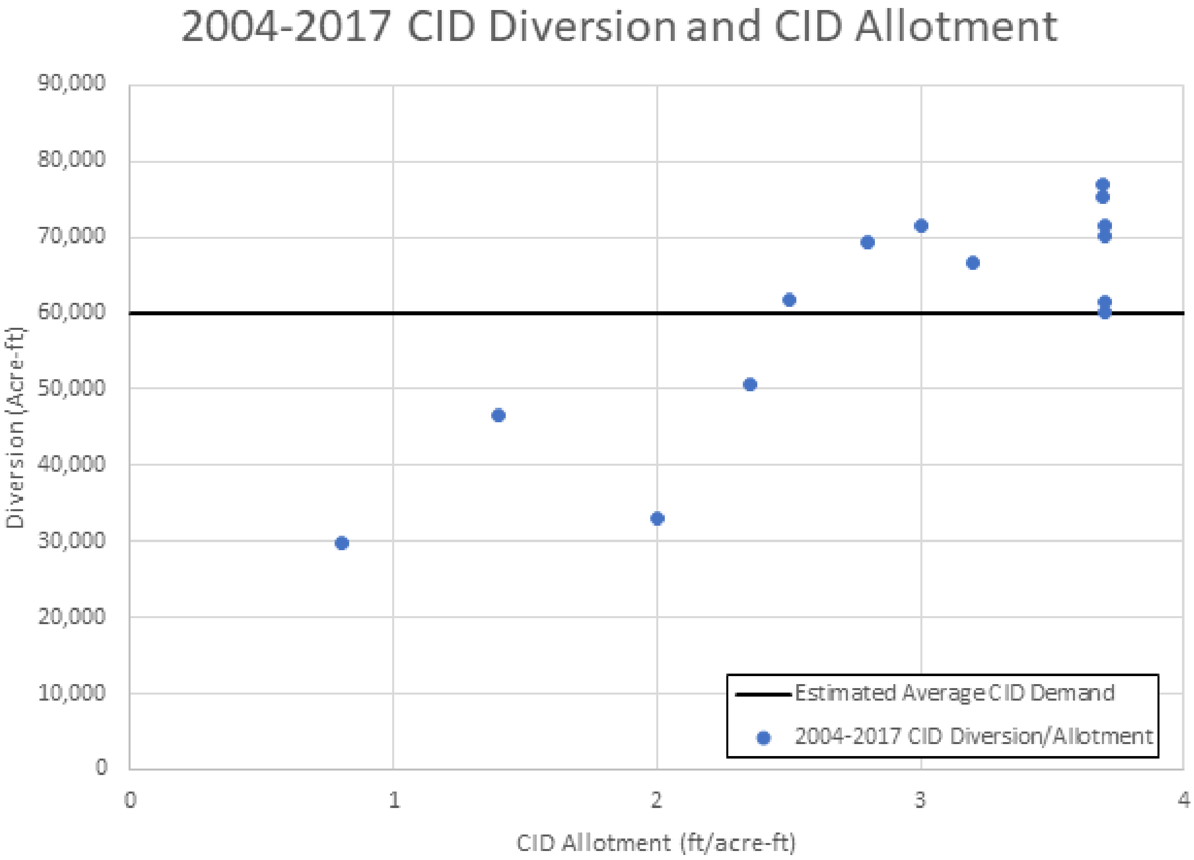

Figure 16. PROM's synthetic CID evapotranspiration data.

3.1.4. Gains and Losses from Acme to Brantley

For the Pecos River Basin Study model runs, a MODFLOW model, Roswell Artesian Basin Groundwater Model (RABGWM) was used to simulate the gains/losses for each storyline between 2010-2099, and the resulting data were used in place of the PROM's gain/loss coefficient calculations for four stretches of the river:

- Acme Gage to Lake Arthur Gage
- Lake Arthur Gage to Artesia Gage
- Artesia Gage to Kaiser Gage
- Kaiser Gage to Brantley Reservoir

Three reach objects were created in the Pecos Basin Study model to incorporate the simulated RABGWM gains/losses into each of the four stretches. Lake Arthur to Artesia already contained a reach object for base inflow in PROM, so the RABGWM simulated gain/losses were simply incorporated into the existing object. The RABGWM simulated gains/losses were converted from monthly values to average daily values to be compatible with the RiverWare model daily timestep. This conversion was done by dividing the monthly value by the number of days in the month. These daily values were then inserted into the appropriate object's designated slot for the 2010-2099 period. For the 1950-2009 model runs, the 2010 gain/loss values were repeated annually.

The BaU Moderate and BaU Dry storylines resulted in negative river flows when river losses from RABGWM were greater than simulated river flow. To offset this negative response, additional model objects were created along each of the four reaches listed above, and a rule was created so that any negative inflow was zeroed out by adding local inflow. An important caveat is that when the river is dry, this knowledge is not transferred to the RABGWM model. RABGWM assumes that the river is continuous in its calculations, thus the river drying in RiverWare is not accounted for in the RABGWM calculations.

An example of the additional objects created for the Acme to Lake Arthur gains/losses is shown in Figure 17.

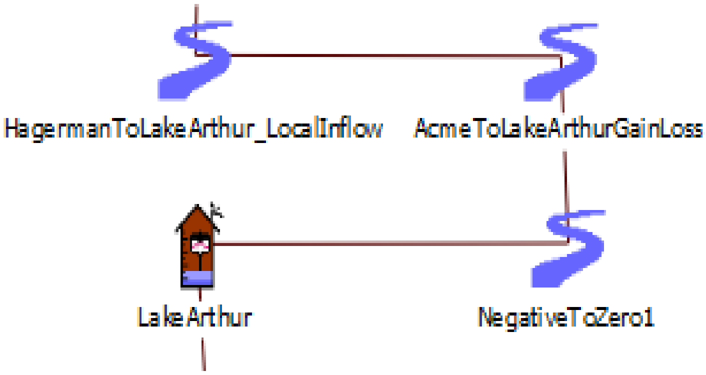

Figure 17. Example of the additional objects created to implement the MODFLOW's gains/losses.

The AcmeToLakeArthurGainLoss object is where Modflow's gains/losses are placed and the NegativeToZero1 is where if the AcmeToLakeArthurGainLoss object calculates a negative outflow, the NegativeToZero1 object will add water to the system to result in 0 cfs flow for that day instead of a negative flow.

3.1.5. Local Inflows and Additional Bias Correction

The Pecos Basin has many minor tributaries and areas where local surface flow can enter in these reaches:

- Local inflow into Santa Rosa
- Santa Rosa to Puerto De Luna
- Puerto De Luna to Sumner
- Acme Local Inflows (Dunlap to Hagerman)
- Hagerman to Lake Arthur
- Lake Arthur to Artesia

A bias correction factor for these areas was applied to each storyline so that the Average modeled 1950-2009 FSID entitlement and CID allotment would equal the historical average FSID entitlement and CID allotment for 1950-2009.

To simulate these local inflows, which are sporadic and not modeled, calculated historic data within PROM for each local inflow were used. Estimates of local inflow were derived from historic 1941-2016 data to generate monthly average values, which were then converted to average daily values (Figure 18). Because the daily values were obtained from monthly values, local inflows are constant during each month and do not exhibit the natural sporadic variability. One thing to note is that there is only one set of monthly averaged values for the Santa Rosa to Puerto De Luna and Puerto De Luna to Sumner local inflows. The one averaged data set is used for both locations. The Santa Rosa to Puerto de Luna reach used the FSID bias correction factor to calculate the modeled historical average for local inflows for the reach, while the Puerto De Luna to Sumner reach used the CID bias correction factor.

For all local inflows except the Acme local inflow, reach objects that were already in the model were used. Adding local inflows into the model required an additional object below Acme Gage due to unrealistic results at the Acme gage because of constant local inflow results from using monthly flow averages to calculate daily values. This would result in flow at the Acme gage rarely, if ever, going below 5 cfs—an unrealistic result that would preclude a proper analysis of river drying on the Pecos, which in reality occurs fairly frequently. Acme flow dropping below 5 cfs is an indicator of the beginning of river intermittency between the Taiban and Acme Gage, a major physical phenomenon being analyzed as part of this study.

After calculating historical monthly averages for each local inflow point, also referred to as synthetic local inflows, a multistep process was taken to not only estimate interannual variations in local inflows, but also to bias correct the synthetic local inflows based on the storylines, so that the storylines’ 1950-2009 average FSID entitlement and CID allotment equal historical averages.

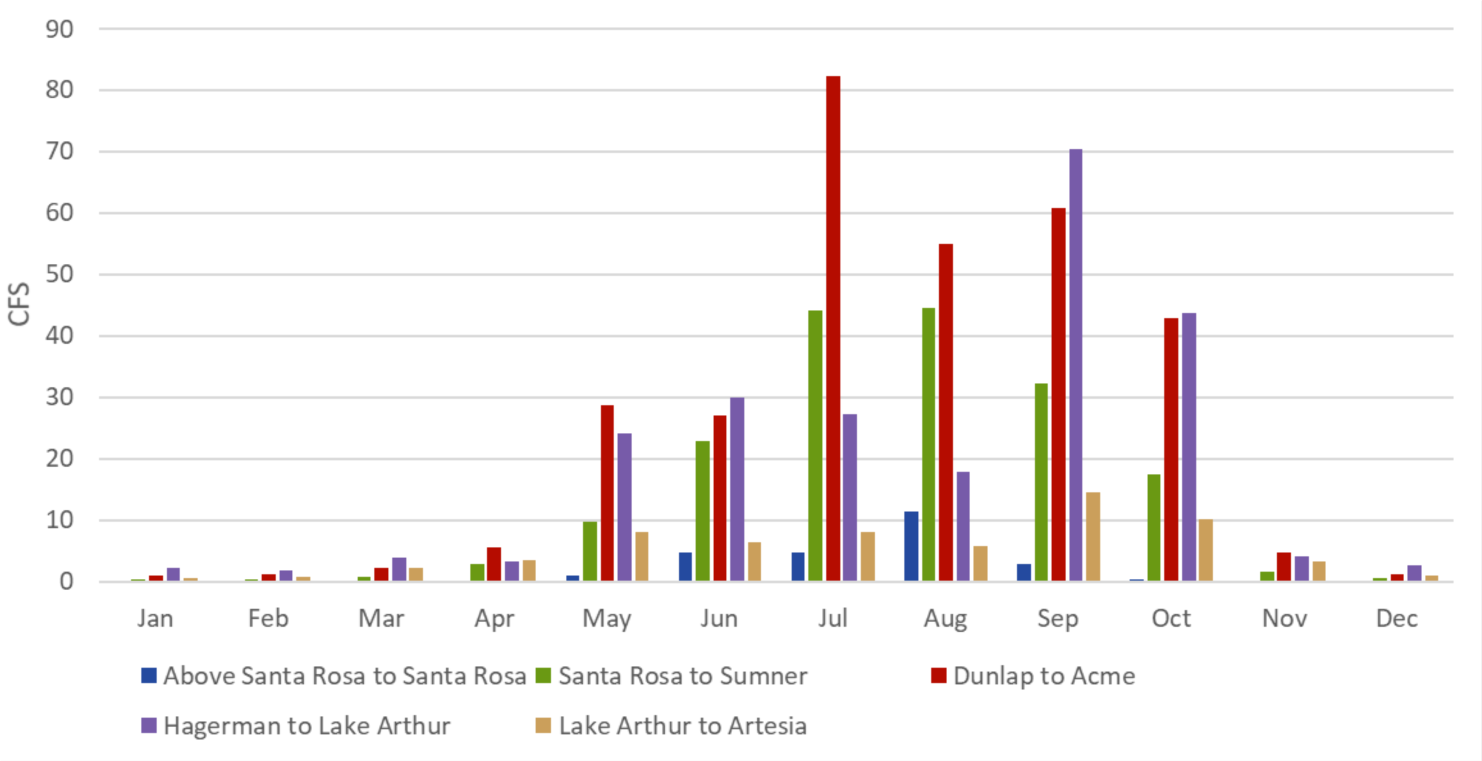

Figure 18. Historical monthly averaged flow in cfs for local inflows.

To incorporate annual variability in the synthetic local inflows, variability in gaged tributary flows was used as a proxy for estimating local inflows. Total annual flows were calculated for each year from 1950 to 2009 for the Rio Hondo, Rio Felix and Rio Peñasco. The Rio Hondo and Rio Felix were averaged to represent variability in local inflows to the northern reaches (Acme to Hagerman and above) while the Rio Felix and Rio Peñasco were averaged to represent variability in local inflows to the lower reaches. For each year, the ratio of the total annual flow relative to the long-term average for the tributary pair was calculated, and this ratio was applied to that year’s local inflows for the respective stream reaches using that tributary pair as a proxy. For example, in a year in which the Rio Hondo and Rio Felix collectively averaged 10% more flow than normal, synthetic local inflow data for that year for the four upstream reaches were estimated by adding 10% to the synthetic average daily values for each day of the year. The below equation represents the calculations up to this point.

$$X_i^j = S^j * \frac{\left((H_i + F_i) - (\overline{H + F})\right)}{(\overline{H + F})}$$

Where:

X_i^j is the local inflow for any given day,

i is the year (1950-2009)

j the day of the year. (1-365). For years with a leap day, the leap day (February 29th) is set to equal the value of the previous day (February 28th).

H_i and F_i are the summed annual flows for a given year for the Rio Hondo and Rio Felix (or Rio Felix and Rio Peñasco), respectively. ($\overline{H+F}$) is the average annual flow of the Rio Hondo plus Rio Felix (or Rio Felix and Rio Peñasco) between 1950-2009.

S^j is the synthetic value for one of the local inflows for a given day of the year. Note that this equation applies only to the reaches from Acme northwards, Rio Hondo (H) would be replaced with Rio Peñasco (P) local inflows associated with reaches south of Acme.

This process results in daily values for 6 local inflows for 5 storylines.

The final step done to the 1950-2009 local inflows was adding a bias-correction factor to each local inflow so that the averaged historical FSID entitlement and CID allotment equaled the modeled historical value for each storyline. For this process the local inflows were separated so that the local inflow that effects FSID (i.e., Santa Rosa to Puerto de Luna local inflow) would be bias corrected first. This first correction is because this local inflow affects both FSID entitlement and CID Allotment, while the other local inflows affect the CID Allotment only. A bias correction factor for each storyline was calculated so that when applied to the Santa Rosa to Puerto de Luna local inflow, the averaged historical 1950-2009 FSID entitlement would equal the averaged FSID entitlement modeled in each storyline. After this factor was found for each storyline for the Santa Rosa to Puerto de Luna local inflow, a factor was similarly calculated for the rest of the local inflows, determined based off of the CID allotment. This results in two different factors, one for the local inflow that effects FSID (FSID factor) and one for the local inflows that only effect CID (CID factor) for each storyline. Table 4 shows the final FSID and CID factors.

Table 4. Bias Correction Factors

Storyline	FSID Factor	CID factor
BaU Moderate	0.39	0.50
BaU Dry	0.32	0.60
BaU HMLS	0.33	1.56
RE Increased Monson	0.28	0.04
RE Median	0.18	0.31

These factors are applied across not only 1950-2009, but for the entire 1950-2099 period. Figure 19 shows the final 1950-2009 local inflow for each storyline for Lake Arthur to Artesia.

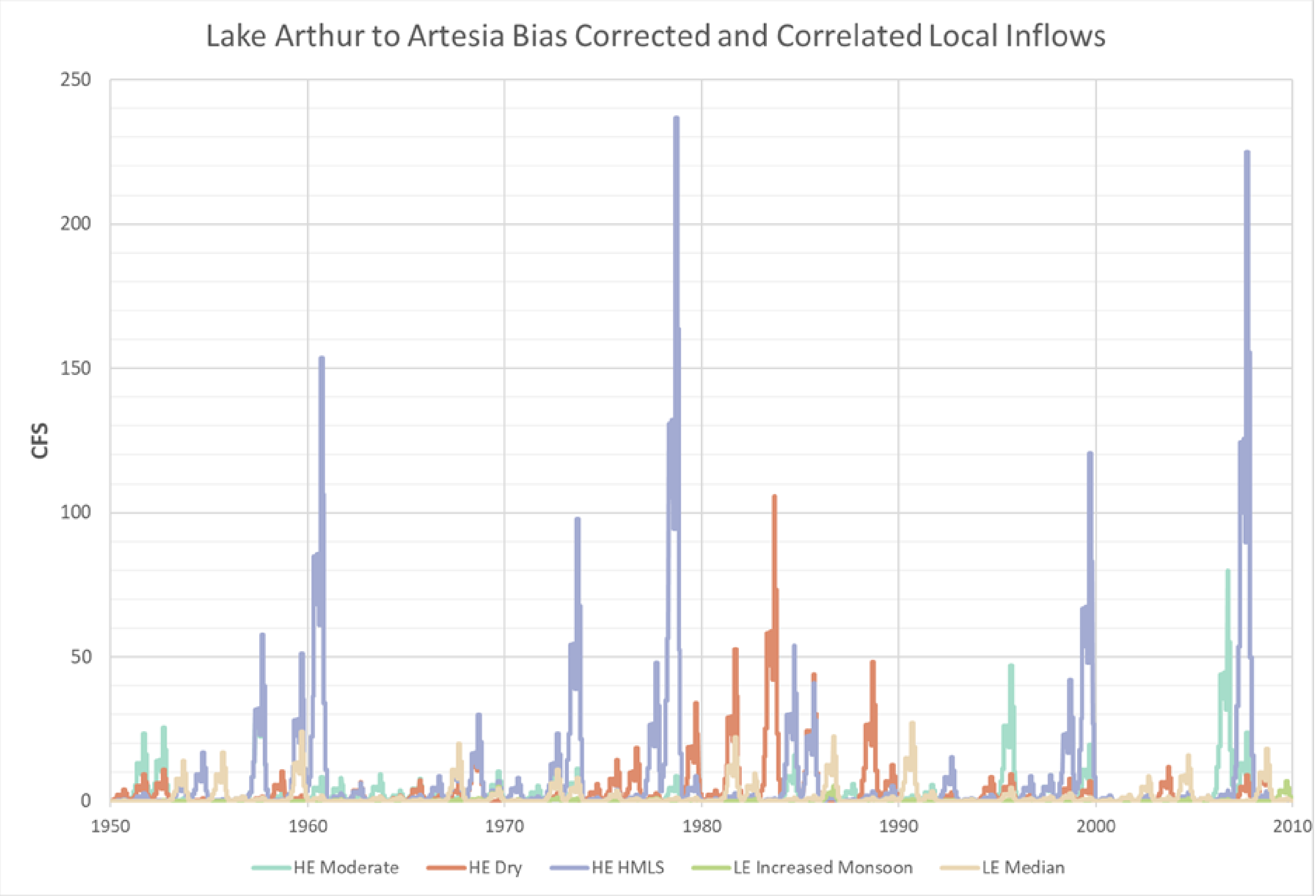

Figure 19. Final modeled 1950-2009 local inflows for each storyline for Lake Arthur to Artesia. These local inflows incorporate both bias-correction and correlating the flows to the nearest tributaries.

The next step to incorporate local inflows was adding a trend to represent each storyline for post-2010. For each storyline, the same tributary pairs that were used to add annual variability to the historical local inflows were used to model future local inflows. The projected trends in these tributary flows were modeled for each storyline, and values for average flow in each tributary pair in 2010 and 2099 were calculated. Using these two values, a single linear trend was estimated for each storyline, in the form of a percentage change each year relative to the year 2010. This percent difference was then applied to the bias-corrected synthetic annual local inflow data for each reach starting with 2010 by using the following equation:

$$\boldsymbol{Z_i = Z_{i-1} + (Z_{2010} * P)}$$

Where:

$\boldsymbol{Z_i}$ is the local inflows for specified year, and

$\boldsymbol{i}$ is the year ranging from 2011-2099.

$\boldsymbol{Z_{i-1}}$ is the previous year’s annual local inflow,

Z_{2010} is the bias-corrected synthetic annual local inflow in 2010, and

P is the percent change as estimated from the pertinent tributary pair.

To add interannual variability to the future projections of local inflows, first the total modeled flows for the 2010-2099 period were calculated, along with the annual flows for each year. Then, each year’s flows were converted to a percentage of the total flows in the entire period, and this was multiplied by the sum of $\mathbf{Z}$ (i.e. the total local inflows to a given reach over the entire period) to provide an annual value of local inflows for each year that corresponds to the modeled behavior of the proxy tributaries in that year. The resulting output is a suite of annual local inflows that have been bias corrected, vary dependent on interannual variations in associated modeled tributary flows, and follow the same overarching trends as these associated tributaries. The final step is to break the annual values into daily ones by using the original bias-corrected synthetic daily data to proportionally calculate each day for every storyline and local inflow.

The local inflows added between 1950 and 2009 was the amount necessary for the modeled historical average FSID entitlement and CID allotment in each storyline to equal the 1950-2009 historical averages. Post-2010, a trend is applied to the local inflows based on nearby tributary modeled flows, resulting in an increase or decrease in the local inflows by 2070-2099.

Figure 20 is a depiction of the average difference between 1950-2009 local inflows and 2070-2099 local inflows. Figure 21 shows the same local inflows as Figure 19, i.e. Lake Arthur to Artesia, only for 2010-2099.

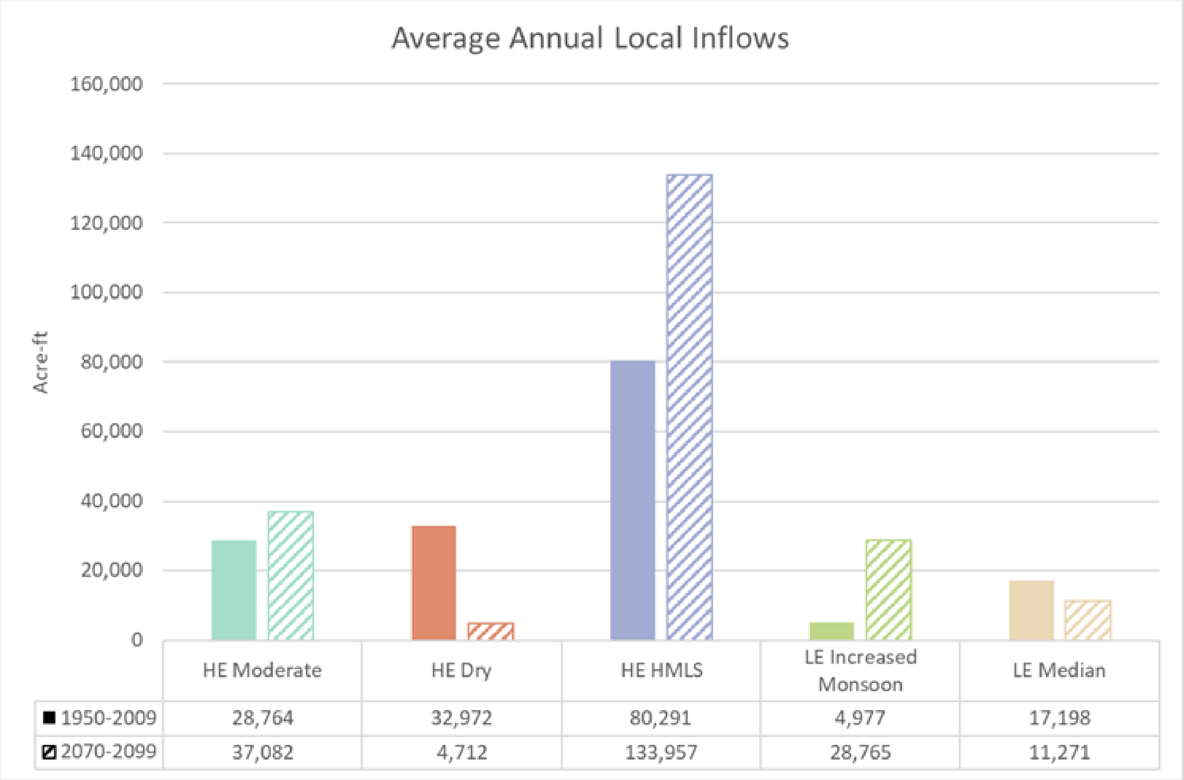

	HE Moderate	HE Dry	HE HMLS	LE Increased Monsoon	LE Median
■ 1950-2009	28,764	32,972	80,291	4,977	17,198
▨ 2070-2099	37,082	4,712	133,957	28,765	11,271

Figure 20. Average annual local inflows added to PROM for 1950-2009 and 2070-2099.

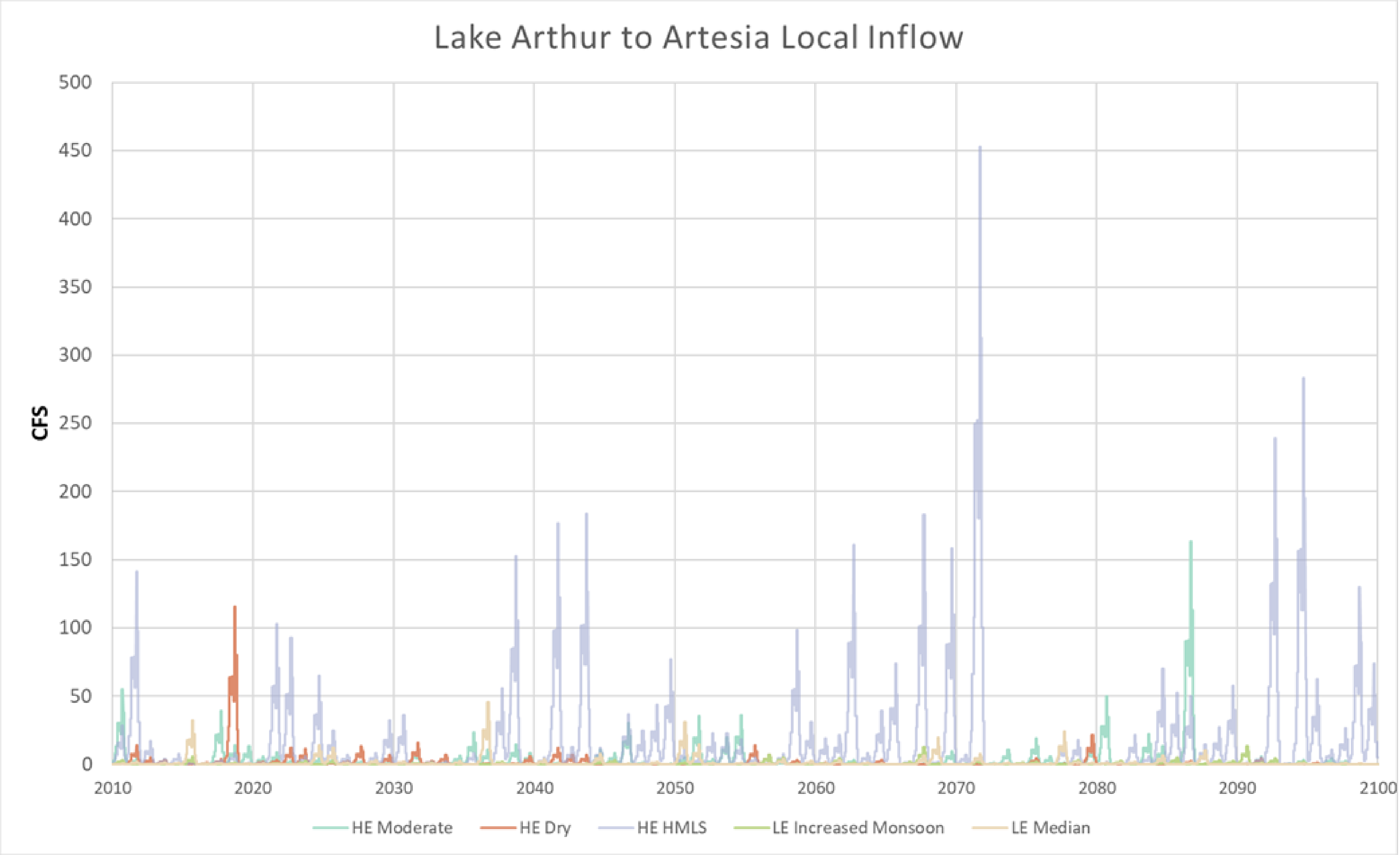

Figure 21. Final 2010-2099 local inflows for each storyline for Lake Arthur to Artesia. These local inflows incorporate both bias-correction, correlating the flows to the nearest tributaries, and the trends of the nearest tributaries.

3.2. Surface Water Irrigation Districts Implementation

3.2.1. Fort Sumner Irrigation District

FSID's entitlement is based on an the sum of the two-week average gaged flow at the Puerto De Luna Gage and Above Santa Rosa Gages, minus the Below Santa Rosa gage, representing the "natural flows" of the Pecos (i.e., what would arrive at the Fort Sumner Diversion Dam if Santa Rosa and Sumner Reservoirs did not exist). In PROM, the entitlement calculation is done daily instead of a two-week average. Also in PROM, Puerto De Luna baseflow varies between 59 cfs during the summer to 85 cfs in the winter. This was an average calculation for the baseflow, based on historical data and added to the model during PROM's creation. This yearly fluctuation was left alone and assumed constant through all time periods and storylines, because generally, baseflow in the Santa Rosa area has been steady throughout the period of record. In addition, there was no modeling done of this baseflow or knowledge of how it would change in the future, especially in terms of each storyline. It is always assumed that FSID diverts their full allotment even if they do not use all of it, except when they forebear, which is generally consistent with normal operations.

For FSID, shortages were analyzed and calculated by the following equation:

$$\boldsymbol{Diversion\ Shortage} \\ = \boldsymbol{Max}(\boldsymbol{Depletion}/\boldsymbol{Efficiency} - \boldsymbol{Amount\ Diverted}, \mathbf{0})$$

Where:

$$\boldsymbol{Depletion} = \boldsymbol{Irrigated\ Area} * \boldsymbol{Evapotranspiration\ Rate} * (\mathbf{1} \\ + \boldsymbol{Incidental\ Loss\ Rate})$$

(CADSWES, 2017)

Where:

Efficiency (representation of irrigation efficiency and is the value within "Minimum Efficiency" slot in PROM) is 50%,

"***Incidental Loss Rate***" is 15%, and

"***Irrigated Area***" is 5,859 acres (4,687.2 acres for Upper FSID and 1,171.8 acres for Lower FSID).

The amount diverted by FSID can be greater than their irrigation requirements, resulting in a negative value for shortages, hence the maximum within the diversion shortage equation. These equations, which are generally standard in calculating shortages in RiverWare, are overridden in PROM due to how the FSID entitlement calculation works. To remedy this, shortages were calculated using the same method in an Excel spreadsheet as a post-processing step.

3.2.2. Carlsbad Irrigation District

In PROM, the CID “Irrigation Diversion Requested” is based on a diversion ratio that is user specified in the model setup. This diversion ratio is calculated using average historic releases to CID on any given day based on nearest 0.5 foot-per-acre CID allotment (i.e., 0.5, 1, 1.5, 2, 2.5, 3, 3.5 foot-per-acre). Irrigation depletions in the model are calculated from evapotranspiration rates which do not coincide with the diversion ratio in the model. This discrepancy results in the “Requested Diversion” and “Depletion” slots not matching up, which can create additional shortages when none should exist. When using the PROM for accounting and annual planning runs, “Depletion” and “Shortages” for CID are not evaluated, so this discrepancy is not an issue. However, the Pecos Basin study requires “Diversions” driven by “Depletions” so that estimated shortages at CID can be effectively analyzed. To compete this task, three rules from the PROM 7.0 ruleset (i.e., *CID Depletion Equals Diversion*, *CID Diversion Requested*, and *Zero CID Diversion Requested*) were turned off. Turning those three rules off allows the model to calculate diversion requested for CID based on calculated “Depletions” instead of being tied to the “Incoming Available Water”. This change, in turn, allows the model to calculate “Diversion Shortage” based on “Depletions” instead of having it equal to zero for the entire run. The “Incoming Available Water” remains a function of CID allotment and is calculated by the following equation from the *CID Unrestricted Water Supply* and *CID Restricted Water Supply* rules in the PROM 7.0 ruleset:

$$\begin{aligned} &\boldsymbol{Incoming\ Available\ Water} \\ &= \boldsymbol{Min}\left(\boldsymbol{Min}\left(\frac{\boldsymbol{CurrentCIDDiversionRate} * \boldsymbol{Irrigated\ Acreage}}{\boldsymbol{DeliveryEfficiency}}\right.\right. \\ &\left.* \boldsymbol{DiversionRatio}, \boldsymbol{Max\ CID\ Diversion}\right), \boldsymbol{Max}\ (\boldsymbol{Water\ Currently\ Available\ in\ Avalon}, \mathbf{0})\Big) \end{aligned}$$

Where:

> ***DiversionRatio*** is a constantly updated value taking into account CID Allotment and the use of Black River water.
>
> ***CurrentCIDDiversionRate*** is a look-up value based on the CID allotment and historical percent of water used out of that allotment for any given day of the year.

As ***CurrentCIDDiversionRate*** values are based on historical diversion values, these values were modified to reflect calculated demand instead of historical averages. These changes result in the ***CID.Diversion*** being completely reliant on the model calculated irrigation demand, driven mainly by evapotranspiration. “Diversions” and “Depletions” for both *CID Diversion*, and, *UpperFSID* and *LowerFSID* assume a full irrigation season for all irrigated acres (20,055 acres for CID and 5,859 acres for FSID). These changes also required increasing Avalon’s target storage from 1,500 to 2,000 acre-ft within *Triggers.Storage* so that Avalon would hold sufficient water to contend with the new *CID.Diversion Requested* values that resulted from these changes. CID still calculates shortages the same way FSID does, using the equations in the FSID section. For CID, the efficiency is 0.5 and the incidental loss rate is 10%.

3.3. Settlement Implementation

As part of the additions added to PROM for the Pecos Basin Study, a yearly Settlement Delivery value is estimated, representing water released from Brantley Reservoir for delivery to the state line in accordance with the 2003 Pecos Settlement (See Sectin 3.1.3. *Pecos Settlement Agreement* in the main report). Calculating the Settlement Delivery value requires first calculating the Project Water Supply. The model annually estimates Project Water Supply on November 1st using the following equation:

$$\text{Project Water Supply} = \text{Total Volume of Water Diverted to CID that Year} + 0.65 * \text{Santa Rosa Storage} + 0.75 * \text{Sumner Storage} + \text{Brantley Storage} + \text{Avalon Storage}$$

The storage values used are the storages for the day prior to the calculation (i.e., October 31st). If the Project Water Supply is less than 50,000 acre feet, then the release for the settlement is zero. If the Project Water Supply is between 50,000 acre feet and 90,000 acre-ft, then the following equation is used:

$$\text{Settlement Release} = \frac{50{,}000\ \text{acre}-\text{ft}}{(25{,}055\ \text{acre}-\text{Total acres in CID owned by ISC}) * 1.35\ \text{carriage loss}} * \text{Total acres in CID owned by ISC} * 1.176\ \text{carriage loss}$$

If the Project Water Supply is above 90,000 acre-ft then the following equation is used:

$$\text{Settlement Release} = \frac{90{,}000\ \text{acre}-\text{ft}}{(25{,}055\ \text{acre}-\text{Total acres in CID owned by ISC}) * 1.35\ \text{carriage loss}} * \text{Total acres in CID owned by ISC} * 1.176\ \text{carriage loss}$$

Based on Project Water Supply, the Settlement Release is determined using the appropriate equation, and released at a constant rate over the month of November.

3.4. Drought and Drying Analysis

Two methods were used to analyze drought and drying conditions along the Pecos River for the Pecos Basin Study: the flow at Acme Gage and the percent bypass available at FSID.

3.4.1. Drying at Acme

The Acme Gage discharge has been used to inform flow management decisions to meet the objective to keep the river continuously flowing since 2003. Since 2000, there have been 5 years that had significant drying along the Pecos River (i.e., 3 years with over 100 days in which flows at Acme dropped below 5 cfs and 2 years with 50 to 100 days). Intermittency of the Pecos River between the USGS Taiban and Acme Gages (shown in the map in Figure 9 in Section 2.2.3. *Surface Water/Groundwater Interactions*) generally begins to occur once the Acme Gage drops below 5 cfs. Therefore, in the model drying at Acme is defined as an average daily discharge of under 5 cfs at the Acme Gage. Drying at Acme only occurs between May through November. The model uses criteria from the 2016 BO to try to simulate keeping the river continuous for the entire run period. However, active management of the river to minimize drying has only occurred since 2003. Since the model is assuming active management over the entire run, model results during 1950-2009 indicate fewer drying days than actually occurred in that time.

Because of this, flow at Acme gage was analyzed in the model to demonstrate drying for the three storylines over the 150-year time frame. PROM recently went through a few modifications to model different requirements called for within the 2016 BO. The 2016 B called for water management changes that resulted in changes on how the reach associated with the Acme gage is modeled and operated in terms of target flows. These operational changes resulted in rules prioritizing different flow rates at the Acme and Taiban gages, depending on how wet/dry the year is. This flow prioritization decreases the amount of times flow at Acme drops below 5 cfs in the model, resulting in lower simulated drying percentages compared to previous historic HDB values. This comparison is present in the analysis and comparison in the main text and graphs.

3.4.2. FSID Bypass Flows

Bypass is available when FSID receives their maximum 100 cfs entitlement, which allows additional water sent downstream to continue flowing in the main channel of the Pecos River. The 2016 Biological Opinion (2016 BO, USFWS 2017) has multiple criteria for determining if a year is critically dry, one of which is calculating the percentage of time during irrigation season that bypass is available at FSID. If the percentage of time that bypass is available during irrigation season is 20% or lower, then that year is considered critically dry.

FSID is entitled to divert up to 100 cfs of the natural flow of the river during irrigation season (termed “Entitlement”). While FSID’s entitlement is calculated on a two-week average, we modeled this entitlement on a daily basis. The model assumes that FSID will always take their entire entitlement. The model also assumes that while groundwater gains between Santa Rosa Reservoir and Sumner Reservoir may vary daily, they are constant year-to-year. Similar to reality, the model calculates FSID’s entitlement by taking the sum of the Above Santa Rosa Gage and the Puerto De Luna Gage minus Santa Rosa Reservoir outflow. As both of these gages are above the effects of the irrigation districts, none of the Water Footprints and Water Management Strategies caused any changes to FSID’s baseline entitlements. Because this was one of the two parameters that PROM was bias-corrected to for the 1950-2009 period, both the modeled and observed 1950-2009 average FSID entitlement are equal to each other.

As the FSID entitlement in the model is calculated daily instead of every second week, a 5 cfs buffer is applied when evaluating the percent of time that irrigation season had bypass.

3.5. CMIP Acknowledgements and Permissions

3.5.1. Acknowledgements

"We acknowledge the World Climate Research Programme's Working Group on Coupled Modelling, which is responsible for CMIP, and we thank the climate modeling groups (listed in the table below) for producing and making available their model output. For CMIP the U.S. Department of Energy's Program for Climate Model Diagnosis and Intercomparison provides coordinating support and led development of software infrastructure in partnership with the Global Organization for Earth System Science Portals."

3.5.2. Modeling Groups and Their Terms of Use

The "official" model and group names given in the table below should be used in all presentations and publications (e.g., in tables and figure legends).

Output from yellow highlighted models is available for unrestricted use. Output from the others may only be used for non-commercial research and educational purposes. [See complete "Terms of Use": http://cmip-pcmdi.llnl.gov/cmip5/terms.html]

Modeling Center (or Group)	Institute ID	Model Name
Commonwealth Scientific and Industrial Research Organization (CSIRO) and Bureau of Meteorology (BOM), Australia	CSIRO-BOM	ACCESS1.0
Beijing Climate Center, China Meteorological Administration	BCC	BCC-CSM1.1 BCC-CSM1.1(m)
Canadian Centre for Climate Modelling and Analysis	CCCMA	CanESM2
National Center for Atmospheric Research	NCAR	CCSM4
Community Earth System Model Contributors	NSF-DOE-NCAR	CESM1(BGC) CESM1(CAM5)
Centro Euro-Mediterraneo per I Cambiamenti Climatici	CMCC	CMCC-CM
Centre National de Recherches Météorologiques / Centre Européen de Recherche et Formation Avancée en Calcul Scientifique	CNRM-CERFACS	CNRM-CM5
Commonwealth Scientific and Industrial Research Organization in collaboration with Queensland Climate Change Centre of Excellence	CSIRO-QCCCE	CSIRO-Mk3.6.0

LASG, Institute of Atmospheric Physics, Chinese Academy of Sciences and CESS,Tsinghua University	LASG-CESS	FGOALS-g2
The First Institute of Oceanography, SOA, China	FIO	FIO-ESM
NOAA Geophysical Fluid Dynamics Laboratory	NOAA GFDL	GFDL-CM3 GFDL-ESM2G GFDL-ESM2M
NASA Goddard Institute for Space Studies	NASA GISS	GISS-E2-R
National Institute of Meteorological Research/Korea Meteorological Administration	NIMR/KMA	HadGEM2-AO
Met Office Hadley Centre (additional HadGEM2-ES realizations contributed by Instituto Nacional de Pesquisas Espaciais)	MOHC (additional realizations by INPE)	HadGEM2-CC
Institute for Numerical Mathematics	INM	INM-CM4
Institut Pierre-Simon Laplace	IPSL	IPSL-CM5A-MR IPSL-CM5B-LR
Japan Agency for Marine-Earth Science and Technology, Atmosphere and Ocean Research Institute (The University of Tokyo), and National Institute for Environmental Studies	MIROC	MIROC-ESM MIROC-ESM-CHEM
Atmosphere and Ocean Research Institute (The University of Tokyo), National Institute for Environmental Studies, and Japan Agency for Marine-Earth Science and Technology	MIROC	MIROC5
Max-Planck-Institut für Meteorologie (Max Planck Institute for Meteorology)	MPI-M	MPI-ESM-MR MPI-ESM-LR
Meteorological Research Institute	MRI	MRI-CGCM3
Norwegian Climate Centre	NCC	NorESM1-M

4. PROM Set-up for Strategy Runs of the Pecos River Basin Study

This section discusses important aspects of and alterations to the RiverWare® Pecos River Operations Model (PROM) for the strategy runs of the Pecos River Basin Study. For additional information about PROM see Reclamation 2020.

4.1. Strategies and Water Footprints Overview

Two main overall Water Management Strategies were modeled:

- **Reducing Irrigation Water Consumption within Each Irrigation District.** This group of Water Management Strategies looked at the potential impacts of reducing irrigation water consumption in each irrigation district.

- **Increasing On-Farm Efficiency in Surface-Water Irrigation Districts.** Increasing irrigation water-use efficiency involves improvements to on-farm efficiency (i.e., increasing the proportion of water applied to crops that is used by those crops, and reducing the proportion that is either lost to evaporation or runs off or infiltrates to surface or groundwater).

For a description of the strategies, see Section 7.1. in the main report.

4.2. Reducing Irrigation Water Consumption within Each Irrigation District

The Reducing Irrigation Water Consumption within Each Irrigation District Strategies were selected based on the results of the BaU Moderate storyline baseline run and modeled with a percent reduction to irrigated acreage.

In BaU Moderate storyline’s preliminary PROM runs, the 20% and 25% Reduction to Districts strategies resulted in the 2070 to 2099 average FSID entitlement and CID allotment approximately equal to what those variables were in the 1950 to 2009 period. For most parameters, the final values for 2070 to 2099 for the BaU Moderate Storyline for the 20 and 25% Reductions to Districts strategies ended up being less similar to the 1950 to 2009 values than the preliminary results. To choose when these reductions would be modeled, the Moderate Baseline storyline was again analyzed. The reanalysis showed consistent results until around the year 2055. After 2055 FSID annual daily diversion shortage increased, Acme drying increased, CID shortage’s increased, CID allotment decreased, and Settlement releases decreased in comparison to the rest of the run. It is at this apparent threshold point in the model that the 20% and 25% reductions to CID and

FSID were implemented, so that both CID and the Settlement deliveries would stay relatively consistent with pre-2055 values. To keep the reduction in acreage to all irrigation districts equal to reduction of acreage to only PVACD an additional 5% was added to PVACD so that the acreage reduced in the 20% to all irrigation districts is about equal to 25% acreage reduced in PVACD. This also applies to the acreage reduced in the 25% to all irrigation districts about equal to the 30% acreage reduced in PVACD.

The effect of changes in pumping/stresses on the Roswell Artesian Basin takes about 10 years to be reflected in changes in baseflow to the river. Because of this 10-year lag, PVACD pumping was reduced from the model ten years earlier, in 2045, to allow for the reductions in groundwater pumping in RABGWM to affect the gains/losses that are inserted into the altered PROM model by 2055.

These model strategies required three additional RABGWM runs that had PVACD reducing their acreage by 20%, 25%, and 30% in 2045. These acreage reductions provided new gains/losses for the Acme to Brantley stretch of the Pecos for the associated PROM runs. For the 25% and 30% reductions to PVACD runs, the new gains/losses were the only parameters that had to change in PROM. The reduction of acreage to all three irrigation districts not only required changing the groundwater gain/losses, but also required manipulation in the "Irrigated Area" slot in the *UpperFSID*, *LowerFSID*, and *CID Diversion* water user objects. The *UpperFSID*, *LowerFSID*, and *CID Diversion* water user objects required directly inputting the new change in acreage in the Table 5.

Table 5. Acreage under Surface Water Strategies

Strategy	CID (acres)	Upper FSID (acres)	Lower FSID (acres)
Baseline	20,000	4,687.2	1,171.8
20% Acreage Reduction	16,000	3749.76	937.414
25% Acreage Reduction	15,000	3515.4	878.85

In addition to changing the values in the "Irrigated Area" slots, an additional row was added to the "IrrigableAcres" slot in the *CID Diversion Data* object. This slot is used in the allotment calculation for CID as it takes into account the additional 5,000 acre-ft that was acquired from CID by the Interstate Stream Commission (ISC), as described in the 2003 Pecos Settlement Agreement (NM Interstate Stream Commission, 2003). This additional row was then set equal to the value in the first row decreased by the amount of acreage that CID was reduced for the 20% and 25% strategies. Along with the additional slot, the *IrrigableAcres* function in the rules is manipulated so that pre-2055 the model would use the top row in the "IrrigableAcres" slot and post-2055 the model would use the newly created bottom row.

4.3. Increased Irrigation Efficiency Strategy

Increasing On-farm efficiency is affected differently depending on the irrigation district. For FSID, all it essentially does is reduce the shortages that occur. This is due to how the model was set-up. It was set-up so that FSID will take all the water down their canals and farmers will only use what is needed to meet the depletions for the crops, while the rest of the water stays within the canals as return flow through their two drains. It will not cause a large impact to the groundwater, again, because of how the model is set-up. The model does a split calculation that calculates how much of the return flow should go to the groundwater and how much should go to the surface water, which stays constant throughout the entire run. Only water that was not used in the depletion for the crops is used in this return flow split. Another thing to not is that, because the model actually requests all of the water, it will actually calculate the incorrect shortages for FSID. I actually have to do post-processing in an Excel sheet that Tom showed me to calculate the correct shortages that FSID has. This is laid out in an Appendix.

CID is much simpler than FSID. CID diverts what it needs including the extra for the on-farm efficiency (so if the model calculates a depletion of 5 acre-ft and CID has an efficiency of .5, 10-acre-ft will get diverted). All of the water that gets diverted is lost as CID has no return flow or groundwater objects in the model.

To quantify the effects of hypothetical water conservation actions that improve irrigation efficiencies, we modeled an exponential increase in on-farm efficiency from 50% in 2010 to 75% in 2050 We used an exponential increase over time since we are assuming that there will be early adopters of efficiency improvement methods. In PROM, irrigation efficiency is represented by the “Minimum Efficiency” slot. The amount of depletion by irrigation that would happen if enough water is available is called “Depletion Requested”. “Depletion Requested” would be the value of water needed if no water is lost within the irrigation process, but as no irrigation process is 100% efficient, the “Minimum Efficiency” is used to account for any losses in the irrigation process. The actual amount of water needed to divert for any given day is thus called “Diversion Requested”, and is calculated by:

$$Diversion\ Requested = \frac{Depletion\ Requested}{Minimum\ Efficiency}$$

It was assumed that instead of a constant linear trend in irrigation efficiency, the efficiency would evolve slowly at first and then rapidly toward the end. To do this an exponential equation was created:

$$y = ax\hat{\ }n$$

Where y is the on-farm efficiency from 0.5 (current levels) to 0.75 and x is the number of days between the first of 2010 and the first of 2050. This uses the assumption that on-farm efficiency on the first day of 2010 is 0.5 and that will exponentially rise until the first day in 2050 when it will reach the max efficiency of 0.75. We used an exponential increase over time since we are assuming that there will be early adopters of efficiency improvement methods, followed by an increasing number of farmers who adopt these methods over time. Note that in addition to the calculations for on-farm efficiency, we assume that the efficiency for water conveyed to the farm remains 85% from 1950 to 2099.

Using those values for x and y, a and n were calculated so that:

$$a = 0.75$$

and

$$n = -0.04228$$

The resulting curve is shown in Figure 22.

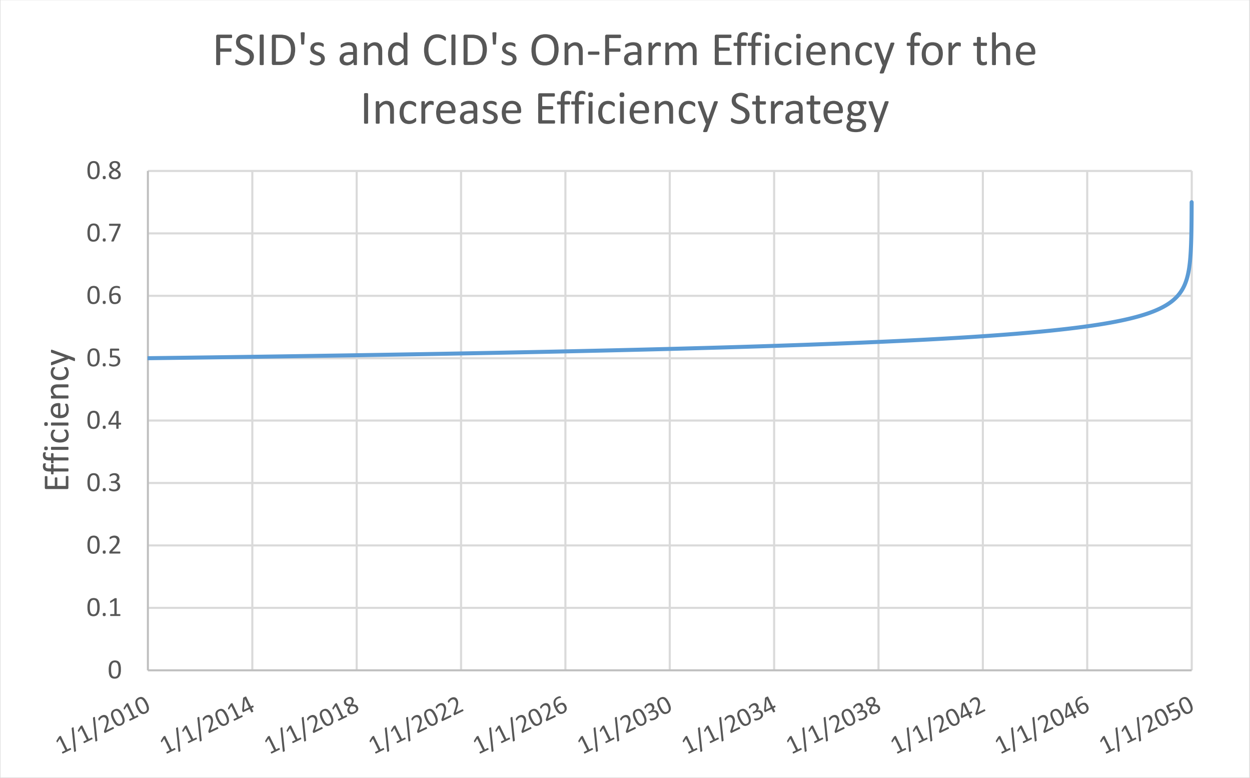

Figure 22. On-farm efficiency for FSID and CID under the increase efficiency strategy.

4.4. Water Footprint Analyses

4.4.1. PVACD

To calculate the PVACD footprint starting in 2010, RABGWM was rerun assuming that no groundwater was pumped. The resulting new gains/losses from RABGWM replaced the previous gains/losses in PROM. PROM was then run with the new gains/losses.

4.4.2. FSID

To calculate FSID’s footprint starting in 2010, PROM was run assuming that FSID would not divert water and that all of FSID’s entitled was water stored in Sumner Reservoir. It is unknown what would actually happen to FSID’s entitled water without FSID operations. There were two operational assumptions that could be made for the water that FSID would have received either:

- Store all the water in Sumner Reservoir, or
- Release all the water into the mainstem of the Pecos River

Determining FSID’s footprint starting in 2010 required first changing the value in *FSID Diversion Data.MaxDemand* from 100 cfs to 0 cfs. In addition, links between the *FSID Diversion* object and the mainstem of the Pecos were removed as well as links between *FSIDMainDrain* and *FSIDLowerDrain* objects were also removed.

4.4.3. CID

To calculate CID’s footprint starting in 2010, PROM was run assuming that CID would not divert water. This was accomplished by setting the value in the *CID Diversion Data.CSIDIrrigatedArea* to zero. Through an initialization rule, this slot sets the entire time series of the *CID Diversion.IrrigatedArea* slot, which tells the diversion object that there are zero acres to be irrigated throughout the modeled period. This modification resulted in the model not sending any water to the *CID Diversion* object.

4.4.4. ESA Operations

To calculate the footprint of ESA operations, PROM was run assuming that there would be no ESA flow targets. Not only did the model have to be altered, but also the ruleset. Some of the changes made may have been redundant but were done to make sure that none of the ESA operations are engaged in the model. In the rules:

- “ESA Release On or Off” was altered so that the *SumnerData.ESA Release On or Off* slot was always set to off. This keeps flows at Sumner Reservoir from being released at Sumner for ESA purposes.

- The *ESAFlowDemand.AcmeTargets* and *ESAFlowDemand.TiabanTargets* tables were set to all zeros, so the model would not release any water at Sumner Reservoir for those gage targets.

- In the *SumnerData* object, every day in the *ESA_BarrPumping* was set to 0 and the *FCPMaxStorage* slot was set to 0. This caused no pumping from the Barr Pumps to occur and for Sumner to not store Fish Conservation Pool (FCP) water.

- The *NMISCLease.MaximumDiversionRate* slot was set to zero and the link between this object and the main channel was disconnected. This removed any of the Vaughan (VCP) pumped water.

- The Seven Rivers Exchange Data object *PumpingRate*, Volume375, and Volume750 were all set to 0 and the object was unlinked from the rest of the model. The purpose of this change was to remove the Seven River pumping that exchanges water from the pumping for ESA water (FCP) at Sumner Reservoir from the model.

5. References

Center for Advanced Decision Support for Water and Environmental Systems (CADSWES), 2017. RiverWare Technical Documentation Version 7.0, Objects, 1478 pp.

Estrada-Lopez, M., 2015. CID Allotment History [Microsoft Excel File], U.S. Department of Interior, Bureau of Reclamation, Albuquerque, NM. Accessed 5/15/2017.

Leavesley, G.H.; Lichty, R.W.; Troutman, B.M.; and Saindon, L.G., 1983. Precipitation runoff modeling system--user's manual. U.S. Geological Survey Water Resources Investigations Report 83-4238, , 207.

Liang, X., D. P. Lettenmaier, E. F. Wood, and S. J. Burges, 1994: A Simple hydrologically Based Model of Land Surface Water and Energy Fluxes for GSMs, J. Geophys. Res., 99(D7), 14,415-14,428.

Mizukami, Naoki, Martyn P. Clark, Kevin Sampson, Bart Nijssen, Yizin Mao, Millary McMillan, Roland J. Viger, Stevel L Markstrom, Lauren E. Hay, Ross Woods, Jeffrey R. Arnold, and Levi D. Brekke, 2015; MizuRoute version 1: a river network routing tool for a continental domain water resources applications; Geoscientific Model Development 9 (2016)2223-2238; doi:10.5.194/grr:d-92223-20116.

Reclamation, 2014. Downscaled CMIP3 and CMIP5 Climate and Hydrology Projections: Release of Hydrology Projection, Comparison with preceding Information, and Summary of User Needs. Prepared by Reclamation, Technical Services Center, Denver, Colorado. 110pp.

Reclamation, 2020. Pecos River Operations Model Updated Documentation. Contains Boroughs and Stockton 2010 documentation and updates. Albuquerque Area Office, Albuquerque New Mexico.

Sun, L., Stevens, L. E., Buddenberg, A., Dobson, J. G., Easterling, D. R., & Easterling, D. R. (2015). Regional surface climate conditions in CMIP3 and CMIP5 for the United States. (July). https://doi.org/10.7289/V5RB72KG

USFWS, 2017 (2016 BO). Final Biological Opinion for the Carlsbad Project Water Operations and Water. Supply Conservation, 2016-2026. Consultation Number 02ENNM00-2016-F-0506. Field Supervisor, Fish and Wildlife Service, New

Mexico Ecological Services Field Office (NMESFO), Albuquerque, New Mexico December 5, 2017. https://www.fws.gov/southwest/es/newmexico/documents/BO/2016-F-0506_Carlsbad_Project_Water_Operations_BiOp_Final.pdf.

U. S. Global Change Research Program; 2018; *Fourth National Climate Assessment.* November 2018. Doi: 10.7930/NCA4.2018. Available at https://nca2018.globalchange.gov/chapter/front-matter-about/.|

Wood, A.W., L.R. Leung, V. Sridhar, and D.P. Lettenmaier, 2004. "Hydrologic Implications of Dynamical and Statistical Approaches to Downscaling Climate Model Outputs," Climatic Change, 15(62):189-216.

Pecos River-New Mexico Basin Study

Groundwater Appendix

Acronyms and Abbreviations

BaU	Business as Usual
BGW	Balleau Groundwater
CID	Carlsbad Irrigation District
DBSA	Daniel B. Stephens and Associates
ETS	segmented evapotranspiration package
FSID	Fort Sumner Irrigation District
HMLS	High Monsoon/Low Snowpack storyline
MODFLOW	a modular hydrologic model developed by the USGS
NMOSE	New Mexico Office of State Engineer
PROM	Pecos River Operations Model
PVACD	Pecos Valley Artesian Conservancy District
RABGWM	Roswell Artesian Basin Groundwater Model
RCH	Recharge Package
RCP	Representative Concentration Pathway
RE	Reduced Emissions
SSP&A	S. S. Papadopulos and Associates
USGS	U.S. Geological Survey

Contents

1. Groundwater Model Development 1
2. Storyline Modeling 3
3. Strategies Modeling and Water Footprint Analyses 4
4. Post-Processing 5
5. Baseline Projections of Future Climate and Hydrology 7
5.1. RABGWM Modeling and Model Assumptions 7
5.2. Methods 9
5.3. Results 12
6. Baseline Modeling Results 15
6.1. Groundwater Budget Components 15
6.2. Groundwater Level Elevations 19
6.3. River Gains and Losses 24
7. Water Management Strategy Modeling Results 27
7.1. Storyline Baseline Figures 28
7.2. 20% Reduction Figures 33
7.3. 25% Reduction Figures 38
7.4. 30% Reduction Figures 43
7.5. River Gains and Losses Figures 48
8. PVACD Water Footprint Analysis 66
8.1. Modeled Simulation of Water Level Changes in Each Storyline with No PVACD Pumping Stresses 66
8.2. PVACD Groundwater Level Footprints 72
9. FSID Shallow Aquifer Modeling 79
9.1. Background 79
9.2. RiverWare Ground Water Storage Objects 80
9.3. Fort Sumner Valley Ground Water Objects 80
9.4. Summary of Data Used to Develop the Fort Sumner Groundwater Objects and Associated Reaches 82
9.5. RiverWare Report Outlining Various User Input Parameters Related to Groundwater Simulation in the Fort Sumner Area 92
9.5.1. Fort Sumner Groundwater Objects 92
9.5.2. FSID Drains 96
10. References 99

1. Groundwater Model Development

The MODFLOW (Harbaugh et. al, 2000) groundwater model of the Roswell Basin was initially developed by Daniel B. Stephens and Associates (DBSA, 1995). In their 1995 report, DBSA describes the review of hydrologic and geologic data and the development of the groundwater model in detail. In summary, DBSA reviewed considerable information on the hydrology and geology of the Roswell Basin and developed a conceptual framework of the groundwater flow system based on that review. That framework consisted of a two-layer groundwater system separated by a confining unit. The upper layer consisted of an unconfined shallow aquifer extending about 65 miles in a north- south direction and about 10 to 12 miles in an east-west direction with the Pecos River located along the eastern margin of the aquifer. The lower layer consisted of the regional carbonate aquifer associated with the San Andres Formation. The regional aquifer extends from beneath the alluvial aquifer west to the location where the water table intersects the base of the regional aquifer, which is about 15 miles west from the western margin of the shallow aquifer. Generally speaking, recharge to the regional and shallow aquifers migrates towards the river along the eastern margin. Groundwater that is not intercepted by wells discharges either to the river or to riparian vegetation within the area of the shallow aquifer, predominantly along the river corridor.

Results of the calibration and verification process indicated that the model reasonably reproduced measured calibration targets. However, these targets did not include conditions prior to 1967, and the calculated seasonal baseflow gain between Acme and Artesia did not correspond well with the measured data.

The model prepared by DBSA was reviewed and evaluated by New Mexico Office of the State Engineer (NMOSE) staff. This review and evaluation identified several concerns regarding some of the model structure and parameter values used in the DBSA model. One of the major concerns was with the use of a general head boundary condition to represent a part of the inflow to the regional carbonate aquifer. While the exact mechanisms for inflows is subject to some debate, the linkage of inflow to rather arbitrarily specified water levels constrains the calculated water levels in the aquifer and could result in understating the effects of pumping. Other concerns dealt with the level of complexity in parameter distributions, initial conditions, poor simulation of seasonal baseflow changes, and complex estimates of some recharge components.

As a result of these concerns, Eric Keyes and others from the NMOSE staff made a number of revisions to the DBSA model. The general boundary condition for inflow to the regional aquifer was removed and replaced with a specified inflow along the aquifer’s western boundary. A more systematic method for estimating some recharge components was developed. The calibration period was extended back in time to incorporate data prior to 1967. The simulation period was extended back to 1900 to allow examination of early conditions in the basin.

Using the revised model structure and parameterization, the model was recalibrated to water-level data and baseflow gains in the reach from Acme to Artesia. The recalibration also included an evaluation of model's ability to simulate spring flow and the decline in spring flow that is noted in the historical record. The recalibration process was conducted using a trial- and-error approach that was guided by various statistical measures and graphical summaries of model performance. The recalibration process produced a model that reasonably replicated measured groundwater levels and baseflow gains. The revised model also reasonably simulated historical declines in spring flow.

The NMOSE model of the Roswell Basin groundwater system was further reviewed and evaluated by a committee composed of NMOSE staff, S. S. Papadopulos and Associates (SSP&A), and Balleau Groundwater (BGW). This review focused on the suitability of the model to evaluate results associated with changes in pumping that might be considered in conjunction with a proposed plan to achieve or maintain compliance with the Pecos River Compact and the Decree issued by the U. S. Supreme Court in Texas v. New Mexico. This review noted several areas where changes in model structure or parameters might be appropriate to improve the model in terms of its suitability for the evaluations that might be conducted. Based on the model review, SSP&A was charged with the task of implementing, testing, and evaluating improvements or changes to the model that were suggested by the committee.

To accomplish its task, SSP&A followed accepted procedures for developing groundwater models that are described in various technical literature such as ASTM. Since many of the steps in the model development process had already been accomplished through the work of DBSA and the NMOSE, SSP&A was able to focus on the model calibration process. To facilitate the calibration process, parameter estimation software was used, PEST-ASP (Doherty 2001). In keeping with the U.S. Geological Survey (USGS) guidelines on groundwater modeling (Hill, 1998), parameterization was kept as simple as possible to reduce the number of parameters being estimated. The utilization of parameter estimation methods in the calibration process improves data evaluation and typically improves the model's calibration.

In 2014 the NMOSE staff (Keyes) incorporated updates through 2013. These updates focused on extension of the pumping datasets. The resulting model, provided by Keyes in 2014, is the current version of the Roswell Artesian Basin groundwater model (RABGWM) used to perform the basin change simulations.

2. Storyline Modeling

Basin change simulations using the RABGWM were built from a set of baseline simulations. The baseline RABGWM climate projection simulations consist of a Base Case, simulating repeated 2010 conditions for the period from 2010 through 2099, and five storylines (see Section 4.3. *Storyline Projections* in the main report for more detail). Three of these storylines were derived from the Representative Concentration Pathway (RCP 8.5) climate projections, associated with Business as Usual (BaU) global actions in the coming years.

- BaU Moderate
- BaU Dry
- BaU High Monsoon/Low Snowpack (HMLS)

Two other scenarios were derived from the Reduced Emissions (RE) RCP 4.5 climate projections, which are associated with substantial efforts to reduce global emissions in the future

- Reduced Emissions Increased Monsoon, and
- Reduced Emissions Median

We modeled these five storylines to project future basin conditions for several parameters, including groundwater. See Section 4.2.6. Roswell Artesian Basin Groundwater Model for an overview of the modeling process. To project future conditions, we used a Groundwater Base Case. The groundwater model simulates conditions from a typical historical year, 2010 (the Base Case year), and repeats those annual conditions through 2099. The same pattern of repeated stresses (pumping, recharge, etc.) provides a baseline against which changes in other model simulations (e.g., storylines, water footprint analyses, and strategy runs) can be compared. Repeating seasonal conditions from the 2010 Base Case year provides a simulation period of 90 years with only seasonal cycling of stresses and no trending or variation in the annual stresses. Section 5.1 *RABGWM Modeling and Modeling Assumptions* shows the 2020 year conditions compared to historical conditions.

Modeling groundwater conditions for the five storylines required modifications to the Groundwater Base Case recharge, pumping, and evapotranspiration to create the stresses associated with each of the five storylines. Results from each of these five storylines were evaluated in terms of their deviation from the Base Case simulation.

Simulation results were extracted and provided to the Pecos River Operations Model (PROM) as input for the associated PROM simulation.

3. Strategies Modeling and Water Footprint Analyses

A series of simulations for Water Management Strategies for the three irrigation districts[1] were performed, based on the five storyline simulations, with modifications reflecting potential adaptations to the projected climate conditions. See Section 7.1.1. *Reducing Irrigation Water Diversions within Each Irrigation District* in the main report. Strategies consist of:

- 20% Reduction to All Districts (PVACD in 2045 and FSID and CID in 2055)
- 25% Reduction to All Districts (PVACD in 2045 and FSID and CID in 2055)
- 25% Reduction to PVACD starting in 2045
- 30% Reduction to PVACD starting in 2045
- Increasing Efficiency of Surface Water Districts from 50% in 2010 to 75% by 2050

Due to the spatial extents of the three irrigation districts and the Roswell Artesian Basin Aquifer, RABGWM simulations were only required for strategies reflecting changes to PVACD. Changes to FSID and CID do not result in a modification of the RABGWM simulation. RABGWM adaptation simulations were only necessary for the strategies that include changes to PVACD pumping starting in 2045. For each strategy affecting the RABGWM simulation, a series of strategy levels were performed to simulate pumping reductions to determine if there is an appropriate level of adjustment specific to each climate change projection. For example, PVACD pumping is simulated with reductions of 20, 25 and 30%:

- 20% Reduction to PVACD
- 25% Reduction by PVACD Strategy
- 30% Reduction by PVACD Strategy

Additionally, water footprint analyses were performed to assess the relative effects of the three irrigation districts, as well as ESA activities, on the river. With regards to groundwater, only PVACD has a “footprint” affecting groundwater conditions in the RAB, so when assessing groundwater footprints, only PVACD was examined.

---

[1] Fort Sumner Irrigation District (FSID), Carlsbad Irrigation District (CID), and Pecos Valley Artesian Conservancy District (PVACD).

4. Post-Processing

Post processing consisted of extracting simulated values of water levels and fluxes. Specifically, water levels at PVACD monitoring wells within the RABGWM domain were extracted and plotted for each of the simulations. In addition, water budget components were summarized in order to evaluate each model run as a diagnostic step. Simulated fluxes between the Pecos River and the shallow alluvium were captured and processed by subreaches:

(0) Basin Seepage (84 river cells + 3 drain cells)
(1) Above Lake Arthur Gage
(2) Lake Arthur Gage to Artesia Gage
(3) From Artesia Gage to Kaiser Gage
(4) From Kaiser Gage to Lake McMillan
(5) Lake McMillan/Brantley Reservoir, Major Johnson Springs

Results presented in this report focus on the total for the basin, and the subreach from Lake Arthur Gage to Artesia Gage for perspective from one river sections demonstrating the most change.

5. Baseline Projections of Future Climate and Hydrology

5.1. RABGWM Modeling and Model Assumptions

Groundwater in the artesian and shallow aquifers flows towards the Pecos River, located along the eastern margin of the basin. Most groundwater that is not intercepted by wells discharges either to the Pecos River or is consumed by riparian vegetation along the river corridor.

Groundwater flow is simulated using a MODFLOW model, the RABGWM. Figure 1 shows the well locations used for input into the RABGWM. RABGWM simulates irrigation of roughly 110,000 acres in PVACD. In reality, this number varies by year; however, in order to focus the groundwater analyses on long-term trends rather than any specific annual stresses or variations, the groundwater model was configured to simulate conditions from a typical historical year (the Base Case year), 2010, and repeats those conditions through 2099. In Figure 1, 2010 stresses are indicated by the labeled red bar. Box and whisker plots of the quartiles and outliers, respectively, indicate that the 2010 values are within the range and typical variation for the historical period. Pumping for 2010 is between the historical mean and median.

The year 2010 was selected as the Base Case year since it is relatively recent and has values of pumping, agricultural recharge and precipitation that are consistent with those from the last 30 years. Note that agricultural recharge in 2010 was slightly below the mean and median, while the 2010 precipitation was slightly above the mean and median. Groundwater pumping in 2010 was close in volume to the historical median (Figure 1) and consistent with use over the prior 30 years. While 2010 pumping is towards the lower end of pumping during the last five complete years of the 1900-2013 RABGWM simulation period, the combination of pumping, agricultural recharge and precipitation stresses being consistent with the last 30 years and 2010 being relatively recent, support the choice of 2010 as the base year. Repeating seasonal conditions from the 2010 Base Case year provides a simulation period of 90 years with only seasonal cycling of stresses and no trending or variation in the annual stresses. The pattern of repeated2010 stresses (pumping, recharge, etc.) provides a baseline against which Storyline and Strategy changes in the other simulations can be compared.

Selecting a Base Case year, in this case 2010, has implications regarding the specific values for a variety of model inputs and outputs, but in no way changes the fundamental process of evaluating impacts from Storylines, Water Footprints, and Water Management Strategies. Using pumping as an example, if a different Base Case year is selected, differences between that year and 2010 pumping may affect timing of when the system reaches specific conditions but does not affect trending and the associated evaluation between Storyline and Strategy impacts. For example, if a pumping rate higher than the 2010 rate is used, then pumping in all subsequent years would also be higher and would reach water rights or physical limits sooner than what would happen under projections using the 2010 Base Case. By the same logic, starting with values lower than the 2010 pumping rate would mean that water rights or physical limits would be reached later in the simulation. While this does not affect the comparison between projections, it is worth considering when assessing other factors such as timing and duration of changes.

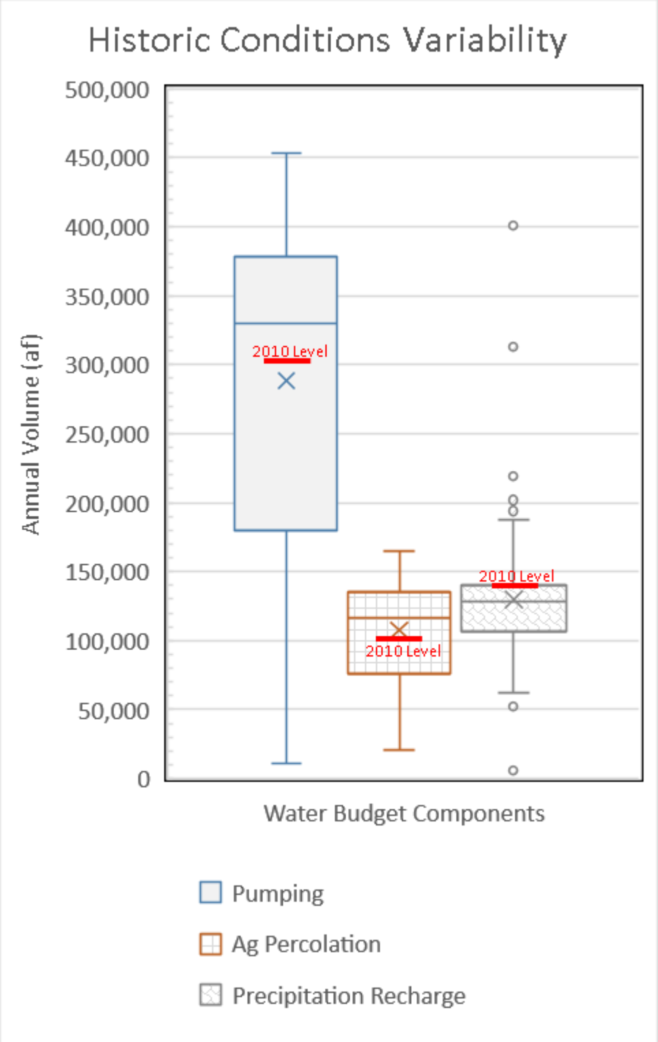

Figure 1. Historical water budget components showing that the Base Case year 2010 falls within the typical range. The whiskers represent the range of historical pumping, agricultural percolation (return flows), and precipitation recharge. The box represents quartiles, the X is the mean value, and the dots represent outliers.

All model runs use the same initial water levels: simulated water levels from the historical RABGWM simulation at the end of 2009. These initial water levels represent the transient conditions at the end of 2009. From these initial values, water levels in the Base Case simulations then adjust in response to the repeated 2010 stresses. The water level changes in the Base Case simulation reflect adjustment of the basin as it moves towards equilibrium with the repeated 2010 stresses. These minor Base Case water-level adjustments can be seen in Section 7. *Storyline Baseline Figures* in this appendix. While the simulated Base Case water levels exhibit some minor changes as the basin storage adjusts to the repeated 2010 stresses, these changes are consistent across all model runs, therefore canceling out when assessing storyline and/or Water Management Strategy impacts relative to the storyline baseline.

Agricultural recharge for 2010 is just slightly below the mean and median, while the 2010 precipitation is slightly above the mean and median. These inputs combine to represent 2010 conditions, which are well within the range of a typical historical year.

- **Pumping** limited in the model to 3.5 acre-feet/acre. Once pumping rates reached this level, the level did not increase—regardless of demands indicated by storyline trending. This limit only needed to be invoked for the Dry Storyline.

- **Evapotranspiration** was adjusted to reflect increased demand associated with increasing temperatures.

- **Recharge** was adjusted to reflect trends in precipitation and pumping.

- **Recharge proportions** remained the same for the simulation period as a percentage of both precipitation and agricultural pumping.

- **Irrigated area** was kept fixed at 110,000 acres and is compatible with the 2010 Water Master's report for the Roswell Aquifer Basin total acreage of about 113,000 acres. Pumping adjustments were used as surrogates for adjustments of irrigated acreage

- **Western boundary recharge** was held constant for all storylines, reflecting the long response time associated with impacts of climate changes on inflows at the western boundary of the model. Published discussions (e.g., Duffy and Gelhar 1978, Newton et al. 2012, Eastoe and Rodney 2014, and Rawling et al. 2014) depict a process of Artesian Aquifer recharge from the Western Boundary on the order of hundreds to thousands of years.

5.2. Methods

For recharge, the RABGWM storyline simulations, precipitation trending applied to stresses within the model domain was based on gages within the active domain (BitterLake, RoswellWSOAirport, RoswellFAAAirport, Hagerman, Hope, Artesia, LakeAvalon). Annual trends from each of these gages was extracted and combined to provide two trends, (1) trending within the RABGWM domain and (2) trending in the region west of the RABGWM domain.

For the recharge rate within the RABGWM domain:

- If year= 2010, the Recharge Package (RCH) package data of 2010 are used.
- If year >2010, the following formula was used to calculate the new rate:

$$RCH_i^j = RCH_{2010}^j * \left(1 + \gamma * (i - 2010)\right)$$ [ii]

Where:

RCH_i^j	Recharge rate for year *i* and month *j*
i	Year ranging from 2011 to 2099

j	Month ranging from 1 to 12
γ	Adjusting parameter for the recharge rate with respect to the precipitation change

For example, RCH_{2010}^{j} is the recharge rate at month j of 2010.

The first set of trending was applied to the RCH to change recharge by a consistent amount each year for the simulation. Western boundary recharge was not modified for any runs presented in this report based on a number of factors including:

- Uncertainty in the response time of the Roswell Artesian Aquifer to western boundary recharge
- Recent estimates of resident time ranging from 1300 to 5600 years (Eastoe and Rodney2014) are much longer than the simulation period
- Basic calculations suggest that for typical properties between the Pecos River and the Sacramento mountains, even after 100 years storage adjustments would still dominate Sacramento-mountain recharge changes—resulting in minimal gradient impacts at the Pecos River within that time period

Evapotranspiration in the RABGWM MODFLOW simulation is incorporated using the segmented evapotranspiration package (ETS) (Banta, 2000). Simulated evapotranspiration was adjusted based on annual trends in evapotranspiration for the region, in the same manner as the Riverware Pecos River Operations Model (PROM). Trends were applied to the segmented evaporation package to produce a consistent change in evapotranspiration with each year.

For the maximum ETS rate:

- If year= 2010, the ETS package data of 2010 are used.
- If year >2010, the following formula was used to calculate the new rate:

$$MaxRat_{i}^{j} = MaxRat_{2010}^{j} * \left(1 + \beta * (i - 2010)\right)$$

Where:

$MaxRat_{i}^{j}$	Maximum ETS rate for year *i* and month *j*
i	Year ranging from 2011 to 2099
j	Month ranging from 1 to 12

β	Adjusting parameter with respect to the ETS change

For example, $MaxRat_{2010}^{j}$ is the ETS rate at month *j* of 2010.

Pumping was adjusted to reflect the precipitation trends for each storyline as a fixed proportion (developed based on regression of historical pumping and precipitation). The adjusted precipitation trend was applied to pumping to create a consistent change in pumping for each year.

For pumping:

- If year= 2010, the well package data of 2010 are used.
- If year >2010, the following formula was used to calculate the new rate:

$$Q_i^j = Q_{2010}^j * \left(1 + (\propto_2 * \theta + \beta) * (i - 2010)\right)$$

Where:

Q_i^j	Pumping rate for year and month j
i	Year ranging from 2011 to 2099
j	Month ranging from 1 to 12
$\propto_2$	Adjusting parameter with respect to precipitation change for the non-western boundary cells
θ	Constant factor equal to -0.47
β	Adjusting parameter with respect to the ETS change

For example, Q_{2010}^j is the pumping rate at month j of 2010.

The tables below summarize the trends associated with each of the factors.

Table 1. Parameters used to generate model boundary conditions for the baseline model runs.

Models	Alpha2[(1)] (non-WB pmp) *(precip based)*	Theta *(precip to pmp)*	Beta *(ET based)*	Gamma[(2)] *(precip based)*	Remarks
Base Case	0.0	0.00	0.00	0.0	No climate trend added
BaU Moderate	-1.811×10^{-3}	-0.47	3.152×10^{-3}	-1.811×10^{-3}	
BaU Dry	-9.660×10^{-3}	-0.47	3.693×10^{-3}	-9.660×10^{-3}	

BAU HMLS	1.894x10^{-3}	-0.47	2.468x10^{-3}	1.894x10^{-3}
RE Increased Monsoon	1.797x10^{-3}	-0.47	3.118x10^{-4}	1.797x10^{-3}
RE Median	-3.509x10^{-4}	-0.47	4.018x10^{-4}	-3.509x10^{-4}

(1) Precipitation trending applied to stresses within the model domain was based on gages within the active domain (Bitter Lake, Roswell WSO Airport, Roswell FAA Airport, Hagerman, Hope, Artesia, Lake Avalon)

Table 2. Annual factors for the baseline model runs

Model	Pumping	ETS	RCH(1)
Base case	0	0	0
BaU Moderate	4.003x10^{-3}	3.152x10^{-3}	-1.810 x10^{-3}
BaU Dry	8.233x10^{-3}	3.693x10^{-3}	-9.660 x10^{-3}
BAU HMLS	1.578x10^{-3}	2.468x10^{-3}	1.894 x10^{-3}
RE Increased Monsoon	-5.328x10^{-4}	3.118x10^{-4}	1.797x10^{-3}
RE Median	5.667x10^{-4}	4.018x10^{-4}	-3.509x10^{-4}

(1) Precipitation trending applied to stresses within the model domain was based on gages within the active domain (BitterLake, RoswellWSOAirport, RoswellFAAAirport, Hagerman, Hope, Artesia, LakeAvalon)

5.3. Results

Simulated water budgets for the runs are presented in this Appendix. Figures in Section 7.1. *Storyline Baseline Figures* show the water budget component differences between the Base Case and the BaU Moderate, BaU Dry, BAU HMLS, RE Increased Monsoon, and RE Median Storylines.

The figures demonstrate the changes in water budget, compared to the Base Case, for each of the five storylines. In each storyline, the slopes of the water budget terms reflect the trend applied to each stress, demonstrating the results of each storyline. Comparing these figures demonstrates the magnitude of change associated with each storyline. The greatest changes are associated with the BaU Dry Storyline, while the RE Median Storyline results in the least amount of change.

Simulated water levels and river-aquifer exchange are discussed in Section 6.3. *River Gains and Losses*, and figures are included in Section 7.5. *River Gains and Losses Figures* for each of the baseline simulations (Groundwater Base Case plus five storyline simulations) in this appendix. Changes in the exchange between river and aquifer are summarized in these sections for the five storylines with plots the net change in flux from the aquifer to the river (RIVnet = RIVin - RIVout) for each storyline.

Base case simulated water levels, demonstrate the adjustment between initial conditions and the repeated 2010 stresses. The differences between the Base Case and the five storylines reflect conditions in each storyline. Water levels for the BAU HMLS, RE Increased Monsoon, and RE Median Storylines are quite similar to the Base Case. The BaU Moderate Storyline simulated water levels are on the order of 50 feet lower than the Base Case in 2099. The BaU Dry Storyline results in significantly greater changes, with projected water levels dropping by hundreds of feet over the simulation period.

As with the simulated water budget components and the water levels, changes range from minor, for the BAU HMLS and RE Median Storylines, to significant, for the BaU Dry Storyline, with the BaU Moderate and RE Increased Monsoon Storylines having moderate, but opposite, impacts. Four of the five storylines are similar in that the aquifer gains more from the river, and that there is a reduction in the amount of water seeping from the aquifer to the river. The differences are primarily in the magnitudes. The exception is the RE Increased Monsoon Storyline, where the aquifer gains less from the river, associated with higher simulated water level predictions.

The net result of the storylines on the Pecos River is discussed in Section 6.3. *River Gains and Losses*, and figures are included in Section 7.5. *River Gains and Losses Figures*. These plots demonstrate the relative magnitude of change in surface water gains between the five storylines, as previously discussed, as well as the differences in transitions.

- RE Increased Monsoon Storyline conditions result in increasing river gains, reflecting generally increasing water levels.
- The BAU HMLS and RE Median Storylines produce a minor and linear response, with small river-gain decreases over the simulation period.
- The BaU Moderate Storyline demonstrates increasing response and nonlinearity reflecting changes to the system associated with the larger changes to simulated water budgets and water levels.
- The BaU Dry Storyline also demonstrates increasing rates of river losses, and also exhibits a rather pronounced shift in the net river gains after about 2060, suggesting that the system is starting to approach some sort of limiting condition. While beyond the scope of the current investigation, this change in trend probably reflects the decreasing potential for additional change in seepage as the BaU Dry Storyline no longer has opportunities for river gains and becomes dominated by river losses.

The magnitude and differences in behavior associated with BaU Dry Storyline results also suggest careful consideration of the limitations associated with the current level of MODFLOW- Riverware coupling. As currently configured MODFLOW does provide aquifer-river seepages for the Riverware simulation, but the representation of Riverware-simulated dry river conditions are not represented in the MODFLOW simulation. Synchronization of this sort of information between the two models will improve the predictive ability of the models for the simulation of storylines with increasing changes.

6. Baseline Modeling Results

Modeling results summarize the simulated change in conditions between the 2010 Groundwater Base Case run and the baselines for each of the five storylines. These runs are intended to provide insight to the results of a range of climate projections without any changes in management practices.

6.1. Groundwater Budget Components

Figures in this subsection show differences in water budget components between the Base Case and five storyline simulations. Terms listed in the legends of those figures are:

- ***Net Storage***: the difference in net storage between the Groundwater Base Case conditions and the baseline conditions for each of the five storylines.
- ***RIV net:*** net river-aquifer seepage difference between the Groundwater Base Case and climate-projection simulations (MODFLOW sign convention)
- ***RIV leakage in***: the difference in river-to-aquifer seepage between the Groundwater Base Case and climate- projection simulations
- ***RIV leakage out:*** the difference in aquifer-to-river seepage between the and storyline simulations
- ***ET segment:*** the difference in evapotranspiration between the Groundwater Base Case and climate-projection simulations.
- ***Well in:*** the change in agricultural recharge between the Groundwater Base Case and climate- projection simulations.
- ***Well out:*** the change in pumping between the Groundwater Base Case and climate-projection simulations.
- ***Rch:*** change in precipitation-based recharge between the Groundwater Base Case and climate- projection simulations.
- ***Deactivated injection wells:*** change in agricultural recharge associated with dry cells in the climate-projection simulation.
- ***Deactivated extraction wells:*** change in pumping associated with dry cells in the climate- projection simulation.

In each case, some components have increased, and others decreased, reflecting the results of simulated climate changes. Note that minor jumps in any of the time series reflect model grid cells going dry. These changes are small enough to not significantly change the outcomes and conclusions of these simulations.

MODFLOW sign conventions are used in in this subsection, so that negative values indicate extraction from the aquifer. For example, the WELOUT series in in this subsection represents the total pumping in the RABGWM simulations. Four of the five storylines simulate increased pumping, additional extraction, of increasing amounts for the BaU Moderate, BaU Dry, BAU HMLS, and RE Median Storylines. The RE Increased Monsoon Storyline exhibits decreasing pumping, reflecting the trend of decreasing demand in that storyline.

Figures in this subsection provide a lumped summary of storyline inputs and results. For example, as indicated by the signs on the RCH terms, recharge as an input increases for the BAU HMLS and RE Increased Monsoon Storylines, while decreasing for the BaU Moderate, BaU Dry, and RE Median Storylines. The simulated ET, ET Segment, for the five storylines reflects both the increase rate in each storyline and the simulated water levels. While all five storylines have increasing ET rates, simulated ET increases for the BAU HMLS and RE Increased Monsoon Storylines and decreases for the other storylines. Decreasing ET reflects simulated water levels falling below the root zones, reducing the simulated amount of ET despite increasing ET rates in those storylines.

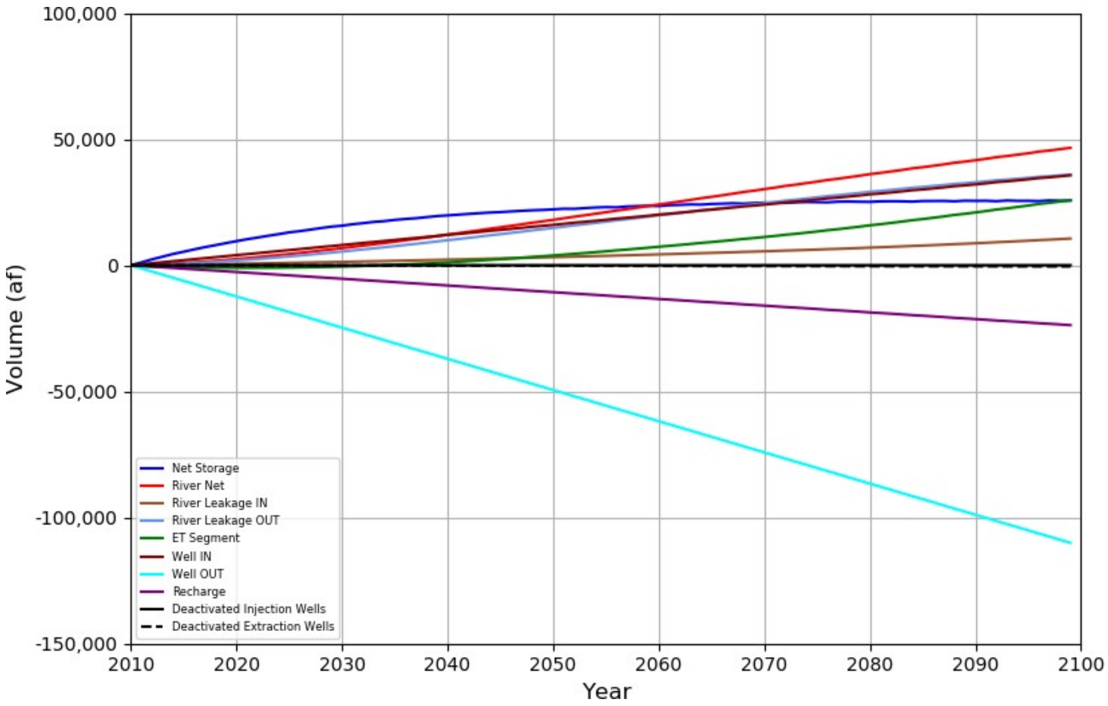

Figure 2. Water-budget component differences: BaU Moderate Storyline minus the Groundwater Base Case.

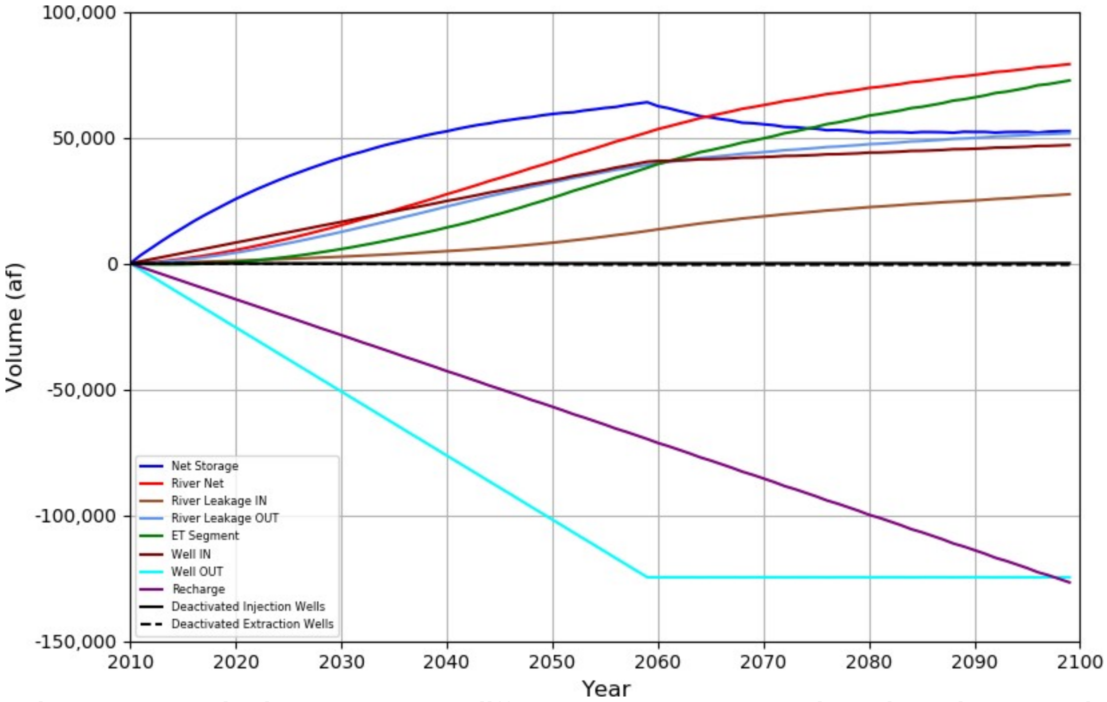

Figure 3. Water-budget component differences: BaU Dry Storyline minus the Groundwater Base Case.

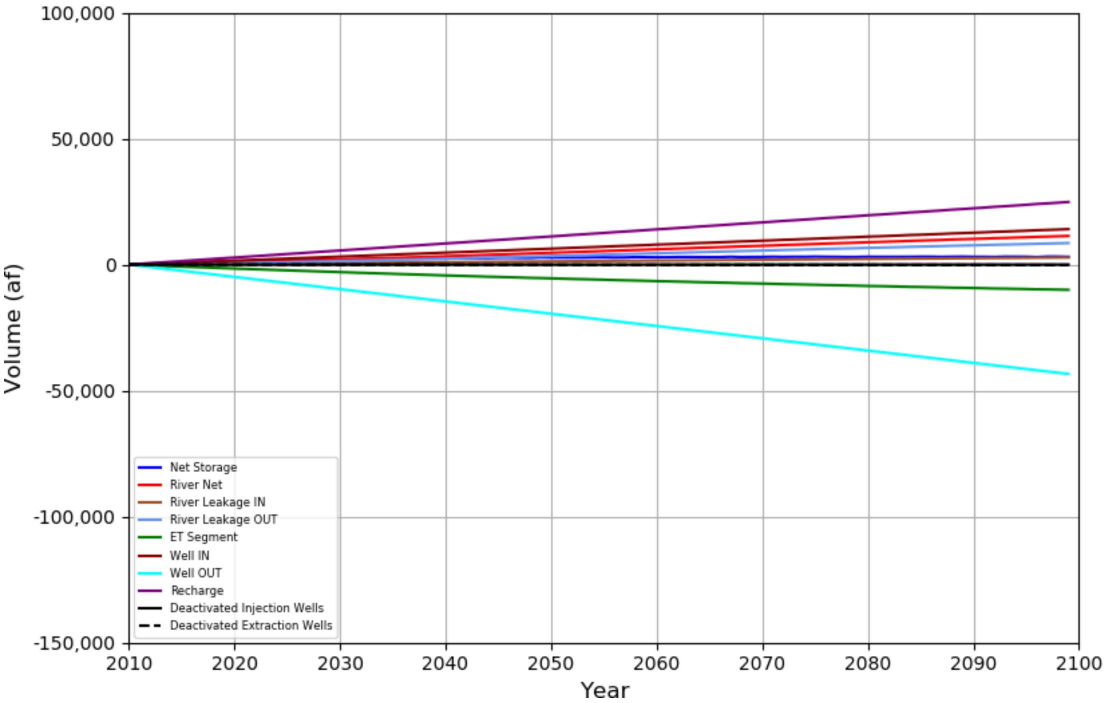

Figure 4. Water-budget component differences: BAU HMLS Storyline minus the Groundwater Base Case.

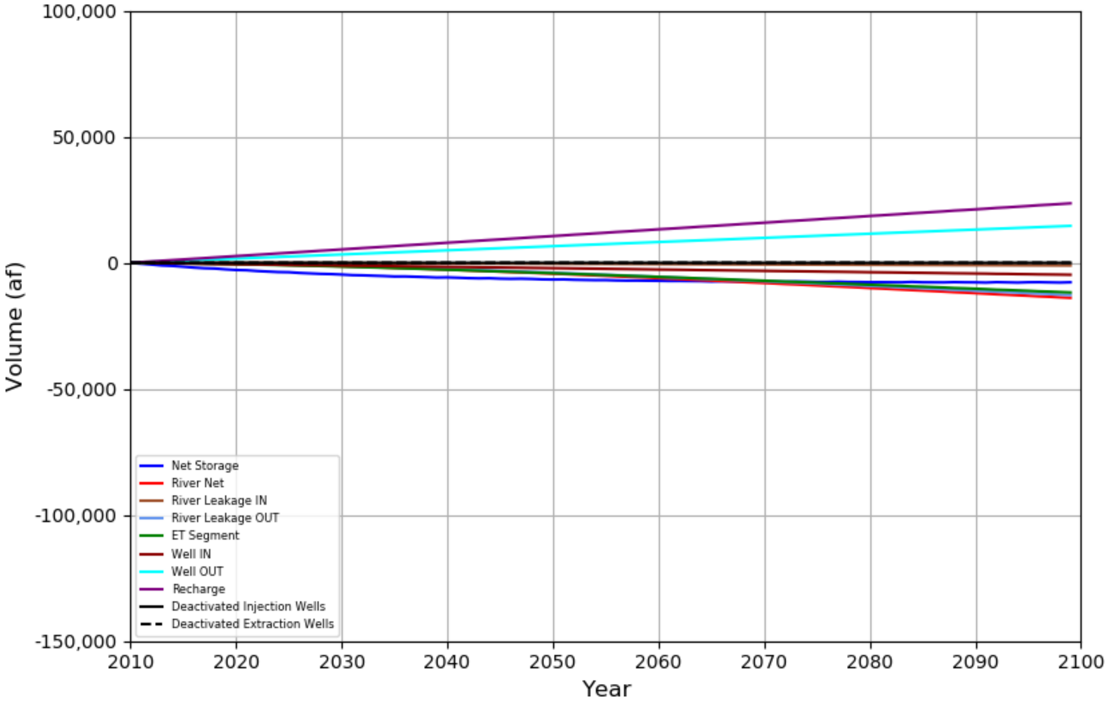

Figure 5. Water-budget component differences: RE Increased Monsoon Storyline minus the Groundwater Base Case.

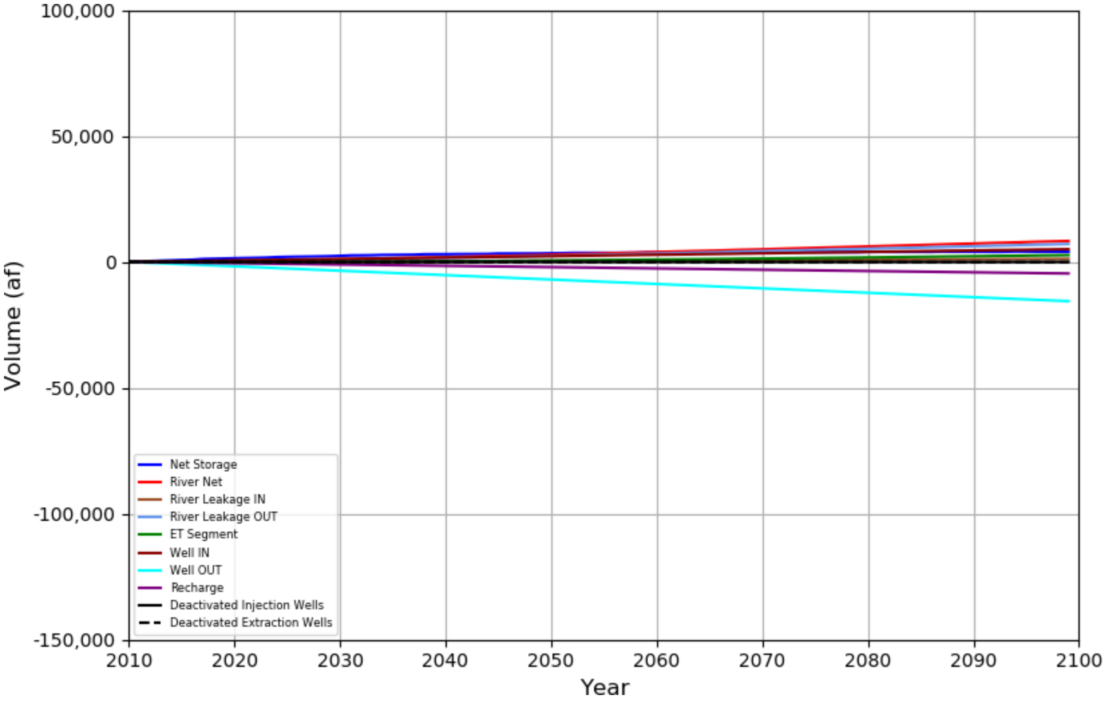

Figure 6. Water-budget component differences: RE Median Storyline minus the Groundwater Base Case.

6.2. Groundwater Level Elevations

Simulated water levels at selected PVACD monitoring-well locations are shown in figures in this subsection. Each figure provides a time series of the simulated water levels at each well associated with the Groundwater Base Case and the five climate-change storylines. While there is considerable difference among the wells regarding the amount of seasonal fluctuation in water levels, the wells generally exhibit similar climate change results. See the main report, Section 5.5.2. *Pecos River Groundwater Gains from Acme Gage to Artesia*.

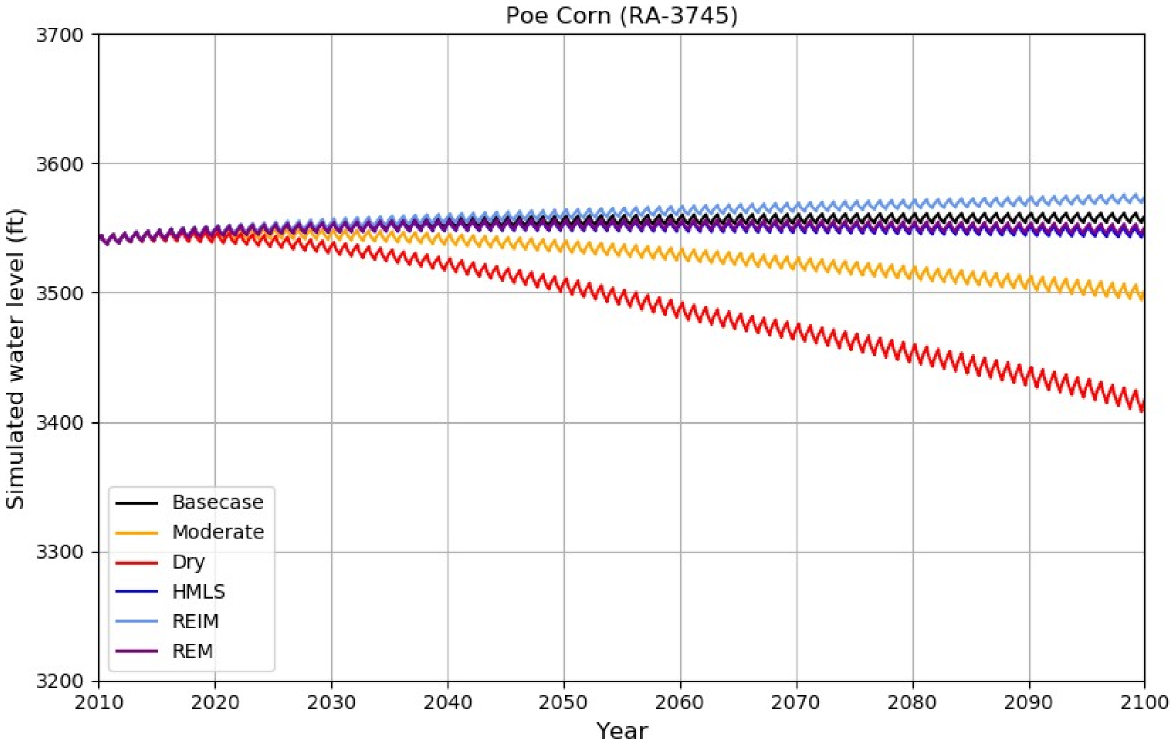

Figure 7. Simulated water-level elevations at the Poe Corn (RA-3745) observation well (storyline baselines without Water Management Strategies)

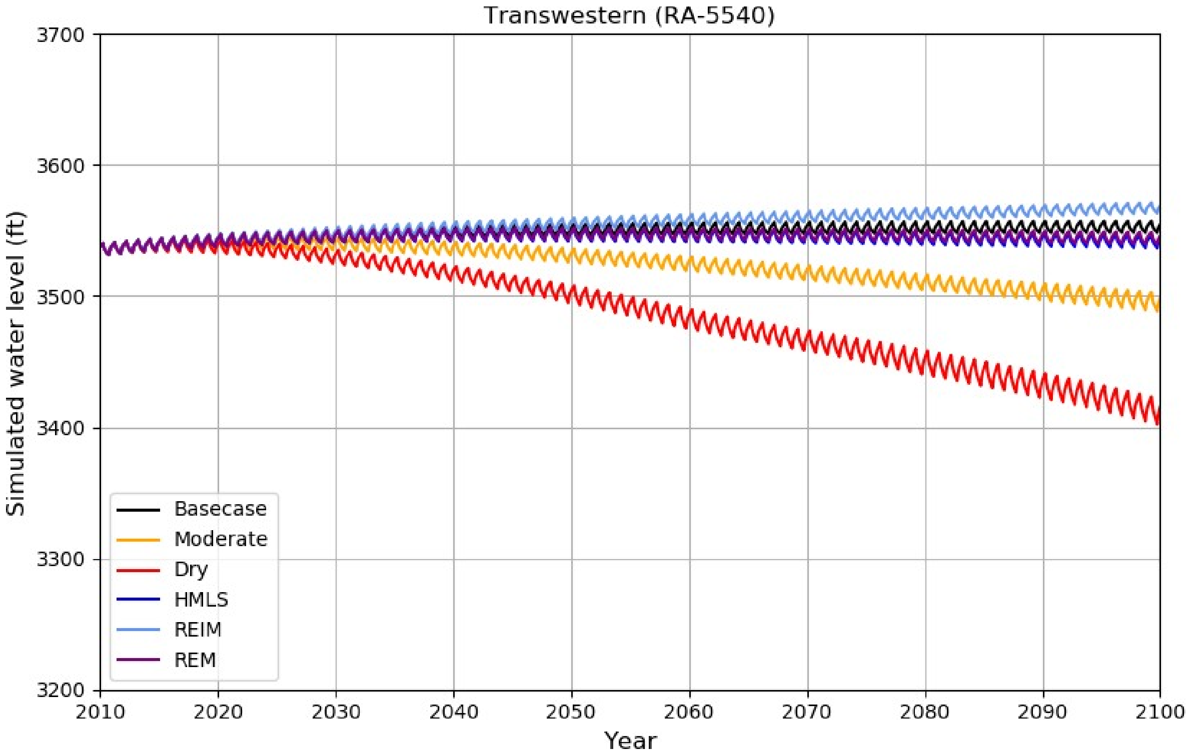

Figure 8. Simulated water-level elevations at the Transwestern (RA-5540) observation well (storyline baselines without Water Management Strategies)

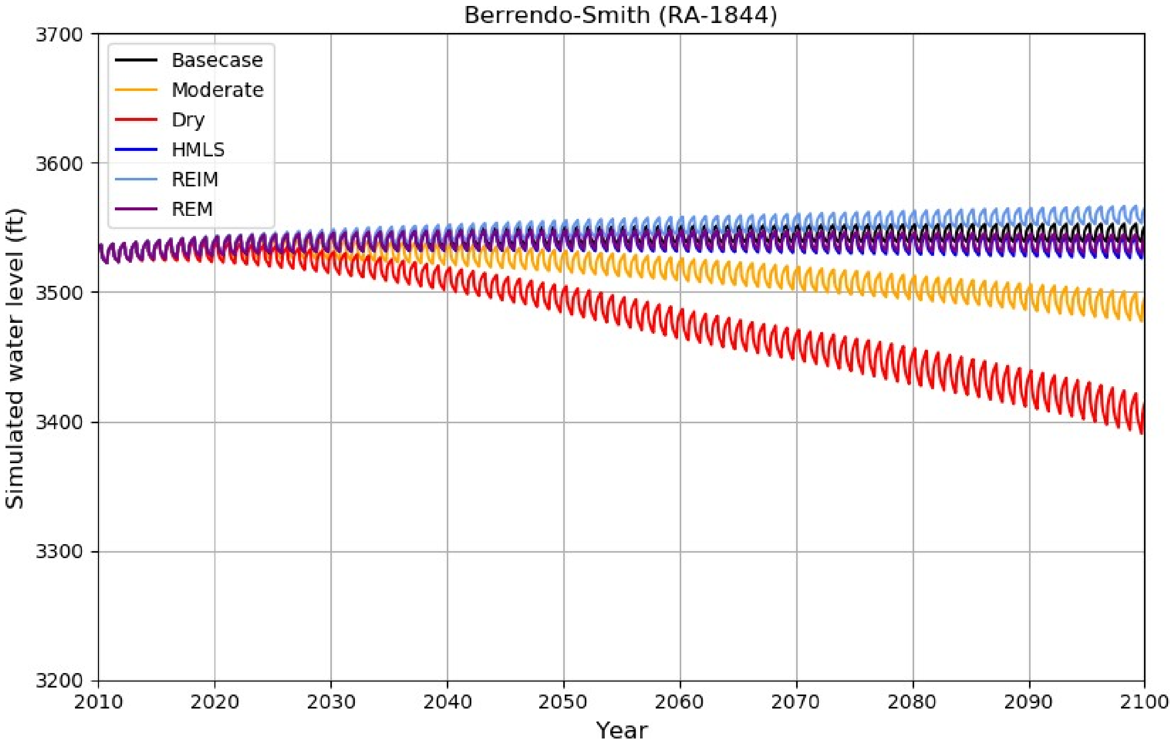

Figure 9. Simulated water-level elevations at the Berrendo-Smith (RA-1844) observation well (storyline baselines without Water Management Strategies)

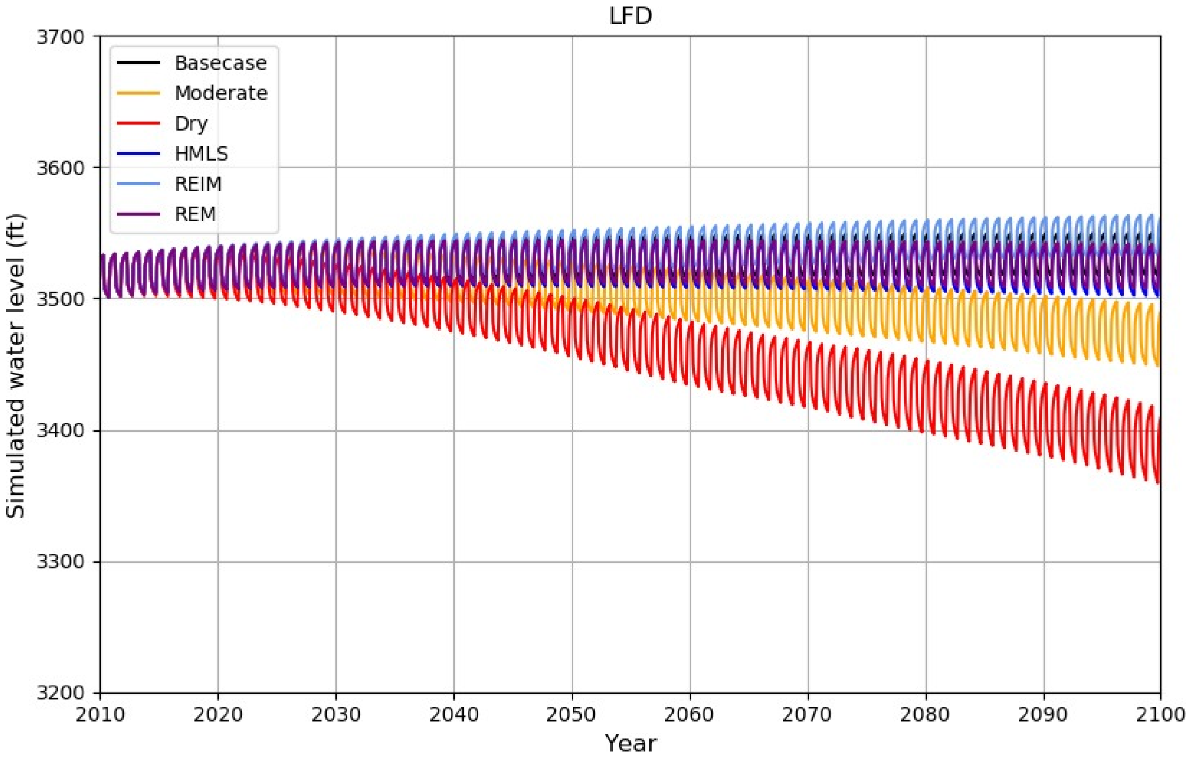

Figure 10. Simulated water-level elevations at the LFD observation well (storyline baselines without Water Management Strategies).

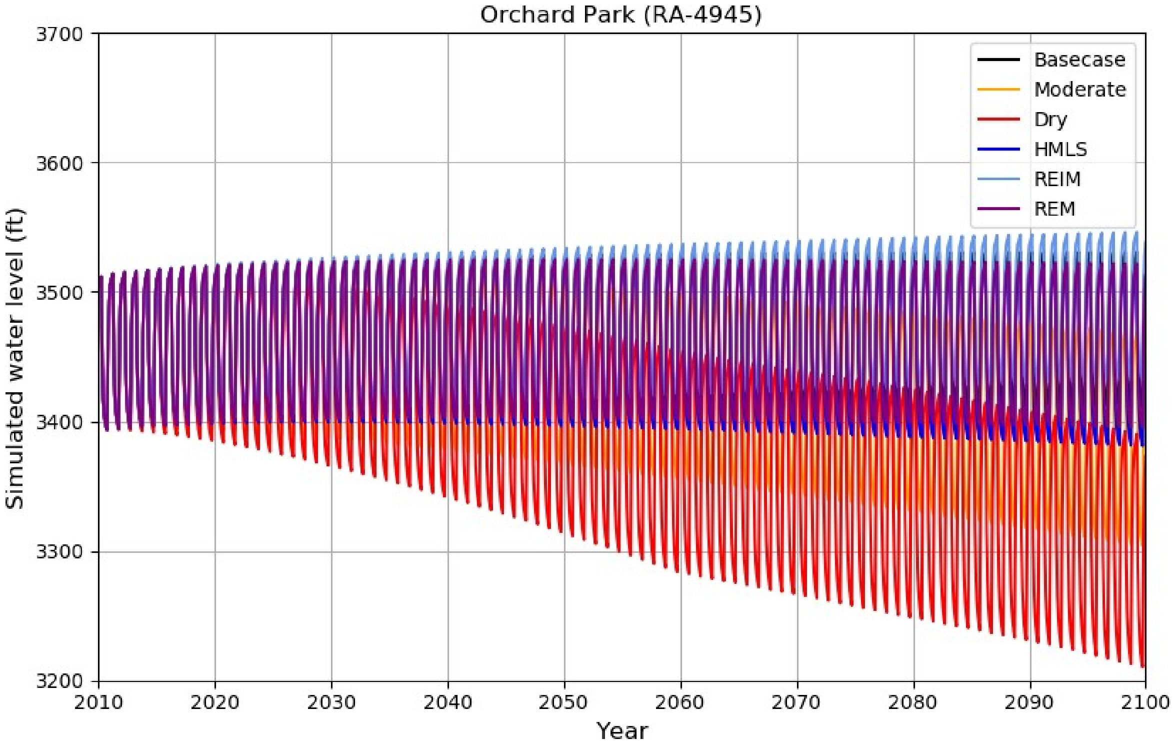

Figure 11. Simulated water-level elevations at the Orchard Park (RA-4945) observation well (storyline baselines without Water Management Strategies).

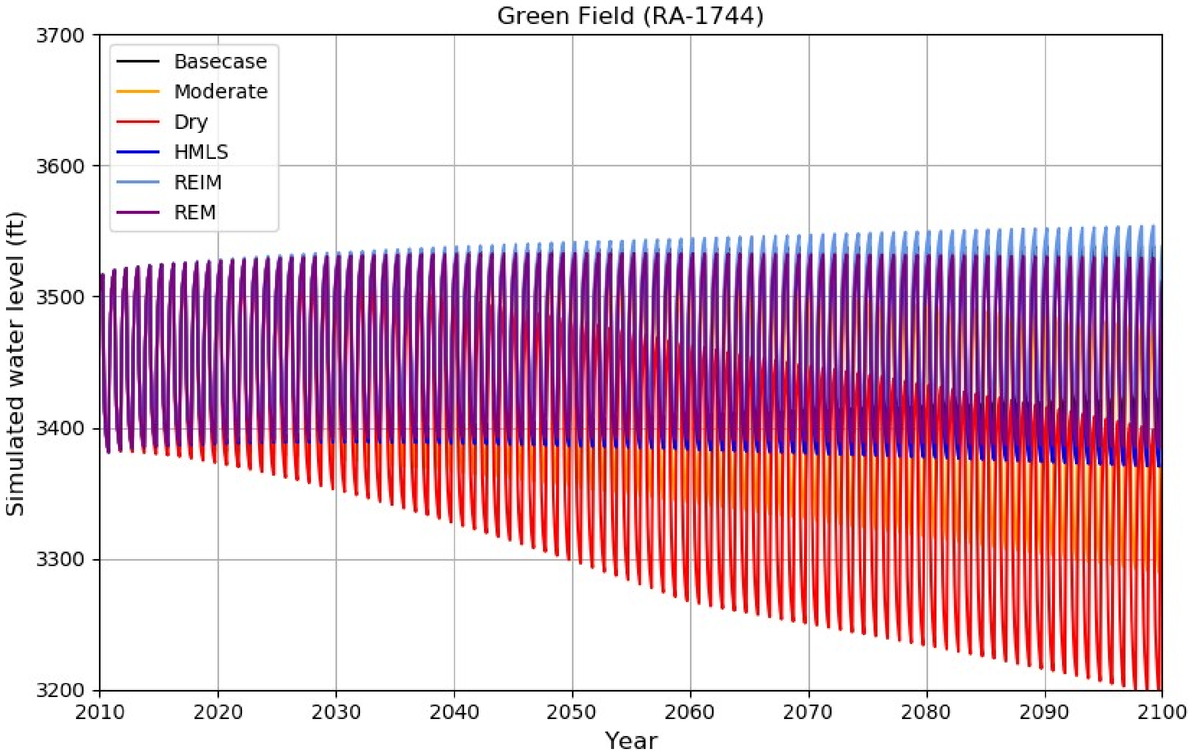

Figure 12. Simulated water-level elevations at the Green Field (RA-1744) observation well (storyline baselines without Water Management Strategies).

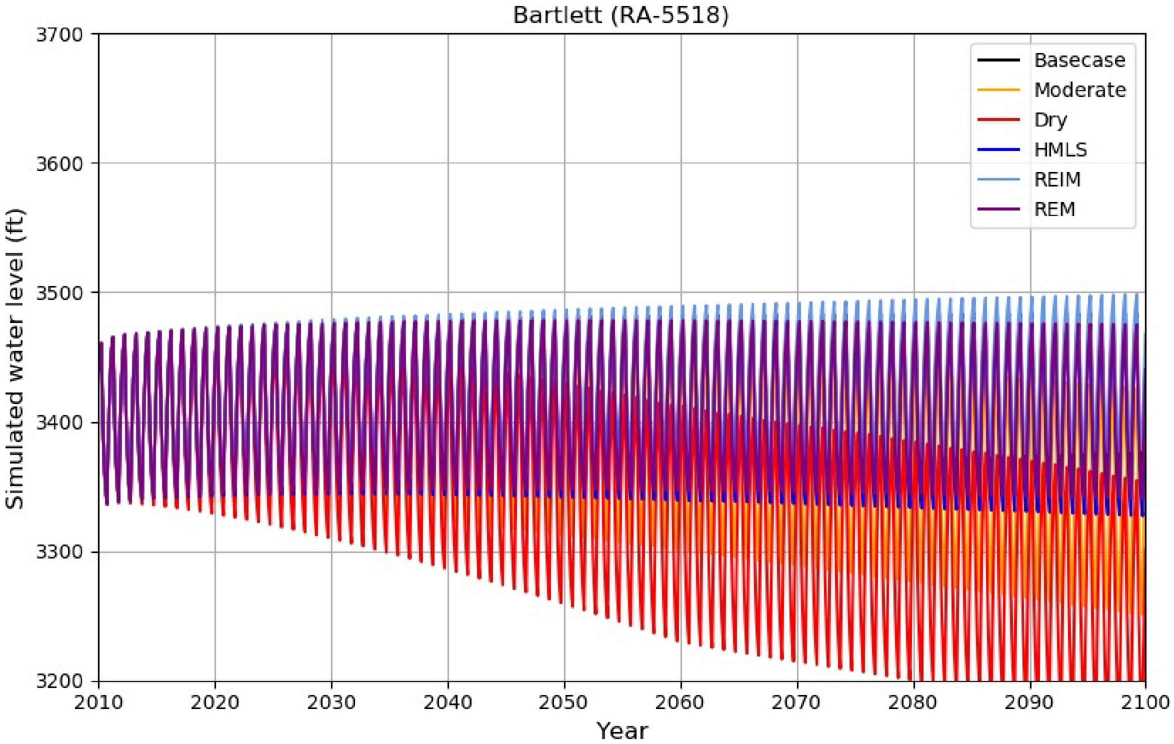

Figure 13. Simulated water-level elevations at the Bartlet (RA-5518) observation well (storyline baselines without Water Management Strategies).

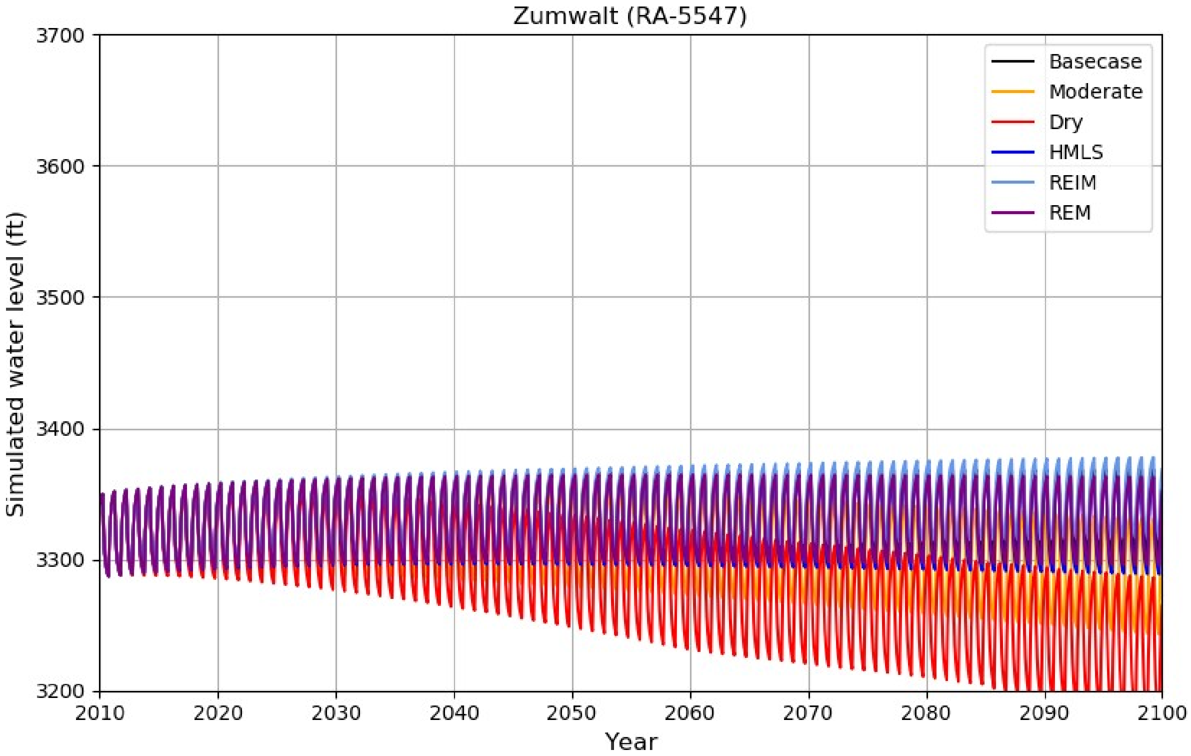

Figure 14. Simulated water-level elevations at the Zumwalt (RA-5547) observation well (storyline baselines without Water Management Strategies).

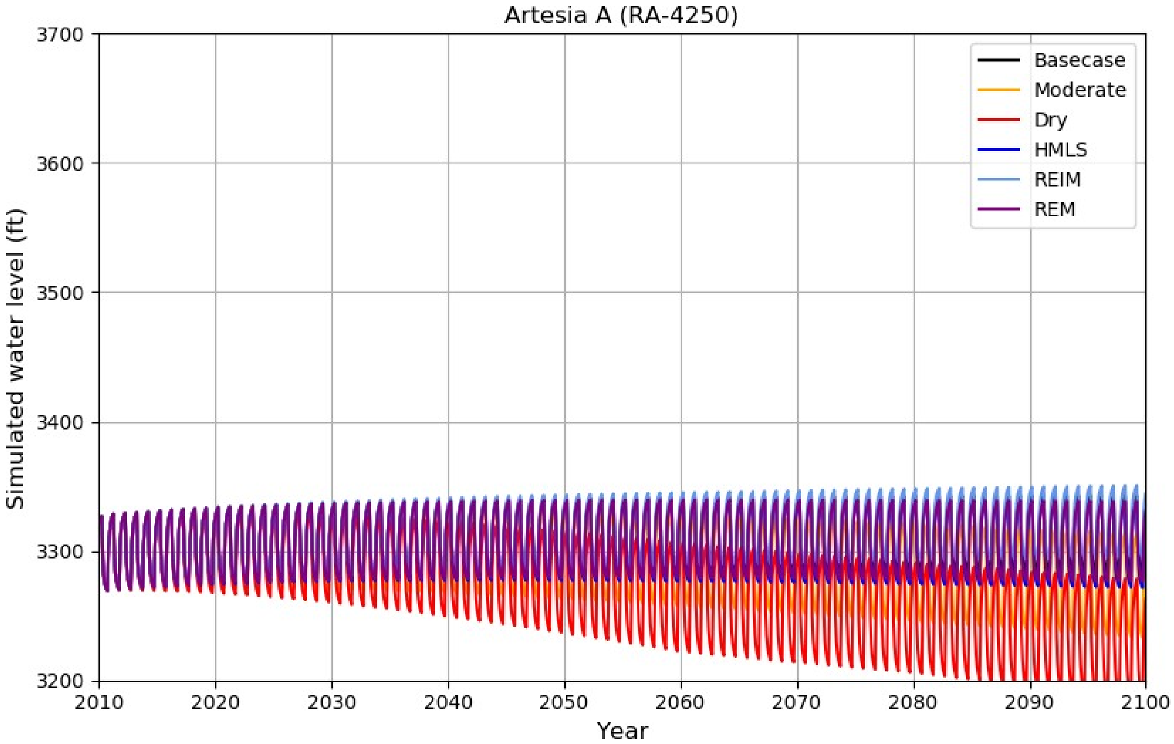

Figure 15. Simulated water-level elevations at the Artesia A (RA-4250) observation well (storyline baselines without Water Management Strategies).

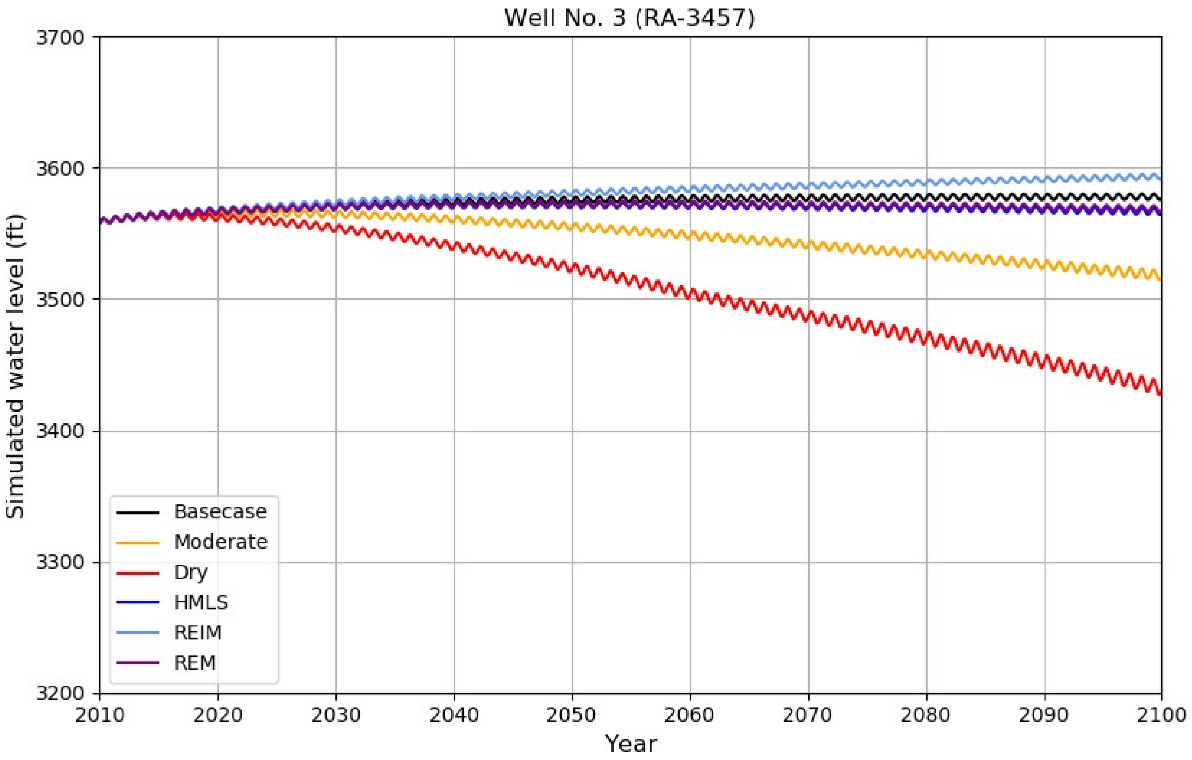

Figure 16. Simulated water-level elevations at the Well No. 3 (RA-3457) observation well (storyline baselines without Water Management Strategies).

6.3. River Gains and Losses

Figures in this subsection illustrate simulated climate storyline changes to river-aquifer exchanges. Five curves depicting net river seepage are included in Figure 17, one for each storyline. MODFLOW sign conventions are used, so that any positive values represent flux into the aquifer, and negative values are flux moving out of the aquifer. Therefore, in Figure 17, positive values of net river seepage indicate river losses and negative indicate river gains. Figure 18 and Figure 19 are river gain difference plots for the entire RABGWM model, including flow to springs, and for the reach between the Lake Arthur and Artesia gages, respectively. In each plot, the time series show the difference in River Gain between the Groundwater Base Case simulation and the five storylines, on an annual basis.River gain in these plots is the same as RIV net in the Figure 17, except the sign is changed, reflecting flow to/from the river, and the values are summarized on an annual basis in acre-feet.

River gains decrease for all storyline except the RE Increased Monsoon (Figure 18). The RE Median and BAU HMLS Storyline baselines have the least amount of decrease, while the BaU Dry Storyline baseline has the most. While the rate of change in river gains approach a constant value for the BAU HMLS and BaU Moderate Storyline baselines, the BaU Dry Storyline rate of river-gain change decreases in later time periods. This appears to indicate limiting conditions: water levels have dropped to the point where river gain cannot decrease any further.

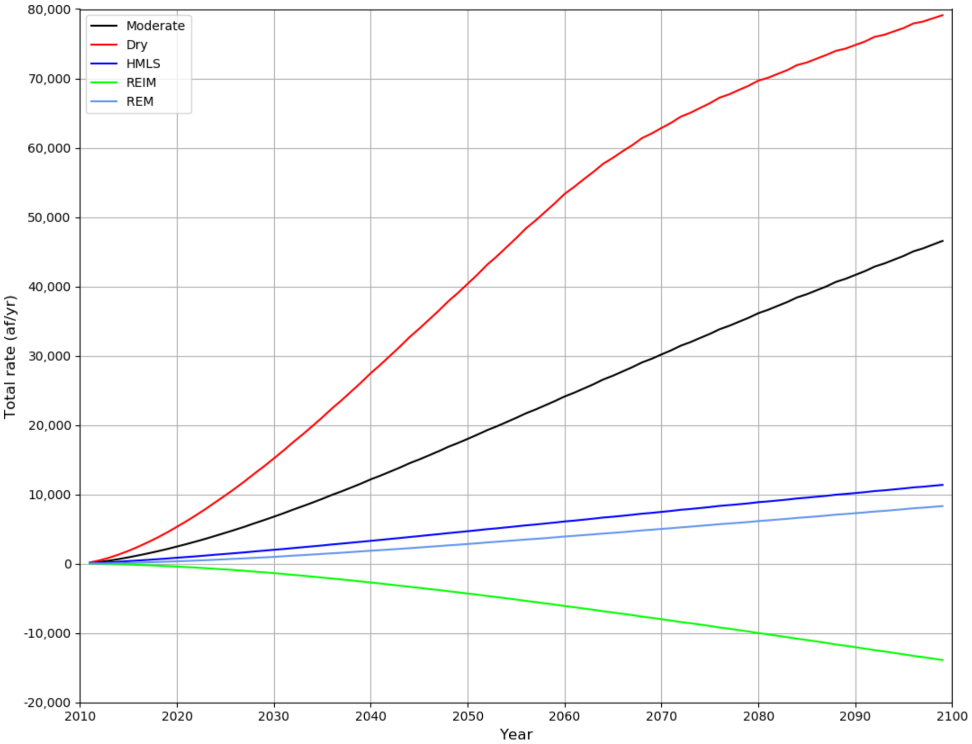

Figure 17. Net river seepage in storyline baselines without Water Management Strategies.

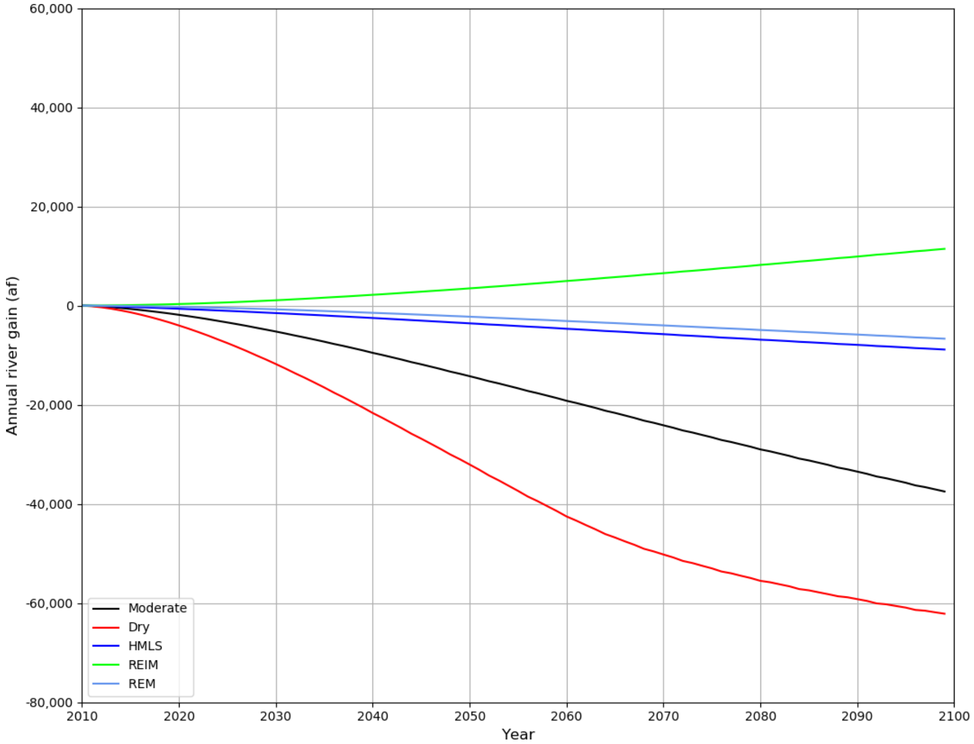

Figure 18. Simulated annual river gain difference (storyline minus the Groundwater Base Case) for the Roswell Artesian Basin, without Water Management Strategies

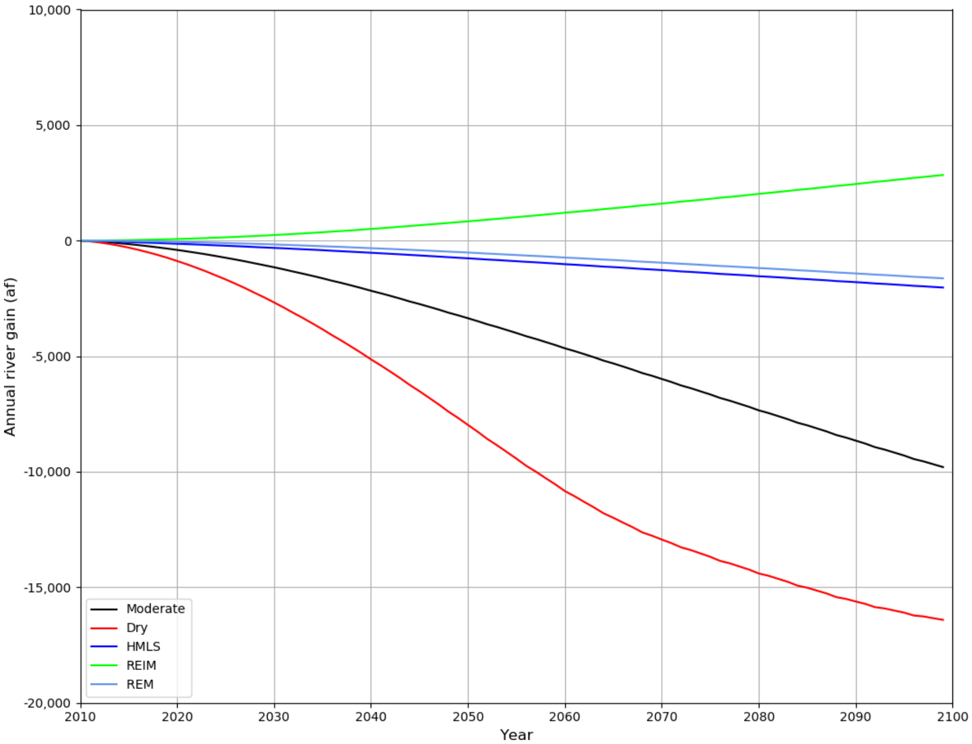

Figure 19. Simulated annual river gain difference (storyline minus Base Case) for the stretch from Lake Arthur Gage to Artesia Gage, without Water Management Strategies.

7. Water Management Strategy Modeling Results

These strategies consisted of reducing water consumption by the irrigation districts by varying amounts. As described in the main report, Section 7.1.1. *Reducing Irrigation Water Diversions within Each Irrigation District* , modeled strategies were a 20% , 25%, and 30% Reduction to PVACD starting in 2045.

Three RABGWM adaptation simulations were performed, incorporating a step decrease in PVACD pumping in 2045. Additionally, as part of the water footprint analyses, the total effect of PVACD on the groundwater was isolated by simulation of zero PVACD pumping after 2010. Pumping reduction in 2045 represents adjustments in total irrigated acreage. Adjustments consisted of reducing pumping by 20, 25 and 30%, to represent climate induced adaptation in irrigated acreage initiated in 2045. The resulting river gains/losses provided the PROM with storyline and adaptation values of gains/losses for the PROM simulations.

Figures in this subsection demonstrate both the storyline results and relative benefit and duration of the three Water Management Strategies. Simulated hydrographs of the PVACD wells within the RABGWM for the Groundwater Base Case (year 2010 conditions repeated throughout the period of record). Seasonal fluctuations vary between the PVACD wells, with increasing fluctuations for wells in areas where water levels show greater fluctuation between irrigation and non-irrigation seasons. For all wells, the BAU HMLS and RE Median storylines create only modest declines in water levels, conditions for the BaU Moderate and BaU Dry storylines result in increasing amounts of water level declines, and water levels rise under RE Increased Monsoon Storyline conditions.

Simulated response to Water Management Strategies shows that each strategy are sufficient to offset any decreases in water levels in the BAU HMLS and RE Median storylines. For the BaU Moderate projections, the simulated response indicates that a 30% adaptation is warranted, but even this strategy would only provide an offset for a limited amount of time before the BaU Moderate Storyline conditions bring water levels down again. The simulation results indicate that under BaU Dry Storyline conditions, none of the modeled Water Management Strategies are sufficient to offset the predicted declines in water levels: water level changes from the Base Case do not return to zero following strategy implementation in this storyline, even briefly.

Analogous to Figure 18, simulated monthly river seepage is summarized for the BaU Moderate, BaU Dry, BAU HMLS, RE Increased Monsoon and RE Median storylines in Section 7.5. *River Gains and Losses Figures*. As with the figures in Section 6. *Baseline Modeling Results* in this appendix, these figures use the MODFLOW convention: positive values indicate water moving into the aquifer, so a positive Net River Seepage indicates water lost from the river and moving into the ground. Implementing Water Management Strategies is not sufficient to offset the simulated change of the BaU Moderate and BaU Dry storylines. For the BAU HMLS, RE Increased Monsoon and RE Median Storylines, all Water Management Strategies evaluated are able to offset the changes in anticipated river seepage conditions, with varying amounts of lag that reflect the climatic conditions of each storyline.

Simulated annual river gain differences (storyline minus baseline results) for the five storylines, and each of the Water Management Strategies, is provided in Section 7.5. *River Gains and Losses Figures*. Each figure consists of four graphs: (a) – (d). The information in graphs (a) and (b) is identical to (c) and (d), respectively. Graphs (a) and (b) provide results in units of acre-feet, a more common unit for assessing storage and pumping, while graphs (c) and (d) provide results in units of cfs, a more common unit when assessing river flow. For each storyline, (a) and (c) depict annual river gain differences for the entire Roswell Artesian Basin, while (b) and (d) depict for the stretch between the Lake Arthur and Artesia Gages. These graphs are quite similar to figures in Sections 7.1 through 7.4, but provide a spatial breakout demonstrating how individual reaches may respond differently than the system as a whole.

7.1. Storyline Baseline Figures

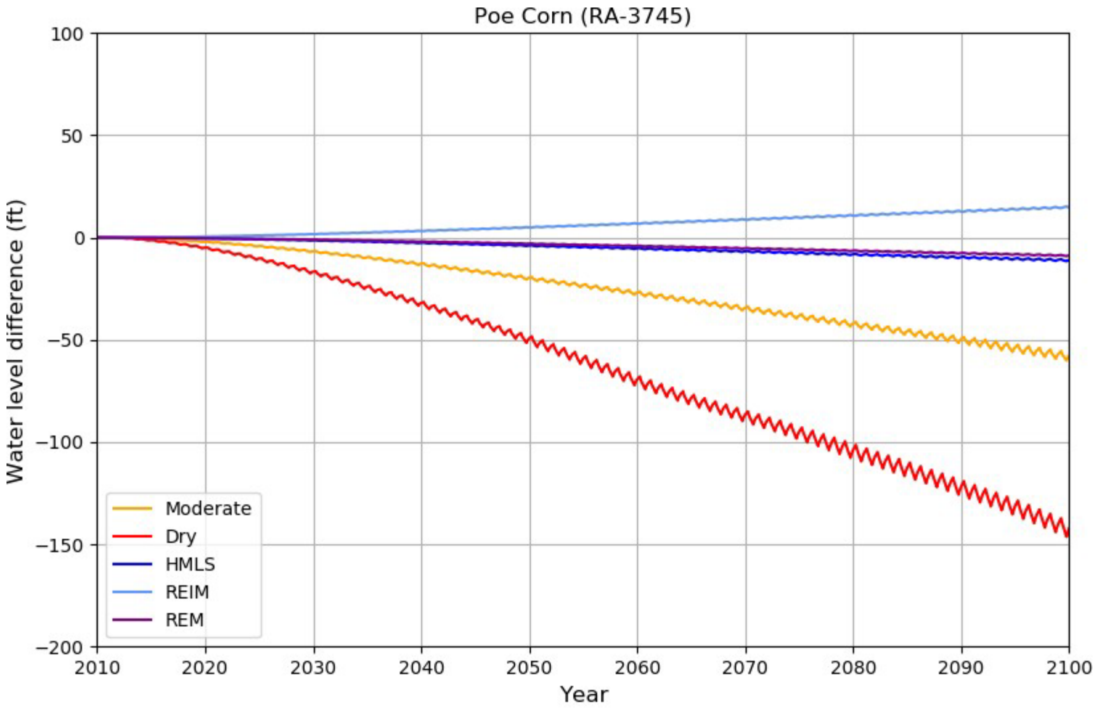

Figure 20. Change in simulated water levels for the Poe Corn (RA-3745) observation well for climate change storylines, without Water Management Strategies (storyline minus Groundwater Base Case).

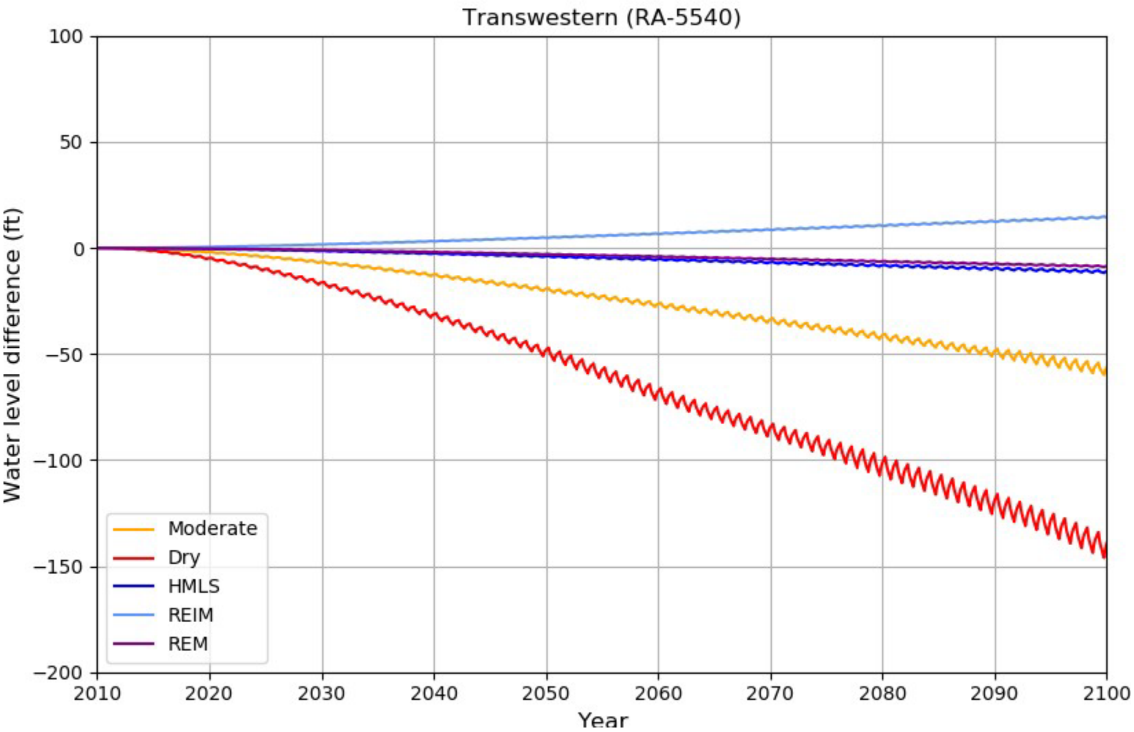

Figure 21. Change in simulated water levels at the Transwestern (RA-5540) observation well for climate change storylines, without Water Management Strategies (storyline minus Groundwater Base Case).

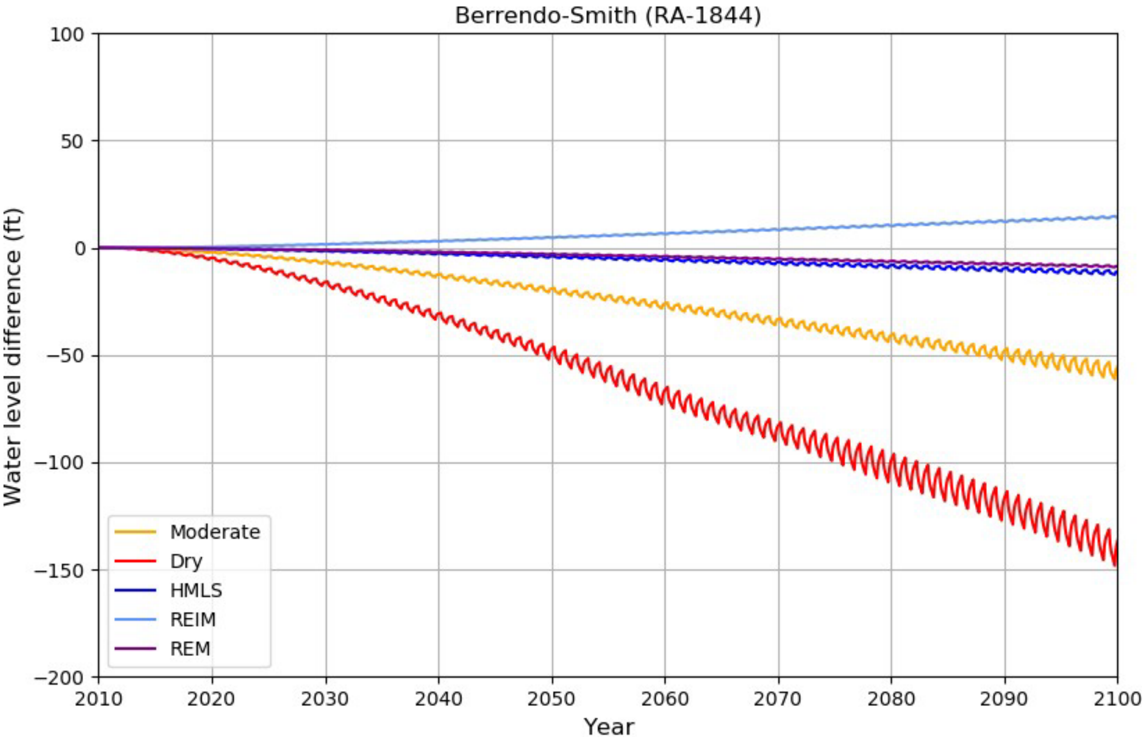

Figure 22. Change in simulated water levels at the Berrendo-Smith (RA-1844) observation well for climate change storylines, without Water Management Strategies (storyline minus Groundwater Base Case).

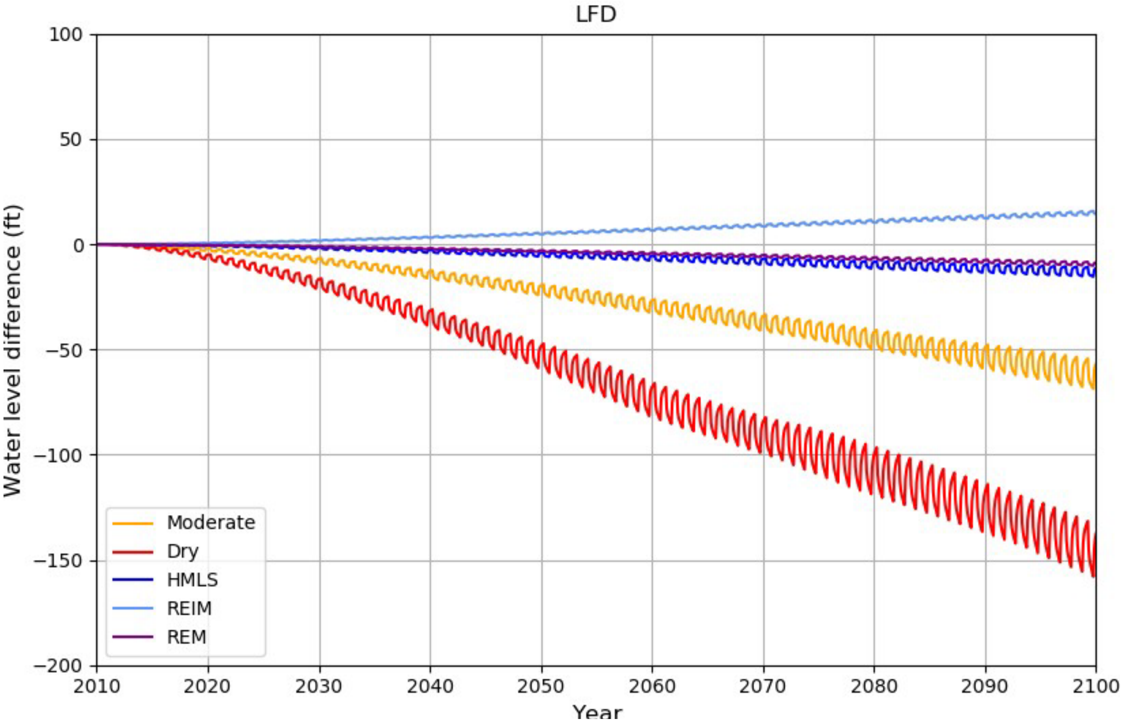

Figure 23. Change in simulated water levels at the LFD observation well for climate change storylines, without Water Management Strategies (storyline minus Groundwater Base Case).

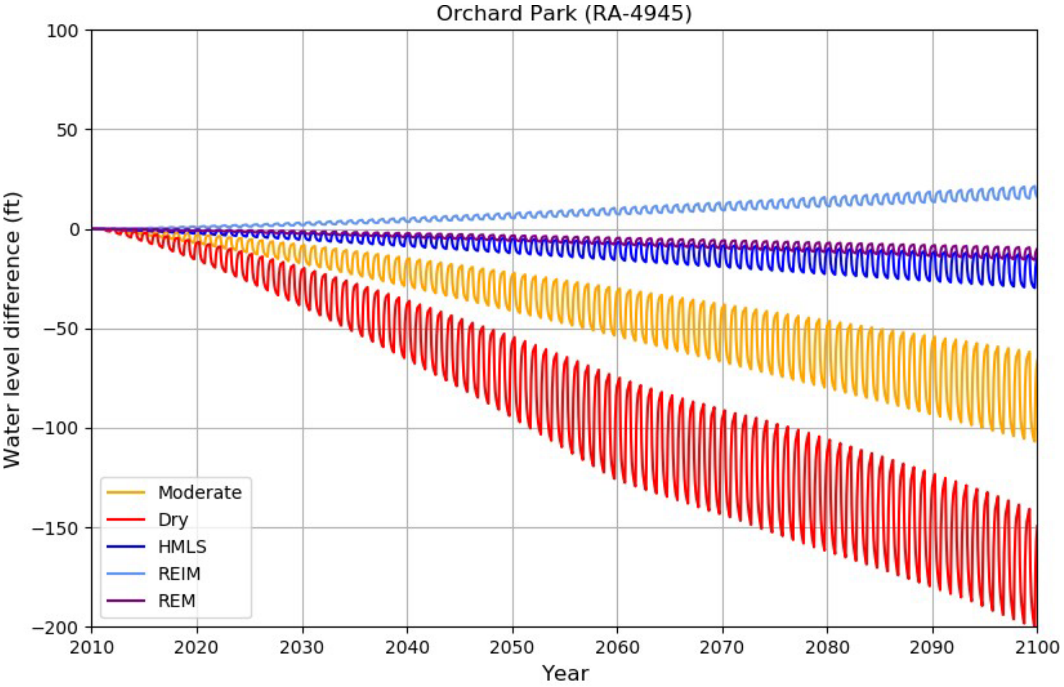

Figure 24. Change in simulated water levels at the Orchard Park (RA-4945) observation well for climate change storylines, without Water Management Strategies (storyline minus Groundwater Base Case).

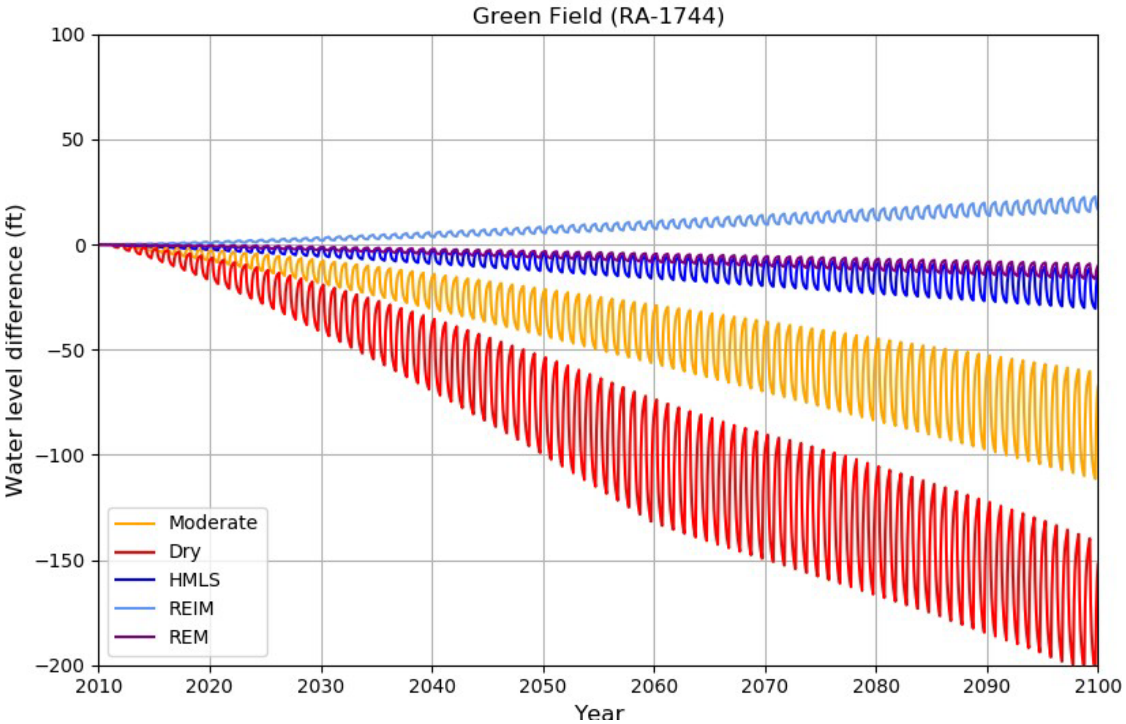

Figure 25. Change in simulated water levels at the Green Field (RA-1744) observation well for climate change storylines, without Water Management Strategies (storyline minus Groundwater Base Case).

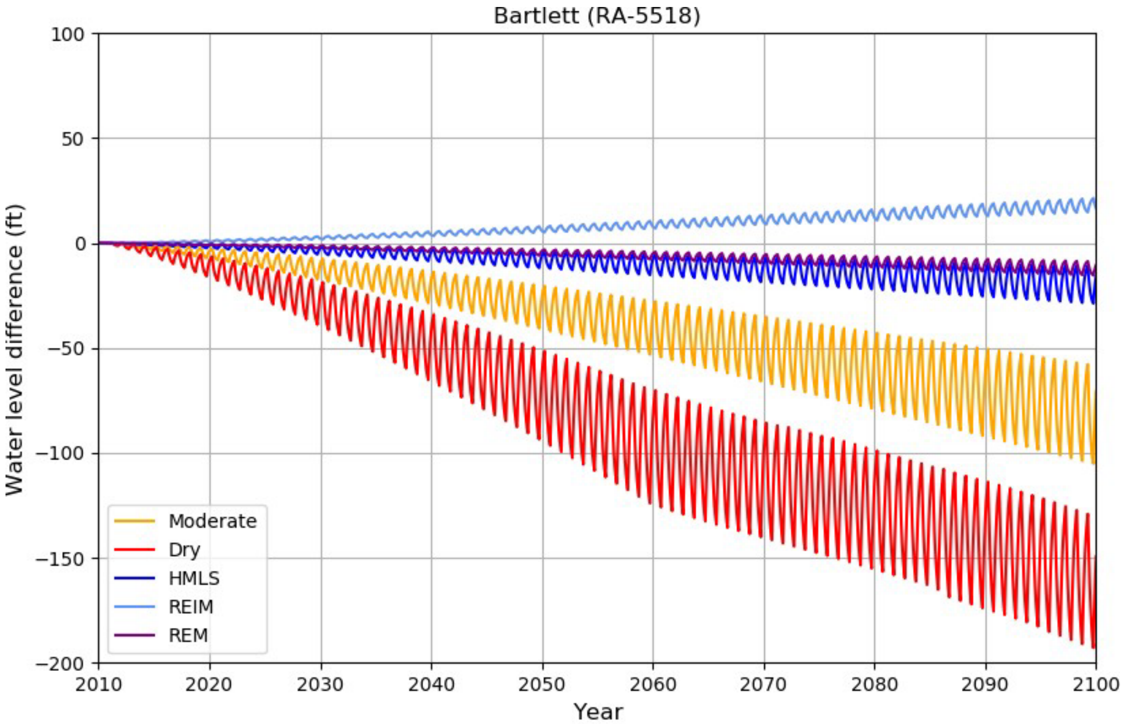

Figure 26. Change in simulated water levels at the Bartlett (RA-5518) observation well for climate change storylines, without Water Management Strategies (storyline minus Groundwater Base Case).

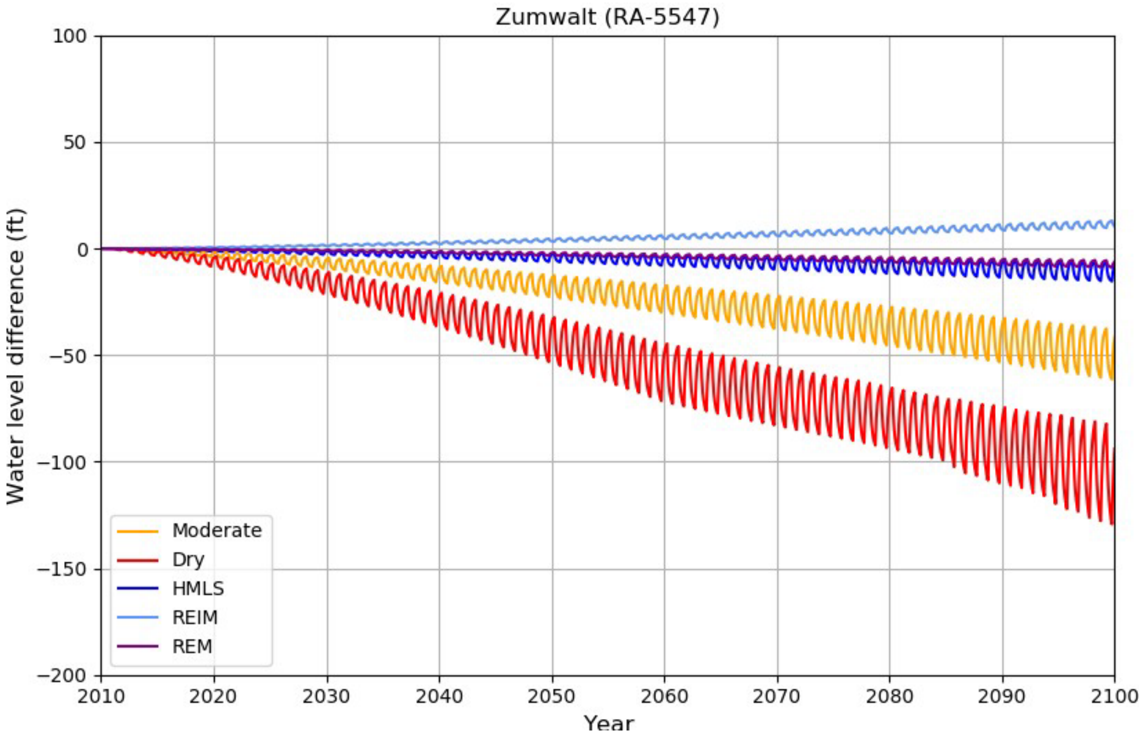

Figure 27. Change in simulated water levels at the Zumwalt (RA-5547) observation well for climate change storylines, without Water Management Strategies (storyline minus Groundwater Base Case)

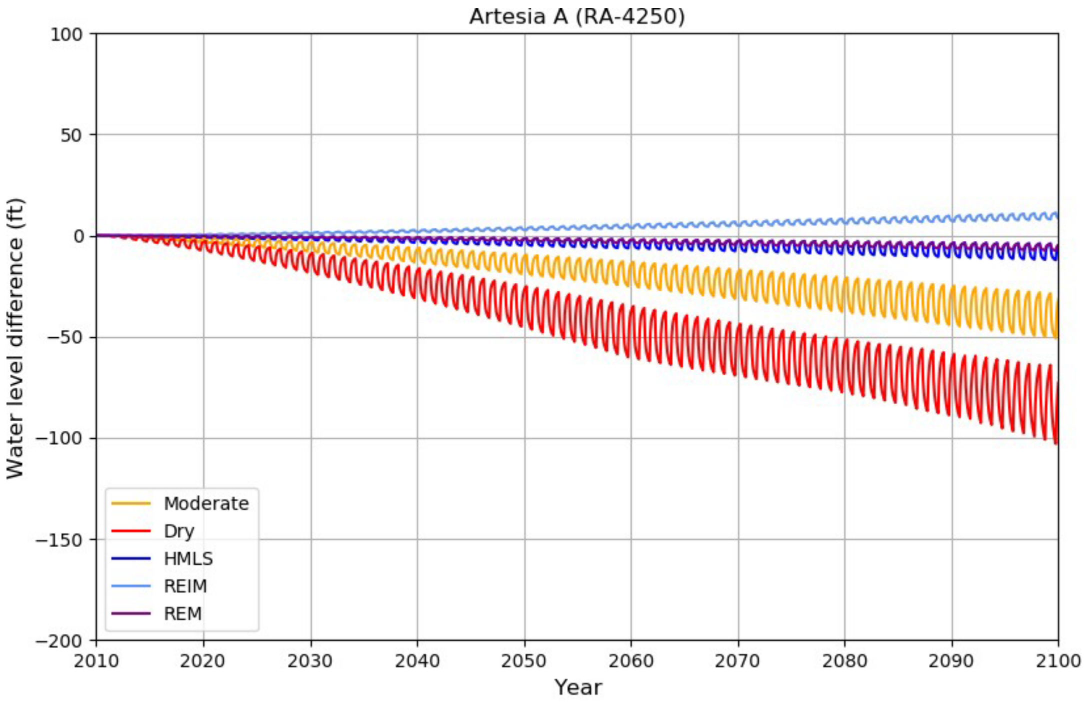

Figure 28. Change in simulated water levels at the Artesia A (RA-4250) observation well for climate change storylines, without Water Management Strategies (storyline minus Groundwater Base Case).

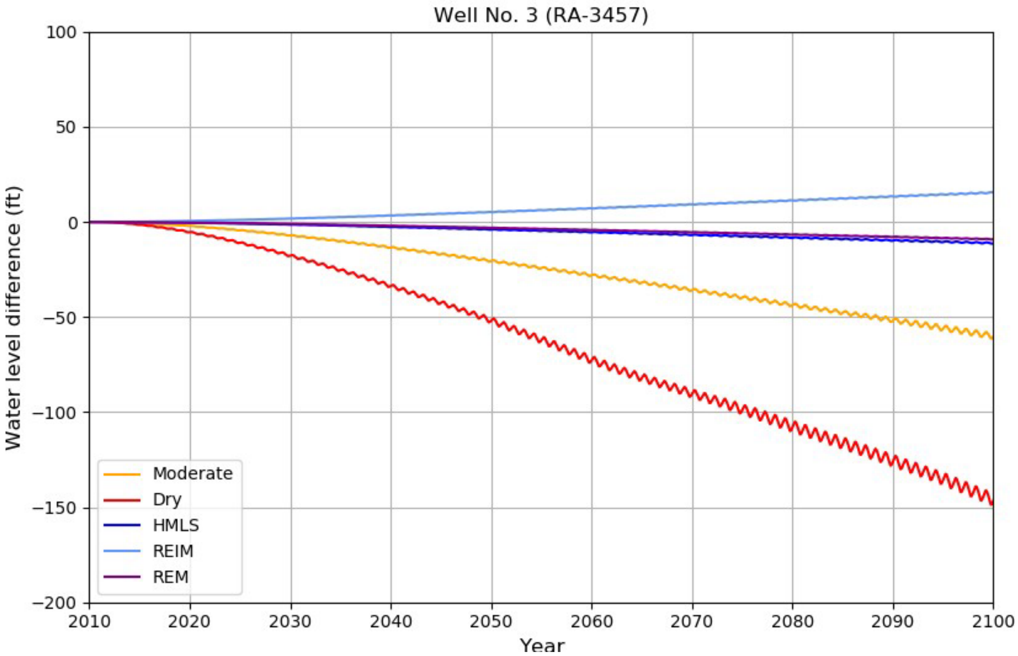

Figure 29. Change in simulated water levels at the Well No. 3 (RA-3457) observation well for climate change storylines, without Water Management Strategies (storyline minus Groundwater Base Case).

7.2. 20% Reduction Figures

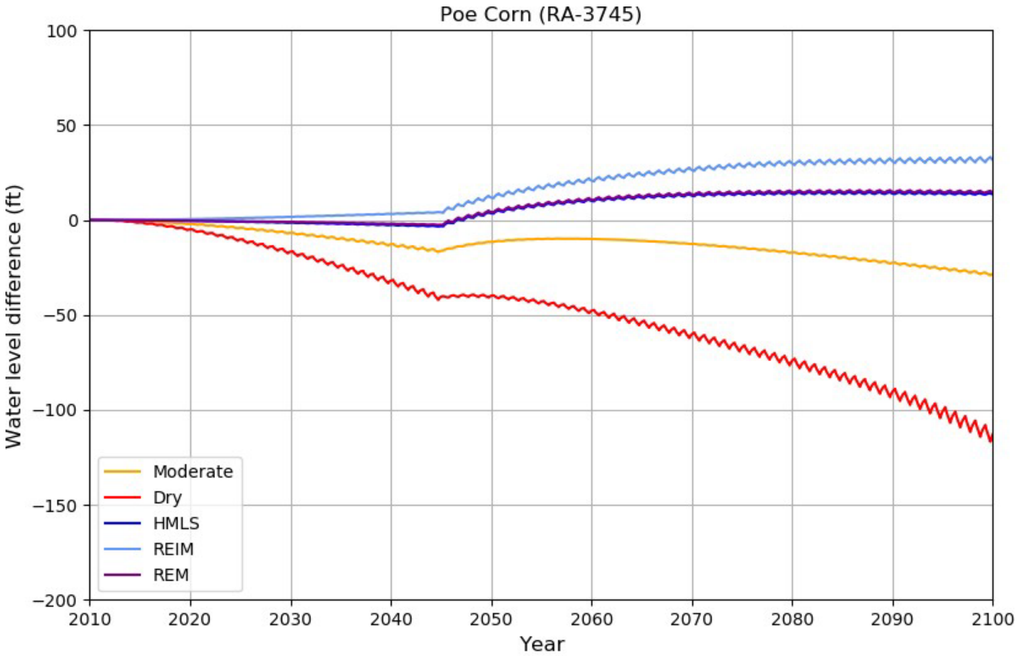

Figure 30. Change in simulated water levels at the Poe Corn (RA-3745) observation well for climate change storylines, with a 20% reduction in irrigation pumping in 2045 (storyline minus Groundwater Base Case).

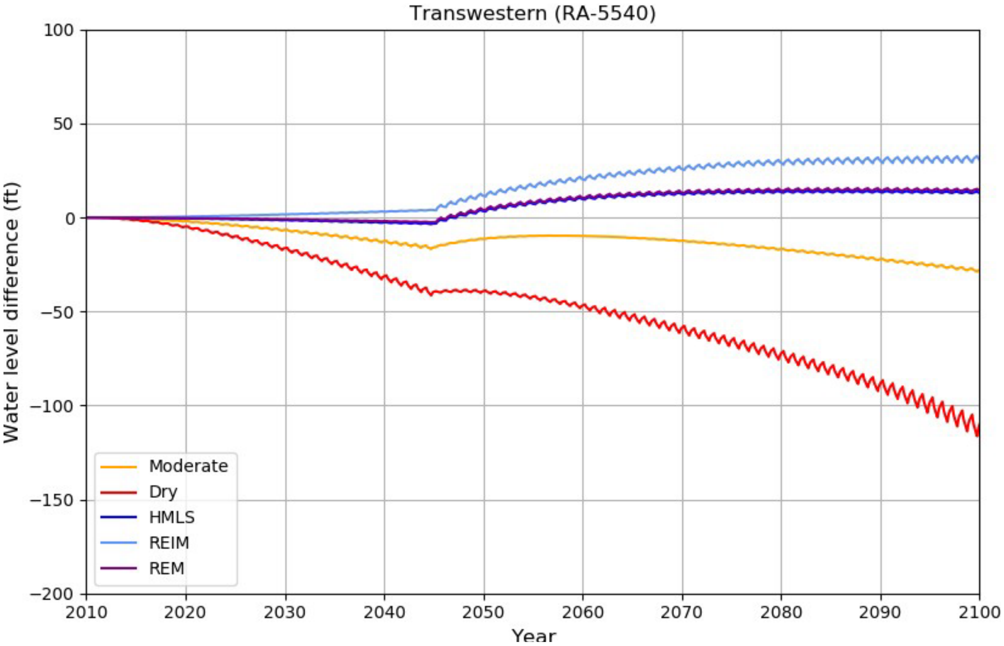

Figure 31. Change in simulated water levels at the Transwestern (RA-5540) observation well for climate change storylines, with a 20% reduction in irrigation pumping in 2045 (storyline minus Groundwater Base Case).

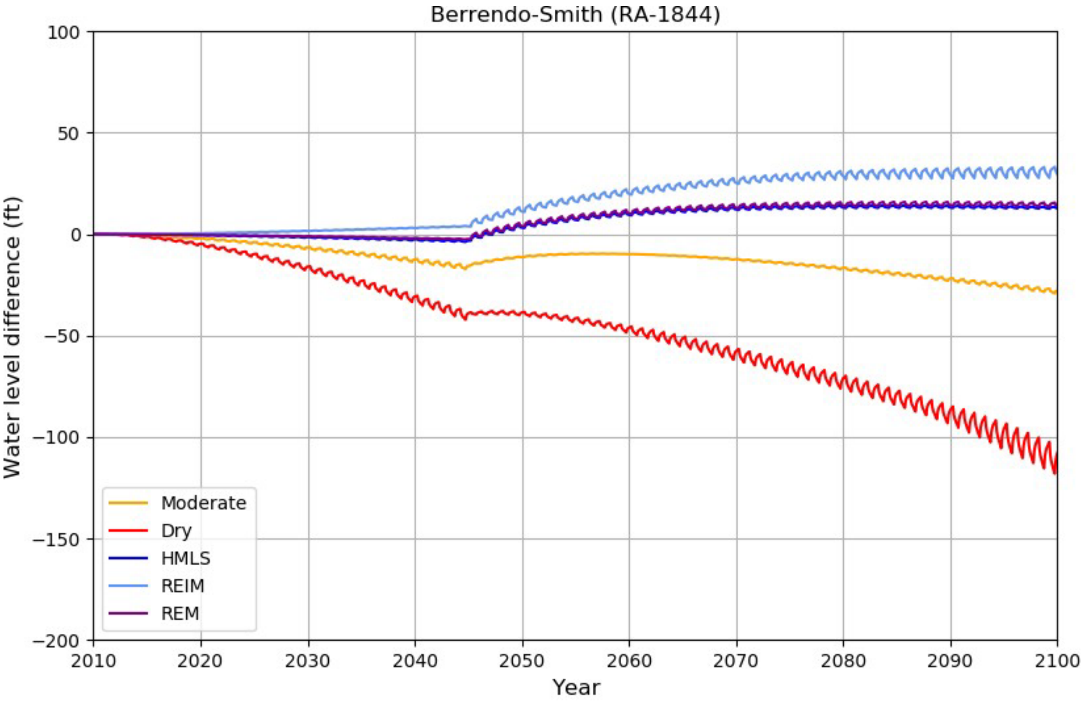

Figure 32. Change in simulated water levels at the Berrendo-Smith (RA-1844) observation well for climate change storylines, with a 20% reduction in irrigation pumping in 2045 (storyline minus Groundwater Base Case).

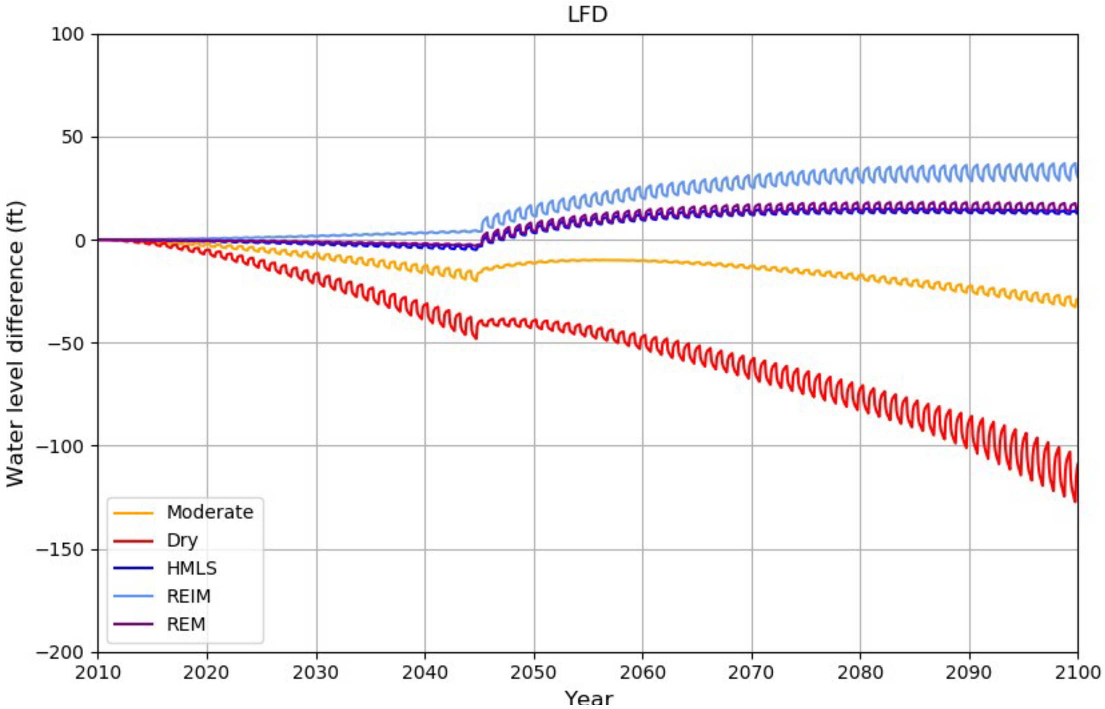

Figure 33. Change in simulated water levels at the LFD observation well for climate change storylines, with a 20% reduction in irrigation pumping in 2045 (storyline minus Groundwater Base Case).

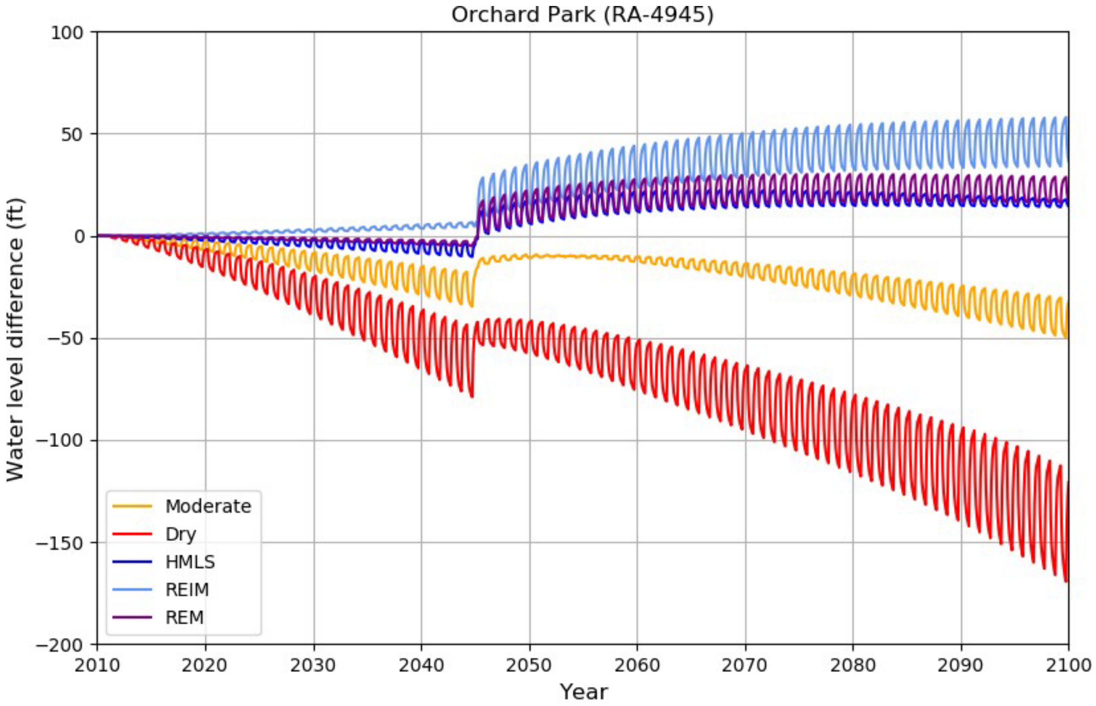

Figure 34. Change in simulated water levels at the Orchard Park (RA-4945) observation well for climate change storylines, with a 20% reduction in irrigation pumping in 2045 (storyline minus Groundwater Base Case).

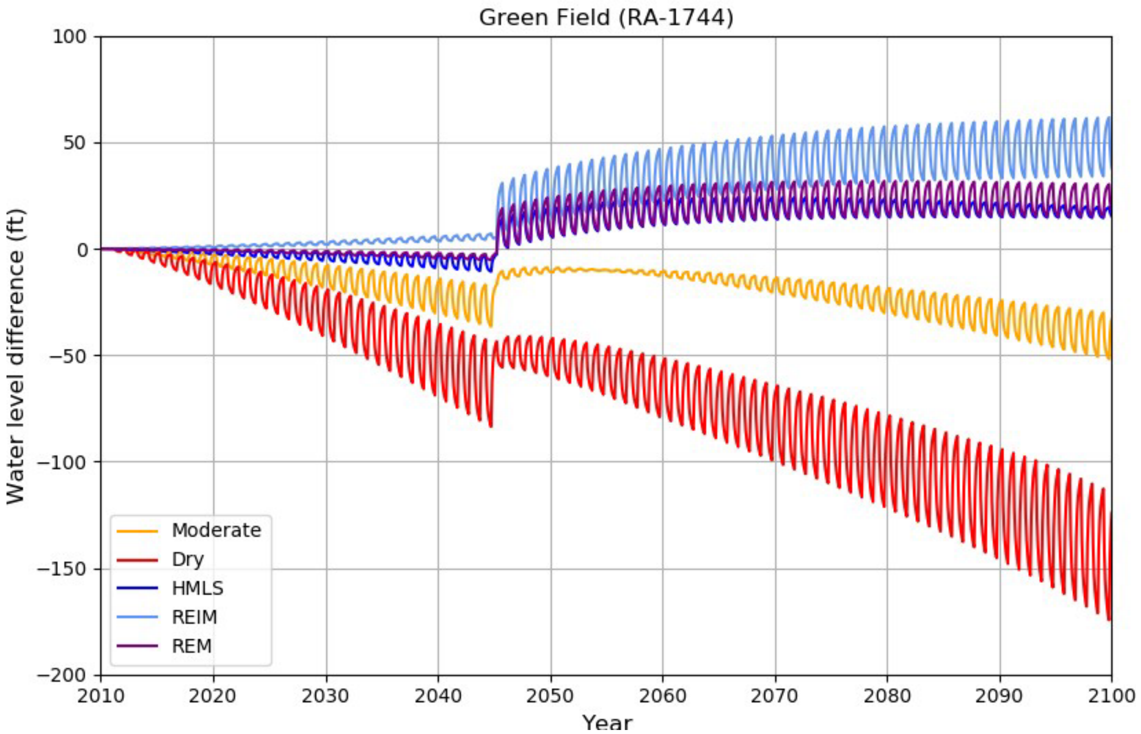

Figure 35. Change in simulated water levels at the Green Field (RA-1744) observation well for climate change storylines, with a 20% reduction in irrigation pumping in 2045 (storyline minus Groundwater Base Case).

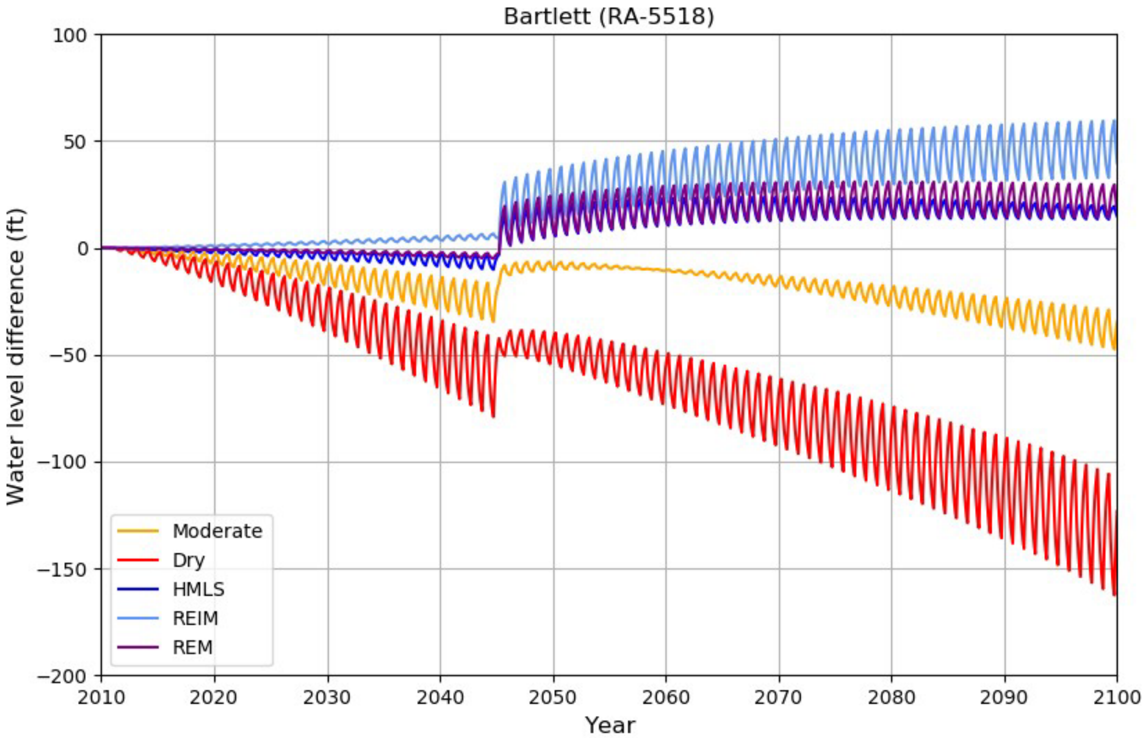

Figure 36. Change in simulated water levels at the Bartlett (RA-5518) observation well for climate change storylines, with a 20% reduction in irrigation pumping in 2045 (storyline minus Groundwater Base Case).

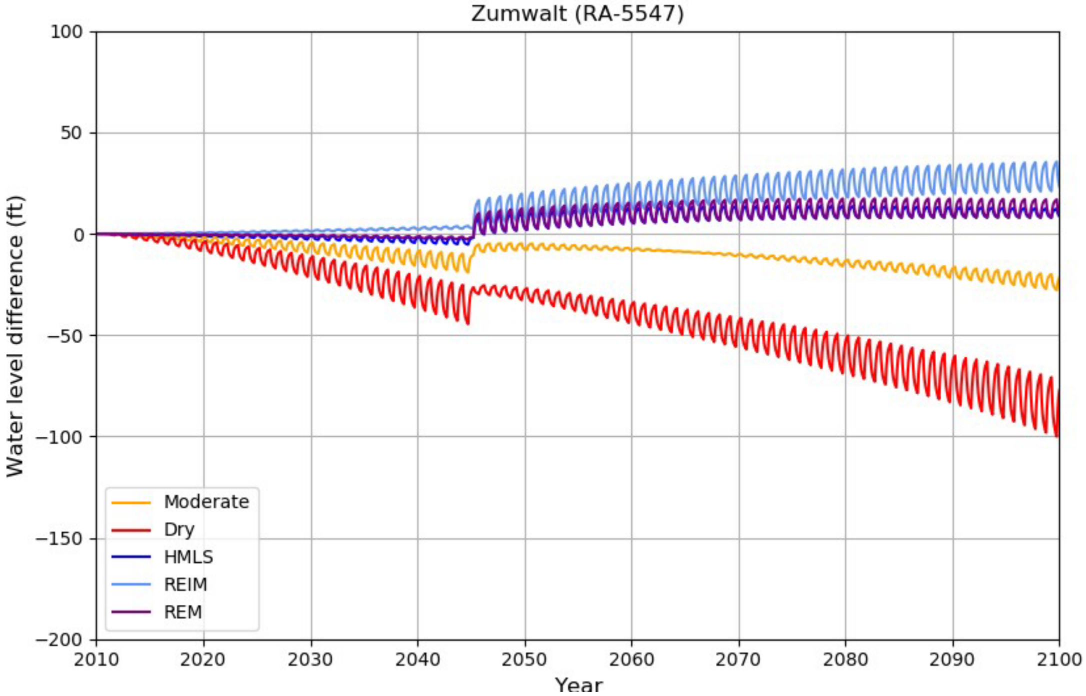

Figure 37. Change in simulated water levels at the Zumwalt (RA-5547) observation well for climate change storylines, with a 20% reduction in irrigation pumping in 2045 (storyline minus Groundwater Base Case).

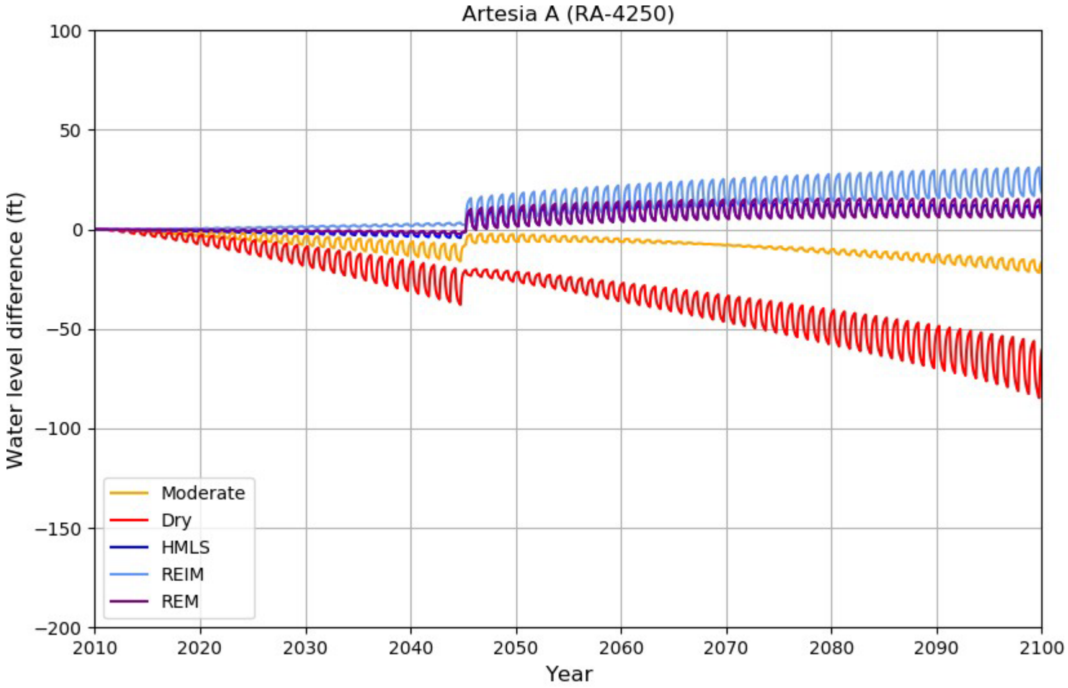

Figure 38. Change in simulated water levels at the Artesia A (RA-4250) observation well for climate change storylines, with a 20% reduction in irrigation pumping in 2045 (storyline minus Groundwater Base Case).

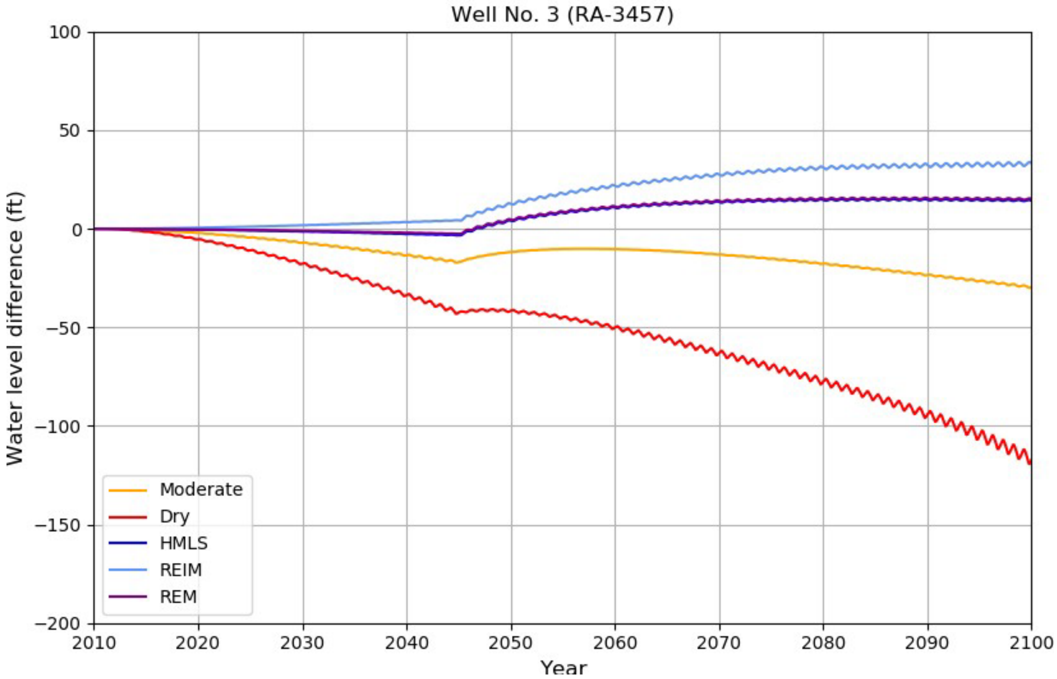

Figure 39. Change in simulated water levels at the Well No 3. ((RA-3457) observation well for climate change storylines, with a 20% reduction in irrigation pumping in 2045 (storyline minus Groundwater Base Case).

7.3. 25% Reduction Figures

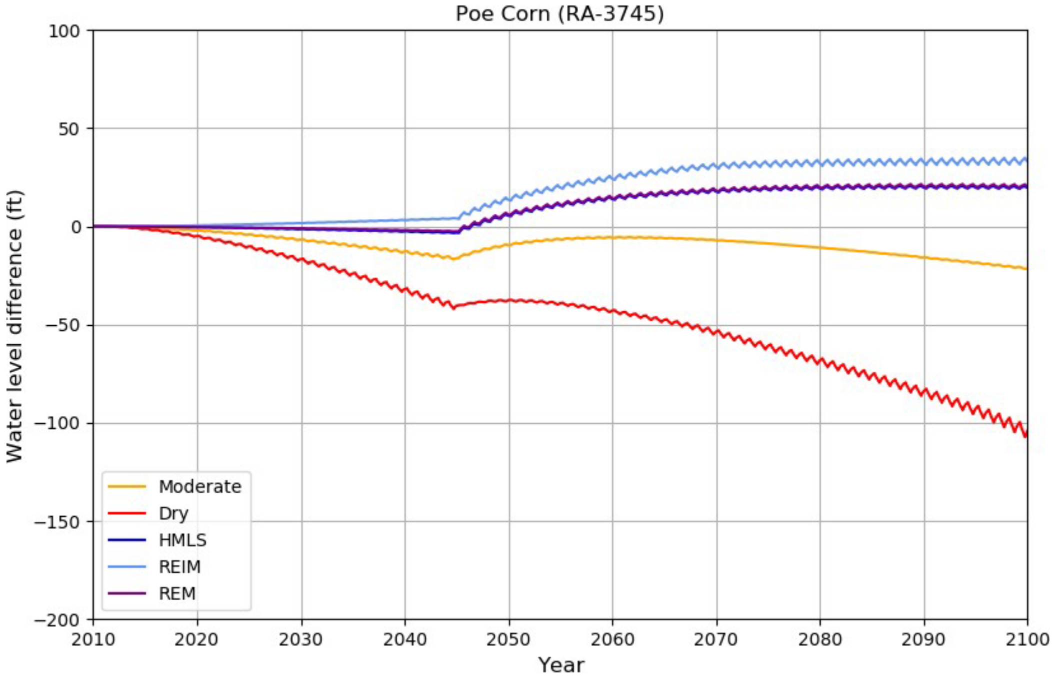

Figure 40. Change in simulated water levels at the Well No 3. ((RA-3457) observation well for climate change storylines, with a 25% reduction in irrigation pumping in 2045 (storyline minus Groundwater Base Case).

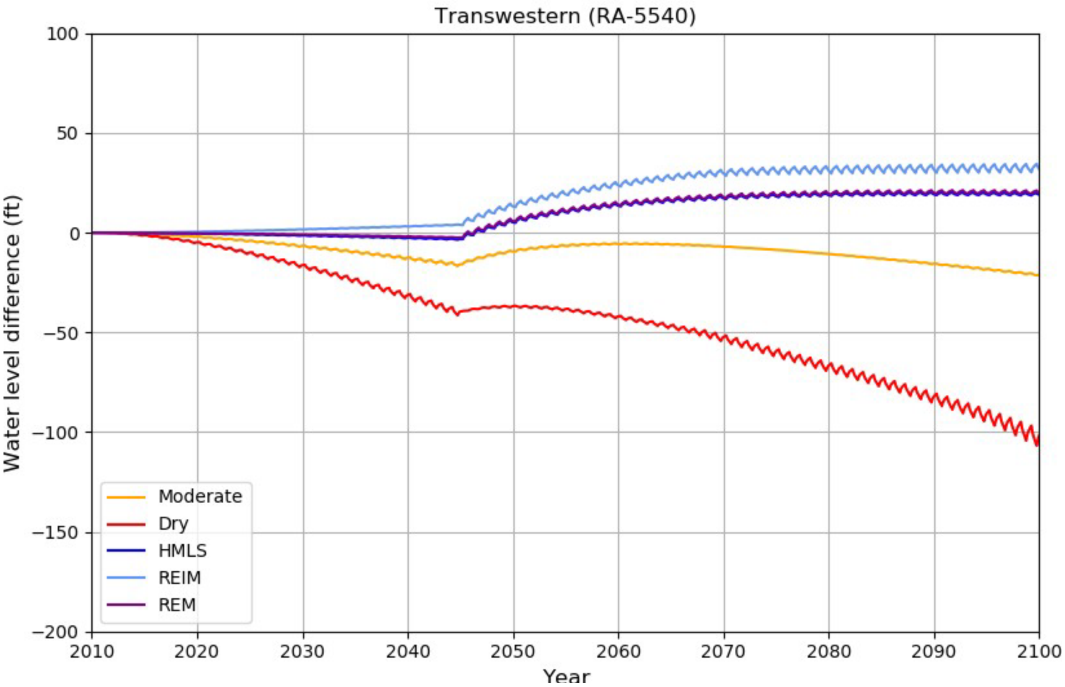

Figure 41. Change in simulated water levels at the Transwestern (RA-5540) observation well for climate change storylines, with a 25% reduction in irrigation pumping in 2045 (storyline minus Groundwater Base Case).

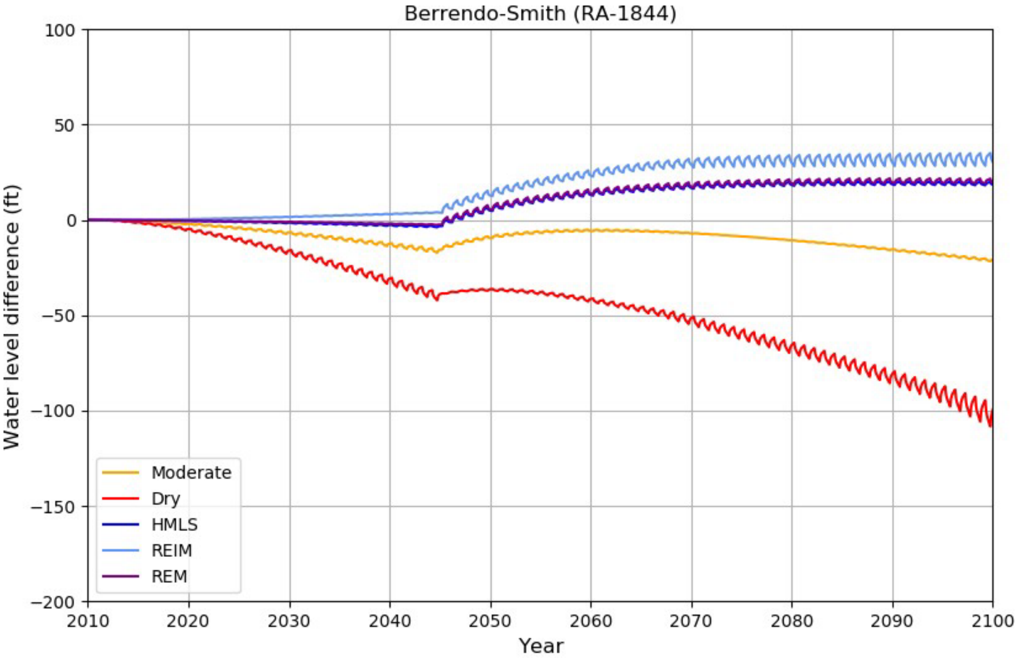

Figure 42. Change in simulated water levels at the Berrendo-Smith ((RA-1844) observation well for climate change storylines, with a 25% reduction in irrigation pumping in 2045 (storyline minus Groundwater Base Case).

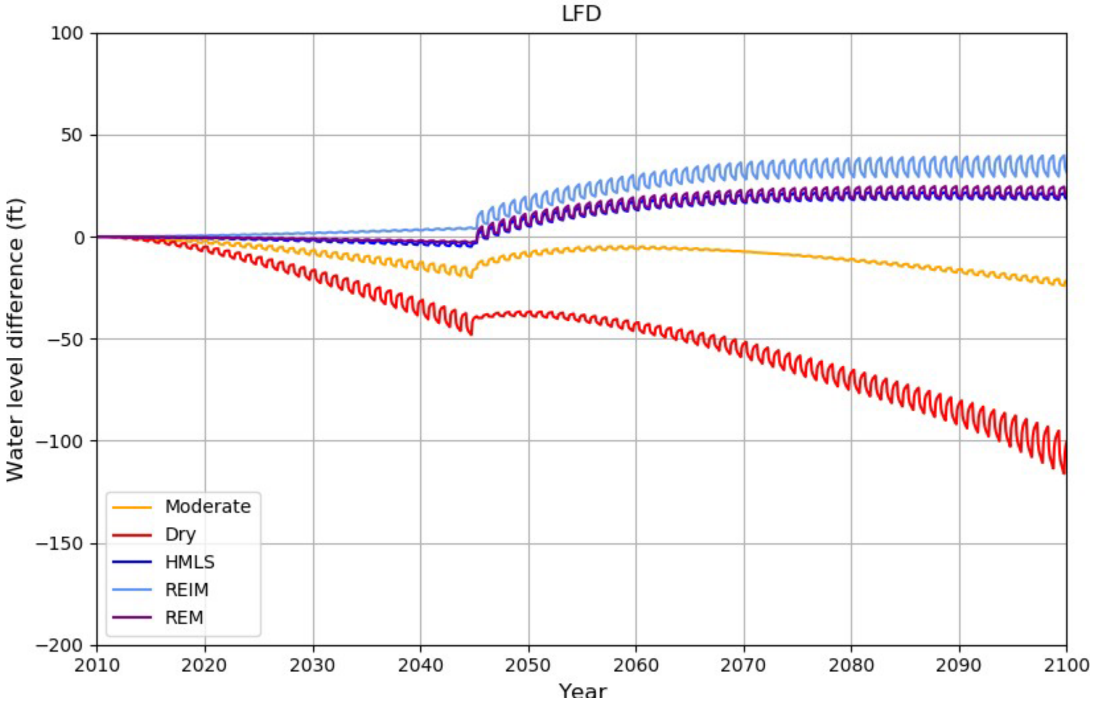

Figure 43. Change in simulated water levels at the LFD observation well for climate change storylines, with a 25% reduction in irrigation pumping in 2045 (storyline minus Groundwater Base Case).

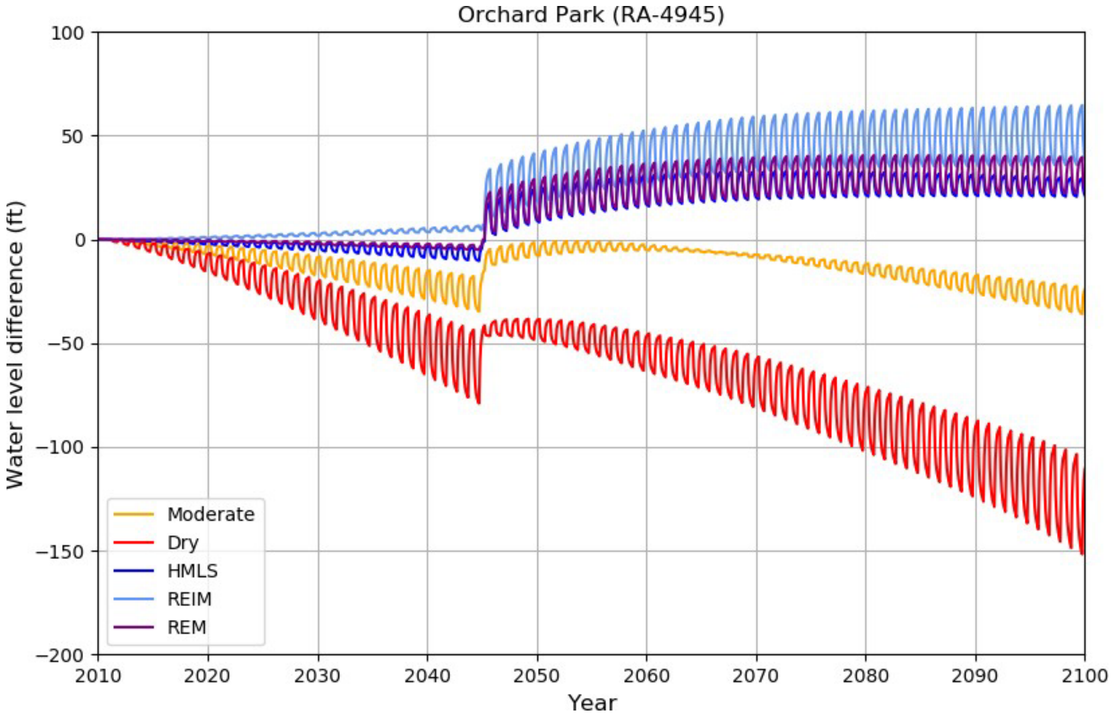

Figure 44. Change in simulated water levels at the Orchard Park (RA-4945) observation well for climate change storylines, with a 25% reduction in irrigation pumping in 2045 (storyline minus Groundwater Base Case).

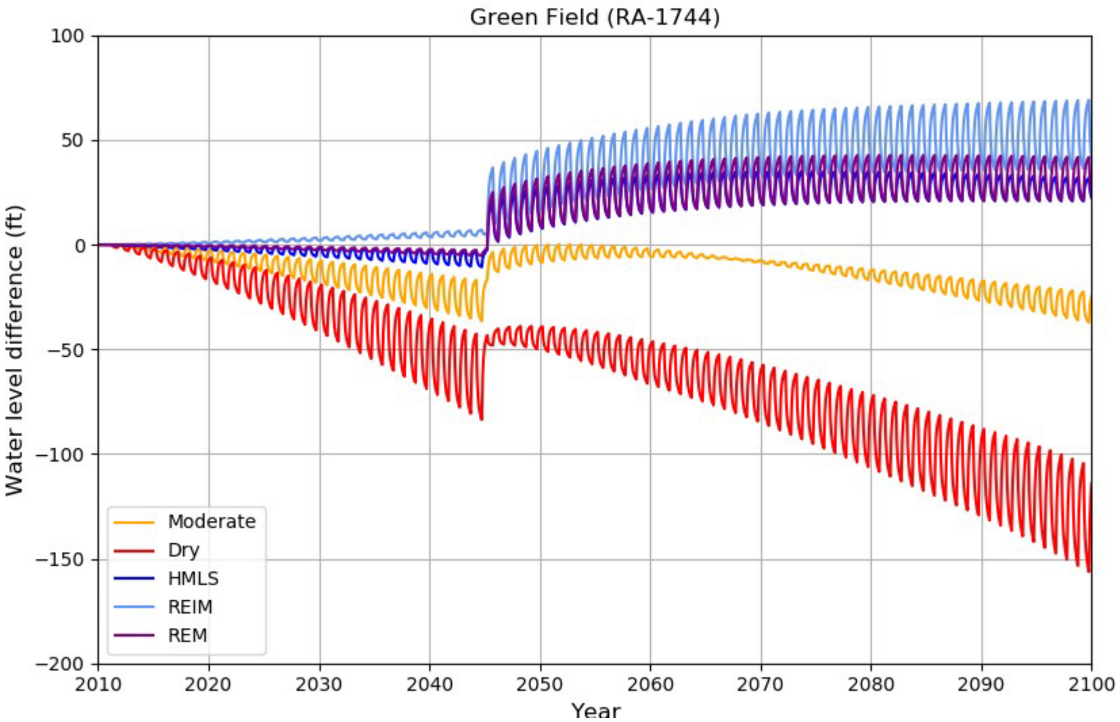

Figure 45. Change in simulated water levels at the Green Field (RA-1744) observation well for climate change storylines, with a 25% reduction in irrigation pumping in 2045 (storyline minus Groundwater Base Case).

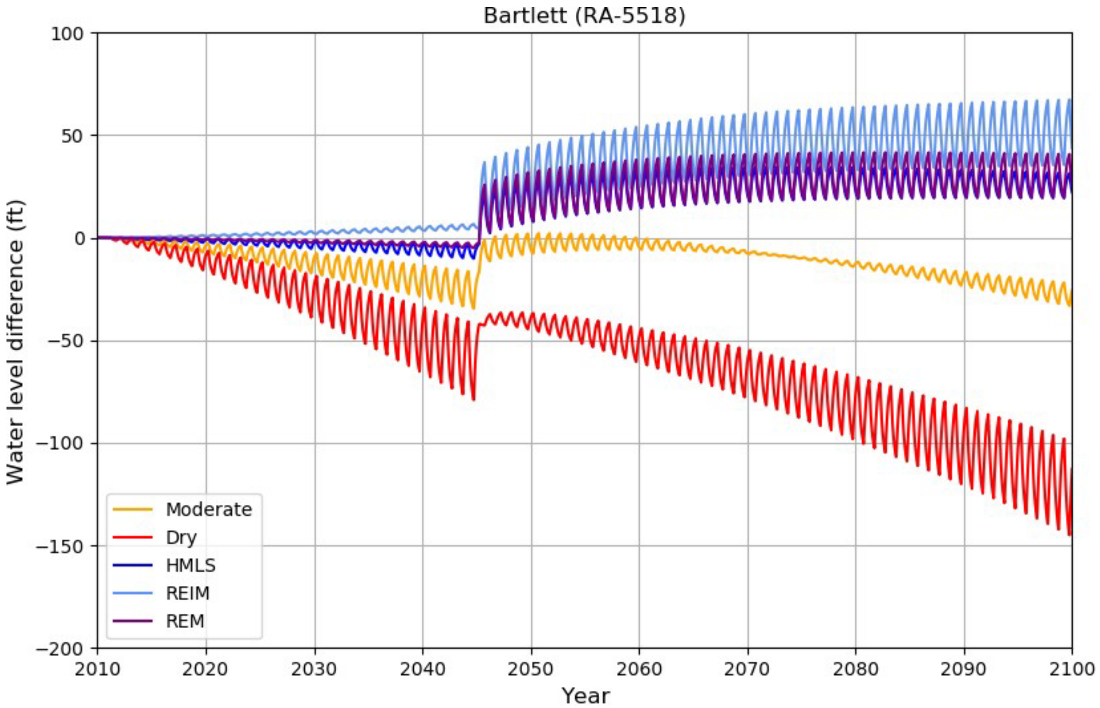

.

Figure 46. Change in simulated water levels at the Bartlett (RA-5518) observation well for climate change storylines, with a 25% reduction in irrigation pumping in 2045 (storyline minus Groundwater Base Case).

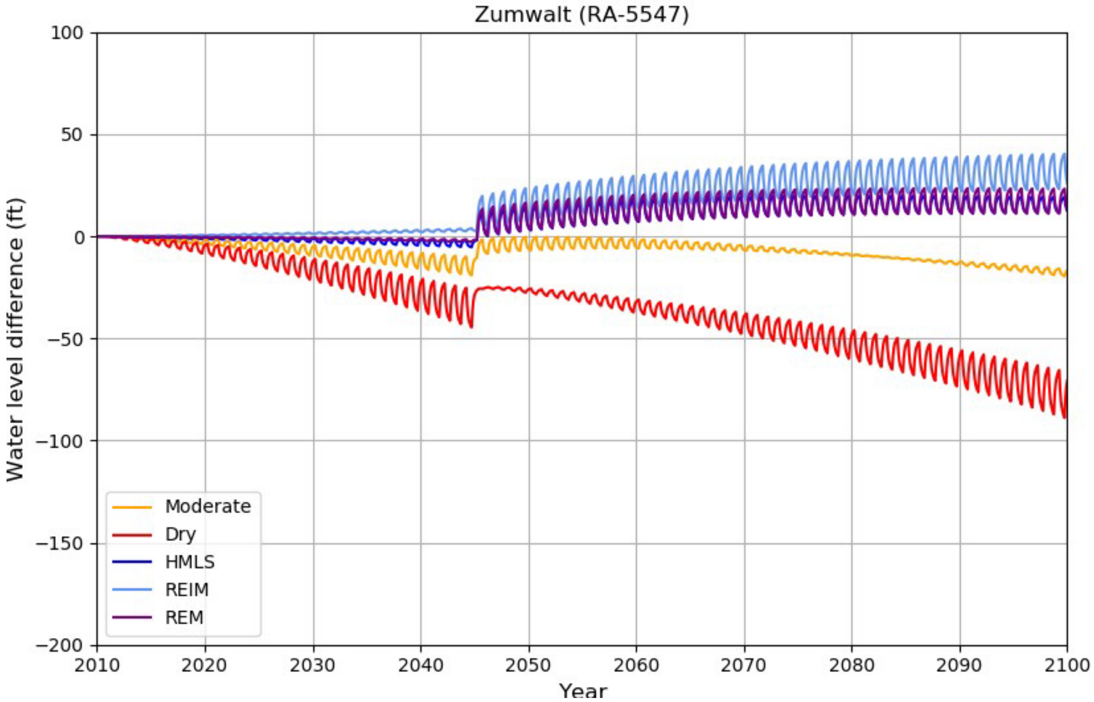

Figure 47. Change in simulated water levels at the Zumwalt (RA-5547) observation well for climate change storylines, with a 25% reduction in irrigation pumping in 2045 (storyline minus Groundwater Base Case).

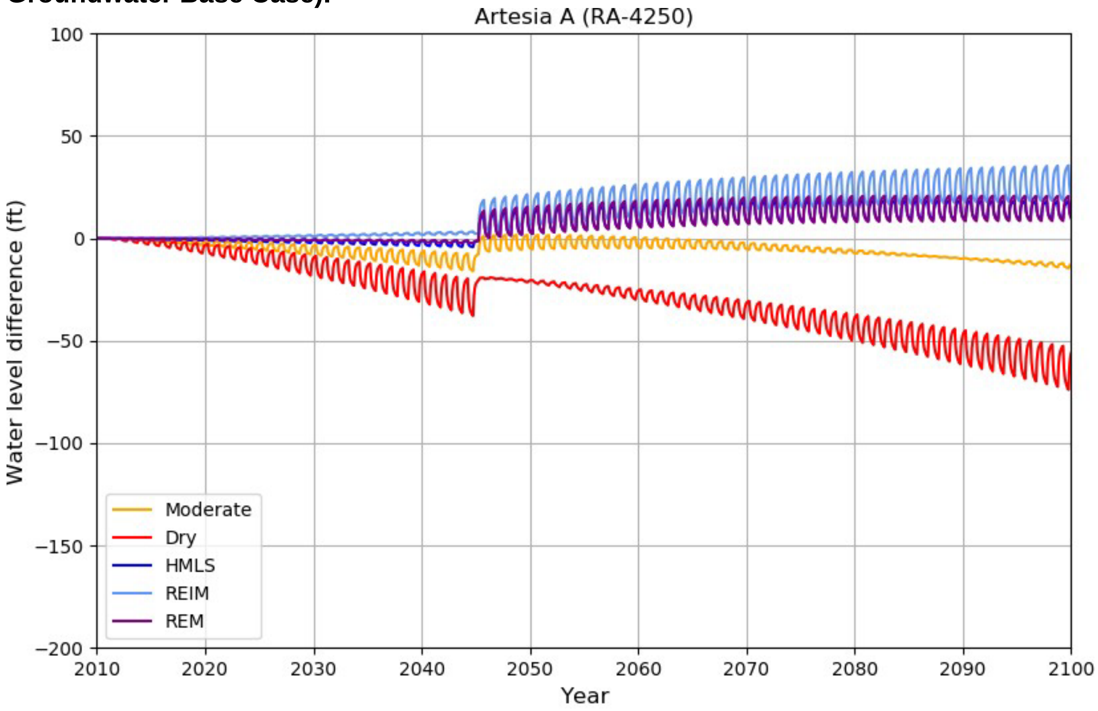

Figure 48. Change in simulated water levels at the Artesia A (RA-4250) observation well for climate change storylines, with a 25% reduction in irrigation pumping in 2045 (storyline minus Groundwater Base Case).

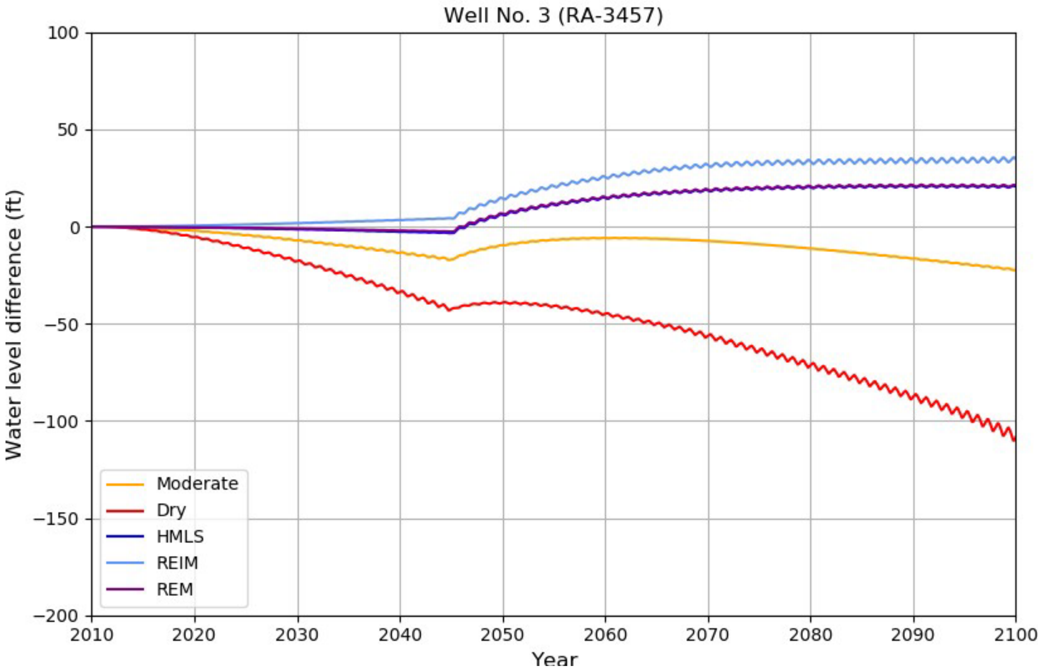

Figure 49. Change in simulated water levels at the Well No. 3 (RA-3457) observation well for climate change storylines, with a 25% reduction in irrigation pumping in 2045 (storyline minus Groundwater Base Case).

7.4. 30% Reduction Figures

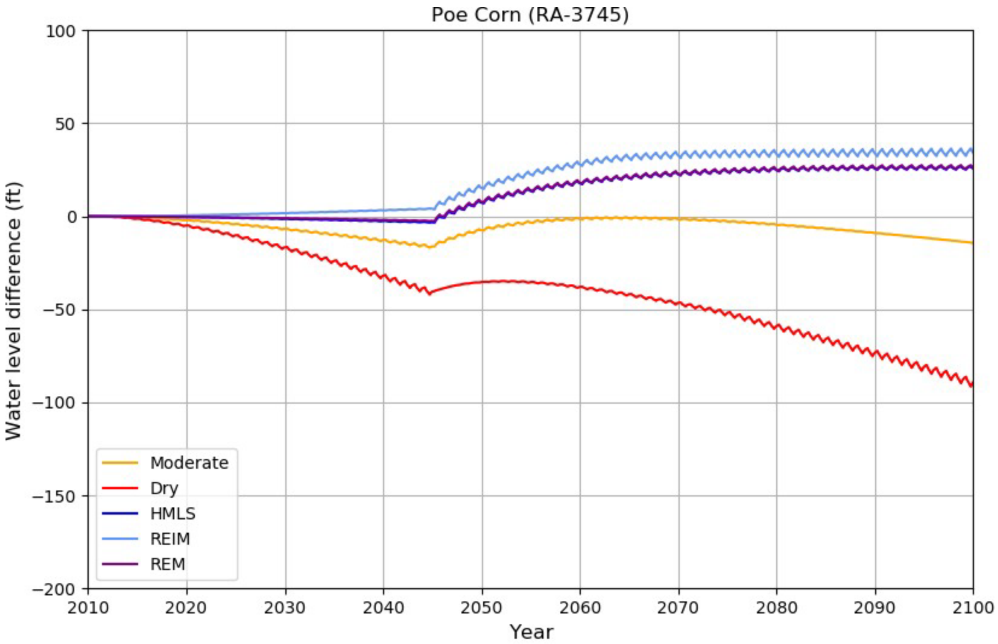

Figure 50. Change in simulated water levels at the Poe Corn (RA-3745) observation well for climate change storylines, with a 30% reduction in irrigation pumping in 2045 (storyline minus Groundwater Base Case).

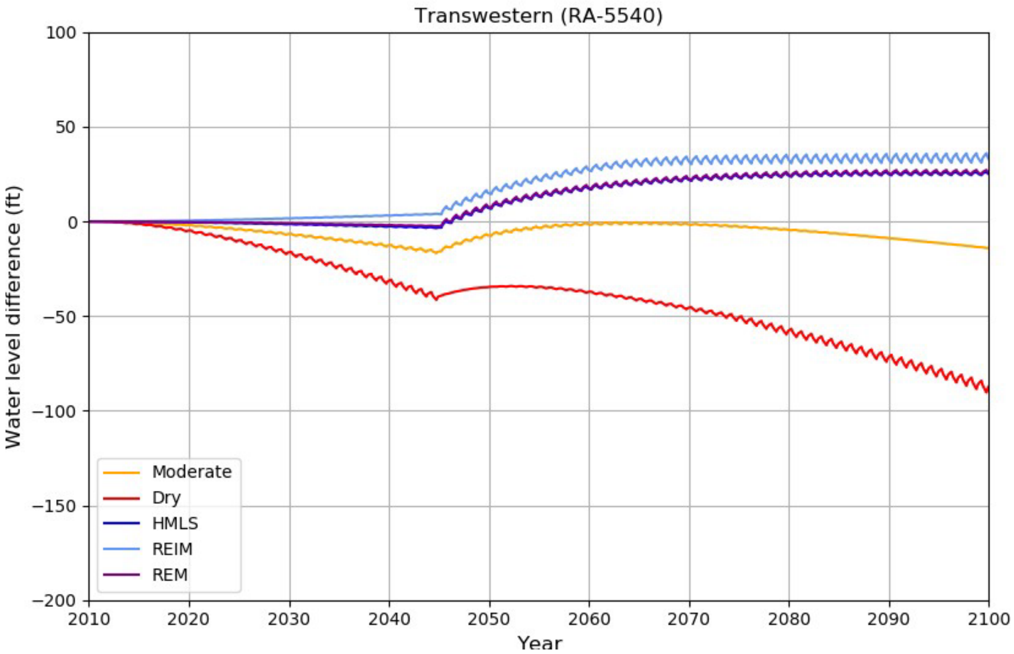

Figure 51. Change in simulated water levels at the Transwestern (RA-5540) observation well for climate change storylines, with a 30% reduction in irrigation pumping in 2045 (storyline minus Groundwater Base Case).

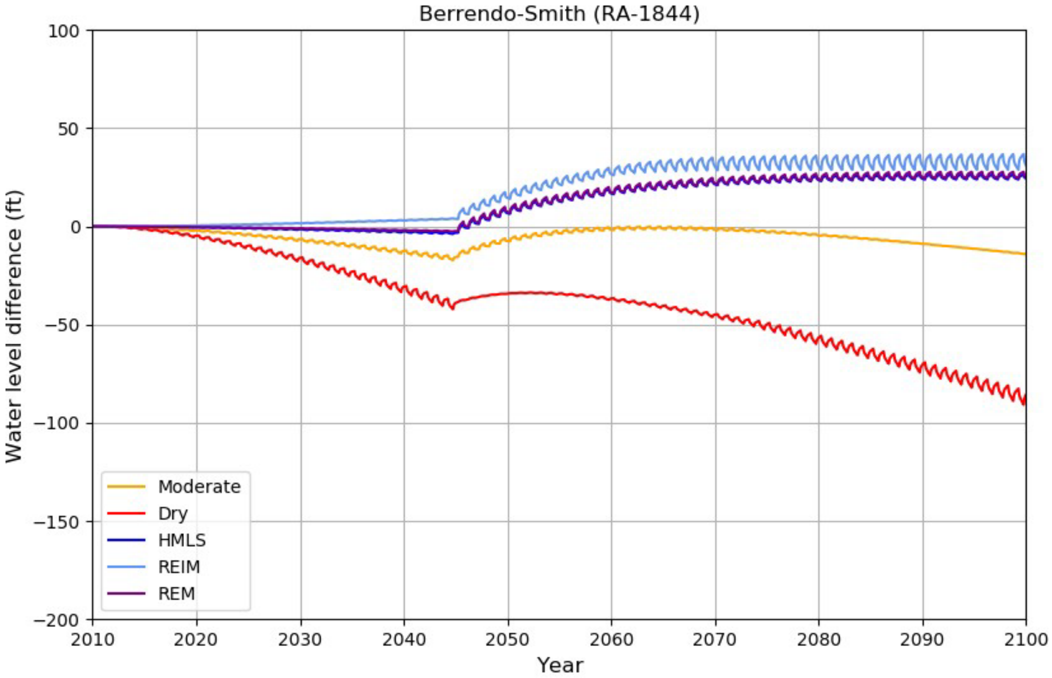

Figure 52. Change in simulated water levels at the Berrendo Smith (RA-1844) observation well for climate change storylines, with a 30% reduction in irrigation pumping in 2045 (storyline minus Groundwater Base Case).

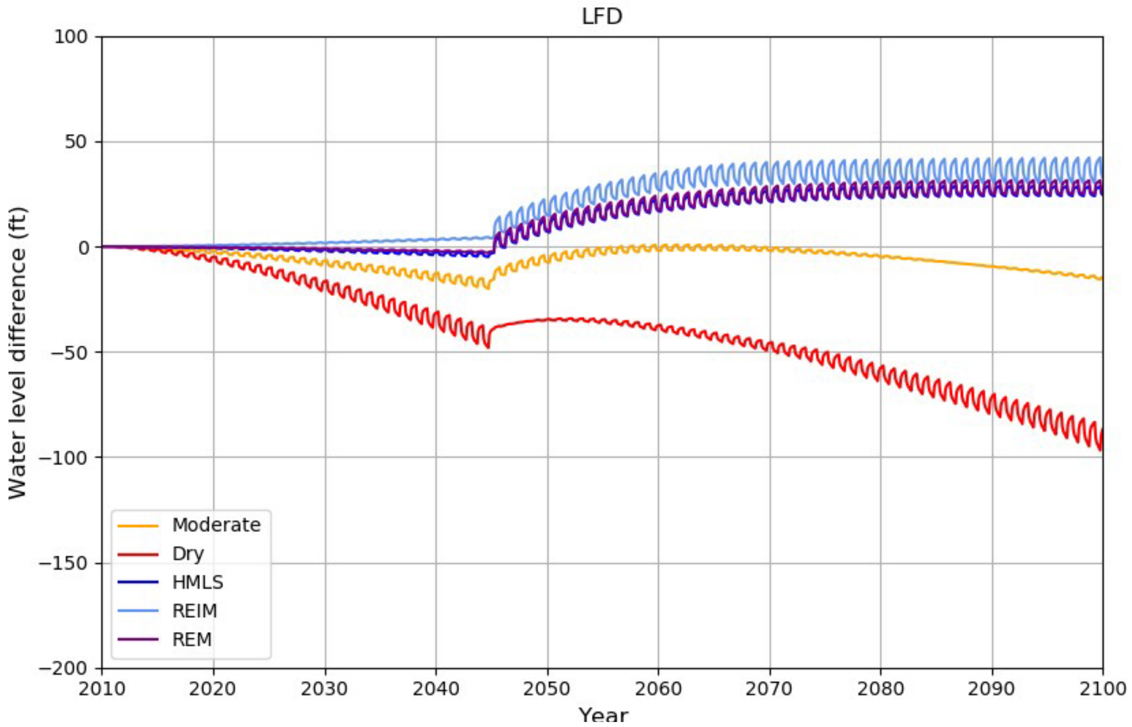

Figure 53. Change in simulated water levels at the LFD observation well for climate change storylines, with a 30% reduction in irrigation pumping in 2045 (storyline minus Groundwater Base Case).

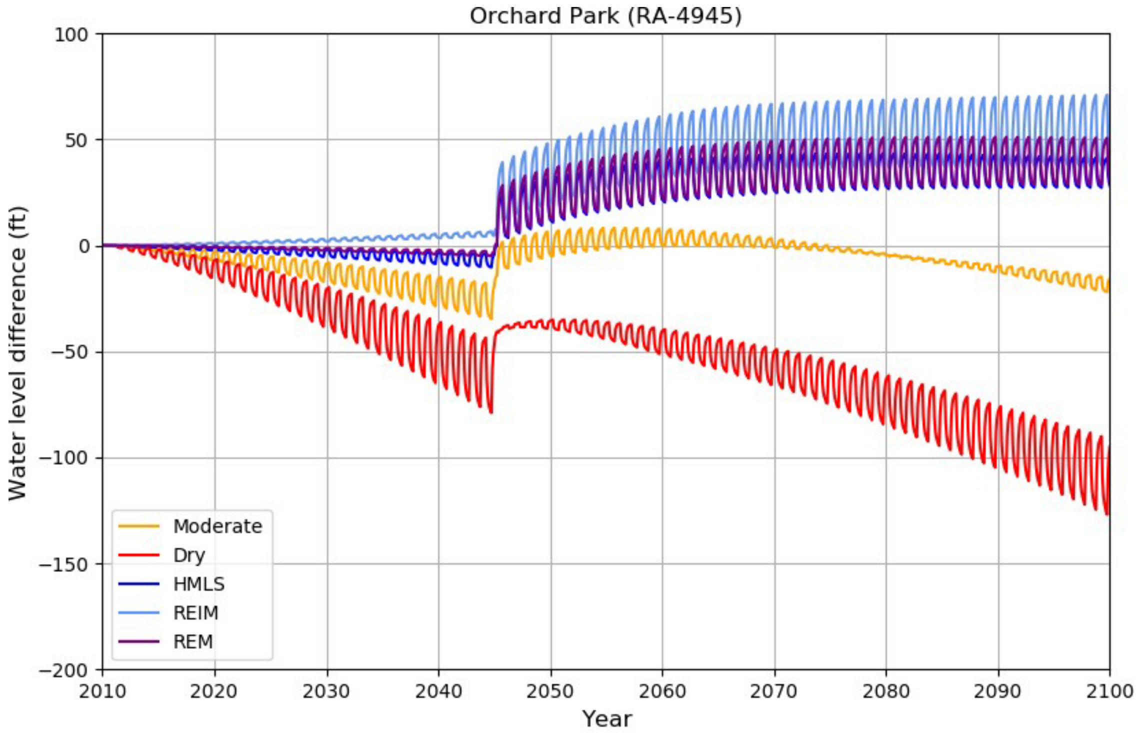

Figure 54. Change in simulated water levels at the Orchard Park (RA-4945) observation well for climate change storylines, with a 30% reduction in irrigation pumping in 2045 (storyline minus Groundwater Base Case).

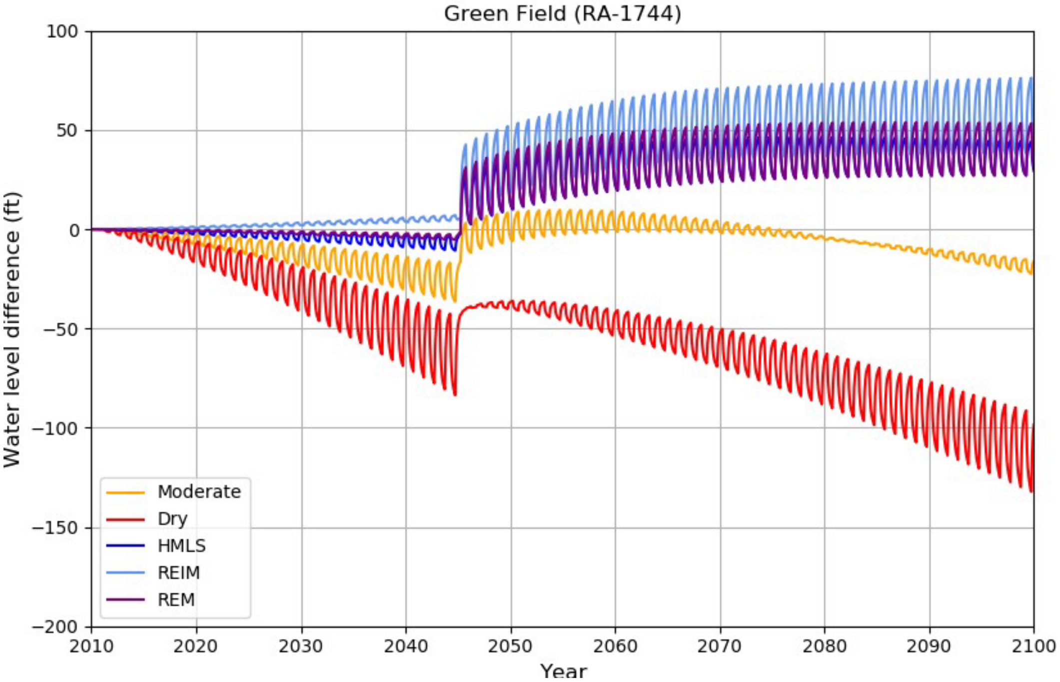

Figure 55. Change in simulated water levels at the Green Field (RA-1744) observation well for climate change storylines, with a 30% reduction in irrigation pumping in 2045 (storyline minus Groundwater Base Case).

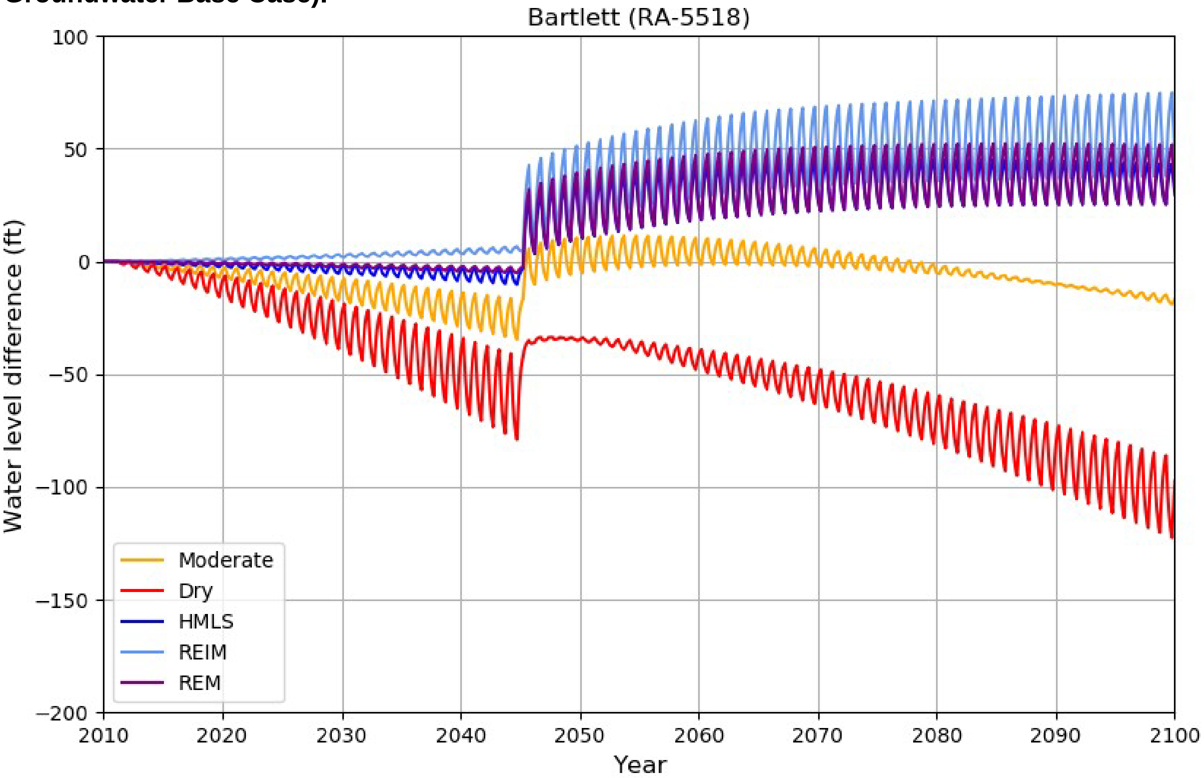

Figure 56. Change in simulated water levels at the Bartlett (RA-5518) observation well for climate change storylines, with a 30% reduction in irrigation pumping in 2045 (storyline minus Groundwater Base Case).

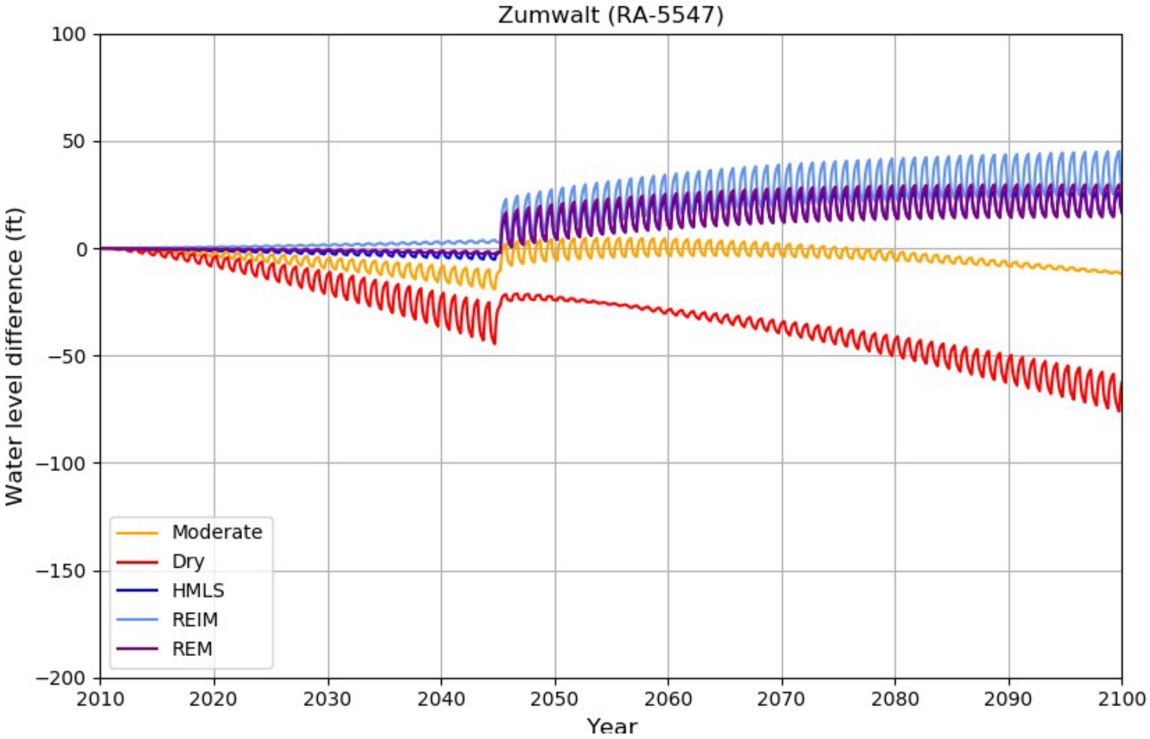

Figure 57. Change in simulated water levels at the Zumwalt (RA-5547) observation well for climate change storylines, with a 39% reduction in irrigation pumping in 2045 (storyline minus Groundwater Base Case).

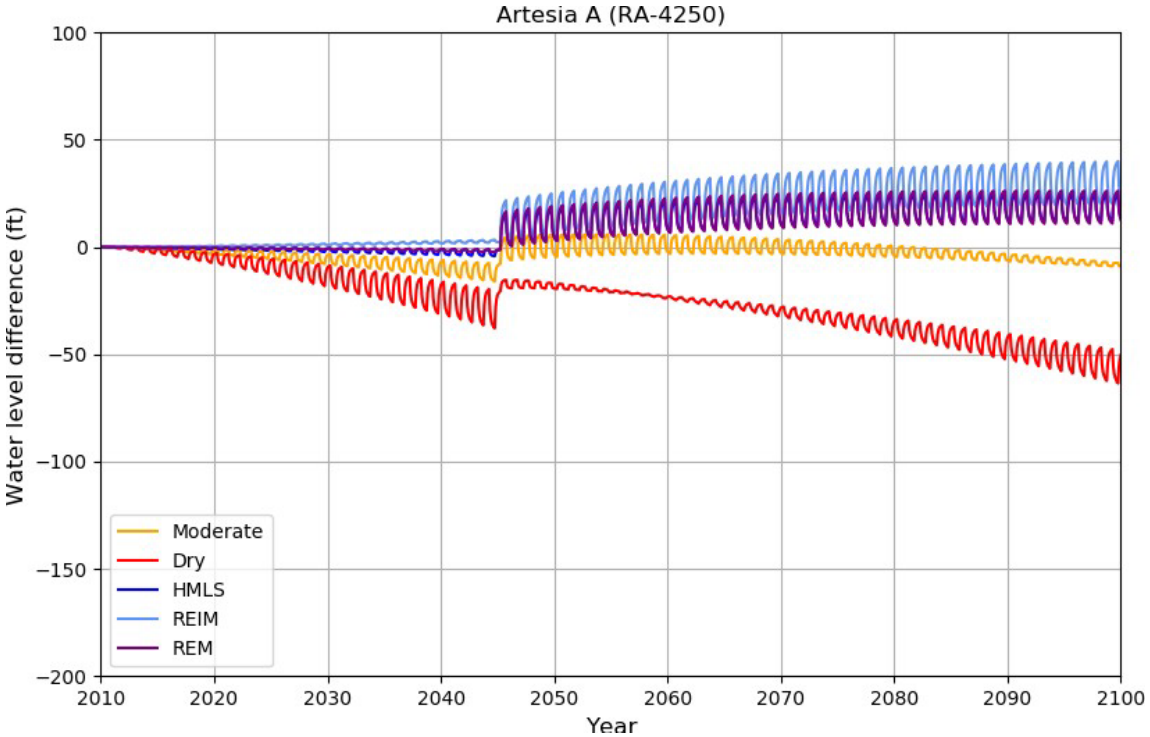

Figure 58. Change in simulated water levels at the Artesia A (RA-4250) observation well for climate change storylines, with a 30% reduction in irrigation pumping in 2045 (storyline minus Groundwater Base Case).

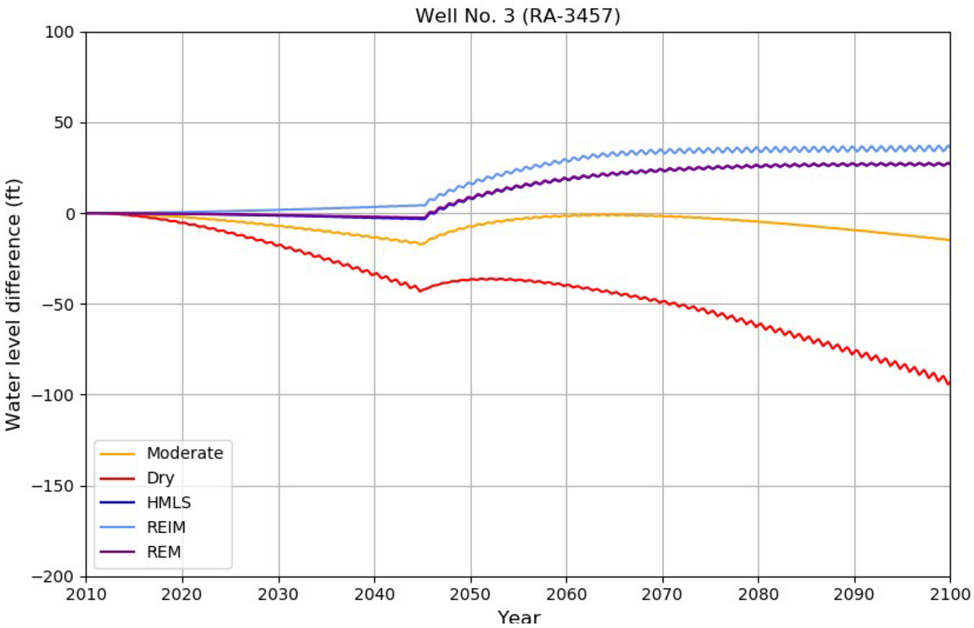

Figure 59. Change in simulated water levels at the Well No. 3 (RA-3457) observation well for climate change storylines, with a 30% reduction in irrigation pumping in 2045 (storyline minus Groundwater Base Case).

7.5. River Gains and Losses Figures

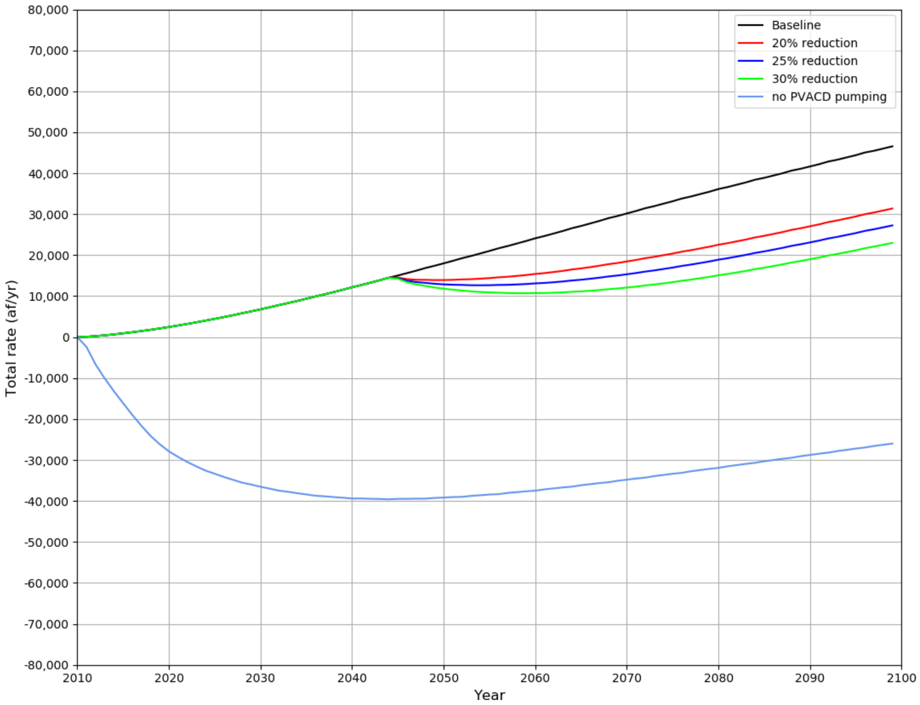

Figure 60. Net river seepage for BaU Moderate Storyline, Water Management Strategies, and PVACD footprint analysis.

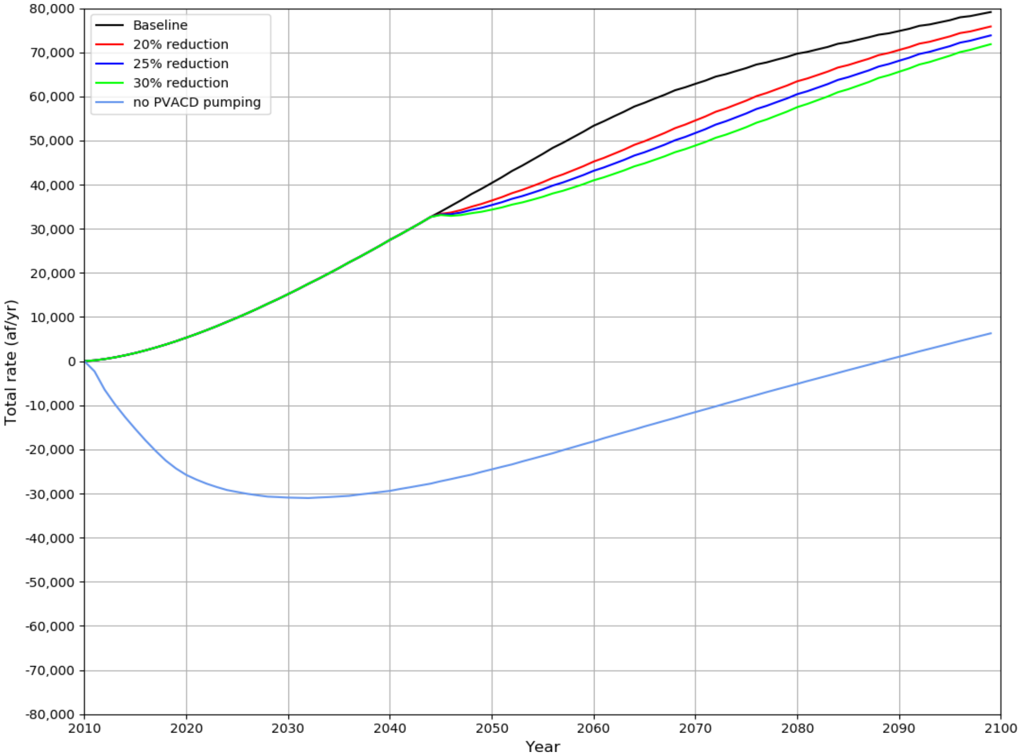

Figure 61. Net river seepage for BaU Dry Storyline, Water Management Strategies, and PVACD footprint analysis.

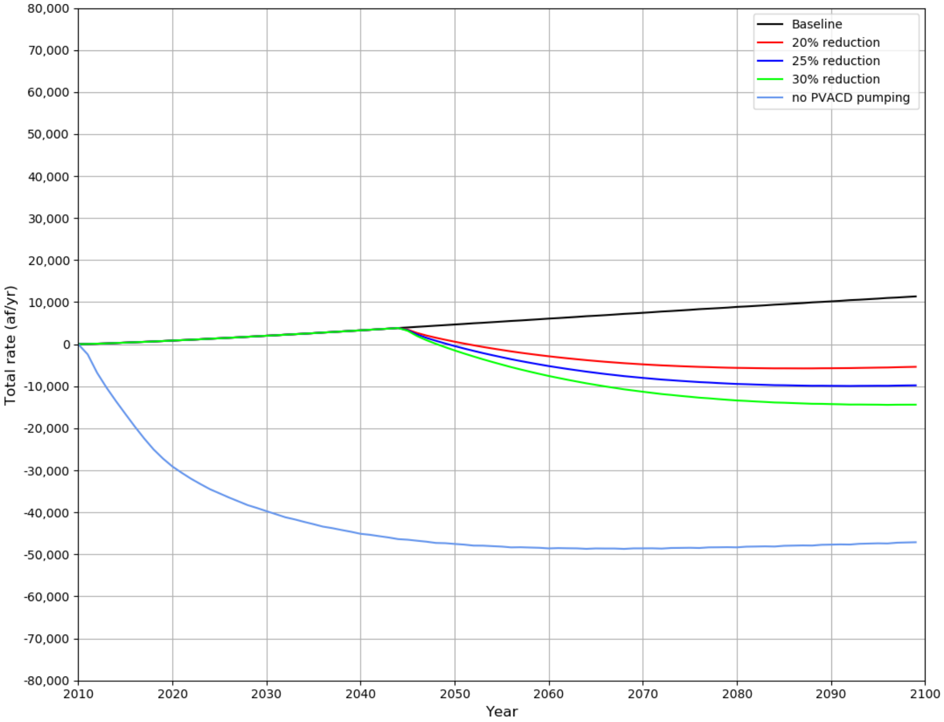

Figure 62. Net river seepage for BAU HMLS Storyline, Water Management Strategies, and PVACD footprint analysis.

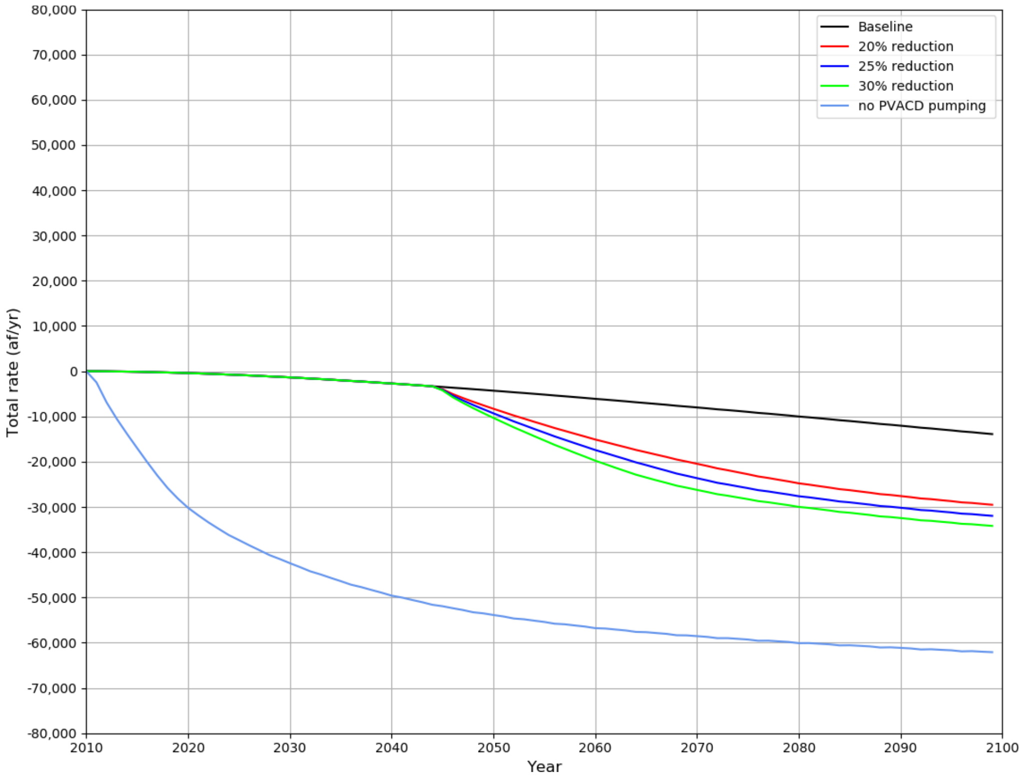

Figure 63. Net river seepage for RE Increased Monsoon Storyline, Water Management Strategies, and PVACD footprint analysis.

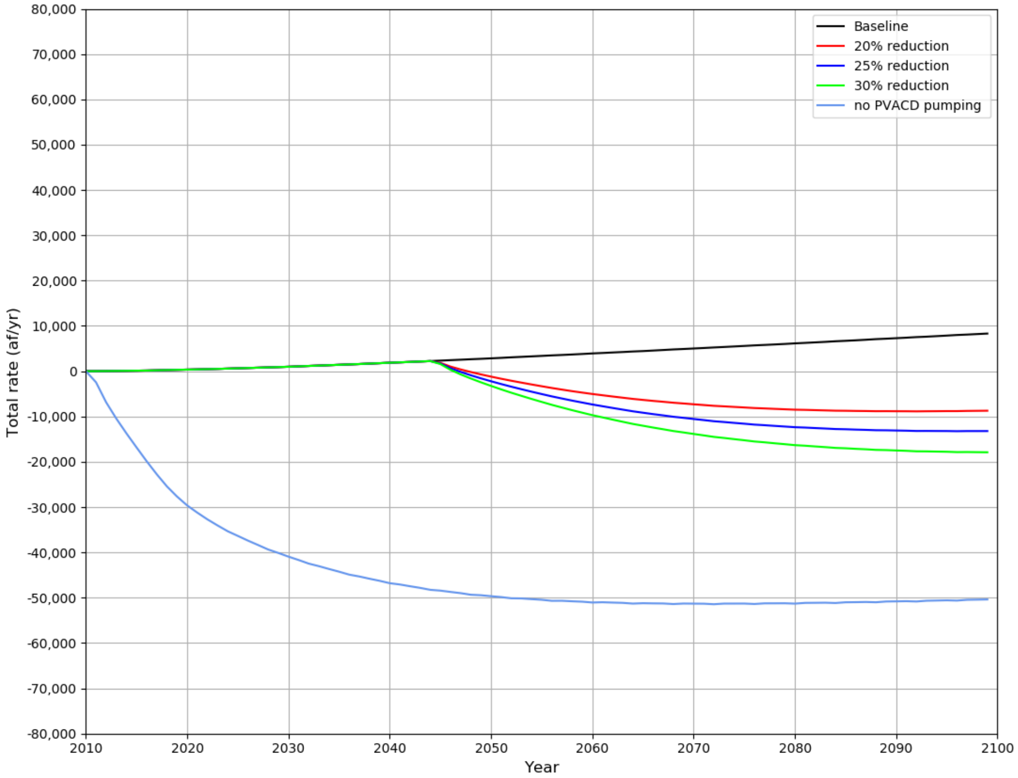

Figure 64. Net river seepage for RE Median Storyline, Water Management Strategies, and PVACD footprint analysis.

(a) Roswell Artesian Basin (AF)

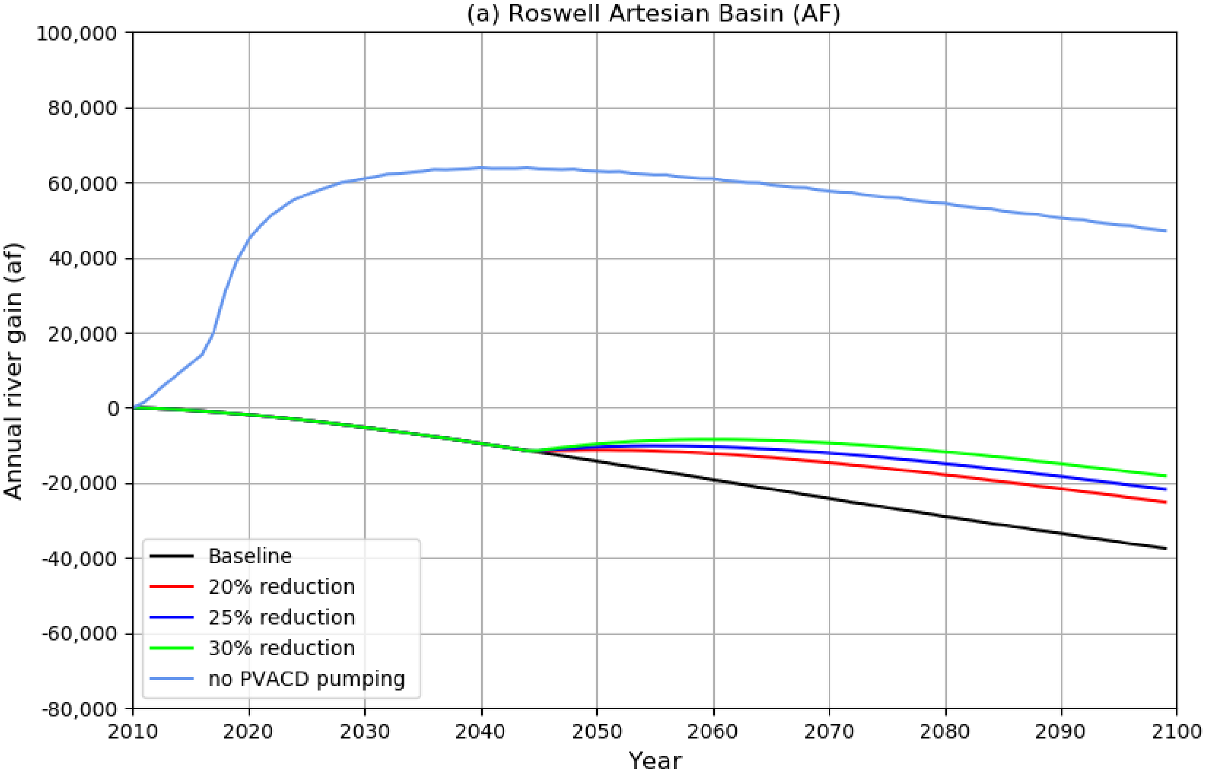

(b) between Lake Arthur and Artesia gauges(AF)

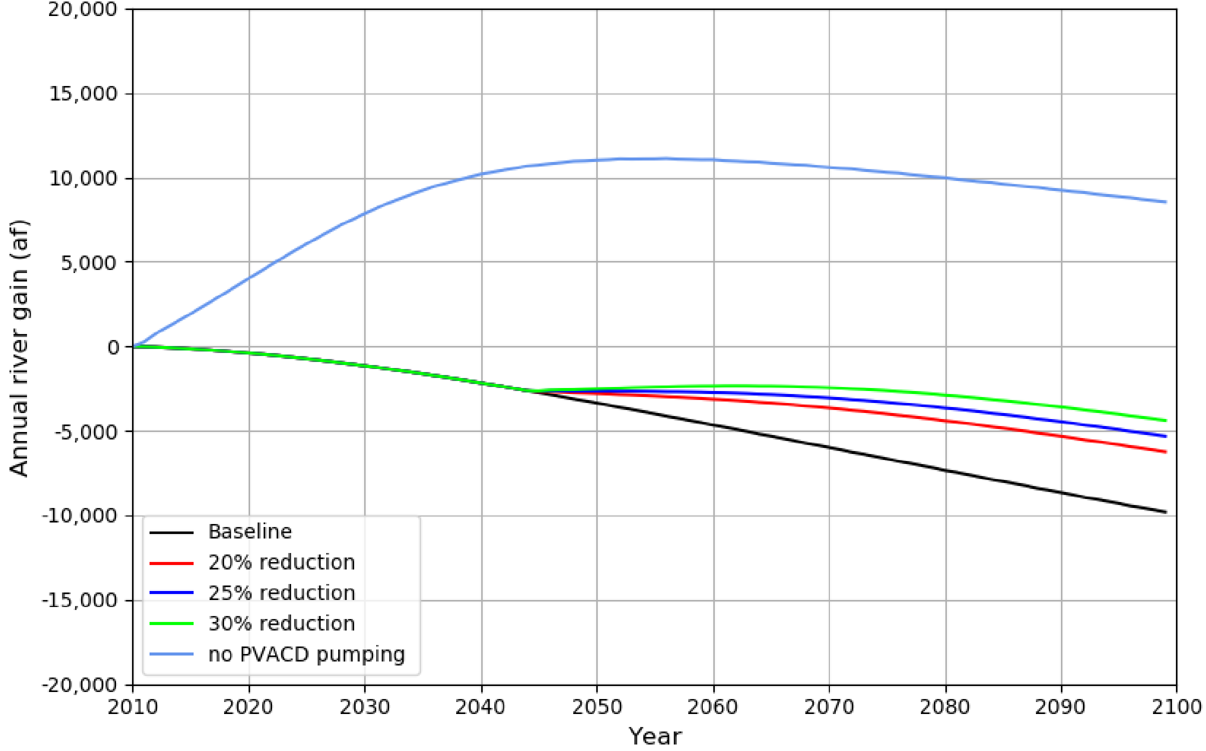

Figure 65. Simulated annual river gain differences associated with BaU Moderate Storyline and Water Management Strategies.

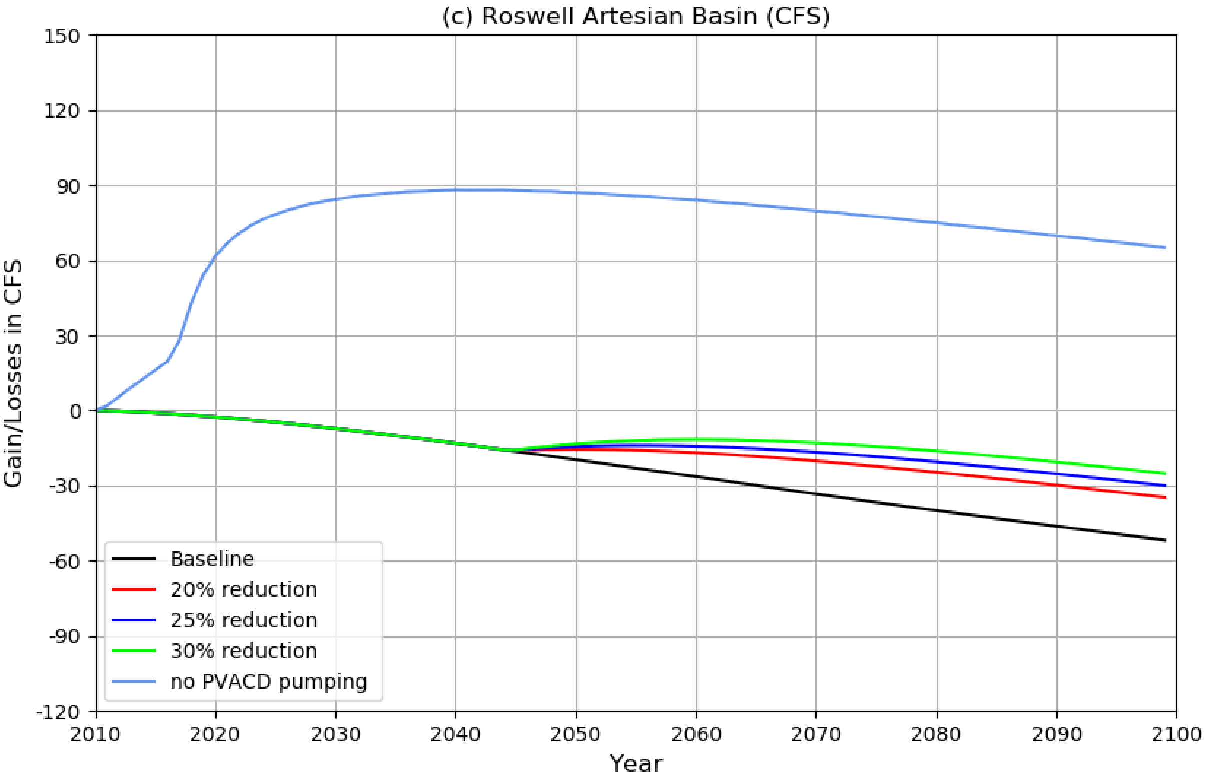

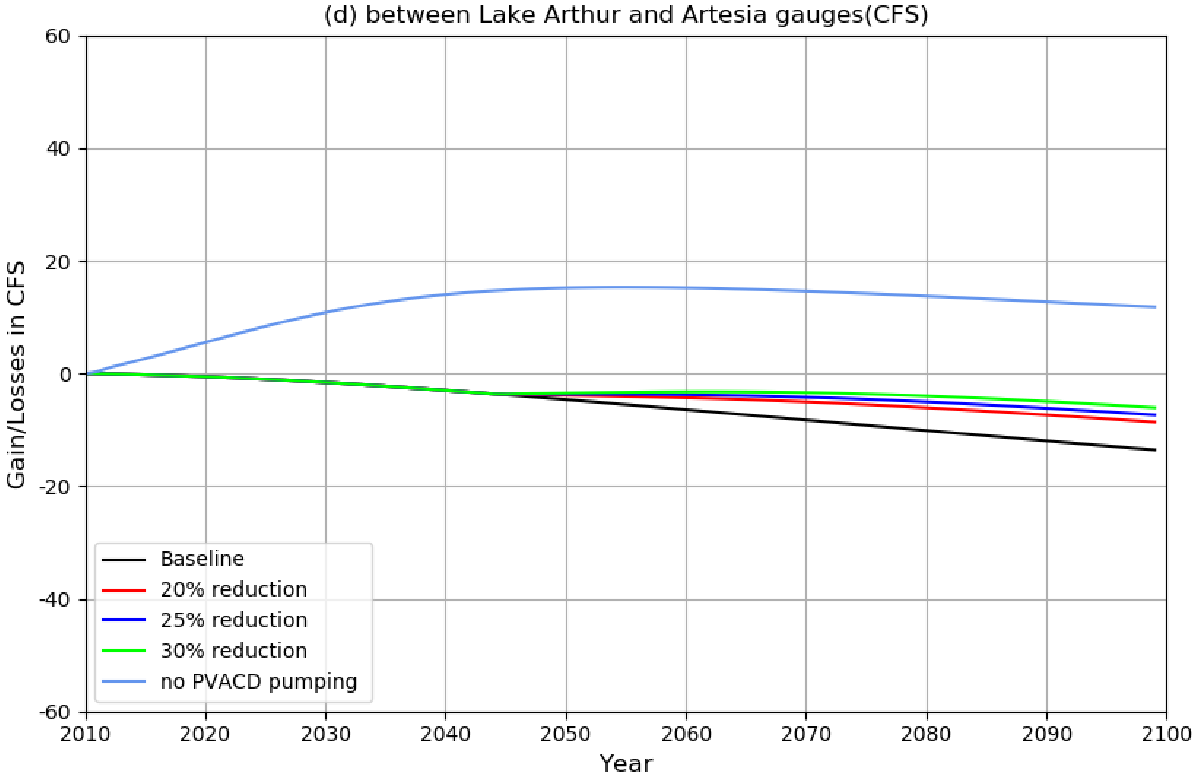

Figure 66. Simulated annual river gain differences associated with BaU Moderate Storyline and Water Management Strategies.

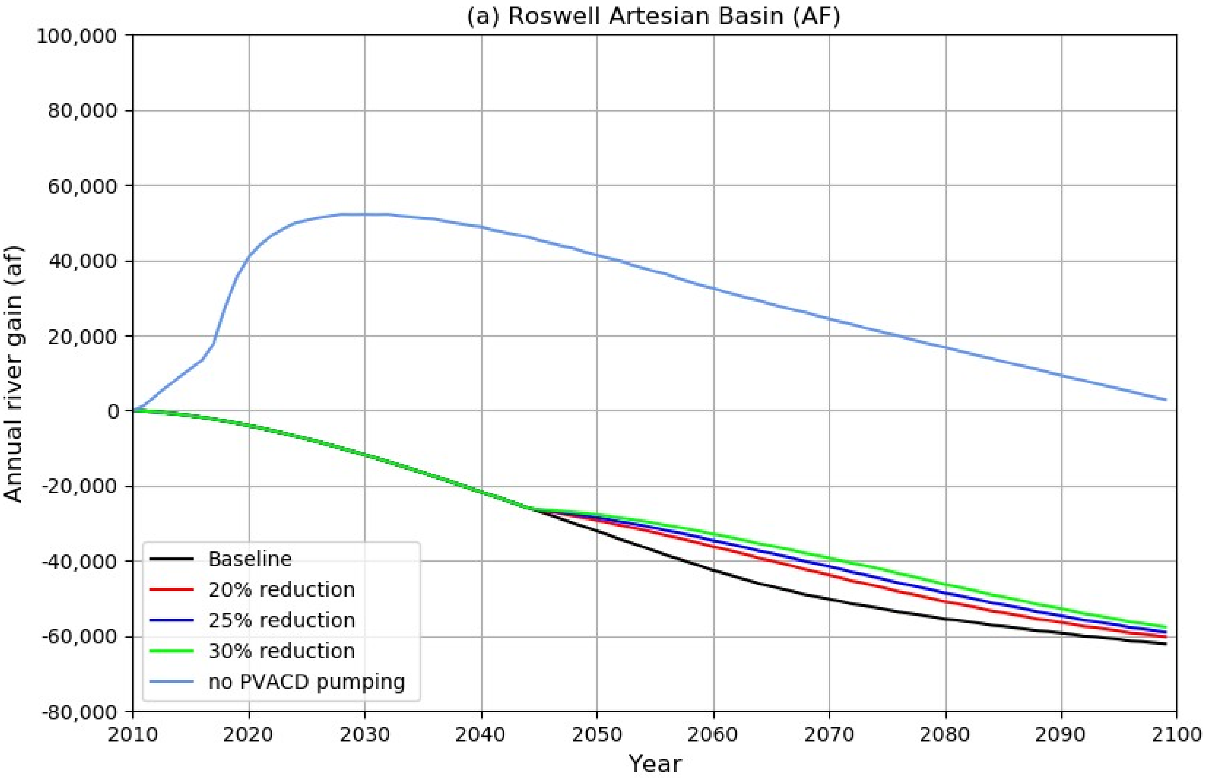

(a) Roswell Artesian Basin (AF)

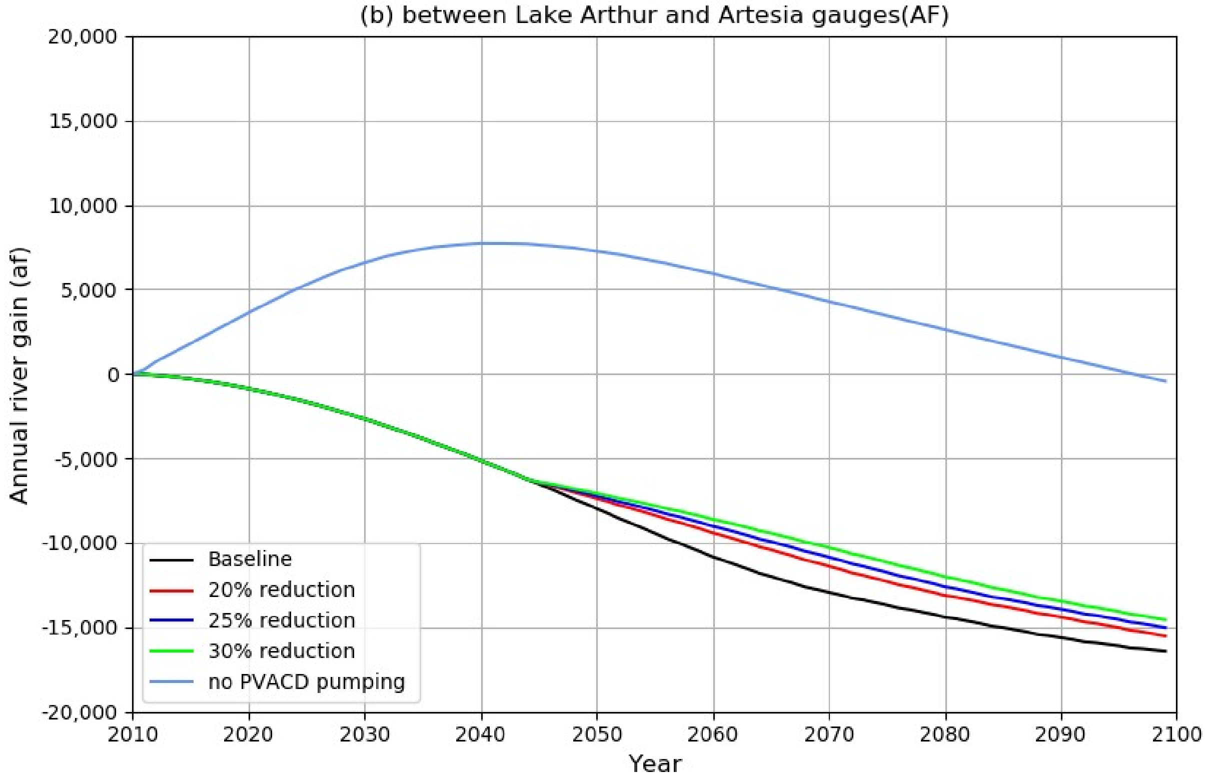

(b) between Lake Arthur and Artesia gauges(AF)

Figure 67. Simulated annual river gain differences associated with BaU Dry Storyline and Water Management Strategies.

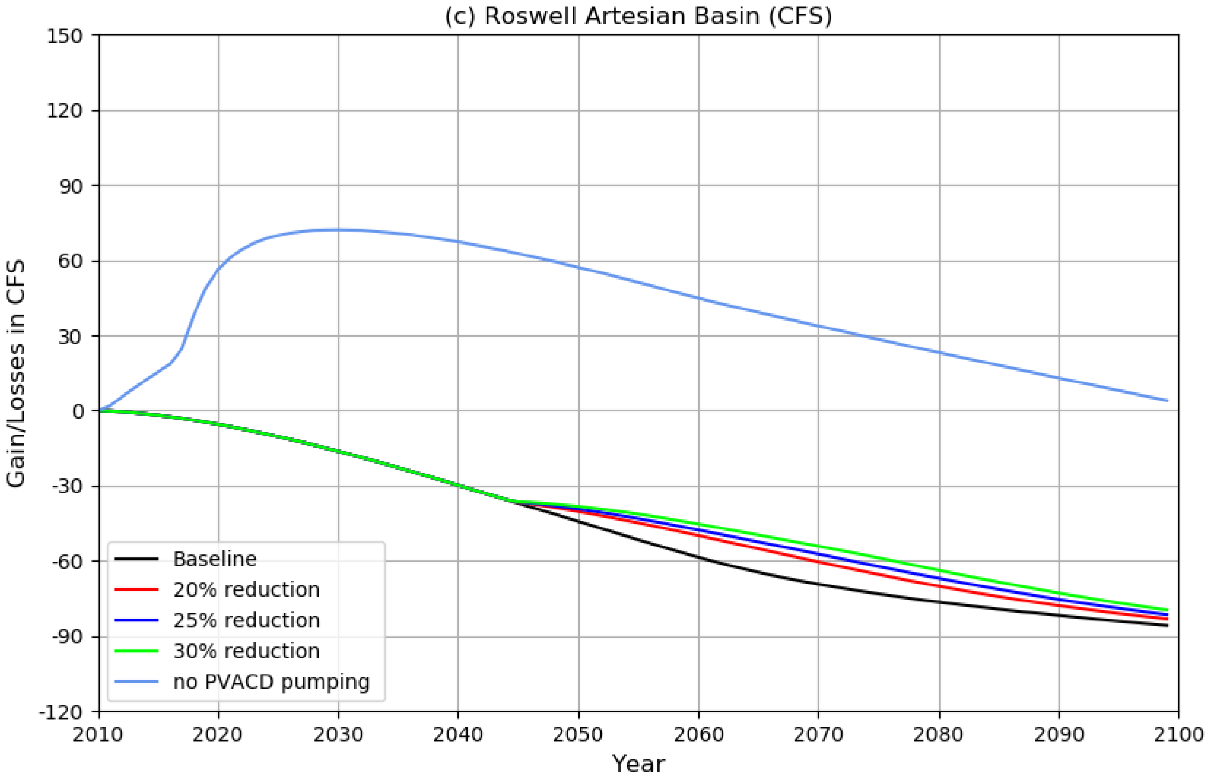

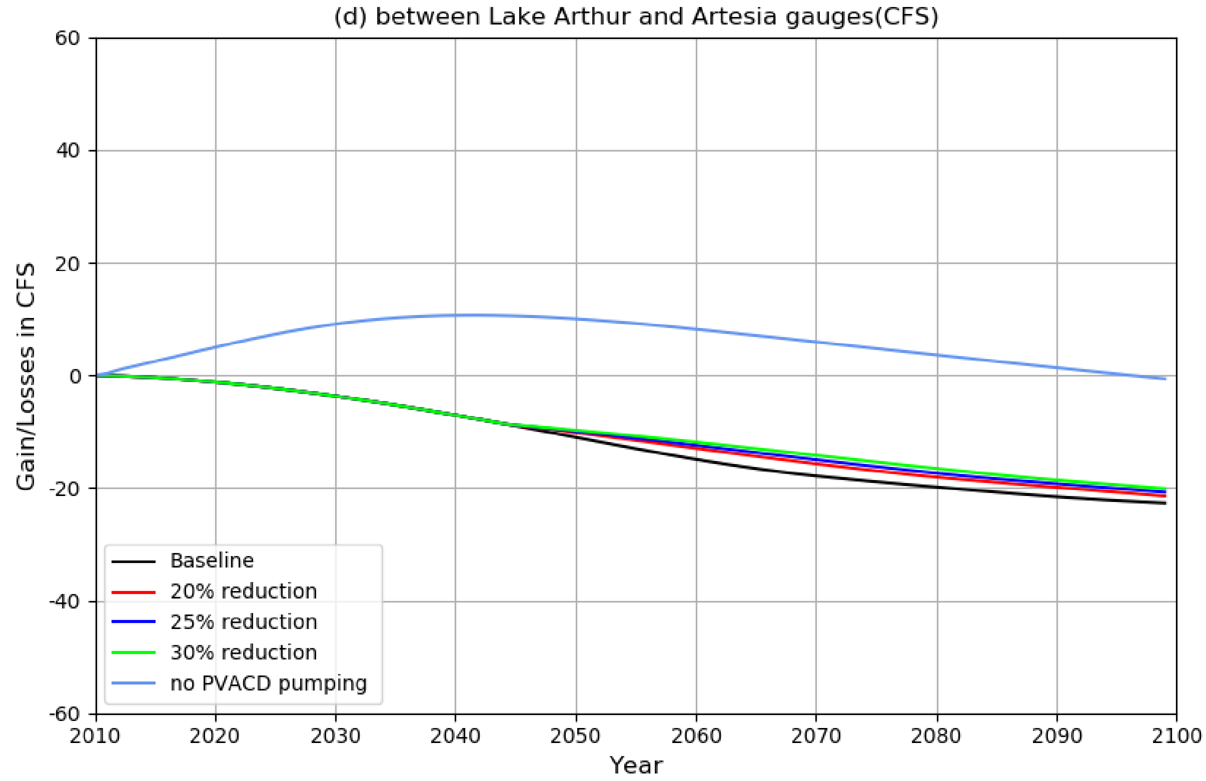

Figure 68. Simulated annual river gain differences associated with BaU Dry Storyline and Water Management Strategies.

(a) Roswell Artesian Basin (AF)

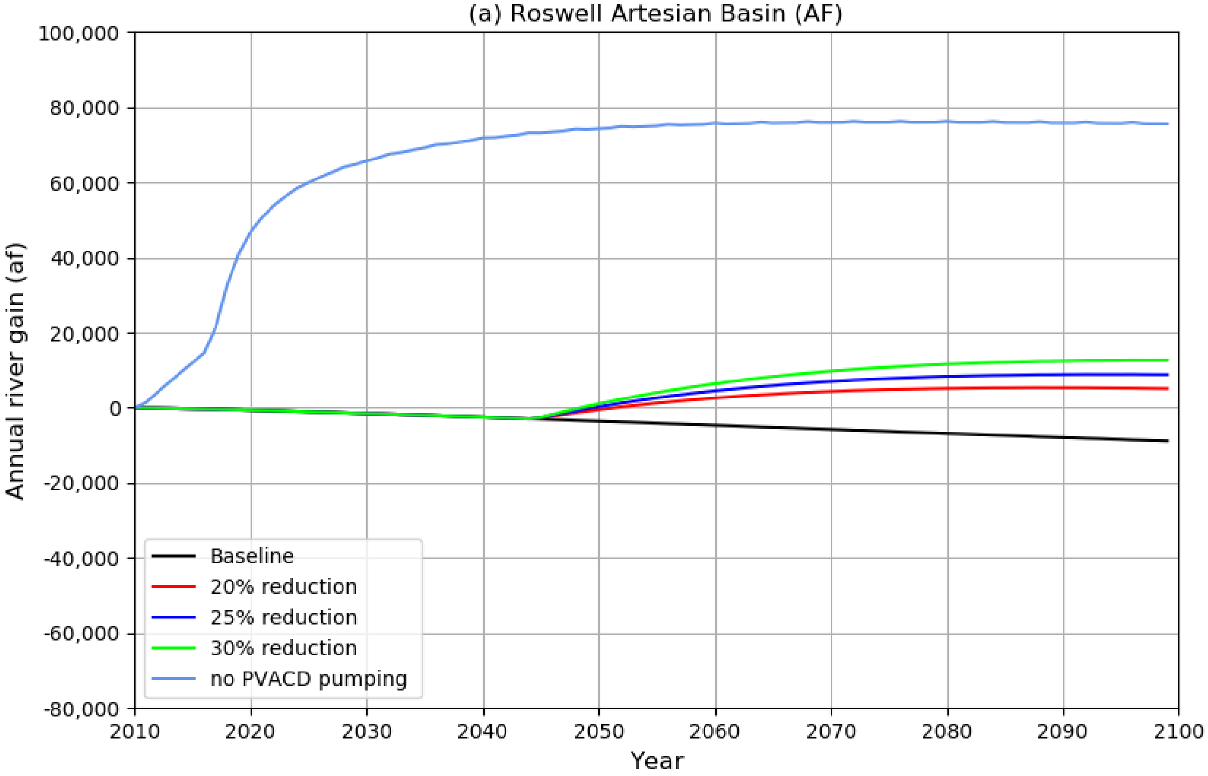

(b) between Lake Arthur and Artesia gauges(AF)

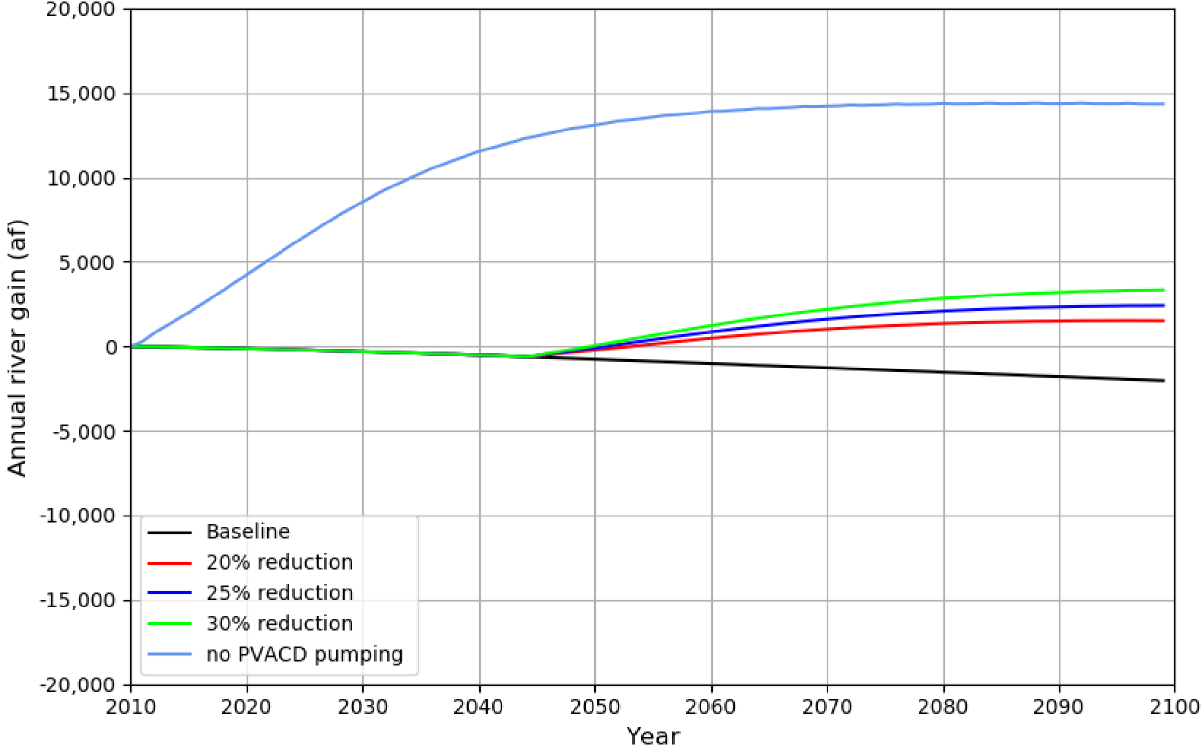

Figure 69. Simulated annual river gain differences associated with BAU HMLS Storyline and Water Management Strategies.

(c) Roswell Artesian Basin (CFS)

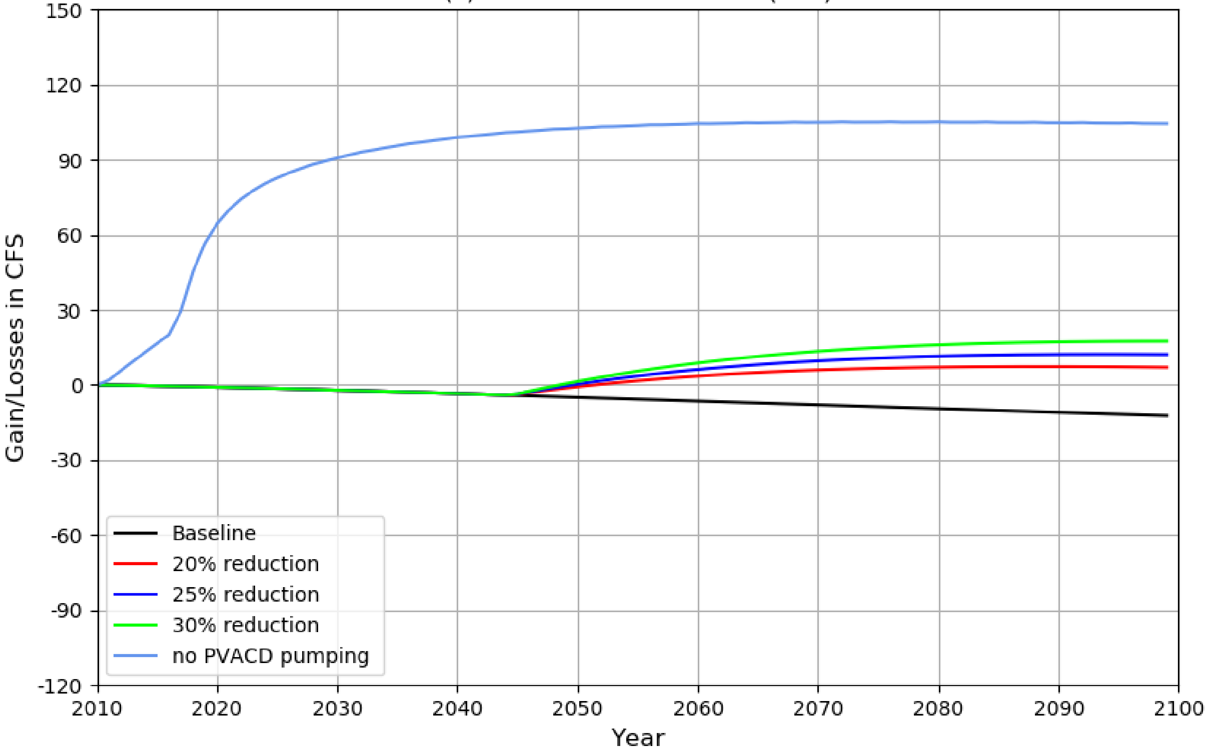

(d) between Lake Arthur and Artesia gauges(CFS)

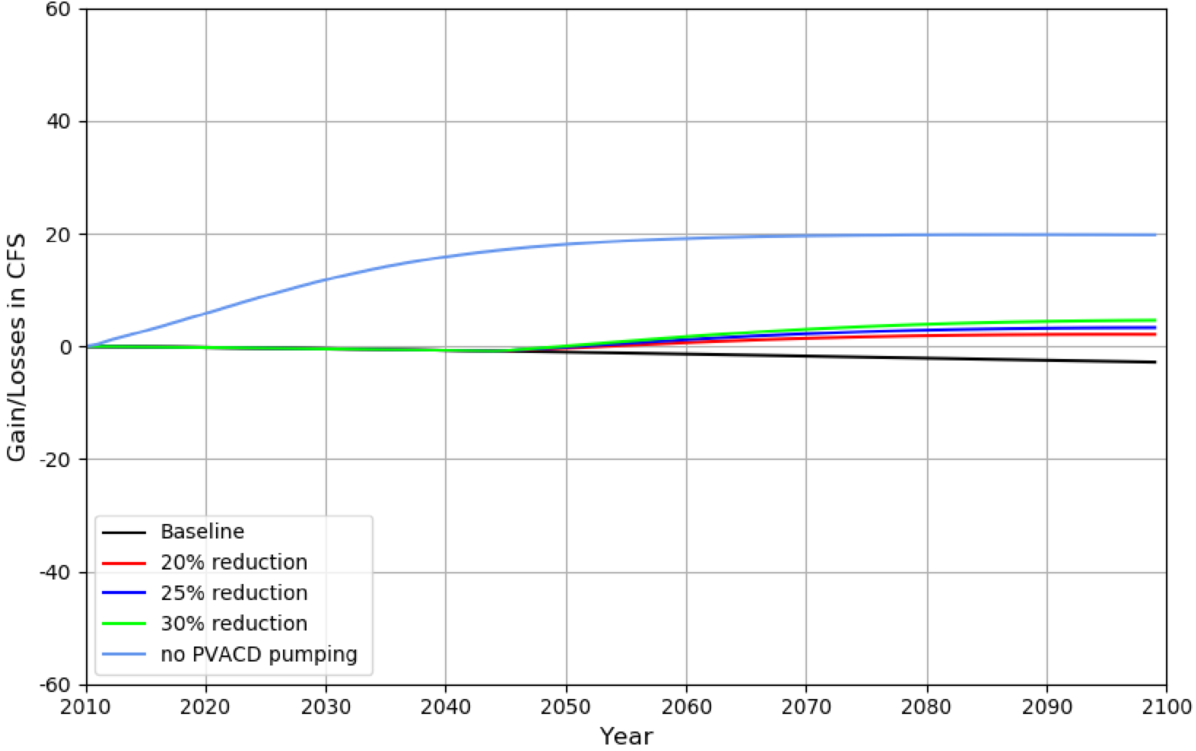

Figure 70. Simulated annual river gain differences associated with BAU HMLS Storyline and Water Management Strategies.

(a) Roswell Artesian Basin (AF)

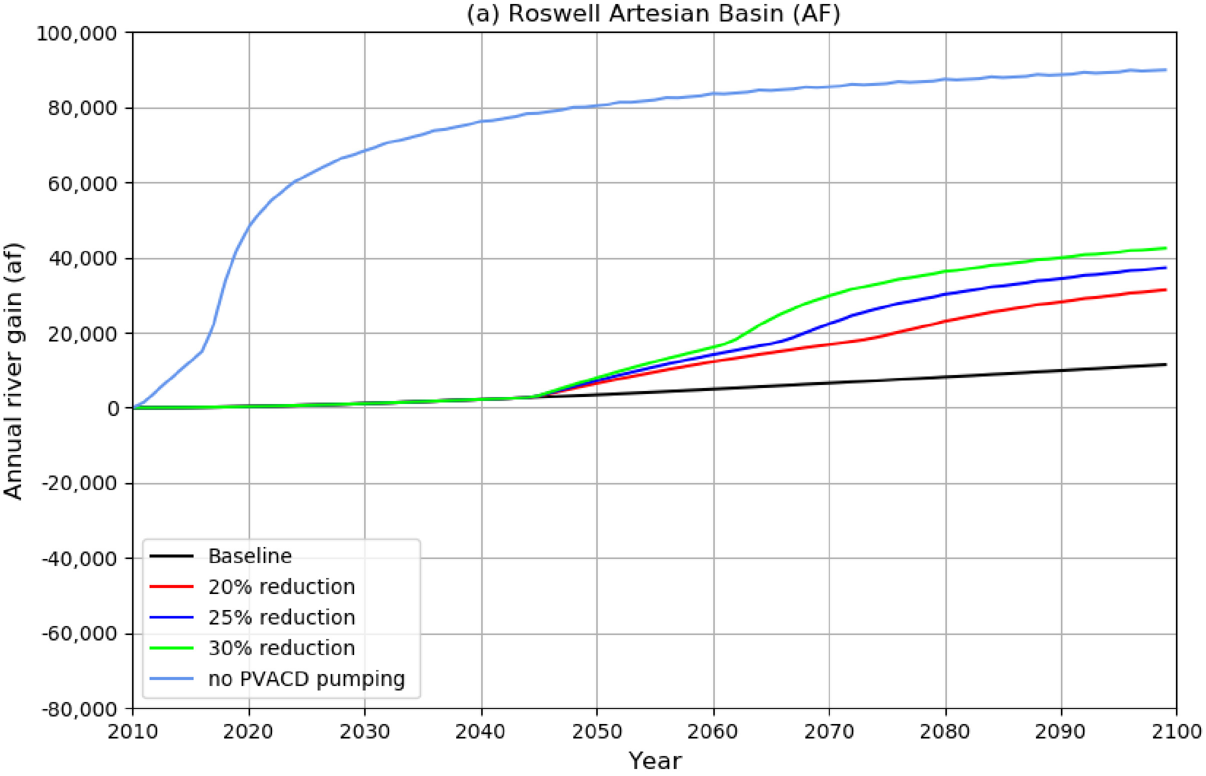

(b) between Lake Arthur and Artesia gauges(AF)

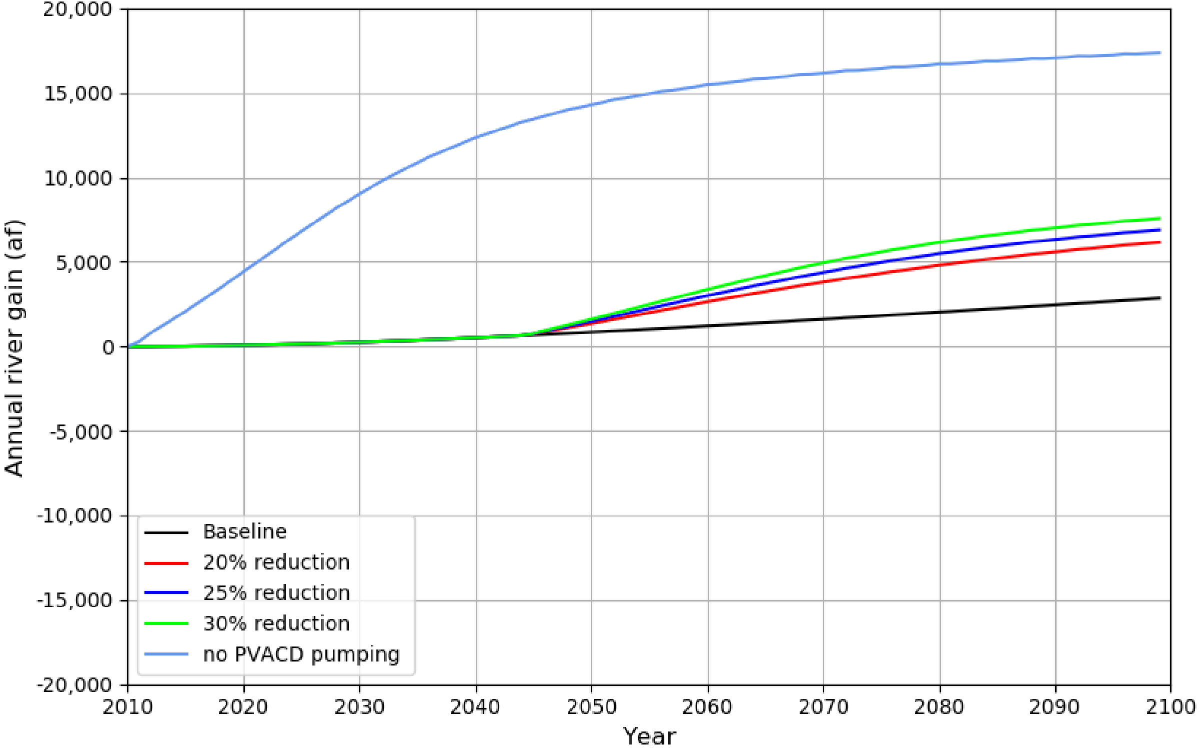

Figure 71. Simulated annual river gain differences associated with RE Increased Monsoon Storyline and Water Management Strategies.

(c) Roswell Artesian Basin (CFS)

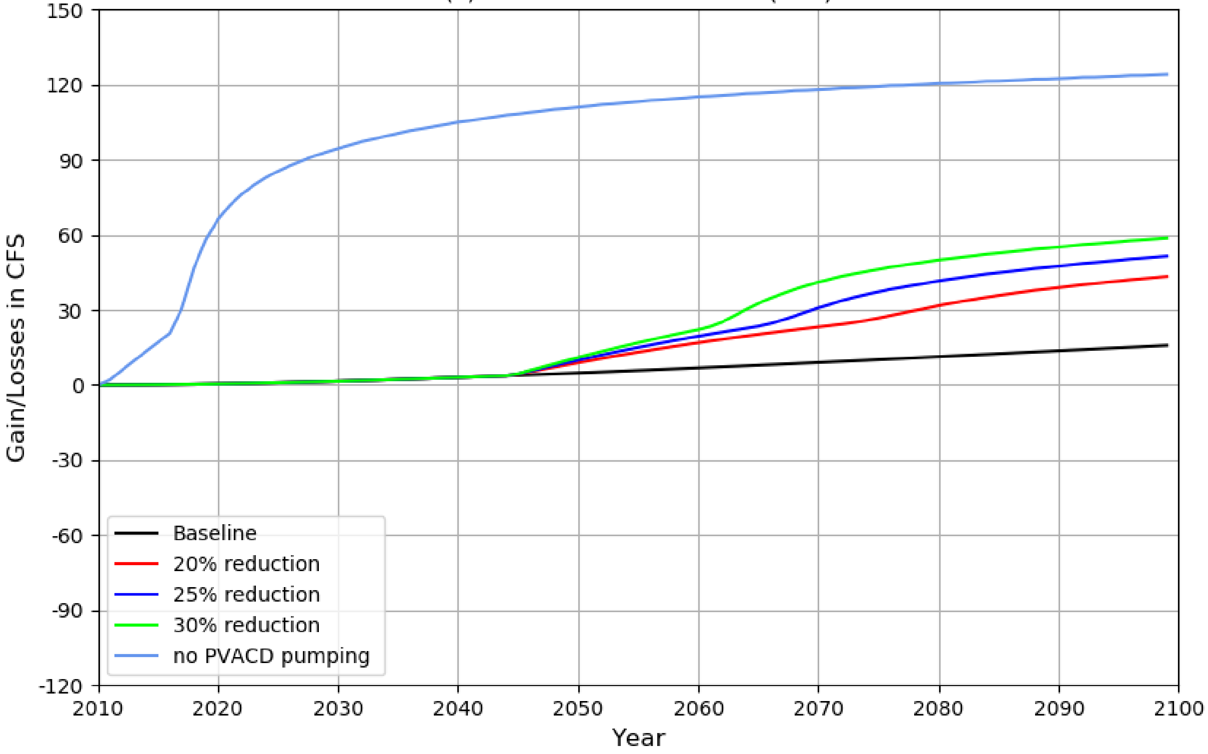

(d) between Lake Arthur and Artesia gauges(CFS)

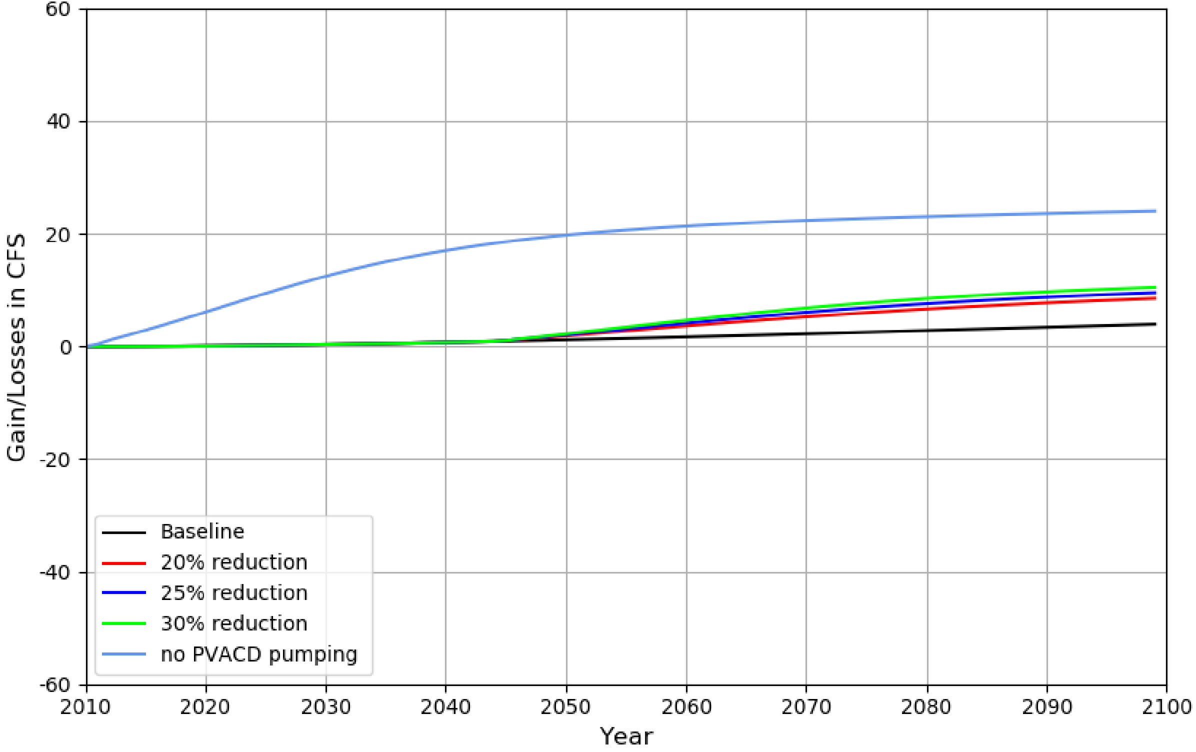

Figure 72. Simulated annual river gain differences associated with RE Increased Monsoon Storyline and Water Management Strategies.

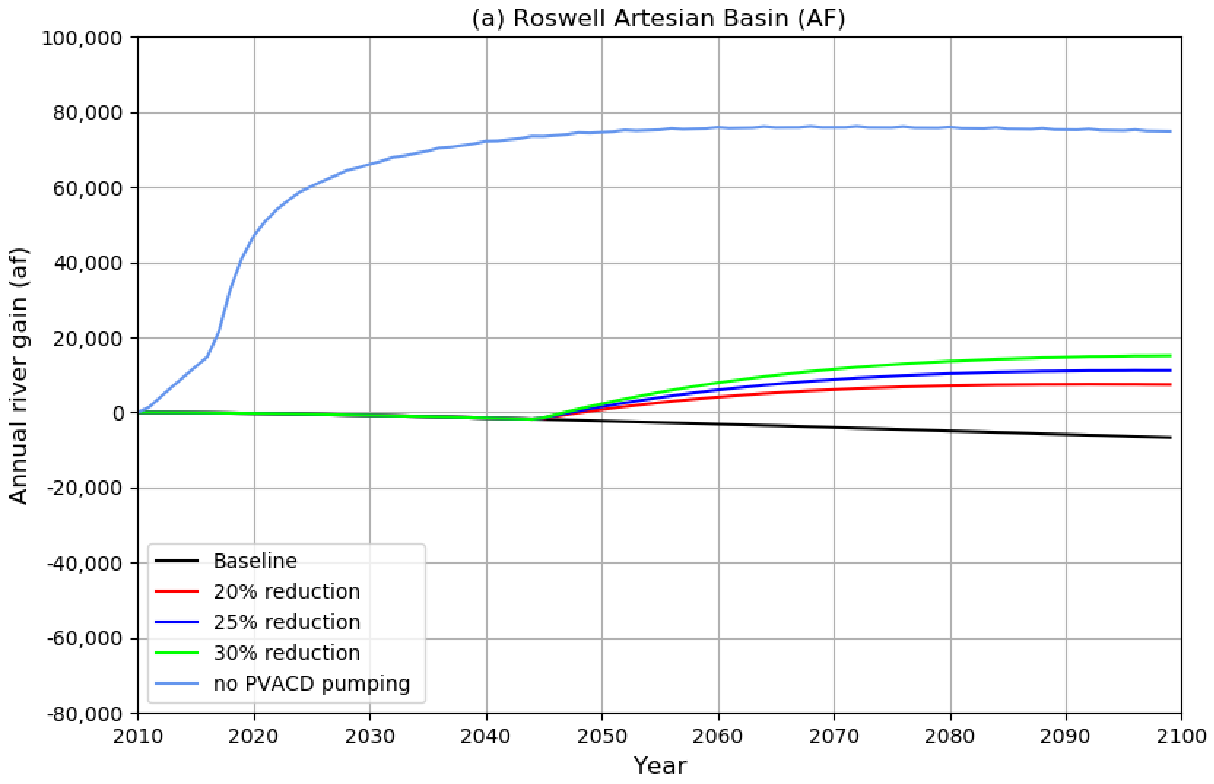

(a) Roswell Artesian Basin (AF)

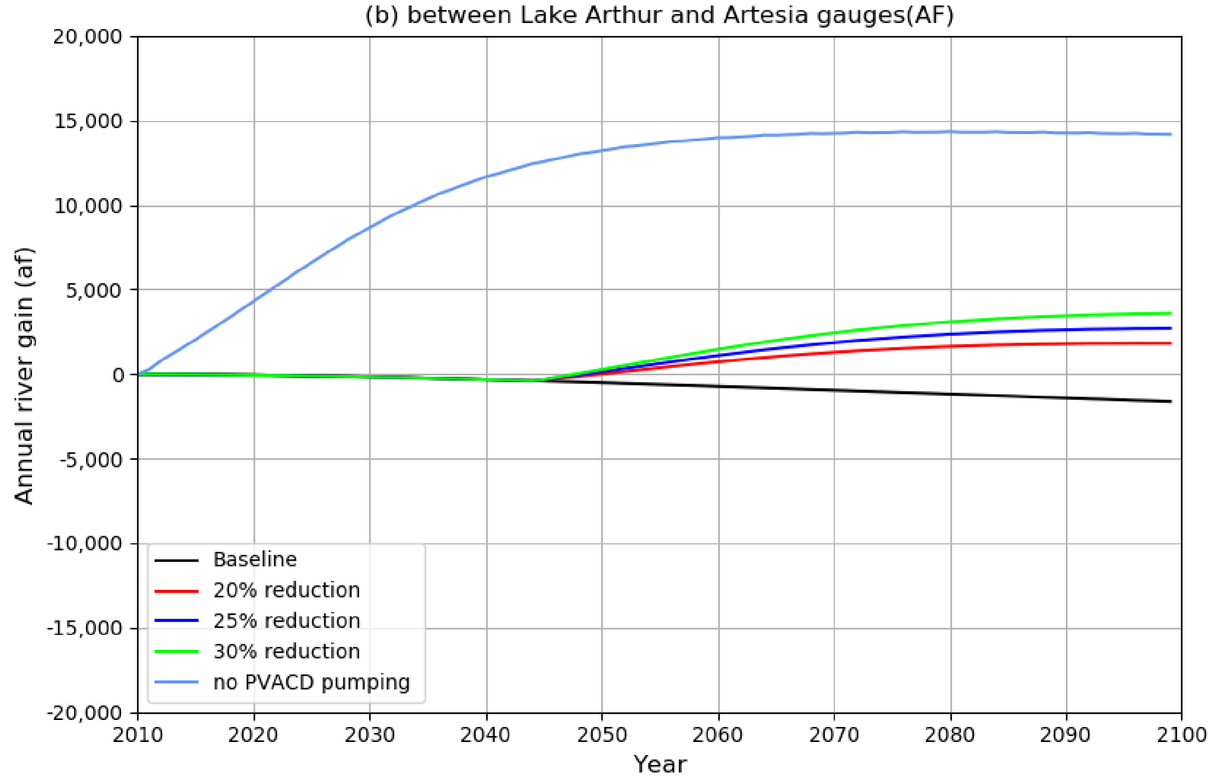

(b) between Lake Arthur and Artesia gauges(AF)

Figure 73. Simulated annual river gain differences associated with RE Median Storyline and Water Management Strategies (Storyline Base Case).

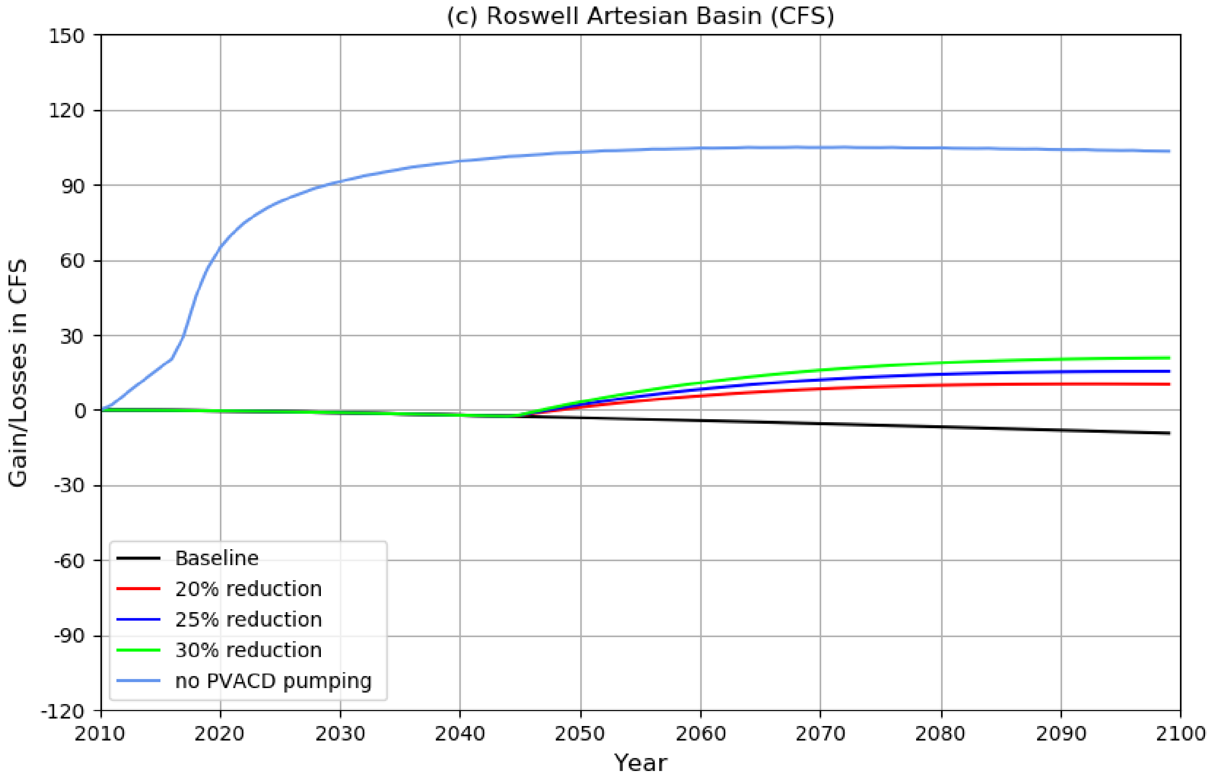
(c) Roswell Artesian Basin (CFS)

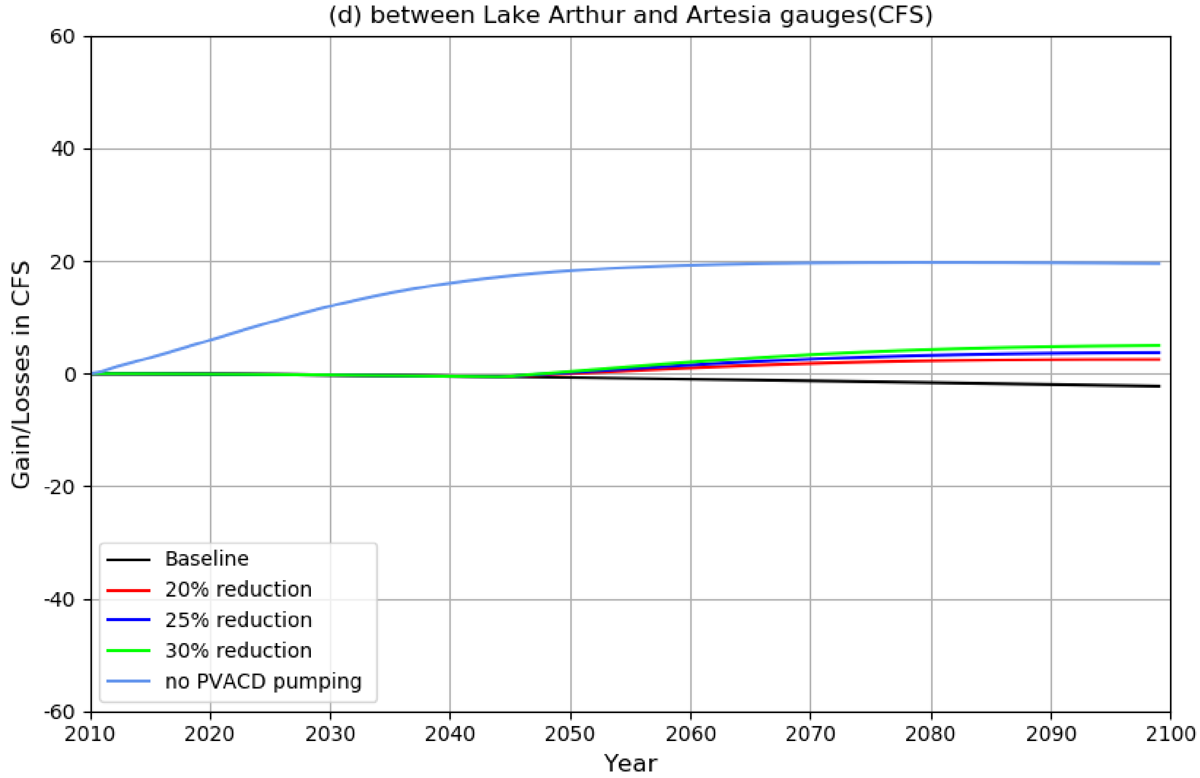
(d) between Lake Arthur and Artesia gauges(CFS)

Figure 74. Simulated annual river gain differences associated with RE Median Storyline and Water Management Strategies (Storyline Base Case)..

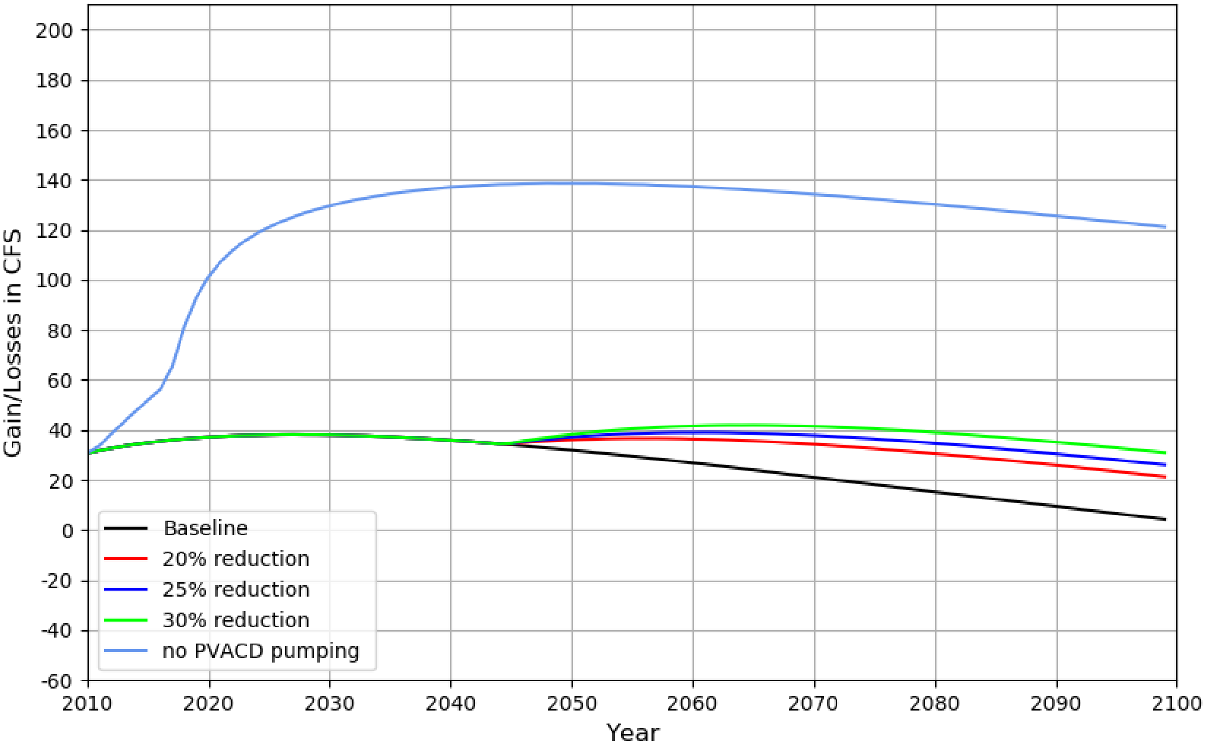

(a) Roswell Artesian Basin (AF)

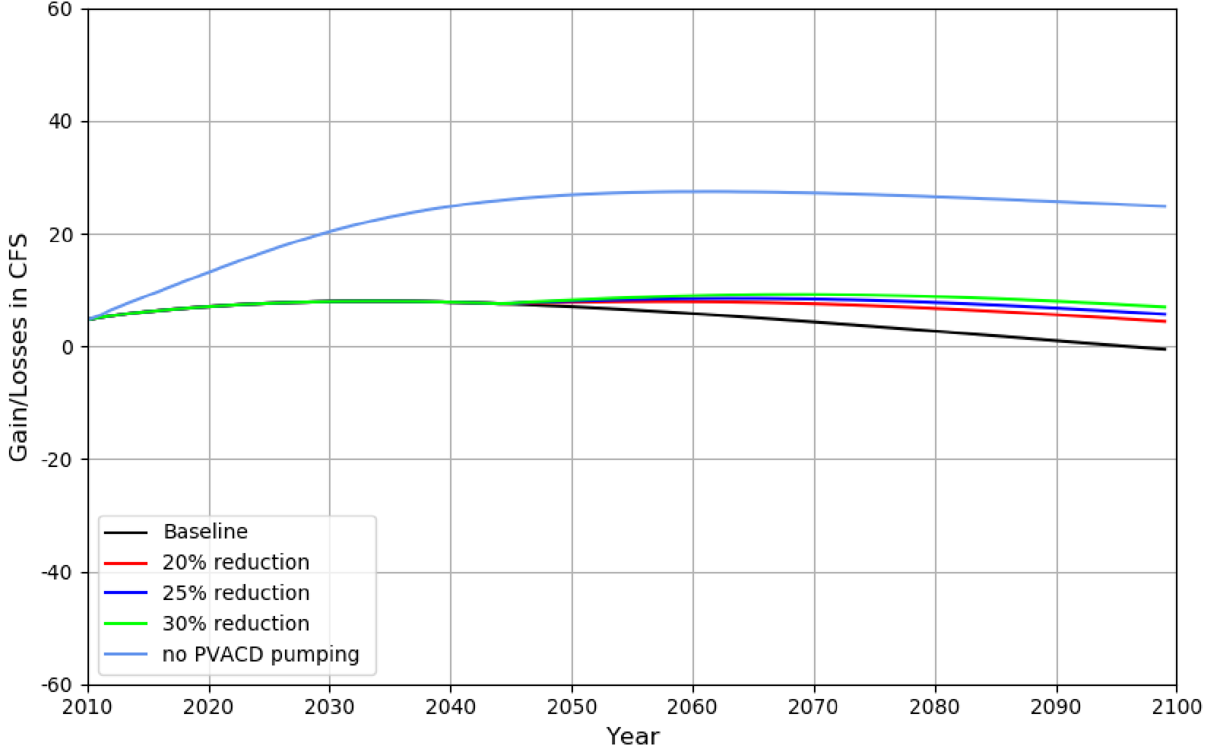

(b) between Lake Arthur and Artesia gauges(AF)

Figure 75. Simulated annual river gain associated with BaU Moderate Storyline and Water Management Strategies.

(a) Roswell Artesian Basin (AF)

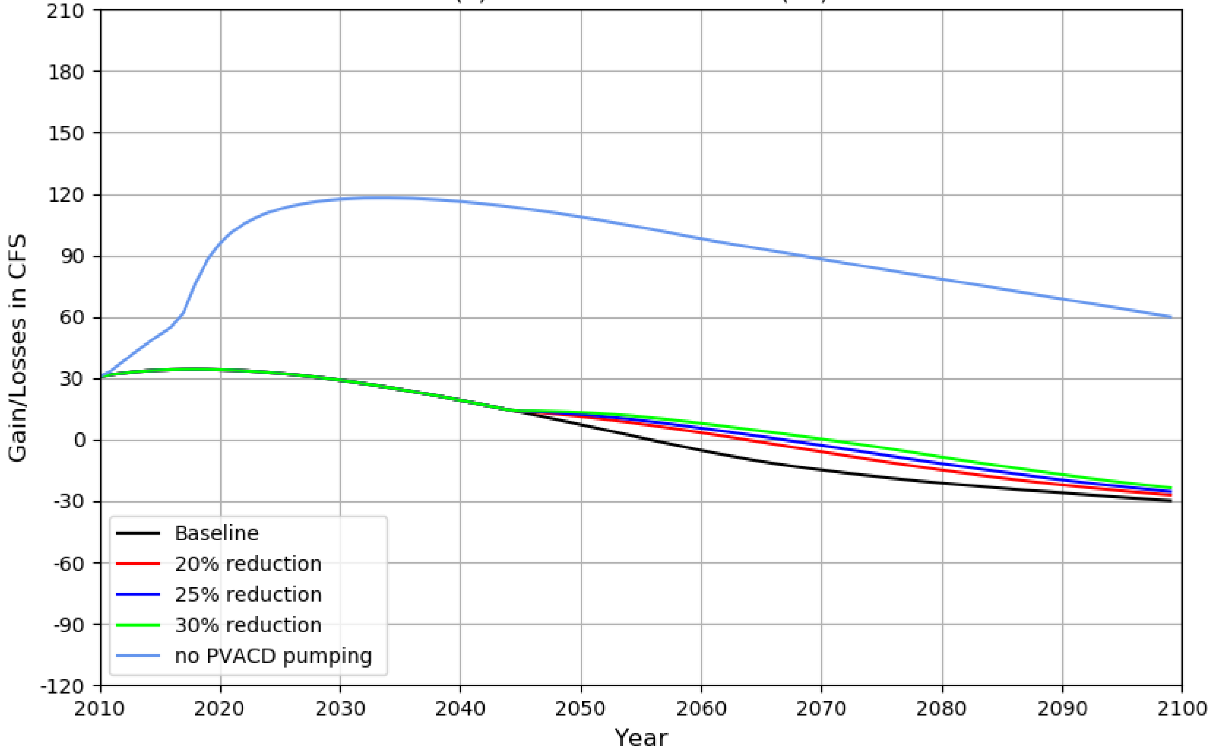

(b) between Lake Arthur and Artesia gauges(AF)

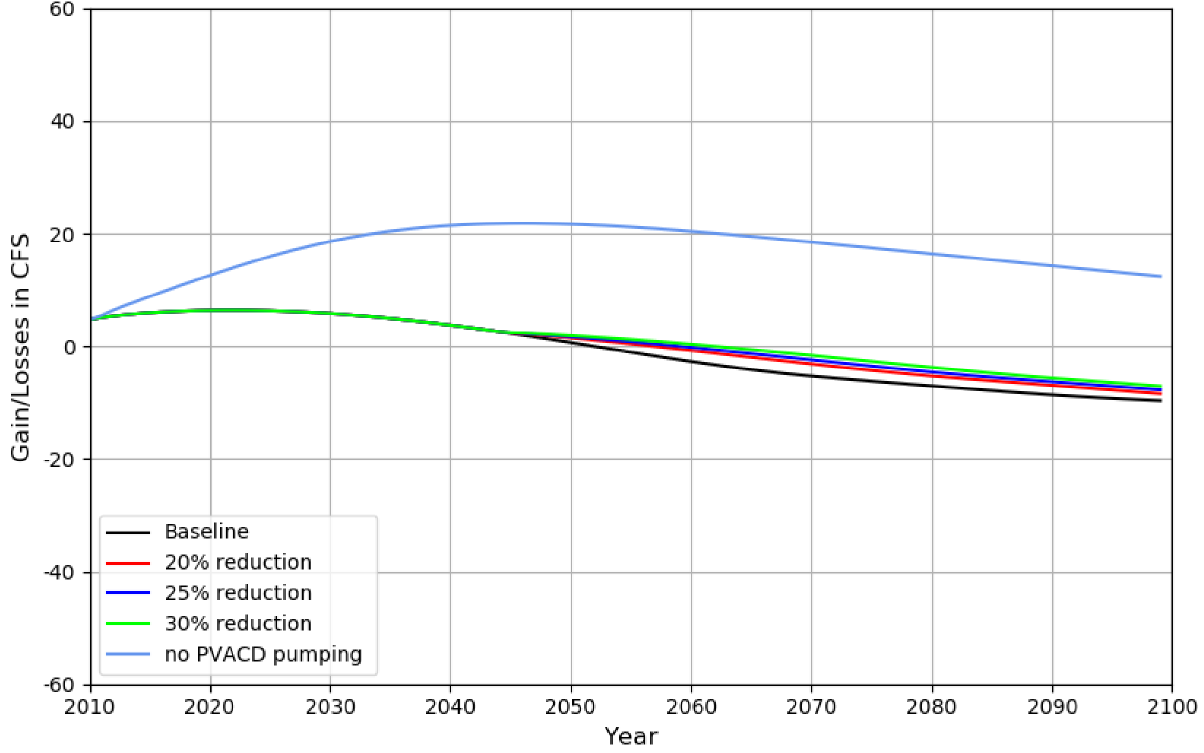

Figure 76. Simulated annual river gain associated with BaU Dry Storyline and Water Management Strategies.

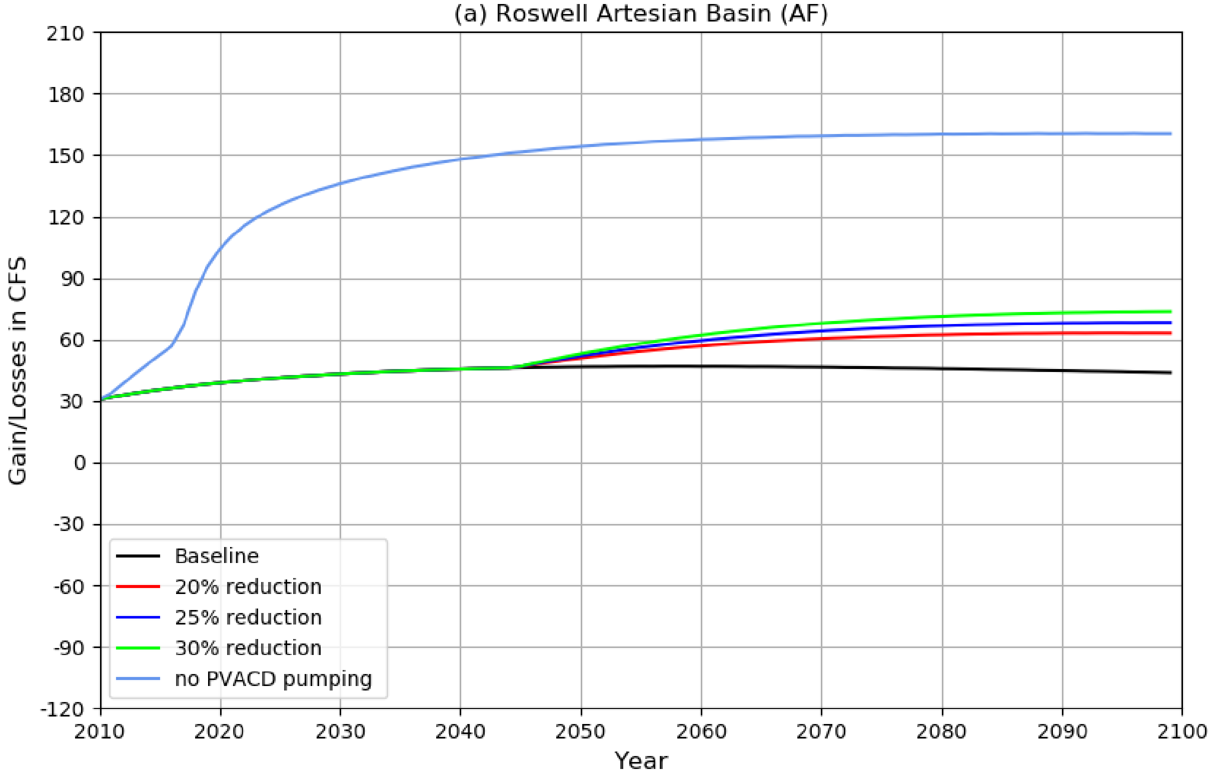

(a) Roswell Artesian Basin (AF)

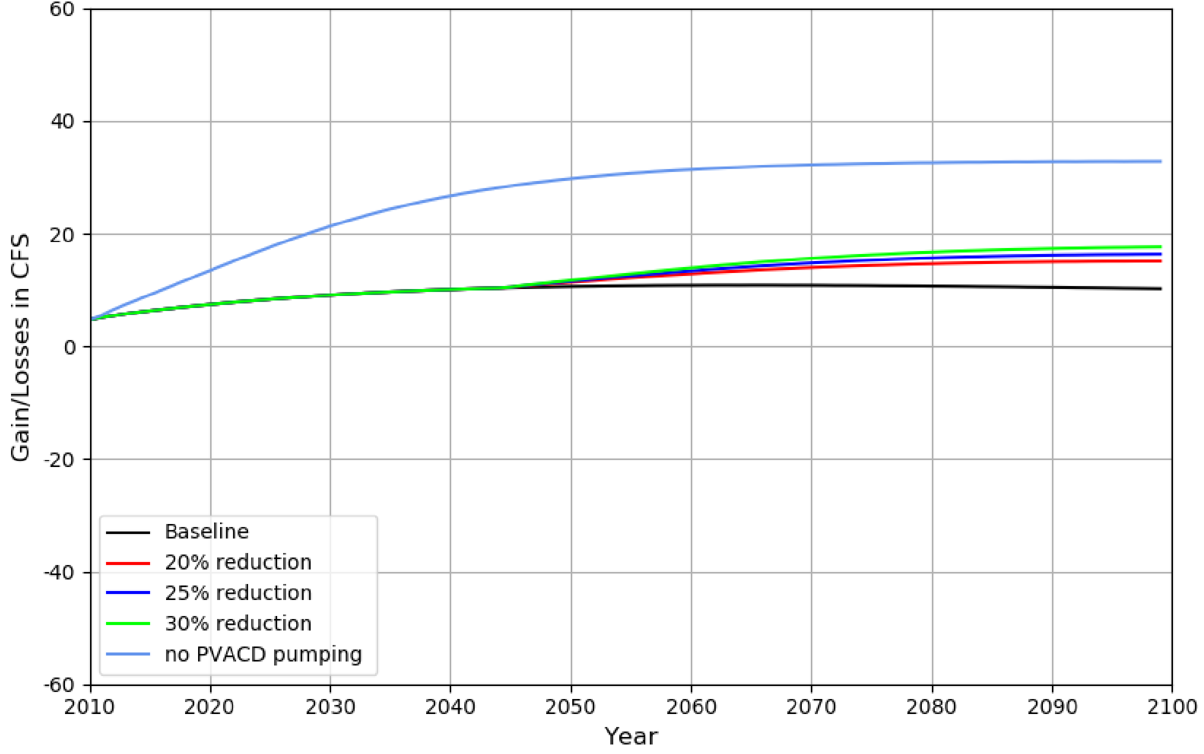

(b) between Lake Arthur and Artesia gauges(AF)

Figure 77. Simulated annual river gain associated with BAU HMLS Storyline and Water Management Strategies.

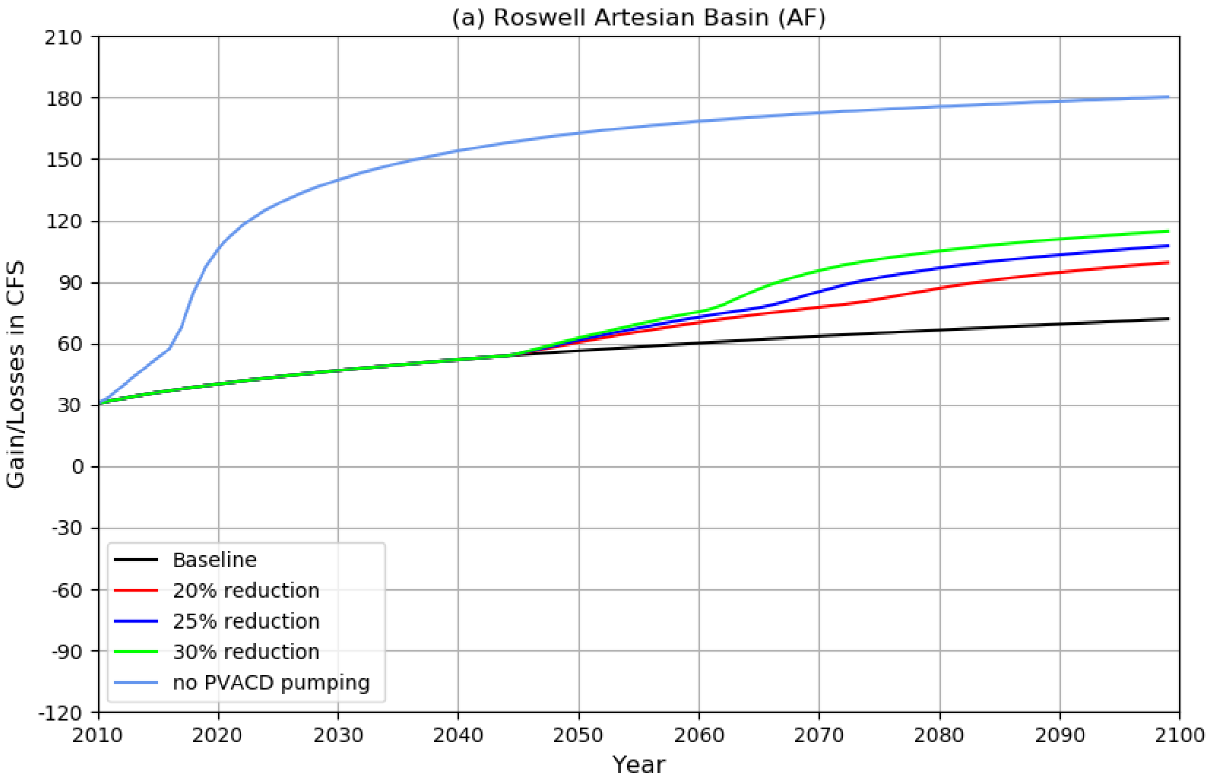

(a) Roswell Artesian Basin (AF)

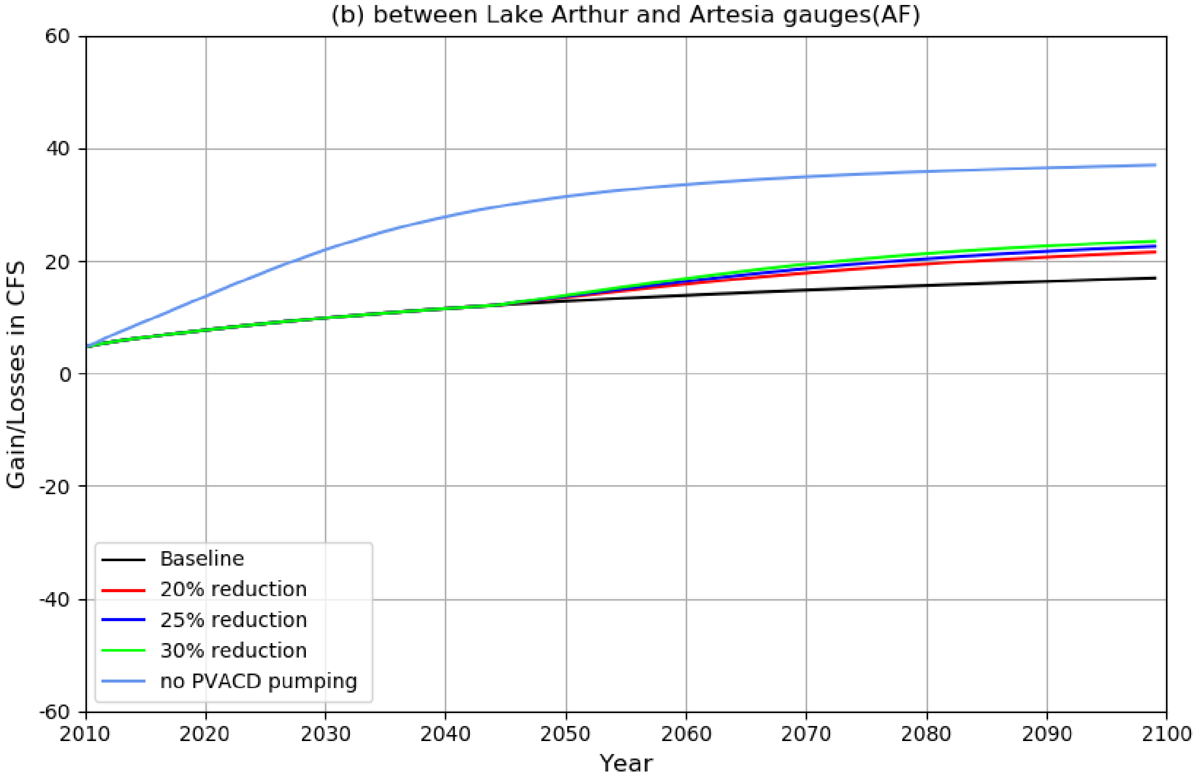

(b) between Lake Arthur and Artesia gauges(AF)

Figure 78. Simulated annual river gain associated with BAU HMLS Storyline and Water Management Strategies.

(a) Roswell Artesian Basin (AF)

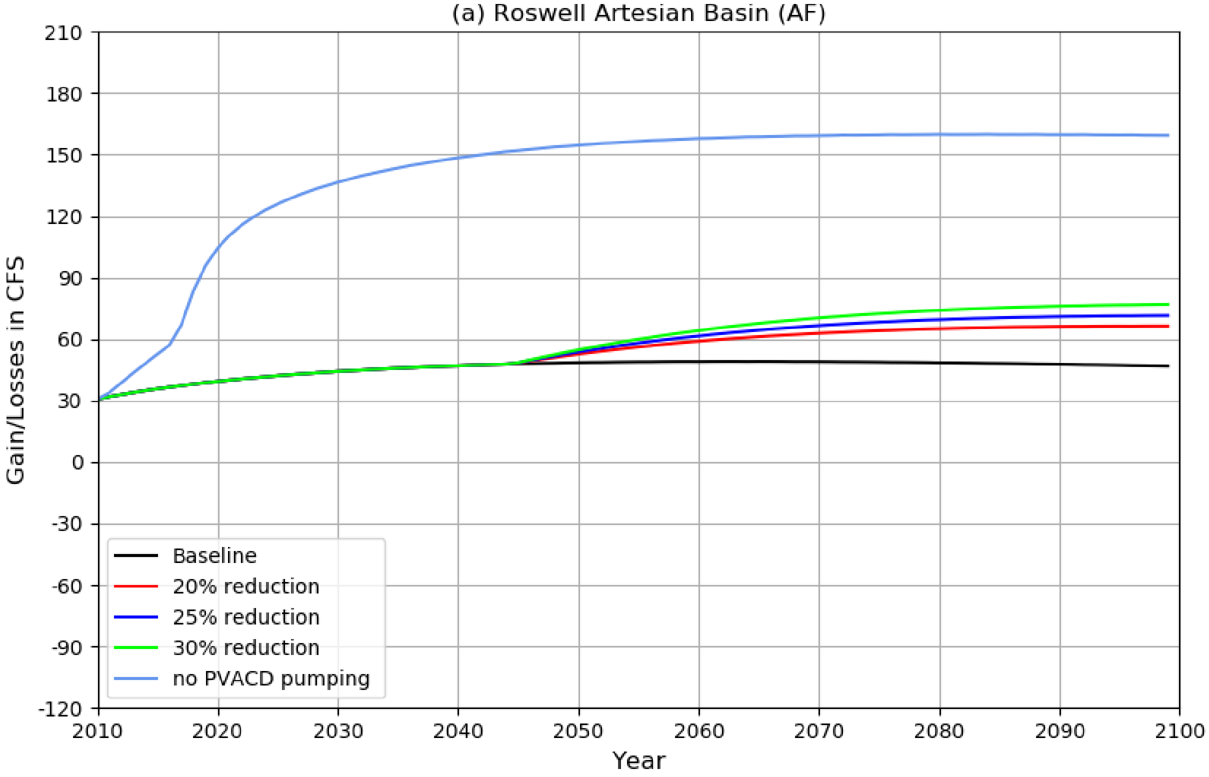

(b) between Lake Arthur and Artesia gauges(AF)

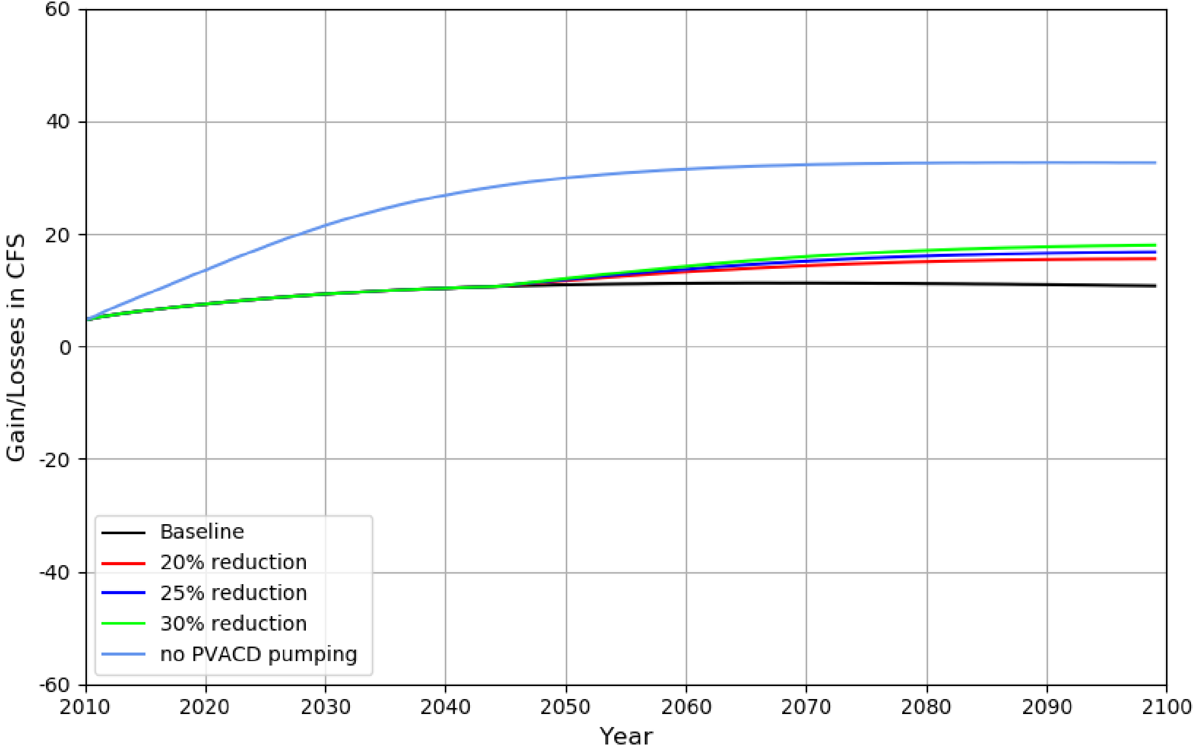

Figure 79. Simulated annual river gain associated with RE Median Storyline and Water Management Strategies.

8. PVACD Water Footprint Analysis

8.1. Modeled Simulation of Water Level Changes in Each Storyline with No PVACD Pumping Stresses

As part of the groundwater modeling work done for this study, changes in water levels were simulated for the five storylines without PVACD pumping stresses. Changes in simulated water levels relative to the Groundwater Base Case are shown in Figures 80-89 below. In general, after an initial period of adjustment following removal of PVACD pumping stresses, in most cases water levels plateau at around the same level, regardless of storyline, when the artesian water level reaches its maximum elevation, limited from further rise as artesian springs begin flowing again. Towards the end of the century, however, in the dry and moderate storylines, water levels begin to fall again, though they still remain above the Groundwater Base Case conditions.

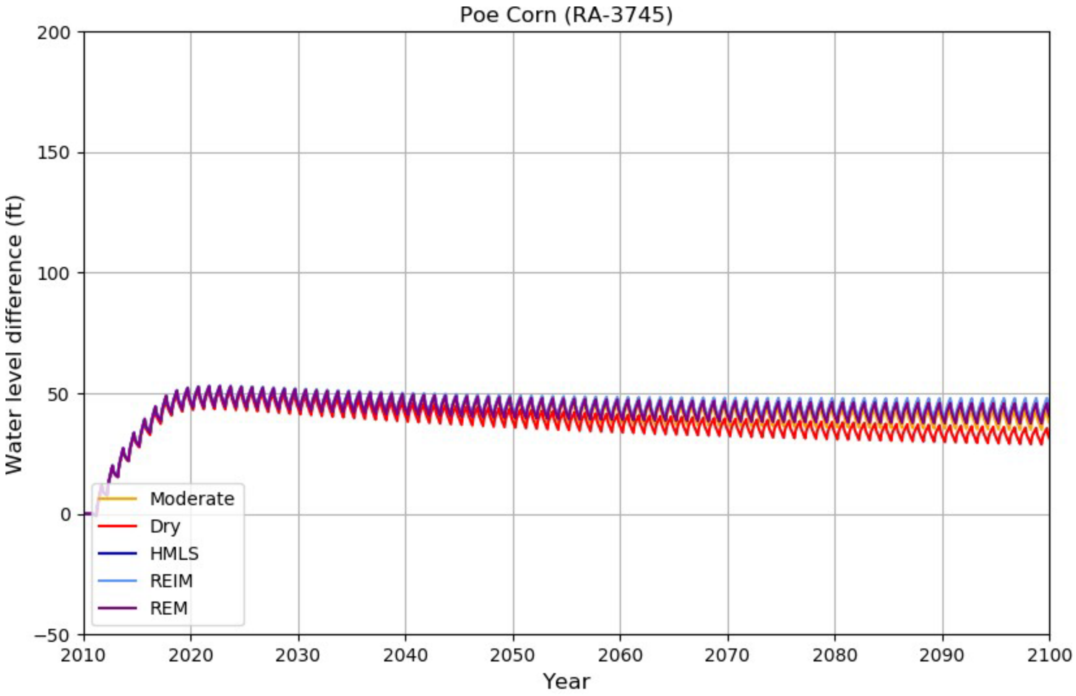

Figure 80. Change in simulated water levels at Poe Corn (RA-3745) observation well for climate change storylines, no PVACD footprint (storyline minus Groundwater Base Case).

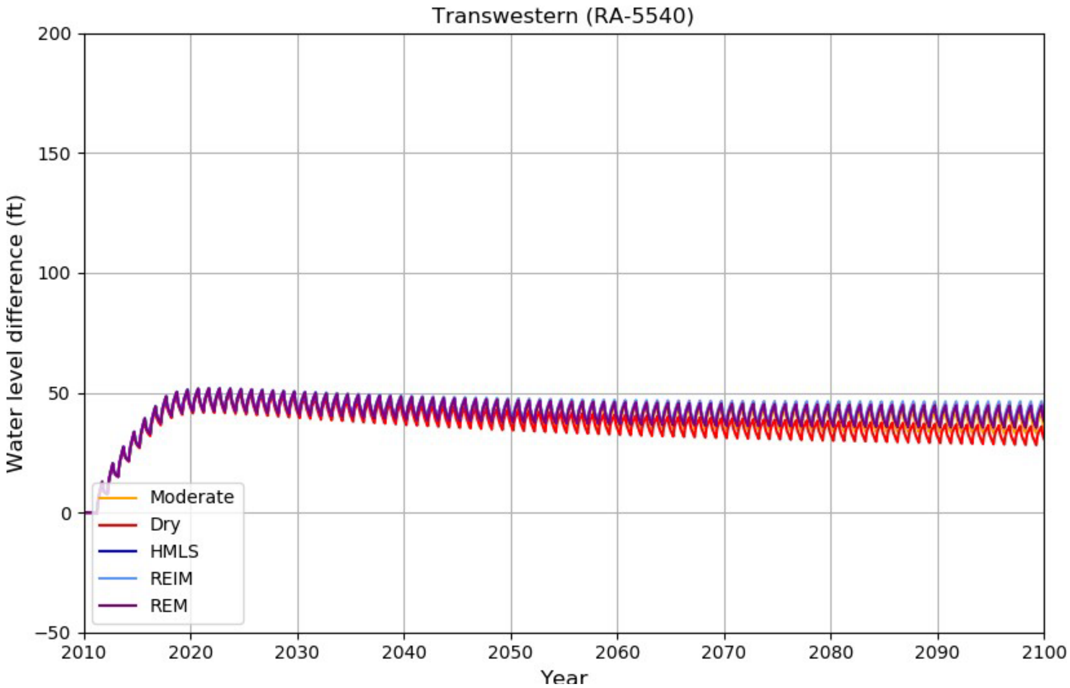

Figure 81. Change in simulated water levels at the Transwestern (RA-5540) observation well for climate change storylines, no PVACD footprint (storyline minus Groundwater Base Case).

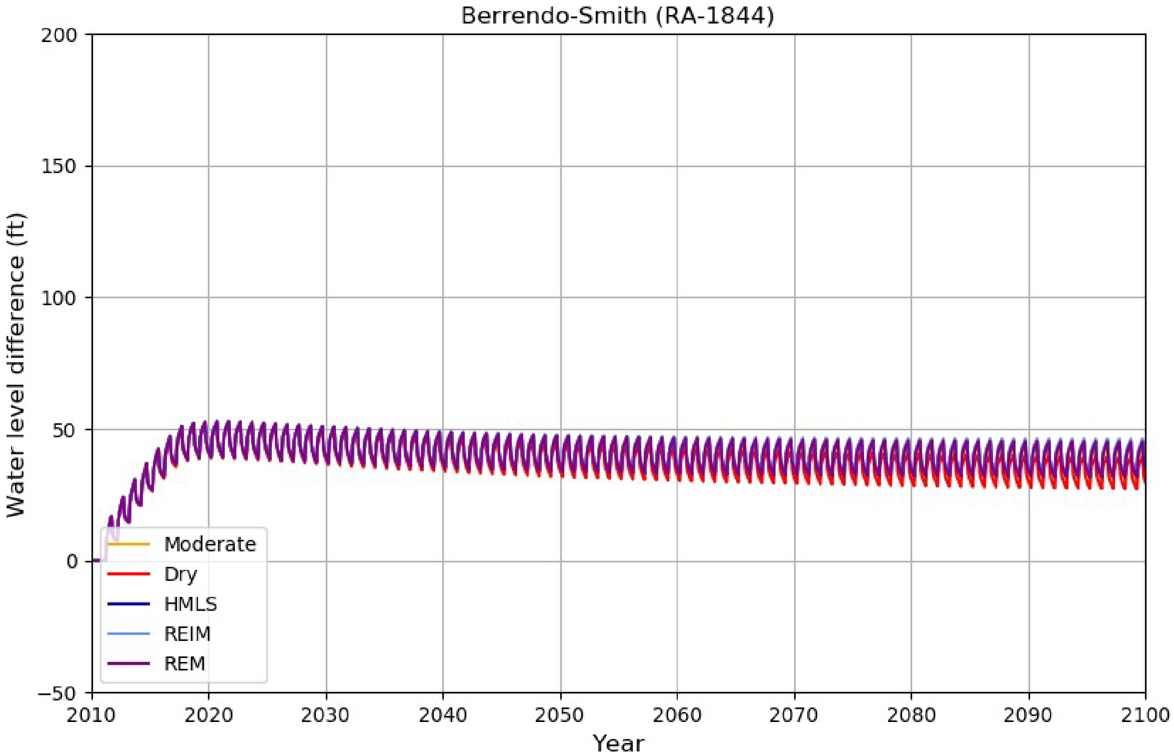

Figure 82. Change in simulated water levels at the Berrendo Smith (RA-1844) observation well for climate change storylines, no PVACD footprint (storyline minus Groundwater Base Case).

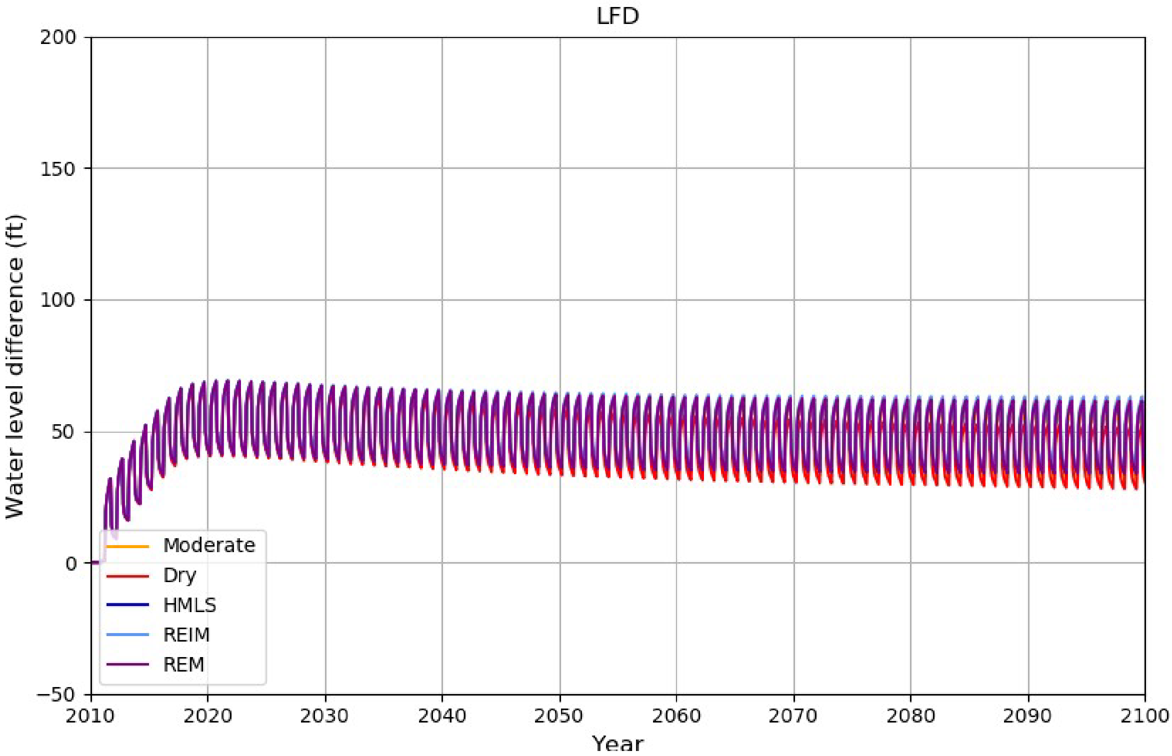

Figure 83. Change in simulated water levels at the LFD observation well for climate change storylines, no PVACD footprint (storyline minus Groundwater Base Case).

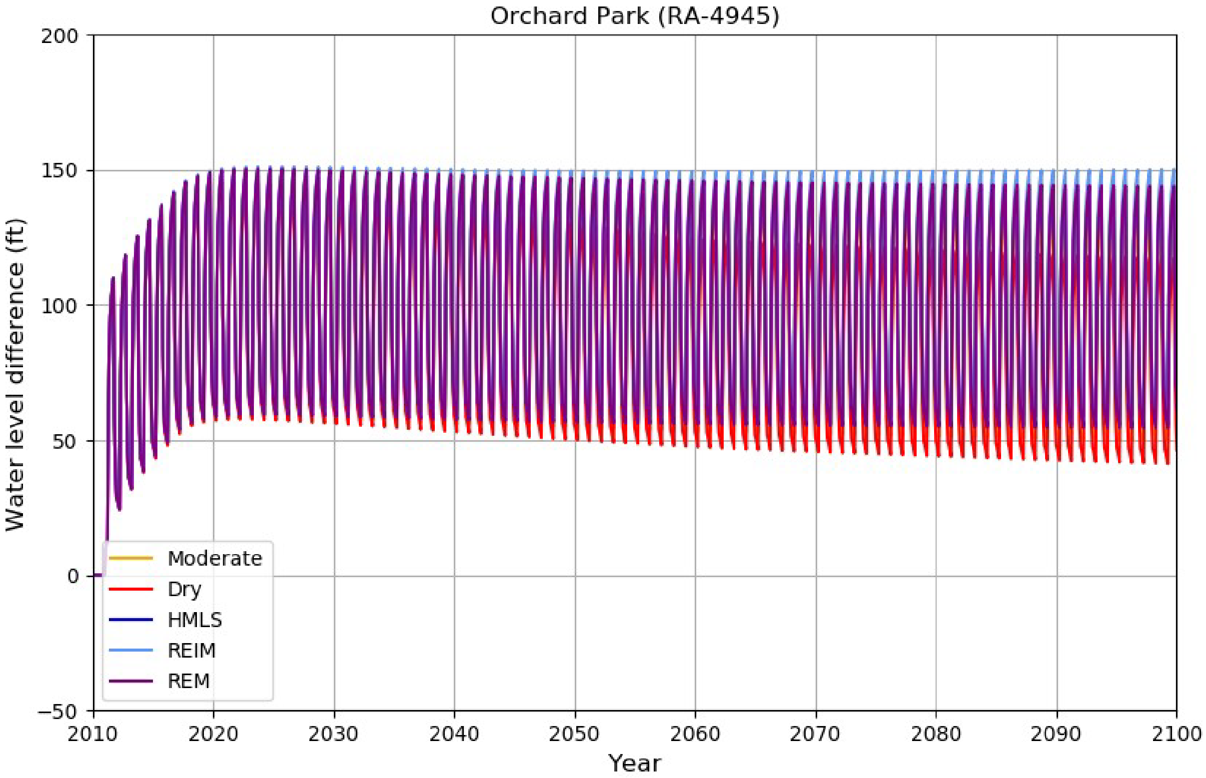

Figure 84. Change in simulated water levels at the Orchard Park (RA-4945) observation well for climate change storylines, no PVACD footprint (storyline minus Groundwater Base Case).

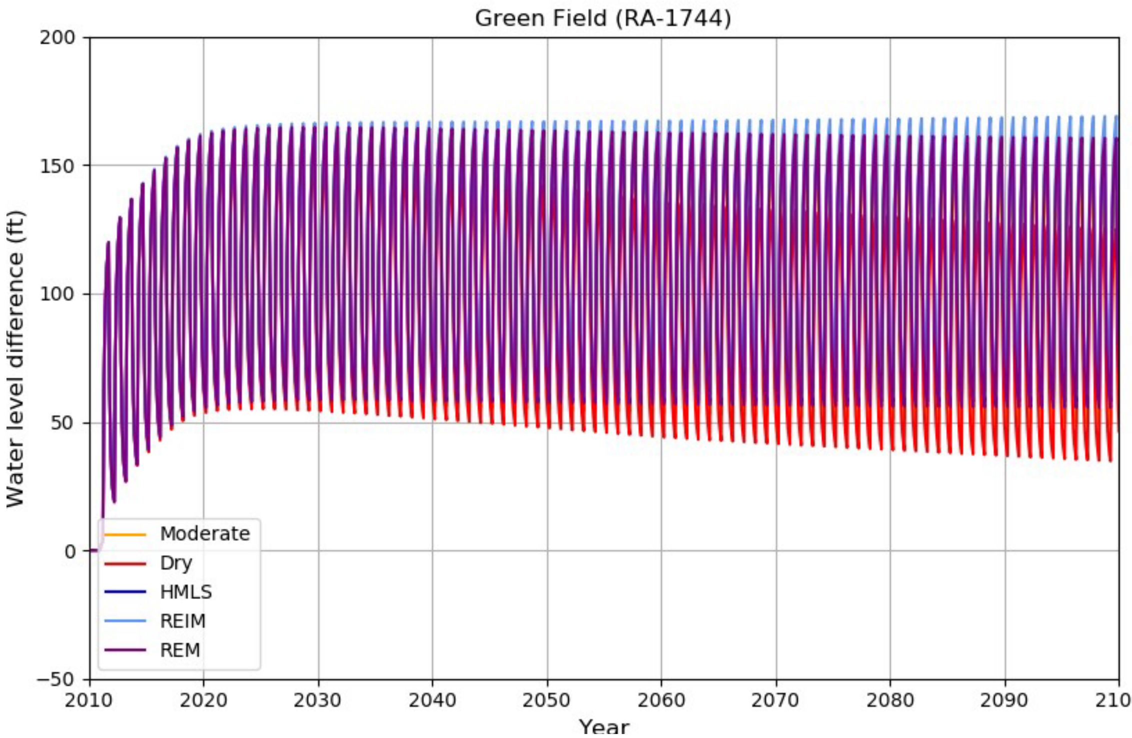

Figure 85. Change in simulated water levels at the Green Field (RA-1744) observation well for climate change storylines, no PVACD footprint (storyline minus Groundwater Base Case).

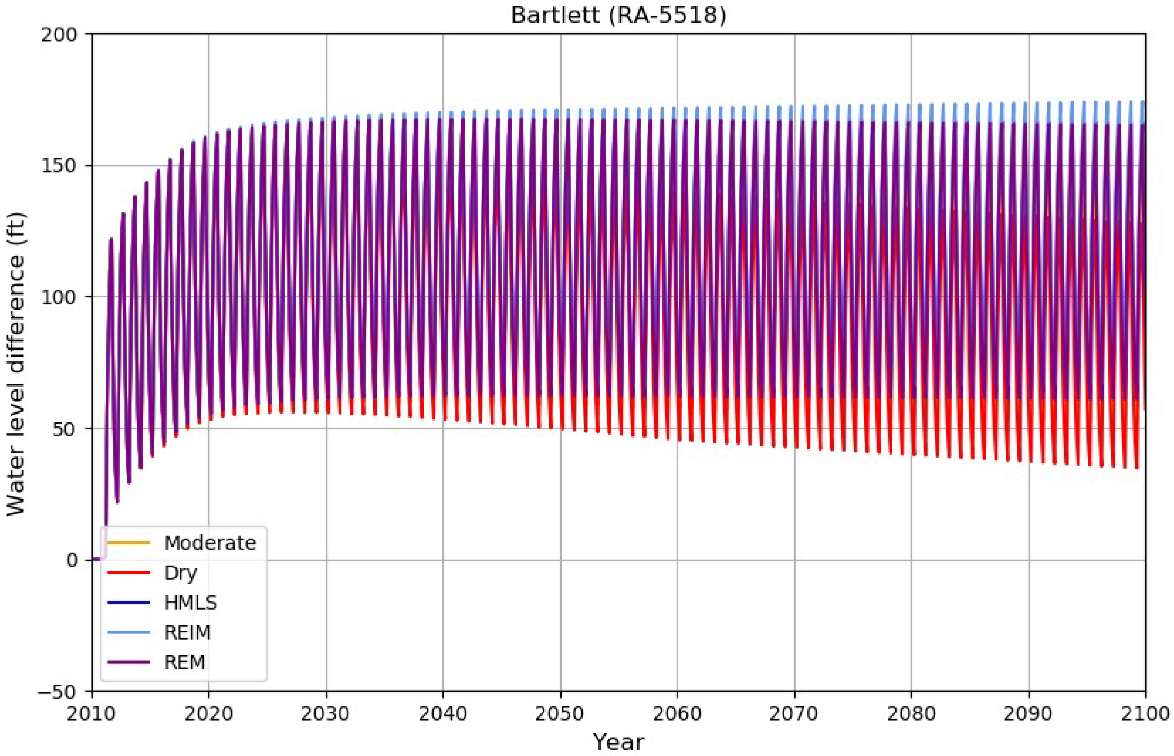

Figure 86. Change in simulated water levels at the Bartlett (RA-5518) observation well for climate change storylines, no PVACD footprint (storyline minus Groundwater Base Case).

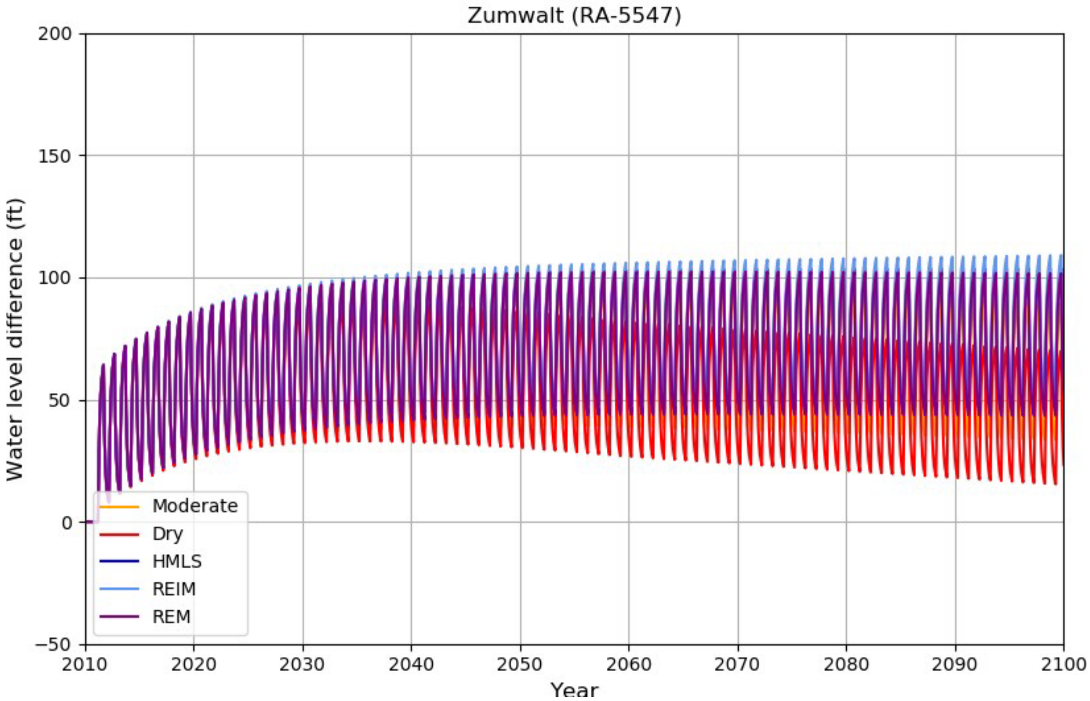

Figure 87. Change in simulated water levels at the Zumwalt (RA-5547) observation well for climate change storylines, no PVACD footprint (storyline minus Groundwater Base Case).

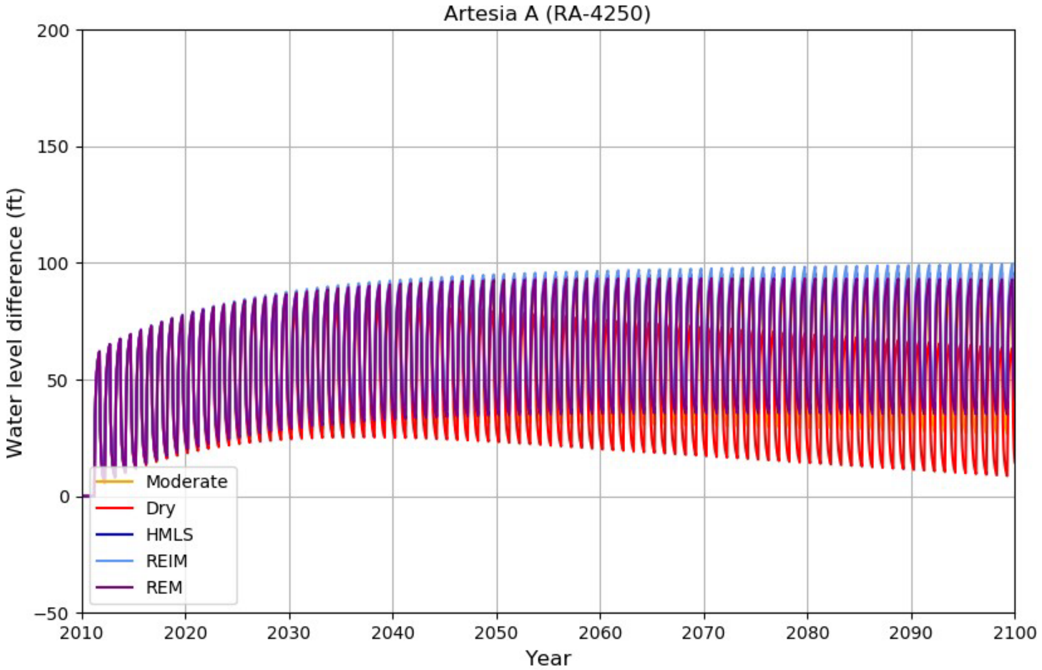

Figure 88. Change in simulated water levels at the Artesia A (RA-4250) observation well for climate change storylines, no PVACD footprint (storyline minus Groundwater Base Case).

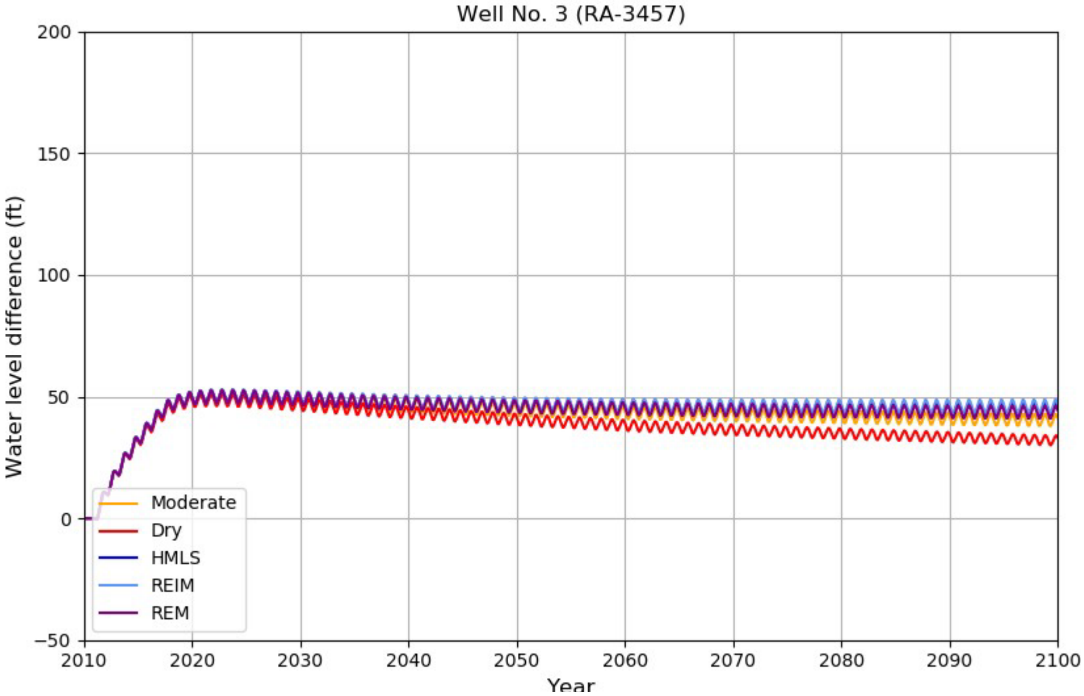

Figure 89. Change in simulated water levels at the Well No. 3 (RA-3457) observation well for climate change storylines, no PVACD footprint (storyline minus Groundwater Base Case).

8.2. PVACD Groundwater Level Footprints

PVACD's footprint on groundwater levels in the Roswell Artesian Basin was estimated by comparing two sets of simulation runs of the RABGWM, one run that models the baseline in each storyline (see Section 5.5.1. *Roswell Artesian Basin Groundwater Levels*), and a second set of runs modeling these baselines without PVACD pumping stresses (see the Groundwater Appendix, Section 8.1). The water footprint analysis results were not explicitly simulated, but were instead generated from differencing these two simulations, and as a result do not distinguish between differences in the two simulations caused by PVACD and differences caused by other factors (for example, effects caused by disconnection of the RAB and the Pecos River). For this footprint analysis, we assumed that the differences in PVACD pumping dominate other differences between those simulations. An explicitly modeled simulation of the footprint, however, could produce different estimates of the PVACD footprints.

As expected, the PVACD water footprint on groundwater levels in the Roswell Artesian Basin is significant for each storyline. PVACD's footprint is larger than any storyline impact. In general, the size of the PVACD footprint is mostly dependent on the differences in the baseline conditions in the five storylines, since the footprint compares simulated water levels with and without the impacts of PVACD. Without the impacts of PVACD, water levels in the RAB would quickly rise, but only by a certain amount before aquifer levels reach the surface, allowing artesian springs to begin flowing again and limiting further water level increases. As a result, the differences between the Groundwater Base Case and the simulated groundwater levels without the impact of PVACD tend to be relatively consistent between storylines (see the Groundwater Appendix, Section 8), while the differences between the Groundwater Base Case and the baselines for each storyline tend to diverge.

As an example, at the LFD observation well (Figure 93), simulated groundwater levels when the storylines are modeled without considering PVACD pumping stresses are roughly 50 feet higher than the Groundwater Base Case in all storylines by the end of the century, while under the baseline storyline conditions (see Section 5.5.1 in the main report and Section 7.1, Figure 23 in this appendix), the storylines range from a groundwater level increase over the same period, relative to the Groundwater Base Case, of about 20 feet in the RE Increased Monsoon Storyline to a decrease of nearly 150 feet in the BaU Dry Storyline. As a result, our estimates of the PVACD footprint at the LFD observation well by the end of the century range from approximately 30 feet of drawdown (reducing from a 50-foot increase to a 20 foot increase) in the RE Increased Monsoon Storyline to a drawdown of almost 200 feet (from a 50-foot increase to a 150-foot decrease) in the BaU Dry Storyline (Figure 93).

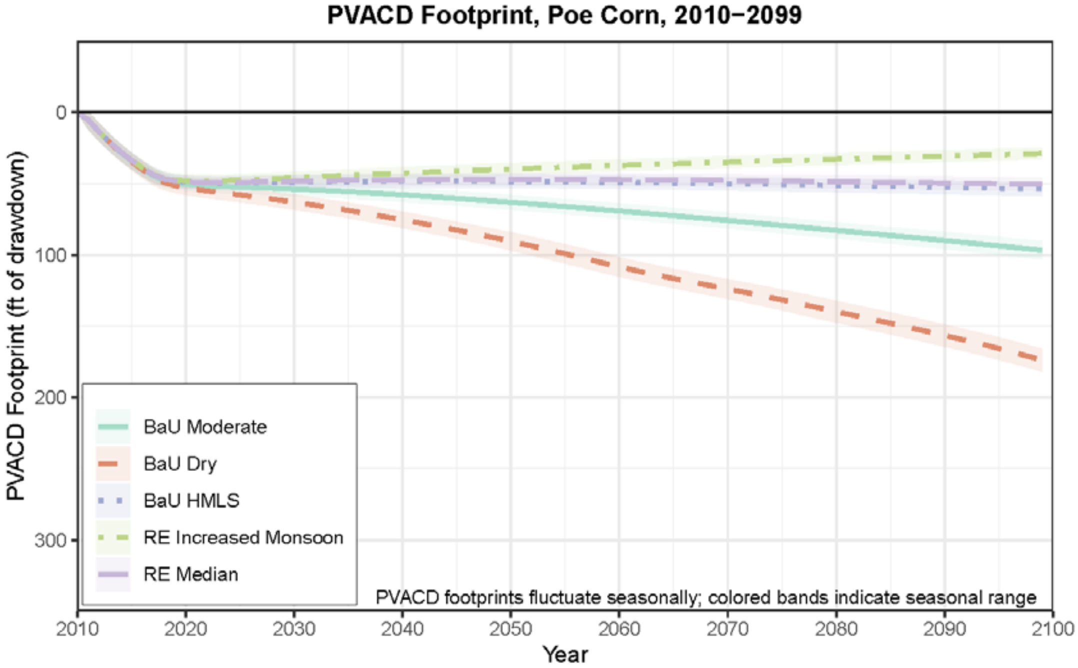

Figure 90. RAB groundwater levels: Estimated water footprint at Poe Corn (RA-3745) observation well in the five storylines, in feet of additional drawdown.

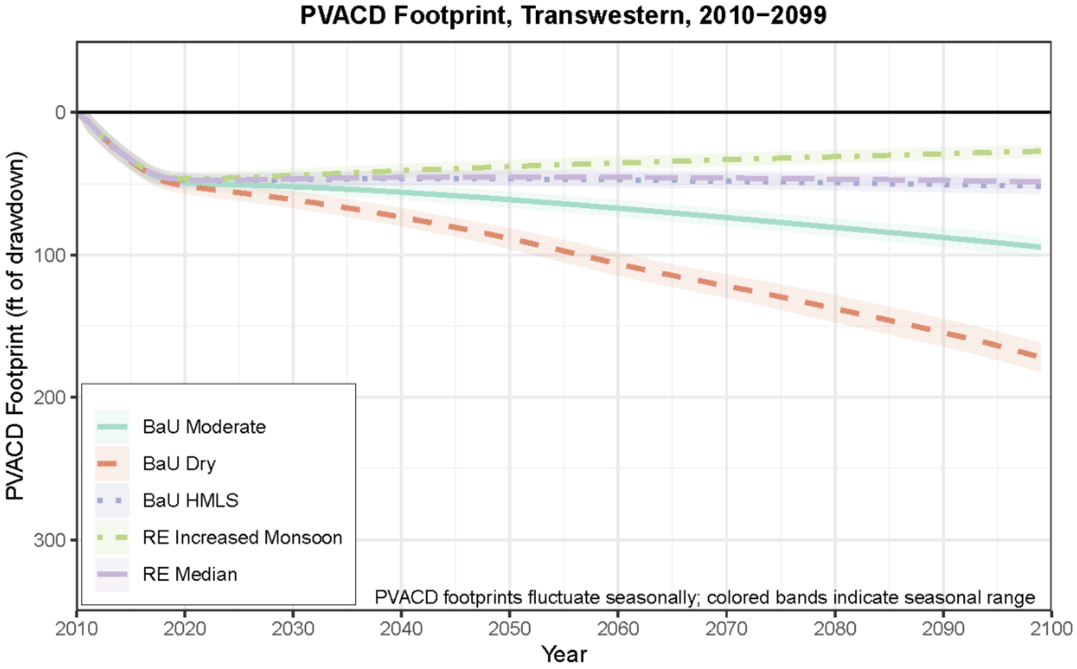

Figure 91. RAB groundwater levels: Estimated water footprint at Transwestern (RA-5540) observation well in the five storylines, in feet of additional drawdown.

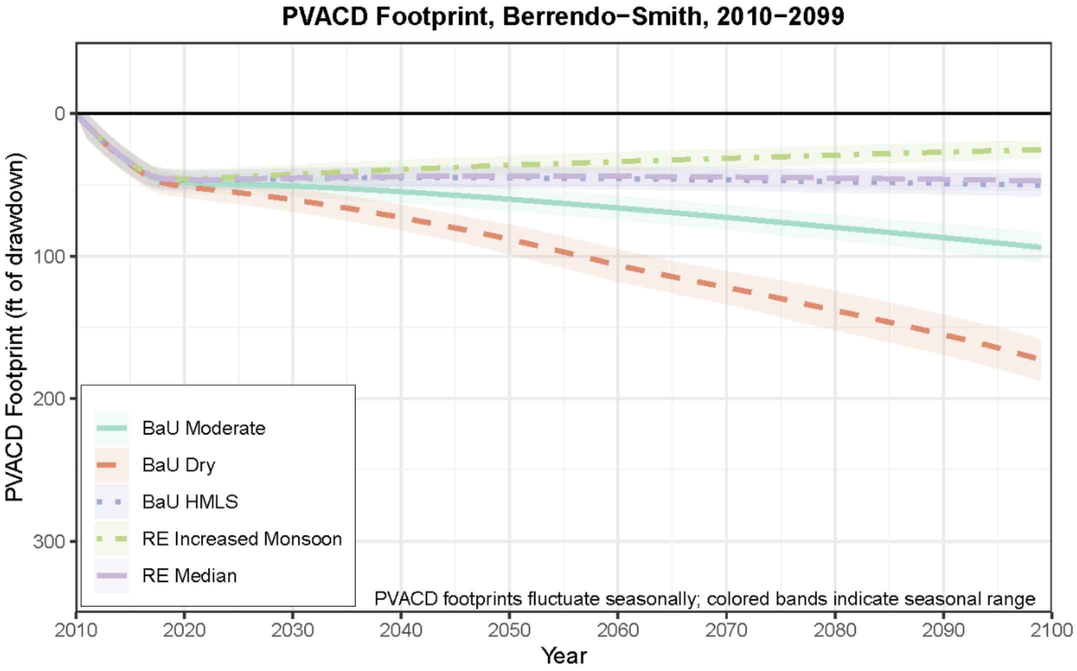

Figure 92. RAB groundwater levels: Estimated water footprint at footprint at Berrendo Smith (RA-1844) observation well in the five storylines, in feet of additional drawdown.

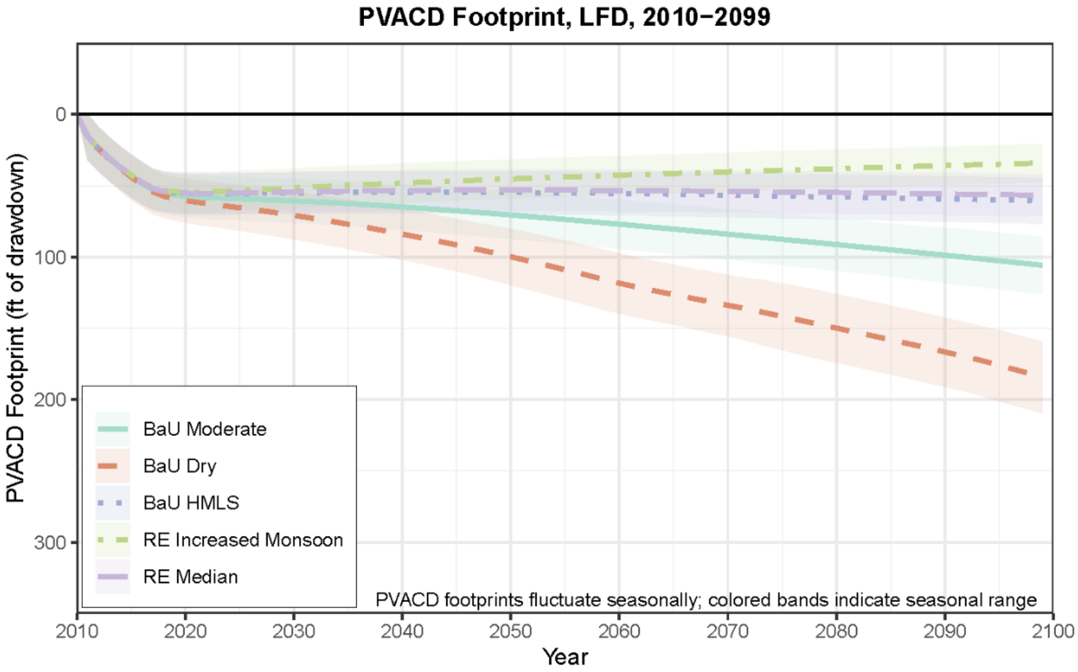

Figure 93. RAB groundwater levels: Estimated water footprint at LFD observation well in the five storylines, in feet of additional drawdown.

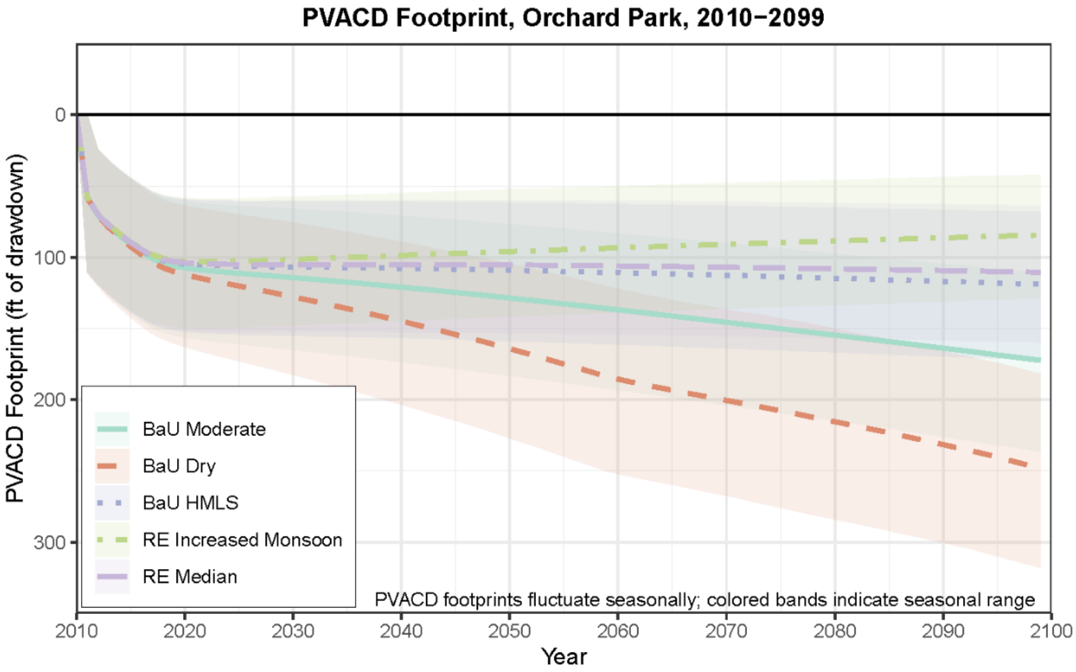

Figure 94. RAB groundwater levels: Estimated water footprint at Orchard Park (RA-4945) observation well in the five storylines, in feet of additional drawdown.

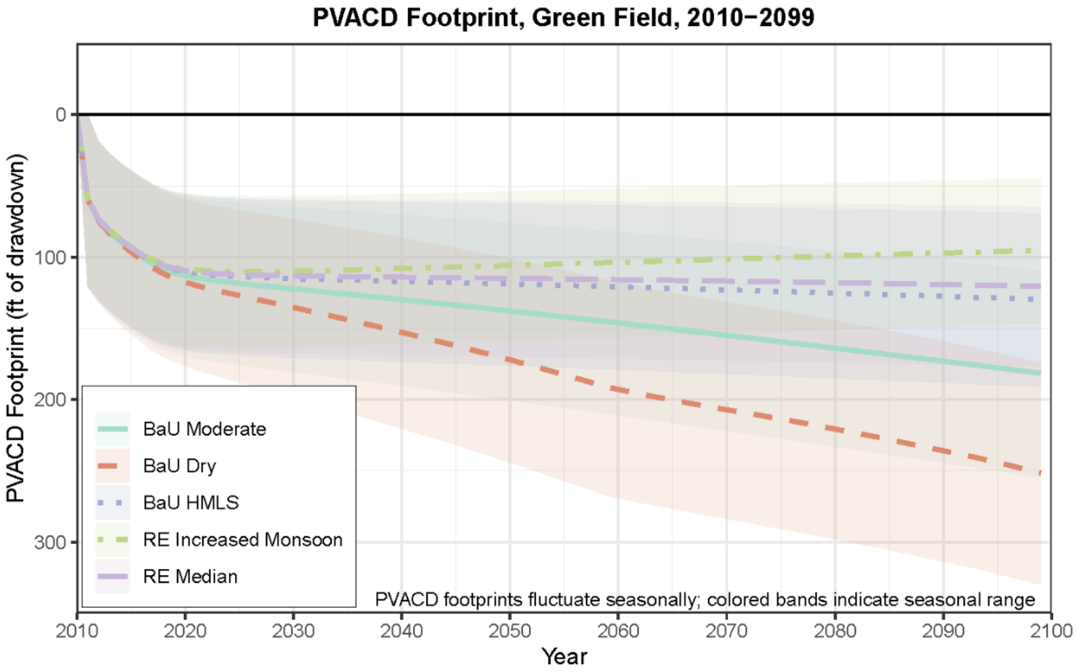

Figure 95. RAB groundwater levels: Estimated water footprint at Green Field (RA-1744) observation well in the five storylines, in feet of additional drawdown.

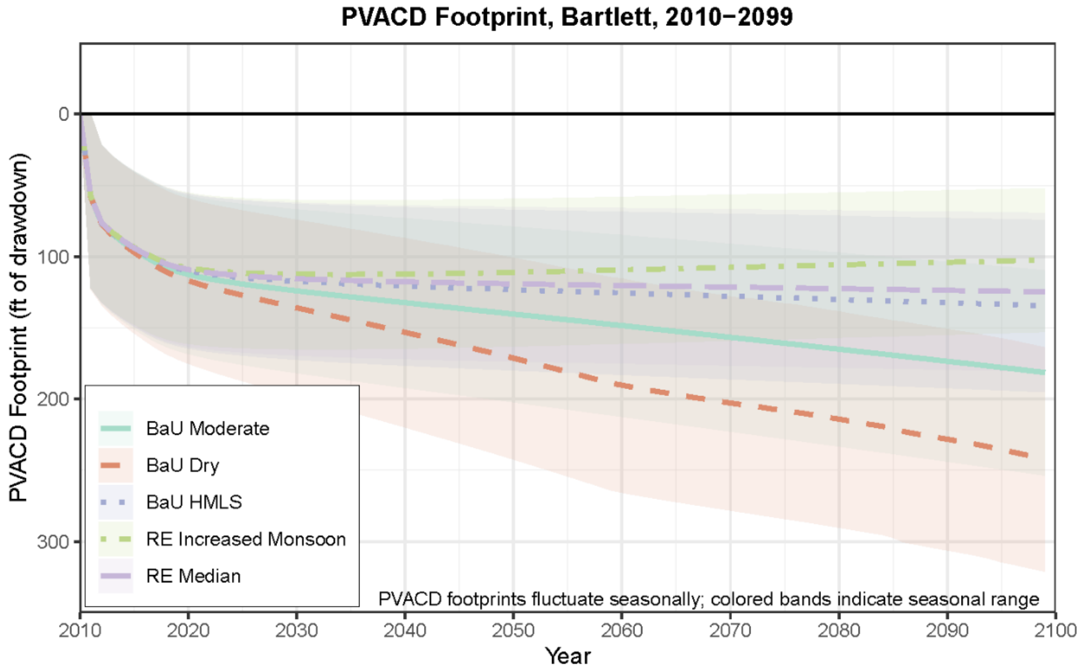

Figure 96. RAB groundwater levels: Estimated water footprint at Bartlett (RA-5518) observation well in the five storylines, in feet of additional drawdown.

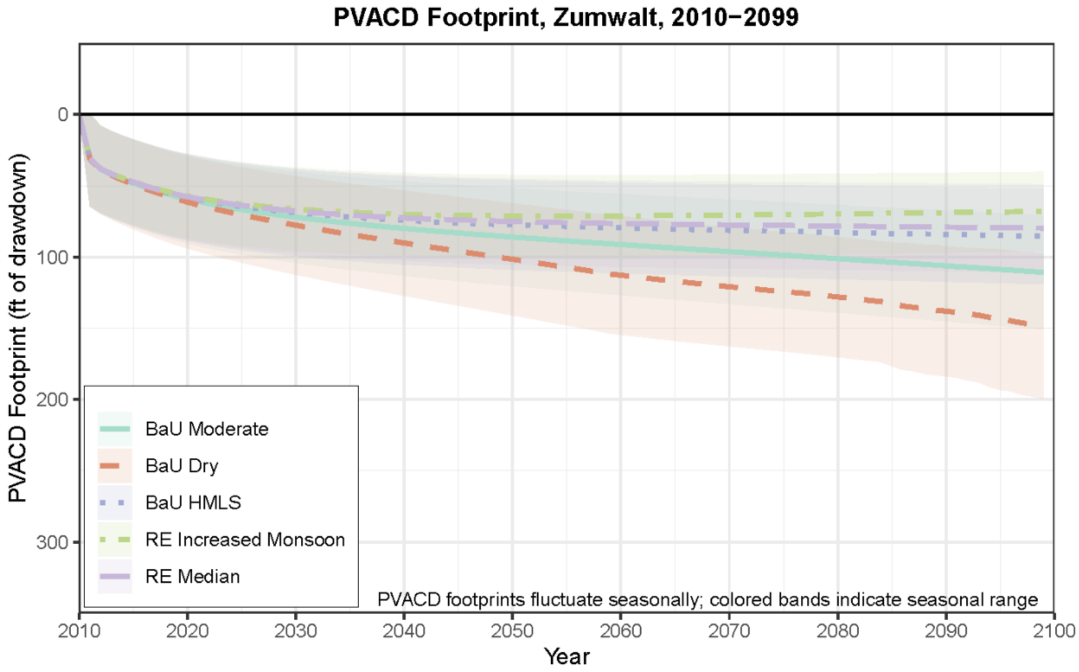

Figure 97. RAB groundwater levels: Estimated water footprint at Zumwalt (RA-5547) observation well in the five storylines, in feet of additional drawdown.

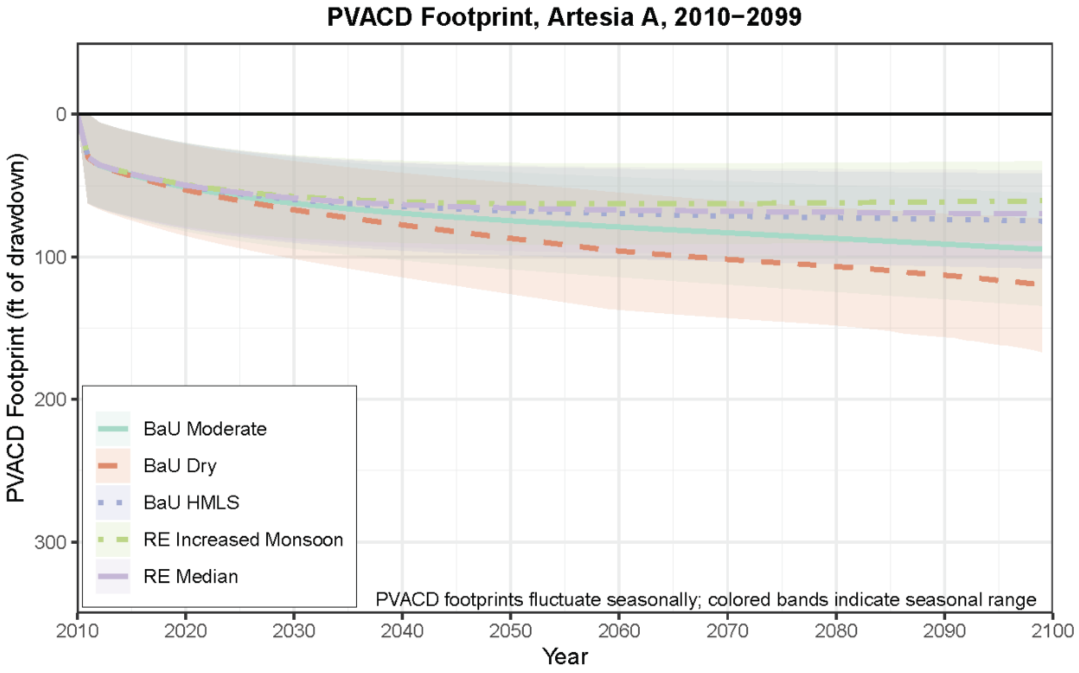

Figure 98. RAB groundwater levels: Estimated water footprint at Artesia A (RA-4250) observation well in the five storylines, in feet of additional drawdown.

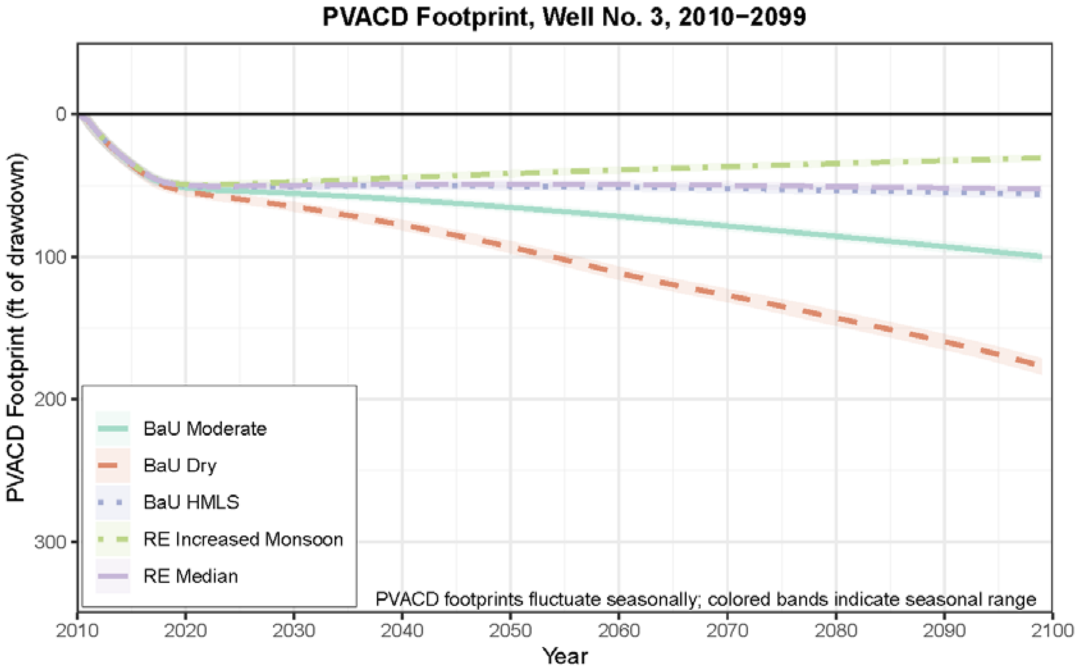

Figure 99. RAB groundwater levels: Estimated water footprint at Well No. 3 (RA-3457) observation well in the five storylines, in feet of additional drawdown.

9. FSID Shallow Aquifer Modeling

9.1. Background

This memorandum summarizes the steps to improve shallow groundwater simulations within the Pecos River Operations Model (PROM) in the vicinity of the Fort Sumner Irrigation District (FSID). The memo was derived from a combination of a draft memo by Emile Sawyer, New Mexico Interstate Stream Commission (NMSIC) and working files left by Larry Grey, Bureau of Reclamation (Reclamation). Model development was initiated and funded by Pecos River Basin Study being conducted jointly by the New Mexico Interstate Stream Commission (NMSIC) and the Bureau of Reclamation (Reclamation).

The Fort Sumner Underground Water Basin (FSUWB) is State Administrative Region delineated by the New Mexico State Engineer. Management of water resources in the Fort Sumner Valley and the FSUWB are of critical importance in meeting the needs of both the 25,055 irrigated acres in the Carlsbad Project and the threatened Pecos bluntnose shiner (shiner). Additionally, compliance with the water delivery requirements of the Pecos River Compact is essential. The Pecos Basin Study in New Mexico was proposed to develop a robust groundwater model for the FSUWB; however, circumstances lead to a decision to use RiverWare ground water objects instead to provide modeling elements that simulate scenarios for essential effective conjunctive management activities for groundwater and surface water in the Pecos Basin.

Previous to this development, within RiverWare, river losses and irrigation return flows in the vicinity of FSID were applied by empirically derived relationships. The relationships did not capture well, new operations or extreme swings in hydrology. With new RiverWare capabilities (groundwater objects) we could approximate head based flow between FSID's irrigated fields, shallow groundwater, irrigation drains and the Pecos River in the vicinity of FSID.
Data Collection

Presumably, user input parameters for the groundwater objects and associated fluxes were derived from a Geographical Information System (GIS) database that included but was not limited to New Mexico Office of the State Engineer's administrative well data, soil strata information and topographical/bathymetric survey data collected at strategic locations within FSID (Appendix 1).

9.2. RiverWare Ground Water Storage Objects

RiverWare ground water storage objects model a simple fill and spill underground body of water. Inflow to an object is given to the object either via user input or a link from a slot from another object. Storage and Outflow values are then calculated based on a mass balance performed on the object and the selected user input methods available in RiverWare. The user must input a value for Storage at the initial timestep of the run for the object to solve successfully (CADWES, 2015).

9.3. Fort Sumner Valley Ground Water Objects

A total of nine (9) ground water objects were developed for the Fort Sumner Valley. These ground water objects were connected within the PROM model to the network of river and drain reaches spanning from just below Fort Sumner dam to the confluence of Taiban Creek. These objects are named from upstream to downstream and east to west in the model accordingly: Eastside 1, Eastside 2, Eastside 3, Eastside 4; Sumner to FSID, FSID to Sand Gate, Sand Gate to Main Drain, Vaughan Wells, and Main Drain to Taiban (Figure 100).

Each groundwater object requires data to fill RiverWare data slots that contain the information for the groundwater objects to interact with the larger model. These slots are set up for the user in RiverWare by choosing a method for the appropriate slots. The Head Based Groundwater Grid method is used to enable connections to other objects. The method relies on beginning of timestep water elevations and hydraulic conductivities for all linked objects. The groundwater objects located within the river corridor (Sumner to FSID, FSID to Sand Gates and Sand Gate to Main Drain) are set to suffer both wetted sand evaporation and evapotranspiration.

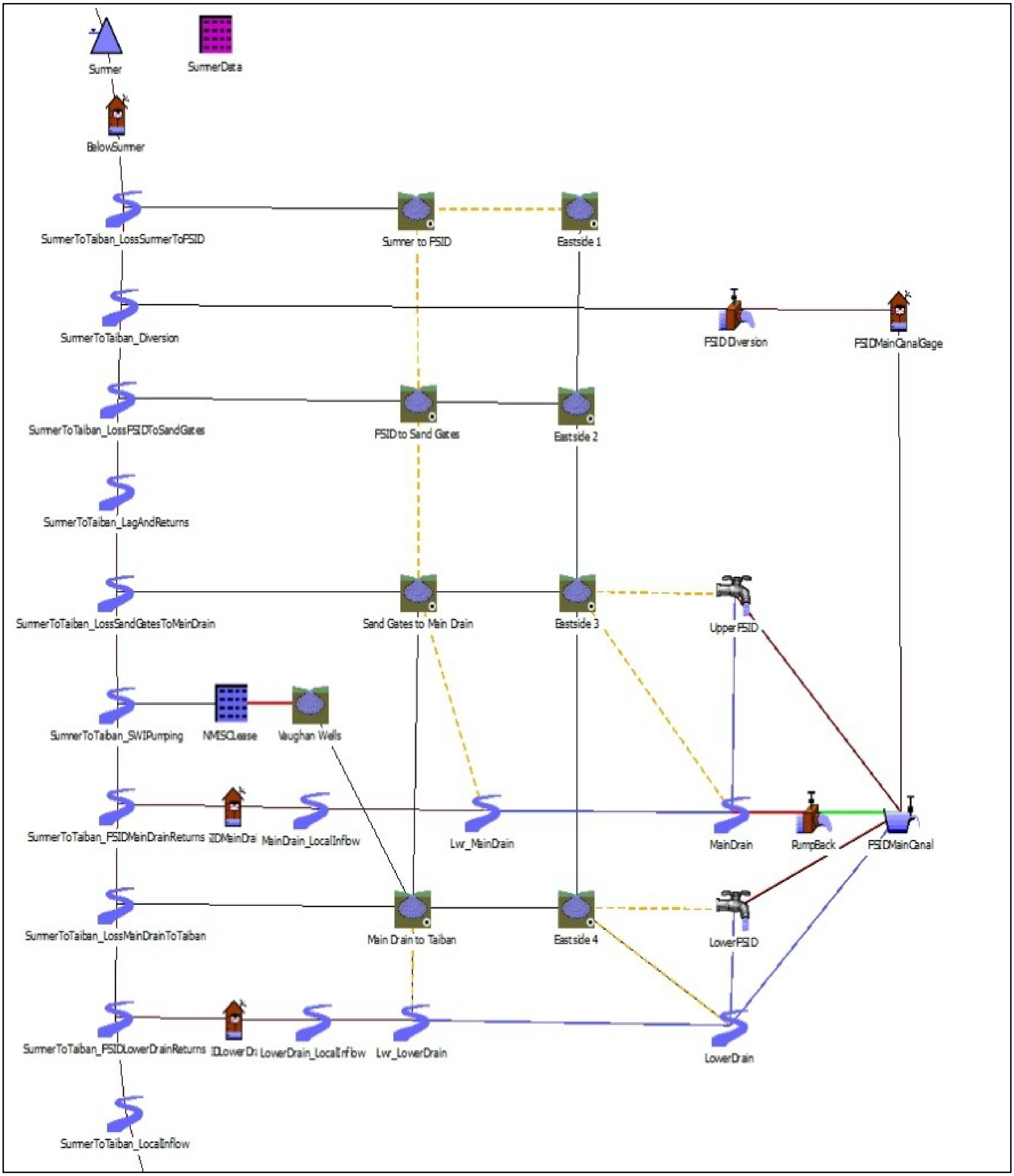

Figure 100. PROM Layout- FSID Groundwater

9.4. Summary of Data Used to Develop the Fort Sumner Groundwater Objects and Associated Reaches

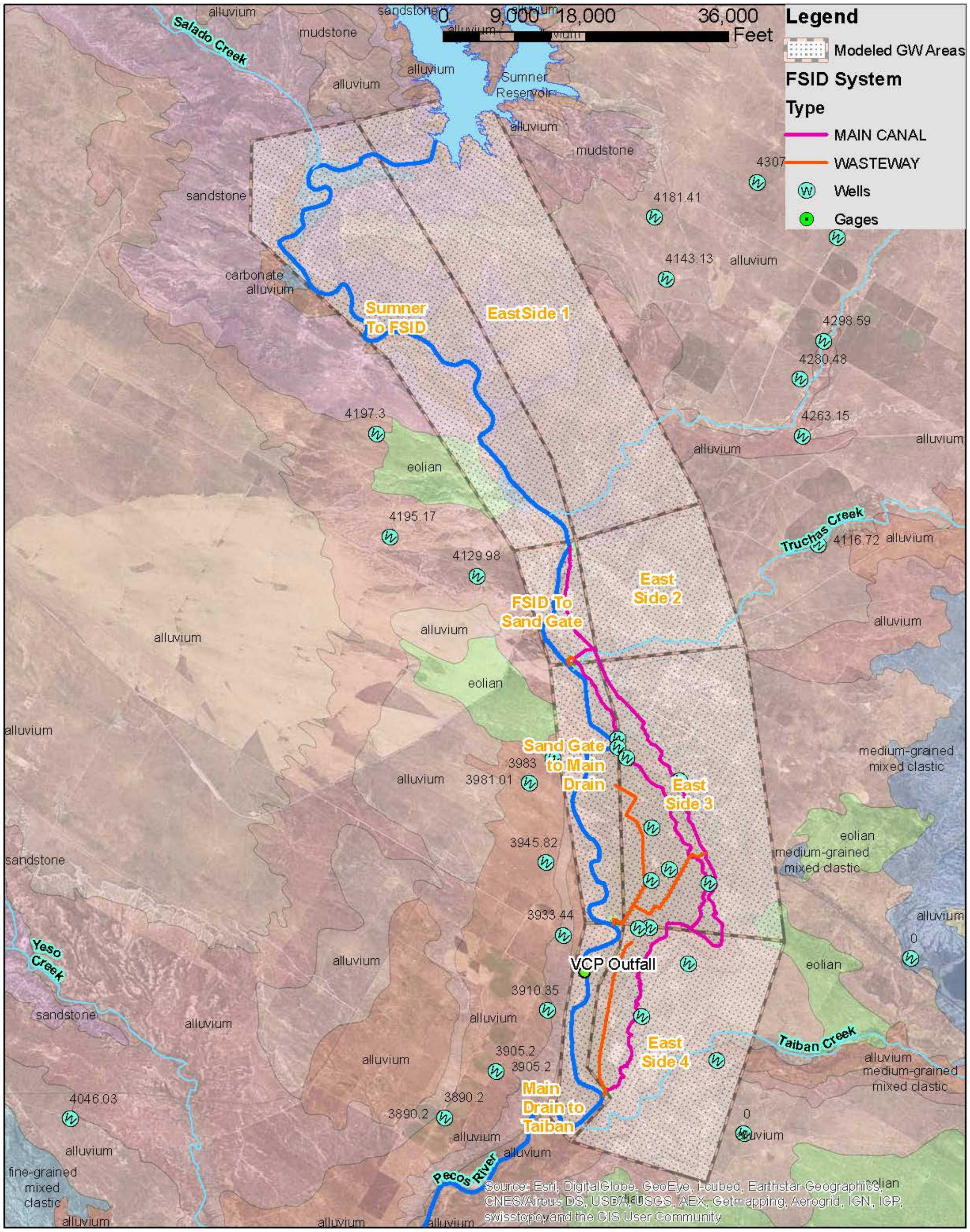

Source: Esri, DigitalGlobe, GeoEye, i-cubed, Earthstar Geographics, CNES/Airbus DS, USDA, USGS, AEX, Getmapping, Aerogrid, IGN, IGP, swisstopo, and the GIS User Community

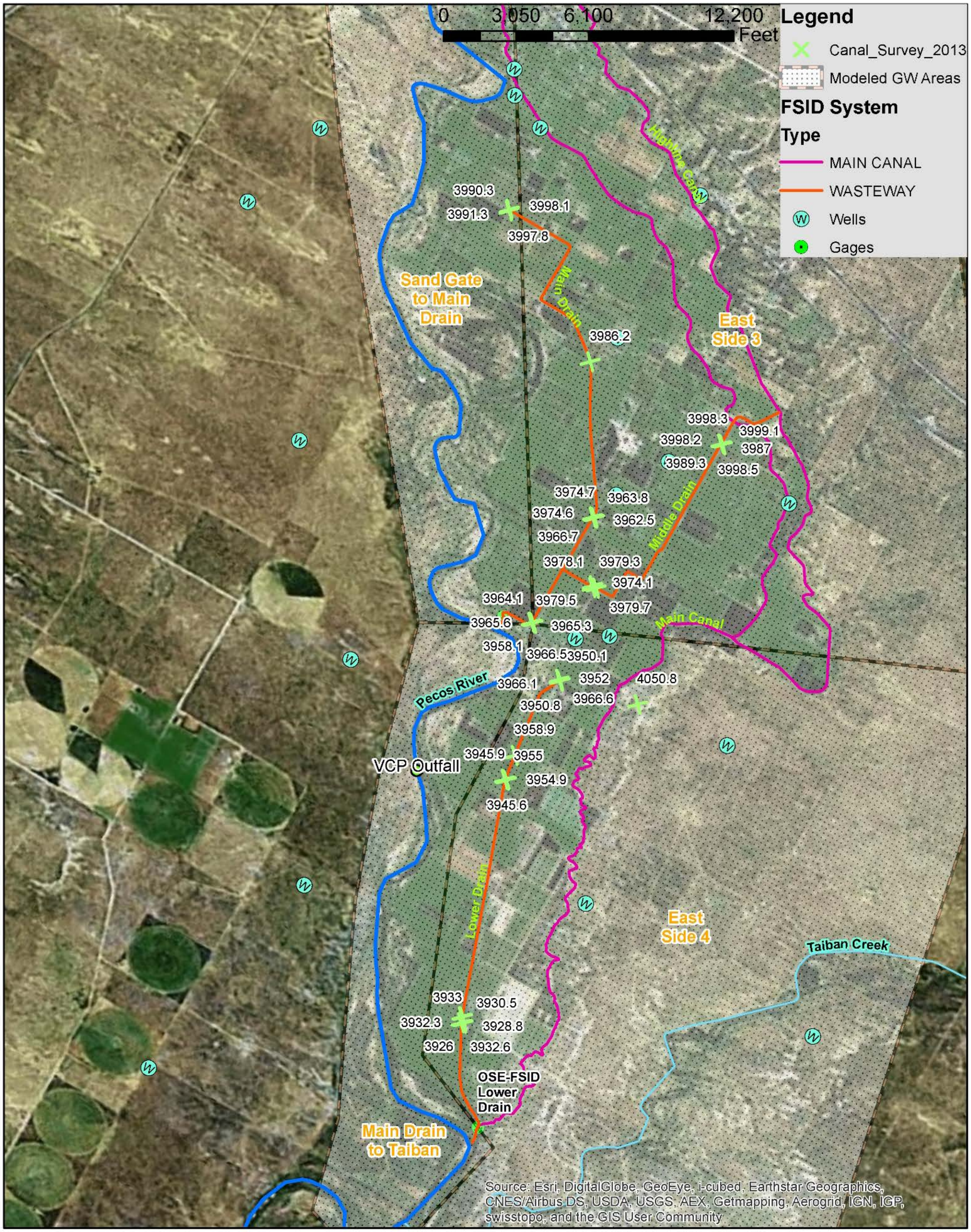

Source: Esri, DigitalGlobe, GeoEye, i-cubed, Earthstar Geographics, CNES/Airbus DS, USDA, USGS, AEX, Getmapping, Aerogrid, IGN, IGP, swisstopo, and the GIS User Community

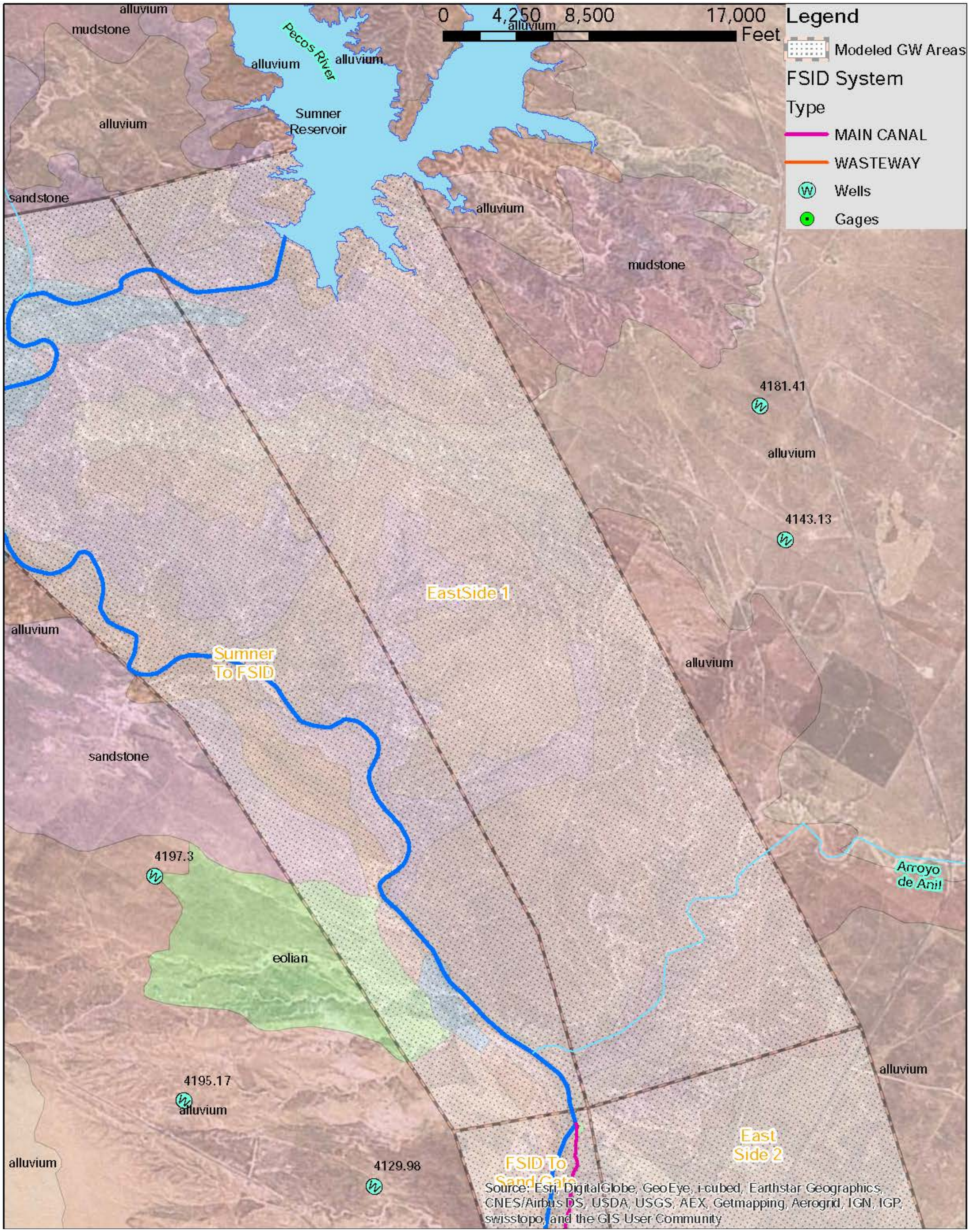

Source: Esri, DigitalGlobe, GeoEye, i-cubed, Earthstar Geographics, CNES/Airbus DS, USDA, USGS, AEX, Getmapping, Aerogrid, IGN, IGP, swisstopo, and the GIS User Community

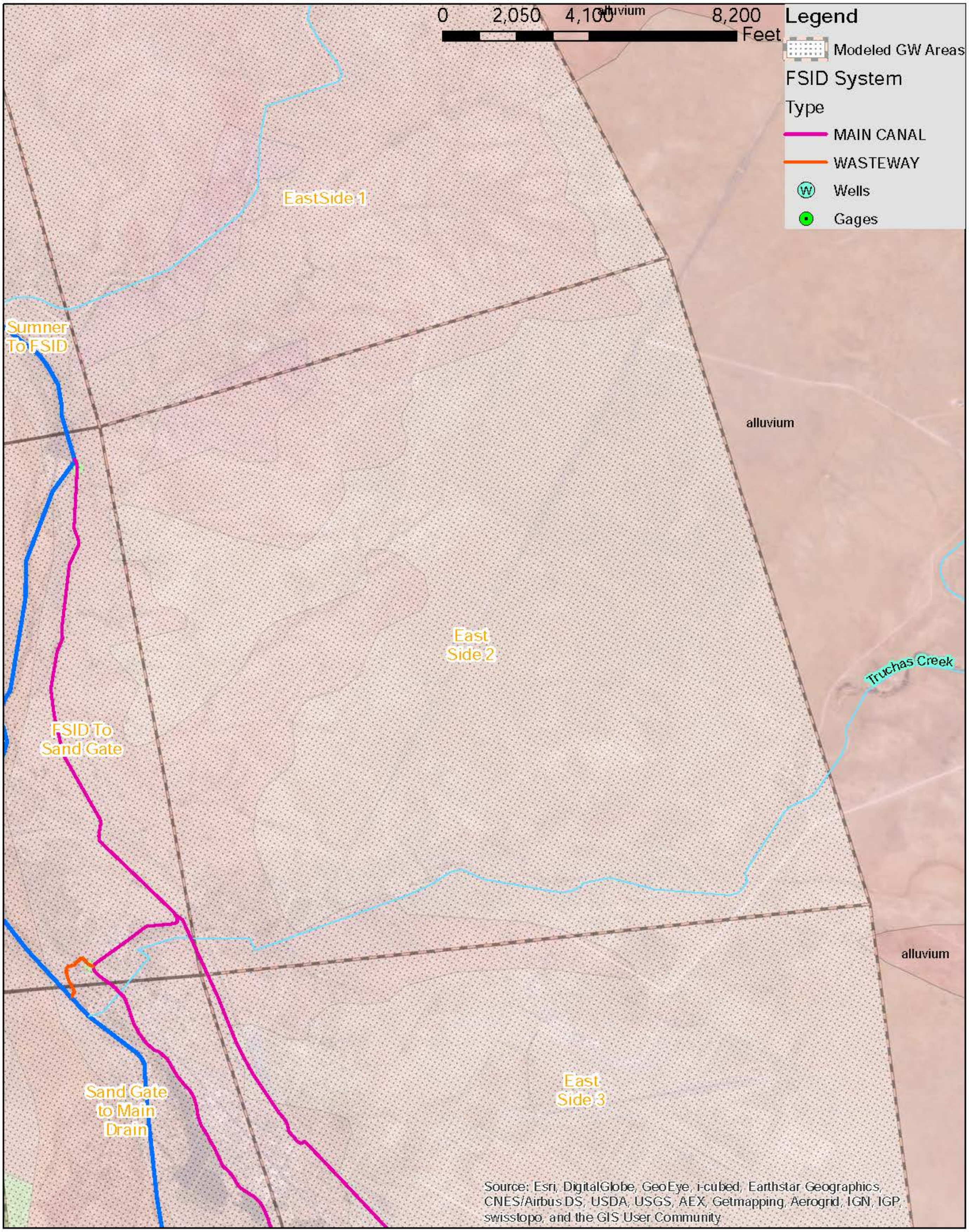

Source: Esri, DigitalGlobe, GeoEye, i-cubed, Earthstar Geographics, CNES/Airbus DS, USDA, USGS, AEX, Getmapping, Aerogrid, IGN, IGP, swisstopo, and the GIS User Community

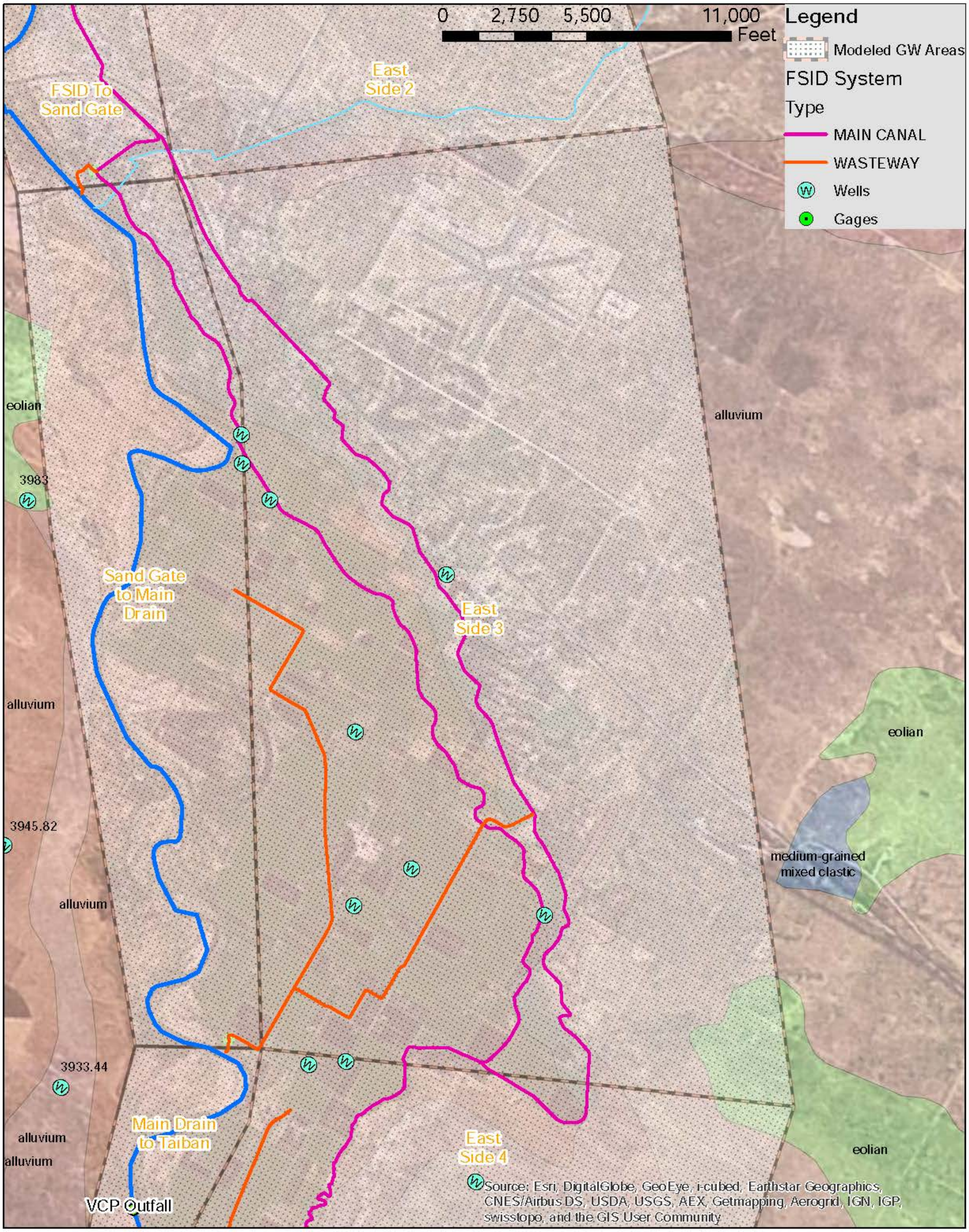

Source: Esri, DigitalGlobe, GeoEye, i-cubed, Earthstar Geographics, CNES/Airbus DS, USDA, USGS, AEX, Getmapping, Aerogrid, IGN, IGP, swisstopo, and the GIS User Community

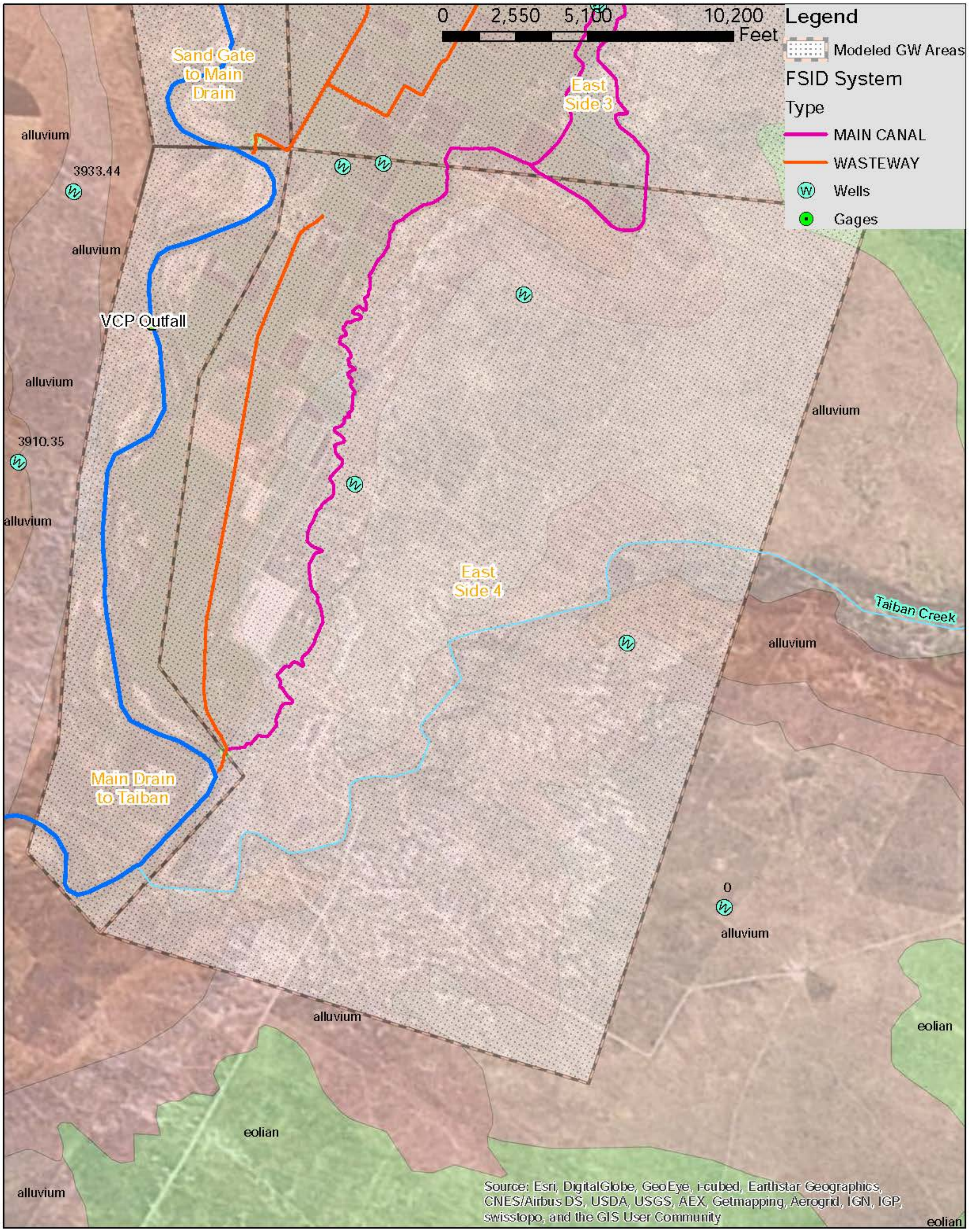

Source: Esri, DigitalGlobe, GeoEye, i-cubed, Earthstar Geographics, CNES/Airbus DS, USDA, USGS, AEX, Getmapping, Aerogrid, IGN, IGP, swisstopo, and the GIS User Community

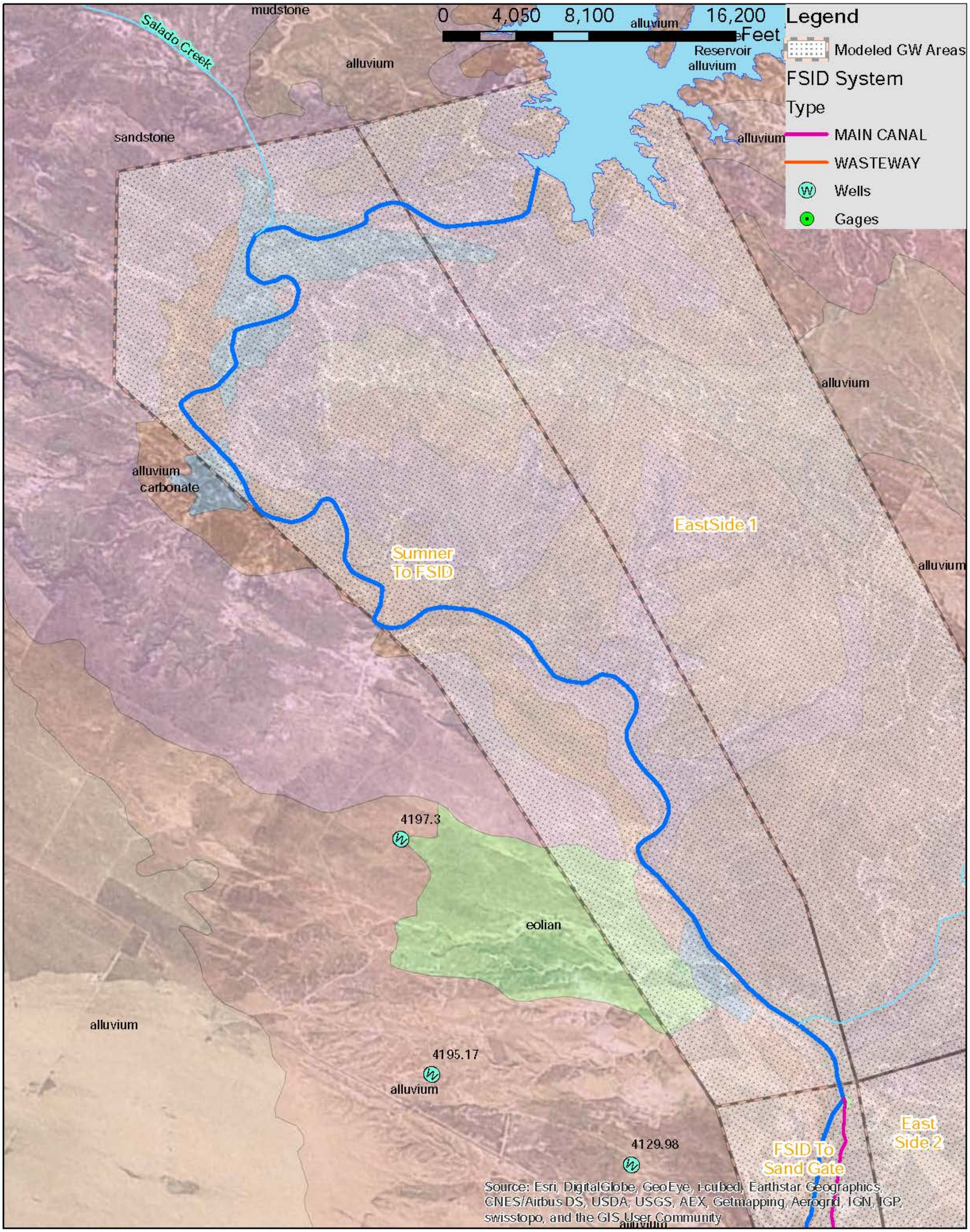

Source: Esri, DigitalGlobe, GeoEye, i-cubed, Earthstar Geographics, CNES/Airbus DS, USDA, USGS, AEX, Getmapping, Aerogrid, IGN, IGP, swisstopo, and the GIS User Community

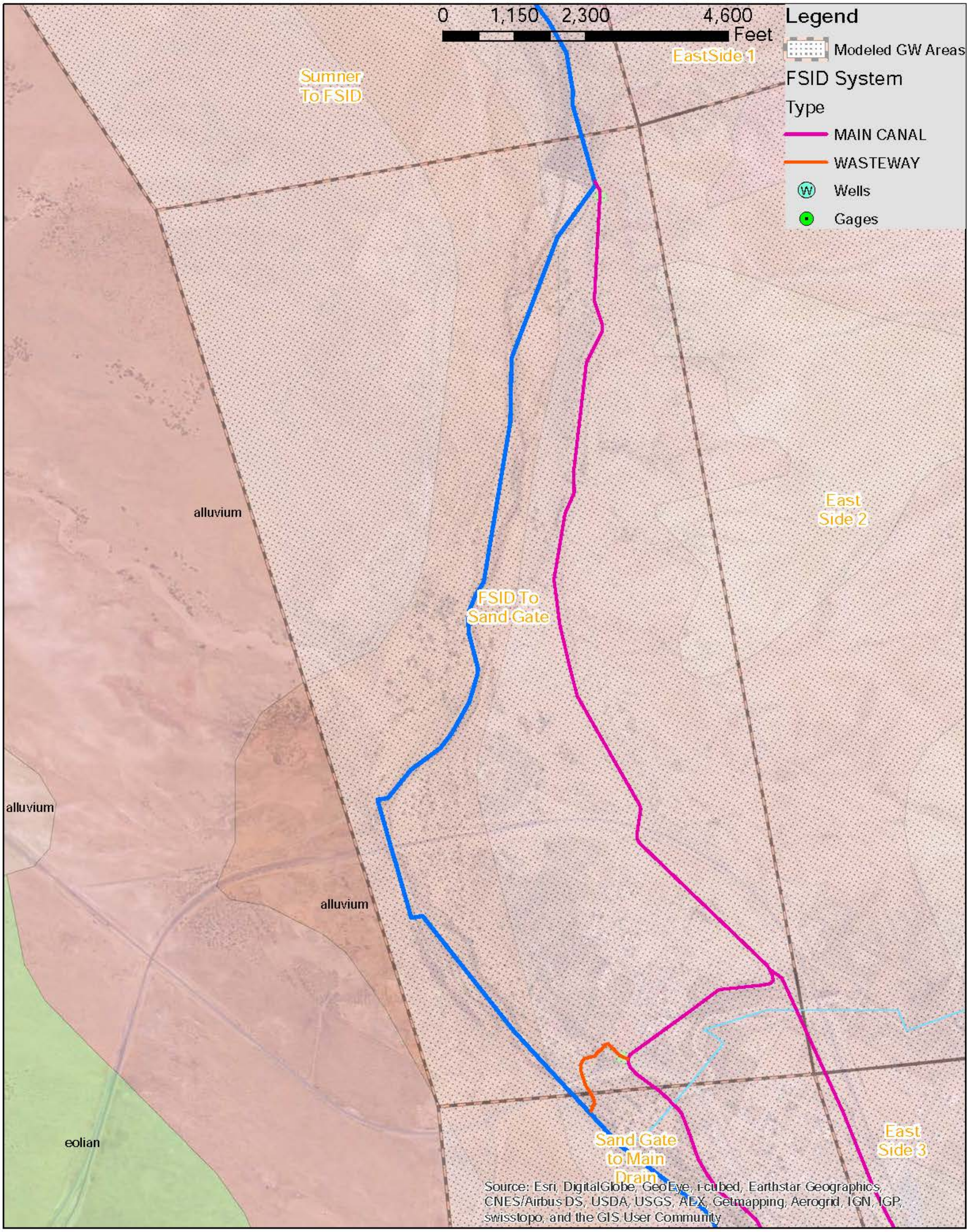

Source: Esri, DigitalGlobe, GeoEye, i-cubed, Earthstar Geographics, CNES/Airbus DS, USDA, USGS, AEX, Getmapping, Aerogrid, IGN, IGP, swisstopo, and the GIS User Community

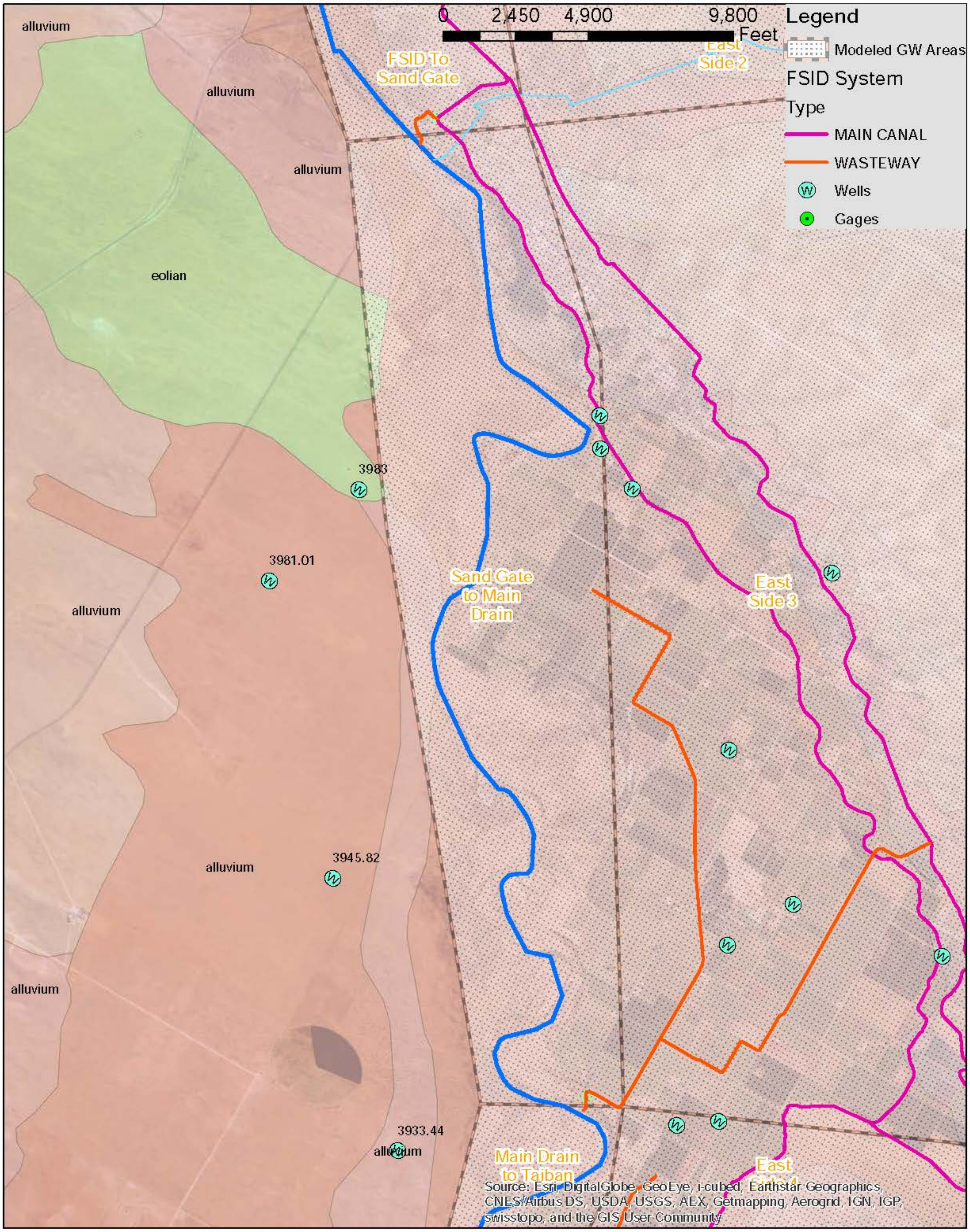

Source: Esri, DigitalGlobe, GeoEye, i-cubed, Earthstar Geographics, CNES/Airbus DS, USDA, USGS, AEX, Getmapping, Aerogrid, IGN, IGP, swisstopo, and the GIS User Community

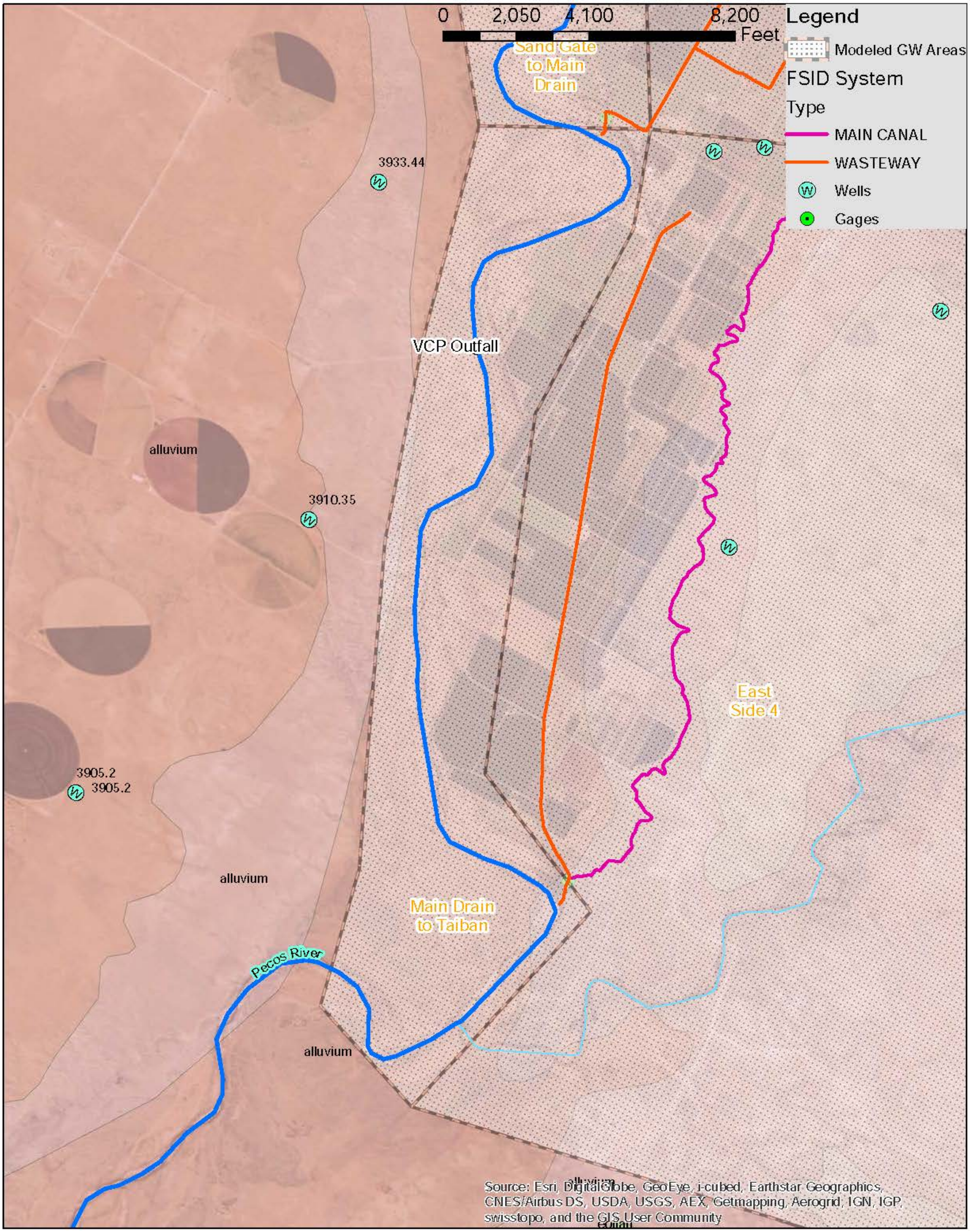

Source: Esri, DigitalGlobe, GeoEye, i-cubed, Earthstar Geographics, CNES/Airbus DS, USDA, USGS, AEX, Getmapping, Aerogrid, IGN, IGP, swisstopo, and the GIS User Community

9.5. RiverWare Report Outlining Various User Input Parameters Related to Groundwater Simulation in the Fort Sumner Area

9.5.1. Fort Sumner Groundwater Objects

9.5.1.1. Eastside 1

Slot	Value	Units
Anisotropy Ratio	1.00	NONE
Aquifer Area	16,873.28	acre
Aquifer Length	52,500.00	ft
Aquifer Thickness	100.00	ft
Aquifer Width	14,000.00	ft
Conductance Downstream	342.96	ft^2/day
Conductance Right	3,684.21	ft^2/day
Hydraulic Conductivity	8.00	ft/day
Specific Yield	0.20	NONE

9.5.1.2. Eastside 2

Slot	Value	Units
Anisotropy Ratio	2.00	NONE
Aquifer Area	4,889.81	acre
Aquifer Length	14,200.00	ft
Aquifer Thickness	100.00	ft
Aquifer Width	15,000.00	ft
Conductance Downstream	449.71	ft^2/day
Conductance Right	1,775.00	ft^2/day
Conductance Upstream	342.96	ft^2/day
Hydraulic Conductivity	15.00	ft/day
Specific Yield	0.20	NONE

9.5.1.3. Eastside 3

Slot	Value	Units
Anisotropy Ratio	2.00	NONE
Aquifer Area	11,019.28	acre
Aquifer Length	30,000.00	ft
Aquifer Thickness	100.00	ft
Aquifer Width	16,000.00	ft
Conductance Downstream	421.05	ft^2/day
Conductance Right	3,135.89	ft^2/day
Conductance Upstream	449.71	ft^2/day
Deep Aquifer Depth	500.00	ft
Deep Aquifer Hydraulic Conductivity	0.50	ft/day
Hydraulic Conductivity	12.00	ft/day
Specific Yield	0.20	NONE

9.5.1.4. Eastside 4

Slot	Value	Units
Anisotropy Ratio	2.00	NONE
Aquifer Area	9,550.05	acre
Aquifer Length	26,000.00	ft
Aquifer Thickness	100.00	ft
Aquifer Width	16,000.00	ft
Conductance Right	3,768.12	ft^2/day
Conductance Upstream	421.05	ft^2/day
Hydraulic Conductivity	20.00	ft/day
Specific Yield	0.20	NONE

9.5.1.5. FSID to Sand Gates

Slot	Value	Units
Anisotropy Ratio	1.00	NONE
Aquifer Area	1,955.92	acre
Aquifer Length	14,200.00	ft
Aquifer Thickness	100.00	ft
Aquifer Width	6,000.00	ft
Conductance Downstream	159.03	ft^2/day
Conductance Left	1,775.00	ft^2/day
Conductance Upstream	254.87	ft^2/day
Hydraulic Conductivity	10.00	ft/day
Soil Limited Evaporation Elevation	4,020.00	ft
Specific Yield	0.10	NONE
Wetted Sand Area	40.00	acre

9.5.1.6. Main Drain to Taiban

Slot	Value	Units
Anisotropy Ratio	1.00	NONE
Aquifer Area	3,461.89	acre
Aquifer Length	26,000.00	ft
Aquifer Thickness	100.00	ft
Aquifer Width	5,800.00	ft
Conductance Left	3,768.12	ft^2/day
Conductance Right	2,015.50	ft^2/day
Conductance Upstream	134.88	ft^2/day
Hydraulic Conductivity	10.00	ft/day
Soil Limited Evaporation Elevation	3,927.00	ft
Specific Yield	0.10	NONE
Wetted Sand Area	144.00	acre

9.5.1.7. Sand Gates to Main Drain

Slot	Value	Units
Anisotropy Ratio	2.00	NONE
Aquifer Area	3,994.49	acre
Aquifer Length	30,000.00	ft
Aquifer Thickness	100.00	ft
Aquifer Width	5,800.00	ft
Conductance Downstream	134.88	ft^2/day
Conductance Left	3,135.89	ft^2/day
Conductance Upstream	159.03	ft^2/day
Hydraulic Conductivity	10.00	ft/day
Soil Limited Evaporation Elevation	3,972.00	ft
Specific Yield	0.10	NONE
Wetted Sand Area	145.00	acre

9.5.1.8. Main Drain to Taiban

Slot	Value	Units
Anisotropy Ratio	1.00	NONE
Aquifer Area	3,461.89	acre
Aquifer Length	26,000.00	ft
Aquifer Thickness	100.00	ft
Aquifer Width	5,800.00	ft
Conductance Left	3,768.12	ft^2/day
Conductance Right	2,015.50	ft^2/day
Conductance Upstream	134.88	ft^2/day
Hydraulic Conductivity	10.00	ft/day
Soil Limited Evaporation Elevation	3,927.00	ft
Specific Yield	0.10	NONE
Wetted Sand Area	144.00	acre

9.5.2. FSID Drains

9.5.2.1. MainDrain

Slot	Value	Units
Conductance	235,224.00	ft^2/day
Diversion Capacity	25.00	cfs
Hydraulic Conductivity	0.50	ft/day
Riverbed Thickness	1.00	ft
Seepage Area	10.80	acre
Streambed Elevation	3,972.30	ft

9.5.2.2. Lwr_MainDrain

Slot	Value	Units
Conductance	10,890.00	ft2/da y
Hydraulic Conductivity	0.50	ft/day
Riverbed Thickness	1.00	ft
Seepage Area	0.50	acre
Streambed Elevation	3,948.80	ft

9.5.2.3. LowerDrain

Slot	Value	Units
Conductance	291,852.00	ft^2/day
Hydraulic Conductivity	1.00	ft/day
Riverbed Thickness	1.00	ft
Seepage Area	6.70	acre
Streambed Elevation	3,938.20	ft

9.5.2.4. Lwr_LowerDrain

Slot	Value	Units
Conductance	10,890.00	ft^2/day
Hydraulic Conductivity	0.50	ft/day
Riverbed Thickness	1.00	ft
Seepage Area	0.50	acre
Streambed Elevation	3,921.40	ft

10. References

Banta, E.R., 2000, MODFLOW-2000, the U.S. Geological Survey Modular Ground-Water Model - Documentation of Packages for Simulating Evapotranspiration with a Segmented Function (ETS1) and Drains with Return Flow (DRT1): U.S. Geological Survey Open-File Report 00-466, 127 p.

DBSA, 1995. Comprehensive Review and Model of the Hydrogeology of the Roswell Basin. Prepared for The New Mexico State Engineer Office. Volume 1. https://www.ose.state.nm.us/Compacts/Pecos/PDF/Roswell-Basin_Vol-I.pdf

Doherty, J., 2001. PEST-ASP Users' manual. Watermark Numerical Computing, Brisbane, Australia.

Duffy, C.J. and L.W. Gelhar, 1978. Recharge and Groundwater Conditions in the Western Region of the Roswell Basin. Partial Technical Completion Report, Project No. A-055-NMEX, New Mexico Water Resources Research Institute.

Eastoe, C.J. and R. Rodney, 2014, Isotopes as Tracers of Water Origin in and Near a Regional Carbonate Aquifer: The Southern Sacramento Mountains, New Mexico, Water 2014, 6, 301- 323

.

Harbaugh, A.W., Banta, E.R., Hill, M.C., and McDonald, M.G., 2000, MODFLOW-2000, the U.S. Geological Survey modular ground-water model -- User guide to modularization concepts and the Ground-Water Flow Process: U.S. Geological Survey Open-File Report 00-92, 121 p.

Hill, M.C., 1992. A computer program (MODFLOWP) for estimating parameters of a transient, three- dimensional, ground-water flow model using nonlinear regression: U.S. Geological Survey Open-File Report 91-484, 358 p.

Newton, B.T., G.C. Rawling, S.S. Timmons, L.A. Land, P.S. Johnson, T.J. Kludt, and J. M. Timmons, 2012. Sacramento Mountains Hydrogeology Study, Open File Report 543, New Mexico Bureau of Geology and Mineral Resources.

Rawling, G.C., B.T. Newton, S.S. Timmons, and L.A. Land, 2014. Hydrogeology of the southern Sacramento Mountains, New Mexico in Geology of the Sacramento Mountains Region, New Mexico Geological Society 65th Annual Fall Field Conference Guidebook.